UNIVERSIDAD PERUANA
CAYETANO HEREDIA

“FILOGENIA, BIOGEOGRAFÍA Y ADAPTACIÓN ECOLÓGICA EN LOS ANDES DE LOS ROEDORES DEL GÉNERO *Thomasomys* COUES, 1884 (RODENTIA: CRICETIDAE)”

TESIS PARA OPTAR EL GRADO DE DOCTOR EN CIENCIAS DE LA VIDA

DENNISSE CINTHYA RUELAS PACHECO

LIMA – PERÚ

2024

UNIVERSIDAD PERUANA
CAYETANO HEREDIA

“PHYLOGENY, BIOGEOGRAPHY, AND ECOLOGICAL ADAPTATION ON THE ANDES OF RODENTS OF THE GENUS *Thomasomys* COUES, 1884 (RODENTIA: CRICETIDAE)”

TESIS PARA OPTAR EL GRADO DE
DOCTOR EN CIENCIAS DE LA VIDA

DENNISSE CINTHYA RUELAS PACHECO

LIMA – PERÚ

2024

DIRECTOR

(DIRECTEUR)

Dr. FABRE, Pierre-Henri

(Université de Montpellier, France)

CO-DIRECTOR

(CO-DIRECTEUR)

Dr. PÉREZ ZÚÑIGA, José Miguel

(Universidad Peruana Cayetano Heredia, Peru)

CO-SUPERVISOR

(CO-ENCADRANT)

Dr. PACHECO TORRES, Víctor Raúl

(Universidad Nacional Mayor de San Marcos, Peru)

THESIS JURY

DR. MÉLANIE DEBIAIS-THIBAUD

PRÉSIDENTE

DR. RINA LASTENIA RAMIREZ MESIAS

EXAMINATRICE

DR. LAURENT GRANJON

EXAMINATEUR

DR. JÉRÔME FUCHS

RAPPORTEUR

DR. ALEXANDRE REIS PERCEQUILLO

RAPPORTEUR

DR. JOSÉ PÉREZ ZÚÑIGA

CO-DIRECTEUR DE THESE

DR. VÍCTOR RAÚL PACHECO TORRES

CO-ENCADRANT

DEDICATION

To my family, who never hesitated to support me despite financial hardships, to my little brother who always motivates me by showing him the way, and to Agatha, my little princess who fills my being with joy.



Design generated using Dall-E.

ACKNOWLEDGMENTS

This thesis is part of a dream that began while I was in my master's program and with which I wanted to materialize the final part of my training as a researcher. This doctorate not only forced me to learn and improve in English, but also to learn French. I tend to be very persistent, and passionate, and fight for what I want despite my pessimism and emotional weakness. However, it is very important to highlight that throughout my journey to this stage, many people have given me the necessary support to keep moving forward, and I would like to thank them here:

I would like to thank Pierre-Henri Fabre (PH) for supporting my doctoral application from the beginning and for his interest in working on a topic I proposed and was beginning to delve into, mountain forest rodents. Throughout all this time, despite his limited time, he kept his confidence in me and gave me the necessary confidence to progress in this thesis. I would also like to thank Víctor Pacheco, with whom I have been working since 2014 on various projects on Peruvian mammals. He gave me the first opportunity by allowing me to do my master's thesis with him, and now, as my co-supervisor in my Ph.D., he reaffirms his trust in my work. Victor is not only my master but also my mentor and a role model in the field of mammalogy.

I would like to thank the members of my thesis committee, Gael Kergoat, Allowen Evin, and Géraldine Veron, for all their advice and encouragement during our meetings about my thesis. I would also like to thank Pierre-Olivier Antoine for always resolving my doubts regarding university administration. I would also like to thank Ulyses Pardiñas, whom I met in a course I took in Ecuador, saw part of the

work I was doing at that time, later invited me to collaborate in the HMW writing taxonomic accounts for some species, and kindly reviewed my project and wrote the recommendation letter for my doctoral application. Many thanks also to José Pérez and Fréderic Delsuc for helping me with my doctoral application and with the cumbersome administrative procedures. Fréderic Delsuc and PH also helped me extend my stay at ISEM last year thanks to two contracts I had with the CNRS and the University of Montpellier.

I would like to thank Nicolás Reyes Amaya (Research Institute of Biological Resources Alexander von Humboldt, Colombia), Juan Diaz Nieto (EAFIT University, Colombia), Santiago Burneo (Museum of Zoology QCAZ, Pontifical Catholic University of Ecuador, Ecuador), Roberto Portela Miguez (Natural History Museum, UK), Robert Voss (American Museum of Natural History, USA), Joseph Cook (Museum of Southwestern Biology, USA), Adam Ferguson and Bruce Patterson (Field Museum of Natural History, USA) for sending tissues and/or specimens for molecular and morphological analysis. Robert Voss also supported my application for the AMNH grants to visit the collection, which was granted to me and allowed me not only to visit the AMNH in 2023 but also the FMNH where Adam Ferguson and Bruce Patterson allowed me to review the collection.

I thank Marie-ka Tilak and Elodie Lauroua for being patient with me and teaching me how to obtain mitogenomes and capture exons. With Marie-ka, I learned a lot from each one of our conversations. To Emmanuel Douzery, who not only taught me the basics in Bash but also performed the first exon capture analyses for *Thomasomys*. To Renaud



Lebrun, thank you for teaching and assisting me in the use of CTscan, reconstructions, and use of Avizo. To Quentin Martinez, who showed me to segment turbinals, shared information and a script that later served as a reference for my own analyses. The discussions we had with PH about my work have been quite fruitful, although it was not the main topic of my thesis, this new topic was quite challenging hard. To Lea Da Cunha, who showed me how to segment the inner ear, which despite not including that part in this thesis due to limited time, is part of my thesis delimitation process, and I will work on it after my thesis defense. I also thank two non-graduate students, María Pumacajia and Rafael Lecaros, who remotely helped me to take photos, measurements, and sample tissues of *Thomasomys* at the Natural History Museum of UNMSM, Peru. To Omar Ruelas, not only for being my little brother and one of the people to whom I dedicate my achievements, but also for being my best friend, and confidant, and for his skill in bioinformatics, which helped me to improve and correct my scripts in R and to understand Bash. To Raisa who helped me taking care of Agatha and staying at my home in Lima while I was doing my Ph.D. in France.

I also want to thank Félix Nesme, who not only supported me emotionally in the last part of my thesis but also became my mom and my personal chef in France. In my almost panic attacks, he always held out his hand and gave me a hug and was with me the times when I had to sleep in the hospital after migraines or when I had surgery. Thank you so much. Additionally, thanks to him, I gained a new family in France, the Nesme family, who welcomed and accepted me without prejudice and made my time in France warmer and more peaceful.

To my super friends Alba Marino and Katherine Vallejos, whom I love, admire, and deeply respect, and with whom I traveled to various places, including Italy and the Czech Republic. Particularly, Alba saved me when I was struggling with bash xD. To Narla Stutz for always helping me with many different matters, from very personal to administrative stuff. To Arthur Naas, with whom we went to Cayenne in French Guiana to present our partial results of the thesis at the LabEx CEBA meeting. Thanks to him, I met other extraordinary people who welcomed me into their home and allowed me to visit the KWATA zoological collection. To my friends Céline Robinet, Moritz Dirnberger, Hamilcar Keilani, Iris Feichtinger, Andrea Kraus, Vicente Crespo, Heitor Bissoli, Jhelam Deshpande, and Marcos Alvez for the time shared and the deep and not-so-deep conversations we had. You all will always be in my heart. To Alexandre Assemat for sharing his thesis with me and enlightening me on how to present mine. To my colleagues at ISEM, Alexis Marion, Lucas Buffan, Killian Gernelle, and many others, for all the time-shared during lunches, áperos, parties, meetings… It was always very interesting to listen to their stories and conversation topics. To my Peruvian colleagues and "mi mancha" or "mis patas" Mabel Alvarado, Jorge Ramirez, Marinoli Rivas, Roxana Castañeda, and others for not forgetting me and giving me the best vibes to finish my thesis and come back to the UNMSM with a richer background.

I extend my gratitude to the institutions that supported my work, including AMNH (United States), INNOVATE-PERU (Peru), ProCiencia (Peru), LabEx CEBA (France), and others, as well as the doctoral schools at Peruvian University Cayetano Heredia (UPCH) and GAIA at the University of Montpellier. Special

thanks to PH and Frederic Delsuc for their financial contributions to my molecular research and imaging studies.

I also wish to acknowledge the administrative staff at UPCH and the University of Montpellier (UM), especially Rebeca Caldas, Miguel Mendoza, Cendrine Jay-Allemand, and Mairec Sullbaran, for their invaluable assistance in navigating the administrative challenges encountered at the start and conclusion of my PhD journey.

To my family, who, despite economic hardships, never forced me to change my career, since biology, especially zoology, is not monetarily profitable, but quite the opposite, they always trusted that somehow, I would find a way to do what I like and not lose my way. And, of course, to Agatha, who came into my life during the first year of my PhD. during the lockdown for the COVID-19 pandemic. She not only accompanied me but also sweetened my days and improved my life. She filled the small room where I lived in Lima and also filled my life during that difficult time of isolation. When I left, it was very hard not to miss her, but I always kept in mind that when I returned, our lives would be better than they were before I left.

Thank you all for being part of this part of my life.

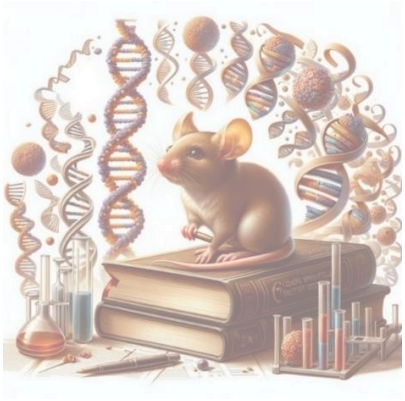

Design generated using Dall-E.

FINANCING SOURCES

- D. Ruelas was supported by a scholarship of the Franco Peruvian School of Life Sciences (2020-2023), one contract with the Université de Montpellier, and another with CNRS (2023).
- Funding for collecting specimens, molecular methods, and scanning was provided by the Agence Nationale de la Recherche (Défi des autres savoirs, Grants DS10, ANR-17-CE02-0005 RHINOGRAD 2017 given to P.-H. Fabre), LabEx Centre d'étude de la biodiversité amazonienne (CEBA, ANR-10-LABX-25-01), and PROCIENCIA (N° PE501078825-2022-PROCIENCIA given to V. Pacheco), INNOVATE-PERU (402-PNICP-PIBA-2014 given to V. Pacheco), and UNMSM (RR 03202-R-18, RR 03556-R-19 given to V. Pacheco).
- Funding for visiting collections was given to D. Ruelas by the American Museum of Natural History (AMNH) and Institut des Sciences de l'Evolution de Montpellier (ISEM).

10% Similitud general

El total combinado de todas las coincidencias, incluidas las fuentes superpuestas, para ca...

Filtrado desde el informe

- Texto citado

Exclusiones

- N.º de fuentes excluidas

Grupos de coincidencias

- 552 Sin cita o referencia 9%
  Coincidencias sin una citación ni comillas en el texto
- 66 Faltan citas 1%
  Coincidencias que siguen siendo muy similar al material fuente
- 0 Falta referencia 0%
  Las coincidencias tienen comillas, pero no una citación correcta en el texto
- 0 Con comillas y referencia 0%
  Coincidencias de citación en el texto, pero sin comillas

Fuentes principales

7%	Fuentes de Internet
9%	Publicaciones
4%	Trabajos entregados (trabajos del estudiante)

Marcas de integridad

N.º de alerta de integridad para revisión

Caracteres reemplazados
439 caracteres sospechosos en N.º de páginas
Las letras son intercambiadas por caracteres similares de otro alfabeto.

Los algoritmos de nuestro sistema analizan un documento en profundidad para buscar inconsistencias que permitirían distinguirla de una entrega normal. Si advertimos algo extraño, lo marcamos como una alerta para que pueda revisarlo.

Una marca de alerta no es necesariamente un indicador de problemas. Sin embargo, recomendamos que preste atención y la revise.

CONTENTS

ABSTRACT

RESUME

RESUMEN

INTRODUCTION 1

1. Sigmodontines in the Tropical Andes 1

2. Overview of the *Thomasomys* genus 7

2.1. Taxonomic status 7

2.2. Diversity and distribution 10

2.3. Karyotype 11

2.4. Morphological species groups 25

2.5. Phylogeny 31

2.6. The non-grouped *Thomasomys* 34

2.7. Challenges and insights 35

2.8. Species concept 38

2.9. Hypothesis 39

OBJECTIVES 40

CHAPTER 1. Unilocus delimitation methods reveal the underestimated species diversity of *Thomasomys* (Rodentia, Cricetidae) 41

Abstract 44

INTRODUCTION 45

MATERIAL AND METHODS 49

RESULTS 57

DISCUSSION 62

CONCLUSIONS 86

ACKNOWLEDGMENTS 87

REFERENCES 88

FIGURES 108

TABLE 1 113

CHAPTER 2. Introduction to the *Thomasomys* (Rodentia: Cricetidae) turbinal bone adaptations: Insights into elevation and environmental challenges 117

Abstract 119

INTRODUCTION 120

METHODS 124

RESULTS 131

DISCUSSION 139

CONCLUSIONS 150

ACKNOWLEDGMENTS 151

REFERENCES 152

APPENDIX 166

FIGURES 170

TABLE 1 176

CHAPTER 3. Three new species of *Thomasomys*-like form from the central Peruvian montane forest and a new perspective of the tribe Thomasomyini 178

Abstract 180

INTRODUCTION 181

MATERIAL AND METHODS 184

RESULTS 191

TAXONOMIC ACCOUNTS 199

DISCUSSION 230

ACKNOWLEDGMENTS 245

REFERENCES 246

APPENDIX 1 267

APPENDIX 2 275

APPENDIX 3 288

APPENDIX 4 290

APPENDIX 5 293

APPENDIX 6 294

APPENDIX 7 295

APPENDIX 8 301

APPENDIX 9 303

FIGURES 304

TABLES 323

GENERAL DISCUSSION 345

CONCLUSIONS 353

REFERENCES 355

SUPPLEMENTARY INFORMATION 372

Supplementary information - Article 1 373

Supplementary information - Article 2 448

Extended abstract in French / Résumé étendu en français : 477

ABSTRACT

The genus *Thomasomys*, a key genus within the Thomasomyini tribe of the Sigmodontinae subfamily, is a focal point for understanding the phylogeny, biogeography, and ecological adaptation of Andean rodents. As the most diverse genus within the Sigmodontinae, *Thomasomys* includes 51 valid species and numerous undescribed ones, predominantly inhabiting Neotropical montane forests and paramos. Its distribution, however, excludes regions like the Guiana Shield, lowland tropical forests, deserts, and oceanic islands. Conflictive findings between early molecular phylogenetic analyses and morphological studies highlight the necessity for an integrated approach encompassing genetic, molecular, and morphological research. This research delves into *Thomasomys* complex taxonomic background, phylogenetic relationships, species diversity, and morphological adaptations, shedding light on its evolutionary history and ecological adaptations in the challenging Andean habitats.

The research encompasses three chapters. Chapter 1 reveals an underestimated species diversity, confirming the monophyly of the genus. The analyses identified ten major clades, demonstrating a complex phylogenetic structure with paraphyletic or polyphyletic relationships among species and challenging the monophyly of some species groups such as Cinereus, Aureus, Gracilis, and Incanus. Unilocus species delimitation methods indicated a higher number of putative species compared to the current taxonomy. It also emphasizes the biogeographical importance of the Marañón area as a geographical barrier influencing species distribution and speciation within *Thomasomys*. Chapter 2 explores the turbinal

bone adaptations in *Thomasomys* species. It suggests that these adaptations are closely tied to elevation and environmental challenges, with a significant positive allometric relationship observed between turbinal surface areas and skull length. Chapter 3 introduces a new genus distinct from *Thomasomys* and describes three new species endemics to the central Peruvian Yungas. This discovery challenges the traditional taxonomic composition of the Thomasomyini tribe, the morphological delimitation of the genera that comprise it, and puts into debate the phylogenetic position of *Rhagomys*.

Together, these chapters shed light on the complex evolutionary history and ecological adaptations of the *Thomasomys* genus, emphasizing the need for integrative research approaches to fully understand the complexities of Andean rodent biodiversity and adaptation.

KEYWORDS

ADAPTATION, RODENTIA, SYSTEMATICS, SOUTH AMERICA,

TROPICAL ANDES

RESUMEN

El género *Thomasomys*, un género clave en de la tribu Thomasomyini de la subfamilia Sigmodontinae, es un punto focal para entender la filogenia, biogeografía y adaptación ecológica de los roedores andinos. Siendo el género más diverso de los Sigmodontinae, *Thomasomys* incluye 51 especies válidas y numerosas no descritas, habitando predominantemente en bosques montanos neotropicales y páramos. Sin embargo, su distribución excluye regiones como el Escudo Guayanés, bosques tropicales de tierras bajas, desiertos e islas oceánicas. Los resultados contradictorios entre análisis filogenéticos moleculares tempranos y estudios morfológicos resaltan la necesidad de un enfoque integral que abarque investigación genética, molecular y morfológica. Esta investigación profundiza en el complejo trasfondo taxonómico de *Thomasomys*, sus relaciones filogenéticas, diversidad de especies y adaptaciones morfológicas, aclarando su historia evolutiva y adaptaciones ecológicas en los desafiantes hábitats andinos.

La investigación abarca tres capítulos. El Capítulo 1 revela una subestimada diversidad de especies, confirmando la monofilia del género. Los análisis identificaron diez clados principales, demostrando una estructura filogenética compleja con relaciones parafiléticas o polifiléticas entre especies y desafiando la monofilia de algunos grupos de especies como Cinereus, Aureus, Gracilis e Incanus. Métodos de delimitación de especies unilocus indicaron un número mayor de especies putativas comparado con la taxonomía actual. También enfatiza la importancia biogeográfica del área del Marañón como una barrera geográfica que influye en la distribución de especies y especiación dentro de *Thomasomys*. El Capítulo 2 explora las adaptaciones de los huesos turbinales en las especies de

Thomasomys. Se sugiere que estas adaptaciones están estrechamente vinculadas a la elevación y los desafíos ambientales, con una relación alométrica positiva significativa observada entre las áreas de superficie turbinal y la longitud del cráneo. El Capítulo 3 introduce un nuevo género distinto de *Thomasomys* y describe tres nuevas especies endémicas de las Yungas peruanas centrales. Este descubrimiento desafía la composición taxonómica tradicional de la tribu Thomasomyini, la delimitación morfológica de los géneros que la componen y pone en debate la posición filogenética de Rhagomys.

Juntos, estos capítulos permiten entender la compleja historia evolutiva y adaptaciones ecológicas del género *Thomasomys*, enfatizando la necesidad de enfoques de investigación integrativos para comprender completamente las complejidades de la biodiversidad y adaptación de los roedores andinos.

PALABRAS CLAVES

ADAPTACIÓN, RODENTIA, SISTEMÁTICA, SUDAMÉRICA, ANDES TROPICALES

RÉSUMÉ

Le genre *Thomasomys*, un genre clé au sein de la tribu des Thomasomyini de la sous-famille des Sigmodontinae, est un point focal pour comprendre la phylogénie, la biogéographie et l'adaptation écologique des rongeurs andins. En tant que genre le plus diversifié au sein des Sigmodontinae, *Thomasomys* comprend 51 espèces valides et de nombreuses autres non décrites, habitant principalement les forêts montagnardes néotropicales et les páramos. Sa distribution exclut cependant des régions comme le Bouclier guyanais, les forêts tropicales de basse altitude, les déserts et les îles océaniques. Les résultats contradictoires entre les analyses phylogénétiques moléculaires précoces et les études morphologiques soulignent la nécessité d'une approche intégrée englobant la recherche génétique, moléculaire et morphologique. Cette recherche se penche sur l'arrière-plan taxonomique complexe, les relations phylogénétiques, la diversité des espèces et les adaptations morphologiques de *Thomasomys*, mettant en lumière son histoire évolutive et ses adaptations écologiques dans les habitats andins exigeants.

La recherche comprend trois chapitres. Le Chapitre 1 révèle une diversité d'espèces sous-estimée, confirmant la monophylie du genre. Les analyses ont identifié dix grands clades, démontrant une structure phylogénétique complexe avec des relations paraphylétiques ou polyphylétiques parmi les espèces et remettant en question la monophylie de certains groupes d'espèces tels que Cinereus, Aureus, Gracilis et Incanus. Les méthodes de délimitation d'espèces unilocus ont indiqué un nombre plus élevé d'espèces putatives par rapport à la taxonomie actuelle. Elles soulignent également l'importance biogéographique de la zone du Marañón comme barrière géographique influençant la distribution des espèces et la spéciation au sein

de *Thomasomys*. Le Chapitre 2 explore les adaptations des os turbinaux chez les espèces de *Thomasomys*. Il suggère que ces adaptations sont étroitement liées à l'élévation et aux défis environnementaux, avec une relation allométrique positive significative observée entre les surfaces des os turbinaux et la longueur du crâne. Le Chapitre 3 introduit un nouveau genre distinct de *Thomasomys* et décrit trois nouvelles espèces endémiques aux Yungas péruviennes centrales. Cette découverte remet en question la composition taxonomique traditionnelle de la tribu des Thomasomyini, la délimitation morphologique des genres qui la composent et met en débat la position phylogénétique de *Rhagomys*.

Ensemble, ces chapitres mettent en lumière l'histoire évolutive complexe et les adaptations écologiques du genre *Thomasomys*, soulignant la nécessité d'approches de recherche intégratives pour comprendre pleinement les complexités de la biodiversité et de l'adaptation des rongeurs andins.

MOTS CLES

ADAPTATION, RODENTIA, SYSTEMATIQUE, AMERIQUE DU SUD, ANDES TROPICALES

INTRODUCTION

1. Sigmodontines in the Tropical Andes

The Andes are one of the most important hotspots of biodiversity and endemism of vertebrates and plants (Ceballos & Ehrlich, 2006; Mittermeier et al., 1998; Myers et al., 2000). As the longest continuous mountain range on Earth, the Andes serve both as dispersal corridors to montane species and as formidable dispersal barriers for lowland forms (Patterson et al., 1992, 2012). The Andes' geological history is marked by a series of morphotectonic segments, each with its own unique characteristics and influences (Gansser, 1973). The Andes are not a unique geologic structure, they consist of a complex interaction among different trends and events of different structural ages since the synchronization of their uplift varies from north to south and from west to east, leading to a complex structural history (Gansser, 1973; Hoorn et al., 2010). The Andes are typically divided into three geological sections: Northern (from Venezuela to northern Peru), Central (northern Peru, Bolivia, Chile, and Argentina), and Southern Andes (Chile and Argentina), being the Northern Andes comparatively younger (Gansser, 1973; Patterson et al., 2012).

The uplift history of the Andes has had significant biological impacts, influencing global climates and creating diverse habitats (Graham, 2009; Hoorn et al., 2010). Over the past 10 million years, continuous uplift and environmental changes have shaped the dynamic, species-rich ecosystems in the Andes and Amazonia (Hoorn et al., 2010). Remarkably, the Andean montane forests (including premontane forests) and paramo, located in the Northern Andes and northern and eastern of the Central Andes, are present from Venezuela to northern

Argentina (Gansser, 1973; Patterson et al., 2012; Tejedor Garavito et al., 2012). These ecosystems, also described as the "moist north-central Andes" (Josse et al., 2003; Kelt & Meserve, 2014) or Tropical Andes (Cazalis et al., 2020; Hazzi et al., 2018), are characterized by it exceptional biodiversity, with a wide range of unique plant and animal species (Antonelli & Sanmartín, 2011; Mittermeier et al., 1998). This diversity is influenced by various factors, including biotic interactions, niche conservatism, and dispersal ability (Antonelli & Sanmartín, 2011). Ecohydrological processes, such as fog regimes, also shape these ecosystems' vegetation and species composition (Aparecido et al., 2018). Montane ecosystems, like Tropical Andes, are also known for their high numbers of endemic species and wide variety of ecosystem services such as water supply and carbon storage (Aparecido et al., 2018).

The subfamily Sigmodontinae, the most diverse mammalian group in the Neotropics, has undergone evolutionary adaptations shaped by ecological and geographical factors, particularly in response to transitions between lowland and montane habitats (Gonçalves et al., 2020; Parada et al., 2015). Through comprehensive phylogenetic analyses and biogeographical history examination, the Andes have been proved as a central source of diversity for these rodents, acting as a macroevolutionary cradle and species attractor with significant dispersal from both Northern and Central-Southern Andes (e.g., Schenk & Steppan, 2018; Vallejos-Garrido et al., 2023). This area showcases elevated speciation, particularly tribes Akodontini and Oryzomyini exhibit higher diversification rates compared to others (Vallejos-Garrido et al., 2023). Their presence in these habitats is also influenced by their ability to adapt to different habitats which is driven by factors

such as habitat selection, behavioral responses, and microhabitat use (Parada et al., 2015; Villarreal et al., 2022). Within montane forests and paramos, these rodents have important roles in the ecosystem, serving as herbivores, seed dispersers, and prey for various predators (e.g.., Noblecilla & Pacheco, 2013; Sahley et al., 2015, 2016).

The Tropical Andes' altitudinal gradient presents unique challenges for biodiversity, including significant temperature fluctuations and variations in oxygen levels, which have deep effects on the adaptation and distribution of species (Cavelier, 1996; Navas, 2002; Patterson et al., 2012; Withers et al., 2016a, 2016b). These environmental soft barriers isolate populations and promote speciation, particularly along the eastern slopes, where are found the montane forests, known for their exceptional species turnover (Weir, 2006). This isolation and the unique ecological conditions have facilitated the emergence of endemic genera, contributing significantly to the speciation and diversification observed. Notable examples include *Aepeomys* (2 species: Pacheco, 2015a), *Anotomys* (1 species: Voss, 2015), *Chibchanomys* (2 species: Voss, 2015), *Chilomys* (7 species: Brito et al., 2022; Pacheco, 2015b), *Handleyomys* (2 species: Gómez- Laverde et al., 2015), *Lenoxus* (1 species: Patton, 2015), *Microryzomys* (2 species: Carleton, 2015), *Neomicroxus* (2 species: Alvarado- Serrano & D'Elía, 2015), *Nephelomys* (14 species: Percequillo, 2015a; Ruelas et al., 2021), *Oreoryzomys* (1 species: Percequillo, 2015b), *Pattonimus* (2 species: Brito et al., 2020), *Tapecomys* (2 species: Salazar-Bravo, 2015), and *Thomasomys* (51 species: Pacheco, 2015c; Pacheco & Ruelas, 2023). Most of them are restricted to the forests of the Northern Andes, except for *Chibchanomys*, *Lenoxus*, *Thomasomys*, *Microryzomys*,

Nephelomys, and *Tapecomys*. Additionally, many other widely distributed genera have endemic species to the Tropical Andes, such as *Akodon*, *Oligoryzomys*, *Neacomys*, *Oxymycterus* and others (e.g., Hurtado & D'Elía, 2019; Hurtado & Pacheco, 2017; Jiménez et al., 2013; Jiménez & Pacheco, 2016; Ruelas & Pacheco, 2022). The diverse climatic conditions, environmental features, and historical contexts across the Andean regions also contribute to the complex adaptations seen in local species (Ojeda & Novillo, 2013). The contrast between the broad geographic ranges of species in eastern Brazil and the more restricted distributions in the Andes further illustrates the impact of the Andes' complex landscape on biodiversity (Ojeda & Novillo, 2013).

The Huancabamba Depression, located between the Northern and Central Andes in the north of Peru, holds significant geographical importance, acting as a constriction point between the Piura and Cajamarca regions, with the lowest elevation recorded at 2145 m in Piura (Alva, 2009; Duellman & Pramuk, 1999). Alongside the Marañón Zone, which encompasses the Marañón River and dry forest, this depression has served as a crucial boundary, demarcating the southern extent of numerous northern species and the northern limit of southern ones (Chapman, 1926; Duellman & Pramuk, 1999). Specifically, for montane-dwelling sigmodontines, such as several species of *Thomasomys* (Pacheco, 2015c), *Nephelomys albigularis* and *N. ricardopalmai* (Ruelas et al., 2021), *Akodon orophilus* (Jiménez et al., 2013), the Huancabamba Depression and the Marañón Zone have played an essential role in shaping their current distribution. Further geographical barriers such as the Táchira Depression (between Colombia and Venezuela), Las Cruces pass (in the Eastern Cordillera of Colombia), Colombian

massif (in Colombia), and the Huallaga river, the Apurímac river valley (in the southeastern Peru) have also been proposed as significant factors influencing the distribution of several taxa (Gutiérrez et al., 2015; Hazzi et al., 2018). Although they have not been properly tested for sigmodontines, likely they are also acting shaping the distribution limits of species of this group (e.g., Hurtado & Pacheco, 2017; Jiménez & Pacheco, 2016; Pacheco, 2015c; Pacheco et al., 2007).

The evolutionary history of sigmodontine rodents in the Tropical Andes is marked by significant diversification events linked to the area's distinct ecological and geological features (Parada et al., 2015; Patterson et al., 2012; Schenk & Steppan, 2018; Vallejos-Garrido et al., 2023). The late Mio-Pliocene period witnessed the emergence of new habitats within the central and northern Andes, leading to the hypothesis that many Andean endemic species originated from Amazonian ancestors. These ancestors may have expanded and adapted to these new biomes, contributing to the rich biodiversity seen today (Upham et al., 2013). Key diversification peaks approximately 6, 3, and 1 million years ago reflect the dynamic interplay between ecological adaptations and geological transformations within the high-elevation Central Andes (Schenk & Steppan, 2018). These rodents' colonization patterns underscore their adaptability to the Tropical Andes' contrasting climates and terrains, from dense montane forests to the open high paramos (Parada et al., 2015; Patterson et al., 2012; Reig, 1986; Schenk & Steppan, 2018). Although the mechanisms and routes of these colonization events remain underexplored, Reig (1986) proposed that the Oryzomyini tribe, including Thomasomyini, originally differentiated in the northern Andes, with early sigmodontines (proto-oryzomyine) potentially arriving in northwestern South

America by rafting from Central America. While the Miocene uplifting of the Andes increased environmental heterogeneity, driving the differentiation of the original oryzomyine stock in montane forests. This process likely led to the adaptation of some genera like *Thomasomys*, *Aepeomys*, and *Chilomys* to Andean environments. Reig (1986) also proposed that Ichthyomyini, likely originating from a *Thomasomys*-like ancestor, adapted to semiaquatic life in mountain streams. Schenk and Steppan (2018) suggested that members of the Phyllotini-Thomasomyini clade, initially widespread in the Brazilian Atlantic Forest, subsequently made a significant leap towards the more demanding environments of the central Andes. This transition underscores the clade's ecological versatility and the role of the Andes as a crucible for sigmodontine speciation. Phyllotini first diversified in the lower-elevation Chaco/Pampas; however, tracing the ancestral roots of the Thomasomyini is challenging due to its members' broad geographical spread (Schenk & Steppan, 2018). Vallejos-Garrido et al. (2023) suggested a Northern Andes origin for the Thomasomyini and Oryzomyini tribes, aligning with Reig's (1986) hypothesis. This contrasts with other hypotheses suggesting origins in the Guiana Highlands/Amazon basin, Central Andes, or Boreal Brazilian region (Maestri & Patterson, 2016; Percequillo et al., 2021; Schenk & Steppan, 2018). Vallejos-Garrido et al.' (2023) findings also align the ancestral range of Abrotrichini, Andinomyini, and Euneomyni tribes with the Central-Southern Andes and suggest an Atlantic-forest origin for Akodontini, and Wiedomyini tribes. However, the origin of the Phyllotini tribe remains unresolved. Focusing on *Oligoryzomys*, Hurtado and D'Elía (2022) highlighted the complex evolutionary pathways of this genus from origin in northern South America through several

environmental and geographical shifts, expanding its range southward and upward into the Andean region and beyond. However, for *Thomasomys*, the most diverse genus of Sigmodontinae primarily inhabiting the Tropical Andes, there are no hypotheses explaining its success in these environments.

These findings emphasize the Tropical Andes' significance as both a barrier and a bridge in the evolutionary history of sigmodontine rodents, facilitating a wide array of adaptive strategies and contributing to the rich biodiversity characteristic of the region. Future research is essential to unravel the detailed mechanisms that have enabled these rodents and other Andean species to thrive in the diverse and often extreme conditions of the Tropical Andes, providing crucial insights for conservation and biodiversity management.

2. Overview of the *Thomasomys* genus

2.1. Taxonomic status

The taxonomy and classification of *Thomasomys* and related genera have undergone various interpretations over the years. The genus *Thomasomys*, initially recognized by Thomas (1906) based on the dental characteristics of its species, has been a subject of taxonomic and phylogenetic debate within the Sigmodontinae subfamily (Pacheco, 2003, 2015c). The nomenclature of *Thomasomys* has been closely linked to related genera such as *Aepeomys*, *Delomys*, and *Wilfredomys*. At different times, *Thomasomys* was placed within the all-encompassing Oryzomyini complex or informally referred to as "thomasomyines" (Hershkovitz, 1962, 1966).

These genera have been viewed alternately as subgenera or even as separate genera themselves in earlier taxonomic treatments (e.g., Cabrera, 1961; Ellerman, 1941; Pine, 1980). Hershkovitz (1962, 1966) proposed the concept of "thomasomyines" as a sylvan grade of rodents with specific characteristics, describing them as "forest-dwelling, broad-footed, long-tailed, 6-mammate, brachydont-pentalophodont mice with wide, short palates, and weakly projecting zygomatic plates." Then, Steadman and Ray (1982) erected the Thomasomyini tribe, formally identifying it based on the combination of short palates and medium- to large-sized pentalophodont molars containing *Thomasomys*, *Rhipidomys* and the fossil genus *Megaoryzomys*. Cerqueira (1982) further endorsed this concept, including *Delomys*, *Phaenomys*, *Rhipidomys*, and *Thomasomys* as extant tribe representatives. Subsequent taxonomic accounts (e.g., Eisenberg & Redford, 1999; McKenna & Bell, 1997) further expanded the tribe to include additional genera and species. However, Voss (1993) contested its validity as a natural group, suggesting that their classification relied solely on shared primitive characteristics.

Pacheco (2003) carried out an extensive cladistic analysis of morphological traits using several New World cricetid rodents, which encompassed *Thomasomys* and its related genera. Contrary to Voss (1993), Pacheco's analysis supported the monophyly of Thomasomyini, which included 11 genera. Pacheco (2003) also suggested the presence of an "Andean thomasomyine clade," which only included *Aepeomys*, *Chilomys*, *Rhipidomys*, and *Thomasomys*. This clade was sister to six other genera found in southeastern Brazil: *Abrawayaomys*, *Juliomys*, *Phaenomys*, *Rhagomys* (with some Andean species), *Wiedomys*, and *Wilfredomys*. However, molecular studies conducted later (e.g., D'Elía et al., 2006; Parada et al., 2015;

Pardiñas et al., 2022; Steppan & Schenk, 2017) provided additional insights, suggesting that the composition of Thomasomyini may require further refinement. Recently Pardiñas et al. (2022) separated *Rhagomys* in its own tribe although sister to his concept of Thomasomyini. These molecular analyses consistently supported a clade composed of *Aepeomys*, *Chilomys*, *Rhagomys*, *Rhipidomys*, and *Thomasomys*. While some issues remain unresolved, the current understanding of the genus *Thomasomys* centers on its position within the Thomasomyini tribe, along with related genera like *Aepeomys*, *Chilomys*, and *Rhipidomys* (Pacheco, 2015c; Pacheco et al., 2015; Pardiñas et al., 2022). Although the monophyly of *Thomasomys* was not recovered in a morphological approach (Pacheco, 2003), it was in most molecular studies (e.g., Brito et al., 2019, 2021; Lee et al., 2022; Pacheco, 2003, 2015c; Pacheco & Ruelas, 2023; Ruelas & Pacheco, 2021). As molecular research advances and includes more taxa and genetic information, our understanding may change. Despite these taxonomic complexities, *Thomasomys* remains an intriguing genus of Neotropical rodents with diverse species and unique characteristics. Currently this genus is widely accepted as valid.

Type species: *Hesperomys cinereus* Thomas, 1882.

Synonyms shown here were taken from Pacheco (2015c):

> *Hesperomys*: Tomes, 1860:219; part (description of *aureus*); not *Hesperomys* Waterhouse.
>
> *Hesperomys* (*Rhipidomys*): Thomas, 1882:108; part (description of *cinereus* and *taczanowskii*); neither *Hesperomys* Waterhouse nor *Rhipidomys* Tschudi.

Hesperomys (*Vesperimus*): Thomas, 1884:449; part (listing of *cinereus* and *taczanowskii*); neither *Hesperomys* Waterhouse nor *Vesperimus* Coues.

Thomasomys Coues, 1884:1275; as subgenus of *Hesperomys*; type species *Hesperomys cinereus* Thomas, by original designation.

Oryzomys: Thomas, 1894:349; part (description of *incanus* and *kalinowskii*); not *Oryzomys* Baird.

Peromyscus (*Thomasomys*): E.- L. Trouessart, 1897:512; part (listing of *cinereus* and *kalinowskii*); not *Peromyscus* Gloger.

Aepeomys: Thomas, 1898:452; part (description of *vulcani*); not *Aepeomys* Thomas.

Thomasomys: Thomas, 1906:443; raised to rank of genus.

Erioryzomys Bangs, 1900:96; type species *Oryzomys monochromos* Bangs, by original designation.

Inomys Thomas, 1917:197; type species *Oryzomys incanus* Thomas, by original designation.

2.2. Diversity and distribution

In the preceding two decades, the systematics of the genus *Thomasomys* have significantly evolved from relying only on morphological characterizations, as exemplified by *T. ucucha* Voss, 2003, to incorporating molecular integrative methods in the most recent descriptions. These methods, notably the use of the Cytb gene, have been essential in substantiating the description of new species, such as *T. andersoni* (Salazar-Bravo & Yates, 2007) and species described thereafter. While the documented diversity of the genus expanded from 44 valid species in 2015

(Pacheco, 2015c) to 51 in 2023 (Table 1) and several candidate species (e.g., Brito et al., 2019, 2021; Lee et al., 2022; Pacheco, 2003, 2015c; Pacheco & Ruelas, 2023; Ruelas & Pacheco, 2021), all of which are restricted to the tropical Andes. Their distribution ranges from northern Venezuela to southern Bolivia, including isolated mountain ranges like the Serranía de la Macarena (Pacheco, 2015c), Cordillera Otishi (Luna & Pacheco, 2002) and Cordillera del Cóndor (Brito et al., 2021). The elevational range they inhabit is extensive, from around 1200 m to 4500 m. It is crucial to note the absence of *Thomasomys* in specific areas, including the Guiana Shield, lowland tropical forests, arid regions, and oceanic islands (Pacheco, 2015c). Most of the holotypes are Peruvian (19) and Ecuadorian (17) and are housed mainly in the American Museum of Natural History (AMNH: 17) and in the Natural History Museum UK (NHMUK: 19) (Table 1).

2.3. Karyotype

The karyotypes observed in *Thomasomys* are generally conservative (Table 2), typically characterized by a diploid number of 2n = 40, 42, or 44, with the notable exception of *T. niveipes*, which has a diploid number of 2n = 24. The variation in the number of autosomal arms is minimal, often resulting in FN = 40, 42, or 44 (Table 2). It is worth mentioning that *Thomasomys* sp. 4 stands out with an FN = 47 (Pacheco et al., 2012).

Table 1. List of described taxa of *Thomasomys*. Abbreviations: AMNH – American Museum of Natural History (AMNH, New York, USA), FMNH – Field Museum of Natural History (Chicago, USA), LSUMZ – Museum of Vertebrate Zoology (Berkeley, USA), MECN – Museo Ecuatoriano de Ciencias Naturales (Quito, Ecuador), MUSM – Museo de Historia Natural de la Universidad Nacional Mayor de San Marcos (Lima, Peru), NHMUK – Natural History Museum (London, UK), USNM – National Museum of Natural History (Washington, USA).

#	**Described taxa**	**Current status**	**Holotype**	**Type locality**	**Distribution**
1	*Thomasomys andersoni* Salazar- Bravo and Yates, 2007	valid	AMNH 268734	"an elfin forest near the headquarters of the Corani hydroelectric plant (17°12′43″S, 65°52′09″W, GPS coordinates, map datum WGS 84) at 2,630 m, Department of Cochabamba, Bolivia."	Bolivia
2	*Thomasomys apeco* Leo and Gardner, 1993	valid	MUSM 7197	"Valle de Los Chochos, ca. 25 km NE Pataz, 3280 m, Parque Nacional Río Abiseo, San Martín, Perú."	Peru
3	*Thomasomys aureus* (Tomes, 1860)	valid	NHMUK 7.1.1.104	Pallatanga, Ecuador (Pacheco 2015)	Ecuador

4	*Thomasomys aureus altorum* Allen, 1914	Synonymized to *aureus* by Musser and Carleton (1993), but used in as subspecies in Brito et al. (2021) without justification	AMNH 36280	“Mt. Pichincha (altitude 11,000 ft.), [Pichincha] Ecuador”	Ecuador
5	*Thomasomys auricularis* Anthony, 1923	valid	AMNH 47697	“Taraguacocha, on trail from Zaruma to Zaraguro, altitude 10,250 feet, Cordillera de Chilla, Provincia del Oro, Ecuador.”	Ecuador
6	*Thomasomys australis* Anthony, 1925	valid	AMNH 38550	“Incachaca, 7700 feet, Prov. Cochabamba, Bolivia.”	Bolivia

7	*Thomasomys baeops* (Thomas, 1899)	valid	NHMUK 98.8.1.7	“Pita R[ío]., above the Chillo Valley, [Pichincha,] Ecuador. Alt. 3500 metres.”	Colombia, Ecuador
8	*Thomasomys bombycinus* Anthony, 1925	valid	AMNH 37740	“Paramillo, Western Andes, [Antioquia,] Colombia; altitude 12,500 ft.”	Colombia
9	*Thomasomys caudivarius* Anthony, 1923	valid	AMNH 47668	“Taraguacocha, Cordillera de Chilla, 10,750 feet [3,277 m], Provincia del Oro, Ecuador.”	Ecuador, Peru
10	*Thomasomys cinereiventer* J. A. Allen, 1912	valid	AMNH 32436	“crest of Western Andes (altitude, 10,340 feet [3,152 m]), 40 miles [64 km] west of Popayan [= Popayán], Cauca, Colombia.”	Colombia
11	*Thomasomys cinereus* (Thomas, 1882)	valid	NHMUK 81.9.7.29	“Cutervo, 9,200′ [2,804 m],” Cajamarca, Peru	Ecuador, Peru
12	*Thomasomys cinnameus* Anthony, 1924	valid	AMNH 67401	“Hacienda San Francisco, east of Ambato, [Tungurahua,] central Ecuador, elevation 8000 feet [2,438 m].”	Colombia, Ecuador

13	*Thomasomys contradictus* Anthony, 1925	valid	AMNH 32955	“Santa Isabel, Quindio Andes, [Quindío,] Colombia; altitude, 12,700 feet [3,871 m].	Colombia
14	*Thomasomys daphne* Thomas, 1917	valid	USNM 194902	“Ocobamba Valley, 9,100 feet [2,774 m],” Cusco, Peru	Peru, Bolivia
15	*Thomasomys dispar* Anthony, 1925	valid	AMNH 33761	“Andalucia, Eastern Andes, Huila, Colombia, elevation 7000 feet.”	Colombia
16	*Thomasomys eleusis* Thomas, 1926	valid	NHMUK 26.4.1.48	“Tambo Jenes, 12,000′ [3,658 m],” Amazonas, Peru.	Peru
17	*Thomasomys emeritus* Thomas, 1916	valid	NHMUK 5.1.1.4	“Montes de Escaguey, alt. 2500 m,” Mérida, Venezuela.	Venezuela
18	*Thomasomys erro* Anthony, 1926	valid	AMNH 68195	“upper slopes of Mt. Sumaco, exact altitude unknown, but probably 8000– 9000 feet [approx. 2,438– 2,743 m] at head of the Rio Suno [= Río Suno], a tributary of the Rio Napo [= Río Napo],” Napo, Ecuador.	Ecuador

19	*Thomasomys fumeus* Anthony, 1924	valid	AMNH 67537	“Hacienda San Francisco, east of Ambato, [Tungurahua,] central Ecuador, elevation about 8000 feet [2,438 m].”	Ecuador
20	*Thomasomys gracilis* Thomas, 1917	valid	USNM 194816	“Matchu [sic] Picchu, 12,000 feet [3,658 m],” Cusco, Peru.	Peru
21	*Thomasomys hudsoni* Anthony, 1923	valid	AMNH 47690	“Bestion [= Bestión], Provincia del Azuay, 10,100 feet [3,078 m], Ecuador.”	Ecuador
22	*Thomasomys hylophilus* Osgood, 1912	valid	FMNH 18583	“Paramo de Tama [= Páramo de Tamá], head of Rio Tachira [= Río Táchira], Santander [= Norte de Santander], Colombia.”	Colombia, Venezuela
23	*Thomasomys incanus* (Thomas, 1894)	valid	NHMUK 94.10.1.4	“Valley of Vitoc [= Río Tulumayo]” Junín, Peru	Peru
24	*Thomasomys fraternus* Thomas, 1927	synonymized to *incanus* by Osgood (1933)	NHMUK 27.11.1.169	“Alcas, 25 miles 5 N.E. of Cerro Junin [, Junín, Peru]. 11,500”	Peru

25	*Thomasomys ischyrus* Osgood, 1914	valid	FMNH 19803	"Tambo Almirante, near Uchco"; defined as "Perú, Amazonas Dept., 65 km E Chachapoyas, near Uchco, Tambo Almirante, 5000 ft (1524 m)"	Peru
26	*Thomasomys kalinowskii* (Thomas, 1894)	valid	NHMUK 94.10.1.2	"Valley of Vitoc [= Río Tulumayo]" Junín, Peru.	Peru
27	*Thomasomys ladewi* Anthony, 1926	valid	AMNH 72113	"Rio Aceramarca, northeast of La Paz [, La Paz], Bolivia, altitude 10,800 feet [3,292 m]."	Bolivia
28	*Thomasomys laniger* (Thomas, 1895)	valid	NHMUK 95.8.1.39	"Bogota"; corrected to Bogotá Region, 8,750 ft (2,667 m), Cundinamarca, Colombia	Colombia
29	*Thomasomys macrotis* Gardner and Romo 1993	valid	LSUMZ 27286	"Puerta del Monte, ca. 30 km NE [of] Los Alisos, ca. 3250 m. [Parque Nacional Río Abiseo], San Martín, Perú."	Peru
30	*Thomasomys monochromos* Bangs, 1900	valid	8348	"Paramo (= Páramo) de Macotama, Sierra Nevada de Santa Marta, 11,000 feet altitude," Magdalena, Colombia	Colombia

31	*Thomasomys nicefori* Thomas, 1921	valid	NHMUK 21.7.1.20	"San Pedro, north of the town [= Medellín]," Antioquia, Colombia	Colombia
32	*Thomasomys niveipes* (Thomas, 1896)	valid	NHMUK 96.11.1.4	"La Oya del Barro, W. Cundinamarca, Colombia"; spelling corrected to La Hoya del Barro [= La Hoya del Barro Blanco], small basin situated at the head of the Río Teusacá and includes the Laguna El Verjón (GómezLaverde et al. 1997)	Colombia
33	*Thomasomys notatus* Thomas, 1917	valid	USNM 194548	"Torontoy," Cusco, Peru.	Peru
34	*Thomasomys onkiro* Luna and Pacheco, 2002	valid	MUSM 13064	"Peru: Department of Cuzco, Province of La Convención, Vilcabamba Cordillera, eastern slope of the Andes, between the Ene and Urubamba rivers, 325 km northwest of city of Cuzco, 11°39′36″S, 73°40′02″W, at 3,350 m elevation in elfi n forest patches of Polylepis, Weinmannia, and Chusquea," corrected to Province of Satipo, Junín department by Quintana Navarrete (2011)	Peru
35	*Thomasomys oreas* Anthony, 1926	valid	AMNH 72130	"Cocopunco [= Cocapunco], about 80 miles north of La Paz, Bolivia, altitude 10,000 feet."	Peru, Bolivia

36	*Thomasomys paramorum* Thomas, 1898	valid	NHMUK 97.11.7.82	“Paramo [= Páramo] south of Chimborazo [= Mt Chimborazo],” defi ned as “Urbina (1°30′S, 78°44′W) just a few kilometers SE of Chimborazo” by Voss (2007), Chimborazo, Ecuador.	Ecuador, Colombia
37	*Thomasomys pardignasi* Brito, Vaca-Puente, Koch, and Tinoco, 2021	valid	MECN 5852	“Ecuador, provincia Morona Santiago, cantón Méndez, parroquia Patuca, Cordillera de Kutukú (02.78722°S, 78.13166°W; elevation 2,215 m)”	Ecuador
38	*Thomasomys popayanus* Allen, 1912	valid	AMNH 32371	“crest of Western Andes (alt. 10,340 ft [3,152 m]), 40 miles [64 km] west of Popayan [= Popayán], Cauca, Colombia.	Colombia
39	*Thomasomys praetor* (Thomas, 1900)	valid	NHMUK 0.3.15.3	“Eastern slope of Paramo [= Páramo] between San Pablo and Cajamarca, [Cajamarca,] Peru,” 4,000 m elevation.	Peru
40	*Thomasomys princeps* (Thomas, 1895)	valid	NHMUK 95.8.1.37	“Bogota,” corrected to Bogotá Region, 8,750 ft (2,667 m), Cundinamarca, Colombia by Musser and Carleton (2005)	Colombia

41	*Thomasomys pyrrhonotus* Thomas, 1886	valid	NHMUK 81.9.7.24	"Tambillo, [Río Malleta,] 5800 ft [1,768 m]," Cajamarca, Peru.	Peru
42	*Thomasomys rosalinda* Thomas and St. Leger, 1926	valid	NHMUK 26.8.6.31	"Goncha, Amazonas, 8500′ [2,591 m]," Peru.	Peru
43	*Thomasomys salazari* Brito, Tinoco, Curay, Vargas, Reyes Puig, Romero and Pardiñas 2019	valid	MECN 5649	"Ecuador, provincia Morona Santiago, cantón Morona, parroquia Zúñac, Parque Nacional Sangay, Guardianía de Atillo (2°11'16.48"S; 78°29'47.55"O, 3508 msnm)"	Ecuador
44	*Thomasomys silvestris* Anthony, 1924	valid	AMNH 66288	"Las Maquinas [= Máquinas], on Santo Domingo trail, west of Corazon [= Corazón], Western Andes, [Pichincha,] Ecuador; altitude 7,000 feet [2,134 m]."	Ecuador
45	*Thomasomys taczanowskii* (Thomas, 1882)	valid	NHMUK 81.9.7.23	"Tambillo, [Río Malleta,] 5800′ [1,768 m]," Cajamarca, Peru.	Ecuador, Peru

46	*Thomasomys ucucha* Voss, 2003	valid	UMMZ 155644	“11,100 ft (3384 m) in the valley of the Río Papallacta (ca. 3–5 km by trail NNW Papallacta), Provincia Napo, Ecuador.”	Ecuador
47	*Thomasomys vestitus* (Thomas, 1898)	valid	NHMUK 98.5.15.3	“Rio Milla [= Río Milla], Merida [= Mérida], 1630 m,” Venezuela	Venezuela
48	*Thomasomys vulcani* (Thomas, 1898)	valid	NHMUK 98.5.1.10	“Mount [Volcán] Pichincha, [Pichincha,] Ecuador, at about 12,000 feet [= 3,658 m].”	Ecuador
49	*Thomasomys burneoi* Lee, Tinoco, and Brito, 2022	valid	MECN 5662	“Ecuador, Provincia de Morona Santiago, cantón Morona, parroquia Zúñac, Parque Nacional Sangay (Sangay National Park), Laguna Negra”	Ecuador
50	*Thomasomys antoniobracki* Ruelas and Pacheco 2021	valid	MUSM 23757	"Campamento Alto Parramata at 2630 m elevation, in Carmen de la frontera district, Huancabamba province, Piura department, Peru"	Peru
51	*Thomasomys lojapiuranus* Pacheco and Ruelas, 2023	valid	MUSM 23758	“Peru, Department of Piura, Province of Huancabamba, Pariamarca Alto”	Peru, Ecuador

52	*Thomasomys shallqukucha* Pacheco and Ruelas, 2023	valid	MUSM 46875	“Peru, Department of Lambayeque, Province of Ferreñafe, District of Kañaris, Geomarca”	Peru
53	*Thomasomys pagaibambensis* Pacheco and Ruelas, 2023	valid	MUSM 40986	“Peru, Department of Cajamarca, Province of Chota, District of Querocoto, Pagaibamba”	Peru

Table 2. Summary of karyotypes reported for species of *Thomasomys*, taken and modified from Pacheco et al. (2012).

Species	2N	FN	X	Y	Country and locality	Reference	Comments
T. andersoni	44	42	?	?	Bolivia: Cochabamba, Corani	Salazar Bravo and Yates (2007)	
T. aff. *aureus*	44	42	A	A	Peru: Río Palca and Yaraccyacu	Gardner and Patton (1976)	Reported as *T. aureus*
T. emeritus	42	40	M	A	Colombia: Cerro Las Banderas, near Merida City (Merida) and Paramo Los Colorados	Aguilera et al. (2000)	Reported as *T. laniger*
T. kalinowskii	44	44	A	A	Peru: Yaraccyacu	Gardner and Patton (1976)	
T. laniger	40	40	M or SM	A	Colombia: Cundinamarca, Carpanta Biological Reserve	Gómez-Laverde et al. (1997)	
T. monochromos	42	42	SM	A	Colombia: San Lorenzo	Gardner and Patton (1976)	
T. niveipes	24	42	M or SM	A	Colombia: Cundinamarca, Carpanta Biological Reserve	Gómez-Laverde et al. (1997)	

T. notatus	44	44	A	A	Peru: Huanuco, Cordillera Carpish	Gardner and Patton (1976)	
T. paramorum	44	42	SM	SM	Ecuador: Mt Pichincha	Gardner and Patton (1976)	Reported as *Thomasomys* sp.
T. paramorum	44	42	A	A	Ecuador	Haynie et al. (2006)	
T. vestitus	44	42	A	A	Colombia: Merida, Santo Domingo, El Baho	Aguilera et al. (2000)	
Thomasomys sp. 4 (sensu Pacheco, 2003)	42	47	A	M	Peru: Huánuco, Palmapampa	Pacheco et al. (2012)	Reported as *Thomasomys* sp., then as *Thomasomys* sp. 4 by Pacheco (2015)
Thomasomys sp. 8 (sensu Pacheco, 2003)	44	44	A	A	Peru: Ayacucho, Yaraccyacu	Gardner and Patton (1976)	Primarily reported as *T. taczanowskii*, then as *T. oreas* by Pacheco et al. (2012)

2.4. Morphological species groups

A critical step in refining the systematics of this genus involved delineating *Thomasomys* sensu stricto (s.s.), considering contradictory findings at the molecular and morphological phylogenetic levels, leading to the proposition of seven morphological groups by Pacheco (2015c) based on morphology, phylogeny, and distribution. The current species classification draws primarily from the works of Pacheco (2003, 2015c), along with contributions of Brito et al. (2019, 2021), Ruelas and Pacheco (2021), Lee et al. (2022), and Pacheco and Ruelas (2023). Pacheco (2015c) also suggested that might be appropriate to give to each species groups a generic status if subsequent research confirms their monophyly. The two genus-group names that are currently available are *Thomasomys* (with *cinereus* Thomas as the type species is) and *Inomys* (with *incanus* Thomas as the type species). While these species groups offer a preliminary framework for understanding *Thomasomys* diversity, ongoing research, and detailed morphological, genetic, and molecular analyses are necessary to confirm and refine these groupings.

a. **Cinereus species group:**

Type species: *Hesperomys* (=*Thomasomys*) *cinereus* Thomas, 1882.

Included species: *australis* Anthony, 1925; *bombycinus* Anthony, 1925; *caudivarius* Anthony, 1923; *cinereiventer* J. A. Allen, 1912; *cinereus* Thomas, 1882; *cinnameus* Anthony, 1924; *contradictus* Anthony, 1925; *daphne* Thomas, 1917; *dispar* Anthony, 1925; *emeritus* Thomas, 1916; *erro* Anthony, 1926; *fumeus* Anthony, 1924; *hudsoni* Anthony, 1923; *hylophilus*

Osgood, 1912; *laniger* Thomas, 1895; *lojapiuranus* Pacheco and Ruelas, 2023; *monochromos* Bangs, 1900; *niveipes* Thomas, 1896; *onkiro* Luna and Pacheco, 2002; *pagaibambensis* Pacheco and Ruelas, 2023; *paramorum* Thomas, 1898; *salazari* Brito, Tinoco, Curay, Reyes-Puig, Romero, and Pardiñas, 2019; *shallqukucha* Pacheco and Ruelas, 2023; *silvestris* Anthony, 1924; *vestitus* Thomas, 1898; *vulcani* Thomas, 1898. Unnamed species *Thomasomys* sp. 3 (sensu Pacheco, 2003), and *Thomasomys* sp. 10 (sensu Pacheco, 2003).

Description: Members of this group are characterized by long and soft dorsal pelage, large and protuberant anuses, absence of genal 1 vibrissae, lack of a rostral tube, and variable auditory bullae (inflated or uninflated). Their carotid circulation is generally primitive (pattern 1). Other features include the absence of capsular processes and the presence of a relatively simple glans penis with no notch on the midventral crater margin. Preputial glands are usually absent.

Distribution: This group consists of small to medium-sized rodents found throughout montane forests from the cordilleras of Venezuela and Colombia to southeastern Bolivia, at elevations from 1198 m to 4500 m. Most species within this group are found in the Northern Andes, from Colombia to northern Peru.

b. **Aureus species group:**

Type species: *Hesperomys* (=*Thomasomys*) *aureus* Tomes, 1860

Included species: *antoniobracki* Ruelas and Pacheco, 2021; *apeco* Leo L. and Gardner, 1993; *aureus* Tomes, 1860 (including *altorum* J. A. Allen, 1914); *auricularis* Anthony, 1923; *burneoi* Lee Jr., Tinoco, and Brito, 2022; *nicefori* Thomas, 1921; *T. pardignasi* Brito, Vaca-Puente, Koch, and Tinoco, 2021; *popayanus* J.A. Allen, 1912; *praetor* Thomas, 1900; *princeps* Thomas, 1895; *pyrrhonotus* Thomas, 1886; *rosalinda* Thomas and St. Leger, 1926. Unnamed species *Thomasomys* sp. 1 (sensu Pacheco, 2003), *Thomasomys* sp. 2 (sensu Pacheco, 2003).

Morphological Traits: This group mainly includes larger *Thomasomys* that have long and soft dorsal pelage, moderately large ears, and a brown-reddish dorsal coloration. These species are characterized by their reddish-brown dorsal pelage. They also possess unique features such as genal 1 vibrissae, a narrow and convergent interorbital region, and a derived carotid circulation pattern (pattern 3). Their upper incisors are opisthodont, and their anteroloph is labially and posteriorly oriented. The presence of a small anterolingual conule in M1 is distinctive. Preputial glands are numerous.

Distribution: These rodents inhabit the montane forests from the cordilleras of Venezuela and Colombia to southeastern Bolivia, at elevations from 1200 m to 4000 m.

c. **Baeops species group:**

Type species: *Oryzomys baeops* Thomas, 1899

Included species: *baeops* Thomas, 1899 and *taczanowskii* Thomas, 1882.

Description: This group includes small to medium-sized *Thomasomys* that have comparatively short dorsal pelage with grayish or brownish coloration, genal 1 vibrissae, and short, relatively broad hindfeet. Their skulls feature a short rostrum and a narrow interorbital region. These rodents usually have a derived carotid circulation (pattern 3) and pointed distal portions of the lateral bacular mounds.

Distribution: These rodents are distributed in the montane forests of the northern Andes, specifically from Colombia to northern Peru, mainly north of the Huancabamba Depression, at elevations from 1150 m to 3800 m.

d. **Gracilis species group:**

Type species: *Thomasomys gracilis* Thomas, 1917

Included species: *andersoni* Salazar-Bravo and Yates, 2007; *gracilis* Thomas, 1917; *oreas* Anthony, 1926. Unnamed species *Thomasomys* sp. 8 (sensu Pacheco, 2003) and *Thomasomys* sp. 9 (sensu Pacheco, 2003).

Description: This group comprises small to medium-sized *Thomasomys* that typically have moderate to long, dense, and soft dorsal pelage, as well as short and relatively broad hindfeet. Their skulls feature a short to moderate rostrum and a narrow interorbital region. These rodents usually have primitive carotid circulation (pattern 1) and bullae that are either uninflated or moderately inflated with short bony tubes.

Distribution: These rodents are found in the montane forests of the southern Andes, ranging from northern Peru to Bolivia, south of the Huancabamba Depression, at elevations from 2000 m to 4270 m.

e. **Incanus species group:**

Species type: *Thomasomys incanus* Thomas, 1894

Included species: *eleusis* Thomas, 1926; *incanus* Thomas, 1894 (including *fraternus* Thomas, 1927); *ischyrus* Osgood, 1914; *kalinowskii* Thomas, 1894; *ladewi* Anthony, 1926; Unnamed species *Thomasomys* sp. 5 (sensu Pacheco, 2003), *Thomasomys* sp. 6 sensu (Pacheco, 2003), *Thomasomys* sp. 7 (sensu Pacheco, 2003).

Description: This group comprises medium-sized *Thomasomys* similar to the Cinereus group but with a derived carotid circulation pattern (pattern 3). Typically, these rodents have a short rostral tube.

Distribution: These rodents are distributed throughout the montane forests of the Southern Andes, from northern Peru to northern Bolivia, south of the Huancabamba Depression at elevations from 2050 m to 3850 m.

f. **Macrotis species group:**

Type species: *Thomasomys macrotis* Gardner and Romo R., 1993

Included species: *macrotis* Gardner and Romo R., 1993

Description: This group is represented only by *T. macrotis*, a large mouse with large ears that shares characteristics with both the Incanus and Aureus groups, including soft and long dorsal pelage, large ears, and a moderately long hindfoot. Their tail is moderately long, with a significant white portion. These rodents exhibit long rostra, a derived carotid circulation (pattern 3), and a rectangular-shaped molar-bearing portion of the maxillae.

Distribution: These rodents are found exclusively in the isolated mountains of the Cordillera Oriental of Peru, between the Río Marañón and Huallaga, south of the Huancabamba Depression, ca 3250 m elevation.

g. **Notatus species group:**

Type species: *Thomasomys notatus* Thomas, 1917

Species included: *notatus* Thomas, 1917.

Description: This group is represented only by *T. notatus* a medium-sized *Thomasomys* that has comparatively short dorsal pelage with distinct countershading. Their hindfeet are short and relatively broad, and they have moderately long tails with a terminal pencil. These rodents feature a short rostrum, narrow interorbital region, primitive carotid circulation (pattern 1), and uninflated bullae with distinct bony tubes. Preputial glands are absent.

Distribution: distributed in the montane forests of the central Andes, including areas in northern and central Peru, south of the Huancabamba Depression, at elevations from 1400 m to 3400 m.

2.5. Phylogeny

In early molecular phylogenetic analyses with very limited taxon sampling, Smith and Patton (1999) and D'Elia et al. (2006) identified *Thomasomys* monophyletic and sister genus to *Chilomys* or *Rhagomys*, respectively. Pacheco (2003) performed a cladistic analysis based on morphological characters, indicating that *Thomasomys* is paraphyletic. Salazar-Bravo and Yates (2007) then used Cytochrome-b (Cytb) sequences from 15 *Thomasomys* taxa to conduct a phylogenetic analysis. Pacheco's (2003) findings were found to be somewhat congruent. Notable clades included: a clade comprising *T. australis*, *T. daphne*, *T. caudivarius*, and *T. cinnameus*, consistent with the Cinereus species group. A clade containing *Thomasomys* sp. 9, *T. oreas*, and *T. andersoni*, consistent with the Gracilis species group (although *T. gracilis* was unrelated). A species pair of *T. aureus* and *T.* sp. 2 (sensu Pacheco 2003), consistent with the Aureus species group. A strongly supported clade of *T. baeops* and *T. taczanowskii*, consistent with the Baeops species group. However, discrepancies between molecular and morphological hypotheses could be attributed to factors like limited taxonomic (15 taxa in molecular analysis versus 53 in morphological analysis), molecular (one marker) coverage, and potential misidentifications. In a multilocus approach, *Thomasomys* has frequently been found monophyletic, except for Parada et al. (2015) findings. More recently but with a better Cytb sampling, *Thomasomys* was found to be monophyletic and well-supported (Brito et al., 2019; 2021; Lee et al., 2015, 2018, 2022; Ruelas & Pacheco, 2021; Pacheco & Ruelas, 2023). The monophyly of the Baeops and Notatus was found to be well-supported but the monophyly of Cinereus group was moderate to weakly supported. Debate surrounds the monophyly status of the Aureus, Incanus,

and Gracilis groups (e.g., Brito et al., 2019, 2021; Lee et al., 2022; Ruelas & Pacheco, 2021; Pacheco & Ruelas, 2023).

Recent findings, although with limitations, have improved our understanding of the *Thomasomys* phylogeny, mainly to define the identity and limits of *T. cinereus*, the type species of the genus (Thomas, 1882), and to show the complex relationships of the most widely distributed *Thomasomys* species, *T. aureus*. *Thomasomys cinereus* had not been included in molecular phylogenetic studies until the work of Brito et al. (2019), who used specimens from Ecuador (Loja and Jimbura). The distribution of *T. cinereus* became a subject of debate when its geographical range was expanded to Ecuador (Moreno Cárdenas & Novillo-Gonzalez, 2020), contradicting the earlier hypothesis of its endemism to the northern Peru (see Pacheco, 2015c). Brito et al.'s (2019) phylogenetic analysis suggested a close relationship between *T. cinereus*, *T. cinnameus*, and *T. hudsoni*, albeit with weak support. Subsequently, Pacheco and Ruelas (2023) conducted a more extensive examination of specimens assigned to *T. cinereus* representing its whole range, revealing that the species represented a complex of four distinct species. This led to define the *T. cinereus* s.s., being found as Peruvian endemic, and describe three new species with small ranges, two Peruvian endemics (*T. shallqukucha* and *T. pagaibambensis*) and one distributed in Peru and Ecuador (*T. lojapiuranus*, identified as *Thomasomys* sp. 2 in Brito et al. (2021)). Notably, Brito et al.'s (2019) analysis of the Cinereus group was marked by several misidentifications (Pacheco and Ruelas, 2023), including erroneous categorization of certain specimens. As an example, specimens reported as *T. cinereus* s.s. by Brito et al. (2019) were not *T. cinereus* s.s. nor any of the new species reported by

Pacheco and Ruelas (2023). These specimens were named *Thomasomys* sp. 2 in Pacheco and Ruelas (2023, not "sp. 2" sensu Pacheco, 2003). Furthermore, both Brito et al. (2019) and Ruelas and Pacheco (2023) identified *Thomasomys* sp. 1 (distinct from "sp. 1" sensu Pacheco, 2003) as a candidate species from Bolivar, Ecuador (MSB 70714).

On the other hand, Pacheco (2015c) and earlier studies noticed that *Thomasomys* species generally exhibit small distribution ranges, with some, like *T. apeco* and *T. rosalinda*, being endemic to very specific localities. *T. aureus*; however, stood out as an exception with a broader distribution from Colombia to Bolivia (Pacheco, 2015c). Pacheco (2003, 2015c) identified two distinct populations within *T. aureus* – one from Cusco, Peru (*Thomasomys* sp. 1) and another from Comarapa, Bolivia (*Thomasomys* sp. 2) – suggesting they were separate species, but he did not formally name them. Posteriorly, Brito et al. (2019) found that *Thomasomys* sp. 1 and *Thomasomys* sp. 2 were paraphyletic, with the former closely related to *T. ladew*i of the Incanus group and the latter related to a broad clade including other members of the Aureus group, such as *T. aureus*, *T. auricularis*, and a *Thomasomys* sp. from El Angel, Ecuador. Ruelas and Pacheco (2021) and Brito et al. (2021), with improved sampling of *T. aureus* specimens, encountered that the Aureus group might not be monophyletic. Incorporating sequences from the *T. aureus* specimens used by Pacheco (2015), Ruelas and Pacheco (2021) discovered that the Aureus group is paraphyletic, comprising two unrelated but well-supported clades – one west and the other east of the Marañón River. While *Thomasomys* sp. 2 was found to be weakly supported at the base of the clade west of the Marañón River. Brito et al. (2021) and Lee et al. (2022)

additionally suggested other candidate species such as *Thomasomys* sp. "Pichincha" and *Thomasomys* sp. "Cajanuma" from Ecuador.

Despite these advances, our understanding of *Thomasomys* phylogeny remains incomplete. Recent studies have primarily focused on the Aureus (mainly on the *T. aureus* complex) and Cinereus groups, leaving other species less explored. The monophyly of certain species and their interrelationships continue to provoke debate. Some relationships identified morphologically by Pacheco (2003), such as *T. baeops* as sister to *T. taczanowskii* or *T. apeco* as sister to *Thomasomys* sp. 1, have been confirmed molecularly (e.g., Brito et al., 2019; Ruelas & Pacheco, 2021). Yet, many relationships remain unclear due to the absence of numerous species from molecular analyses.

2.6. The non-grouped *Thomasomys*

Thomasomys sp. 4 (sensu Pacheco, 2003) presents a unique taxonomic puzzle. It was morphologically differentiated from other *Thomasomys* species, and its karyotype was reported for a population from Huánuco (Table 2; Pacheco et al. 2012), but contrary to the other species it was not included in any species group sensu Pacheco (2015). In the morphological phylogeny, *Thomasomys* sp. 4 was identified as the sister taxon to *Thomasomys* sp. 5 within a larger clade that comprises species attributed to the Incanus group and *Aepeomys*. The exclusion of this candidate species without further explanation by the author raises questions about its association with the species of the Incanus group or even its classification within the *Thomasomys* genus, especially considering the nesting of non-*Thomasomys* species from the *Aepeomys* genus in this clade. Despite being

documented by Pacheco (2003) and Pacheco et al. (2012), there has been no subsequent evaluation or recording of *Thomasomys* sp. 4, leaving its taxonomic status an intriguing unresolved issue.

2.7. Challenges and insights

The genus *Thomasomys*, with its remarkable diversity and complex taxonomy, reflects the adaptability of Andean rodents to the multifaceted ecological niches of the Tropical Andes. The genus faces taxonomic challenges, primarily due to the extensive morphological variation among its species. This variation, as highlighted by Pacheco (2015c) through population studies of species such as *T. aureus*, *T. nicefori*, *T. kalinowskii* and many others, underscores the urgent need for advanced genetic and molecular systematics research. These studies are crucial to refine species classification and provide a complement to morphological analyses.

The genus has been the subject of varied phylogenetic interpretations, with early molecular analyses positioning *Thomasomys* either as a sister genus to *Chilomys* or *Rhagomys*, while morphological studies suggest a paraphyletic nature (Pacheco, 2003; Smith & Patton, 1999; D'Elía et al., 2006). Discrepancies in these findings are attributed to some factors like limited taxon sampling, the choice of molecular markers, and potential specimen misidentifications. However, more recent analyses using Cytb sequences have begun to reconcile these differences, recognizing distinct species groups within *Thomasomys*, such as Cinereus, Notatus, and Baeops, which aligns partially with morphological hypotheses. It is also important to note that the distribution of these species groups can be influenced by factors such as elevation, habitat type, and geographical barriers as pointed out by

Pacheco (2015c). The presence of certain species or groups may be restricted to specific elevational zones within the Andean Mountain ranges. As well as recent studies suggest that the diversity of *Thomasomys* is greater with several candidate species, some of them assessed morphologically but not yet described.

Thomasomys species are high-elevation habitat specialists exclusively inhabiting Neotropical premontane and montane forests, including the paramo (Pacheco, 2015c). Notably, they are absent from specific regions like the Guiana Shield, lowland tropical forests, deserts, and oceanic islands. With 51 valid species and several undescribed ones, *Thomasomys* is the most diverse sigmodontine genus, exhibiting co-occurrence of multiple species in the same montane habitat (Pacheco, 2015b; Pacheco & Ruelas, 2023; Voss, 2003). Their adaptability to varied environmental conditions and ecological niches, particularly in high-elevation environments, distinguishes *Thomasomys* from other diverse sigmodontine genera like *Akodon* and *Oligoryzomys* (Brandão et al., 2021; Hurtado & D'Elía, 2022; Pacheco, 2015b; Pardiñas et al., 2015; Weksler & Bonvicino, 2015). The genus's success could be attributed to its ability to exploit a broad range of resources, although a comprehensive understanding of *Thomasomys* is lacking, hindering the formulation of evolutionary hypotheses regarding its high adaptation and radiation in high-elevation habitats. The wide variation in temperature and humidity along Tropical Andes elevational gradients likely plays a crucial role in shaping the diverse adaptations and success of *Thomasomys* species.

Understanding the ecological adaptations and evolutionary responses of high-elevation specialized species such as *Thomasomys* to the challenging

conditions of montane settings is largely dependent on studying their turbinals. These complex bone structures are found inside the nasal cavity (Parsons, 1967). They are important for respiration and smell, two processes that are necessary for life in high-elevation environments with drastically fluctuating temperatures (Martinez et al., 2020). In cold, high-elevation regions, these structures are especially crucial for controlling the temperature of inhaled air and preserving moisture (Green et al., 2012; Martinez et al., 2023). By examining turbinals, one can gain insight into the morphological adaptations made by these species to enhance their olfactory and respiratory capacities, as well as their evolutionary success in these niches. Martinez et al. (2020) suggested that temperature-adapted evolutionary response, representing convergent evolution in response to similar ecological pressures across different semi-aquatic rodents, could be indicated by larger respiratory turbinals in species living in colder habitats (mediated by elevation). Turbinals also function as markers of more general ecological and physiological adaptations, possibly indicating convergent evolutionary patterns among different species under comparable environmental stressors (e.g., Green et al., 2012; Martinez et al., 2023; Schmidt-Nielsen et al., 1970). Given the diverse distribution and wide morphological range of *Thomasomys*, detailed studies of their turbinals can elucidate the underlying mechanisms of their adaptation, offering valuable data for formulating hypotheses about their evolutionary history and resilience in the fluctuating Andean climates.

Moreover, the unresolved taxonomic status of *Thomasomys* sp. 4 (sensu Pacheco, 2003) underscores the imperative for continued research into the genus's complex relationships and taxonomy. Clarifying the taxonomic identity of this

candidate species is crucial for several reasons. It is imperative to elucidate the taxonomic identity of *Thomasomys* sp. 4 for multiple reasons. First, it aids in improving our comprehension of the richness and evolutionary history of the genus, guaranteeing precise taxonomic classification and identification. Second, figuring out *Thomasomys* sp. 4's status could provide fresh information on the genus's ecological adaptations and niche specializations, especially in high-elevation settings. Third, by identifying various lineages and their distributions—a crucial step in maintaining biodiversity in the Andean regions—it may aid in more general biogeographical and conservation research. Finally, resolving these taxonomic ambiguities may help identify new cryptic species, which will increase our understanding of the evolutionary processes that have shaped the varied range of mice known as *Thomasomys* and its adaptive radiation.

In brief, the complexity and evolving taxonomy of the *Thomasomys* genus highlights the need for further research to clarify its relationships and taxonomy. Comprehensive sampling, accurate species identifications, and continued molecular and morphological studies are essential for a better understanding of this diverse rodent group. Such efforts are vital for unraveling the complex evolutionary history of this genus, ensuring the accuracy of its classification, and understanding its remarkable adaptability to the diverse ecosystems of the Tropical Andes.

2.8. Species concept

The species concept employed in this thesis is the General Lineage or Unified Species Concepts (de Queiroz, 2005, 2007), which defines a species as an independently evolving lineage. It integrates various criteria like morphology,

reproductive isolation, and genetics but doesn't require all criteria simultaneously. This integral approach acknowledges the complexity of species and their evolutionary histories.

2.9. Hypothesis

The hypothesis of this thesis is that the current taxonomic scheme of *Thomasomys* does not represent the specific diversity of the genus, where the morphology of the turbinal bones appears to be a key factor for the evolution and adaptation to high environments.

OBJECTIVES

The general objective of this thesis is to propose a comprehensive framework on the monophyly and species limits of the *Thomasomys* genus using phylogenetic analysis, analyze morphological adaptations to high-elevation environments, and clarify the taxonomic status of a candidate species of *Thomasomys* within the Thomasomyini tribe. This thesis is divided into three chapters, each with a specific objective:

1. **Phylogenetic analyses of *Thomasomys* genus and species limits:** Employ phylogenetic inference analyses on DNA sequences to test the monophyly of the *Thomasomys* genus, assess Pacheco's (2003, 2015) proposed species groups and candidate species, and investigate species diversity using multiple unilocus species delimitation methods.

2. **Study of morphological adaptations in *Thomasomys*:** Analyze the morphological adaptations in the turbinal bones of *Thomasomys* species, based on the Martinez et al.' (2020) statement for high-elevation rodent species, to uncover how these correspond to elevation and environmental challenges, offering insights into the evolutionary responses of *Thomasomys* to diverse high-elevation habitats.

3. **Assessment of the non-grouped *Thomasomys* and taxonomic implications for the *Thomasomys* genus and Thomasomyini tribe:** Examine the candidate species *Thomasomys* sp. 4 within a combined molecular and morphological framework, contributing to the understanding of *Thomasomys* sensu stricto and overall, the composition of the Thomasomyini tribe.

CHAPTER 1. Unilocus delimitation methods reveal the underestimated species diversity of *Thomasomys* (Rodentia, Cricetidae)

By using all available sequences of the mitochondrial cytochrome b gene, this first chapter aimed to determine the monophyly of *Thomasomys*, phylogenetic relationships, and species boundaries through phylogenetic molecular analyses and species delimitation methods. These analyses revealed significant insights into the species diversity of *Thomasomys*. The findings suggest that *Thomasomys* sensu stricto (s.s.) is monophyletic, not all the clades representing species groups are monophyletic, and the species diversity is underestimated, potentially doubling the current number of valid species. The candidate species proposed by some authors could constitute valid species, but detailed taxonomic studies are needed, in addition to the inclusion of holotypes, since some species were found to be paraphyletic. Additionally, a taxon previously identified as *Thomasomys* might represent a new genus within the Thomasomyini tribe, distinct from others already known. The chapter also discusses the Marañón zone, comprised of the Marañón valley and river, as biogeographical barrier influencing the distribution and diversification for major clades and for populations, particularly those previously known under the epithet *aureus*. This chapter advocates for an integrative approach and the use of more genes to better understand the diversity and evolutionary history of this genus.

The corresponding article for this chapter was submitted at Zoologica Scripta on August 15, 2023, and has been accepted for publication in June, 2024. Preliminary

results were presented at the Journée annuelle CEBA (October 4, 2022) and the International Symposium “Cenozoic ecosystems of the Andes-Amazon Region: Landscapes and Organisms” (April 5, 2023 - April 6, 2023).

Cited as:

Ruelas, D., Pacheco, V., Pérez, J., Diaz-Nieto, J., & Fabre, P.-H. (2024). Unilocus delimitation methods reveal the underestimated species diversity of *Thomasomys* (Rodentia, Cricetidae). *Zoologica Scripta*.

Unilocus delimitation methods reveal the underestimated species diversity of *Thomasomys* (Rodentia, Cricetidae)

Dennisse Ruelas[1,2,3,4], Víctor Pacheco[1], Juan Diaz-Nieto[5], José Pérez[6], Pierre-Henri Fabre[2,7]

[1]Museo de Historia Natural, Universidad Nacional Mayor de San Marcos, Lima 11, Peru.

[2]Institut des Sciences de l'Évolution (ISEM, UMR 5554 CNRS-IRD-UM), Université de Montpellier, Place E. Bataillon - CC 064 - 34095, Montpellier Cedex 5, France.

[3]Instituto de Ciencias Biológicas "Antonio Raimondi", Facultad de Ciencias Biológicas, Universidad Nacional Mayor de San Marcos, Lima, Peru.

[4]Doctorado en Ciencias de la Vida, Universidad Peruana Cayetano Heredia, Av. Honorio Delgado 430, Lima, Peru.

[5]Universidad EAFIT, Colombia.

[6]Universidad Peruana Cayetano Heredia, Peru.

[7]Institut Universitaire de France (IUF), Paris, France.

Abstract

Thomasomys is the most diverse genus of the Sigmodontinae subfamily, comprising at least 51 species. Despite recent systematic advances, the monophyly of this genus, the proposed species groups and their content, and the species limits are not yet firmly established. Using a well-sampled mitochondrial dataset, we aim to test the monophyly of the genus, infer phylogenetic relationships among species and species groups and test the limits between described species and candidate species. For this, we used a large matrix of 272 partial non-redundant sequences of the Cytochrome b mitochondrial gene from 40 valid and 20 candidate species. Using probabilistic approaches on this dataset, we inferred *Thomasomys* phylogenetic relationships and explored species boundaries using four unilocus species delimitation methods (ABGD, ASAP, bPTP, and GMYC). *Thomasomys* sensu stricto was recovered monophyletic and well-supported, excluding the candidate species "*Thomasomys*" sp. 4 (sensu Pacheco, 2003). All analyses consistently recovered ten well-supported major clades and several paraphyletic or polyphyletic species. Delimitation methods and genetic divergences estimated that *Thomasomys* comprises between 81 and 93 putative species, thus potentially doubling the species diversity of *Thomasomys*. Such a result clearly calls for an urgent taxonomic revision of this genus and the use of further molecular loci within an integrative taxonomic approach to describe its diversity and understand its evolutionary history.

Keywords: Andes, Thomasomyini, Marañón, phylogeny, Sigmodontinae

INTRODUCTION

The genus *Thomasomys* Coues 1884 of the Thomasomyini tribe is endemic to South America and is distributed along the Andes from Venezuela to Bolivia. *Thomasomys* species include small (e.g., *T. gracilis*), medium (e.g., *T. cinereus*), and large size (e.g., *T. apeco*) species which occur in Andean habitats such as paramo, premontane, and montane forests from 1150 to 4500 m a.s.l. (Pacheco, 2015). This genus, with 51 extant species, is the most speciose of the Sigmodontinae subfamily, including the 44 species recognized by Pacheco (2015) and seven recently described new species: *T. salazari* Brito et al. 2019, *T. pardignasi* Brito et al. 2021, *T. antoniobracki* Ruelas and Pacheco 2021, *T. burneoi* Lee et al. 2022, *T. lojapiuranus* Pacheco and Ruelas 2023, *T. pagaibambensis* Pacheco and Ruelas 2023, and *T. shallqukucha* Pacheco and Ruelas 2023.

Considering *Thomasomys* systematics, its monophyly is still debatable. Pacheco (2003) performed the first morphological inference on the Thomasomyini where he found *Thomasomys* paraphyletic due to the inclusion of *Aepeomys*, *Chilomys*, and *Rhipidomys*. However, molecular studies using the Cytochrome b gene (e.g., Brito et al., 2019, 2021; Lee et al., 2011, 2015, 2018, 2022; Pacheco & Ruelas, 2023; Ruelas & Pacheco, 2021; Salazar-Bravo & Yates, 2007) and mito-nuclear supermatrices (e.g., Schenk & Steppan, 2018; Steppan & Schenk, 2017; Vallejos-Garrido et al., 2023) subsequently found *Thomasomys* as monophyletic (except in Parada et al., 2015) with contrasted phylogenetic support (from moderate to high), and a limited species sampling.

To date, most of the *Thomasomys* species description have been done prior to 1930 mainly by O. Thomas and J.A. Allen (see species list in Musser & Carleton, 2005; Pacheco, 2015). Few species descriptions occurred until recently and the only detailed morphological revision of this genus has been performed by Pacheco (2003). Subsequently, Pacheco (2015) detailed his view of *Thomasomys* sensu stricto (s.s.) distinguishing it from other thomasomyines and, among many other findings, provided an important taxonomic update by identifying and defining seven morphological groups: (*i*) the Cinereus group, distributed from the Andes of Venezuela and Colombia, to southeastern Bolivia; (*ii*) the Incanus group, from northern Peru (south of the Huancabamba depression) to northern Bolivia; (*iii*) the Aureus group, from the cordilleras of Venezuela and Colombia to southeastern Bolivia; (*iv*) the Baeops group, from Colombia to northern Peru (north of the Huancabamba depression); (*v*) the Gracilis group, occurring from northern Peru (south of the Huancabamba depression) to Bolivia; (*vi*) the Macrotis group, found only in the isolated mountains of the Cordillera Oriental of Peru, between the Marañón and Huallaga rivers; and (*vii*) the Notatus group, distributed throughout the northern (south of the Huancabamba depression) and central Peru (see Table S1). In addition, Pacheco (2003, 2015) morphologically identified eleven candidate species (see Table S1), some of which have been included in systematic frameworks (e.g., Parada et al., 2015; Ruelas & Pacheco, 2021; Salazar-Bravo & Yates, 2007), but none of these candidate species have been properly assessed or named, except for *T. ucucha* (Voss, 2003). Similarly in a molecular context, many divergent lineages from Ecuador and Peru have been proposed to be candidate species (e.g., Brito et al., 2019, 2021; Lee et al., 2022; Pacheco & Ruelas, 2023; Ruelas &

Pacheco, 2021).Several authors have concurred finding major clades representing the Baeops, Macrotis, and Notatus groups (sensu Pacheco, 2015) as monophyletic with strong support; however, the Cinereus group usually has been found with moderate to weak support (Brito et al., 2019, 2021; Lee et al., 2015, 2018, 2022; Pacheco & Ruelas, 2023; Ruelas & Pacheco, 2021; Salazar-Bravo & Yates, 2007). In contrast, these authors have often found the major clades representing the Aureus, Gracilis, and Incanus groups to be paraphyletic. The paraphyly of these groups is likely the result of limited gene and species sampling, the contradictory relationships, misidentifications, and the presence of species complexes. As an example, *T. aureus* was considered monotypic (but see remarks in Pacheco, 2015), however, it has been confirmed as a species complex containing at least three additional candidate species from Ecuador –"El Angel," "Cajanuma," and "Pichincha"– (Brito et al. 2021, Lee et al. 2022), increasing the number of candidate species (*Thomasomys* sp. 1 from southern Peru, *Thomasomys* sp. 2 from Bolivia) previously identified by Pacheco (2003) and included in molecular studies (e.g., Ruelas & Pacheco, 2021; Salazar-Bravo & Yates, 2007). These candidate species have been found as part of two molecularly divergent and unrelated clades containing species of the Aureus group, one restricted to species occurring west of the Marañón river and the other in the east of this river (except for *Thomasomys* sp. 2 which is basal to this clade), suggesting limited dispersal along this barrier (Ruelas & Pacheco, 2021). In the Incanus group (sensu Pacheco, 2015), *T. ladewi* and *T. kalinowskii* have been found as paraphyletic (e.g., Brito et al., 2019; Lee et al., 2022; Pacheco & Ruelas, 2023; Salazar-Bravo & Yates, 2007), which generated a discussion about the proper identification of *T. kalinowskii* and its closer

relationship between *T. ladewi* and *T. macrotis* (see more details in Brito et al., 2019; Pacheco and Ruelas, 2023). While in a morphological approach, *T. macrotis* was found as sister to the clade of the species belonging to the Aureus group (see Pacheco, 2003). These contrasted findings underscore the complexity of delineating evolutionary relationships and species diversity within the genus, with contrasted support for the monophyly and relationships within *Thomasomys* and its major clades.

While research on *Thomasomys* has significantly advanced its taxonomy and systematics, the high number of candidate species highlighted by Pacheco (2015) and others (e.g., Brito et al., 2019, 2021; Lee et al., 2015, 2018; Pacheco & Ruelas, 2023), the complex relationships among species and major clades assumed as species groups necessitates a thorough evaluation. Moreover, the contrasting geographical patterns found in the genus, including both widespread species and microendemics, underscores the importance of delineating *Thomasomys* species boundaries to better understand its diversity. In recent years, molecular phylogenies and species exploratory delimitation methods have allowed the evaluation of species boundaries for complex taxa (e.g., Bignotto et al., 2020; Esselstyn et al., 2012; Firkowski et al., 2016; Ramirez et al., 2017; Stervander et al., 2020; Voss et al., 2018); however, their accuracy, which rely on a single gene (usually mitochondrial), has been debated (Cadenillas & D'Elía, 2021; Knowles & Carstens, 2007). Nonetheless, the Cytb gene has been widely used to identify potential species in mammals, some of which have subsequently been validated using multilocus approaches and traditional morphological methods (e.g., da Cruz & Weksler, 2018; Hurtado, 2021; Hurtado & D'Elía, 2018; Lee et al., 2022; Pacheco

& Ruelas, 2023; Suárez-Villota, Carmignotto, et al., 2018; Suárez-Villota, Quercia, et al., 2018; Teta et al., 2013). In the Sigmodontinae, these methods have been successfully applied to estimate the species boundaries of several genera, such as *Oligoryzomys* (Hurtado & D'Elía, 2019), *Brucepattersonius* (Abreu et al., 2021), *Holochilus* (Prado et al., 2021), *Nephelomys* (Ruelas et al., 2021), *Chilomys* (Brito et al., 2022), and also for the Aureus and Cinereus groups of *Thomasomys* (Brito et al., 2021; Pacheco & Ruelas, 2023).Using newly sequenced material, and a new mitochondrial matrix with a dense intra and inter specific sampling, we present the first large-scale phylogenetic analysis of *Thomasomys* to test its monophyly and interspecific relationships and explore the species diversity by implementing multiple species delimitation methods.

MATERIAL AND METHODS

Taxon sampling and taxonomic criteria

Our taxon sampling includes 287 specimens of *Thomasomys*, covering much of the taxonomic and geographical distribution of the genus from Colombia, Ecuador, Peru, and Bolivia (Figure 1). Under the criteria explained here, named hereafter "Taxonomy," specimens analyzed in this study belong to 40 valid species of *Thomasomys* and the remaining 20 represent candidate species or undescribed forms (Table 1). Our taxonomic understanding for the currently valid species follows Pacheco (2003, 2015), Brito et al. (2019, 2021), Ruelas and Pacheco (2021), Lee et al. (2022), and Pacheco and Ruelas (2023). Undescribed forms previously proposed by Pacheco (2003, 2015) and used by other authors (e.g., Brito et al., 2021; Parada et al., 2013; Ruelas & Pacheco, 2021; Salazar-Bravo & Yates,

2007) were included in our taxon sampling as follows: *Thomasomys* sp. 1 (sensu Pacheco 2003) corresponds to specimens from Cusco (Peru) with some external morphological characters similar to *T. aureus* and consequently it has been assigned to such nominal form in most phylogenetic studies (e.g., Brito et al., 2019, 2021; Lee et al., 2011, 2015; Parada et al., 2013; Salazar-Bravo & Yates, 2007; Smith & Patton, 1999) but also as *Thomasomys* sp. 1 by Ruelas & Pacheco (2021); *Thomasomys* sp. 2 (sensu Pacheco 2003) is represented only by one sequence (AMNH 260422) and few specimens (see Pacheco 2015) from Comarapa (Bolivia) which were respectively treated as *T. aureus* (e.g., Brito et al., 2019), *Thomasomys* sp. (e.g., Brito et al., 2021; Lee et al., 2011, 2022), and *Thomasomys* sp. 2 following Pacheco's (2003) criteria (e.g., Salazar-Bravo & Yates, 2007; Ruelas & Pacheco, 2021); *Thomasomys* sp. 3 (sensu Pacheco 2003) is represented by specimens from Puno (Peru) and La Paz (Bolivia) which exhibit morphological characters similar to *T. daphne* and have been treated under this name (e.g., Salazar-Bravo & Yates, 2007; Brito et al., 2019, 2021); *Thomasomys* sp. 4 (sensu Pacheco 2003) includes material from Pasco and Junín (Peru); *Thomasomys* sp. 7 (sensu Pacheco 2003) is represented by specimens from Huánuco (Peru) that share some morphological characters with *T. kalinowskii*; *Thomasomys* sp. 8 (sensu Pacheco 2003) is represented by specimens from Ayacucho (Peru) that share some morphological characters with *T. oreas*; *Thomasomys* sp. 9 (sensu Pacheco 2003) is represented by specimens from Cusco (Peru) that have some morphological characters similar to *T. oreas* and it has been analyzed in previous molecular studies under the latter name (e.g., Smith & Patton, 1999; Lee et al., 2011, 2015, 2018; Brito et al. 2019, 2021), and *Thomasomys* sp. 10 (sensu Pacheco 2003) includes material from Piura

(Peru) that have some morphological characters similar to *T. vulcani*. The candidate species identified as "sp. 4", "sp. 7", "sp. 9", and "sp. 10" have not been previously included in any molecular phylogenetic analyses.

Candidate species and unidentified material (sp.) presented by other authors or labeled as such in the MUSM were coded with the letters A through F as follows: *Thomasomys* sp. A corresponds to material from Junín (MUSM 52861, MUSM 42490) which share some morphological characters with *T. incanus* and were provisionally allocated in the Incanus group (V. Pacheco and D. Ruelas pers. obs.); *Thomasomys* sp. B corresponds to a specimen (MSB 70714) from Bolivar (Ecuador) that was identified as *T. caudivarius* by Salazar-Bravo and Yates (2007) and Lee et al. (2015), and as *Thomasomys* sp. 1 (not the same "sp. 1" sensu Pacheco, 2003) by Brito et al. (2019) and Pacheco and Ruelas (2023), and it was allocated in the Cinereus group; *Thomasomys* sp. C is represented by two specimens (MEPN 12722, MEPN 12742) identified as *Thomasomys* sp. in Brito et al. (2019), *T. aureus* "El Angel" in Brito et al. (2021), and *Thomasomys* sp. "El Angel" in Lee et al. (2022), this material was included in the Aureus group; *Thomasomys* sp. D corresponds to a specimen from Junín (Peru) with some morphological characters shared with *T. incanus* (Pacheco pers. obs.), it was identified as *T.* cf. *incanus* by Pacheco and Ruelas (2023) and allocated in the Incanus group; *Thomasomys* sp. E corresponds to three specimens from Pichincha named as *T. aureus altorum* "Pichincha" in Brito et al. (2021) and *Thomasomys* sp. "Pichincha" in Lee et al. (2022), and were included in the Aureus group; and finally, *Thomasomys* sp. F corresponds to a specimen from Huancavelica (Peru) with some morphological characters that merit its allocation in the Incanus group (D. Ruelas pers. obs.). Other

considerations relative to the identification of material included in our analyses are detailed as follows: specimens QCAZ 15612–15624 and QCAZ 15626–15630 were identified as *T. cinereus* in Brito et al. (2019); however, after delimiting *T. cinereus* s.s., such material was assigned to *Thomasomys* sp. 2 by Pacheco and Ruelas (2023) (not the same "sp. 2" sensu Pacheco, 2003), here we consider the QCAZ material as *T.* aff. *cinereus*. Also, specimen TEL 2243 has been identified as *T. cinnameus* (Lee et al., 2015) and *T. hudsoni* (Lee et al., 2018), here we followed this latter identification. Specimen QCAZ 13243, named as *T. aureus* "Shuncos" in Brito et al. (2021), but after delimiting *T. aureus* s.s. (see Brito et al., 2021; Ruelas & Pacheco, 2021), this material is treated here as *T.* aff. *aureus*. Specimen MUSM 17457, which was treated as "*T. daphne* LAC" in Steppan and Schenk (2017), is named here as *Thomasomys* aff. *oreas* (following its identification at the MUSM). The specimen MVZ 181999 was treated as *T. ischyrus* by Lee et al. (2011) but re-identified as *T. taczanowskii* by Lee et al. (2015), this latter name is used here. Specimen MVZ 166703, referred to as *T. oreas* by Patton and Smith(1999) and as *Thomasomys* sp. 1 (different to "sp. 1" sensu Pacheco, 2003) by Steppan and Schenk (2017), is treated here as *Thomasomys* sp. 9 following Pacheco (2003, 2015). Also, for the following material we used its MUSM identification: specimens MUSM 52676, 52650, 52668, and 18615 are treated as *T.* aff. *ischyrus*; specimens MUSM 14984 from Pasco, and MUSM 34877 and MUSM:DLR430 from Ayacucho are treated as *T.* aff. *kalinowskii*; and specimen MUSM 52644 from Huánuco (Peru) is treated as *T. apeco.*

Finally, sequences AY041205 (Rinehart et al., 2005) and DQ914654 (Salazar-Bravo & Yates, 2007) belong to the same specimen of *T. baeops* (MSB

70704), of which only the second sequence was used here because it is longer (771 bp vs. 727 bp); the sequence of the specimen MECN 5662 was excluded from our sampling because it was named as *T. burneoi* by Lee et al. (2022), but the sequence in GenBank corresponds to *T. salazari*; and lastly, we included the sequence of specimen TEL 2775 as part of our outgroup, although it was initially identified as *Thomasomys* sp. by Lee et al. (2015), it was later re-identified as *Chilomys instans* (Brito et al., 2019, 2022).

Gene sampling, DNA isolation, amplification, and sequencing

We obtained sequences of the mitochondrial Cytochrome b gene (Cytb) from 287 specimens of *Thomasomys*, among which 112 were newly sequenced, and the remaining sequences were obtained from GenBank (see Table 1, Table S2). For newly sequenced material, whole genomic DNA was isolated from fresh tissues (muscle or liver) and dry skins using the GF-1 Nucleic Acid Extraction Kit (Vivantis), High Pure PCR Template Preparation Kit (®Roche), Wizard® SV Genomic DNA Purification System Kit (Promega Corp.), and NucleoMag Tissue Kit (Macherey-Nagel SARL). The tissues and specimens used in this study are housed in the Departamento de Mastozoología of the Museo de Historia Natural of the Universidad Nacional Mayor de San Marcos (MUSM, Lima) and in the Biological Collection at Universidad EAFIT (Colombia). Primers MVZ05 and MVZ16 (Smith & Patton, 1993) were used to amplify partial sequences of the Cytb gene. The thermal cycling conditions for the polymerase chain reaction (PCR) consisted of an initial denaturation of 94°C for 5 minutes, followed by 33 cycles of PCR (denaturation at 93°C for 1 minute, annealing at 45°C for 1 minute, and

extension at 72°C for 1.5 minutes) and a final extension at 72°C for 10 minutes (Ruelas et al., 2020). Amplified products were sent to external companies (Macrogen Inc., Korea, and Eurofins Scientific, France) for purification and Sanger sequencing. We evaluated the quality of the obtained sequences in CodonCode Aligner (CodonCode Corporation, USA) and deposited them in GenBank (OP978392-OP978501, OP991879-OP991881).

Phylogenetic analyses

We used species representatives from other tribes of the Sigmodontinae subfamily as outgroups following Brito et al. (2019): Abrothichini (*Abrothrix olivaceus*), Akodontini (*Akodon aerosus, Akodon boliviensis, Akodon torques, Blarinomys breviceps, Brucepattersonius soricinus, Deltamys kempi, Juscelinomys huanchacae, Kunsia tomentosus, Necromys lasiurus, Oxymycterus rufus, Scapteromys aquaticus,* and *Thaptomys nigrita*), Andinomyini (*Andinomys edax*), Phyllotini (*Auliscomys micropus, Graomys griseoflavus, Phyllotis magister*), Oryzomyini (*Holochilus sciureus, Microryzomys minutus, Nectomys squamipes, Nesoryzomys fernandinae, Oecomys bicolor,* and *Oligoryzomys longicaudatus*), Sigmodontini (*Sigmodon alstoni, Sigmodon arizonae,* and *Sigmodon hispidus*), Wiedomyini (*Wiedomys pyrrhorhinos*), and available sequences of the representative species of the Thomasomyini s.s. (*Chilomys instans, Rhipidomys albujai, Rhipidomys emiliae, Rhipidomys ipukensis, Rhipidomys latimanus, Rhipidomys leucodactylus, Rhipidomys macrurus, Rhipidomys mastacalis,* and *Rhipidomys wetzeli*), and the new Rhagomyini (*Rhagomys longilingua* and *Rhagomys rufescens*), which was previously part of the Thomasomyini (Luna,

2015; Pardiñas et al., 2022). Our ingroup includes the *Thomasomys* species listed in Table 1. All our Cytb matrix sequences were translated to aminoacids and examined for the presence of stop codons using EMBOSS Transeq (https://www.ebi.ac.uk/Tools/st/emboss_transeq/).

We constructed a matrix with all the 329 Cytb gene sequences (including the outgroup) and removed duplicates, this resultant matrix included 272 sequences (including the outgroup) ranging in length between 400 and 801 bp. Only 9 sequences had 40-49.69% missing data on the final matrix, while 201 had 0-5% of missing data, the remaining sequences had between 6% to 39% of missing data. We used exclusively this non-redundant matrix for both phylogenetic inference and species delimitation analyses. All the sequences were aligned using ClustalW (Thompson et al., 1994) implemented in Mega 7 (Kumar et al., 2016). We then used jModelTest via the Akaike Information Criterion to find the substitution model that best fitted our data, which corresponded to GTR+I+G with the following parameters: base frequencies (A= 0. 3175, C= 0.3848, G= 0.0348, T= 0.2592), rate matrix (0.4131, 10.0805, 0.4781, 0.6078, 5.0382, 1.0000), proportion of invariable sites (0.3580), and gamma distribution of the shape parameter (0.6080). We reconstructed the phylogenetic relationships of our sequences using Maximum Likelihood (ML) and Bayesian Inference (BI) analyses implemented in IQ-TREE (Nguyen et al., 2015) and MrBayes 3.2.6 (Ronquist et al., 2012), respectively. For the ML analysis we evaluated nodal support with 5000 bootstrap pseudoreplicates using the ultrafast option (Hoang et al., 2018). BI included two independent Markov chain Monte Carlo (MCMC) analyses for 20 million generations each, sampling every 1000 generations and including one cold chain and three heated chains. We

discarded 25% of the trees as burn-in and used the remaining trees to compute a 50% majority rule consensus and summarize the posterior probabilities (pp) for each node. The ML and BI topologies were edited in iTOL 4 (Letunic & Bork, 2019). We considered well-supported clades when bs > 90% and pp > 0.95 and moderately supported clades with bs between 75 and 89%, and pp between 0.75 and 0.94.

Finally, we estimated pairwise Kimura 2-parameter (K2P) genetic distances among our recovered "species" and major clades using the non-redundant matrix implemented in Mega 7 and plotted in R 4.2.1 (R Core Team, 2022) using the "ggplot2" (Wickham, Chang, et al., 2023) and "dplyr" (Wickham, François, et al., 2023) packages.

Species delimitation

Based on the lineage species concept (de Queiroz, 2005, 2007), we performed four unilocus species delimitation methods: Automatic Barcode Gap Discovery (ABGD: Puillandre et al., 2012), Assemblage of Species by Automatic Partitioning (ASAP: Puillandre et al., 2021); Bayesian implementation of the Poisson Tree Processes (bPTP: Zhang et al., 2013), and the General Mixed Yule Coalescent (GMYC: Fujisawa & Barraclough, 2013; Pons et al., 2006). We implemented the ABGD method, uploading our FASTA alignment into the ABGD web server (https://bioinfo.mnhn.fr/abi/public/abgd/) with the following settings: pmin = 0.001, pmax = 0.10, X = 1.00, and using simple distance. The ASAP method was also implemented in the web server (https://bioinfo.mnhn.fr/abi/public/asap/) using the default settings and simple distance. Similarly, bPTP, was implemented in the

web server version (https://species.h-its.org/; Zhang et al., 2013) using the maximum clade credibility tree obtained from MrBayes (see Phylogenetic analyses section) and running $5x10^5$ MCMC generations with two strategies: Bayesian PTP heuristic (bPTP-h) and Bayesian PTP maximum likelihood (bPTP-ML). For ABGD, ASAP, and bPTP, only the ingroup was used. The single- and multiple-threshold GMYC methods (sGMYC, mGMYC) were implemented in the "splits" package (https://r-forge.r-project.org/projects/splits) of R 4.1.1. For both GMYC analyses we built a time calibrated tree in Beast 2 (Bouckaert et al., 2019) using an uncorrelated log-normal relaxed-clock model, a birth-death tree prior, and multiple secondary calibration points (following Hurtado & D'Elía, 2019) with the same crown age prior estimates of the Sigmodontinae tribes of Parada et al. (2015). We ran the analysis 100 million generations sampling every 16000 generations and evaluated stationarity in Tracer 1.6 (Rambaut et al., 2018). We discarded the first 5% of trees as burn-in and used the remaining trees to compute a 50% majority rule consensus tree. Finally, in order to assess the congruence, we compared the results of these analyses with the initial, or "a priori," species assignment of the sequences referred here as "Taxonomy" (see Table 1).

RESULTS

Phylogenetic relationships

The genus *Thomasomys* was found to be strongly supported as monophyletic (bs= 100, pp= 1), including all our ingroup taxa—except for the undescribed species "*Thomasomys*" sp. 4—and forming a strongly supported clade with *Chilomys* and *Rhipidomys* (bs = 97, pp = 0.91) (Figure 2, Figure S1). From now on, our concept

of *Thomasomys* does not include "*Thomasomys*" sp. 4, whose taxonomic identity will be resolved elsewhere. Our results show that *Thomasomys* is formed by ten well-supported major clades (A–J, see Figure 2) geographically delimited mainly by the Marañón River (Figure S2-S11). Some of these major clades were found congruent with the species groups such as Baeops (clade J) and Notatus (clade E) (Figure 2, Table S3). The Incanus (clades H and I) and Cinereus (clades B, C, D, and four lineages) groups were found represented by monophyletic clades, although with poor phylogenetic support (bs < 75, pp < 0.75) and containing two or three well-supported major clades. Conversely, Aureus (clades F and G, and one independent lineage) and Gracilis (clade A and one independent lineage) groups were represented by paraphyletic clades. Furthermore, *T. macrotis* of the Macrotis group was identified as nested within clade H (Figure 2, Table S3).

In the phylogenetic tree (Fig. 2a-c), Clade A (bs= 100, pp= 1) consists of *T. andersoni* as a sister lineage to a clade formed by *T. oreas*, *T.* aff. *oreas* from Cusco, *Thomasomys* sp. 9, and *Thomasomys* sp. 8. Taxa in this clade occur from central Peru to Bolivia (Figure S2). Clade B (bs= 98, pp= 1) is formed by *T. australis* from Cochabamba, as a sister group to the clade formed by *T. daphne* from Cusco, and *Thomasomys* sp. 3. These taxa are distributed from southern Peru to central Bolivia (Figure S3). Clade C (bs= 95, pp= 0.98) includes (*i*) a well-supported clade formed by *T. contradictus* and *T. bombycinus*, both from Colombia; and (*ii*) another formed by *T. fumeus* from Napo and *Thomasomys* sp. 10 from Piura, *T. bombycinus* and *T. vulcani*, both from Carchi, Ecuador. These taxa are distributed in northern Peru (west of the Marañón river), Ecuador, and Colombia (Figure S4). Clade D (bs= 100, pp= 1) is formed by six moderately to well-supported subclades: (*i*) *T. ucucha* from

Carchi and Imbabura as a sister lineage to the clade *Thomasomys* sp. B and *T. silvestris* (from Cotopaxi and Pichincha); (*ii*) *T. cinereus* from La Libertad and Cajamarca and a clade formed by *T. shallqukucha*, *T. pagaibambensis*, and *T. lojapiuranus*; (*iii*) *T. cinnameus* from Carchi and a clade formed by *T. cinnameus* from Antioquia, *T. hudsoni* from Chimborazo, and *T. paramorum* from Chimborazo; (*iv*) *T. salazari*; (*v*) *T. caudivarius* from Loja; and (*vi*) *T.* aff. *caudivarius* and *T.* aff. *cinereus*. These taxa occur in northern Peru (west of the Marañón river) and Ecuador (Figure S5). Clade E (bs= 100, pp= 1) contains *T. notatus* from Amazonas, Junín, and Cusco, each population in a distinct clade, all well-supported. These taxa occur from central to southern Peru (Figure S6). Clade F (bs= 99, pp= 1) is formed by four well-supported clades: (*i*) a well-supported clade (bs= 100, pp= 1) containing *T.* aff. *aureus* from Shuncos and *T. antoniobracki*; (*ii*) a well-supported clade (bs= 100, pp= 1) including *T. auricularis* from Loja and Azuay and *T. pyrrhonotus* from La Libertad and Lambayeque, a moderately supported clade formed by *T. nicefori* from the Cordillera Occidental of Colombia, a well-supported clade of *T. nicefori* from Frontino (Parque Nacional Natural Las Orquídeas) and from the Cordillera Central of Colombia, and another well-supported clade consisting of *T.* aff. *aureus* from northern Cajamarca, *T. pardignasi*, *T. aureus*, *T. princeps*, *Thomasomys* sp. C, *T. burneoi*, and *Thomasomys* sp. E; (*iii*) *T. praetor* from Ancash; and (*iv*) *T.* aff. *aureus* from Lambayeque and southern Cajamarca. These taxa occur from Colombia to the west of the Marañón river in northern Peru (Figure S7). Clade G (bs= 91, pp= 1) is composed of *T. apeco* from San Martín and Huánuco and a well-supported clade containing *Thomasomys* sp. 1 and *T.* aff. *aureus* from Amazonas, San Martín, and Junín. Taxa in this clade

occur from east of the Marañón river in northern to southern Peru (Figure S8). Clade H (bs= 96, pp= 0.94) is formed by *T. macrotis*, *T. ladewi*, and a clade consisting of *T.* aff. *kalinowskii* from Ayacucho and *Thomasomys* sp. F, all occurring from central Peru to Bolivia (Figure S6). Clade I (bs= 99, pp= 0.96) is divided into five subclades, (*i*) *T.* aff. *kalinowskii* from Pasco and *Thomasomys* sp. 7; (*ii*) *T. incanus*; (*iii*) *T. ischyrus* from Huánuco and Amazonas, each population in a distinct clade; (*iv*) *T.* aff. *ischyrus* from Huánuco; and (*v*) *T. kalinowskii* from Junín and Pasco, both populations in distinct clades; while *Thomasomys* sp. A from Junín was recovered unresolved, because its relationship to the clade *T.* aff. *kalinowskii* from Pasco + *Thomasomys* sp. 7 was poorly supported. Taxa in this clade are distributed from central to southern Peru (Figure S9). Clade J (bs= 100, pp=1) consists of *T. baeops* and *T. taczanowskii*. *T. baeops* is subdivided into three divergent populations from Carchi, Napo, and Bolivar, respectively. Similarly, four divergent populations of *T. taczanowskii* were found to be monophyletic and include lineages from El Oro (Ecuador) + Piura (Peru), La Libertad (Peru), Chimborazo and Morona Santiago (Ecuador), and Piura, Cajamarca, and Lambayeque (Peru). Taxa in this clade occur from northern Peru (west of the Marañón river) to central Ecuador (Figure S10). Additionally, some taxa were recovered unresolved with respect to the major clades. *Thomasomys* sp. D and *T. contradictus* formed a moderately supported clade (bs= 100, pp= 0.77), the former occurring in central Peru and the latter in the Cordillera Central of Colombia (Figure S11). While *T. gracilis* from Cusco, represented by two sequences, was recovered unresolved and basal to the *Thomasomys* s.s. clade. Finally, *T. onkiro* and *T. erro* were always recovered to be

unresolved and placed between clade C + D and clade E, and *Thomasomys* sp. 2 was recovered unresolved and weakly related to clade G (bs = 90%, no pp).

Genetic distances

Interspecific genetic distances between *Thomasomys* species ranged from 3.31% (*T. burneoi* versus *Thomasomys* sp. E) to 18.60% (*T. andersoni* versus *T. apeco*). *Thomasomys* aff. *aureus*, *T. baeops*, *T. bombycinus*, *T. cinnameus*, *T. contradictus*, *T.* aff. *kalinowskii*, *T. nicefori*, *T. notatus*, and *T. pyrrhonotus* showed intraspecific distances greater than 3% (Figure 3, Table S4).

Species delimitation

Our exploratory unilocus species delimitation methods inferred between 81 and 93 putative species (excluding "*Thomasomys*" sp. 4; Figure 2, Table S5) compared to the 40 valid species and 19 candidate species of *Thomasomys* s.s. (Table 1) proposed by taxonomic criteria (see Material and Methods). Analyses based on the p-distances inferred 81 and 82 putative *Thomasomys* species, ABGD and ASAP, respectively, and were the most conservative. In both analyses, *T. apeco*, *T. bombycinus*, *T. cinnameus*, *T. contradictus*, *T. kalinowskii*, *T.* aff. *kalinowskii*, *T. pyrrhonotus*, and *Thomasomys* sp. 3 were each split into two putative species; *T. baeops*, *T. nicefori*, and *T. notatus* were each divided into three putative species. While *T. taczanowskii* was split into four putative species and *T.* aff. *aureus* into five. In the case of *T. ischyrus*, it was found to consist of two putative species by ABGD and three putative species by ASAP. While the phylogeny-based analyses, bPTP and GMYC, estimated between 83 to 94 putative *Thomasomys* species. The bPPT analysis, both bPTP-ML and bPTP-h, estimated 83 putative species, mostly

congruent with those found in the ABGD and ASAP analyses, but additionally, *T.* aff. *caudivarius* was split into two putative species. The GMYC with a single threshold time of 0.194 Mya estimated 90 putative *Thomasomys* species, mostly congruent with those found in the bPTP analysis, but here *T. cinereus* was split into five putative species, *T. hudsoni* into two, and *T. taczanowskii* into six. While the GMYC with multiple thresholds (0.271, 0.154, 0.114, 0.084, and 0.018 Mya) estimated 93 putative species, and the results are like the single threshold results but *T. taczanowskii* was split into seven putative species, *T. kalinowskii* into three, and *T. cinereus* into six putative species. In all analyses, *T.* aff. *aureus* "Shuncos" and *T. antoniobracki* were found as a single putative species, and 26 of the 40 valid species (*T. andersoni*, *T. aureus*, *T. auricularis*, *T. australis*, *T. burneoi*, *T. caudivarius*, *T. daphne*, *T. erro*, *T. fumeus*, *T. gracilis*, *T. incanus*, *T. ladewi*, *T. lojapiuranus*, *T. macrotis*, *T. onkiro*, *T. oreas*, *T. pagaibambensis*, *T. paramorum*, *T. pardignasi*, *T. praetor*, *T. princeps*, *T. salazari*, *T. shallqukucha*, *T. silvestris*, *T. ucucha*, *T. vulcani*) and 15 of the candidate species (*T.* aff. *cinereus*, *T.* aff. *ischyrus*, *T.* aff. *oreas*, *Thomasomys* sp. 1, *Thomasomys* sp. 2, *Thomasomys* sp. 7, *Thomasomys* sp. 8, *Thomasomys* sp. 9, *Thomasomys* sp. 10, *Thomasomys* sp. A, *Thomasomys* sp. B, *Thomasomys* sp. C, *Thomasomys* sp. D, *Thomasomys* sp. E, and *Thomasomys* sp. F) each formed a single putative species congruent with the taxonomic criteria ("Taxonomy").

DISCUSSION

Methodological considerations and limitations

Molecular species delimitation methods are employed when there is a need to determine the boundaries between different species or assess the potential existence of cryptic species within a taxonomic group. Exploratory methods – such as ABGD, ASAP, bPTP, or GMYC – propose new species partitions based on unilocus matrices typically (Puillandre et al., 2012, 2021). Some authors also stated that sometimes these methods tend to overestimate the putative species (Hamilton et al., 2014; Hurtado & D'Elía, 2019; Luo et al., 2018; Puillandre et al., 2012; Zhang et al., 2013). Although it is preferable to use multilocus approaches to infer molecular delimitations (Knowles & Carstens, 2007), unilocus and multilocus methods have found congruent results for some small mammals such as *Oligoryzomys* (Agrellos et al., 2012; da Cruz & Weksler, 2018; González-Ittig et al., 2010; Hurtado & D'Elía, 2019; Teta et al., 2013), *Dromiciops* (Suárez-Villota, Quercia, et al., 2018), and *Octodon* (Cadenillas & D'Elía, 2021). Despite criticisms regarding potential inaccuracies in unilocus gene trees and their representation of the species tree(Cadenillas & D'Elía, 2021), as well as susceptibility to factors like sample size, population size, divergence time, and gene flow (e.g., Cadenillas & D'Elía, 2021; de Abreu-Jr et al., 2020; Knowles & Carstens, 2007; Luo et al., 2018), these methods are widely used. Their appeal lies in not requiring any *a priori* hypotheses and, most importantly, providing an initial step in the integrative taxonomy process by identifying potential candidate species (Puillandre et al., 2012, 2021).

The absence of a consensus on the best unilocus species delimitation method has led researchers to use various methods for comparisons, ensuring robust taxonomic decisions (e.g., Abreu et al., 2021; Hurtado & D'Elía, 2019; Pacheco & Ruelas, 2023; Prado et al., 2021; Ruelas et al., 2021). This practice is crucial for

accuracy, reliability, and avoiding biases, particularly in complex taxa like the rodents of the genus *Thomasomys*. Different methods, with varying assumptions and biases, offer insights into the consistency and accuracy of species boundaries. Within this context, the methods employed herein demonstrated proficiency in recognizing established *Thomasomys* species and other lineages proposed by Pacheco (2003, 2015) based on a morphological approach or other authors on a molecular approach.

Based on our findings, ASAP and ABGD estimations were more conservative, aligning with the present taxonomy and our "Taxonomy" criteria (Figure 2). ABGD identified 81 putative species, which is consistent with its principle of requiring clear genetic distance gaps for species delimitation (Puillandre et al., 2012). While ASAP identified 82 putative species, suggesting one additional species compared to ABGD. This additional species may be attributed to its probabilistic modeling (Puillandre et al., 2021). Both methods use pairwise genetic distances and identify limits by a distance threshold used to partition the data into putative species (Puillandre et al., 2012, 2021). ABGD does not provide a score for each partition, whereas ASAP does. ABGD is sensitive to recent speciation events and dependent on sample sizes. It is efficient when intraspecific diversity is lower than interspecific diversity and warns that for datasets with many species, there is a small chance of finding them all (Puillandre et al., 2012). It is also essential to recognize that ABGD and ASAP are not exempt from issues. They require a careful examination of genetic distances to avert homoplasy. On the other hand, the bPTP and GMYC methods require a pre-existing phylogenetic tree to infer speciation and coalescent processes, estimating branching event rates

(Puillandre et al., 2021; Zhang et al., 2013). The species partition is found by maximizing the likelihood scores of the transitions from interspecific to intraspecific branching processes (Zhang et al., 2013). bPTP proposed 83 putative species, indicating one more species compared to ASAP. This result aligns with its Bayesian principles, which consider uncertainties and model complexity. sGMYC identified 90 putative species, while mGMYC, 93, which reflect GMYC's sensitivity to diversification patterns and its tendency to detect more species based on likelihood models (Luo et al., 2018). The mGMYC model, with increased flexibility and multiple thresholds, surpasses the sGMYC's estimation. This enhanced flexibility allows mGMYC to capture even more nuanced diversification patterns (Luo et al., 2018). Although both GMYC and bPTP could represent more reliable methods for inferring species limits because of their sensitivity to diversification patterns, they also have the potential to introduce bias due to their reliance on unilocus phylogenies. Additionally, the use of calibration points and priors sets for inferring the ultrametric tree may introduce potential bias in GMYC (Zhang et al., 2013). In this study, the calibration was performed for tribes, lacking specific information for the diversification of *Thomasomys* which underscores the need to interpret these results cautiously and consider potential biases in the context of calibration choices.

Species delimitation is an issue highly influenced by the nature of data (e.g., unilocus or multilocus) and method employed (Knowles & Carstens, 2007) and encounters challenges posed by complex biological phenomena. These challenges include introgression, incomplete lineage sorting, geographic structure, and diverse evolutionary forces within widely distributed genera (Scornavacca & Galtier, 2017;

Tomasco et al., 2022), such as *Thomasomys*. These complexities compromise the assumption of a distinct gap between intra- and interspecific distances – as assumed by ABGD and ASAP–, potentially leading to misinterpretations (Baker & Bradley, 2006; Bradley & Baker, 2001; Puillandre et al., 2012, 2021). While combining bPTP and GMYC may enhance methodological robustness, it does not provide a complete resolution to these challenges. Moreover, the presence of cryptic diversity, where genetically distinct species manifest morphological similarity, poses an additional challenge for unilocus methodologies (e.g., Hofmann et al., 2019; Kuchta et al., 2016; Welton et al., 2013). Addressing these limitations requires an interpretation that integrates multilocus methodologies, diverse evolutionary contexts, and acknowledges the potential influence of several biological processes on species delimitation outcomes. Adding additional loci has proven effective, particularly in situations with high population genetic structure and introgressive hybridization, reducing discrepancies between datasets (Dupuis et al., 2012; Kuchta et al., 2016).

In the broader context of systematic analyses, while genetic data can offer more compelling evidence than other sources (e.g., morphology, distribution, behavior), it is crucial not to overlook this evidence. Molecular species delimitation tools give initial species hypotheses that additional methods within integrative taxonomy should confirm. Newly identified candidate species from various delimitation methods should be considered provisional and require confirmation through a comprehensive integrative approach, acknowledging their role as one part of the taxonomic assessment.

Species delimitation

While the estimations derived from the methods used in this study suggest a range of 81 to 93 putative species, it is evident that our understanding of the species diversity within the *Thomasomys* genus remains incomplete. Acknowledging that all these methods come with inherent limitations, a cautious approach leads us to consider the distance-based methods ABGD (81 putative species) and ASAP (82 putative species), as well as the phylogeny-based method bPTP (83 putative species), as potentially more reliable. This consideration aligns closely with the existing taxonomic framework and previous studies, resulting in lesser taxonomic changes and thus representing hypotheses that are well-supported by the available evidence. The difference between the results of these three methods is the split of *T. ischyrus* (Figure 2, Table S5) and *T.* aff. *caudivarius* (Figure 2, Table S5). Nonetheless, it's important to note that we do not dismiss the results of GMYC (both single and multiple thresholds) entirely, even though they appear to overestimate the number of delimited species, as also observed in previous studies (e.g., da Cruz & Weksler, 2018; Hurtado & D'Elía, 2019). This overestimation may be attributed to our limited understanding of the speciation and extinction rates throughout the radiation of *Thomasomys*, factors that significantly influence the accuracy of GMYC.

All the methods unanimously identified 41 putative species (26 valid species and 15 candidate species; Figure 2, Table S5) that agree with the prior identification ("Taxonomy"), while the remaining were further subdivided with one case of merging (*T. antoniobracki* and *T.* aff. *aureus* "Shuncos"). Of the candidate species

consistently recovered as distinct each, *Thomasomys* sp. 2, *Thomasomys* sp. 7, *Thomasomys* sp. 8, *Thomasomys* sp. 9, *Thomasomys* sp. 10, and *T.* aff. *cinereus* had been subject to prior morphological analyses to establish their distinct status (Pacheco, 2003, 2015; Brito et al., 2019; Pacheco and Ruelas, 2023). Regarding the unnamed species *Thomasomys* sp. 1 and *Thomasomys* sp. 2, recent works found none related to *T. aureus* s.s. (Ruelas & Pacheco, 2021; Brito et al., 2021; Lee et al., 2022; this study) supporting Pacheco's (2003, 2015) argument. On the other hand, Pacheco (2015), based on morphological examination and distribution, suggested that karyotypes (2n=44, FN=42) of the populations from Río Palca, Junín, and Yuraccyacu, Ayacucho (Gardner & Patton, 1976) could belong to *Thomasomys* sp. 1. However, our results suggest that *Thomasomys* associated with the *aureus* form from Junín is genetically distinct (Figure 2). So far, *Thomasomys* sp. 1 is only known from a few localities in Cusco and northern Bolivia (Pacheco, 2015; Ruelas & Pacheco, 2021). About *Thomasomys* sp. 2, it was recovered moderately to weakly related to clade F (*aureus* s.s. and allies), in agreement with Ruelas and Pacheco (2021), Brito et al. (2021), and Lee et al. (2022). Anderson (1997) and Pacheco (2003, 2015) provided morphological descriptions, and Pacheco (2015) suggested that this is probably the smallest species in the Aureus group. Currently, the formal description of *Thomasomys* sp. 1 and *Thomasomys* sp. 2 is in progress (Pacheco et al. in prep.). Regarding the unnamed species *Thomasomys* sp. 8 and *Thomasomys* sp. 9 were well-supported each and distinct from *T. oreas* s.s. Previously, Pacheco (2003, 2015) provided morphological differences between these three taxa and suggested that *T. oreas* from Cochabamba (MSB 87126), also used here, belonged to a distant population morphologically

distinct from the type locality in La Paz, Bolivia (about 344 km away). Regarding the candidate species *T.* aff. *cinereus*, some morphological comparisons were provided by Brito et al. (2019), but under the epithet *cinereus* (see Pacheco & Ruelas, 2023). There is no available morphological data for the other candidate species (*Thomasomys* sp. A, *Thomasomys* sp. B, *Thomasomys* sp. C, *Thomasomys* sp. D, *Thomasomys* sp. E, and *Thomasomys* sp. F).

Thomasomys bombycinus, *T. cinnameus*, and *T. contradictus*, were found non-monophyletic and each division was recovered as a putative species (Figure 2, Table S5). First, our Colombian specimens of *T. bombycinus* could be considered part of the s.s. population; however, they were collected more than 110 km away from the type locality in Quindío, Colombia (Anthony, 1925). Compared to the holotype (AMNH 37740), our specimens show distinct morphological characters more congruent with those described by Pacheco (2015) for the population occurring in Paramo Frontino and Santa Bárbara in Antioquia. Meanwhile, the Ecuadorian specimen of *T. bombycinus* (MECN 4957) reported by Brito et al. (2019) should be cautiously considered because the authors presented no evidence for the identification. Second, the genetic distances between our samples from Carchi, Ecuador – more than 200 km far from the type locality (Anthony, 1924) – versus our Colombian specimens suggested that *T. cinnameus* is a species complex concurring with Pacheco's (2015) view, who also indicated that *T. cinnameus* from Antioquia (Colombia) is likely a new candidate species. Third, *T. contradictus* was composed of two non-related clades, one from Vereda las Palomas and Vereda Nori in Sonson, closely related to the Colombian *T. bombycinus*, whereas the other clade also from Vereda Las Palomas in Sonson unexpectedly related to a Peruvian

undescribed species (*Thomasomys* sp. D) from Junín in central Peru. Morphologically, Pacheco (2003, 2015) noted some craniodental differences in the Sonson population compared to *T. contradictus s.s.* from the type locality at Quindío and suggested it could represent a separate species. Consequently, we consider that our *T. contradictus* sister of *Thomasomys* sp. D might correspond to a different entity of *T. contradictus* s.s. The clade closely related to *T. bombycinus* might represent the distinct population of *T. contradictus* suggested by Pacheco (2015) or also be part of the *T. contradictus* s.s.

Thomasomys apeco, *T. pyrrhonotus*, and *Thomasomys* sp. 3 were each consistently split into two putative species (Figure 2, Table S5). First, *T. apeco* was considered as a species known only for the type locality in Amazonas (Pacheco, 2015; Teta & D'Elía, 2019). However, discovering an additional specimen identified as *T. apeco* from Huánuco (MUSM 52644) suggests it might represent a new candidate species rather than a mere extension of the species' known range. Second, contrary to Pacheco's (2015) suggestion of *T. pyrrhonotus* as monotypic, it may represent two distinct entities, one from La Libertad and the other from Lambayeque. To confirm this, it is essential to include specimens from near the type locality in Cajamarca to determine whether both entities represent candidate species or if one is part of the *pyrrhonotus* s.s. Third, our findings about the undescribed species *Thomasomys* sp. 3 align with the morphological observations of Pacheco (2015). However, this taxon was split into two molecular entities (Puno versus La Paz: 2.24%) separated by a distance of approximately 281 km. Further investigation with additional specimens is required to confirm whether this genetic distance is associated with the geographical distance or if other factors are at play.

Thomasomys baeops, *T. nicefori*, and *T. notatus* were each consistently split into three putative species (Figure 2, Table S5). First, Pacheco (2015) found that *T. baeops* exhibited variation in several morphological characters along its distribution, suggesting a regional species-level differentiation. Although our sampling was small and limited to some Ecuadorian localities (Carchi, Napo, and Bolivar), the high intraspecific genetic distance among geographically distant populations (up to 4.54%, Table S4) concurs with this statement, suggesting that *T. baeops* may be composed of more than one taxon. Second, Pacheco (2003, 2015) recognized *T. nicefori* as a valid species and distinct from *T. popayanus*, under which *T. nicefori* was previously considered a synonym (see Voss, 2003). *T. nicefori* has been recorded in both the Western and Central Cordilleras (Pacheco, 2015) in Colombia, although Patiño-Castillo and Solari (2017) suggested that it occurs only in the Central Cordillera. In this study, *T. nicefori* was split into three putative species with high intraspecific distances supporting Pacheco's (2015) interpretation (Figure 3, Table S4). Our specimens come from three different localities in Antioquia (see Table S2) in the Western and Central cordilleras: the first in the Parque Nacional Natural Las Orquídeas (PNNO) at 1827 m a.s.l., the second in Sonson 3087 to 3101 m a.s.l., and the third in Urrao at 3300 m a.s.l.; all far from the type locality. Pacheco (2015) suggested that the Urrao population could be a distinct species based on morphological differences and sympatry with *T. popayanus*, consistent with our findings. Further, integrative studies are needed to confirm whether these three putative taxa represent *T. nicefori* s.s., *T. popayanus*, or another species. Third, in agreement with Pacheco (2015), *T. notatus* was found to be a species complex (Figure 2). We tentatively considered the specimens from

Cusco (MVZ 166706, UMMZ 160588) as *T. notatus* s.s. because the morphology is comparatively similar to the holotype and the type locality of this species is located in "Torontoy," Cusco (Thomas, 1917). Therefore, *T. notatus* from Junín and Amazonas could each represent candidate species. Previously, Pacheco (2015) mentioned some distinctive morphological characters of the Amazonas-Pasco population that might correspond to our sequenced specimens from Amazonas.

Thomasomys taczanowskii, traditionally regarded as monotypic (Pacheco 2015), exhibited substantial genetic divergence, suggesting the presence of four to seven putative species (Figure 2, Table S5). Despite the absence of specimens from the type locality, we posit that the clade containing specimens from Cajamarca and Lambayeque may indeed represent the species s.s., given their proximity to the type locality in Tambillo, Río Malleta, Cajamarca (Thomas, 1882). While the methods used indicate that this is probably a species complex, it is worth noting that no prior morphological studies have explored this possibility.

Thomasomys aff. *caudivarius* exhibited distinct results in our analyses (Figure 2, Table S5). While distance-based methods ABGD and ASAP suggested a single putative species, phylogeny-based methods bPTP and GMYC indicated a division into two putative species, none of them related to *T. caudivarius* s.s. further evidenced by a high genetic distance of 9.39% (Table S4) and Pacheco's (2015) morphological assessment. Additional research is needed to confirm these distinctions and support species-level recognition. In the case of the two putative species scenario, one group comprises specimens from Cajamarca, while the other consists of specimens from Piura, both in northern Peru. However, there is currently

no morphological data to substantiate these divisions. It is possible that this split resulted from incomplete sampling, and further sequencing from both localities, which are in proximity, is necessary. Additionally, if these two putative species are indeed distinct, it is important to consider ecological factors such as the type of forest or elevation in their evaluation to understand this division.

Given its proximity to the type locality (65 km E Chachapoyas, near Uchco, Tambo Almirante, Amazonas) and morphology (Osgood, 1914), we consider that our specimens *T. ischyrus* from Amazonas as valid representatives of the species s.s. In all our analyses, this species was recovered to be a species complex of two or three putative species, with a notable distinction between the specimen from Huánuco and those from Amazonas. On the other hand, the form *T.* aff. *ischyrus* from Huánuco was recovered as a sister of *T. kalinowskii* and with a genetic distance of 6.25% with *T. ischyrus* s.s. (Table S4). These findings are consistent with Pacheco's (2015) suggestion that these specimens may constitute a new species based on their disjunct distribution with respect to *T. ischyrus* s.s. and certain morphological differences.

Likewise, our representatives of *T. kalinowskii* are the closer to the type locality ("Valley of Vitoc [= Río Tulumayo]", Junín) and so here they are considered *T. kalinowskii* s.s. Even though the specimens from Oxapampa, Pasco (MUSM 14984), and Chiquintirca, Ayacucho (MUSM DLR430, MUSM 34977) share some morphological characters with *T. kalinowskii* s.s., they were recovered in different major clades (clade I and H, respectively; Figure 2) and a genetic distance of 9.05% (Table S4). Regarding the specimens from Ayacucho, Pacheco

(2015) mentioned some morphological differences with respect to *T. kalinowskii* s.s., but the specimen from Pasco was not previously evaluated. In addition, Pacheco (2015) provided some morphological differences between *Thomasomys* sp. 7 and *T. kalinowskii* s.s. in the species description of *T. kalinowskii*, but it is grouped herein with *T.* aff. *kalinowskii* from Pasco instead. On the other hand, numerous authors (e.g., Salazar-Bravo and Yates, 2007, Brito et al., 2019; Lee et al., 2022) have found specimen *T. kalinowskii* MVZ 172598– morphologically identified by V. Pacheco in Salazar-Bravo and Yates (2007) and Pacheco (2015) – and *T. ladewi* paraphyletic or unresolved in Cytb-based phylogenies. Brito et al. (2019) suggested that specimen MVZ 172598 needed to be reevaluated as it was more closely related to the Baeops and Notatus groups than to the Incanus group represented only by *T. ladewi*. However, they also considered an *aureus*-like specimen from Cusco (= *Thomasomys* sp. 1 sensu Pacheco, 2003) as part of the Incanus group, with which *T. ladewi* was recovered in a weakly supported clade (Brito et al., 2019: figure 3). We consider this statement to be a misinterpretation, probably due to the small sample size. Here, a broader sampling places *T. kalinowskii* MVZ 172598 within major clade I with other specimens of *T. kalinowskii* from Junín and Pasco and with phylogenetic solid support. This reaffirms Pacheco's (2015) identification based on side-by-side morphological comparisons with the holotype.

Thomasomys aureus s.l. (sensu lato) remains a highly complex and challenging case within the *Thomasomys* taxonomy. Although the type locality of *T. aureus* was not given in the original description (Tomes, 1860), Pacheco (2015) suggested Pallatanga, Ecuador, as the likely location (sensu Pacheco, 2015). This

author also proposed that specimens from Río Tatahuazo, Bolivar Province, Ecuador (MSB 70707 and 70708) could be considered *T. aureus* s.s. because of the proximity to Pallatanga. This allocation was crucial in resolving the taxonomy of this group. Furthermore, Pacheco (2003, 2015) delimited the *aureus* epithet only for some Ecuadorian populations (Bolivar, Napo, Pichincha, Tungurahua, and Morona Santiago). Nonetheless, Pacheco's (2015) hypothesis requires validation through molecular sequences of the holotype, represented only by a dry skin specimen (NHMUK ZD 7.1.1.104: Tomes, 1860). Recently, Brito et al. (2021) refined taxonomy, suggesting that *aureus* s.s. is limited to populations from Azuay, Bolivar, Cañar, and Chimborazo provinces, while the populations from Pichincha and Morona Santiago could represent a distinct taxon. They also suggested that at least four other candidate species allied to *aureus* occur in Ecuador. One of them, *aureus* "Shuncos" from Zamora Chinchipe (QCAZ 13243), was found here to be an additional specimen of the recently described *T. antoniobracki* (Figure 2). This discovery, constituting a new record for Ecuador, warrants confirmation through a morphological examination. On the other hand, *altorum* Allen 1914 – considered a synonym of *aureus* (Pacheco, 2015) –with the type locality in Pichincha (Allen, 1914) is the only name available for any Ecuadorian population distinct to *aureus* s.s. Brito et al. (2021) used this epithet as a subspecies for the *aureus* population from Pichincha – here named *Thomasomys* sp. E – and Cotopaxi (MECN 5053, 5208, 5389) without providing details. Although the authors found these specimens to be paraphyletic to *aureus* s.s. (MECN 74 and 6144), they were scored morphologically together with specimens assigned to *T. aureus* s.s. (Brito et al., 2021: figure 1 and table 3). Ruelas and Pacheco (2021) and Brito et al. (2021)

provided morphological characters for *T. aureus*, but *T. aureus* s.s. sensu Brito et al. (2021) remains imprecise due to including characters from the population assigned to *altorum*. Conservatively, we refrained from using the epithet *altorum* for these specimens, emphasizing the need for a thorough revision and comparison with the holotype (AMNH 36280) for proper validation. Furthermore, the most extreme case of splitting occurred in specimens assigned to *T.* aff. *aureus* (Figure 2), which was expected given their wide distribution (Figure S7, Figure S8). The epithet *aureus* was usually assigned to several taxa, due to some common external characters shared with *aureus* s.s., such as coat color, large body size, and some craniodental characters. Pacheco (2003, 2015) suggested that some populations assigned to *aureus* may merit recognition at the species-level. Here, a putative new species was recovered from San Martín (MUSM 7990) to be distinct from *Thomasomys* sp. 1 and another from central Peru (Amazonas and Junín, this study). Nonetheless, because of its proximity to the type locality of *T. rosalinda* in Goncha, Amazonas (Thomas & St. Leger, 1926), their status need to be further clarified.

Phylogeny and species groups

Our results present a new phylogenetic hypothesis for the genus *Thomasomys* by evaluating representatives of all morphological groups and most valid and candidate species (Table 1). *Thomasomys* s.s. was found to be a monophyletic genus, strongly supported in both the ML and BI analyses (Figure 2). This outcome is consistent with findings from previous molecular studies (e.g., Salazar-Bravo & Yates, 2007; Lee et al., 2018, 2022; Brito et al., 2019, 2021; Ruelas & Pacheco, 2021; Pacheco & Ruelas, 2023) and contrary to the paraphyletic nature obtained in

the morphological phylogeny (Pacheco, 2003) or findings of Parada et al. (2015) in a multilocus approach, who found *T. gracilis* as sister of *Rhagomys longilingua* (phylogenetic support was not provided). However, this relationship may be an artifact because *Rhagomys* has never been found within *Thomasomys* by all other approaches (e.g., Pardiñas et al., 2022). Likewise, the relationships of *Thomasomys* with other genera of the tribe Thomasomyini s.l. (Pacheco, 2015) are still unresolved or weakly supported (e.g., D'Elía et al., 2006; Moreno Cárdenas et al., 2021; Pacheco, 2003; Parada et al., 2015; Pardiñas et al., 2022; Steppan & Schenk, 2017).

Our results align with previous studies in identifying major clades (Figure 2) reflecting some species groups sensu Pacheco (2015): (*i*) The Baeops (Clade J) and Notatus (clade E) groups were each found monophyletic supporting Pacheco's (2003, 2015) morphological view and previous molecular findings (e.g., Lee et al., 2018; Ruelas & Pacheco, 2021; Salazar-Bravo & Yates, 2007). (*ii*) The Cinereus group (clades B, C, D, and four lineages), being by far the largest group, was monophyletic although with weak support. Phylogenetic relationships among its major clades and some species are broadly consistent with the findings of Pacheco (2003), Lee et al. (2018), Brito et al. (2019), Ruelas and Pacheco (2021), and Pacheco and Ruelas (2023). (*iii*) The Aureus group (clades F and G, and *Thomasomys* sp. 2) was found paraphyletic (see Figure 2) in agreement with some molecular findings (e.g., Lee et al., 2015, 2018; Brito et al., 2019; Ruelas & Pacheco, 2021) and challenging both Pacheco's (2003, 2015) morphological perspective and some molecular studies that had found its monophyly, although with low support (e.g., Salazar-Bravo & Yates, 2007; Brito et al., 2021; Lee et al.,

2022). This group appears divided by the Marañón River, with one clade (Aureus "West" group; Figure S7) containing species from the western Marañón River, and another (Aureus "East" group; Figure S8) containing species from the eastern Marañón River. The inclusion of *T. popayanus* and *T. rosalinda* might help to resolve the monophyly of this group. (*iv*) Contrary to Pacheco's (2003) earlier findings and in agreement with Salazar-Bravo & Yates (2007) and Lee et al. (2018), the Gracilis group was recovered as paraphyletic (clade A and one independent lineage: *T. gracilis*; Figure 2). Notably, in an unilocus approach by Brito et al. (2019) and multilocus approach by Steppan and Schenk (2017: figure 4) its monophyly was recovered, although weakly supported. (*v*) Except for the nesting of *T. macrotis* (Macrotis group), the Incanus group was found to be monophyletic (clades H and I) but with low support with earlier literature (Gardner & Romo, 1993; Pacheco, 2003) suggesting a closer relationship between *T. macrotis* and Incanus and Aureus groups based on craniodental similarities. Despite these considerations, based on its autapomorphies (Gardner & Romo, 1993), this species was considered the only member of the Macrotis group (Pacheco, 2015). *Thomasomys macrotis* and members of the Incanus group share several potential synapomorphic characters (e.g., absence of genal 1 vibrissae, derived carotid circulation, long posterior end of nasals; Pacheco, 2015) that might justify a close relationship despite species of both groups being represented by limited molecular data (e.g., Steppan & Schenk, 2017; Ruelas & Pacheco, 2021). Morphological characters and relationships of taxa of these clades require further investigation. This study also initiates the exploration into the relationships among the species of the Incanus group; indicating that a comprehensive assessment of its internal

relationships and monophyly will demand the inclusion of sequences from *T. eleusis*, *T. fraternus* Thomas 1927 (synonym of *T. incanus* but likely to be a valid species, Pacheco, V. in prep.), and the candidate species *Thomasomys* sp. 5 and *Thomasomys* sp. 6.

Additionally, "*Thomasomys*" sp. 4 identified in a morphological phylogeny (Pacheco 2003) as sister to *Thomasomys* sp. 5 within a broader *Thomasomys* clade that also included *Aepeomys* (Pacheco, 2003), has been found to be paraphyletic to *Thomasomys* s.s. (Figure 2). Our phylogenetic findings and high molecular divergences –from 14.58% (versus *T. daphne*) to 19.83% (versus *T. oreas*) – suggest the possibility of a new genus not related to *Thomasomys* containing at least two candidate species from central Peru (Figure 2, Figure S11). These findings on the complex relationships among species and major clades are preliminary and underscore the necessity for comprehensive taxonomic sampling, which should include the examination of holotypes and additional molecular markers. Such efforts are essential to draw robust conclusions about the relationships within the genus *Thomasomys* and the Thomasomyini tribe.

Distributional patterns

Thomasomys species predominantly inhabit different habitats of the Tropical Andes like montane forests and paramos (Pacheco, 2015), with some endemic species isolated in Sub-Andean cordilleras (Neill, 2005; Wurdack, 2017). These Sub-Andean micro-endemics are*:* (*i*) *T. erro* found in the subalpine rainforest and upper montane rainforest in the Volcan Sumaco in northern Ecuador (Anthony, 1926; Salgado Loza et al., 2021), but also in the Ecuadorian Cordillera Oriental (Pacheco,

2015), (*ii*) *T. onkiro* in the elfin forest of the Cordillera Vilcabamba (or Cordillera Otishi) in central Peru (Luna & Pacheco, 2002), and (*iii*) *T. pardignasi* in the Cordillera del Cóndor and Kutukú (Brito et al., 2021). These findings underscore the genus' adaptation to unique habitats and the role of geographical isolation in species diversity. But also, isolation may have led to *T. erro* and *T. onkiro* being unresolved in the phylogeny (Figure 2). Several isolated cordilleras remain understudied due to their remote and challenging accessibility, presenting opportunities for discovering further new species or divergent populations. We urge extensive sampling in sub-Andean zones, such as in the Cordillera Azul, Cordillera Yanachaga, Cordillera Otishi, or Cordillera Escalera, which form discontinuous eastern Andean mountain chains (Espurt et al., 2008; Neill, 2005; Pfiffner & Gonzalez, 2013; Wurdack, 2017).

Pacheco (2015) suggested that species (except for *T. aureus*) and species groups (except for the Cinereus and Aureus groups) have disjunct distributions due to the Huancabamba depression and the Marañón river, which are significant barriers promoting allopatric diversification in Andean fauna (Duellman & Pramuk, 1999; Guzman et al., 2021; Weigend, 2002, 2013). Notably, the Marañón river and its dry valley (namely the Marañón Zone) have been identified as formidable dispersal barriers for diverse vertebrate species, including small mammals (Hurtado & Pacheco, 2017; Jiménez et al., 2013; Pacheco & Ruelas, 2023, 2023; Ruelas et al., 2021), birds (Hazzi et al., 2018; Winger & Bates, 2015), reptiles (Koch et al., 2006), and certain plant groups (Marcelo-Peña et al., 2016; Särkinen et al., 2011). For *Thomasomys*, a highly montane specialist genus, the Marañón Zone significantly influenced the distribution and mitochondrial divergence among major

clades (Figure 2; Figures S4-S10). Located in the upper Marañón watershed, the Marañón Dry Valley traverses seven regions in Peru, disrupting the continuity of humid mountain forests (Duellman & Pramuk, 1999; Marcelo-Peña et al., 2016; Winger, 2017). Due to its position relative to the Huancabamba depression, eastern leeward trade winds, and the circulation of cold air in central valleys, this valley experiences exceptionally arid climatic conditions (Duellman & Pramuk, 1999; Killeen et al., 2007). Such environmental challenges pose dispersal difficulties in a specialized species. The topology suggests that *Thomasomys* species are divided across this barrier, with different clades occupying the western and eastern sides, aligning with Pacheco's (2015) statement for the eastern distribution of Notatus, Incanus, Macrotis, and Gracilis groups. Similarly, the Huancabamba depression also might influence the species distribution, separating monotypic species with isolated populations in the western Marañón river. The habitat in this depression is mostly open shrubby vegetation or dry forests (Linares-Palomino, 2004), preventing the dispersion of species living at humid and high elevation habitats, such as *Thomasomys* (Pacheco & Ruelas, 2023). In addition, Pacheco and Ruelas (2023) proposed that small rivers on the western slope of the Peruvian Andes might have acted as dispersal barriers, alongside the Huancabamba depression. Both these geomorphological structures might have structured populations of *T. pyrrhonotus*, *T.* aff. *aureus*, and *T. taczanowskii*, that were found to be species *complex*.

Likewise, species like *T. aureus* s.l., *T. notatus*, or *T. oreas* s.l., previously thought to have wide distributions (see maps in Pacheco, 2015), are now suggested to include several potential cryptic species (Figure 2) with isolated and smaller ranges. Such is the case of the recently described species *T. lojapiuranus*, *T.*

shallqukucha, and *T. pagaibambensis*, which were previously thought to be part of a widely distributed *T. cinereus* s.l. (Pacheco & Ruelas, 2023). Factors such as the Marañón Zone, Huancabamba depression, and the Huallaga river have been identified as significant barriers influencing the divergence of *Thomasomys* aff. *aureus* (Figure 2, Figure S7, Figure S8), a pattern observed in other small rodents too, such as *Akodon* (Jiménez et al., 2013; Jiménez & Pacheco, 2016) and *Neacomys* (Hurtado & Pacheco, 2017). As a general pattern, *Thomasomys* encompasses species with limited ranges including microendemic species like *T. macrotis*, *T. rosalinda*, or *T. onkiro* (Pacheco, 2015; Teta & D'Elía, 2019) highlighting this pattern. In conclusion, the role of geographical features (like rivers, valleys, depressions, and isolated mountain chains) in shaping the distribution patterns of *Thomasomys* still awaits a formal biogeographic analysis that goes beyond inferences based on geographical distribution and phylogenies.

Species diversity and challenges

Our mitochondrial phylogenetic analyses confirm that *Thomasomys* is by far the most speciose genus in the subfamily Sigmodontinae and that its species diversity is still greatly underestimated, especially in view of our limited geographic sampling (Figures 1, 2). Likewise, this study marks a significant step in the molecular systematics of *Thomasomys*, providing the first mitochondrial phylogenetic analyses of 15 taxa previously not assessed: 11 Peruvians (*T. ischyrus*, *T. incanus*, *T.* aff. *aureus*, *T.* aff. *caudivarius*, *T.* aff. *ischyrus*, *T.* aff. *kalinowskii*, *Thomasomys* sp. 7, *Thomasomys* sp. 8, *Thomasomys* sp. 10, *Thomasomys* sp. A, and

Thomasomys sp. F) and three Colombians (*T. contradictus*, *T. nicefori*, and *T. princeps*).

Our findings recovered at least 81 putative species which include 41 candidate species for *Thomasomys* – according to ABGD delimitation method, the most conservative– primarily distributed in Peru, with six candidate species identified by Pacheco (2003, 2015) confirmed as monophyletic and molecularly divergent (*Thomasomys* sp. 1, *Thomasomys* sp. 2, *Thomasomys* sp. 7, *Thomasomys* sp. 8, *Thomasomys* sp. 9, and *Thomasomys* sp. 10). However, some splits may also be due to divergence between distant populations of widely distributed *Thomasomys* species, such as *T. notatus* with about 1058 km (Fig. 1b). This suggests potential cryptic species within distant populations, echoing patterns seen in other Andean species, such as the *Phyllotis xanthopygus* complex (Jayat et al., 2021; Ojeda et al., 2021; Teta et al., 2018), the *Phyllotis andium* complex (Rengifo & Pacheco, 2015, 2018), or the *Nephelomys albigularis* complex (Percequillo, 2003; Ruelas et al., 2021).

The scope for discovering additional species remains promising as further evaluation of specimens from northern South America and Bolivia unfolds. Specifically, a significant pool of unexamined species includes seven valid species from Colombia (*T. cinereiventer*, *T. dispar*, *T. hylophilus*, *T. laniger*, *T. monochromos*, *T. niveipes*, *T. popayanus*), two from Venezuela (*T. emeritus*, *T. vestitus*), and two from Peru (*T. eleusis* and *T. rosalinda*), all of which were not part of this study. Moreover, two candidate species – *Thomasomys* sp. 5 and *Thomasomys* sp. 6 (sensu Pacheco 2003) – and many distinct populations belonging

to valid species (see remarks in Pacheco, 2015) were also not included. Clearly, the current species diversity of *Thomasomys* is expected to surpass by far the estimates within this study. This study also highlights challenges in species boundary resolution due to the limited distribution records, and the necessity for comprehensive molecular and morphological approach. Some *Thomasomys* species, known only from their type localities or from a few close localities, will require further studies such as *T. fumeus, T. hudsoni*, and *T. ucucha* (Brito et al., 2019; Pacheco, 2003, 2015; Teta & D'Elía, 2019; Voss, 2003). Although range extensions and morphological comparisons were not provided precisely for these species, we have adopted these species assignments by Brito et al. (2019). But it is important to stress that the molecular sequences attributed to these species should be validated, as they are not from specimens from the type localities or the type series. Our findings align with some prior studies but also reveal new relationships. As an example, based on morphological inferences, Pacheco (2003, 2015) found *T. fumeus* and *Thomasomys* sp. 10 to be closely related, a relationship further confirmed in our study (Figure 2). Furthermore, in contrast to Brito et al. (2019), who found that *T. hudsoni* and *T. paramorum* belong to the same clade along with *T. niveipes,* our findings align with Pacheco and Ruelas (2023) in placing these two species within the same clade as *T. cinnameus* s.l., likely influenced by our larger species sampling. Further research is crucial to refine our understanding of the evolutionary relationships within *Thomasomys*. This requires integrating additional data sources and advanced analytical methods to overcome the limitations posed by incomplete knowledge of species distributions and their evolutionary history.

Considering the significant morphological variations in *Thomasomys* as reported by Pacheco (2015), along with the candidate species proposed by many authors, and the findings of this study, it is essential to incorporate molecular data from type series. This approach is crucial for precisely delineating species boundaries and, consequently, for accurately determining the composition and validity of species groups. While recent years have seen an increase in recognized valid species, with numbers rising from 44 to 51, molecular sequences are predominantly available from the most recent type series (see Table 1, Table S2). Most *Thomasomys* species were described before the widespread use of molecular techniques. Therefore, sequencing genetic material from historical holotypes, primarily housed at the Natural History Museum of London (NHMUK, 19 holotypes) and the American Museum of Natural History (AMNH, 17 holotypes), is a critical step for accurate species identification. Furthermore, the significance of new collections from type localities cannot be rule out, particularly as many holotypes are over a century old. Relying only on these old specimens for complete information could be limited, making new collections in type localities is crucial for gathering additional data spanning morphology, genomics, behavior, karyology, and more.

As a pivotal tool, species delimitation not only contributes to systematics, evolution, or ecology but also exerts influence over conservation efforts and policy-making. Except for Colombia, several *Thomasomys* species have been included in national red lists in different categories of threat (Table S6): one species in Venezuela (Romero & Pacheco, 2015), 13 in Ecuador (Tirira, 2021), 15 in Peru (MINAGRI, 2014), and two in Bolivia (MMAyA, 2009). In the case of Ecuador

and Peru, they represent more than half of their *Thomasomys* species. While globally, the IUCN (https://www.iucnredlist.org/) has listed nine species on the Red List. Another critical role of species delimitation is underscored by its contribution to unveiling micro-endemism, a phenomenon usually underestimated. A clear understanding of these intricacies is crucial, especially for species proposed as complexes, both in this study and in various others (e.g., Pacheco, 2003, 2015; Brito et al., 2019, 2021; Ruelas & Pacheco, 2021; Lee et al., 2022). The reassessment of many listed species may occur, potentially amplifying the number of species designated as highly vulnerable, driven by factors such as their restricted range and habitat loss.

CONCLUSIONS

This study improves our understanding of the diversity and evolutionary history of *Thomasomys*, emphasizing the need of integrating molecular data with other evidence and employing multiple species delimitation methods to make well-informed taxonomic decisions. This study found that the *Thomasomys* genus is monophyletic after removing the divergent "*Thomasomys*" sp. 4 and identified numerous well-supported species and potential candidates within *Thomasomys*, highlighting taxonomic complexities and the importance of robust species descriptions through morphological and ecological studies. Additionally, the phylogenetic analysis challenged previous taxonomic notions, and underscored the Marañón zone as a significant geographic barrier. Furthermore, over 42 candidate species were suggested, with methods such as ABGD, ASAP, and bPTP proving higher efficiency than GMYC (single and multi-threshold) estimating from up to

83 putative species. Most of the recognized species were each monophyletic and well-supported by all the analyses. The candidate species sensu Pacheco (2003), such as *Thomasomys* sp. 1, *Thomasomys* sp. 2, *Thomasomys* sp. 7, *Thomasomys* sp. 8, *Thomasomys* sp. 9, and *Thomasomys* sp. 10, are recommended for formal recognition after a taxonomic revision. While the other candidate species require a more thorough examination, including incorporating additional morphological data.

The future research should encompass a multi-faceted approach, incorporating taxonomic revisions (integrating molecular data, morphology, and ecology), exploring isolated and underexplored areas, especially in the sub-Andean zones, for discovering new species, obtaining molecular data from holotypes and type series, particularly for pre-molecular era descriptions, which is essential for improving taxonomic accuracy. Understanding microendemism and ecological and evolutionary dynamics will provide broader ecosystem insights. Finally, collaborative interdisciplinary efforts will facilitate an integrative understanding of *Thomasomys*, contributing to refined taxonomy and improved conservation strategies.

ACKNOWLEDGMENTS

We thank Elizabeth Escobar, Diego Marcelo, Yangjosé Perez, Andderson Solis, Carlos Jiménez, Edith Salas, Heidi Quintana, Jessica Amanzo, Marina Villalobos, and other colleagues for collecting the specimens and tissues used here. We also thank Guillermo D'Elía (Universidad Austral de Chile, Chile) for his support in the molecular analysis at the beginning of the project; Omar Ruelas for his support

using the “ggplot” package; Lina García-Loaiza (Instituto Alexander von Humboldt, Colombia) for sharing with us the sequence of *T. princeps*; Roberto Portela Miguez for sharing with us the photographs of the holotypes of *Thomasomys* housed at The Natural History Museum (NHM, London); Jorge Brito for sharing with us photos of *T. bombycinus* from Ecuador (MECN 4957); and Marie-Ka Tilak (Université de Montpellier, France) for helping us in the obtention of the sequences of Colombian specimens. We thank the *platform GenSeq* from the LabEx CeMEB (Montpellier) for DNA extraction facilities, and especially Erick Desmarais et Frédérique Cerqueira for their help and time. We want to thank Frédéric Delsuc for his help, advice, and support considering this project. DR was supported by a scholarship of the Franco Peruvian School of Life Sciences. This work was supported by CONCYTEC through the PROCIENCIA program within the framework of the “Basic Research Projects” contest 2022-01, according to contract No. PE501078825-2022-PROCIENCIA, by the contract N° 402-PNICP-PIBA-2014 (INNOVATE-PERU), by the RR 03202-R-18 and RR 03556-R-19 of the Universidad Nacional Mayor de San Marcos, by the Institut Universitaire de France (IUF) and the LabEx Centre d’étude de la biodiversité amazonienne (CEBA, ANR-10-LABX-25-01). This publication is contribution No ISEM 2024-136 SUD of the Institut des Sciences de l’Evolution de Montpellier (UMR 5554 – CNRS-IRD).

REFERENCES

Abreu, E. F., Jung, D. M. H., Christoff, A. U., Valiati, V. H., Jansa, S. A., & Percequillo, A. R. (2021). Systematics of *Brucepattersonius* Hershkovitz, 1998 (Rodentia, Sigmodontinae): Molecular species delimitation and morphological

analyses suggest an overestimation in species diversity. *Systematics and Biodiversity*, *19*(6), 544–570. https://doi.org/10.1080/14772000.2021.1890270

Agrellos, R., Bonvicino, C. R., Rosa, E. S. T., Marques, A. A. R., D'Andrea, P. S., & Weksler, M. (2012). The taxonomic status of the Castelo dos Sonhos Hantavirus reservoir, *Oligoryzomys utiaritensis* Allen 1916 (Rodentia: Cricetidae: Sigmodontinae). *Zootaxa*, *3220*(1), Article 1. https://doi.org/10.11646/zootaxa.3220.1.1

Allen, J. A. (1914). Two new mammals from Ecuador. *Bulletin of the American Museum of Natural History*, *33*, 585–597.

Anderson, S. (1997). Mammals of Bolivia, taxonomy and distribution. *Bulletin of the American Museum of Natural History*, *231*, 1–652.

Anthony, H. E. (1924). Preliminary report on Ecuadorean mammals No. 6. *American Museum Novitates*, *139*, 1–9.

Anthony, H. E. (1925). New species and subspecies of *Thomasomys*. *American Museum Novitates*, *178*, 1–4.

Anthony, H. E. (1926). Preliminary report on Ecuadorean mammals No. 7. *American Museum Novitates*, *240*, 1–6.

Baker, R. J., & Bradley, R. D. (2006). Speciation in mammals and the genetic species concept. *Journal of Mammalogy*, *87*(4), 643–662. https://doi.org/10.1644/06-MAMM-F-038R2.1

Bignotto, T. S., Maniglia, T. C., Gomes, V. N., Oliveira, I. J. de, Agostinho, C. S., Prioli, S. M. A. P., & Prioli, A. J. (2020). Genetic evidence for a species complex within the piranha *Serrasalmus maculatus* (Characiformes, Serrasalmidae) from three Neotropical river basins based on mitochondrial

DNA sequences. *Genetics and Molecular Biology*, *43*(1), e20190131. https://doi.org/10.1590/1678-4685-gmb-2018-0131

Bouckaert, R., Vaughan, T. G., Barido-Sottani, J., Duchêne, S., Fourment, M., Gavryushkina, A., Heled, J., Jones, G., Kühnert, D., De Maio, N., Matschiner, M., Mendes, F. K., Müller, N. F., Ogilvie, H. A., du Plessis, L., Popinga, A., Rambaut, A., Rasmussen, D., Siveroni, I., … Drummond, A. J. (2019). BEAST 2.5: An advanced software platform for Bayesian evolutionary analysis. *PLOS Computational Biology*, *15*(4), e1006650. https://doi.org/10.1371/journal.pcbi.1006650

Bradley, R. D., & Baker, R. J. (2001). A test of the genetic species concept: Cytochrome-b sequences and mammals. *Journal of Mammalogy*, *82*(4), 960–973. https://doi.org/10.1644/1545-1542(2001)082<0960:ATOTGS>2.0.CO;2

Brito, J., Tinoco, N., Curay, J., Vargas, R., Reyes-Puig, C., Romero, V., & Pardiñas, U. F. J. (2019). Diversidad insospechada en los Andes de Ecuador: Filogenia del grupo "cinereus" de *Thomasomys* y descripción de una nueva especie (Rodentia, Cricetidae). *Mastozoología Neotropical*, *26*(2), 308–330. https://doi.org/10.31687/saremMN.19.26.2.0.04

Brito, J., Tinoco, N., Pinto, C. M., García, R., Koch, C., Fernandez, V., Burneo, S., & Pardiñas, U. F. J. (2022). Unlocking Andean sigmodontine diversity: Five new species of *Chilomys* (Rodentia: Cricetidae) from the montane forests of Ecuador. *PeerJ*, *10*, e13211. https://doi.org/10.7717/peerj.13211

Brito, J., Vaca-Puente, S., Koch, C., & Tinoco, N. (2021). Discovery of the first Amazonian *Thomasomys* (Rodentia, Cricetidae, Sigmodontinae): A new species from the remote Cordilleras del Cóndor and Kutukú in Ecuador. *Journal*

of Mammalogy, *102*(2), 615–635. https://doi.org/10.1093/jmammal/gyaa183

Cadenillas, R., & D'Elía, G. (2021). The number of species of degus (genus *Octodon*) is currently underestimated: An appraisal of species limits and their phylogenetic relationships (Rodentia: Hystricomorpha: Octodontidae). *Molecular Phylogenetics and Evolution*, *159*, 107111. https://doi.org/10.1016/j.ympev.2021.107111

da Cruz, M. de O. R., & Weksler, M. (2018). Impact of tree priors in species delimitation and phylogenetics of the genus *Oligoryzomys* (Rodentia: Cricetidae). *Molecular Phylogenetics and Evolution*, *119*, 1–12. https://doi.org/10.1016/j.ympev.2017.10.021

de Abreu-Jr, E. F., Pavan, S. E., Tsuchiya, M. T. N., Wilson, D. E., Percequillo, A. R., & Maldonado, J. E. (2020). Museomics of tree squirrels: A dense taxon sampling of mitogenomes reveals hidden diversity, phenotypic convergence, and the need of a taxonomic overhaul. *BMC Evolutionary Biology*, *20*(1), 77. https://doi.org/10.1186/s12862-020-01639-y

de Queiroz, K. (2005). A unified concept of species and its consequences for the future of taxonomy. *Proceedings of the California Academy of Sciences*, *56*(18), 196–215.

de Queiroz, K. (2007). Species concepts and species delimitation. *Systematic Biology*, *56*(6), 879–886. https://doi.org/10.1080/10635150701701083

D'Elía, G., Luna, L., González, E. M., & Patterson, B. D. (2006). On the Sigmodontinae radiation (Rodentia, Cricetidae): An appraisal of the phylogenetic position of *Rhagomys*. *Molecular Phylogenetics and Evolution*, *38*(2), 558–564. https://doi.org/10.1016/j.ympev.2005.08.011

Duellman, W. E., & Pramuk, J. B. (1999). Frogs of the genus *Eleutherodactylus* (Anura: Leptodactylidae) in the Andes of northern Peru. *Scientific Papers, 13*, 1–78.

Dupuis, J. R., Roe, A. D., & Sperling, F. A. H. (2012). Multi-locus species delimitation in closely related animals and fungi: One marker is not enough. *Molecular Ecology*, *21*(18), 4422–4436. https://doi.org/10.1111/j.1365-294X.2012.05642.x

Espurt, N., Brusset, S., Baby, P., Hermoza, W., Bolaños, R., Uyen, D., & Déramond, J. (2008). Paleozoic structural controls on shortening transfer in the Subandean foreland thrust system, Ene and southern Ucayali basins, Peru. *Tectonics*, *27*(3), TC3009.

Esselstyn, J. A., Evans, B. J., Sedlock, J. L., Anwarali Khan, F. A., & Heaney, L. R. (2012). Single-locus species delimitation: A test of the mixed Yule–coalescent model, with an empirical application to Philippine round-leaf bats. *Proceedings of the Royal Society B: Biological Sciences*, *279*(1743), 3678–3686. https://doi.org/10.1098/rspb.2012.0705

Firkowski, C. R., Bornschein, M. R., Ribeiro, L. F., & Pie, M. R. (2016). Species delimitation, phylogeny and evolutionary demography of co-distributed, montane frogs in the southern Brazilian Atlantic Forest. *Molecular Phylogenetics and Evolution*, *100*, 345–360. https://doi.org/10.1016/j.ympev.2016.04.023

Fujisawa, T., & Barraclough, T. G. (2013). Delimiting species using single-locus data and the generalized mixed yule coalescent approach: A revised method and evaluation on simulated data sets. *Systematic Biology*, *62*(5), 707–724.

https://doi.org/10.1093/sysbio/syt033

Gardner, A. L., & Patton, J. L. (1976). Karyotypic variation in oryzomyine rodents (Cricetinae) with comments on chromosomal evolution in the neotropical cricetine complex. *Occasional Papers of the Museum of Zoology*, *49*, 1–48.

Gardner, A. L., & Romo, M. R. (1993). A new *Thomasomys* (Mammalia: Rodentia) from the Peruvian Andes. *Proceedings of the Biological Society of Washington*, *106*(4), 762–774. https://doi.org/10.4135/9781412994064.n303

González-Ittig, R. E., Salazar-Bravo, J., Barquez, R. M., & Gardenal, C. N. (2010). Phylogenetic relationships among species of the genus *Oligoryzomys* (Rodentia, Cricetidae) from Central and South America. *Zoologica Scripta*, *39*(6), 511–526. https://doi.org/10.1111/j.1463-6409.2010.00446.x

Guzman, B. K., García-Bravo, A., Allauja-Salazar, E. E., Mejía, I. A., Guzmán, C. T., & Oliva, M. (2021). Endemism of woody flora and tetrapod fauna, and conservation status of the inter-Andean Seasonally Dry Tropical Forests of the Marañón valley. *Global Ecology and Conservation*, *28*, e01639. https://doi.org/10.1016/j.gecco.2021.e01639

Hamilton, C. A., Hendrixson, B. E., Brewer, M. S., & Bond, J. E. (2014). An evaluation of sampling effects on multiple DNA barcoding methods leads to an integrative approach for delimiting species: A case study of the North American tarantula genus Aphonopelma (Araneae, Mygalomorphae, Theraphosidae). *Molecular Phylogenetics and Evolution*, *71*, 79–93. https://doi.org/10.1016/j.ympev.2013.11.007

Hazzi, N. A., Moreno, J. S., Ortiz-Movliav, C., & Palacio, R. D. (2018). Biogeographic regions and events of isolation and diversification of the

endemic biota of the tropical Andes. *Proceedings of the National Academy of Sciences of the United States of America*, *115*(31), 7985–7990. https://doi.org/10.1073/pnas.1803908115

Hoang, D. T., Chernomor, O., von Haeseler, A., Minh, B. Q., & Vinh, L. S. (2018). UFBoot2: Improving the ultrafast bootstrap approximation. *Molecular Biology and Evolution*, *35*(2), 518–522. https://doi.org/10.1093/molbev/msx281

Hofmann, E. P., Nicholson, K. E., Luque-Montes, I. R., Köhler, G., Cerrato-Mendoza, C. A., Medina-Flores, M., Wilson, L. D., & Townsend, J. H. (2019). Cryptic diversity, but to what extent? Discordance between single-locus species delimitation methods within mainland Anoles (Squamata: Dactyloidae) of northern central America. *Frontiers in Genetics*, *10*. https://www.frontiersin.org/articles/10.3389/fgene.2019.00011

Hurtado, N. (2021). A new species of the genus *Oligoryzomys* (Rodentia: Cricetidae) from Peru. *Journal of Mammalogy*, *102*(3), 931–946. https://doi.org/10.1093/jmammal/gyab030

Hurtado, N., & D'Elía, G. (2018). A new species of long-tailed mouse, genus *Oligoryzomys* Bangs, 1900 (Rodentia: Cricetidae), from the Bolivian Yungas. *Zootaxa*, *4500*(3), 341. https://doi.org/10.11646/zootaxa.4500.3.3

Hurtado, N., & D'Elía, G. (2019). An assessment of species limits of the South American mouse genus *Oligoryzomys* (Rodentia, Cricetidae) using unilocus delimitation methods. *Zoologica Scripta*, *48*(5), 557–570. https://doi.org/10.1111/zsc.12365

Hurtado, N., & Pacheco, V. (2017). Revision of *Neacomys spinosus* (Thomas, 1882) (Rodentia: Cricetidae) with emphasis on Peruvian populations and the

description of a new species. *Zootaxa*, *4242*(3), 401. https://doi.org/10.11646/zootaxa.4242.3.1

Jayat, J. P., Teta, P., Ojeda, A. A., Steppan, S. J., Osland, J. M., Ortiz, P. E., Novillo, A., Lanzone, C., & Ojeda, R. A. (2021). The *Phyllotis xanthopygus* complex (Rodentia, Cricetidae) in central Andes, systematics and description of a new species. *Zoologica Scripta*, *50*(6), 689–706. https://doi.org/10.1111/zsc.12510

Jiménez, C. F., & Pacheco, V. (2016). A new species of grass mouse, genus *Akodon* Meyen, 1833 (Rodentia, Sigmodontinae), from the central Peruvian Yungas. *Therya*, *7*(3), 449–464. https://doi.org/10.12933/therya-16-336

Jiménez, C. F., Pacheco, V., & Vivas, D. (2013). An introduction to the systematics of *Akodon orophilus* Osgood, 1913 (Rodentia: Cricetidae) with the description of a new species. *Zootaxa*, *3669*(3), Article 3. https://doi.org/10.11646/zootaxa.3669.3.2

Killeen, T. J., Douglas, M., Consiglio, T., Jørgensen, P. M., & Mejia, J. (2007). Dry spots and wet spots in the Andean hotspot. *Journal of Biogeography*, *34*(8), 1357–1373. https://doi.org/10.1111/j.1365-2699.2006.01682.x

Knowles, L. L., & Carstens, B. C. (2007). Delimiting species without monophyletic gene trees. *Systematic Biology*, *56*(6), 887–895. https://doi.org/10.1080/10635150701701091

Koch, C., Venegas, P., & Böhme, W. (2006). A remarkable discovery: Description of a big-growing new gecko (Squamata: Gekkonidae: Phyllopezus) from northwestern Peru. *Salamandra*, *42*, 145–150.

Kuchta, S. R., Brown, A. D., Converse, P. E., & Highton, R. (2016). Multilocus phylogeography and species delimitation in the Cumberland Plateau

salamander, *Plethodon kentucki*: Incongruence among data sets and methods. *PloS One*, *11*(3), e0150022. https://doi.org/10.1371/journal.pone.0150022

Kumar, S., Stecher, G., & Tamura, K. (2016). MEGA7: Molecular evolutionary genetics analysis version 7.0 for bigger datasets. *Molecular Biology and Evolution*, *33*(7), 1870–1874. https://doi.org/10.1093/molbev/msw054

Lee, T. E., Boada-Terán, C., Scott, A. M., Burneo, S. F., & Hanson, J. D. (2011). Small mammals of Sangay National Park, Chimborazo Province and Morona Santiago Province, Ecuador. *Occasional Papers, Museum of Texas Tech University*, *305*, 1–16.

Lee, T. E., Ritchie, A. R., Vaca-Puente, S., Brokaw, J. M., Camacho, M. A., & Burneo, S. F. (2015). Small mammals of Guandera Biological Reserve, Carchi Province, Ecuador and comparative Andean small mammal ecology. *Occasional Papers, Museum of Texas Tech University*, *334*, 1–17.

Lee, T. E., Tinoco, N., & Brito, J. (2022). A new species of Andean mouse of the genus *Thomasomys* (Cricetidae, Sigmodontinae) from the eastern Andes of Ecuador. *Vertebrate Zoology*, *72*, 219–233. https://doi.org/10.3897/vz.72.e78219

Lee, T. E., Tinoco, N., Feller, M. J., Gomez, D., Hanson, J. D., Camacho, A. M., & Burneo, S. F. (2018). Mammals of Yacuri National Park, Loja Province, Ecuador. *Occasional Papers, Museum of Texas Tech University*, *357*, 1–17.

Letunic, I., & Bork, P. (2019). Interactive Tree Of Life (iTOL) v4: Recent updates and new developments. *Nucleic Acids Research*, *47*(W1), W256–W259. https://doi.org/10.1093/nar/gkz239

Linares-Palomino, R. (2004). Los Bosques Tropicales Estacionalmente Secos: I. El

concepto de los bosques secos en el Perú. *Arnaldoa*, *11*(1), 85–102.

Luna, L. (2015). Genus *Rhagomys* Thomas, 1886. In J. L. Patton, U. F. J. Pardiñas, & G. D'Elía (Eds.), *Mammals of South America. Volume 2, Rodents* (pp. 580–583). The University of Chicago Press.

Luna, L., & Pacheco, V. (2002). A new species of *Thomasomys* (Muridae: Sigmodontinae) from the Andes of southeastern Peru. *Journal of Mammalogy*, *83*(3), 834–842.

Luo, A., Ling, C., Ho, S. Y. W., & Zhu, C.-D. (2018). Comparison of methods for molecular species delimitation across a range of speciation scenarios. *Systematic Biology*, *67*(5), 830–846. https://doi.org/10.1093/sysbio/syy011

Marcelo-Peña, J. L., Huamantupa, I., Särkinen, T., & Tomazello, M. (2016). Identifying conservation priority areas in the Marañón valley (Peru) based on floristic inventories. *Edinburgh Journal of Botany*, *73*(1), 95–123. https://doi.org/10.1017/S0960428615000281

MINAGRI. (2014). Decreto Supremo que aprueba la actualización de la lista de clasificación y categorización de las especies amenazadas de fauna silvestre legalmente protegidas. *El Peruano*, 520497–520504.

MMAyA. (2009). *Libro rojo de la fauna silvestre de vertebrados de Bolivia*. Ministerio de Medio Ambiente y Agua.

Moreno Cárdenas, P. A., Tinoco, N., Albuja, L., & Patterson, B. D. (2021). A new species of *Rhagomys* (Rodentia, Sigmodontinae) from southeastern Ecuador. *Journal of Mammalogy*, *102*(1), 123–138. https://doi.org/10.1093/jmammal/gyaa104

Neill, D. (2005). Cordillera del Cóndor: Botanical treasures between the Andes and

the Amazon. *Plant Talk*, *41*, 17–21.

Nguyen, L.-T., Schmidt, H. A., von Haeseler, A., & Minh, B. Q. (2015). IQ-TREE: A fast and effective stochastic algorithm for estimating maximum-likelihood phylogenies. *Molecular Biology and Evolution*, *32*(1), 268–274. https://doi.org/10.1093/molbev/msu300

Ojeda, A. A., Teta, P. V., Jayat, J. P., Lanzone, C., Cornejo, P., Novillo, A., & Ojeda, R. A. (2021). Phylogenetic relationships among cryptic species of the *Phyllotis xanthopygus* complex (Rodentia, Cricetidae). *Zoologica Scripta*, *50*(3), 269–281. https://doi.org/10.1111/zsc.12472

Osgood, W. H. (1914). Mammals of an expedition across northern Peru. *Field Museum of Natural History, Zoological Series*, *10*, 143–185.

Pacheco, V. (2003). *Phylogenetic analyses of the Thomasomyini (Muroidea: Sigmodontinae) based on morphological data* [Ph.D. dissertation]. The City University of New York.

Pacheco, V. (2015). Genus *Thomasomys* Coues, 1884. In J. L. Patton, U. F. J. Pardiñas, & G. D'Elia (Eds.), *Mammals of South America. Volume 2, Rodents* (pp. 617–682). The University of Chicago Press.

Pacheco, V., & Ruelas, D. (2023). Systematic revision of *Thomasomys cinereus* (Rodentia: Cricetidae: Sigmodontinae) from northern Peru and southern Ecuador, with descriptions of three new species. *Bulletin of the American Museum of Natural History*, *461*, 1–71.

Parada, A., D'Elía, G., & Palma, R. E. (2015). The influence of ecological and geographical context in the radiation of Neotropical sigmodontine rodents. *BMC Evolutionary Biology*, *15*(172), 1–17. https://doi.org/10.1186/s12862-

015-0440-z

Parada, A., Pardiñas, U. F. J., Salazar-Bravo, J., D'Elía, G., & Palma, R. E. (2013). Dating an impressive Neotropical radiation: Molecular time estimates for the Sigmodontinae (Rodentia) provide insights into its historical biogeography. *Molecular Phylogenetics and Evolution*, *66*(3), 960–968. https://doi.org/10.1016/j.ympev.2012.12.001

Pardiñas, U. F. J., Tinoco, N., Barbière, F., Ronez, C., Cañón, C., Lessa, G., Koch, C., & Brito, J. (2022). Morphological disparity in a hyperdiverse mammal clade: A new morphotype and tribe of Neotropical cricetids. *Zoological Journal of the Linnean Society*, zlac016. https://doi.org/10.1093/zoolinnean/zlac016

Patiño-Castillo, E., & Solari, S. (2017). Morphometric patterns in assemblages of Cricetid rodents from the Central and Western Cordilleras of Colombia. *Therya*, *8*(1), 53–62. https://doi.org/10.12933/therya-17-459

Percequillo, A. R. (2003). *Sistemática de Oryzomys Baird, 1858: Definição dos grupos de espécie e revisão taxonómica do grupo albigularis (Rodentia, Sigmodontinae)* [Ph.D. dissertation]. Universidade de São Paulo, Brazil.

Pfiffner, O. A., & Gonzalez, L. (2013). Mesozoic–Cenozoic evolution of the western margin of South America: Case study of the Peruvian Andes. *Geosciences*, *3*(2), Article 2.

Pons, J., Barraclough, T. G., Gomez-Zurita, J., Cardoso, A., Duran, D. P., Hazell, S., Kamoun, S., Sumlin, W. D., & Vogler, A. P. (2006). Sequence-based species delimitation for the DNA taxonomy of undescribed insects. *Systematic Biology*, *55*(4), 595–609. https://doi.org/10.1080/10635150600852011

Prado, J. R. do, Knowles, L. L., & Percequillo, A. R. (2021). New species

boundaries and the diversification history of marsh rat taxa clarify historical connections among ecologically and geographically distinct wetlands of South America. *Molecular Phylogenetics and Evolution*, *155*, 106992. https://doi.org/10.1016/j.ympev.2020.106992

Puillandre, N., Brouillet, S., & Achaz, G. (2021). ASAP: Assemble species by automatic partitioning. *Molecular Ecology Resources*, *21*(2), 609–620. https://doi.org/10.1111/1755-0998.13281

Puillandre, N., Lambert, A., Brouillet, S., & Achaz, G. (2012). ABGD, Automatic Barcode Gap Discovery for primary species delimitation. *Molecular Ecology*, *21*(8), 1864–1877. https://doi.org/10.1111/j.1365-294X.2011.05239.x

R Core Team. (2022). *R: A language and environment for statistical computing* [R]. R Foundation for Statistical Computing. URL https://www.R-project.org/

Rambaut, A., Drummond, A. J., Xie, D., Baele, G., & Suchard, M. A. (2018). Posterior summarization in Bayesian phylogenetics using Tracer 1.7. *Systematic Biology*, *67*(5), 901–904. https://doi.org/10.1093/sysbio/syy032

Ramirez, J. L., Birindelli, J. L., Carvalho, D. C., Affonso, P. R. A. M., Venere, P. C., Ortega, H., Carrillo-Avila, M., Rodríguez-Pulido, J. A., & Galetti, P. M. (2017). Revealing hidden diversity of the underestimated neotropical ichthyofauna: DNA barcoding in the recently described genus *Megaleporinus* (Characiformes: Anostomidae). *Frontiers in Genetics*, *8*, 149. https://doi.org/10.3389/fgene.2017.00149

Rengifo, E. M., & Pacheco, V. (2015). Taxonomic revision of the Andean leaf-eared mouse, *Phyllotis andium* Thomas 1912 (Rodentia: Cricetidae), with the description of a new species. *Zootaxa*, *4018*(3), Article 3.

Rengifo, E. M., & Pacheco, V. (2018). Phylogenetic position of the Ancash leaf-eared mouse *Phyllotis definitus* Osgood 1915 (Rodentia: Cricetidae). *Mammalia*, *82*(2), 153–166. https://doi.org/10.1515/mammalia-2016-0138

Rinehart, T. A., Grahn, R. A., & Wichman, H. A. (2005). SINE extinction preceded LINE extinction in sigmodontine rodents: Implications for retrotranspositional dynamics and mechanisms. *Cytogenetic and Genome Research*, *110*(1–4), 416–425. https://doi.org/10.1159/000084974

Romero, V., & Pacheco, V. (2015). Rata andina olivácea, *Thomasomys hylophilus*. In J. P. Rodríguez, A. García-Rawlins, & F. Rojas-Suárez (Eds.), *Libro rojo de la fauna venezolana* (4th ed., p. 43). Provida y Fundación Empresas Polar.

Ronquist, F., Teslenko, M., van der Mark, P., Ayres, D. L., Darling, A., Höhna, S., Larget, B., Liu, L., Suchard, M. A., & Huelsenbeck, J. P. (2012). MrBayes 3.2: Efficient Bayesian phylogenetic inference and model choice across a large model space. *Systematic Biology*, *61*(3), 539–542. https://doi.org/10.1093/sysbio/sys029

Ruelas, D., & Pacheco, V. (2021). A new species of *Thomasomys* Coues, 1884 (Rodentia: Sigmodontinae) from the montane forests of northern Peru with comments on the "aureus" group. *Revista Peruana de Biología*, *28*(3), e19912. https://doi.org/10.15381/rpb.v28i3.19912

Ruelas, D., Pacheco, V., Inche, B., & Tinoco, N. (2021). A preliminary review of *Nephelomys albigularis* (Tomes, 1860) (Rodentia: Cricetidae), with the description of a new species from the Peruvian montane forests. *Zootaxa*, *5027*(2), 175–210. https://doi.org/10.11646/zootaxa.5027.2.3

Ruelas, D., Pacheco, V., & Jiménez, C. F. (2020). Range extension and

phylogenetic relationships of *Akodon josemariarguedasi* (Rodentia: Cricetidae) with comments on the aerosus species group. *Mammalia*, *84*(2), 207–213. https://doi.org/10.1515/mammalia-2018-0209

Salazar-Bravo, J., & Yates, T. L. (2007). A new species of *Thomasomys* (Cricetidae: Sigmodontinae) from central Bolivia. In D. A. Kelt, E. P. Lessa, J. Salazar-Bravo, & J. L. Patton (Eds.), *The quintessential naturalist honoring the life and legacy of Oliver P. Pearson* (pp. 747–774). University of California Press.

Salgado Loza, J. A., Mothes, P. A., & Córdova, M. D. (2021). New observations on the recent eruptive activity of Sumaco Volcano (Ecuador), based on geochronology, stratigraphy and petrography. *Journal of South American Earth Sciences*, *112*, 103568. https://doi.org/10.1016/j.jsames.2021.103568

Särkinen, T. E., Marcelo-Peña, J. L., Yomona, A. D., Simon, M. F., Pennington, R. T., & Hughes, C. E. (2011). Underestimated endemic species diversity in the dry inter-Andean valley of the Río Marañón, northern Peru: An example from *Mimosa* (Leguminosae, Mimosoideae). *Taxon*, *60*(1), 139–150. https://doi.org/10.1002/tax.601012

Schenk, J. J., & Steppan, S. J. (2018). The role of geography in adaptive radiation. *The American Naturalist*, *192*(4), 415–431. https://doi.org/10.1086/699221

Scornavacca, C., & Galtier, N. (2017). Incomplete lineage sorting in mammalian phylogenomics. *Systematic Biology*, *66*(1), 112–120. https://doi.org/10.1093/sysbio/syw082

Smith, M. F., & Patton, J. L. (1993). The diversification of South American murid rodents: Evidence from mitochondrial DNA sequence data for the akodontine

tribe. *Biological Journal of the Linnean Society*, *50*(3), 149–177. https://doi.org/10.1006/bijl.1993.1052

Smith, M. F., & Patton, J. L. (1999). Phylogenetic relationships and the radiation of sigmodontine rodents in South America: Evidence from cytochrome b. *Journal of Mammalian Evolution*, *6*(2), 89–128.

Steppan, S. J., & Schenk, J. J. (2017). Muroid rodent phylogenetics: 900-species tree reveals increasing diversification rates. *PLOS ONE*, *12*(8), e0183070. https://doi.org/10.1371/journal.pone.0183070

Stervander, M., Hansson, B., Olsson, U., Hulme, M. F., Ottosson, U., & Alström, P. (2020). Molecular species delimitation of larks (Aves: Alaudidae), and integrative taxonomy of the genus *Calandrella*, with the description of a range-restricted African relic taxon. *Diversity*, *12*(11), 428. https://doi.org/10.3390/d12110428

Suárez-Villota, E. Y., Carmignotto, A. P., Brandão, M. V., Percequillo, A. R., & Silva, M. J. de J. (2018). Systematics of the genus *Oecomys* (Sigmodontinae: Oryzomyini): Molecular phylogenetic, cytogenetic and morphological approaches reveal cryptic species. *Zoological Journal of the Linnean Society*, *184*(1), 182–210. https://doi.org/10.1093/zoolinnean/zlx095

Suárez-Villota, E. Y., Quercia, C. A., Nuñez, J. J., Gallardo, M. H., Himes, C. M., & Kenagy, G. J. (2018). Monotypic status of the South American relictual marsupial *Dromiciops gliroides* (Microbiotheria). *Journal of Mammalogy*, *99*(4), 803–812. https://doi.org/10.1093/jmammal/gyy073

Teta, P., & D'Elía, G. (2019). The least known with the smallest ranges: Analyzing the patterns of occurrence and conservation of South American rodents known

only from their type localities. *Therya*, *10*(3), 271–278. https://doi.org/10.12933/therya-19-886- ISSN 2007-3364

Teta, P., Jayat, J. P., Lanzone, C., & Ojeda, A. (2018). Geographic variation in quantitative skull traits and systematic of southern populations of the leaf-eared mice of the *Phyllotis xanthopygus* complex (Cricetidae, Phyllotini) in southern South America. *Zootaxa*, *4446*(1), Article 1. https://doi.org/10.11646/zootaxa.4446.1.5

Teta, P., Jayat, J. P., Ortiz, P. E., & D'elía, G. (2013). The taxonomic status of *Oligoryzomys brendae* Massoia, 1998 (Rodentia, Cricetidae), with comments on the availability of this name. *Zootaxa*, *3641*(4), Article 4. https://doi.org/10.11646/zootaxa.3641.4.9

Thomas, O. (1882). On a collection of rodents from north Peru. *Proceedings of The Zoological Society of London*, *1882 (part I)*, 98–111.

Thomas, O. (1917). Preliminary diagnoses of new mammals obtained by the Yale-National Geographic Society Peruvian expedition. *Smithsonian Institution Miscellaneous Collections*, *68*, 1–3.

Thomas, O., & St. Leger, J. (1926). LXXIV.—*The Spedan Lewis South American Exploration* .—V. *Mammals obtained by Señor E. Budin in Neuquen*. *Annals and Magazine of Natural History*, *18*(108), 635–641. https://doi.org/10.1080/00222932608633560

Thompson, J. D., Higgins, D. G., & Gibson, T. J. (1994). CLUSTAL W: Improving the sensitivity of progressive multiple sequence alignment through sequence weighting, position-specific gap penalties and weight matrix choice. *Nucleic Acids Research*, *22*(22), 4673–4680. https://doi.org/10.1093/nar/22.22.4673

Tirira, D. (2021). *Lista Roja de los mamíferos del Ecuador* (3rd ed.). Asociación Ecuatoriana de Mastozoología, FundaciónMamíferos y Conservación, Pontificia Universidad Católica del Ecuador y Ministeriodel Ambiente, Agua y Transición Ecológica del Ecuador.

Tomasco, I. H., Giorello, F. M., Boullosa, N., Feijoo, M., Lanzone, C., & Lessa, E. P. (2022). The contribution of incomplete lineage sorting and introgression to the evolutionary history of the fast-evolving genus Ctenomys (Rodentia, Ctenomyidae). *Molecular Phylogenetics and Evolution*, *176*, 107593. https://doi.org/10.1016/j.ympev.2022.107593

Tomes, R. F. (1860). Notes on a second collection of Mammalia made by Mr. Fraser in the Republic of Ecuador. *Proceedings of The Zoological Society of London*, *1860*, 211–221.

Vallejos-Garrido, P., Pino, K., Espinoza-Aravena, N., Pari, A., Inostroza-Michael, O., Toledo-Muñoz, M., Castillo-Ravanal, B., Romero-Alarcón, V., Hernández, C. E., Palma, R. E., & Rodríguez-Serrano, E. (2023). The importance of the Andes in the evolutionary radiation of Sigmodontinae (Rodentia, Cricetidae), the most diverse group of mammals in the Neotropics. *Scientific Reports*, *13*(1), Article 1. https://doi.org/10.1038/s41598-023-28497-0

Voss, R. S. (2003). A new species of *Thomasomys* (Rodentia: Muridae) from eastern Ecuador, with remarks on mammalian diversity and biogeography in the Cordillera Oriental. *American Museum Novitates*, *3421*, 1–47.

Voss, R. S., Díaz-Nieto, J. F., Jansa, S. A., & Angermann, R. (2018). A revision of *Philander* (Marsupialia, Didelphidae). Part 1, *P. quica*, *P. canus*, and a new species from Amazonia. *American Museum Novitates*, *3891*, 1–70.

https://doi.org/10.1206/3891.1

Weigend, M. (2002). Observations on the biogeography of the Amotape-Huancabamba Zone in northern Peru. *Botanical Review*, *68*(1), 38–54.

Weigend, M. (2013). Observaciones adicionales sobre la biogeografía de la zona de Amotape-Huancabamba en el norte del Perú: Definiendo el límite suroriental. *Revista Peruana de Biología*, *11*(2), 127–134. https://doi.org/10.15381/rpb.v11i2.2447

Welton, L. J., Siler, C. D., Oaks, J. R., Diesmos, A. C., & Brown, R. M. (2013). Multilocus phylogeny and Bayesian estimates of species boundaries reveal hidden evolutionary relationships and cryptic diversity in Southeast Asian monitor lizards. *Molecular Ecology*, *22*(13), 3495–3510. https://doi.org/10.1111/mec.12324

Wickham, H., Chang, W., Henry, L., Pedersen, T. L., Takahashi, K., Wilke, C., Woo, K., Yutani, H., Dunnington, D., Posit, & PBC. (2023). *ggplot2: Create elegant data visualisations using the grammar of graphics* (3.4.4) [Computer software]. https://cran.r-project.org/web/packages/ggplot2/index.html

Wickham, H., François, R., Henry, L., Müller, K., Vaughan, D., Software, P., & PBC. (2023). *dplyr: A grammar of data manipulation* (1.1.3) [Computer software]. https://cran.r-project.org/web/packages/dplyr/index.html

Winger, B. M. (2017). Consequences of divergence and introgression for speciation in Andean cloud forest birds. *Evolution*, *71*(7), 1815–1831. https://doi.org/10.1111/evo.13251

Winger, B. M., & Bates, J. M. (2015). The tempo of trait divergence in geographic isolation: Avian speciation across the Marañon Valley of Peru. *Evolution*, *69*(3),

772–787. https://doi.org/10.1111/evo.12607

Wurdack, K. J. (2017). A new disjunct *Dendrothrix* (Euphorbiaceae, tribe Hippomaneae): A Guiana Shield element in sub-Andean cordilleras of Ecuador and Peru. *PhytoKeys*, *86*, 117–130. https://doi.org/10.3897/phytokeys.86.14761

Zhang, J., Kapli, P., Pavlidis, P., & Stamatakis, A. (2013). A general species delimitation method with applications to phylogenetic placements. *Bioinformatics*, *29*(22), 2869–2876. https://doi.org/10.1093/bioinformatics/btt499

FIGURES

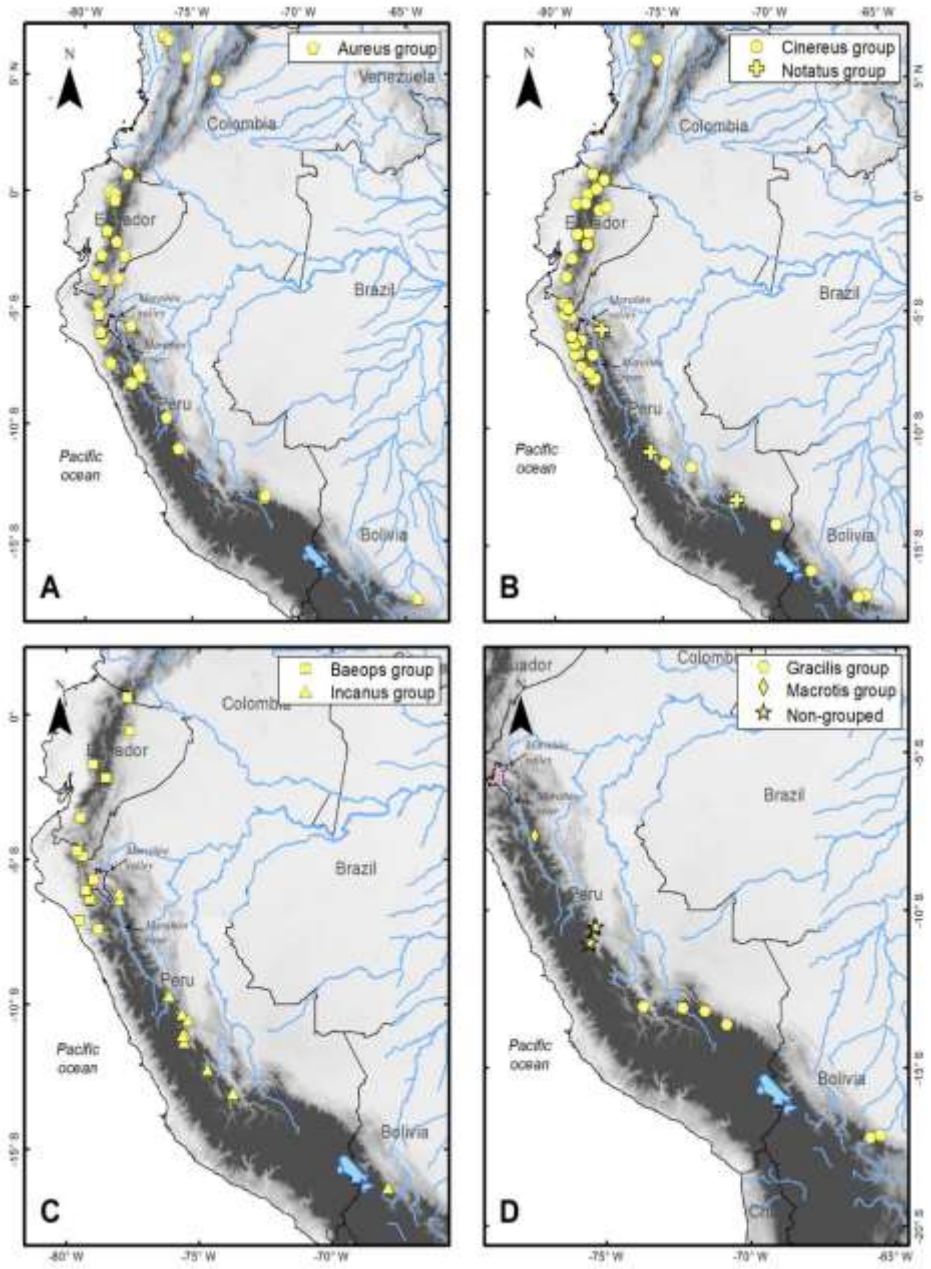

Figure 1. Geographical coverage of the taxonomic sampling of the species of the species groups: Aureus (A), Baeops (C), Cinereus (B), Gracilis (D), Incanus (C), Macrotis (D), Notatus (B), and the non-grouped taxon (D). Species contained in each species group (sensu Pacheco 2015) are shown in Table 1. Localities are listed in Table S2.

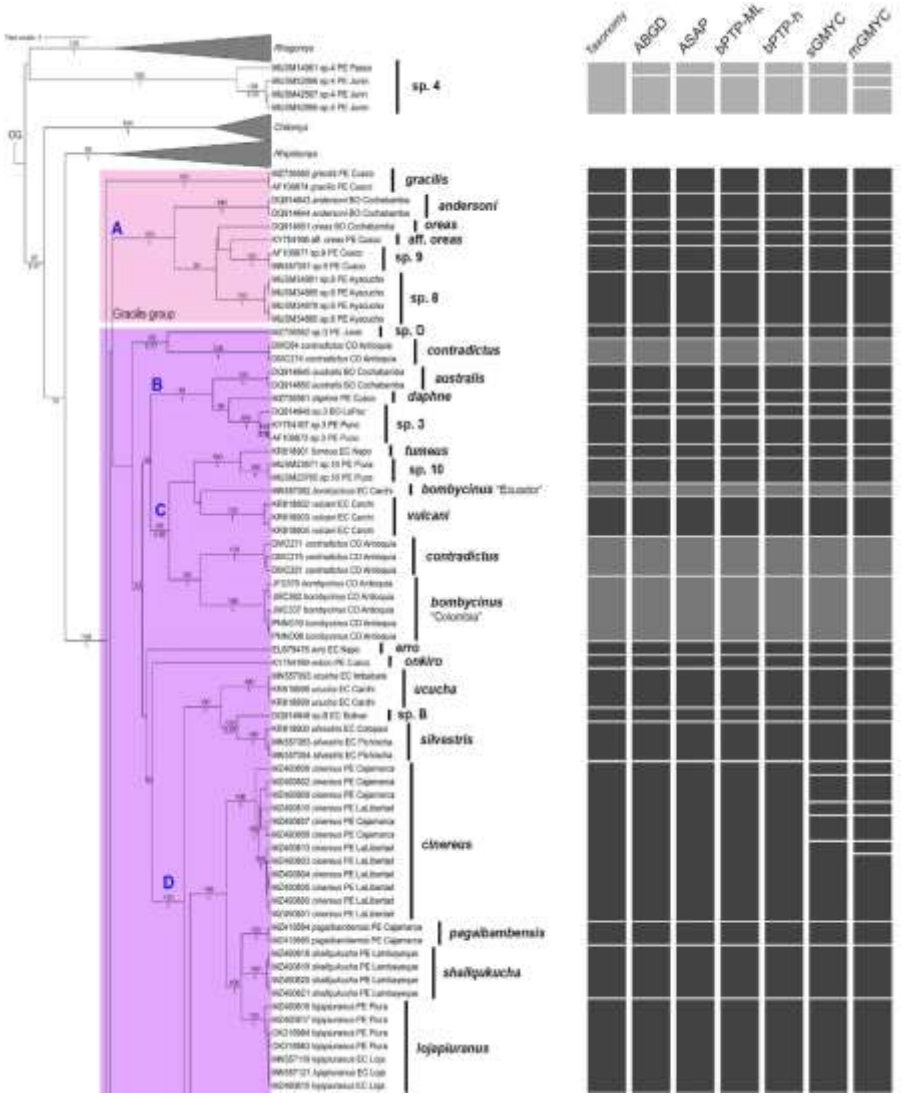

Figure 2 (part A). Ultrametric tree based on Cytb DNA sequences of the genus *Thomasomys* reconstructed by Bayesian analysis in BEAST 2. Numbers in the branches indicate support values of the adjacent node retrieved in the maximum likelihood analysis (Bootstrap values, above) and the Bayesian inference (posterior probability, below). Only values more than 75 % of bs or 0.75 of pp are shown. Titles of color columns indicate the "Taxonomy" criteria (see Material and Methods) and the species delimitation methods employed (ABGD, ASAP, bPTP-h, bPTP-ML, sGMYC, and mGMYC); major clades are identified with letters in blue (A-J); boxes in different colors indicate the species inferred with each method;

the number of species estimated is given at the bottom. Letters in blue indicate the major clades. Country abbreviations: BO– Bolivia, CO– Colombia, EC– Ecuador, PE– Peru.

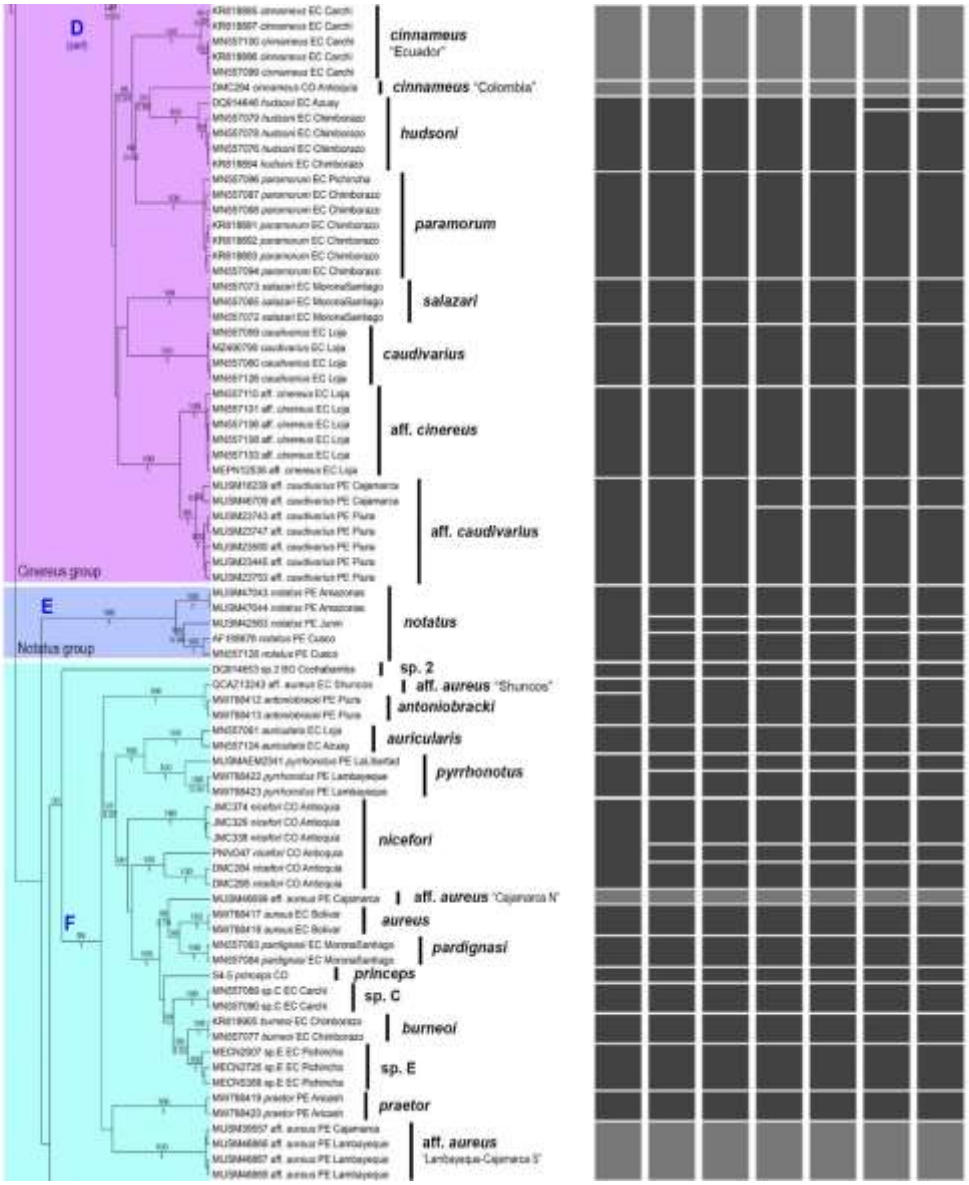

Figure 2 (Part B)

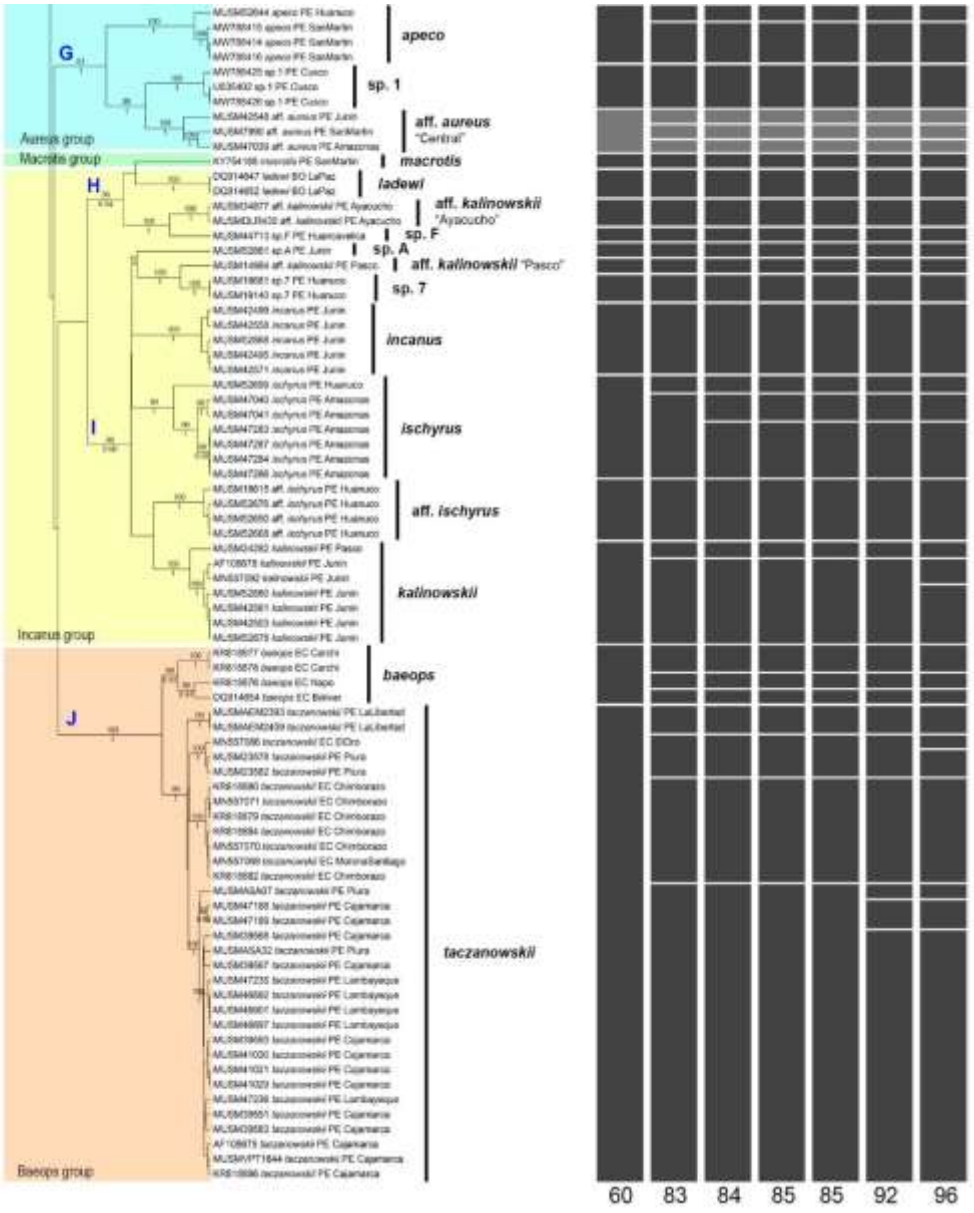

Figure 2 (Part C)

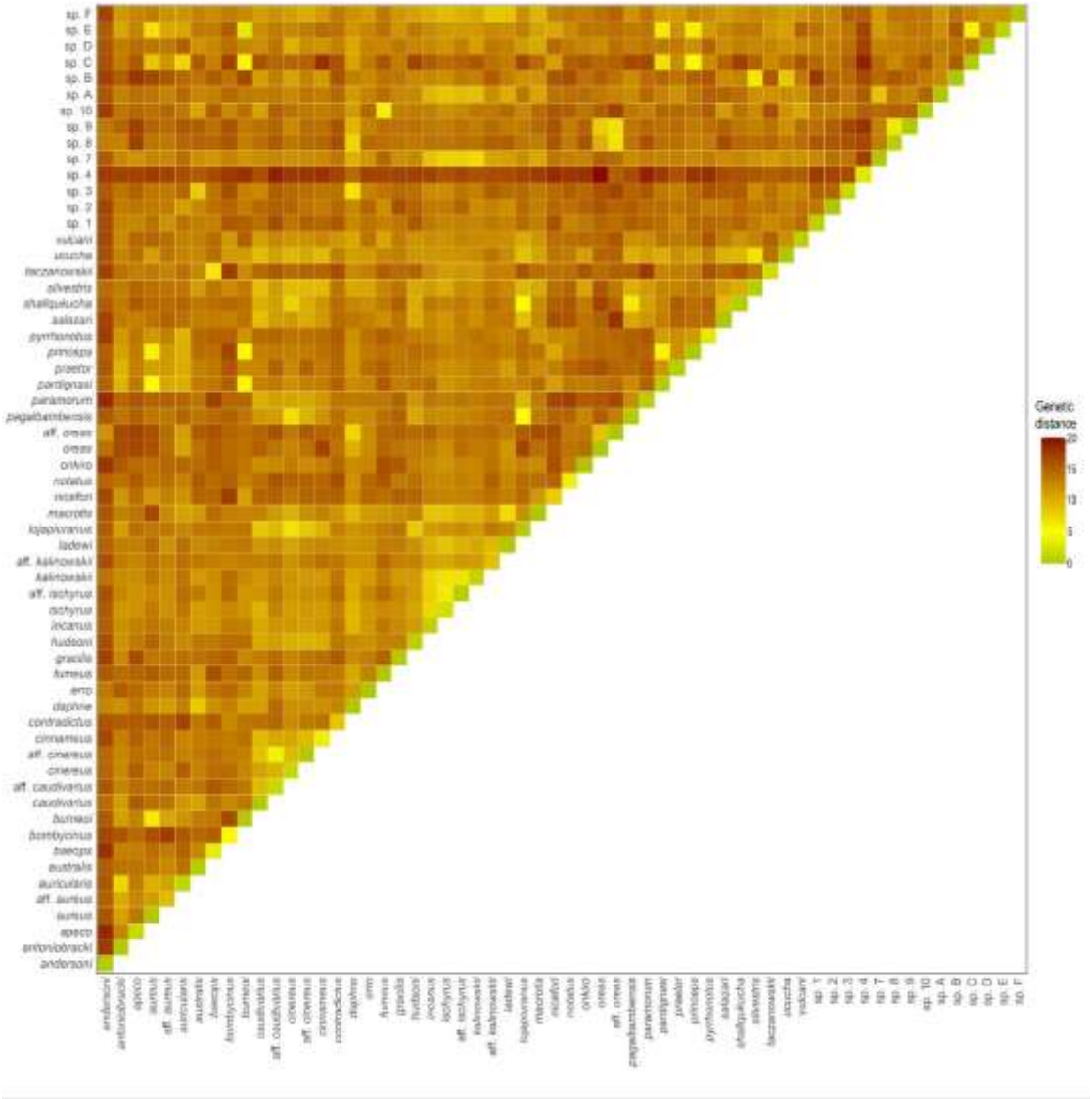

Figure 3. Heat map showing genetic distances between *Thomasomys* species analyzed in this study. For the values, see Table S4.

TABLE 1

Table 1. Cytochrome-b mitochondrial gene sequences of *Thomasomys* used in the molecular analysis gathered from GenBank and obtained in this study (see Table S2). See the taxonomic criteria ("Taxonomy") in Material and Methods for the taxon names. Species with sequences of the type series are marked with asterisks.

Taxa	Species group sensu Pacheco (2015)	Genbank	This study	Total	Non-redundant
*Thomasomys andersoni**	Gracilis	2	0	2	2
*Thomasomys antoniobracki**	Aureus	2	0	2	2
*Thomasomys apeco**	Aureus	3	1	4	4
Thomasomys aureus	Aureus	2	0	2	2
Thomasomys aff. *aureus*	Aureus	1	8	9	9
Thomasomys auricularis	Aureus	3	0	3	2
Thomasomys australis	Cinereus	2	0	2	2
Thomasomys baeops	Baeops	4	0	4	4
Thomasomys bombycinus	Cinereus	1	5	6	6
*Thomasomys burneoi**	Aureus	2	0	2	2
Thomasomys caudivarius	Cinereus	4	0	4	4

Thomasomys aff. *caudivarius*	Cinereus	0	7	7	7
Thomasomys cinereus	Cinereus	14	0	14	12
Thomasomys aff. *cinereus*	Cinereus	18	1	19	6
Thomasomys cinnameus	Cinereus	5	1	6	6
Thomasomys contradictus	Cinereus	0	5	5	5
Thomasomys daphne	Cinereus	1	0	1	1
Thomasomys erro	Cinereus	1	0	1	1
Thomasomys fumeus	Cinereus	1	0	1	1
Thomasomys gracilis	Gracilis	2	0	2	2
Thomasomys hudsoni	Cinereus	5	0	5	5
Thomasomys incanus	Incanus	0	6	6	5
Thomasomys ischyrus	Incanus	0	7	7	7
Thomasomys aff. *ischyrus*	Incanus	0	4	4	4
Thomasomys kalinowskii	Incanus	2	8	10	7
Thomasomys aff. *kalinowskii*	Incanus	0	3	3	3
Thomasomys ladewi	Incanus	2	0	2	2
*Thomasomys lojapiuranus**	Cinereus	11	0	11	7
*Thomasomys macrotis**	Macrotis	1	0	1	1
Thomasomys nicefori	Aureus	0	6	6	6
Thomasomys notatus	Notatus	2	3	5	5

Thomasomys onkiro	Cinereus	1	0	1	1
Thomasomys oreas	Gracilis	1	0	1	1
Thomasomys aff. *oreas*	Gracilis	1	0	1	1
*Thomasomys pagaibambensis**	Cinereus	4	0	4	2
Thomasomys paramorum	Cinereus	10	0	10	7
*Thomasomys pardignasi**	Aureus	3	0	3	2
Thomasomys praetor	Aureus	3	0	3	2
Thomasomys princeps	Aureus	1	0	1	1
Thomasomys pyrrhonotus	Aureus	3	1	4	3
*Thomasomys salazari**	Cinereus	13	0	13	3
*Thomasomys shallqukucha**	Cinereus	5	0	5	4
Thomasomys silvestris	Cinereus	3	0	3	3
Thomasomys taczanowskii	Baeops	14	26	40	32
Thomasomys ucucha	Cinereus	3	0	3	3
Thomasomys vulcani	Cinereus	3	0	3	3
Thomasomys sp. 1 (sensu Pacheco 2003)	Aureus	3	0	3	3
Thomasomys sp. 2 (sensu Pacheco 2003)	Aureus	1	0	1	1
Thomasomys sp. 3 (sensu Pacheco 2003)	Cinereus	3	0	3	3

Thomasomys sp. 4 (sensu Pacheco 2003)	Non-grouped	0	9	9	4
Thomasomys sp. 7 (sensu Pacheco 2003)	Incanus	0	2	2	2
Thomasomys sp. 8 (sensu Pacheco 2003)	Gracilis	0	4	4	4
Thomasomys sp. 9 (sensu Pacheco 2003)	Gracilis	2	0	2	2
Thomasomys sp. 10 (sensu Pacheco 2003)	Cinereus	0	2	2	2
Thomasomys sp. A	Incanus	0	2	2	1
Thomasomys sp. B	Cinereus	1	0	1	1
Thomasomys sp. C	Aureus	2	0	2	2
Thomasomys sp. D	Cinereus	1	0	1	1
Thomasomys sp. E	Aureus	3	0	3	3
Thomasomys sp. F	Incanus	0	1	1	1
Total	**7**	**175**	**112**	**287**	**230**

CHAPTER 2. Introduction to the *Thomasomys* (Rodentia: Cricetidae) turbinal bone adaptations: Insights into elevation and environmental challenges

The second chapter of this thesis explores the hypothesis that mammals in high-elevation habitat exhibit morphological adaptations specifically tailored to conserve heat and moisture. It hypothesizes that *Thomasomys* species found at higher elevations will possess enlarged and more developed respiratory turbinals to face their greater need for warming and humidifying air in the Tropical Andes. Using turbinal surface areas as a proxy for thermoregulatory efficiency, this study investigates the complex relationship between elevation, environmental conditions, and morphological adaptations, using X-ray micro-computed tomography (CT). This approach aims to shed light on the evolutionary adaptations that underpin the success of *Thomasomys* in the montane forests. Additionally, it is discussed the methodology for sizing by size and total surface, highlighting how different approaches can yield varying results.

The article derived from this chapter is yet to be published but is intended for submission to the Journal of Mammalogy following the submission of the thesis manuscript. Preliminary results were presented at the Journée des Doctorants (JDD) of the ISEM in 2023 (June 15, 2023).

Cite as: **Ruelas, D**., Fabre, P.-H., Pacheco, V., & Martinez, Q. (in rev.). Introduction to the *Thomasomys* (Rodentia: Cricetidae) turbinal bone adaptations: Insights into elevation and environmental challenges. *Journal of Mammalogy*.

Introduction to the *Thomasomys* (Rodentia: Cricetidae) turbinal bone adaptations: Insights into elevation and environmental challenges

Dennisse Ruelas[1,2,3], Pierre-Henri Fabre[3,4,5], Víctor Pacheco[1], Quentin Martinez[3,6]

[1]Museo de Historia Natural, Universidad Nacional Mayor de San Marcos, Lima 11, Peru.

[2]Doctorado en Ciencias de la Vida, Universidad Peruana Cayetano Heredia, Av. Honorio Delgado 430, Lima, Peru.

[3]Institut des Sciences de l'Évolution (ISEM, UMR 5554 CNRS-IRD-UM), Université de Montpellier, Place E. Bataillon - CC 064 - 34095, Montpellier Cedex 5, France.

[4]Mammal Section, Department of Life Sciences, The Natural History Museum, SW7 5DB London, United Kingdom.

[5]Institut Universitaire de France (IUF), Paris, France.

[6]Staatliches Museum für Naturkunde Stuttgart, DE-70191, Stuttgart, Germany

Abstract

Turbinal bones in mammals, due to their role in thermoregulation and olfaction, are effective indicators for studying ecological habits. Hypothetically, larger respiratory turbinals aid in heat and moisture retention, particularly in challenging environments like high elevations. The Andes, with their diverse landscapes and high biodiversity, provide an ideal environment for such studies. Among Andean endemics, the *Thomasomys* genus, mostly restricted to montane forests and paramos, exhibits high species diversity and adaptability across various elevational zones. This makes it a prime candidate for exploring the relationship between ecological niches, habitat selection, and turbinal morphology. Using 3D CT-scans of *Thomasomys* turbinal bones, our analysis aims to understand the interplay between turbinal adaptations, elevation-related challenges, and environmental factors represented by PCA-summarized bioclimatic variables. Our study reveals consistent turbinal characteristics among *Thomasomys* species, showing (*i*) isometry or slight positive allometric relationships with skull length, (*ii*) absence of an evolutionary trade-off between the naso- and maxilloturbinals, and surprisingly, between the respiratory and olfactory turbinals; (*iii*) influence of the elevation on turbinal surface area, lower-elevation species having comparatively smaller turbinal surface areas; and (*iv*) the bioclimatic variables showed significant correlations with proportion of the respiratory and olfactory turbinals. Therefore, our results align with the general hypothesis that large respiratory turbinals may help in coping with harsh environmental conditions. However, the positive correlation between the elevation and the olfactory turbinal surface areas remains puzzling and may result from various ecological confounding factors. Overall, this study sheds light on the

complex adaptations of turbinal bones and their interactions with environmental factors, contributing to our understanding of mammalian ecomorphology in montane forest habitats.

Key words: Andes, heat and moisture conservation, montane forest, olfaction, Sigmodontinae

INTRODUCTION

The study of anatomical adaptations in response to environmental factors is a cornerstone of evolutionary biology. Turbinal bones in the nasal cavity of tetrapods, particularly in mammals, are complex structures with dual roles in thermoregulation and olfaction (e.g., Parsons 1967; Schmidt-Nielsen et al. 1970; Hillenius 1992; Van Valkenburgh et al. 2011, 2014; Green et al. 2012; Yee et al. 2016; Martinez et al. 2018, 2020, 2023a; b; Wagner and Ruf 2019; Smith et al. 2021). Turbinal bones can be categorically subdivided into two primary functional compartments: (*i*) the anterior part contains the respiratory turbinals that warm and moisten inspired air before reaching the lungs optimizing respiratory efficiency, and (*ii*) the posterior part contains the olfactory turbinals, which are involved in olfaction thanks to their olfactory epithelium and their connection to the olfactory bulb (Schmidt-Nielsen et al. 1970; Green et al. 2012; Smith et al. 2012; Pang et al. 2016; Martinez et al. 2023c). Due to these combined roles, turbinal bones have emerged as potential ecological proxies for inferring the dietary habits and other ecological habits of mammals (e.g., Van Valkenburgh et al. 2011, 2014; Green et al. 2012; Martinez et al. 2018, 2020, 2023c; a; b). Exploring the complexities of turbinals not only unveils the complexity of physiological processes (Green et al. 2012) but also provides a

unique perspective on how environmental conditions act as strong selective forces driving evolutionary change. Some studies suggested a link between the relative surface area of the respiratory turbinals and the environmental conditions linked to the elevation and the latitude, although none have rigorously tested this hypothesis (Van Valkenburgh et al. 2011, 2014; Green et al. 2012; Martinez et al. 2020, 2023a; b).

When examining the effects of elevation and environmental conditions, specialized functions of turbinals become particularly relevant. At higher elevations, the air is often thinner and cooler, with meager oxygen levels, posing challenges for effective respiration and thermoregulation (Spence and Tingley 2020). So, selection related to habitat conditions would be expected to act mainly on respiratory turbinals more so than olfactory turbinals. Respiratory turbinals are mostly represented by the naso- and the maxilloturbinal and are mostly covered by a highly vascularized respiratory epithelium composed of ciliated structures and mucus glands (Harkema et al. 2006; Barrios et al. 2014; Ruf 2020; Smith and Bonar 2022; Martinez et al. 2023a). As organisms adapt to these conditions, changes in turbinal structure may occur to optimize respiratory efficiency. For example, the demands of warm and water retention are greater for species living at high elevations with cold and dry environments than those living lower with more temperate and mesic environments (Withers et al. 2016a; b). Similarly, the olfactory turbinals underscore their significance in detecting scents, which can be vital for survival and reproduction (Moulton 1967; Green et al. 2012; Martinez et al. 2023a). Different environments may expose organisms to distinct odors, influencing their ability to find food, avoid predators, and communicate with conspecifics.

Therefore, studying how elevation and environmental conditions impact the structure and function of olfactory turbinals contributes to our understanding of how animals adapt to their environment.

With its heterogeneous landscapes, the Andes offer an exceptional opportunity to study adaptive traits. Organisms inhabiting these regions have evolved a diverse array of morphological and physiological traits to cope with harsh conditions (Voss 1988; Monge and Leon-Velarde 1991; Rezende et al. 2005; Withers et al. 2016a; Schenk and Steppan 2018) such as high elevation, low temperature, or varying humidity (e.g., high in montane and premontane forests, low in puna). High-elevation species face the dual challenges of colder temperatures and increased respiratory demands due to lower oxygen levels (Withers et al. 2016a; b; Luna et al. 2017; Butaric and Klocke 2018). The Andean environments are home to a rich diversity of rodents (Patterson et al. 2012; Vallejos-Garrido et al. 2023), making them a prime group for investigating adaptive traits.

In the realm of Andean mammalian diversity, the *Thomasomys* genus stands out for its remarkable adaptability to varying high elevational zones, exclusively inhabiting montane forests (including premontane forests) and páramos. It spans an impressive range of 3350 m elevation (from 1150 to 4500 m) with most species inhabiting between 2000 to 3500 m (Supplementary Data SD1). These species generally have very limited distribution ranges (see maps and remarks in Pacheco 2015). The mean annual temperatures of these forests vary, with upper montane forests (2500 to 3500 m) experiencing 7 to 15°C and lower montane forests (1500 to 2500 m), 15 to 19°C (Young and León 1999). In some localities can have

minimum temperatures of 4°C. Significantly, *Thomasomys* species are completely absent from certain geographic areas, such as the Guiana Shield, lowland tropical forests, desert regions, and oceanic islands (Pacheco 2003, 2015; Pacheco et al. 2015). Furthermore, *Thomasomys* being the most diverse genus of sigmodontine rodents, with 51 valid species and several undescribed species (Pacheco 2015; Pacheco and Ruelas 2023; Ruelas et al. 2024), many species co-occur within the same montane habitat – until five in the same locality – with most exhibiting semi-arboreal or scansorial behavior (Leo L and Gardner 1993; Voss 2003; Brito M et al. 2012; Pacheco 2015). Morphologically, the genus spans a wide range, from the smaller *T. daphne* (head and body length= 80 mm) to the larger *T. apeco* (head and body length= 238 mm), with corresponding weights varying from 14 g to 335 g (Pacheco 2015). Such distribution patterns and morphological diversity underline *Thomasomys*' high ecological specialization and adaptation to mountain niches, with elevational gradients being crucial for habitat selection. In contrast, other diverse genera like *Akodon* (42 species) and *Oligoryzomys* (32 species), have fewer species confined to high-elevation environments (Pardiñas et al. 2015; Weksler and Bonvicino 2015; Brandão et al. 2021; Hurtado and D'Elía 2022). This contrasts with the success of *Thomasomys* in these habitats, potentially linked to their specific adaptations to the environmental conditions of high-altitude forests. In semi-aquatic rodents, Martinez et al. (2020) proposed that respiratory turbinals may be larger in species living in colder habitats (mediated by elevation), indicating a temperature-adapted evolutionary response, a pattern that could represent convergent evolution in response to similar ecological pressures across different species. The high variation and diversity within a single genus underscore its adaptability to diverse

environmental conditions and ecological niches, allowing for the exploitation of a broad range of resources. However, despite its ecological success, the limited comprehensive understanding of *Thomasomys* impedes the formulation of evolutionary hypotheses regarding its adaptation and radiation in high-elevation habitats. The fluctuating environmental conditions across the Andean elevational gradients likely impose considerable selective pressures on the morphology of *Thomasomys* species, contributing to their varied adaptations and ecological success.

Therefore, the *Thomasomys* species are a perfect model to test the hypothesis that mammals through high-elevation habitats may display distinct morphological adaptations specifically linked to their capacity to conserve heat and moisture. In this sense, we expect that *Thomasomys* species inhabiting higher elevations present larger respiratory turbinals due to their increased need for warm air. By using turbinal surfaces as a proxy for homeothermic function, our study aims to unravel the complex interplay between elevation and environmental variables with morphological structures obtained by X-ray micro-computed tomography (CT), shedding light on the evolutionary success of *Thomasomys*.

METHODS

Specimens

We employed 45 adult specimens of *Thomasomys* species preserved in alcohol which include 19 species (Appendix 1). The use of ethanol-preserved specimens ensures that the anterior part of the respiratory turbinal is not damaged due to the cleaning methods, which is an important factor for a quantitative approach at this

taxonomic scale. These specimens were collected in Peru and Colombia between 1500 m and 3380 m a.s.l. (Supplementary Data SD2). Specimens are housed in the Museum of Natural History of the Universidad Nacional Mayor de San Marcos (MUSM, Lima) and the Field Museum of Natural History (FMNH, Chicago). Species identification was made by D. Ruelas and V. Pacheco following Ruelas et al.' (2024) nomenclature. Also, we downloaded CT-scans of the skull of *T. aureus* (MEPN 6144) from MorphDbase (https://www.morphdbase.de/).

Because there is no phylogenetic hypothesis based on a multilocus phylogeny, we grouped the *Thomasomys* species based on the morphological species groups proposed by Pacheco (2015). Our specimens belong to six of them: the Aureus group (n= 10) with mainly large-sized species distributed from 2117 to 3217 m a.s.l; the Baeops group (n= 10) with small-sized species distributed from 1500 to 2950 a.s.l.; the Cinereus group (n= 11) with small and medium-sized species distributed from 2200 to 3290 m a.s.l.; the Gracilis group (n= 1) with small species distributed 2880 m a.s.l.; the Incanus group (n= 11) with medium-sized species distributed from 2200 to 3380 m a.s.l.; and the Notatus group (n= 2) comprised by the medium-sized *T. notatus* distributed from 1900 to 1920 m a.s.l (Supplementary Data SD2).

Data acquisition

The acquisition of 3D data was performed using an EasyTom 150 microtomograph with a voxel size ranging from 0.018 to 0.027 mm. Using a combination of unstained ethanol-preserved specimens and classical CT technology will only image bony structures (materials with high density) and provide strictly comparable

results with most studies on turbinals that are mostly based on dry skulls. Turbinals from the left side of the skull were segmented following Martinez et al. (2018, 2023a) with Avizo Lite v. 9.0.1 (Fisher Scientific Inc., USA). In cases where the left side of the skull was damaged due to the use of snap traps for mouse collection, the left side of the skull was replaced by the right side. The turbinals were manually segmented every two or three images, and an interpolation was employed to bridge the gaps in segmentation. All the interpolated images were then checked to correct any potential errors.

Variables

Explanatory variable sets were generated as follows:

Size.— We extracted the skull length (SL, in mm) from the reconstructed CT data with Avizo Lite v. 9.0.1. It was measured from the most anterior part of the nasal to the most posterior part of the occipital (Supplementary Data SD3).

Turbinal surface area.— We extracted the surface area of the segmented turbinals using Avizo Lite v. 9.0.1. (Supplementary Data SD3). We merged the turbinal surface areas (Fig. 1) into respiratory (naso- and maxilloturbinal) and olfactory (other turbinals considering the semicircular lamina) turbinals following the turbinal functional partitioning by Martinez et al. (2018, 2020, 2023a). In rodents, the epithelial cover of the maxilloturbinal is widely accepted (Martinez et al. 2023a; b). While the nasoturbinal is predominantly covered by respiratory epithelium, there is limited comparative histology data, and this covering can vary significantly among mammalian species (e.g., Smith and Bhatnagar 2004; Smith and Rossie 2008; Smith et al. 2012; Yee et al. 2016; Herbert et al. 2018; Martinez et al. 2023a).

Therefore, we separately analyzed the naso- and the maxilloturbinal to evaluate the potential impact of this functional partitioning on our findings (see Martinez et al. 2018, 2020 for a similar methodology).

Elevation.— These data (in meters) were extracted from the Museum collection's databases. If the elevation was not provided, it was estimated based on either the geographic coordinates or details of the location where the specimen was collected (Appendix 1).

Bioclimatic variables.— We retrieved climatic data variables with a resolution of 2.5 arc-min from the WorldClim 2.1 database (https://www.worldclim.org) for the period of 1970-2000 (Fick and Hijmans 2017). The 19 bioclimatic variables available were retrieved as follows: BIO1 = Annual mean temperature; BIO2 = Mean diurnal range (mean of monthly (max temp - min temp)); BIO3 = Isothermality (BIO2/BIO7) (×100); BIO4 = Temperature seasonality (standard deviation ×100); BIO5 = Max temperature of warmest month; BIO6 = Min temperature of coldest month; BIO7 = Temperature annual range (BIO5-BIO6); BIO8 = Mean temperature of wettest quarter; BIO9 = Mean temperature of driest quarter; BIO10 = Mean temperature of warmest quarter; BIO11 = Mean temperature of coldest quarter; BIO12 = Annual precipitation; BIO13 = Precipitation of wettest month; BIO14 = Precipitation of driest month; BIO15 = Precipitation seasonality (coefficient of variation); BIO16 = Precipitation of wettest quarter; BIO17 = Precipitation of driest quarter; BIO18 = Precipitation of warmest quarter; and BIO19 = Precipitation of coldest quarter (Supplementary Data SD3). To simplify this data, a principal component analysis (PCA) was conducted on the

correlation matrix following Souquet et al. (2019). The explanatory variables for the model were limited to only the PC axes that accounted for 5% or more of the variance. Additionally, we explored the individual influence of the most important variables on the PC axes selected previously.

Data correction

In the study of turbinal structures, researchers commonly recommend two forms of correction to account for variations: sizing by (*i*) overall body size, using metrics such as skull length, body length, or mass, and (*ii*) by total turbinal surface area (TTSA) (e.g., Green et al. 2012; Martinez et al. 2018, 2020). Our research incorporates both types of corrections to better understand the implications for the functional morphology and adaptive significance of turbinal structures. (i) Adjusting by body size allows for comparing morphological traits and shapes without size bias, aiding in the detection of morphological differences and the exploration of evolutionary and ecological adaptations (e.g., Green et al. 2012; Porto et al. 2013; Weaver and Grossnickle 2020; Mitchell et al. 2023). Here, sizing by SL helps gauge the proportion and relative size of turbinals within the skull, supporting the hypothesis that larger turbinals are indicative of better adaptation to colder, higher elevation environments. (ii) Sizing by TTSA provides insight into the balance between respiratory (related to heat and moisture conservation) and olfactory capabilities, offering insights into ecological adaptations and evolutionary biology (e.g., Martinez et al. 2018, 2020, 2023a). We hypothesize to shift towards higher respiratory and lower olfactory proportions in adaptation to colder, elevated environments following Martinez et al.'s (2020) findings.

To account for the SL, we performed log-transformed linear regressions (or ordinary least-squares regression) between the skull length as independent variable and the respiratory (RTSA), olfactory (OTSA), and total turbinal surface areas (TTSA) as dependent variables (Warton et al. 2006; Green et al. 2012). While accounting for the TTSA, we performed log-transformed linear regressions between the TTSA as an independent variable and both RTSA and OTSA as dependent variables. For our subsequent analyses, we employed residuals from these analyses which are respectively referred to as *(i)* relative respiratory turbinal surface area, *(ii)* relative olfactory surface area, and *(iii)* relative total turbinal surface area. This method of using ordinary least-squares regression is endorsed for allometry studies due to its proficiency in managing measurement errors and accurately depicting allometric scaling (Kilmer and Rodríguez 2017).

Quantitative analyses

To delve into the interplay between nasoturbinal and maxilloturbinal and between respiratory and olfactory turbinal surface areas of *Thomasomys* and their potential correlation after accounting for the size effect, an initial step involved assessing the normality of the variables (relative surface areas), accomplished through the Shapiro-Wilk test. Given the non-normal distribution identified in both nasoturbinal (W= 0.909, P= 0.002) and maxilloturbinal (W= 0.935, P= 0.014) surface areas, as well as in the RTSA (W= 0.906, P= 0.001) and OTSA (W= 0.915, P= 0.003), we used Kendall's Tau correlation coefficient for analysis, a method supported by Bolboacă and Jäntschi (2006) and Ghent (1963) for its effectiveness with non-

normal data. This approach helps determine the extent to which changes in one variable are associated with changes in another (Jarantow et al. 2023).

Subsequently, to assess the influence of elevation and bioclimatic factors on turbinal surface areas, we conducted linear regression analyses. In these analyses, the relative surface areas of turbinals were defined as dependent variables, with elevation and bioclimatic variables – represented by PCs–, as independent variables. Given the non-normal distribution of relative turbinal surface areas when sized by SL, which included both positive and negative values, we opted for the Yeo-Johnson transformation (Johnson 1949) to normalize the data. This method, distinguished for its robustness and adaptability, and is notably proficient in handling data with varying signs, effectively normalizing it according to the Z family of distributions (Chou et al. 1998; Santos-Fernandez 2014). Conversely, for the data sized by TTSA, which displayed a normal distribution for both respiratory ($W = 0.985$, $P = 0.807$) and olfactory turbinals ($W = 0.982$, $P = 0.691$), we proceeded without transformation. Although, using PCs simplify the analysis, capturing essential climatic variations to understand ecological influences and respiratory adaptations, we also analyzed the impact of individual variables for deeper insights.

Lastly, to visually underscore our study's scope, we incorporated the phylogenetic tree of *Thomasomys* taken from Ruelas et al. (2024). This inclusion serves to demonstrate the extension of our sampling. However, the absence of four taxa within the phylogeny and the necessity to merge by a mean population with different altitudinal ranges posed a significant constraint. Opting to remove these

taxa or meaning our species would have resulted in a reduction of our sample size, thereby compromising the comprehensiveness of our analysis. Consequently, we did not undertake phylogeny-based analyses such as phylogenetic generalized least squares (PGLS), prioritizing the integrity of our sample representation (Fig. 2).

For all these analyses, we used the "devtools" (Wickham et al. 2022), "factoextra" (Kassambara and Mundt 2020), "FactoMiner" (Lê et al. 2008), "ggplot2" (Wickham et al. 2023), "Johnson" (Santos-Fernandez 2014), "reshape2" (Wickham 2020), and "smplot2" (Min and Zhou 2021) packages within the R version 4.1.3 environment (R Core Team 2022) and RStudio (RStudio Team 2023).

RESULTS

Turbinal morphology

Turbinals of all the *Thomasomys* species analyzed showed consistent morphological patterns in scroll complexity and size (Fig. 1, Supplementary Data SD4, Supplementary Data SD5, Supplementary Data SD6). The genus *Thomasomys* presents two respiratory turbinals (nasoturbinal and maxilloturbinal) located in the anterior portion of the rostrum and seven olfactory turbinals (semicircular lamina, frontoturbinal 1, frontoturbinal 2, ethmoturbinal I, interturbinal, ethmoturbinal II, and ethmoturbinal III) located posteriorly (Fig. 2).

The nasoturbinal has two lamellae: the first, shorter lamella is dorsal and located closer to the nasal bone, exhibiting variations such as simple (e.g., *T. antoniobracki*, *T. daphne*, *T. taczanowskii*), or branching (e.g., *T. ischyrus*, *T. pagaibambensis*). The second, longer lamella branches and scrolls angularly

(clockwise on the right nasoturbinal and counterclockwise on the left nasoturbinal). Branches can be short or long. Typically, when the scroll is a complete turn or less, it is like a square (e.g., *T. antoniobracki*); when it is one or 1.5 turns, it is triangular-shaped or square-shaped (e.g., *T.* aff. *kalinowskii*, *T.* cf. *pyrrhonotus*). Along the nasoturbinal, the middle section is notably more robust in some species, such as those in the Incanus group and in larger species of the Cinereus group (Fig. 2; Supplementary Data SD4, Supplementary Data SD6). However, the robustness can also remain relatively constant, as observed in *T. taczanowskii* or *T. daphne* (Fig. 2; Supplementary Data SD4). In addition, the posterior part of the nasoturbinal comes into slight contact with the anterior part of ethmoturbinal I, and this contact varies in extent, being more significant in some species, such as *T. ischyrus*, *T. kalinowskii*, and *T.* sp. 6, and less pronounced in others, like *T. notatus* or *T. aureus*.

The maxilloturbinal, attached to the maxillary bone and located under the nasoturbinal, exhibits considerable variation along its length (Fig. 2; Supplementary Data SD4). The maxilloturbinal has one or two roots and two major lamellae: the first, longer lamella ascends and comes closer to the nasoturbinal, scrolling dorsally and angularly for one complete turn (clockwise on the left maxilloturbinal and counterclockwise on the right maxilloturbinal). This lamella typically features one or two small branches, but occasionally, it is simple (as seen in *T. daphne* and *T.* aff. *aureus*). The second lamella is shorter, ventrally angular scrolled, and sometimes branches in the middle into two or three slightly straight sub-lamellae, one longer than the others. Along the maxilloturbinal, the robustness can also remain relatively constant from the anterior to the posterior part, but the posterior portion always tapers to a sharp point, being unattached to the maxillary bone (Fig.

2; Supplementary Data SD4). The maxilloturbinals are anteriorly placed similarly to the nasoturbinal. Both structures are of similar size and respectively positioned ventrally and dorsally in the rostrum. However, significant exceptions exist, as detailed in Figure 2. Notably, in *T.* cf. *caudivarius* and *T.* aff. *incanus*, the nasoturbinal is more elongated than the maxilloturbinal (Fig. 2; Supplementary Data SD6).

The semicircular lamina, which is the uppermost olfactory turbinal, displays notable variation in its structure (Fig. 2). The semicircular lamina is anteroposteriorly elongated and protruded medially in the dorsoventral direction. This protrusion joins the dorsal side of the ethmoturbinal I. The frontoturbinal 1 has two lamellae, one on the right side and the other on the left, both exhibiting a slight ventral scroll, typically less than one full turn. Sometimes, the lamellae closer to the semicircular lamina may feature a single straight small projection, as observed in *T. pagaibambensis* or *T. ischyrus*. The frontoturbinal 2 is typically composed of one lamella that is slightly scrolled ventrally, as seen in species like *T. oreas*. However, in less common cases, it consists of two divergent lamellae, one positioned dorsally and the other ventrally in relation to their orientation within the nasal cavity. Both lamellae are slightly scrolled, with the dorsal one being shorter and the ventral one being longer, as seen in *T. kalinowskii*. Usually, frontoturbinal 1 is as long as frontoturbinal 2 except for *T.* cf. *dispar* and *T. daphne* (Fig. 2). The ethmoturbinal I, being the largest olfactory turbinal, exhibits a prominent projection towards the rostral side. Its structure is characterized by a delicate, intricate arrangement of thin scrolls and plates. The ethmoturbinal I protrudes medially in the dorsoventral direction, which is notably wide in *T. daphne* and *T. antoniobracki*,

and its anterior part extends to the posterodorsal region of the nasoturbinal. The interturbinal consists of a single lamella that is slightly ventrally scrolled, typically less than one full turn. It is the simplest turbinal, and its structure remains relatively consistent with minimal variation along its length. The ethmoturbinal II formed two lamellae, one lamella dorsal and straight and the other lamella ventral and slightly scrolled, less than one full turn. The ethmoturbinal III formed one slightly scrolled lamella, which sometimes has a small projection in the middle before scrolling, as observed in species of the Incanus group. In most *Thomasomys* species, the frontoturbinals, interturbinals, and ethmoturbinals are notably elongated, except for smaller species like *T. daphne* and *T. taczanowskii*, where these structures are shorter (Fig. 2).

Correlation analyses and allometric relationships

To explore the interplay between turbinal surface areas and skull length (SL), we generated an array of regression plots involving the three distinct categories—respiratory turbinal surface area (RTSA), olfactory turbinal surface area (OTSA), and total turbinal surface area (TTSA). The results demonstrated statistically significant correlations in each comparison, with RTSA (Adjusted R^2= 0.57, P= 1.25e-09, S= 2.22, Fig. 3A), OTSA (Adjusted R^2= 0.594, P= 3.54e-10, S=2.05, Fig. 3B), and TTSA (Adjusted R^2= 0.603, P = 2.2e-10, S= 2.11, Fig. 3C) all showing isometry or positive allometry. These findings underscore that in general, large members of the *Thomasomys* genus, showcase similar or more expansive turbinal surface areas when compared to their smaller counterparts (Fig. 3). Interestingly, the large *Thomasomys* species such as *T. antoniobracki* (SL: 44.76-43.86 mm;

occurring at 2630 and 2720 m) and *T.* aff. *aureus* (SL: 40.58-40.85 mm; occurring at 3217 m) from the Aureus group, consistently displays less expansive turbinal surface areas when compared to their smaller counterparts, like *T. taczanowskii* from the Baeops group (SL= 26.94-29.63 mm; occurring between 1500 to 2950 m), than the general trend (Fig. 3). It is also interesting to notice that some mid-sized species of the Cinereus like *T.* sp. 10 (SL= 32.85 mm; occurring at 2630 and 2780 m) and *T. pagaibambensis* (SL= 33.43 mm; occurring at 2946 m) and Incanus like *T. kalinowskii* (SL= 30.47-33.25 mm; inhabiting at 2757 m) and *T. ischyrus* (SL= 31.09-32.05 mm; inhabiting at 2757 and 2900 m) groups occurring in similar elevations but different localities (see appendix 1; Supplementary Data SD2) showed turbinal surface areas comparatively as large as the large-sized species (Fig. 2, Supplementary Data SD5). Moreover, we did not uncover a direct correlation between SL, as a proxy for body size, and elevation, indicating that *Thomasomys* species of various sizes coexist across a similar elevation range, specifically between 2000 to 3000 m (Supplementary Data SD7). This distribution pattern is evident across different *Thomasomys* groups, including Aureus, Baeops, Cinereus, and Incanus, highlighting a complex relationship between size and other factors, beyond the influence of elevation alone, including the monophyletic nature of each group.

Size corrected turbinal

Through correlation analyses, it was found that after accounting for the size effect, there is a positive correlation between the relative nasoturbinal and maxilloturbinal turbinal surface areas (tau = 0.669, P = 8.546e-13) and between the relative

respiratory and olfactory turbinal surface areas (tau = 0.570, P = 4.093e-09). These findings underscore that smaller nasoturbinals are associated with smaller maxilloturbinals (Fig. 4A, Supplementary Data SD5). Smaller relative RTSA in *Thomasomys* species, like *T. taczanowskii*, tend to coincide with smaller OTSA (Fig. 4B, Supplementary Data SD5), while species with larger RTSA, like *Thomasomys* sp. 10, *T. ischyrus* or *T.* aff. *incanus*, exhibit larger OTSA. Notably, larger species in the Aureus group and smaller species in the Baeops group consistently showed smaller turbinal surface areas in both nasoturbinals and maxilloturbinals, as well as RTSA and OTSA. Conversely, mid-sized species in the Cinereus and Incanus groups displayed more extensive turbinals. Overall, our results suggest an absence of an evolutionary trade-off between the naso- and maxilloturbinals, as well as between the respiratory and olfactory turbinals.

Bioclimatic variables

The 19 bioclimatic variables retrieved from WorldClim were summarized using a PCA, and only two axes were needed to explain most variance (PC1: 74.78%, PC2: 16.06%) (Supplementary Data SD8, Supplementary Data SD9). BIO6 demonstrated a significant contribution of the PC1, as indicated by its coefficient of 0.507 and reflects the temperature dynamics (Supplementary Data 9). Similarly, BIO14, BIO17, and BIO19 significantly shaped PC2 with loadings of 0.268, 0.238, and 0.236, respectively, reflecting their influence on precipitation patterns (Supplementary Data 9).

Effect of environmental variables on the turbinals size

Remarkably, elevation displays a statistically significant but slightly weak positive relationship with relative RTSA (Adjusted $R^2 = 0.0753$, $P = 0.038$, Fig. 5A), while relative OTSA exhibits a stronger and significant positive correlation with elevation (Adjusted $R^2 = 0.152$, $P = 0.005$, Fig. 5B), meaning a clear trend where species inhabiting lower-elevation habitats often display smaller relative RTSA and OTSA (Supplementary Data S6). Moreover, there is a statistically significant, moderate positive relationship between elevation and TTSA (Adjusted $R^2 = 0.152$, $P = 0.005$, Fig. 5C). Species groups with the widest elevation range, such as the Cinereus and Incanus groups, exhibited a dispersed pattern in the analysis involving RTSA (Fig. 5A), while their OTSA showed a slightly increasing trend (Fig. 5B). However, for the other groups, the relationship between RTSA or OTSA and elevation was not as evident. Collectively, these findings highlight the significant impact of elevation on the complex morphology of turbinal surface areas in *Thomasomys* species. Furthermore, species size does not seem to linked to elevation (Supplementary Data 1, Supplementary Data 7), as *Thomasomys* species of varying sizes are found cohabiting within the same elevation ranges.

The linear regression results showed varying associations between the principal components (PC1 and PC2) representing bioclimatic variables and the relative turbinal surface areas (RTSA, OTSA, and TTSA) in the *Thomasomys* species (Fig. 5D-I). In the case of PC1, the associations with turbinal surface areas (RTSA, OTSA, and TTSA) were not statistically significant (Fig. 5D-F). Regarding species groups, the Incanus and Cinereus groups showed an increasing pattern of RTSA in relation to PC1 (Fig. 5D), which was not observed when examining OTSA against PC1 (Fig. 5E). The Aureus group exhibited a slight decreasing pattern of

OTSA concerning PC1 (Fig. 5E). For the other groups, no distinct pattern was observed. Similar to PC1, PC2 showed no significant associations with turbinal surface areas (Fig. 5G-I). Moreover, there were no clear patterns of increase or decrease in OTSA or RTSA with respect to PC2 within the species groups. Upon individually analyzing the bioclimatic variables (Table 1, Supplementary Data SD10), a slight correlation was observed between BIO 12 (annual precipitation) and the relative RTSA (Adjusted R^2= 0.0684, P= 0.0458). No significant correlations were found in the other cases. Surprisingly, there is no significant correlation between elevation and this environmental variable (Adjusted R^2= 0.00502, P= 0.275; Supplementary Data SD11).

Effect of environmental variables on the total surface area

Regressions showed strong and highly significant relationships between the respective turbinal surface area (respiratory or olfactory) and the total surface area (Fig. 6A-B). Regarding the influence of elevation and environmental variables (Fig. 6C-H), the PC1 of bioclimatic variables showed a more significant impact on both RTSA (Adjusted R^2 = 0.299, P = 6.15e-05) and OTSA (Adjusted R^2 = 0.299, P = 6.13e-05) compared to elevation or the PC2 of bioclimatic variables, which did not show statistical significance. On the other hand, the presence of opposite signs in the slopes in the regressions between turbinal surfaces areas against both elevation and bioclimatic variables (PC1 and PC2) can be attributed to the positive correlation between respiratory and olfactory turbinal surface areas (Fig. 4B) and the fact that the TTSA is the sum of the RTSA and OTSA.

When it comes to the species groups, the species belonging to the Cinereus and Aureus groups showed a slight decreasing pattern of the RTSA and a slightly increasing pattern of the OTSA with respect to the elevation. The remaining groups did not display any increasing or decreasing pattern in any variable. Upon individually analyzing the bioclimatic variables (Table 1, Supplementary Data SD12), significant correlations were found in almost all the bioclimatic variables and the relative RTSA and relative OTSA, except for variables related to the temperature, such as BIO5 (Max temperature of warmest month), BIO8 (Mean temperature of wettest quarter), and BIO10 (Mean temperature of warmest quarter), and as well as for BIO1 (Annual mean temperature) but only for relative OTSA. This suggests a nuanced relationship between proportions of the turbinal surface areas and environmental factors.

DISCUSSION

High-elevation adaptations

High-elevation adaptations in small mammals have been studied with a focus on some physiological responses, usually associated with the metabolic rate (e.g., Schippers et al. 2012; Arias-Reyes et al. 2021), breathing (e.g., Arias-Reyes et al. 2021), blood oxygen-carrying capacity (e.g., Tufts et al. 2013; Lui et al. 2015; Arias-Reyes et al. 2021), and water loss (e.g., Cortés et al. 1990, 2003; Withers et al. 2016b). To our knowledge, this study is the first statistical evidence using turbinal surface areas as a proxy of heat and moisture conservation related to environmental factors focused on high-elevation forests. Here, we found that in *Thomasomys* there is a significant correlation between the relative RTSA, when

sizing by SL, and the elevation (Fig. 5A, Supplementary Data SD6). This finding aligns with the hypothesis that species living in high elevation may have some morpho-physiological adaptation helping them to minimize heat loss and to cope with the harsh environmental conditions (e.g., Van Valkenburgh et al. 2004, 2011; Green et al. 2012; Withers et al. 2016b; a; Martinez et al. 2020, 2023a; b).

Therefore, our results suggest that mid-sized species inhabiting high elevations demonstrate a more efficient respiratory system (Fig. 5A-C). Specifically, this fact may be linked to the surface increase of the respiratory epithelium that is richly vascularised, thus contributing in warming up the inspired air. Indeed, some studies (e.g., Jackson and Schmidt-Nielsen 1964; Schmidt-Nielsen and Jackson 1964; Schmidt-Nielsen et al. 1970; Caputa 1979) have properly demonstrated that rabbits and some rodents employ their maxilloturbinals during inhalation to increase the temperature of the inspired air, helping it quickly reach the body temperature. This mechanism is a crucial adaptation to maintain optimal internal body temperature. However, when it comes to heat and moisture conservation during exhalation, there is a wide variation among species, suggesting a degree of specialization (Xi et al. 2016, 2023; Arias-Reyes et al. 2021).

Using SL sizing, our regression results are non-significant for the bioclimatic variables related to temperature and precipitation (except only for annual precipitation against RTSA, which was significant), independently or merged together in the PCA (Fig. 5D-F, Supplementary Data SD10). Such an absence of correlation when considering the size does not necessarily indicate that the *Thomasomys* species do not have thermal adaptations to cope with their

environment. Rather, it suggests that factors other than temperature and precipitation might play a more substantial role in their ecological adaptations. As an example, in canid and arctoid carnivorans, Green et al. (2012) did not find a significant relationship between RTSA and climate, as estimated by latitude. Which may suggest that the size of respiratory turbinals is not strongly driven by climate-related factors. Instead, other ecological parameters, such as diet and habitat, appear to have a more significant impact (Green et al. 2012). However, when examining the functional partitioning of turbinal surface areas (TTSA adjusting), the PC1 of bioclimatic variables shows significant correlations with the relative RTSA (Fig. 6E-F). Specifically, RTSA is positively correlated with five temperature-related variables (BIO1, BIO3, BIO6, BIO9, and BIO11) and eight precipitation-related variables (BIO12, BIO13, BIO14, BIO16, BIO17, BIO18, and BIO19). In contrast, it negatively correlates with three temperature variables (BIO2, BIO4, and BIO7) and one precipitation variable (BIO15) (Table 1, Supplementary Data SD12). These correlations indicate potential adaptations of *Thomasomys* species to their environmental conditions, with a greater proportion of respiratory turbinals related to the diverse temperatures and precipitation levels of their habitats. These habitats include diverse ecosystems, spanning pre-montane, montane, and páramo regions across different phytoregions and ecoregions in the Tropical Andes (Tejedor Garavito et al. 2012). The diverse climatic conditions in these habitats, influenced by factors such as Pacific and Atlantic winds, the rain shadow effect (Kattan et al. 2004) and atmospheric circulation patterns (Killeen et al. 2007), create a complex environment. Precipitation, in particular, plays an essential role in determining the structure and nutrient dynamics of Tropical Andes, with variations influenced by

forest structure and topography (Clark et al. 2014; Shrestha et al. 2021). These complex environmental conditions have likely led to unique adaptations in *Thomasomys* species, as reflected in their respiratory turbinal proportions, facilitating survival in a complex mosaic of Andean habitats. Characteristics such as complex scrolling, increased turbinal size at higher elevations and in areas of high precipitation, and variable turbinal proportions correlating with specific temperature and precipitation conditions, likely underscore their evolutionary responses.

The traditionally held view that mammals are more restricted in high-altitude range than birds (Withers et al. 2016a), due to oxygen scarcity associated with lower barometric pressure at higher elevations (Dill et al. 1964; Peacock 1998; Withers et al. 2016a; Spence and Tingley 2020) is challenged by recent evidence. Recent findings of rodents living up to 6739 meters in Atacama suggest that mammals might be more resilient and adaptable to high elevations than previously assumed (Storz et al. 2023). Mammalian adaptations that allow them to thrive in high-elevation, low-oxygen environments are influenced by factors like genetic pre-adaptation, developmental adaptation, and short-term phenotypic acclimation (Monge and Leon-Velarde 1991; Storz et al. 2010b; Li et al. 2021). Large respiratory turbinals, as seen in *Thomasomys*, are essential for efficient oxygen uptake, especially at high elevations. Their surfaces, covered with moist mucous membranes, humidify, warm, and filter incoming air, optimizing oxygen absorption covered by moist mucous membranes that help to humidify, warm, and filter the incoming air (e.g., Van Valkenburgh et al. 2004, 2014; Withers et al. 2016a; b;

Martinez et al. 2023a; Yuk et al. 2023), which is essential for effective gas exchange in these habitats.

Thomasomys, predominantly inhabiting diverse high-elevation forests up to 2000 m (Supplementary Data SD1, Supplementary Data SD2), have unequivocally evolved specific adaptations for these environments as hypothesized here. Their successful colonization and diversification in high-elevation forests during the Pliocene (Parada et al. 2015) clearly highlights their efficient and early adaptation to such ecosystems. This is further evidenced by our findings that *Thomasomys* species inhabiting at higher elevations (i.e., *T. pagaibambensis* at 2946 m, *T. caudivarius* at 3290 m, *T.* aff. *incanus* at 3380 m) exhibit significantly larger and more complexly scrolled turbinals in comparison to their counterparts at lower elevations (i.e., *T. taczanowskii* from Cajamarca at 1500 m) (Fig. 2, Supplementary Data SD6). These morphological features provide increased epithelial surface area and mucous membranes, enhancing respiratory efficiency in thin-air conditions.

Other adaptive factors, such as epithelium thickness, venous system expansion, and specialized aquaporin distributions in turbinals, are hypothesized to play a role in high-elevation habitat adaptation (Gallardo et al. 2008, Smith et al. 2022). However, the link between bony respiratory turbinals and physiological traits like basal metabolic rate or body temperature remains unclear (Martinez et al. 2023b). Future research should focus on exploring cellular-level changes in high-elevation species using histology and diceCT techniques. This approach will make it possible to identify specific alterations associated with the venous system, mucus glands, or ciliated structures.

The interdependence of respiratory and olfactory turbinals

While this study primarily emphasizes the respiratory turbinals of *Thomasomys* as a proxy of heat and moisture conservation, olfactory turbinals provide insights into the potential olfactory capabilities. Notably, we found a positive correlation between the relative surface area of the respiratory and olfactory turbinals (Fig. 4B). The existence of such a correlation between both types of turbinals carries potential biological implications, hinting at possible co-dependence in response to certain environmental or physiological factors. The absence of an evolutionary trade-off between the naso- and maxilloturbinals (Fig. 4A), in line with findings in small mammals (Martinez et al. 2023b), contrasts with the unexpected absence of a trade-off between olfactory and respiratory turbinals (Fig. 4B). Traditionally, an evolutionary trade-off between these turbinals has been observed in several mammal groups (e.g., Van Valkenburg et al. 2011, Green et al. 2012, Martinez et al. 2018, 2020), suggesting that turbinals may not be as developmentally constrained as previously thought, allowing for diverse patterns in response to selective pressures. Our results, potentially influenced by focusing on closely related species from the same genus, indicate that evolutionary trade-offs in turbinal morphology may vary across different taxonomic categories. Such a diverse array of turbinal surface area observed along elevational gradients could be related to the speciation process among *Thomasomys*, likely driven by varying habitats at different elevations.

The significant correlation found between OTSA and PC1 of bioclimatic variables (Supplementary Data SD12), specifically the seven temperature-related

variables (BIO2, BIO3, BIO4, BIO6, BIO7, BIO9, BIO11) and all precipitation-related variables (BIO12-BIO19), can also be explained by considering the ecological and biological significance of olfaction capabilities in mammals. Olfaction is essential for the survival of most mammals, serving functions such as finding food, identifying mates and offspring, avoiding threats, and demarcation of territory (e.g., Buck and Axel 1991; Rosell and Sanda 2006; Niimura 2012; Poddar-Sarkar and Brahmachary 2014; McClanahan and Rosell 2020). Not only allometry explains size and relative size of olfactory turbinals that have also been shown to evolve according to diet, lifestyle, or prey detection (Green et al. 2012; Martinez et al. 2018). Ongoing debates exist about the functional link between the size of olfactory turbinals and correlated olfactory capabilities such as olfactory sensitivity, particularly in carnivores and insectivores (Green et al. 2012, Martinez et al. 2018, 2023a, c). Herbivores, like rabbits, exhibit highly sensitive olfaction despite their diet (Schalken 1976; Schaal et al. 2003). Their unique nose-wiggling behavior aids in detecting chemical molecules and pheromones, crucial for environmental navigation and mating (Melo and González-Mariscal 2010; Kromin and Ignatova 2014). In *Thomasomys* species, which have diverse diets ranging from herbivory to omnivory (López-Arévalo et al. 1993; Pacheco 2015; Sahley et al. 2016), enhanced olfactory capabilities could be critical for locating varied food sources, especially in diverse montane environments from the Andes. Studies based on stomach contents (Noblecilla and Pacheco 2013) and fecal analysis (Sahley et al. 2015, 2016) have found dietary variations, mid-sized species like *T. notatus* and *T. kalinowskii*, as well as the larger *T.* aff. *aureus*, mainly disperse seeds, while smaller species, such as *Thomasomys* sp. 8 (identified as *T. oreas*), exhibit more varied or

insectivorous diets. While the mid-sized species *T. laniger* was found as an opportunistic eater, consuming more insects during the rainy season and a diverse range of seeds when fruits are abundant (López-Arévalo et al. 1993).

Here, we found that the mid-sized species of the Cinereus and Incanus groups, likely seed dispersors, have more turbinal surface than *T. aureus*, a larger species (Fig. 3). The correlation between OTSA and bioclimatic variables (Table 1, Supplementary Data SD12) suggests an adaptive trend to environmental pressures from montane ecosystems where climatic conditions also affect food availability although difficult to test due to lack of ecological data for this genus. Despite this scarcity, discrete observation on the olfactory turbinals of *T. pardignasi* and *T. aureus* of the Aureus group lead Brito et al. (2021) to hypothesize that these species are omnivorous. This hypothesis was based on the fact that these species may have complex olfactory turbinals (found to be related to earthworm consumption; Martinez et al. 2018) and their hypsodont teeth, which could be a response to an herbivorous diet. However, this hypothesis requires more quantitative evidence about the olfactory turbinals across a wide range of sigmodontine species prior to full validation. To determine a more definitive link between olfactory turbinals and diet in *Thomasomys* species, additional research, particularly feces and stomach content analyses, is essential because very little is known about its diet.

Other factors influencing the evolution of turbinals

Our findings reveal that, in general, larger *Thomasomys* species have larger respiratory turbinal surface area relative to their skull size compared to their counterparts (positive allometry, s = 2.22, Fig. 3A). This aligns with previous

studies in murine rodents, as well as on the scale of small non-flying mammals and Carnivora, where the correlation between the respiratory turbinals and skull length shows positive allometry (s = 2.21, 2.49, and 2.27, respectively; Green et al., 2012; Martinez et al., 2018, 2020). Similarly, the correlation between the maxilloturbinal and skull length on the scale of mammals also shows positive allometry (s = 2.60; Martinez et al., 2023b). However, outside this general trend, some large *Thomasomys* species, such as those of the Aureus group, tend to have relatively less respiratory surface area relative to their skull size compared to their counterparts (Fig. 3A). Additionally, Green et al. (2012) found an isometric relationship between the surface area of respiratory turbinals and the volume of the nasal chamber, suggesting that larger caniform species tend to have relatively less respiratory surface area compared to the volume of their nasal chamber. This reduction was likely interpreted as decreased heat retention and water conservation demands, as larger species have a lower surface area to volume ratio, which may reduce heat loss (Green et al., 2012). Overall, this demonstrates that results may vary using different size proxies.

The ethmoturbinals (= olfactory turbinals) hold significant taxonomic relevance. Notable observations by Pacheco (2015), Pacheco and Ruelas (2023), and Brito et al. (2021) highlight distinct variations in olfactory turbinal sizes across different species. Mid-sized species *T. caudivarius*, *T. incanus*, *T. ischyrus*, and *T. kalinowskii* along with the smaller species *T. taczanowskii* exhibit larger olfactory turbinals. In contrast, the large-sized species *T. aureus* and the mid-sized species *T. auricularis, T. cinereus, T. lojapiuranus*, *T. notatus*, and *T. shallqukucha* tend to have olfactory turbinals of moderate size. Meanwhile the mid-sized species *T.*

pagaibambensis, *T. pardignasi*, and *T. pyrrhonotus* stand out with small and poorly developed olfactory turbinals. These observations, primarily based on external examinations, underline the potential of ethmoturbinals as a taxonomic tool. Here, based on quantitative data, we found that small-sized species tend to have smaller olfactory turbinals (e.g., *T. taczanowskii*, *T. daphne*) and the mid- and large-sized species (e.g., *T. pagaibambensis, T. ischyrus*), larger olfactory turbinals. We have also noticed that species groups of *Thomasomys* not only aid in species diagnosis but also appear to influence the distribution of certain features (i.e., in the xy plots, in the boxplots). For instance, species groups like Aureus, Cinereus or Incanus displayed noticeable slight increasing or decreasing trends in some analyses and in the remaining groups no trend was noticed. This observation is significant because even though we did not incorporate a phylogenetic context, it is possible that some of these trends are associated with phylogenetic inertia. Indeed, comparative observation as well as phylogenetic comparative analyses found a significant phylogenetic signal related to turbinal variation (e.g., Green et al. 2012; Martinez et al. 2018, 2020, 2023c). These findings underscore the need for detailed analysis to support the taxonomic and evolutionary significance of olfactory turbinal variations in *Thomasomys* species.

Another influencing factor could be the development of the anterior part of ethmoturbinal I, which in some mammals is covered by respiratory epithelium (Smith et al. 2007; Martinez et al. 2020; Ruf 2020). We observed some variation in this aspect in *Thomasomys* (Fig. 2), but this may not significantly affect the overall pattern due to its relatively small area. Additionally, histological analysis would be

needed to accurately define this area and explore potential variations between species.

Our study included a significant representation of the small-sized and widely distributed species *T. taczanowskii*, ranging from 1500 m to 2950 m in elevation (Appendix 1). Notably, the turbinal surface areas (both respiratory and olfactory) of *T. taczanowskii* showed relative consistency across all elevations, with no apparent pattern in any of the variables analyzed (Figs. 5, 6). Additionally, we observed size and turbinal surface area variations between two adult specimens of the mid-sized *T. notatus*, aged ~3 and 5 (following Pacheco and Ruelas, 2023). Typically, taxonomic studies focus on ages 3 and 4, as older specimens can have flatter and broader skulls, which might affect statistical analyses (pers. obs.). Our observations suggest that in *Thomasomys*, age may significantly influence morphological characteristics, with the younger specimen having smaller turbinals than the older one. Despite being based on only two specimens, these findings align with other studies (Mason et al. 2020; Ito et al. 2022) showing turbinal size and complexity differences between juvenile and adult stages in some species.

We previously propose that turbinals of *Thomasomys* might reflect adaptations to life in high-elevation environments. Considering an Amazonian origin for the Thomasomyini tribe – which includes Tropical Andes specialist genera *Aepeomys*, *Chilomys*, and *Thomasomys*, along with the widely distributed *Rhipidomys* – and their subsequent migration into the Andes (Schenk and Steppan 2018), it seems likely that their ancestral forms possessed smaller or less developed turbinals. The scans provided by Brito et al. (2022: figure 13) reveal that in Andean

rodents such as *Chilomys instans* and *C. georgeledecii* (ranging from 1502 to 2350 m), the turbinals are less scrolled and simpler compared to those in *C. neisi* (ranging from 2500 to 2900 m) and *C. percequilloi* (ranging from 1090 to 3400 m); meanwhile, the turbinals in the lowland species *Rhipidomys leucodactylus* (FMNH 68654) were observed to be less developed and less scrolled than those in *Thomasomys* (pers. obs.). This observation indicates a significant evolutionary adaptation to high-altitude environments, such as montane forests, leading to their successful radiation in these challenging habitats. To substantiate this hypothesis, comprehensive molecular studies involving multiple genetic loci are necessary. Furthermore, examining adaptations in other high-elevation rodents, like the deer mouse *Peromyscus maniculatus* (Snyder 1982; Storz et al. 2007, 2010a), provides valuable comparisons for understanding potential genetic adaptations in *Thomasomys*. This broader view will enhance our understanding of the evolutionary and ecological significance of respiratory turbinals in adapting *Thomasomys* to diverse environmental conditions.

CONCLUSIONS

This study highlights how different correction methods —sizing by SL versus TTSA— significantly influence our interpretation of the relationship between turbinal morphology and environmental factors in *Thomasomys* species within the Tropical Andes. Sizing by SL, we found that elevation significantly impacts turbinal size, hinting at an evolutionary adaptation to varying altitudes. However, no significant correlation was found with bioclimatic variables. Conversely, sizing by TTSA shows a strong correlation with the PC1 of bioclimatic variables, but not with elevation or the PC2, indicating diverse functional distributions of turbinal

areas. These findings underscore the importance of using multiple correction methods to fully understand the complex interplay between ecology and anatomy in biological adaptations.

Our findings also elucidate the complex adaptations of *Thomasomys* species' turbinals to the diverse Tropical Andes environments, highlighting the significant role of morphology and allometry in response to elevation and bioclimatic variables. Larger species exhibit more extensive turbinal areas, suggesting adaptations for high-elevation habitats. The significant correlation between turbinal proportions and environmental factors also emphasizes the ecological adaptability of *Thomasomys* across these habitats. These findings challenge traditional views on mammalian altitude adaptations, underlining the complexity of evolutionary responses in *Thomasomys* and pointing towards a co-evolution of respiratory and olfactory turbinals. Future research should delve deeper into the genetic and physiological mechanisms underlying these patterns, using advanced methodologies such as histology and diceCT, to unravel the complex evolutionary history and ecological success of *Thomasomys* in the Andean landscapes.

ACKNOWLEDGMENTS

We thank Elizabeth Escobar, Diego Marcelo, Maria Peralta, Carlos Jiménez, Edith Salas, Mariela Leo, Jessica Amanzo, Marina Villalobos, and other colleagues for collecting the specimens used here. We thank Anthony Pauca for software support in obtaining bioclim variables and Omar Ruelas for assistance with the "ggplot" package. We also thank Adam Ferguson (Field Museum of Natural History,

Chicago) for lending us some specimens. We thank Renaud Lebrun for their help with the CT facilities. CT data acquisitions were performed using the micro-computed tomography (μCT) facilities of the MRI platform member of the national infrastructure France-BioImaging supported by the French National Research Agency (Grant ANR-10-INBS-04, “Investments for the future”) and those of the Laboratoire d’Excellence Centre Méditerranéen de l’Environnement et de la Biodiversité (LabEx CeMEB, ANR10-LABX-0004). Funding was provided by the Agence Nationale de la Recherche (Défi des autres savoirs, Grants DS10, ANR-17-CE02-0005 RHINOGRAD 2017, PHF), and Prociencia (N° PE501078825, VP). DR was supported by a scholarship of the Franco Peruvian School of Life Sciences. This is a contribution of ISEM 2024-X, Univ Montpellier, CNRS, EPHE, IRD, Montpellier, France.

REFERENCES

Arias-Reyes, C., J. Soliz, and V. Joseph. 2021. Mice and rats display different ventilatory, hematological, and metabolic features of acclimatization to hypoxia. Frontiers in Physiology 12:647822.

Barrios, A. W., G. Núñez, P. Sánchez Quinteiro, and I. Salazar. 2014. Anatomy, histochemistry, and immunohistochemistry of the olfactory subsystems in mice. Frontiers in Neuroanatomy 8.

Bolboacă, S. D., and I. Jäntschi. 2006. Pearson versus Spearman, Kendall’s tau correlation analysis on structure-activity relationships of biologic active compounds. Leonardo Journal of Sciences 5:179–200.

Brandão, M. V., A. R. Percequillo, G. D’Elía, R. Paresque, and A. P. Carmignotto. 2021. A new species of *Akodon* Meyen, 1833 (Rodentia: Cricetidae:

Sigmodontinae) endemic from the Brazilian Cerrado. Journal of Mammalogy 102:101–122.

Brito, J. et al. 2022. Unlocking Andean sigmodontine diversity: five new species of *Chilomys* (Rodentia: Cricetidae) from the montane forests of Ecuador. PeerJ 10:e13211.

Brito, J., S. Vaca-Puente, C. Koch, and N. Tinoco. 2021. Discovery of the first Amazonian *Thomasomys* (Rodentia, Cricetidae, Sigmodontinae): a new species from the remote Cordilleras del Cóndor and Kutukú in Ecuador. Journal of Mammalogy 102:615–635.

Brito M, J., W. R. Teska, and R. Ojala-Barbour. 2012. Descripción del nido de dos especies de *Thomasomys* (Cricetidae) en un bosque alto-andino en Ecuador. Therya 3:263–268.

Buck, L., and R. Axel. 1991. A novel multigene family may encode odorant receptors: a molecular basis for odor recognition. Cell 65:175–187.

Butaric, L. N., and R. P. Klocke. 2018. Nasal variation in relation to high-altitude adaptations among Tibetans and Andeans. American Journal of Human Biology 30:e23104.

Caputa, M. 1979. Temperature gradients in the nasal cavity of the rabbit. Journal of Thermal Biology 4:283–286.

Chou, Y.-M., A. M. Polansky, and R. L. Mason. 1998. Transforming Non-Normal Data to Normality in Statistical Process Control. Journal of Quality Technology 30:133–141.

Clark, K. E. et al. 2014. The hydrological regime of a forested tropical Andean catchment. Hydrology and Earth System Sciences 18:5377–5397.

Cortés, A., M. Rosenmann, and C. Baez. 1990. Función del riñón y del pasaje nasal en la conservación de agua corporal en roedores simpátridos de Chile central. Revista chilena de historia natural:279–291.

Cortés, A., C. Tirado, and M. Rosenmann. 2003. Energy metabolism and thermoregulation in Chinchilla brevicaudata. Journal of Thermal Biology 28:489–495.

Dill, D. B., E. F. Adolph, and C. G. Wilber. 1964. Handbook of Physiology: Adaptation to the Environment. American Physiological Society.

Fick, S. E., and R. J. Hijmans. 2017. WorldClim 2: new 1-km spatial resolution climate surfaces for global land areas. International Journal of Climatology 37:4302–4315.

Ghent, A. W. 1963. Kendall's "Tau" coefficient as an index of similarity in comparisons of plant or animal communities. The Canadian Entomologist 95:568–575.

Green, P. A., B. Van Valkenburgh, B. Pang, D. Bird, T. Rowe, and A. Curtis. 2012. Respiratory and olfactory turbinal size in canid and arctoid carnivorans. Journal of Anatomy 221:609–621.

Harkema, J. R., S. A. Carey, and J. G. Wagner. 2006. The nose revisited: a brief review of the comparative structure, function, and toxicologic pathology of the nasal epithelium. Toxicologic Pathology 34:252–269.

Herbert, R. A., K. S. Janardhan, A. R. Pandiri, M. F. Cesta, and R. A. Miller. 2018. Nose, Larynx, and Trachea. Pp. 391–435 in Boorman's Pathology of the Rat (A. W. Suttie, ed.). 2nd edition. Academic Press, Boston.

Hillenius, W. J. 1992. The evolution of nasal turbinates and mammalian

endothermy. Paleobiology 18:17–29.

Hurtado, N., and G. D'Elía. 2022. Historical biogeography of a rapid and geographically wide diversification in Neotropical mammals. Journal of Biogeography 49:781–793.

Jackson, D. C., and K. Schmidt-Nielsen. 1964. Countercurrent heat exchange in the respiratory passages*. Proceedings of the National Academy of Sciences 51:1192–1197.

Jarantow, S. W., E. D. Pisors, and M. L. Chiu. 2023. Introduction to the Use of Linear and Nonlinear Regression Analysis in Quantitative Biological Assays. Current Protocols 3:e801.

Kassambara, A., and F. Mundt. 2020. factoextra: Extract and Visualize the Results of Multivariate Data Analyses. <https://cran.r-project.org/web/packages/factoextra/index.html> (23 January 2024).

Kattan, G. H., P. Franco, V. Rojas, and G. Morales. 2004. Biological diversification in a complex region: a spatial analysis of faunistic diversity and biogeography of the Andes of Colombia. Journal of Biogeography 31:1829–1839.

Killeen, T. J., M. Douglas, T. Consiglio, P. M. Jørgensen, and J. Mejia. 2007. Dry spots and wet spots in the Andean hotspot. Journal of Biogeography 34:1357–1373.

Kilmer, J. T., and R. L. Rodríguez. 2017. Ordinary least squares regression is indicated for studies of allometry. Journal of Evolutionary Biology 30:4–12.

Kromin, A. A., and Yu. P. Ignatova. 2014. Objective Method for Registration of the Sniffing Component of the Search Behavior in Rabbits Subjected to Food Deprivation. Bulletin of Experimental Biology and Medicine 156:522–525.

Lê, S., J. Josse, and F. Husson. 2008. FactoMineR: An R package for multivariate analysis. Journal of Statistical Software 25:1–18.

Leo L, M., and A. L. Gardner. 1993. A new species of a giant *Thomasomys* (Mammalia: Muridae: Sigmodontinae) from the Andes of northcentral Peru. Proceedings of the Biological Society of Washington 106:417–428.

Li, M. et al. 2021. The hypoxia adaptation of small mammals to plateau and underground burrow conditions. Animal Models and Experimental Medicine 4:319–328.

López-Arévalo, H., O. Montenegro, and A. Cadena. 1993. Ecología de los pequeños mamíferos de la reserva biológica carpanta, en la cordillera oriental Colombiana. Studies on Neotropical Fauna and Environment 28:193–210.

Lui, M. A. et al. 2015. High-altitude ancestry and hypoxia acclimation have distinct effects on exercise capacity and muscle phenotype in deer mice. American Journal of Physiology - Regulatory, Integrative and Comparative Physiology 308:R779–R791.

Luna, F., H. Naya, and D. E. Naya. 2017. Understanding evolutionary variation in basal metabolic rate: An analysis in subterranean rodents. Comparative Biochemistry and Physiology Part A: Molecular & Integrative Physiology 206:87–94.

Martinez, Q. et al. 2018. Convergent evolution of an extreme dietary specialisation, the olfactory system of worm-eating rodents. Scientific Reports 8:17806.

Martinez, Q. et al. 2020. Convergent evolution of olfactory and thermoregulatory capacities in small amphibious mammals. Proceedings of the National Academy of Sciences 117:8958–8965.

Martinez, Q. et al. 2023a. Turbinal bones are still one of the last frontiers of the tetrapod skull: hypotheses, challenges and perspectives. PaleorXiv. <https://paleorxiv.org/2gm95/> (22 August 2023).

Martinez, Q. et al. 2023b. Mammalian maxilloturbinal evolution does not reflect thermal biology. Nature Communications 14:4425.

Martinez, Q., M. Courcelle, E. Douzery, and P.-H. Fabre. 2023c. When morphology does not fit the genomes: the case of rodent olfaction. Biology Letters 19:20230080.

McClanahan, K., and F. Rosell. 2020. Conspecific recognition of pedal scent in domestic dogs. Scientific Reports 10:17837.

Melo, A. I., and G. González-Mariscal. 2010. Communication by olfactory signals in rabbits: its role in reproduction. Vitamins and Hormones 83:351–371.

Min, S. H., and J. Zhou. 2021. smplot: An R package for easy and elegant data visualization. Frontiers in Genetics 12:1–10.

Mitchell, D. R., E. Sherratt, and V. Weisbecker. 2023. Facing the facts: Adaptive trade-offs along body size ranges determine mammalian craniofacial scaling. Biological Reviews:1–29.

Monge, C., and F. Leon-Velarde. 1991. Physiological adaptation to high altitude: oxygen transport in mammals and birds. Physiological Reviews 71:1135–1172.

Moulton, D. G. 1967. Olfaction in mammals. American Zoologist 7:421–429.

Niimura, Y. 2012. Olfactory receptor multigene family in vertebrates: from the viewpoint of evolutionary genomics. Current Genomics 13:103–114.

Noblecilla, M. C., and V. Pacheco. 2013. Dieta de roedores sigmodontinos (Cricetidae) en los bosques montanos tropicales de Huánuco, Perú. Revista

Peruana de Biología 19:317–322.

Pacheco, V. 2003. Phylogenetic analyses of the Thomasomyini (Muroidea: Sigmodontinae) based on morphological data. Ph.D. dissertation, The City University of New York, New York.

Pacheco, V. 2015. Genus *Thomasomys* Coues, 1884. Pp. 617–682 in Mammals of South America. Volume 2, Rodents (J. L. Patton, U. F. J. Pardiñas & G. D'Elia, eds.). The University of Chicago Press, Chicago.

Pacheco, V., J. L. Patton, and G. D'Elía. 2015. Tribe Thomasomyini Steadman and Ray, 1982. Pp. 571–574 in Mammals of South America. Volume 2, Rodents (J. L. Patton, U. F. J. Pardiñas & G. D'Elía, eds.). The University of Chicago Press, Chicago.

Pacheco, V., and D. Ruelas. 2023. Systematic revision of *Thomasomys cinereus* (Rodentia: Cricetidae: Sigmodontinae) from northern Peru and southern Ecuador, with descriptions of three new species. Bulletin of the American Museum of Natural History 461:1–71.

Pang, B. et al. 2016. The influence of nasal airflow on respiratory and olfactory epithelial distribution in felids. The Journal of Experimental Biology 219:1866–1874.

Pardiñas, U. F. J. et al. 2015. Genus *Akodon* Meyen, 1833. Pp. 144–204 in Mammals of South America. Volume 2, Rodents (J. L. Patton, U. F. J. Pardiñas & G. D'Elía, eds.). The University of Chicago Press, Chicago.

Parsons, T. S. 1967. Evolution of the nasal structure in the lower tetrapods. American Zoologist 7:397–413.

Patterson, B. D., S. Solari, and P. M. Velazco. 2012. The role of the Andes in the

diversification and biogeography of Neotropical mammals. Pp. 351–378 in Bones, Clones, and Biomes (B. D. Patterson & L. P. Costa, eds.). The University of Chicago Press, Chicago.

Peacock, A. J. 1998. Oxygen at high altitude. BMJ : British Medical Journal 317:1063–1066.

Poddar-Sarkar, M., and R. L. Brahmachary. 2014. Pheromones of Tiger and Other Big Cats. Neurobiology of Chemical Communication (C. Mucignat-Caretta, ed.). CRC Press/Taylor & Francis, Boca Raton (FL).

Porto, A., L. T. Shirai, F. B. de Oliveira, and G. Marroig. 2013. Size variation, growth strategies, and the evolution of modularity in the mammalian skull. Evolution 67:3305–3322.

R Core Team. 2022. R: A language and environment for statistical computing. R, R Foundation for Statistical Computing, Vienna, Austria. <URL https://www.R-project.org/>.

Rezende, E. L., F. R. Gomes, C. K. Ghalambor, G. A. Russell, and M. A. Chapelli. 2005. An evolutionary frame of work to study physiological adaptation to high altitudes. Revista chilena de historia natural 78:323–336.

Rosell, F., and J. Sanda. 2006. Potential risks of olfactory signaling: the effect of predators on scent marking by beavers. Behavioral Ecology 17:897–904.

RStudio Team. 2023. RStudio: Integrated Development Environment for R. R, R Core Team, RStudio, PBC, Boston, MA. <www.rstudio.com/>.

Ruelas, D., V. Pacheco, J. Pérez, J. Diaz-Nieto, and P.-H. Fabre. 2024 Unilocus delimitation methods reveal the underestimated species diversity of *Thomasomys* (Rodentia, Cricetidae). Zoologica Scripta.

Ruf, I. 2020. Ontogenetic transformations of the ethmoidal region in Muroidea (Rodentia, Mammalia): new insights from perinatal stages. Vertebrate Zoology 70:383–415.

Sahley, C. T., K. Cervantes, V. Pacheco, E. Salas, D. Paredes, and A. Alonso. 2015. Diet of a sigmodontine rodent assemblage in a Peruvian montane forest. Journal of Mammalogy 96:1071–1080.

Sahley, C. T., K. Cervantes, E. Salas, D. Paredes, V. Pacheco, and A. Alonso. 2016. Primary seed dispersal by a sigmodontine rodent assemblage in a Peruvian montane forest. Journal of Tropical Ecology 32:125–134.

Santos-Fernandez, E. 2014. Johnson: Johnson Transformation. R, . <https://rdrr.io/cran/Johnson/> (22 January 2024).

Schaal, B., G. Coureaud, D. Langlois, C. Giniès, E. Sémon, and G. Perrier. 2003. Chemical and behavioural characterization of the rabbit mammary pheromone. Nature 424:68–72.

Schalken, A. P. M. 1976. Three types of pheromones in the domestic rabbit, *Oryctolagus cuniculus* (L). Chemical Senses 2:139–155.

Schenk, J. J., and S. J. Steppan. 2018. The role of geography in adaptive radiation. The American Naturalist 192:415–431.

Schippers, M.-P., O. Ramirez, M. Arana, P. Pinedo-Bernal, and G. B. McClelland. 2012. Increase in Carbohydrate Utilization in High-Altitude Andean Mice. Current Biology 22:2350–2354.

Schmidt-Nielsen, K., F. R. Hainsworth, and D. E. Murrish. 1970. Counter-current heat exchange in the respiratory passages: Effect on water and heat balance. Respiration Physiology 9:263–276.

Schmidt-Nielsen, K., and D. C. Jackson. 1964. Countercurrent heat exchange in the respiratory passages. Science (New York, N.Y.) 144:567.

Shrestha, D. et al. 2021. Detection of Spatial Rainfall Variation over the Andean Region Demonstrated by Satellite-Based Observations. Atmosphere 12:1204.

Smith, T. D. et al. 2007. Scaling of the first ethmoturbinal in nocturnal strepsirrhines: Olfactory and respiratory surfaces. The Anatomical Record 290:215–237.

Smith, T. D., and K. P. Bhatnagar. 2004. Microsmatic primates: Reconsidering how and when size matters. The Anatomical Record Part B: The New Anatomist 279B:24–31.

Smith, T. D., and C. J. Bonar. 2022. The nasal cavity in agoutis (*Dasyprocta* spp.): a micro-computed tomographic and histological study. Vertebrate Zoology 72:95–113.

Smith, T. D., A. Curtis, K. P. Bhatnagar, and S. E. Santana. 2021. Fissures, folds, and scrolls: The ontogenetic basis for complexity of the nasal cavity in a fruit bat (*Rousettus leschenaultii*). The Anatomical Record 304:883–900.

Smith, T. D., T. P. Eiting, and K. P. Bhatnagar. 2012. A quantitative study of olfactory, non-olfactory, and vomeronasal epithelia in the nasal fossa of the bat *Megaderma lyra*. Journal of Mammalian Evolution 19:27–41.

Smith, T. D., and J. B. Rossie. 2008. Nasal fossa of mouse and dwarf lemurs (Primates, Cheirogaleidae). The Anatomical Record: Advances in Integrative Anatomy and Evolutionary Biology 291:895–915.

Snyder, L. R. G. 1982. 2,3-diphosphoglycerate in high- and low-altitude populations of the deer mouse. Respiration Physiology 48:107–123.

Souquet, L. et al. 2019. Back to the wild: does feralization affect the mandible of non-commensal house mice (Mus musculus domesticus)? Biological Journal of the Linnean Society 126:471–486.

Spence, A. R., and M. W. Tingley. 2020. The challenge of novel abiotic conditions for species undergoing climate-induced range shifts. Ecography 43:1571–1590.

Storz, J. F. et al. 2007. The molecular basis of high-altitude adaptation in deer mice. PLoS Genetics 3:e45.

Storz, J. F. et al. 2023. Extreme high-elevation mammal surveys reveal unexpectedly high upper range limits of Andean mice. bioRxiv. <https://www.biorxiv.org/content/10.1101/2023.08.22.554215v1> (8 January 2024).

Storz, J. F., A. M. Runck, H. Moriyama, R. E. Weber, and A. Fago. 2010a. Genetic differences in hemoglobin function between highland and lowland deer mice. The Journal of Experimental Biology 213:2565–2574.

Storz, J. F., G. R. Scott, and Z. A. Cheviron. 2010b. Phenotypic plasticity and genetic adaptation to high-altitude hypoxia in vertebrates. The Journal of Experimental Biology 213:4125–4136.

Tejedor Garavito, N. et al. 2012. Evaluación del estado de conservación de los bosques montanos en los Andes tropicales: Ecosistemas 21:148–166.

Tufts, D. M., I. G. Revsbech, Z. A. Cheviron, R. E. Weber, A. Fago, and J. F. Storz. 2013. Phenotypic plasticity in blood–oxygen transport in highland and lowland deer mice. The Journal of Experimental Biology 216:1167–1173.

Vallejos-Garrido, P. et al. 2023. The importance of the Andes in the evolutionary radiation of Sigmodontinae (Rodentia, Cricetidae), the most diverse group of

mammals in the Neotropics. Scientific Reports 13:2207.

Van Valkenburgh, B. et al. 2011. Aquatic adaptations in the nose of carnivorans: evidence from the turbinates: Aquatic adaptations in the nose of carnivorans. Journal of Anatomy 218:298–310.

Van Valkenburgh, B. et al. 2014. Respiratory and olfactory turbinals in feliform and caniform carnivorans: the influence of snout length. The Anatomical Record 297:2065–2079.

Van Valkenburgh, B. V., J. Theodor, A. Friscia, A. Pollack, and T. Rowe. 2004. Respiratory turbinates of canids and felids: a quantitative comparison. Journal of Zoology 264:281–293.

Voss, R. S. 1988. Systematics and ecology of ichthyomyine rodents (Muroidea): patterns of morphological evolution in a small adaptive radiation. Bulletin of the American Museum of Natural History 188:259–493.

Voss, R. S. 2003. A new species of *Thomasomys* (Rodentia: Muridae) from eastern Ecuador, with remarks on mammalian diversity and biogeography in the Cordillera Oriental. American Museum Novitates 3421:1–47.

Wagner, F., and I. Ruf. 2019. Who nose the borzoi? Turbinal skeleton in a dolichocephalic dog breed (*Canis lupus familiaris*). Mammalian Biology 94:106–119.

Warton, D. I., I. J. Wright, D. S. Falster, and M. Westoby. 2006. Bivariate line-fitting methods for allometry. Biological Reviews 81:259–291.

Weaver, L. N., and D. M. Grossnickle. 2020. Functional diversity of small-mammal postcrania is linked to both substrate preference and body size. Current Zoology 66:539–553.

Weksler, M., and C. R. Bonvicino. 2015. Genus *Oligoryzomys* Bangs, 1900. Pp. 417–436 in Mammals of South America. Volume 2, Rodents (J. L. Patton, U. F. J. Pardiñas & G. D'Elía, eds.). The University of Chicago Press, Chicago.

Wickham, H. 2020. reshape2: Flexibly Reshape Data: A Reboot of the Reshape Package. <https://cran.r-project.org/web/packages/reshape2/index.html> (23 January 2024).

Wickham, H. et al. 2023. ggplot2: Create elegant data visualisations using the grammar of graphics. <https://cran.r-project.org/web/packages/ggplot2/index.html> (16 October 2023).

Wickham, H., J. Hester, W. Chang, J. Bryan, and RStudio. 2022. devtools: Tools to Make Developing R Packages Easier. <https://cran.r-project.org/web/packages/devtools/index.html> (16 January 2024).

Withers, P., C. E. Cooper, S. K. Maloney, F. Bozinovic, and A. P. Cruz-Neto. 2016a. Physiological adaptations to extreme environments. Pp. 290–392 in Ecological and environmental physiology of mammals (P. Withers, C. E. Cooper, S. K. Maloney, F. Bozinovic & A. P. Cruz-Neto, eds.). Oxford Academic, Oxford, UK.

Withers, P., C. E. Cooper, S. K. Maloney, F. Bozinovic, and A. P. Cruz-Neto. 2016b. Physiological characteristics of mammals. Pp. 146–289 in Ecological and environmental physiology of mammals (P. Withers, C. E. Cooper, S. K. Maloney, F. Bozinovic & A. P. Cruz-Neto, eds.). Oxford Academic, Oxford, UK.

Xi, J. et al. 2016. Anatomical Details of the Rabbit Nasal Passages and Their Implications in Breathing, Air Conditioning, and Olfaction. Anatomical record

(Hoboken, N.J. : 2007) 299:853–868.

Xi, J., X. A. Si, and M. Malvè. 2023. Nasal anatomy and sniffing in respiration and olfaction of wild and domestic animals. Frontiers in Veterinary Science 10:1172140.

Yee, K. K., B. A. Craven, C. J. Wysocki, and B. Van Valkenburgh. 2016. Comparative morphology and histology of the nasal fossa in four mammals: gray squirrel, bobcat, coyote, and white-tailed deer. Anatomical Record (Hoboken, N.J.: 2007) 299:840–852.

Young, K. R., and B. León. 1999. Peru's humid Eastern montane forests: an overview of their physical settings, biological diversity, human use and settlement, and conservation needs. Centre for Research on Cultural and Biological Diversity of Andean Rainforests (DIVA), Denmark.

Yuk, J., M. M. H. Akash, A. Chakraborty, S. Basu, L. P. Chamorro, and S. Jung. 2023. Morphology of pig nasal structure and modulation of airflow and basic thermal conditioning. Integrative and Comparative Biology 63:304–314.

APPENDIX

Appendix 1. List of collection localities and specimens of *Thomasomys* analyzed in this study. Abbreviations: MUSM – Museo de Historia Natural de la Universidad Nacional Mayor de San Marcos (Lima), FMNH – Field Museum of Natural History (Chicago), and MEPN – Museo de Historia Natural "Gustavo Orcés V." de la Escuela Politécnica Nacional (Quito). Sex: f – female, m – male.

Thomasomys antoniobracki (n= 2): PERU: Piura, Huancabamba, El Carmen de la Frontera, Minera Majaz, Campamento Alto Parramata, -4.894 -79.368, 2630 m (2m: MUSM 23754, 23755).

Thomasomys aureus (n= 1): ECUADOR: Bolivar, Cruz de Lizo, Tatahuazo river, -1.72 -79, 2600 m (1f: MEPN 6144).

Thomasomys* aff. *aureus (n= 2): PERU: Junín, Tarma, Huasahuasi, San Pedro de Churco, -11.030 -75.543, 3217 m (2m: MUSM 52859, 52860).

Thomasomys* aff. *caudivarius (n= 3): PERU: Cajamarca, San Ignacio, Tabaconas, Piedra Cueva in Cerro Coyona (Tabaconas-Namballe National Sanctuary), -5.268 -79.270, 3290 m (1m: MUSM 46711). Piura, Huancabamba, El Carmen de la Frontera, Minera Majaz, Campamento Alto Parramata, -4.90 -79.37, 2762 m (2f: MUSM 23562, 23750).

Thomasomys daphne (n= 3): PERU: Cusco, Paucartambo, Kosñipata, La Esperanza, -13.178 -71.605, 2880 m (2f: MUSM 20014, 20017; 1m FMNH 175229).

Thomasomys* cf. *dispar (n= 2): COLOMBIA: Huila, San Agustin, San Antonio, 1.948 -76.500, 2200 m (1f: FMNH 72397, 1?: FMNH 72400)

Thomasomys incanus (n= 2): PERU: Pasco, Oxapampa, Oxapampa, San Alberto, -10.531 -75.350, 2788 m (1m: MUSM 46187). Junín, Tarma, Huasahuasi, San Pedro de Churco, -11.030 -75.552, 3309 m (1m: MUSM 52873).

Thomasomys* aff. *incanus (n= 2): PERU: San Martín, Mariscal Cáceres, Huicungo, P.N. Río Abiseo, La Playa, -7.645 -77.48, 2650 m (2m: MUSM 7985, 8002).

Thomasomys ischyrus (n= 3): PERU: Huánuco, Huánuco, Chinchao, Caserio San Pedro de Carpish, -9.72418 -76.0994, 2757 m (1f: MUSM 18346; 1m: MUSM 18347); Huánuco, Pachitea, Chaglla, Palmapampa, -9.88667 -75.88944, 2900 m (1h: MUSM 17848).

Thomasomys kalinowskii (n= 2): PERU: Huánuco, Huánuco, Chinchao, Caserio San Pedro de Carpish, -9.724 -76.099, 2757 m (1m: 18374; 1f: MUSM 18381).

Thomasomys* aff. *kalinowskii (n= 1): PERU: Pasco, Oxapampa, Oxapampa, San Alberto, 7Km al este de Oxapampa, limite este del P. N. Yanachaga Chemillen, -10.55 -75.4, 2200 m (1m: MUSM 14993).

Thomasomys notatus (n= 2): PERU: Cusco, Paucartambo, Kosñipata, Suecia, km 138.5 Carretera Shintuya, -13.100 -71.567, 1900 m (1f: MUSM 17021), -13.101 -71.569, 1920 m (1f: FMNH 170690).

Thomasomys pagaibambensis (n= 1): PERU: Cajamarca, Chota, Querocoto, Agua de la Montaña, -6.371 -79.153, 2946 (1m: MUSM 39737).

Thomasomys* cf. *pyrrhonotus (n= 2): PERU: Piura, Huancabamba, El Carmen de la Frontera, Habas Pite, -5.091 -79.344, 2117 m (1m: MUSM 55555); Piura, Huancabamba, El Carmen de la Frontera, Machete, -5.096 -79.347, 2169 m (1m: MUSM 55553).

Thomasomys taczanowskii (n= 10): PERU: Cajamarca, San Miguel, La Florida, San Miguel, La Florida, Agua Azul, -6.885 -79.075, 1500 m (2f: MUSM 15066, 15067); Cajamarca, Chota, Querocoto, Peña Brava, -6.354 -79.140, 2265 m (1f: MUSM 39741); Cajamarca, Chota, Querocoto, Agua de la Montaña, -6.371 -79.153, 2933 m (2m: MUSM 39735, 39738). Lambayeque, Ferreñafe, Uyurpampa, -6.220 -79.362, 2827 m (1f: MUSM 21802). Piura, Huancabamba, El Carmen de la Frontera, Habas Pite, -5.091 -79.344, 2117 m (3m: MUSM 55562, 55567, 55558); Piura, Huancabamba, El Carmen de la Frontera, Machete, -5.096 -79.346, 2169 m (1m: MUSM 55583).

***Thomasomys* sp. 1 (sensu Pacheco, 2003)** (n= 3): PERU: Cusco, Paucartambo, Kosñipata, Morro Leguia, carretera Paucartambo-Pillcopata, km 135, -13.197 -71.5767, 2250 m (1m: MUSM 9349); Cusco, Paucartambo, Kosñipata, Pillahuata, -13.162 -71.620, 2460 m (1m: MUSM 19581); Cusco, Quispicanchi, Marcapata, Amacho, -13.575 -70.926, 2750 m (1m: FMNH 75588).

***Thomasomys* sp. 6 (sensu Pacheco, 2003)** (n= 1): PERU: Pasco, Oxapampa, Huancabamba, Santa Bárbara -10.339 -75.642, 3368 (1f: MUSM 46249).

***Thomasomys* sp. 9 (sensu Pacheco, 2003)** (n= 1): PERU: Cusco, Paucartambo, Kosñipata, La Esperanza, -13.178 -71.605, 2880 m (1m: MUSM 20023).

***Thomasomys* sp. 10 (sensu Pacheco, 2003)** (n= 2): PERU: Piura, Huancabamba, El Carmen de la Frontera, Minera Majaz, Campamento Alto Parramata, -4.894 -79.368, 2630 m (1f: MUSM 23763); Piura, Huancabamba, El Carmen de la Frontera, Minera Majaz, Campamento Alto Parramata, -4.901 -79.372, 2780 m (1m: MUSM 23764).

FIGURES

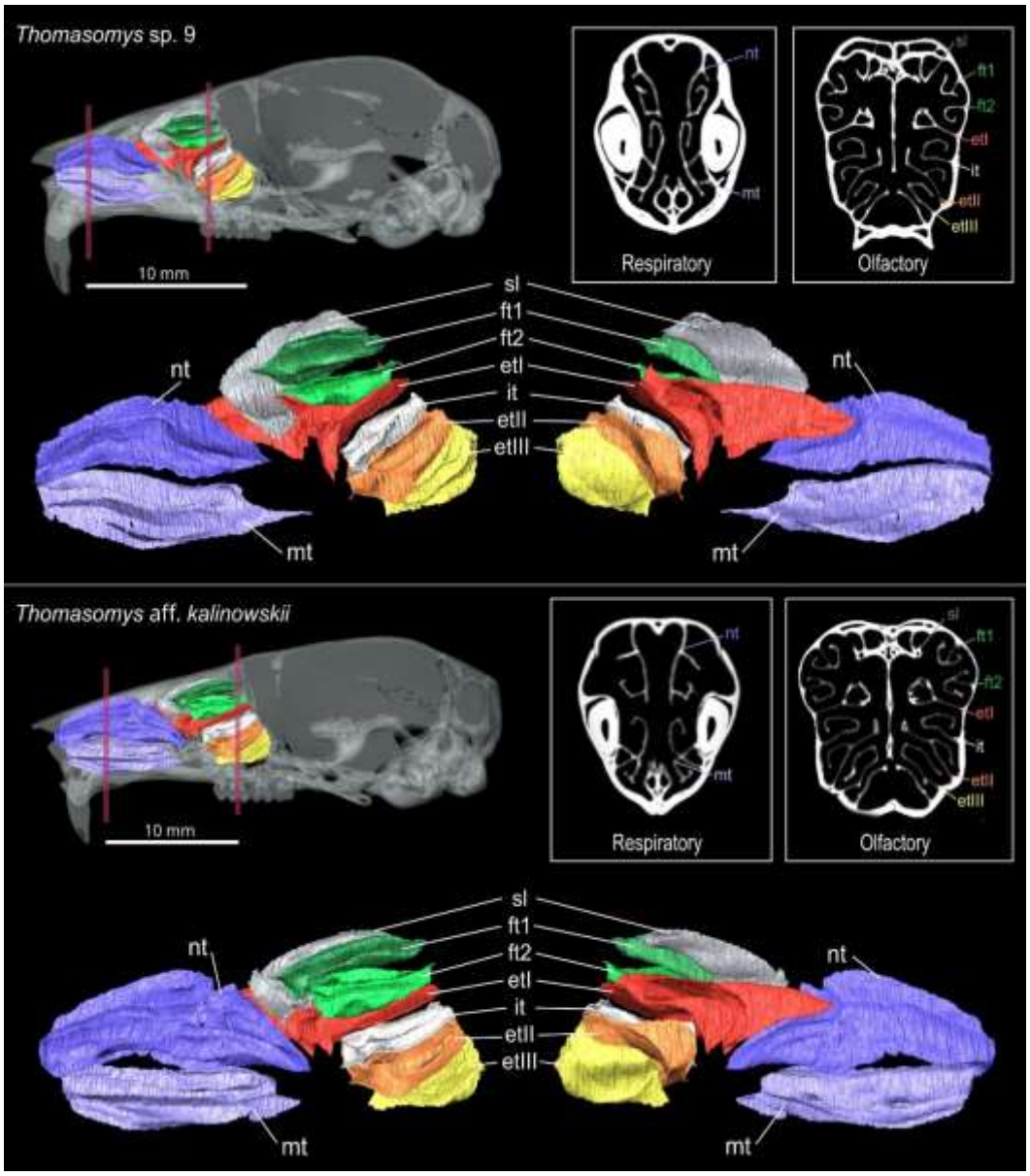

Figure 1.— Sagittal plane of the skull and coronal cross-section and 3D representations of turbinal bones of *Thomasomys* sp. 9 and *T.* aff. *kalinowskii*. Abbreviations: nt – nasoturbinal, mt – maxilloturbinal, sl – semicircular lamina, ft1 – frontoturbinal 1, ft2 – frontoturbinal 2, it – interturbinal, etI – ethmoturbinal I, etII – ethmoturbinal II, etIII – ethmoturbinal III.

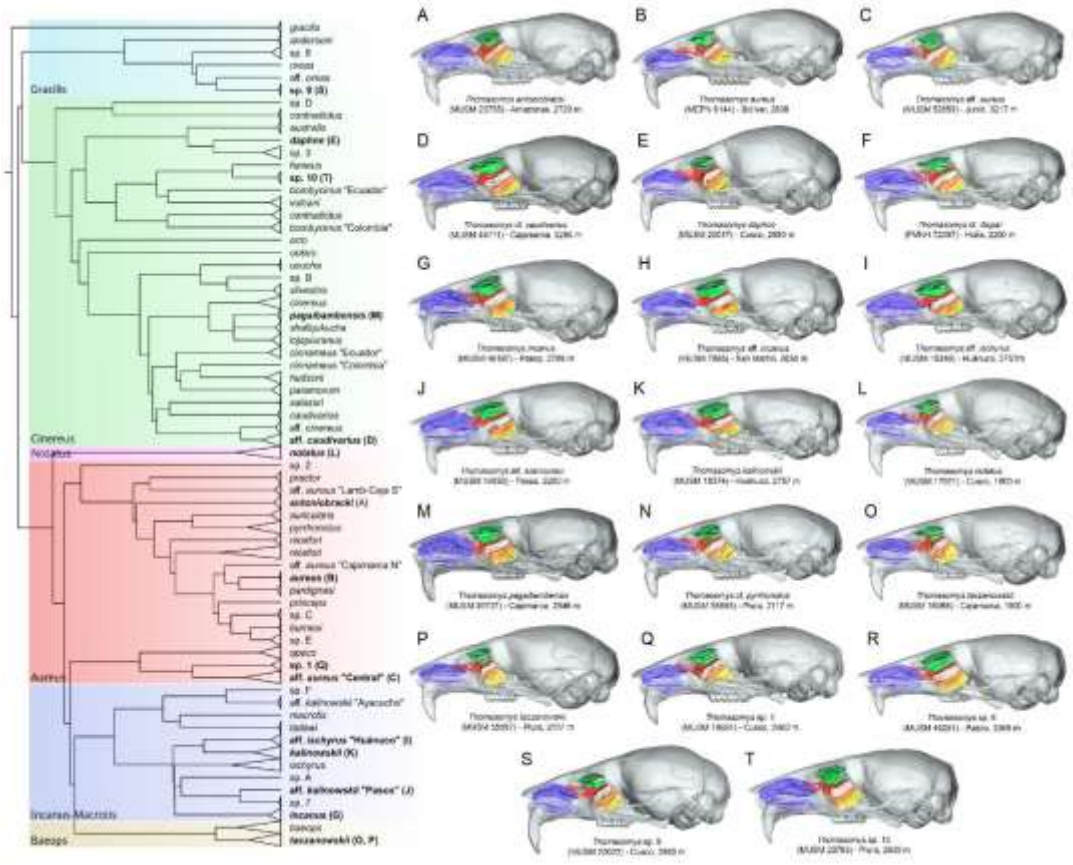

Figure 2.— Phylogeny and morphological diversity of the turbinal bones of the *Thomasomys* species. The phylogenetic tree is derived from Ruelas et al. (2024) and associated with 3D representations of turbinal bones and coronal cross-section along the *Thomasomys* species used in this study (A-T).

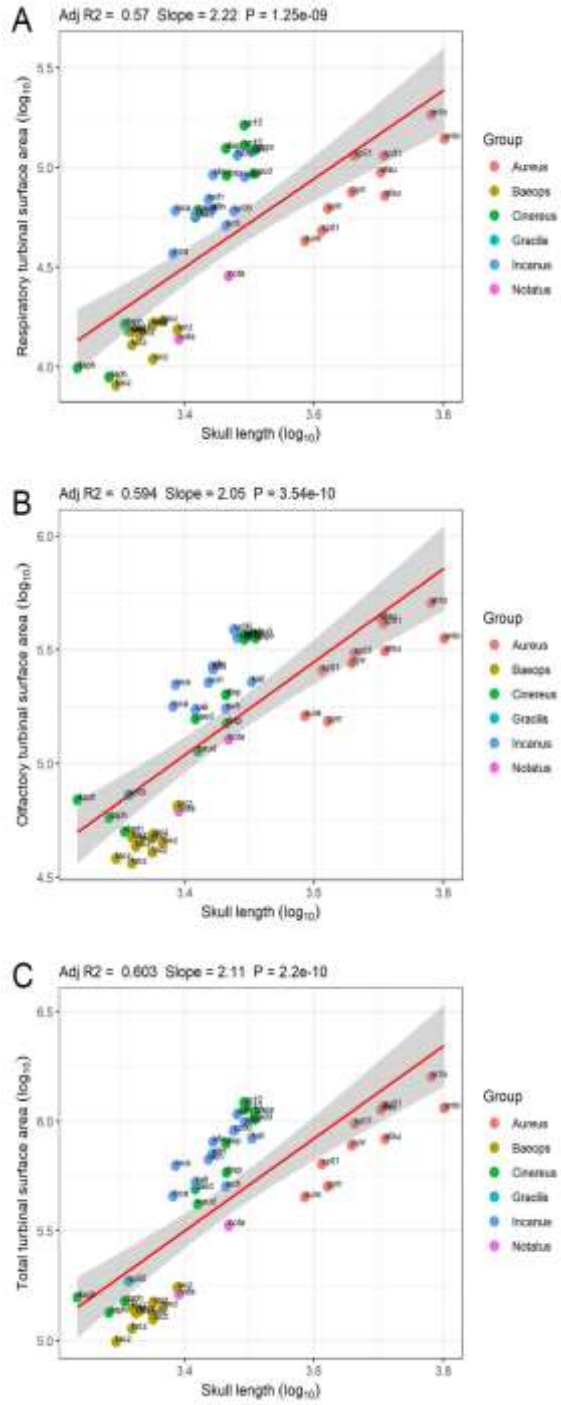

Figure 3.— Log-transformed linear regression plot of (A) respiratory turbinal surface area against skull length, (B) olfactory turbinal surface area against skull length, and (C) total turbinal surface area against skull length. Colors represent the species groups sensu Pacheco (2015). Abbreviations for species are shown in Supplementary Data SD3.

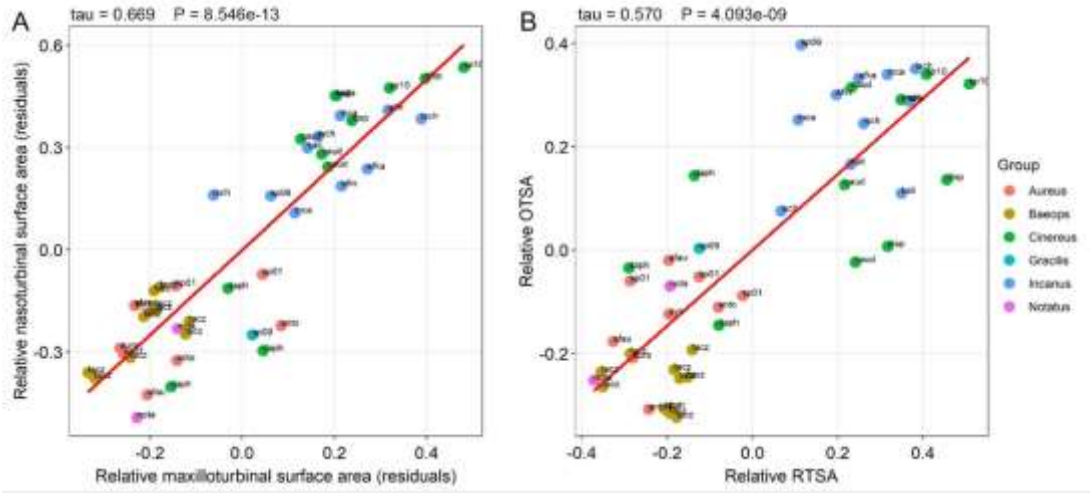

Figure 4.— Plot of Kendall's tau correlation between (A) residuals of nasoturbinal and maxilloturbinal surface areas and (B) residuals of olfactory (OTSA) and respiratory (RTSA) turbinal surface areas of *Thomasomys*. Colors represent the species groups sensu Pacheco (2015). Abbreviations for species are shown in Supplementary Data SD3.

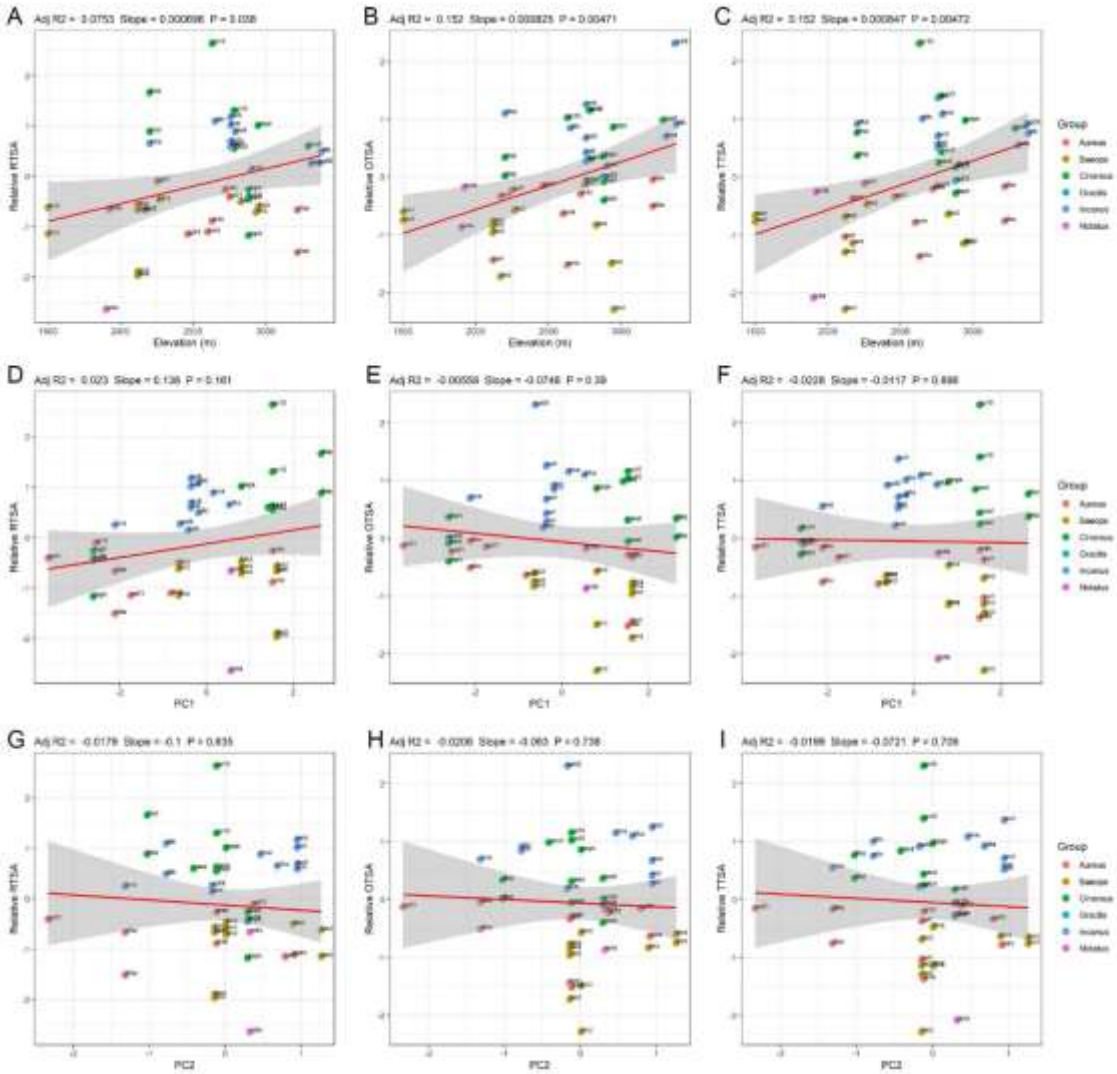

Figure 5.— Log regressions (red line) of (A) relative respiratory turbinal surface area (RTSA) against elevation, (B) relative olfactory turbinal surface area (OTSA) against elevation, (C) relative total turbinal surface area (TTSA) against elevation, (D) relative RTSA against PC1, (E) relative OTSA against PC1, (F) relative TTSA against PC1, (G) relative RTSA against PC2, (H) relative OTSA against PC2, (I) relative TTSA against PC2. Colors represent the species groups sensu Pacheco (2015). Abbreviations for species are shown in Supplementary Data SD3.

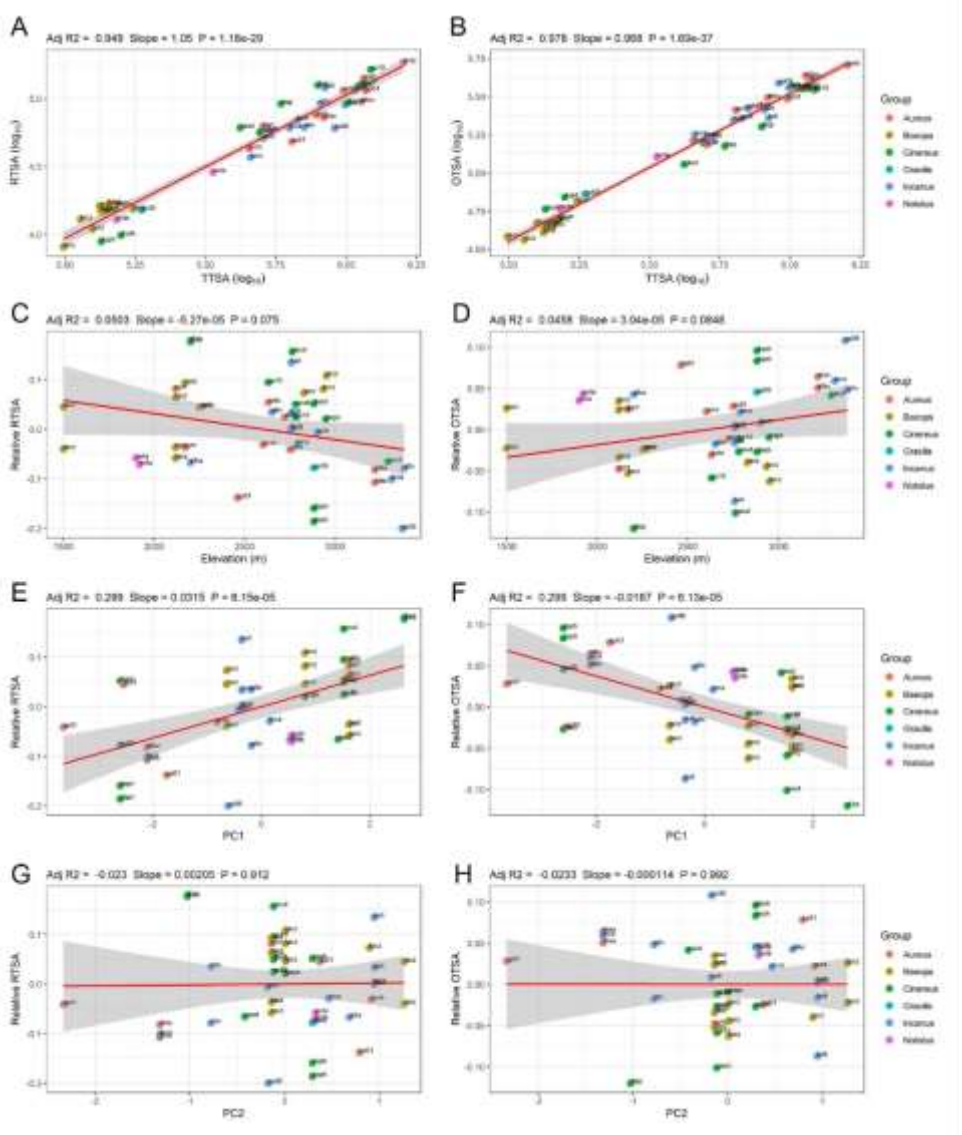

Figure 6.— Analyses using turbinal surface areas corrected by TTSA. Log-log regressions (red line) of (A) respiratory turbinal surface area (RTSA) against total turbinal surface area (TTSA), (B) olfactory turbinal surface area (RTSA) against total turbinal surface area (TTSA). Regressions using the correction by total turbinal surface area: (C) relative RTSA against elevation, (D) relative OTSA against elevation, (E) relative RTSA against PC1, (F) relative OTSA against PC1, (G) relative RTSA against PC2, (H) relative OTSA against PC2. Colors represent the species groups sensu Pacheco (2015). Abbreviations for species are shown in Supplementary Data SD3.

TABLE 1

Linear regression of turbinal surface areas sized by skull length and TTSA against 19 bioclimatic variables. Significant P-values are shown in bold. Abbreviations are explained in Methods.

BioClim variables	Skull length sized									TTSA sized					
	relative RTSA			relative OTSA			relative TTSA			relative RTSA			relative OTSA		
	R^2	slope	P	R^2	slope	P	R^2	slope	P	R^2	slope	P	R^2	slope	P
BIO01	-0.023	0.0055	0.947	-0.004	-0.0617	0.371	-0.013	-0.0474	0.505	0.074	0.0137	**0.039**	0.064	-0.0077	0.052
BIO02	0.017	-0.1680	0.191	-0.007	0.0094	0.414	-0.023	0.0040	0.973	0.238	-0.0375	**0.000**	0.247	0.0227	**0.000**
BIO03	0.020	0.0382	0.175	0.025	-0.0358	0.152	-0.021	-0.0082	0.753	0.384	0.0103	**0.000**	0.375	-0.0060	**0.000**
BIO04	0.046	-0.0080	0.085	-0.016	0.0023	0.591	-0.021	-0.0013	0.759	0.260	-0.0014	**0.000**	0.245	0.0008	**0.000**
BIO05	-0.017	-0.0403	0.607	-0.011	-0.0495	0.477	-0.009	-0.0553	0.439	-0.007	0.0056	0.411	-0.012	-0.0028	0.491
BIO06	-0.011	0.0374	0.469	0.017	-0.0597	0.190	-0.014	-0.0292	0.536	0.261	0.0156	**0.000**	0.245	-0.0090	**0.000**
BIO07	0.022	-0.0894	0.167	0.003	0.0604	0.296	-0.023	0.0075	0.900	0.307	-0.0212	**0.000**	0.306	0.0126	**0.000**
BIO08	-0.020	-0.0287	0.724	0.009	-0.0840	2.410	0.000	-0.0730	0.323	0.049	0.0123	0.079	0.039	-0.0068	0.101
BIO09	-0.019	0.0292	0.674	-0.002	-0.0586	0.341	-0.016	-0.0346	0.585	0.136	0.0157	**0.007**	0.123	-0.0089	**0.011**
BIO10	-0.023	-0.0105	0.896	-0.009	-0.0541	0.448	-0.013	-0.0488	0.505	0.035	0.0109	0.116	0.028	-0.0061	0.141

BIO11	-0.019	0.0299	0.667	-0.003	-0.0572	0.353	-0.016	-0.0340	0.592	0.136	0.0157	**0.007**	0.122	-0.0089	**0.011**
BIO12	0.068	0.0009	**0.046**	-0.023	0.0000	0.906	-0.013	0.0003	0.519	0.217	0.0001	**0.001**	0.231	-0.0001	**0.000**
BIO13	0.017	0.0044	0.194	-0.015	-0.0018	0.551	-0.023	0.0002	0.950	0.177	0.0009	**0.002**	0.166	-0.0005	**0.003**
BIO14	0.032	0.0106	0.124	-0.011	-0.0045	0.470	-0.023	0.0002	0.978	0.283	0.0022	**0.000**	0.317	-0.0014	**0.000**
BIO15	0.016	-0.0173	0.200	-0.018	0.0055	0.651	-0.023	-0.0004	0.975	0.171	-0.0034	**0.003**	0.198	0.0022	**0.001**
BIO16	0.028	0.0019	0.138	-0.023	-0.0001	0.907	-0.020	0.0004	0.724	0.144	0.0003	**0.006**	0.140	-0.0002	**0.007**
BIO17	0.026	0.0028	0.147	-0.006	-0.0015	0.391	-0.023	-0.0002	0.929	0.300	0.0006	**0.000**	0.336	-0.0004	**0.000**
BIO18	0.044	0.0028	0.089	-0.023	-0.0003	0.862	-0.019	0.0007	0.671	0.196	0.0004	**0.001**	0.200	-0.0003	**0.001**
BIO19	0.014	0.0022	0.207	0.002	-0.0016	0.302	-0.022	-0.0004	0.795	0.287	0.0006	**0.000**	0.317	-0.0003	**0.000**

CHAPTER 3. Three new species of *Thomasomys*-like form from the central Peruvian montane forest and a new perspective of the tribe Thomasomyini

In the third chapter of this thesis, the taxon identified out of *Thomasomys* sensu stricto in Chapter 1 is analyzed within the context of the Thomasomyini tribe. To ascertain the phylogenetic placement of this taxon, it was performed exhaustive assessment that merges both qualitative and quantitative morphological analyses with molecular data derived from mitochondrial and nuclear genes. Our findings also place this novel form outside the realm of currently recognized thomasomyine genera (*Aepeomys*, *Chilomys*, *Rhipidomys*, and *Thomasomys*). Consequently, we assert that the clade formed by these specimens constitutes a new genus, characterized by three lineages that are both molecularly divergent and morphologically distinct. In recognition of these discoveries, we describe this new genus and its associated species, all of which are endemic to the central Peruvian montane forests. The inclusion of new genetic sequences from *Aepeomys*, *Chilomys*, and *Rhipidomys* has further enabled a refined discussion on the composition of the Thomasomyini tribe and the evolutionary standing of *Rhagomys*.

Disclaimer: In this chapter are described a new genus and three new species. For this purpose, informal names for these entities ("Oxapampa," "Tarma," "Satipo") are used for avoiding future inconveniences related to the formal naming under the

International Code of Zoological Nomenclature. The manuscript and taxonomic accounts format follow the AMNH Novitates guideline (Knight, 2014).

Cited as: **Ruelas, D.**, Fabre, P.-H., & Pacheco, V. (in prep.). Description of three new *Thomasomys*-like species from the central Peruvian montane forest and a new perspective of the Thomasomyini tribe.

Three new species of *Thomasomys*-like form from the central Peruvian montane forest and a new perspective of the tribe Thomasomyini

Dennisse Ruelas[1,2,3,4], Víctor Pacheco[1,2], Pierre-Henri Fabre[4,5]

[1]Museo de Historia Natural, Universidad Nacional Mayor de San Marcos, Lima 11, Peru.

[2]Instituto de Ciencias Biológicas "Antonio Raimondi", Facultad de Ciencias Biológicas, Universidad Nacional Mayor de San Marcos, Lima, Peru.

[3]Doctorado en Ciencias de la Vida, Universidad Peruana Cayetano Heredia, Av. Honorio Delgado 430, Lima, Peru.

[4]Institut des Sciences de l'Évolution (ISEM, UMR 5554 CNRS-IRD-UM), Université de Montpellier, Place E. Bataillon - CC 064 - 34095, Montpellier Cedex 5, France.

[5]Institut Universitaire de France (IUF), Paris, France.

Abstract

The genus *Thomasomys*, currently considered a monophyletic genus, holds the distinction of being the most diverse within the Sigmodontinae subfamily. However, a molecular previous study identified *Thomasomys*-like specimens that challenged the monophyletic status of *Thomasomys* and the composition of the Thomasomyini tribe. To resolve the phylogenetic position of this form, we

developed a comprehensive study, combining qualitative and quantitative morphological analyses with molecular data using 13 mitochondrial genes and 5 nuclear genes. Our results found this new form outside the currently known thomasomyine genera (*Aepeomys*, *Chilomys*, *Rhipidomys*, and *Thomasomys*). Therefore, we propose the clade conformed by these specimens represents a new genus composed by three lineages molecularly divergent and morphologically distinct. In light of these findings, we formally describe this novel genus and its associated new species, which are all endemic to the central Peruvian yungas. The addition of new sequences of *Aepeomys*, *Chilomys*, and *Rhipidomys* allowed us to discuss the composition of the Thomasomyini tribe and the position of *Rhagomys*.

Keywords: Andes, new genus, Pasco, Sigmodontinae

INTRODUCTION

Rodents of the Thomasomyini tribe are widely distributed across forested habitats in tropical South America, predominantly in the Andean forests and the Amazon basin (Pacheco et al., 2015; Tribe, 2015). Its composition has been in constant debate due to the adding and removing genera that are now considered Sigmodontinae *insertis sedis* or part of other tribes (see for more details Pacheco et al., 2015; Pardiñas et al., 2022). Pacheco et al. (2015) defined Thomasomyini to include *Aepeomys*, *Chilomys*, *Rhagomys*, *Rhipidomys*, and *Thomasomys*, supported by both morphological (e.g., Pacheco, 2003; Pacheco et al., 2015; Voss, 2003) and molecular evidence (e.g., D'Elía et al., 2006; Parada et al., 2015; Smith & Patton, 1999; Steppan & Schenk, 2017). However, Pardiñas et al. (2022) proposed excluding *Rhagomys* due to its distinct morphology, suggesting the establishment

of Rhagomyini as a new monotypic tribe. Following Pacheco et al. (2015) and recent changes and additions (Brito et al., 2017, 2019, 2021, 2022; Campos et al., 2022; García et al., 2020; Lee et al., 2022; Pacheco & Ruelas, 2023; Pardiñas et al., 2022; Ruelas & Pacheco, 2021), this tribe contains 87 species, spanning two genera characterized by limited species diversity and narrow geographic ranges (*Aepeomys* and *Chilomys*), alongside two highly diversified and widely distributed genera (*Rhipidomys* and *Thomasomys*).

Thomasomys, the genus that gives name to the tribe, is the most diverse genus in the Sigmodontinae subfamily; however, its relationships with respect to the other members of the Thomasomyini tribe have not been consistent nor well-supported in all these studies (e.g., Brito et al., 2019; Parada et al., 2015; Ruelas et al., 2024; Steppan & Schenk, 2017). Based on morphology, Pacheco (2003) identified *Thomasomys* as paraphyletic when intermixed with *Rhipidomys* and *Chilomys*, encompassing multiple undescribed species. Although Pacheco (2003) phylogenetic results inferred *Aepeomys* as embedded within *Thomasomys*, he provided details of external and craniodental characters for *Thomasomys* sensu stricto (s.s.) and chose to not include *Aepeomys* in it. Subsequently, Pacheco (2015b), based on his morphological findings (Pacheco, 2003), known molecular phylogenies and distributional patterns, delimited *Thomasomys* and recognized seven morphological groups: Aureus, Baeops, Cinereus, Gracilis, Incanus, Macrotis, and Notatus, most of which have been recovered monophyletic in a molecular approach (e.g., Brito et al., 2019; Lee et al., 2022; Pacheco & Ruelas, 2023; Steppan & Schenk, 2017). The unnamed species proposed by Pacheco (2003) were provisionally subsumed into recognized species (Pacheco, 2015), with the

exception of "*Thomasomys*" sp. 4. Indeed, Pacheco (2003) identified "*Thomasomys*" sp. 4 as the sister of *Thomasomys* sp. 5 within a broad clade of *Thomasomys*, which also included species from the Incanus group, encompassing *Aepeomys*. However, more recently, Ruelas et al. (2024) conducted a phylogenetic analysis using the Cytochrome b mitochondrial gene, revealing that "*Thomasomys*" sp. 4 is potentially paraphyletic in relation to other *Thomasomys* species. In addition, Ruelas et al. (2024) suggested that this may represent a complex containing at least two candidate species. These findings challenge the composition of the Thomasomyini tribe once again. On the other hand, although there is not a formal description of "*Thomasomys*" sp. 4, it was morphologically scored and characterized by Pacheco (2003) based on specimens from Pasco, and its karyotype from Huánuco is known (Pacheco et al., 2012). It stands out from other *Thomasomys* species due to unique characteristics such as a biarmed Y chromosome and biarmed autosomal pairs 1, 5, and 20, as well as FN = 47 (Pacheco et al., 2012). Pacheco (2012) proposed that these distinctive features may indicate species-level divergence.

With the discovery of additional museum material, this contribution aims to perform a taxonomic revision of "*Thomasomys*" sp. 4 based on a morphological (qualitative and quantitative analyses) and molecular approach to provide a description of this new taxa, including morphological comparisons and detailed anatomical evidence, partially based on micro-computed tomography (micro-CT) and a molecular analysis using 13 mitochondrial genes and five nuclear genes. Additionally, because of the inclusion of all the Thomasomyini genera we discuss the composition of this tribe and the position of *Rhagomys*.

MATERIAL AND METHODS

Source of Material: For the morphological assessment, we examined a total of 114 adult specimens belonging to "*Thomasomys*" sp. 4 (Pacheco 2003, Ruelas et al. 2024). These specimens were collected from three regions in Peru: Junín (n = 46), Huánuco (n= 2), and Pasco (n = 67). For comparative purposes, we directly examined skulls and skins of species of the genera *Aepeomys*, *Chilomys*, *Rhipidomys*, and *Thomasomys*, including holotypes, which are housed at the American Museum of Natural History (AMNH, New York), Field Museum (FMNH, Chicago), and Museo de Historia Natural of the Universidad San Marcos (MUSM, Lima). In addition, we examined high-quality photos of some holotypes housed at the Natural History Museum (NHMUK, London). For quantitative analyses, we measured specimens of "*Thomasomys*" sp. 4 (n= 50) and, due to the relationships recovered in the morphological phylogeny (Pacheco 2003), *Aepeomys lugens* (n= 12) and species of the Incanus group of *Thomasomys* such as *T. eleusis* (n= 4), *T. incanus* (n= 7), *T. ischyrus* (n= 16), *T. kalinowskii* (n= 7), and *T. ladewi* (n= 5). Additionally, we included specimens of *Thomasomys cinereus* (n= 8) and *T. shallqukucha* (n= 9). All specimens of "*Thomasomys*" sp. 4 used in this study and collection localities are listed in appendix 1 and mapped in figure 1.

Groups: In light of the possibility that "*Thomasomys*" sp. 4 may encompass multiple distinct entities, as was proposed (Ruelas et al. 2024), and with an improved geographic sampling, we have delineated three distinct groups – two of them representing the lineages found by Ruelas et al. (2024) – each associated with isolated populations. These groups are designated as "Oxapampa," found in the

Oxapampa Province, Oxapampa District in Pasco; "Satipo," occurring in the Satipo Province, Pampa Hermosa District in Junín; and "Tarma," inhabiting the montane forest of the Huasahuasi District, San Pedro de Churco in Junín.

Molecular Analyses

DNA Isolation: We isolated the whole DNA from six specimens of "*Thomasomys*" sp. 4 from Satipo (Junín), Tarma (Junín), and Oxapampa (Pasco) in Peru. Additionally, DNA from *Akodon josemariarguedasi* (n= 1), *Aepeomys lugens* (n= 2), *Chilomys instans* (n= 2), *Rhipidomys gardneri* (n= 1), and *Thomasomys* spp. (n= 39) was also isolated. The specimens we sequenced in this study are listed in table 1. DNA isolation was performed using the DNeasy Blood and Tissue Kit from Qiagen, following the manufacturer's instructions. The final elution was carried out in either water or the elution buffer. To fragment the DNA, we utilized sonication with an ultrasonic cleaning unit. We followed the Illumina library preparation procedure, including steps like blunt-end repair, adapter ligation, adapter fill-in, and indexing PCR, as developed by Meyer and Kircher (2010) with modifications outlined by Tilak et al. (2015). Using these libraries, we captured exon using myBaits Custom Kit (Daicel Arbor Biosciences, United States) following the manufacturer's instructions. The tagged DNA libraries were pooled and subsequently sequenced as single-end reads by an external service provider (Novogene Co., United Kingdom). To prepare the data, we removed adapter fragments using Fastp (Chen et al., 2018). Subsequently, we assembled the mitochondrial genomes using Mitofinder (Allio et al., 2020). We recovered the exons using hybpiper (Johnson et al., 2016). We compared our newly obtained

mitogenes and nuclear genes with sequences available from public databases (NCBI, OrthoMaM v12: Allio et al., 2024). Finally, sequence alignment was carried out using MACSE 2 (Ranwez et al., 2018) and MUSCLE (Edgar, 2004).

Phylogenetic Analyses: For phylogenetic analyses, we used sequences of "*Thomasomys*" sp. 4 (n= 14) and *Aepeomys* (n= 2), *Chilomys* (n= 4), *Rhipidomys* (n= 4), and *Thomasomys* (n= 42) as ingroup. For the outgroup, we included sequences of representatives of species of the tribes Abrawayaomyini (*Abrawayaomys ruschii*), Abrothrichini (*Abrothrix andina*, *Notiomys edwardsii*), Akodontini (*Akodon josemariarguedasi*, *Akodon montensis*, *Akodon torques*, *Brucepattersonius soricinus*, *Lenoxus apicalis*, *Necromys amoenus*, *Oxymycterus nasutus*, *Oxymycterus rufus*), Andinomyini (*Andinomys edax*, *Punomys kofordi*), Euneomyini (*Euneomys chinchilloides*, *Irenomys tarsalis*), Ichthyomyini (*Rheomys raptor*), Neomicroxini (*Neomicroxus bogotensis*), Oryzomyini (*Holochilus sciureus*, *Melanomys caliginosus*, *Nephelomys albigularis*, *Nephelomys keaysi*, *Oligoryzomys stramineus*, *Oryzomys palustris*), Phyllotini (*Calomys musculinus*, *Calomys venustus*, *Eligmodontia moreni*, *Eligmodontia typus*, *Phyllotis darwini*, *Phyllotis haggardi*), Reithrodontini (*Reithrodon auritus*), Rhagomyini (*Rhagomys longilingua*, *Rhagomys rufescens*, *Rhagomys septentrionalis*), Sigmodontini (*Sigmodon hispidus*), and Wiedomyini (*Juliomys pictipes*, *Wiedomys cerradensis*, *Wilfredomys oenax*) as outgroup. We constructed three matrices, one with 13 mitochondrial protein-coding genes (ND1, ND2, COX1, COX2, ATP8, ATP6, COX3, ND3, ND4L, ND4, ND5, ND6, and CYTB), the second with five nuclear genes (GHR, ACP5, RAG1, RBP3, and BRCA1), and the third a supermatrix

resulting of concatenation of the first two matrixes. For details of ingroup and outgroups for each dataset see appendix 2.

Phylogenetic relationships were inferred using both maximum likelihood (ML) and Bayesian inference (BI) incorporating the best-fit nucleotide substitution models as identified by ModelFinder (Kalyaanamoorthy et al., 2017) with option partition models (Chernomor et al., 2016), using the Bayesian Information Criterion (BIC, Schwarz, 1978), respectively. We conducted partitioned ML using IQ-TREE 1.6.3 (Chernomor et al., 2016; Nguyen et al., 2015), performing 5000 nonparametric bootstrap replicates to identify the best tree and calculate bootstrap support (bs) values. Partitioned Bayesian analyses were performed using MrBayes 3.2.6 (Ronquist et al., 2012), running simulations for 10 million generations with four simultaneous Markov chains. Trees were sampled every 1000 generations per chain, and the initial 25% of trees were discarded as burn-in. The remaining trees were employed to generate a 50% majority rule consensus tree, and Bayesian posterior probabilities (pp) were assigned to each node. Convergence of chains was assessed using the effective sample size (ESS) indicator, ensuring it exceeded 200 for all priors, as confirmed using Tracer 1.7 (Rambaut et al., 2018).

Genetic Distances: We calculated corrected genetic distances using Cytochrome b (CYTB) gene sequences of "*Thomasomys*" sp. 4, applying the Kimura 2-parameter model using MEGA 7.0 (Kumar et al., 2016).

Morphological and Morphometric Analyses

Given the potential classification of "*Thomasomys*" sp. 4 as a new genus and a species complex based on Ruelas et al. (2024) findings, we conducted

morphological analyses separately for genus and species levels due to differences in resolution, taxonomic scope, and methodological approaches. Genus-level analysis focused on broader traits, while species-level analysis identified subtle differences crucial for species identification. This separation ensures accurate classification by addressing both broad and specific morphological characteristics.

Age Criteria: The relative age was based on molar toothwear following Pacheco and Ruelas (2023), so we consider specimens in age classes 3 and 4 as "adults," while specimens in age classes 0–1 as "juveniles," and specimens in age class 2 as "subadults."

Morphology: Terminology and definitions for general morphological features followed Carleton and Musser (1989) and Voss (1988, 2003), Reig (1977), for anatomical features of Thomasomyini followed Pacheco (2003, 2015b), Brito et al. (2021), and Pacheco and Ruelas (2023), for teeth morphology nomenclature Carleton and Musser (1989) and Hershkovitz (1994). Additionally, descriptions of the soft palate were based on Carleton (1980), and stomach anatomy following Carleton (1973).

Scanning: We scanned the skull of two specimens of "*Thomasomys*" sp. 4, one from Oxapampa, Pasco (MUSM 11340) and another from Satipo, Junín (MUSM 40820), and one specimen of *Aepeomys lugens* (NHMUK 1905.2.5.15). Specimens used are preserved in ethanol and not dyed. The acquisition of 3D data was performed using the traditional protocol with an EasyTom 150 microtomograph, achieving a voxel size ranging from 0.018 to 0.021 mm. Image reconstruction, segmentation, and visualization were performed using Avizo Lite

v. 9.0.1 (Fisher Scientific Inc., USA). We segmented the left turbinal bones following Martinez et al. (2018) and Ruelas et al. (in rev.: Chapter 2). Scans and segmentation of *Thomasomys* cf. *pyrrhonotus* (MUSM 55555) was taken from Ruelas (in rev.: Chapter 2).

External and Craniodental Measurements: We measured only adult specimens. Weight (W) in grams (g) and external measurements (TL: total length, T: tail length, F: hindfoot length, E: ear length) in millimeters (mm) were transcribed from specimen labels and the Collections' database. Additionally, 21 craniodental and mandibular measurements were obtained using a dial caliper (error: ± 0.1 mm) following Luna and Pacheco's (2002) and Ruelas and Pacheco's (2021): greatest length of skull (GLS), condyloincisive length (CIL), condylomolar length (CML), length of orbital fossa (LOF), length of nasals (LN), diastema length (LD), length of incisive foramina (LIF), length of maxillary toothrow (LM), breadth of incisive foramina (BIF), breadth of rostrum (BR), breadth of palatal bridge (BPB), breadth of first upper molar (BM1), breadth of nasals (BN), least interorbital breadth (LIB), zygomatic breadth (ZB), rostral length (RL), braincase breadth (BB), breadth of zygomatic plate (BZP), depth of incisor (DI), height of braincase (HBC), mesopterygoid fossa breadth (MFB), and length of mandibular toothrow (MN). Furthermore, we used the ratio "Tail%" (= LT/HBL × 100) to quantify proportions of the tail with respect to head-and-body length for descriptive purposes.

Quantitative analyses: We calculated summary statistics (average, standard deviation, and minimum and maximum values) for each morphological variable within each species. To facilitate univariate and multivariate analyses, we

constructed two matrices: (*i*) for genus-level analysis, including "*Thomasomys*" sp. 4, *Aepeomys*, and *Thomasomys* species, and (*ii*) for species-level analysis, only including "*Thomasomys*" sp. 4 specimens.

For both matrices, we used the Royston Test for assessing multivariate normality and the Anderson-Darling test for univariate normality. Given that the measurements differed by order of magnitude, the data were log-transformed. Morphological variables were checked for high degrees (>0.80) of correlation using Spearman's coefficient, and highly correlated variables were discarded. We carried out a principal component analysis (PCA) based on a variance–covariance matrix to ordinate specimens in a multivariate space. This method simplifies multivariate data to key indices, exposing trends, clusters, and outliers, and clarifies relationships among observations and variables for a concise data overview (Jolliffe & Cadima, 2016). We used the PC scores that explained most of the variation to undertake an analysis of variance (ANOVA). For the second matrix, we also performed a post hoc Tukey–Kramer test for unbalanced groups ($P < 0.05$). The Tukey–Kramer test facilitates the comparison among unequal group sizes across all possible pairs of group means. Moreover, the test plays a crucial role in managing the overall risk of Type I errors (false positives) that could arise during multiple comparisons, thereby ensuring the reliability of the findings (Keselman et al., 1976; Keselman & Rogan, 1977).

For the second matrix, we also performed a non-parametric permutational multivariate analysis of variance (PERMANOVA) with a post hoc using 1000 iterations only on the second matrix to test for significant differences ($P < 0.05$) in

craniodental variables among groups ("Oxapampa," "Tarma," "Satipo"). Additionally, we carried out a discriminant function analysis (DFA) to assess the correct allocation of specimens by estimating the percentage of correct classification using 10000 Jackknife replicates.

We performed all our analyses in R (R Core Team, 2022) within the RStudio 2023.06.2 environment (RStudio Team, 2023), using the following packages: "MVN" (Korkmaz et al., 2021) for normality, "caret" (Kuhn et al., 2023) for the correlation matrix, "devtools" (Wickham et al., 2022), "pairwiseAdonis" (Martinez Arbizu, 2020), and "vegan" (Oksanen et al., 2022) for PERMANOVA," "maptools" (Bivand & Lewin-Koh, 2023) for PCA, "DTK" (Lau, 2013) for Tukey-Kramer tests, and "MASS" for DFA.

RESULTS

Phylogenetic inference

We obtained three matrices: a concatenated mitochondrial matrix of 11334 bp, a concatenated nuclear matrix of 6148 bp, and a supermatrix of 17482 bp. Detailed information about variable sites, potentially parsimony informative sites, and singleton sites is provided in appendix 3 while the best models used for each partition are listed in appendix 4.

Our phylogenetic trees found different topologies with the notable inclusion of *Rhagomys* within the clade containing the tribe Thomasomyini (fig. 2, appendix 5, appendix 6). The Thomasomyini tribe, only including *Aepeomys*, *Chilomys*, *Rhipidomys*, *Thomasomys*, and "*Thomasomys*" sp. 4, was well-supported only in

the nuclear genes analysis (bs = 98, pp= 0.96). *Rhagomys* was nested within the Thomasomyini clade but remained unresolved in the ML analysis of mitochondrial genes (appendix 5) and the supermatrix BI analysis (appendix 6).

In all analyses, "*Thomasomys*" sp. 4 was unequivocally monophyletic (mitochondrial: bs= 100, pp= 1; nuclear: bs = 100, pp = 1; concatenated: bs= 100, pp= 1). The phylogenetic position of "*Thomasomys*" sp. 4 was variable, it was sister to *Thomasomys* in the nuclear genes and supermatrix analyses (appendix 6, fig. 2) but sister to *Rhipidomys* in the mitochondrial gene analyses (appendix 5). Moreover, "*Thomasomys*" sp. 4 was composed of three well-supported clades and molecularly divergent which correspond to the delimited groups "Oxapampa" (bs = 100, pp = 1), "Tarma" (bs = 100, pp = 1), and "Satipo." Consequently, these groups are henceforth referred to as lineages.

Genetic distances

Our findings reveal that the corrected genetic distance between the "Satipo" and "Oxapampa" lineages is 6.37±0.8%, between "Tarma" and "Oxapampa" is 5.4±0.75% and between "Tarma" and "Satipo" is 6.98±0.77%. Meanwhile, the intraspecific distances are notably smaller, with "Oxapampa" with 0.287% and "Tarma" with 0.092%.

Qualitative analyses

"*Thomasomys*" sp. 4 displays a range of unique external and cranial features that differentiate it from members of the *Thomasomys* genus as well as other genera

within the Thomasomyini tribe (figs. 3, 4, 5,; table 2). Some of the most important differences are explained as follows:

Externally, "*Thomasomys*" sp. 4 has a slightly countershaded body pelage (like *Aepeomys*), contrasting with the moderate to distinct countershading found in *Rhipidomys* while variable countershading in *Thomasomys* (no countershaded in *T. gracilis, T. bombycinus, T. daphne, T. ladewi, T. kalinowskii, T. hylophilus, T. caudivarius, T. ucucha, T. monochromos, T. onkiro*). Mystacial vibrissae are shorter than in *Chilomys, Rhipidomys,* and *Thomasomys*. Genal I vibrissae is present (like in *Chilomys*, *Rhipidomys*) versus absent in *Aepeomys* while in *Thomasomys* it is usually absent but is also polymorphic for some species, present in some populations. The claw of hallux is longer than in *Aepeomys*. Dark metatarsal patches are absent (like in *Aepeomys*) versus present in *Rhipidomys* and *Chilomys* and variable but usually present in *Thomasomys*. A gap between the hypothenar and thenar pads of hindfeet is present as compared to *Aepeomys* and *Chilomys* versus absent in *Rhipidomys.* The fifth digits of pes are shorter (like in *Aepeomys*) than in *Chilomys, Rhipidomys* and *Thomasomys*. Ungual tuft is denser than in *Chilomys* but less dense than in *Aepeomys* while in *Rhipidomys* and *Thomasomys* is variable. The tail is bicolored versus monocolored or indistinctly bicolored in *Aepeomys*, *Chilomys, Rhipidomys* (except *R. latimanus* and *R. macconnelli*), and *Thomasomys*. Pencil tail is short, like in *Aepeomys*, *Chilomys* and *Thomasomys* (except *T. erro* and *T. notatus*) versus present in *Rhipidomys*. The tail, respect to the body size, is shorter than in *Aepeomys, Chilomys, Rhipidomys*, and *Thomasomys*.

Cranially, nasals are broader than *Aepeomys* and *Chilomys*, extending beyond the premaxillae versus subequal to the premaxilla or slightly extended beyond the premaxillae in *Chilomys*. A rostral tube (formed by the lateral walls of the nasals and premaxilla) is present (like in *Aepeomys*) while absent in *Chilomys*, *Rhipidomys* and, *Thomasomys* (except *T. erro* and *T. incanus*). The rostrum is longer (like in *Aepeomys*) than in *Chilomys*, while variable in *Rhipidomys* and *Thomasomys*. The lacrimal bones are larger than in *Aepeomys.* The turbinal bones are more complex (more scrolled and with additional branches) than in *Aepeomys*, *Chilomys*, *Rhipidomys*, and *Thomasomys* (fig. 5). The anterodorsal frontal sinuses are more inflated than in *Aepeomys*, *Rhipidomys*, and most *Thomasomys*. The supraorbital ridges are absent (like in *Aepeomys*) versus present and well-developed in *Rhipidomys* while variable in *Thomasomys* (present in species of the Aureus group, *T. ladewi*, and *T. macrotis*). The masseteric tubercles are reduced (like in *Chilomys*) versus prominent in *Aepeomys*. The incisive foramina are shorter (like in *Aepeomys* and *Chilomys*) than in *Rhipidomys* and *Thomasomys*. The palate is shorter than in *Aepeomys* and *Chilomys* but longer than in *Rhipidomys* and *Thomasomys*. The mesopterygoid fossa is wider than in *Chilomys* and *Rhipidomys*. The sphenopalatine vacuities are absent or barely as narrow slits on one or both sides of the basisphenoid-presphenoid suture (like in *Chilomys* and *Rhipidomys*) versus moderately perforated, usually elongated, in *Aepeomys* and *Thomasomys*. The zygomatic arches converged anteriorly (like in *Aepeomys* and most *Thomasomys*) or are barely subparallel versus subparallel in *Chilomys* and *Rhipidomys*. The zygomatic plates are slated backward from the maxillary root (like in Aepeomys) versus vertical in *Chilomys*, *Rhipidomys*, and *Thomasomys* (except

T. aureus complex, *T. incanus*, *T. kalinowskii*, and *T. caudivarius*). The upper incisors are orthodonts or slightly opisthodonts (similar to *Aepeomys*) in contrast to *Chilomys*, which has proodont or orthodont incisors and *Rhipidomys*, which has opisthodont incisors, while *Thomasomys* exhibits proodont, orthodont, and opisthodont incisors. The capsular processes are absent (similar to *Aepeomys*) while present in *Chilomys* and *Rhipidomys*. The gall bladder is absent versus present in *Aepeomys*, *Chilomys*, and *Thomasomys* (except *T. oreas*).

Specimens identified as "*Thomasomys*" sp. 4 exhibit significant variation in a suite of morphological characters that is better interpreted as composed of three main lineages: "Oxapampa," "Tarma," and "Satipo" (figs. 6-13). Differences between these lineages are listed in table 3, and some of the most important differences are explained as follows: externally, the ventral pelage is light gray in "Oxapampa" and "Tarma" and yellowish in "Satipo", the hindfoot is larger in "Oxapampa" and "Tarma" lineages than in "Satipo" (F: 26–32 mm and 26–30 mm vs. 22–28.5 mm). The tail is bicolored in "Oxapampa" and faintly bicolored in "Tarma" and "Satipo" lineages and has more scales per cm in "Satipo" (23 scales vs. 21 scales in the others), hair on the scales is short and dark in "Oxapampa" and "Tarma", while longer and whitish in "Satipo." Digital pads are more swollen in "Oxapampa" and "Tarma" lineages. Digital ungual tuft is longer in "Tarma" and "Satipo" lineages. Thenar of the manus is larger than hypothenar in "Tarma" and "Satipo" vs. subequal in "Oxapampa". Plantar skin is darker in "Tarma" and "Satipo." Cranial characters also provide evidence for the distinction of these lineages. For instance, anterior border of nasal is rounded in "Oxapampa" and triangular in "Tarma" and "Satipo." Infraorbital foramen is narrower in "Tarma"

and “Satipo.” Zygomatic notch is shallower in “Oxapampa” and “Tarma”, while zygomatic plate in “Satipo” is wider. Incisive foramen is shorter in “Satipo.” Subsquamosal fenestra is larger than postglenoid foramen in “Tarma” and “Satipo” and subequal to postglenoid foramen in “Oxapampa.” Paraoccipital process is small and broad in “Oxapampa” and “Satipo” and long and thin in “Tarma.” Squamosal ridge is slightly developed in “Tarma” vs. shallow in “Oxapampa” and “Satipo”. Orbicular apophysis of malleus is larger in “Oxapampa” and “Satipo,” Mandible ramus is narrower in “Tarma.” Coronoid process is longer in “Oxapampa” than in “Tarma” and “Satipo.” Anteromedian flexus is deeper in “Satipo.” The m2 anterocingulum is longer in “Oxapampa” and “Tarma.” The m2 ectolophid is present in “Oxapampa” and “Satipo.” The m2 ectostylid is only present in “Tarma.”

Quantitative analyses

Descriptive statistics for adult specimens of “*Thomasomys*” sp. 4 “Oxapampa” (N = 28), “Tarma” (N = 14), and “Satipo” (N = 7) are provided in table 4 and for the other thomasomyine species are in appendix 7. Both the multivariate (H = 118.83, P = 0.55e-19) and univariate (appendix 8) normality tests confirmed that the data is not consistent with normal distribution assumptions. In the first matrix, six of our 22 variables (GLS, CIL, LOF, LM, ZB, MFB, and MN) exhibited a high correlation (>0.75). While in the second matrix, only the variables GLS and CIL had a high correlation (appendix 9). We removed the highly correlated variables from our subsequent analyses based on these results.

For the first matrix, PCA revealed that the first three principal components (PC1, PC2, and PC3) collectively explain 76.33% of the total variance in the dataset

(fig. 14, table 5). Variables with high loadings on these components are critical in distinguishing between the morphological differences in the dataset. PC1, representing 43.59% of the total variance, is mainly explained by high positive loadings of BZP (0.602) and DI (0.397). PC2, explaining 24.55% of the variance, is mainly explained by loadings of DI (0.480) and MFB (-0.526). PC3, responsible for 8.20% of the total variance, is mainly explained by the loadings of BN (-0.515) and MFB (0.535). The PCA plots revealed distinct morphospaces occupied by each taxon (fig. 14). In the PC1 versus PC2 plot, three groupings are evident, (*i*) *Aepeomys lugens* and *T. incanus* which occupy close but separate morphospaces, (*ii*) the remaining *Thomasomys* species, and (*iii*) the "*Thomasomys*" sp. 4 lineages (fig. 14A). In the PC1 versus PC3 plot, three groupings can be differentiated, (*i*) *Aepeomys lugens*, (*ii*) *T. incanus*, and (*iii*) the remaining taxa (fig. 14B). In the PC2 versus PC3 plot, two groupings can be distinguished, (*i*) the "*Thomasomys*" sp. 4 lineages and (*ii*) the remaining species (fig. 14C). These distinct groupings indicate that the variables used are effective in distinguishing between these taxa. Notably, "*Thomasomys*" sp. 4 lineages were consistently recovered as independently grouped and separated from the other species in the PC1 vs. PC2 and PC 2 vs. PC3 plots. The ANOVA conducted for PC1, PC2 and PC3 scores reveals significant differences in these components among these taxa (PC1: F= 114.78, P= 2.2e-16; PC2: F= 84.10, P= 2.2e-16; PC3: F= 24.49, P= 2.2e-16). These results confirm that the morphological traits captured by these PCs effectively distinguish between the assessed taxa and validate the distinct groupings observed in the PCA plots, particularly highlighting the distinctiveness of the "*Thomasomys*" sp. 4 lineages compared to *Aepeomys lugens* and *Thomasomys* species.

For the second matrix, the MANOVA results showed that the "*Thomasomys*" sp. 4 lineages ("Oxapampa," "Tarma," and "Satipo") have a statistically significant proportion of the total variation (F = 5.217, P = 0.001). The pairwise comparison results revealed that the differences between these pairs are also statistically significant: "Oxapampa" versus "Tarma" (F = 4.634, P = 0.003), "Oxapampa" versus "Satipo" (F = 4.260, P = 0.003), and "Tarma" versus "Satipo" (F = 8.866, P = 0.003). These findings suggest a considerable differentiation among the "*Thomasomys*" sp. 4 lineages. PCA revealed that the first three principal components (PC1, PC2, and PC3) collectively explain 52.37% of the total variance in the dataset (fig. 15A, 15B, table 6). PC1, representing 22.10% of the total variance mainly explained by high loadings of BN (0.690), DI (0.373), and MFB (-3.71). PC2, explaining 18.13% of the total variance, is mainly explained by high loadings of BIF (0.613) and LIF (0.513), and DI (-0.276). PC3, responsible for 12.14% of the total variance, is mainly explained by high negative loadings of BZP (-0.667) and BPB (-0.530). The analysis of variance (ANOVA) conducted for PC1, PC2 and PC3 scores reveals significant differences in these components among lineages (PC1: F= 7.364, P= 0.0017; PC2: F= 10.323, P= 0.0002; PC3: F= 8.008, P= 0.001), indicating that each exhibit distinct mean PC1, PC2, and PC3 values. The post-hoc analysis for unbalanced groups along PC1 found significant differences between "Tarma" and "Oxapampa" (P = 0.002) and between "Tarma" and "Satipo" (P = 0.017), while PC2 and PC3 showed significant differences between "Oxapampa" and "Satipo" (PC2: P = 0.0002; PC3: P = 0.018) and between "Tarma" and "Satipo" (PC2: P = 0.0004; PC3: P = 0.0006) which provides evidence that lineages are distinct from each other, thereby statistically confirming that each

lineage occupies a different morphospace. While no significant difference were found when comparing “Oxapampa” and “Satipo” (P = 0.930) in PC1 and “Oxapampa” and “Tarma” in PC2 (P = 0.957) and PC3 (P = 0.119). The LDA highlights the variance distribution explained by the first two linear discriminants (LD1 and LD2), with LD1 explaining 51.46% and LD2 explaining 48.54% of the total variance (fig. 15C; table 6). These results underscore the distribution of variance across variables and their influence on LD1 and LD2, emphasizing the role of these variables in discriminating among lineages. The Jackknife results provide a breakdown of the number of specimens correctly classified into each lineage, showing that 25 specimens of “Oxapampa,” six specimens of “Satipo,” and 14 specimens of “Tarma” were correctly classified by the LDA model. Additionally, it highlights that a few misclassifications occurred, with one specimen of “Oxapampa” being incorrectly classified as “Satipo” and three specimens of “Oxapampa” as “Tarma,” while one specimen of “Satipo” was incorrectly classified as “Oxapampa.”

TAXONOMIC ACCOUNTS

In light of the evidence mentioned above, which suggests that “*Thomasomys*” sp. 4 is distinct molecularly and morphologically from other thomasomyine genera, and within it, the lineages “Oxapampa,” “Satipo,” and “Tarma” each correspond to distinct species-level lineages. Considering that there are currently no available names for any of them, we proceed with the formal taxonomic description of this newly proposed genus and its three species.

Tribe Thomasomyini Steadman and Ray, 1982

"*Thomasomys*" sp. 4 new genus

Montane forest mouse

Figures 3A, 4A, 5A, 5B, 6, 7, 8, 9, 10, 11, 12, 13, 16, 17, 18

Thomasomys sp. 4: Pacheco, 2003

Thomasomys sp.: Pacheco, Córdova, and Velásquez, 2012

"*Thomasomys*" sp. 4: Ruelas et al. 2024

Type species: "*Thomasomys*" sp. 4 "Oxapampa" sp. nov.

Contents: Three species are described here as "*Thomasomys*" sp. 4 "Oxapampa" sp. nov., "*Thomasomys*" sp. 4 "Tarma" sp. nov., and "*Thomasomys*" sp. 4 "Satipo" sp. nov.

Diagnosis: "*Thomasomys*" sp. 4, a small-bodied thomasomyine rodent, can be distinguished from other thomasomyine genera by its slightly short mystacial vibrissae; presence of genal I vibrissae; claw of the hallux elongated; absence of dark metatarsal patches; tail short and bicolored, pencil tail short; nasals broad and cuminate; presence of a rostral tube; rostrum long; lacrimal bone small; turbinal bones very scrolled and complex, anterodorsal frontal sinuses slightly inflated; supraorbital ridges absent; masseteric tubercle reduced; incisive foramina short; palate moderately long; posterolateral palatal pits simple and small; mesopterygoid fossa wide and typically sided; zygomatic arches converged anteriorly to slightly subparallel; zygomatic plate slanted backward from the maxillary root; capsular

process of the mandible absent; orthodontic or slightly opisthodont upper incisors; anteroflexus of M1 small.

Morphological Description: "*Thomasomys*" sp. 4 is a small rodent genus (TL = 213–260 mm) with long, soft, and dense dorsal fur. Dorsal and ventral pelage are slightly countershaded. Dorsal pelage is brownish and slightly grayish or olive brown with hairs slate colored at the base. Ventral pelage is whitish, light gray, and washed with yellowish or brownish, individual hairs slate colored basally. The ears are moderately long (E = 17–22 mm). Postauricular patches are absent. The mystacial vibrissae are short or barely long, reaching slightly beyond the pinnae's posterior border when laid back alongside the head (by about half the pinnae length). The supraorbital vibrissae are relatively long, reaching beyond the pinnae's posterior border when laid back alongside the head. The genal 1 vibrissae are present. Submental vibrissae are present. The tail is slightly short or nearly equal in length to the combined length of the head and body (Tail % = 48.5–56.68). It is comparatively thick, bicolored or slightly bicolored. The pencil tail is short or slightly long and dark or whitish. The metacarpals are pale brownish or whitish without patches. Claws of the hallux are elongated. Ungual tuft is dense. Digit II of manus is larger than digit V. The hindfeet are moderately long (F = 22–32 mm) with no metatarsal patch, and dense ungual tufts. The plantar surface of the hind foot is pale. The thenar and hypothenar pads are distinctly separated by a gap. Digit I of the hind foot (hallux) is elongated, its claw surpasses the first interphalangeal joint of digit II. Digit V of the hind foot is relatively long, with its claw reaching about halfway along the second phalanx of digit IV.

"*Thomasomys*" sp. 4 features a moderately long skull (CIL= 29.90–32.12 mm), characterized by a flat or barely convex profile, notably lacking a frontal bump. The rostrum is relatively long and moderately broad. A rostral tube is present, and the gnathic process is of moderate size. The nasals are elongated, either rounded or cuminate in shape, extended beyond the premaxillae, with narrow posterior margins extending posteriorly beyond the premaxillae and reaching the lacrimal bones. The turbinal bones are very scrolled and complex and represented by two respiratory turbinals (nasoturbinal and maxilloturbinal) located in the anterior portion of the rostrum and seven olfactory turbinals (semicircular lamina, frontoturbinal 1, frontoturbinal 2, ethmoturbinal I, interturbinal, ethmoturbinal II, and ethmoturbinal III) located posteriorly. The zygomatic notches of the skull range from comparatively deep to slightly shallow. The lacrimal bones are very small and lack a posterior process. Anterodorsal frontal sinuses are slightly inflated. The interorbital region is narrow (LIB = 5.74–6.51 mm) and hourglass-shaped with rounded margins. The braincase is broad and slightly rounded. The interparietal bone is wide and extends moderately in an anteroposterior direction and nearly flat anteriorly. The zygomatic arches are either subparallel or converge anteriorly to a moderate extent. Zygomatic plates are moderately broad and slanted backward from the maxillary root. Maseteric tubercles are reduced. The postglenoid foramina are small, placed anterior to the subsquamosal fenestra, which is relatively larger or of the same size. The tegmen tympani is robust, covering the squamosal's suspensory process. The carotid circulation is pattern 2. The paraoccipital process is simple and notably small or very small, exhibiting a slight curvature. The incisive foramina are short, not extending to reach the anterior margins of the first upper molars. The

maxillary septum is long, although it is less than half the length of the incisive foramina. The palate is short and wide (following Hershkovitz, 1962). The mesopterygoid fossa of the species is wide and typically sided. The sphenopalatine vacuities are absent with no perforations on the dorsal roof of the mesopterygoid fossa or barely as narrow slits on each side of the basisphenoid-presphenoid suture. The parapterygoid fossa is triangular-shaped. The foramina ovalia are moderate to small. The alisphenoid struts are present and sometimes incomplete. The middle lacerate foramina are narrow. The auditory bullae are small, flask-shaped, and slightly inflated, complementing the slightly long and narrow Eustachian tube. Malleus lamina is usually rectangular shaped. The basioccipital bone is moderately broad. The mastoid region of the skull is imperforate, yet a mastoid fenestra is usually present.

Teeth: The upper incisors are either orthodont or slightly opisthodont, featuring a yellowish or orangish enamel on their anterior surfaces. The upper molar rows are moderately long (LM= 4.78-5.28 mm) and parallel. The molars are brachyodont and pentalophodont. Molars do not exhibit interpenetration of the labial and lingual flexi; both labial and lingual cingula are not developed; and accessory labial roots are absent. Size-wise, the first molar is larger than the second, while the third molar is the smallest, a pattern consistent in both the maxilla and mandible.

Mandible: The coronoid process of the mandible is distinctly narrow, very elongated, and falciform, featuring a prominently deep sigmoid notch. The angular process is notably short and placed anterior to the condylar process. In the lower

incisor alveolus, the capsular process is either completely absent or indistinct. The mental foramen is located below the diastemal border on the lateral surface of the mandible.

Palatal rugae: "*Thomasomys*" sp. 4 has three diastema palatal rugae and five incomplete (interdental) transverse palatal ridges. Additionally, the i4 ridge may be shorter compared to the others.

Gall bladder: Absent.

Distribution: "*Thomasomys*" sp. 4 is distributed in the central montane forest of Peru in the Junín, Huánuco (see remarks), and Pasco department at elevation from 2200 to 3368 m.

Taxonomic Comparisons: Externally, "*Thomasomys*" sp. 4 compared to *Aepeomys* has genal I vibrissae present, longer claw of hallux, less dense ungual tuft, and shorter bicolored tail (vs. long and monocolored tail). Cranially, "*Thomasomys*" sp. 4 has broader nasals, slightly larger lacrimal bone, more scrolled and complex turbinal bones, more inflated anterodorsal frontal sinuses, reduced masseteric tubercle (vs. prominent), slightly shorter palate, absence sphenopalatine vacuities or barely as narrow slits (vs. moderately perforated), broader zygomatic plate, orthodont or slightly opisthodont upper incisors (vs. always slightly opisthodont), and gall bladder is absent.

Externally, "*Thomasomys*" sp. 4 compared to *Chilomys* has shorter mystacial vibrissae, absence of dark metatarsal patches, denser ungual tuft, relatively shorter fifth digit of pes, shorter and bicolored tail (vs. long and

monocolored tail). Cranially, "*Thomasomys*" sp. 4 has broader nasals that extend beyond the premaxilla (vs. subequal or slightly extended beyond the premaxilla), a rostral tube developed (vs. absent), longer rostrum, more scrolled and complex turbinal bones, absence of supraorbital ridges (vs. slightly developed), shorter palate, wider mesopterygoid fossa, zygomatic arches converging anteriorly or slightly subparallel (vs. subparallel), broader zygomatic plate, zygomatic plate slanted backward from the maxillary root (vs. vertical), orthodont or slightly opisthodont upper incisors (vs. proodont or orthodont), absence of capsular process, gall bladder absent.

"*Thomasomys*" sp. 4 and *Rhipidomys* exhibit several distinctive features in their external morphology and cranial characteristics. Externally, "*Thomasomys*" sp. 4 has slightly countershaded body pelage (vs. moderately to distinctly countershaded), shorter mystacial vibrissae, presence of genal I vibrissae (vs. usually absent), absence of dark metatarsal patches, presence of a gap between hypothenar and thenar pads of hind feet (vs. absence), shorter fifth digit of pes, shorter pencil tail, shorter tail. Cranially, "*Thomasomys*" sp. 4 has rostral tube developed, more scrolled and complex turbinals, more inflated anterodorsal frontal sinuses, absence of supraorbital ridges, shorter incisive foramina, wider mesopterygoid fossa, zygomatic arches converging anteriorly or slightly subparallel (vs. typically subparallel), zygomatic plate slanted backward from the maxillary root (vs. vertical), orthodont or slightly opisthodont upper incisors (vs. only opisthodont), absence of capsular process.

“*Thomasomys*” sp. 4 and *Thomasomys* exhibit several distinctive features in their external morphology and cranial characteristics. Externally, "*Thomasomys*" sp. 4 has shorter mystacial vibrissae, absence of dark metatarsal patches (vs. usually present, except in *T. bombycinus*), shorter fifth digits of pes, bicolored and shorter tail relative to head body length (vs. long monocolored tail and often with terminal white tip). Cranially, “*Thomasomys*” sp. 4 has a rostral tube (vs. absent, except in *T. erro* and *T. incanus*), more scrolled and complex turbinal bones, shorter incisive foramina, broader zygomatic plate and slanted backward from the maxillary root (vs. vertical, except in *T. aureus*, *T. incanus*, and *T. caudivarius*), sphenopalatine vacuities absent or barely as narrow slits (vs. moderately perforated), absence of the gall bladder (vs. present, except in *T. oreas*).

Remarks: Pacheco et al. (2012) examined the karyotypes of “*Thomasomys*” sp. 4, involving a male (MUSM 17826) and a female (MUSM 17827) collected at 20 km southeast of Chaglla, in the Chaglla District, Pachitea Province, Huánuco Department, between May 15 and 26, 2000, at an elevation of 3020 m (09º53'12" S, 75º53'22" W). We examined (MUSM 17836) and a female (MUSM 17837) from the same locality and collection and confirm they have the diagnostic characters of “*Thomasomys*” sp. 4, and likely to belong to the “Oxapampa” lineage or to an unnamed lineage. The specimens from Huánuco, compared to the “Oxapampa” lineage, has a straight anterior border of nasals (vs. rounded), narrower infraorbital foramen, narrower zygomatic plate, deep and large posterolateral palatal pits, one on each side, postglenoid foramen is small and anterior to a larger subsquamosal fenestra. These differences may be attributed to age differences, as both specimens fall into the age category 2.

"Thomasomys" sp. 4 "Oxapampa", new species

Figures 3A, 4A, 5A, 6, 9, 10A, 11A, 12A, 13A, 16

Thomasomys sp. 4, Pacheco 2003

Thomasomys sp., Pacheco, Córdova, and Velásquez 2012 (see remarks)

"*Thomasomys*" sp. 4, Ruelas et al. 2024; part

Holotype: An adult male specimen housed in the Museo de Historia Natural de la Universidad Nacional Mayor de San Marcos (MUSM 10571), collected by Sergio Solari on October 30, 1994 (original field number SS 880). The holotype is preserved as skin and skull in good condition.

Paratypes: 11 specimens from the type locality (MUSM 11447, 11457, 14964, 14968, 14969, 14973, 14975, 14976, 14980, 14981)

Type locality: Peru, Pasco Department, Oxapampa Province, Oxapampa District, San Alberto, W Parque Nacional Yanachaga Chemillen (10.55° S, 75.4° W), at 2600 m elevation. Locality number 3 in figure 1.

Diagnosis: "*Thomasomys*" sp. 4 "Oxapampa" differs from its congeners by the following combination of morphological characters: tips of the ventral pelage light gray; tail bicolored; hairs on the tail scales short and dark; thenar and hypothenar pads of the hind foot close; plantar surface pale; supercilliary vibrissae present; tail pencil short and dark; digital pads of the foot very swollen; digital ungual tuft short; thenar and hypothenar of the manus subequal; anterior border of nasals rounded; infraorbital foramen slightly wide; zygomatic notch shallow;

zygomatic plate moderately broad; incisive foramen very short; subsquamosal fenestra subequal in size to postglenoid foramen; paraoccipital process small and broad; posterior process of the zygomatic arch slightly developed; maxillo-palatal sutura reaches M2 anterior border; squamosal ridge shallow; occipital condyle very swollen; orbicular apophysis of malleus elongated; mandible ramus broad; and coronoid process long; anteromedian flexus deep; m2 anterocingulum long; m2 ectolophid present.

Morphological Description: "*Thomasomys*" sp. 4 "Oxapampa" is a small species (HBL = 213–247 mm) with long, soft, and dense dorsal fur. Dorsal pelage is brownish and slightly grayish with hairs slate colored at the base. Ventral pelage is light gray or washed with pale brown, individual hairs slate colored basally. Dorsal and ventral pelage are slightly countershaded. The ears are moderately long (E = 18.5–22 mm). Postauricular patches are absent. The mystacial vibrissae are barely long, reaching slightly beyond the pinnae's posterior border when laid back alongside the head (by about half the pinnae length). The supraorbital vibrissae are also relatively long, reaching beyond the pinnae's posterior border when laid back alongside the head. The genal 1 vibrissae are absent. Submental vibrissae are present. The tail is nearly equal in length to the combined length of the head and body (Tail % = 51.46). It is comparatively thick, slightly bicolored, and lacks a white tip. The pencil tail is short and white. The metacarpals are pale brownish or whitish. Digit II of manus is larger than digit V. The hindfeet are moderately long (HFL = 26–32 mm) with no metatarsal patch, and dense ungual tufts. The plantar surface of the hind foot is pale. The thenar and hypothenar pads are distinctly separated. Digit I of the hind foot (hallux) is elongated, its claw surpasses the first

interphalangeal joint of digit II. Digit V of the hind foot is long, with its claw reaching about halfway along the second phalanx of digit IV.

Cranium: The skull is moderately large (GLS = 29.9–32.12 mm) with a flat or barely convex profile, without a bump on the frontal region. The rostrum is clearly long and moderately narrow. There is a developed rostral tube, and the gnathic process is somewhat small. The nasals are long and rounded; the posterior margins are narrow, slightly extending posteriorly to the lacrimal bones and beyond the premaxillae. The turbinal bones are very scrolled and complex and represented by two respiratory turbinals (nasoturbinal and maxilloturbinal) located in the anterior portion of the rostrum and seven olfactory turbinals (semicircular lamina, frontoturbinal 1, frontoturbinal 2, ethmoturbinal I, interturbinal, ethmoturbinal II, and ethmoturbinal III) located posteriorly. The zygomatic notches are shallow. The lacrimal bones are very small. The interorbital region is narrow and hourglass shaped with rounded margins, and the frontal sinuses are slightly inflated. The braincase is broad and rounded. The interparietal is wide and moderately long anteroposteriorly. The zygomatic arches might converge anteriorly or be squarish. The zygomatic plates are moderately broad and vertically oriented. The posterior margin of the inferior zygomatic root is dorsal to the anterior margin of M1. The zygomatic processes of the maxilla and the squamosal are closely approximated; the jugal is slender. The postglenoid foramen is almost the same size as subsquamosal fenestra. The tegmen tympani is robust, covering the squamosal's suspensory process. The carotid circulation is pattern 2, identified by the presence of a stapedial foramen, squamosal-alisphenoid groove, and sphenofrontal foramen. The optic foramen is of moderate size. The paraoccipital process is very small,

slightly curved, and not bifurcated. The incisive foramina are short and do not reach the anterior margins of the first upper molars; the maxillary septum is long but less than half the incisive foramina length. The palate is short and wide. The mesopterygoid fossa is slightly rounded and narrow with subparallel sides without a median posterior process of the palate. The sphenopalatine vacuities are small and simple or absent. The parapterygoid fossa is triangular, shallow, and without vacuities. The foramina ovalia are moderate in size. The alisphenoid struts are present and sometimes incomplete. The middle lacerate foramina are narrow. The posterolateral palatal pits are simple and small. The auditory bullae are small, flask shaped, and sligthly inflated; the Eustachian tube is slightly long and narrow, with one spine that does not reach the alisphenoid; the stapedial foramen of the bulla is inconspicuous while the carotid canal is conspicuous. The basioccipital is moderately broad, and the mastoid is usually perforate. The lamina of the malleus is squarish, and the orbicular apophysis is elongated with a shallow basal constriction on the anterior margin and absent on the posterior margin. The processus brevis of the incus is slightly elongated, slender, and delicate.

Teeth: The upper incisors are orthodont with yellowish enamel on their anterior surfaces. The rows of upper molars are moderately long (LM = 4.78–5.28 mm). The upper molars are brachyodont and pentalophodont. These molars do not exhibit interpenetration of the labial and lingual flexi; labial and lingual cingula are not developed. The procingulum of first upper molar (M1) is slightly smaller than protocone-paracone cusp pair; the anteromedian flexus is distinct; the anteroloph is conspicuous and merges with the anterolabial conule; the paraflexus is oriented transversally to the median mure; the mesoloph is well developed and reaches

perpendicularly the labial margin of the tooth; the protoflexus is oriented transversally; the metaflexus curves slightly; and the posteroloph is missing. Second upper molar (M2) exhibits a strong anteroloph with a recurved paraflexus; the mesoloph is narrow, complete, and reaches the labial margin of the tooth; the metaflexus is deep and recurved; and the posteroloph is coalesced with the metacone. Third upper molar (M3) is half of the M2, only its paraflexus is oriented transversally, and its hypoflexus is absent. On the lower molars, the main cuspids are conspicuous and slightly alternating. The rows of lower molars are moderately long (5.06–5.6 mm). The first lower molar (m1) shows a weak anteromedian flexid; the protolophid and anterolophid are short and quickly merge; the anterolabial and anterolingual cingula are poorly developed; the mesoflexid is narrow and recurved; the entoflexid is coalesced with the entoconid; the posteroflexid is deep and almost straight; the ectolophid is well developed and reaches perpendicularly the labial margin of the tooth; the hypoflexid is narrow and oriented perpendicularly; and the mesolophid is narrow and coalesced with entoconid. On the second lower molar (m2), the mesolophid is short and coalesced with entoconid; the anterolabial cingulum is small; the ectolophid is developed and reaches perpendicularly the labial margin of the tooth. The third lower molar (m3) has a squarish occlusal shape; the hypoflexid is narrow and oriented perpendicularly; the hypoconulid is developed.

Mandible: The coronoid process of the mandible is distinctly narrow, very elongated, and falciform, resulting in a deep sigmoid notch. The angular process is moderately extended and aligns with the level of the condylar process. The capsular

process is either wholly absent or barely distinct. The mental foramen is below the diastema border on the lateral surface of the mandible.

Palatal rugae: This species has three diastema palatal rugae and five incomplete (interdental) transverse palatal ridges.

Stomach: The stomach is classified as unilocular-hemiglandular type (Carleton, 1973; Pacheco, 2003). It features an unequal distribution of cornified and glandular epithelia, with the cornified epithelium constituting almost one-third. The incisura angularis is notably shallow. The thick bordering fold crosses the lesser curvature of the stomach slightly anterior to the incisura angularis.

Gall bladder: Absent

Karyotype: 2n = 42, FN = 47, most autosomes are acrocentrics, except for pairs 1, 5, and 20, which are metacentrics (Pacheco et al., 2012). The sexual pair comprises a autocentric X chromosome and a metacentric Y chromosome (Pacheco et al., 2012). Noteworthy secondary constrictions were observed in the medial region of the long arm of the X sexual pair and the distal region of the long arm of autosomal pair 10.

Measurements of Holotype: GLS, 31.64; CIL, 27.51; CML, 17.65; LOF, 9.16; LN, 13.05; LD, 8.24; LIF, 5.98; LM, 4.97; BIF, 2.43; BR, 5.54; BPB, 3.24; BM1, 1.55; BN, 4.26; LIB, 6.03; ZB, 15.09; RL, 11.97; BB, 13.26; BZP, 2.66; DI, 1.57; HBC, 9.04; MFB, 2.66; MN, 5.21. Measurements of additional specimens are provided in table 4.

Distribution: "*Thomasomys*" sp. 4 "Oxapampa" is distributed in the montane forest of Oxapampa in the Pasco Department from 2200 to 3368 m elevation.

Taxonomic Comparisons: "*Thomasomys*" sp. 4 "Oxapampa" compared to "*Thomasomys*" sp. 4 "Tarma" differs by its tail long and bicolored (vs. short and faintly bicolored tail); pencil tail white (vs. dark); digital ungual tuft shorter; thenar of the manus subequal than hypothenar (vs. larger than hypothenar); thenar and hypothenar pads of the hindfoot closer (vs. widely separated); plantar skin on the hind foot paler; anterior border of nasals rounded (vs. triangular); infraorbital foramen wider; incisive foramen shorter; palatal slightly straight or with a small median process (vs. slightly rounded); subsquamosal fenestra subequal to postglenoid foramen (vs. larger than postglenoid foramen); paraoccipital process smaller and broader; jugal shorter; squamosal ridge shallow (vs. conspicuous); orbicular apophysis of malleus larger; occipital condyle more swollen; mandible ramus broader; coronoid process longer; m2 ectolophid present; both m2 ectostylid and m3 ectolophid absent.

"*Thomasomys*" sp. 4 "Oxapampa" compared to "*Thomasomys*" sp. 4 "Satipo" has light gray tips on its ventral pelage, in contrast to the yellowish tips in "Satipo." Bicolored tail with 21 scales/cm and short, dark hair on the scales (vs. a faintly bicolored tail with 23 scales/cm and long, whitish hair); pencil tail longer; digital ungual tuft shorter; thenar of the manus subequal than hypothenar (vs. larger than hypothenar); thenar and hypothenar pads of the hind foot are closely approximated (vs. widely separated pads); digital pads of the foot more swollen;

supercilliary vibrissae present, anterior border of nasals are rounded (vs. triangular); infraorbital foramen wider; zygomatic notch more shallow; zygomatic plate narrower; subsquamosal fenestra are subequal to postglenoid foramen (vs. larger than postglenoid foramen); maxillo-palatal suture reaches M2 anterior border (vs. surpasses M2 anterior border); manubrium of malleus broader; occipital condyle more swollen; coronoid process is longer; anteromedian flexus less deep; M1 mesoloph, M2 anteroloph, M2 mesoloph, and M3 anteroloph less elongated; m1 metaconid less massive; m2 anterocingulum more elongated.

Natural history: This species occurs in diverse habitats of the Cordillera Yanachaga in Oxapampa. This semi-isolated cordillera, a prominent feature in the Peruvian Amazon, is nestled within the Department of Pasco (Catchpole, 2012). Its strategic location between the Amazonian plain to the east and the Andean Cordillera to the west, about 80 km from the true Amazonian plain, provides a range of ecological environments. The Cordillera Yanachaga is separated from the Andean massif by the Río Huancabamba, a geographical demarcation that contributes to its distinct ecological character, underscores its geographical uniqueness (Vivar Pinares, 2006). Adjacent to the east lie the lower, northward-oriented San Matías-San Carlos and El Sira cordilleras, together dividing the sub-basins of the Río Pachitea (Brack, 1987). The Cordillera Yanachaga's ecological significance led to the establishment of the Parque Nacional Yanachaga Chemillén in 1986, safeguarding its cultural and biophysical characteristics (Catchpole, 2012). It spans the districts of Oxapampa, Pozuzo, Palcazú, Villa Rica, and Huancabamba, featuring a rich variety of habitats, from dense cloud forests to expansive Puna grasslands (INRENA, 2006). At the higher elevations, between 2700 and 3000 m,

the park is characterized by unique dwarf forests. These forests are notable for their stunted growth, with trees just 1.5 to 2 meters tall, and branches and trunks densely covered with epiphytes, forming ecological islands distinct from the taller montane humid forests. Their ecological uniqueness is further accentuated by thick layers of roots and humus overlying a sandstone substrate, marked by irregular rock outcrops. In this forests, "*Thomasomys*" sp. 4 "Oxapampa" is sympatric with the sigmodontines *Akodon josemariarguedasi*, *Akodon* sp., *Microryzomys minutus*, *Nephelomys keaysi*, *Oligoryzomys destructor*, *Thomasomys* aff. *aureus*, *T. incanus*, *T. kalinowskii*, *T. notatus* (Ruelas et al., 2020, 2021; Vivar Pinares, 2006). Additional specimens reported by Pacheco (2003) that also belong to "*Thomasomys*" sp. 4 "Oxapampa" are LSUMZ 29166, collected in Millpo, E Tambo de Vacas on Pozuzo-Chaglla trail; and LSUMZ 25895, 25897, collected in Santa Cruz, ca. 9 km SSE Oxapampa.

"*Thomasomys*" sp. 4 "Tarma", new species

Figures 7, 9, 10B, 11B, 12B, 13B, 17

"*Thomasomys*" sp. 4: Ruelas et al. 2024; part

Holotype: An adult male specimen housed in the Museo de Historia Natural de la Universidad Nacional Mayor de San Marcos (MUSM 52895), collected by Diego Marcelo on September 01, 2019 (original field number DMC 29). The holotype is preserved as skin and skull in good condition.

Paratypes: Twelve males (MUSM 42508, 42509, 42512, 42515, 42517, 42518, 42565, 42570, 52893, 52899, 52900) and two females (MUSM 42511, 42567) from the type locality.

Type locality: Peru, Junín Department, Tarma Province, Huasahuasi District, San Pedro de Churco (11.03° S, 75.54° W). Locality number 7 in figure 1.

Diagnosis: "*Thomasomys*" sp. 4 "Tarma" differs from its congeners by the following combination of morphological characters: tips of the ventral pelage light gray; tail short and faintly bicolored; hairs on the tail scales short and dark; thenar and hypothenar pads of the hid foot widely separated; plantar surface dark; supercilliary vibrissae present; pencil tail short and dark; digital pads of the foot very swollen; digital ungual tuft long; thenar in the manus longer than hypothenar; anterior border of nasals triangular; infraorbital foramen narrow; zygomatic notch shallow; posterior border of palate slightly rounded; subsquamosal fenestra larger than postglenoid foramen; paraoccipital process long and thin; developed posterior process of the zygomatic arch; maxillo-palatal sutura reaches M2 anterior border; squamosal ridge conspicuous; orbicular apophysis of malleus short; occipital condyle swollen; mandible ramus narrow; m2 ectostylid and m3 ectostylid present.

Morphological Description: "*Thomasomys*" sp. 4 "Tarma" is a small species (HBL = 220–244 mm) with long, soft, and dense dorsal fur. Dorsal pelage is brownish with hairs slate colored at the base. Ventral pelage is light gray and washed with pale brown, individual hairs slate colored basally. Dorsal and ventral pelage are slightly countershaded. The ears are moderately long (E = 17–22 mm). Postauricular patches are absent. The mystacial vibrissae are barely long, reaching

slightly beyond the pinnae's posterior border when laid back alongside the head (by about half the pinnae length). The supraorbital vibrissae are also relatively long, reaching beyond the pinnae's posterior border when laid back alongside the head. The genal 1 vibrissae are absent. Submental vibrissae are present. The tail is on average shorter than the combined length of head and body (Tail% = 51.35), comparatively thick, mostly unicolored, and without a white tip. The pencil tail is short and dark. The metacarpals are pale brownish or whitish. Digit II of manus is larger than digit V. The hindfeet are moderately long (F = 26–30 mm) with no metatarsal patch, and dense ungual tufts. The plantar surface of the hind foot is pale. The thenar and hypothenar pads are widely separated by a gap. Digit I of the hind foot (hallux) is moderately elongated, its claw surpasses the first interphalangeal joint of digit II. Digit V of the hind foot is long, with the claw extending about half the length of the second phalanx of digit IV.

Cranium: The skull is moderately large (GLS = 30.9–31.55 mm) with a flat or barely convex profile, without a bump on the frontal region. The rostrum is relatively long and moderately narrow. A rostral tube is present, and the gnathic process is slightly small. The nasals are long and rounded; the posterior margins are narrow, slightly extending posteriorly to the lacrimal bones and beyond the premaxillae. The zygomatic notches are shallow. The lacrimal bones are very small. The interorbital region is narrow and hourglass shaped with rounded margins, and the frontal sinuses are slightly inflated. The braincase is broad and rounded. The interparietal is wide and moderately long anteroposteriorly. The zygomatic arches converge anteriorly to squarish. The zygomatic plates are moderately broad and vertically oriented. The posterior margin of the inferior zygomatic root is dorsal to

the anterior margin of M1. The zygomatic processes of the maxilla and the squamosal are closely approximated; the jugal is slender. The postglenoid foramen is small and anterior to the subsquamosal fenestra. The postglenoid foramen is the same size as subsquamosal fenestra. The tegmen tympani is robust, covering the squamosal's suspensory process. The carotid circulation is pattern 2, identified by the presence of a stapedial foramen, squamosal-alisphenoid groove, and sphenofrontal foramen. The optic foramen is moderate in size. The paraoccipital process is very small, slightly curved, and not bifurcated. The incisive foramina are short and do not reach the anterior margins of the first molars; the maxillary septum is long but less than half the incisive foramina length. The palate is short and wide. The mesopterygoid fossa is slightly rounded and narrow with subparallel sides without a median posterior process of the palate. The sphenopalatine vacuities are small and simple. The parapterygoid fossa is triangular, shallow, and without vacuities. The foramina ovalia are moderate in size. The alisphenoid struts are present and sometimes incomplete. The middle lacerate foramina are narrow. The auditory bullae are small, flask-shaped, and inflated; the Eustachian tube is slightly long and narrow, with one spine that usually does not reach the alisphenoid; the stapedial foramen of the bulla is inconspicuous while the carotid canal is conspicuous. The basioccipital is moderately broad, and the mastoid is imperforate. Lamina of malleus is squarish, and the orbicular apophysis is short, knob-like, with a basal constriction on the anterior margin and absent on the posterior margin. The processus brevis of the incus is elongated, slender, and delicate.

Teeth: The upper incisors are orthodont with yellowish enamel on their anterior surfaces. The rows of upper molars are moderately long (LM = 4.92–5.26

mm). The upper molars are brachyodont and pentalophodont. These molars do not exhibit interpenetration of the labial and lingual flexi; labial and lingual cingula are not developed. The procingulum of M1 is slightly smaller than the protocone-paracone cusp pair; the anteromedian flexus is distinct; the anteroloph is conspicuous and merges with the anterolabial conule; the paraflexus is oriented transversally to the median mure; the mesoloph is well developed, curved, and reaches perpendicularly to the labial margin of the tooth; the protoflexus is oriented transversally; the metaflexus curves slightly; and the posteroloph is missing. M2 exhibits a strong anteroloph with a recurved paraflexus; the protoflexus is reduced or coalesced; the mesoloph is narrow, very long, curved, and reaches the labial margin of the tooth; the metaflexus is deep and curved; and the posteroloph is coalesced with the metacone. M3 is half of the M2, only its paraflexus is curved; anteroloph is curved and long; and hypoflexus is absent. On the lower molars, the main cuspids are conspicuous and slightly alternating. The rows of lower molars are moderately long (MN = 5.33–5.48 mm). The m1 shows a weak anteromedian flexid; the protolophid and anterolophid are short and quickly merge; the anterolabial and anterolingual cingula are poorly developed; the mesoflexid is narrow and recurved; the entoflexid is coalesced with the entoconid; the posteroflexid is deep and almost straight; the ectolophid is well developed and reaches perpendicularly the labial margin of the tooth; the hypoflexid is narrow and oriented perpendicularly; and the mesolophid is narrow and coalesced with entoconid. On m2, the mesolophid is short and coalesced with entoconid; the anterolabial cingulum is small; the ectostylid is developed. The m3 has a squarish

occlusal shape; the hypoflexid is narrow and oriented perpendicularly; ectolophid is short; the hypoconulid is well developed.

Mandible: The coronoid process of the mandible is distinctly narrow, slightly elongated, and falciform, resulting in a deep sigmoid notch. The angular process is slightly long and reaches the level of the condylar process. The capsular process of the lower incisor alveolus is absent or indistinct. The mental foramen is below the diastemal border on the lateral surface of the mandible.

Palatal rugae: This species has three diastema palatal rugae and five incomplete (interdental) transverse palatal ridges, but the i4 is short, not reaching the palatal midline.

Stomach: The stomach is classified as unilocular-hemiglandular type (Carleton, 1973; Pacheco, 2003). It features an unequal distribution of cornified and glandular epithelia, with the cornified epithelium constituting almost one-third. The incisura angularis is notably shallow. The thick bordering fold crosses the lesser curvature of the stomach slightly anterior to the incisura angularis.

Gall bladder: Absent.

Karyotype: Unknown.

Measurements of Holotype: GLS, 30.9; CIL, 26.91; CML, 17.22; LOF, 8.8; LN, 12.75; LD, 8.7; LIF, 6.24; LM, 5.06; BIF, 2.46; BR, 5.37; BPB, 3.19; BM1, 1.63; BN, 4.32; LIB, 5.85; ZB, 15.33; RL, 11.71; BB, 13.31; BZP, 2.7; DI, 1.25; HBC, 8.84; MFB, 2.71; MN, 5.4. Measurements of additional specimens are provided in table 4.

Distribution: "*Thomasomys*" sp. 4 "Tarma" is distributed in the montane forest of Tarma from 3087 to 3219 m elevation.

Taxonomic Comparisons: "*Thomasomys*" sp. 4 "Tarma" differs from "*Thomasomys*" sp. 4 "Oxapampa" by its tail faintly bicolored (vs. bicolored tail); pencil tail darker (vs. white); digital ungual tuft longer; thenar of the manus larger than hypothenar (vs. subequal than hypothenar); the thenar and hypothenar pads of the hind foot more separated; plantar skin on the hind foot darker; anterior border of nasals triangular (vs. rounded); infraorbital foramen narrower; incisive foramen less short; palatal slightly rounded (vs. straight or with a small median process); subsquamosal fenestra larger than postglenoid foramen (vs. subequal to postglenoid foramen); paraoccipital process longer and thinner; jugal longer; orbicular apophysis of malleus smaller; squamosal ridge conspicuous (vs. shallow); occipital condyle less swollen; mandible ramus narrower; coronoid process shorter; m2 ectolophid absent; m2 ectostylid and m3 ectolophid present.

"*Thomasomys*" sp. 4 "Tarma" differs from "*Thomasomys*" sp. 4 "Satipo" by its light gray tips in the ventral pelage (vs. yellowish tips); tail with 21 scales (vs. 23 scales per cm); hair on the scales of the tail shorter and darker; pencil tail shorter and darker; digital pads in the foot more swollen; plantar skin of hind foot darker; supercilliary vibrissae present; zygomatic notch more shallow (vs. deep); zygomatic plate less broad; incisive foramen slightly longer; palatal slightly rounded (vs. slightly straight or with a small median process); paraoccipital process longer and thinner; jugal longer; maxillo-palatal suture reaches M2 anterior border (vs. surpasses M2 anterior border); orbicular apophysis of malleus smaller;

manubrium of malleus thinner; squamosal ridge conspicuous (vs. shallow); mandible ramus narrower; anteromedian flexus less deep; M1 mesoloph, M2 anteroloph, M2 mesoloph, and M3 anteroloph shorter; m1 metaconid less massive; m2 anterocingulum longer; m2 ectolophid absent; m2 ectostylid and m3 ectolophid present.

Natural history: This species inhabits the Yungas of San Pedro de Churco (locally known as Churco), located on the eastern slopes of the Andes in central Peru's Junín department, at an elevation of 3496 m. Churco's notable placement within the Santuario Nacional Pampa Hermosa buffer zone is crucial for conserving diverse Andean-Amazonian mountain ecosystems ranging from 1130 to 4080 m elevation. The area, influenced by Köppen's HighMontane Dry Tundra (ETH) and Continental Humid Boreal (Dwb) climates, supports a unique assemblage of flora and fauna across its varied forest types, from high montane Queñua and cloud forests to lower montane cloud forests (SERNANP, 2012). In this forest "*Thomasomys*" sp. 4 is sympatric with the sigmodontines *Akodon josemarguedasi* (Ruelas et al., 2020), *Calomys sorellus*, *Microryzomys altissimus*, *M. minutus*, and five species of *Thomasomys* (*Thomasomys* sp. A, *T.* aff. *aureus*, *T. incanus*, *T. kalinowskii*, and *T. notatus*; Ruelas et al. 2024). Medium and large sizd mammals (i.e., *Odocoileus virginianus*, *Pudu mephistopheles*, *Lycalopex culpaeus*, *Puma concolor*, *Conepatus chinga*, *Eira barbara*, *Mustela frenata*, *Tremarctos ornatus*, *Cuniculus taczanowskii*) have also been reported (Melo-Dias et al., 2022).

"*Thomasomys*" sp. 4 "Satipo", new species

Figures 5B, 8, 9, 10C, 11C, 12C, 13C, 18

Holotype: An adult male specimen housed in the Museo de Historia Natural de la Universidad Nacional Mayor de San Marcos (MUSM 40810), collected by Maria Peralta on June 25, 2011 (original field number MCP 989). The holotype is preserved as skin and skull in good condition.

Paratypes: 12 specimens from the type locality, four females (40823, 46089, 46091, 46095) and eight males (MUSM 40811-40813, 46090, 46092, 46098-46101) collected in the type locality.

Type locality: Peru, Junín Department, Satipo Province, Pampa Hermosa District, Calabaza (11.51° S, 74.85° W). Locality number 8 in figure 1.

Diagnosis: "*Thomasomys*" sp. 4 "Satipo" differs from its congeners by the following combination of morphological characters: tips of the ventral pelage yellowish; tail slightly short and faintly bicolored; hairs on the tail scales long and whitish; thenar and hypothenar pads of the hind foot widely separated; plantar surface pale; supercilliary vibrissae absent; pencil tail longer and whitish; digital pads of the foot swollen; digital ungual tuft long; thenar longer than hypothenar in the manus; anterior border of nasals triangular; infraorbital foramen narrow; zygomatic notch deep; zygomatic plate broad; subsquamosal fenestra larger than postglenoid foramen; paraoccipital process small and broad; jugal long; maxillo-palatal sutura surpass M2 anterior border; large orbicular apophysis of malleus; manubrium of malleus very thin; squamosal ridge shallow; occipital condyle swollen; mandible ramus broad; anteromedian flexus deep; M1 mesoloph, M2 anteroloph, M2 mesoloph, and M3 anteroloph very long; m1 metaconid very massive; m2 anterocingulum short.

Morphological Description: "*Thomasomys*" sp. 4 "Satipo" is a small species (HBL = 220–260 mm) with long, soft, and dense dorsal fur. Dorsal pelage is olive brown with hairs slate colored at the base. Ventral pelage is whitish and washed with yellowish, individual hairs slate colored basally. Dorsal and ventral pelage are moderately countershaded. The ears are moderately long (E = 19.5–22 mm) and paler. Postauricular patches are absent. The mystacial vibrissae are short, raising the pinnae' posterior border when laid back alongside the head, sometimes slightly surpassing it. The supraorbital vibrissae are also relatively long, reaching beyond the pinnae's posterior border when laid back alongside the head. The genal 1 vibrissae are absent. Submental vibrissae are present. The tail is on average longer than the combined length of head and body (Tail% = 49.17), comparatively thin, mostly unicolored, and without a white tip. Pencil tail is slightly long and whitish. The metacarpals are brownish. Digit II of manus is larger than digit V. The hindfeet are moderately long (F = 22–28.5 mm) with no metatarsal, and dense ungual tufts. The plantar surface of the hind foot is dark. The thenar and hypothenar pads are separated by a distinct gap. Digit I of the hind foot (hallux) is moderately elongated, its claw extending close to the first interphalangeal joint of digit II. Digit V of the hind foot is long, with the claw extending beyond the length of phalanx 2 of digit IV.

Cranium: The skull is moderately large (GLS = 30.28–30.79 mm) with a flat or barely convex profile, without a bump on the frontal region. The rostrum is relatively long and moderately narrow. A rostral tube is present, and the gnathic process is slightly small. The nasals are long and rounded; the posterior margins are narrow, slightly extending posteriorly to the lacrimal bones and beyond the

premaxillae. The turbinal bones are very scrolled and complex and are represented by two respiratory turbinals (nasoturbinal and maxilloturbinal) located in the anterior portion of the rostrum and seven olfactory turbinals (semicircular lamina, frontoturbinal 1, frontoturbinal 2, ethmoturbinal I, interturbinal, ethmoturbinal II, and ethmoturbinal III) located posteriorly. The zygomatic notches are shallow. The lacrimal bones are very small. The interorbital region is narrow and hourglass-shaped with rounded margins, and the frontal sinuses are slightly inflated. The braincase is broad and rounded. The interparietal is wide and moderately long anteroposteriorly. The zygomatic arches converge anteriorly to squarish. The zygomatic plates are moderately broad and vertically oriented. The posterior margin of the inferior zygomatic root is dorsal to the anterior margin of M1. The zygomatic processes of the maxilla and the squamosal are closely approximated; the jugal is slender. The postglenoid foramen is small and anterior to the subsquamosal fenestra. The postglenoid foramen is the same size as subsquamosal fenestra. The tegmen tympani is robust, covering the squamosal's suspensory process. The carotid circulation is pattern 2, identified by the presence of a stapedial foramen, squamosal-alisphenoid groove, and sphenofrontal foramen. The optic foramen is moderate in size. The paraoccipital process is very small, slightly curved, and not bifurcated. The incisive foramina are short and do not reach the anterior margins of the first molars; the maxillary septum is long but less than half the incisive foramina length. The palate is short and wide. The mesopterygoid fossa is slightly rounded and narrow with subparallel sides without a median posterior process of the palate. The sphenopalatine vacuities are small and simple or absent. The parapterygoid fossa is triangular, shallow, and without vacuities. The foramina ovalia are

moderate in size. The alisphenoid struts are present and sometimes incomplete. The middle lacerate foramina are narrow. The auditory bullae are small, flask shaped, and inflated; the Eustachian tube is slightly long and narrow, with one spine that slightly reaches the alisphenoid; the stapedial foramen of the bulla is conspicuous and the carotid canal is small. The basioccipital is moderately broad, and the mastoid is usually perforated. Lamina of the malleus is narrow and has a rectangular shape, and the orbicular apophysis is moderately long with a basal constriction on the anterior margin and absent on the posterior margin. The processus brevis of the incus is elongated, slender, and delicate.

Teeth: The upper incisors are orthodont with orangish enamel on their anterior surfaces. The rows of upper molars are moderately long (LM = 4.81–4.98 mm). The upper molars are brachyodont and pentalophodont. These molars do not exhibit interpenetration of the labial and lingual flexi; labial and lingual cingula are not developed. The procingulum of M1 is slightly smaller than the protocone-paracone cusp pair; the anteromedian flexus is distinct; the anteroloph is conspicuous and merges with the anterolabial conule; the paraflexus is oriented transversally to the median mure; the mesoloph is well developed and reaches perpendicularly the labial margin of the tooth; the protoflexus is oriented transversally; the metaflexus curves slightly; and the posteroloph is missing. M2 exhibits a strong anteroloph with a recurved paraflexus; the propoflexus is reduced or coalesced; the mesoloph is narrow, complete, and reaches the labial margin of the tooth; the metaflexus is deep and curved; and the posteroloph is coalesced with the metacone. M3 is half of the M2, only its paraflexus is oriented transversally, and its hypoflexus is absent. On the lower molars, the main cuspids are conspicuous

and slightly alternating. The rows of lower molars are moderately long (MN = 5.07–5.3 mm). The first lower molar (m1) shows a weak anteromedian flexid; the protolophid and anterolophid are short and quickly merge; the anterolabial and anterolingual cingula are poorly developed; the mesoflexid is narrow and recurved; the entoflexid is coalesced with the entoconid; the posteroflexid is deep and almost straight; the ectolophid is well developed and reaches perpendicularly the labial margin of the tooth; the hypoflexid is narrow and oriented perpendicularly; and the mesolophid is narrow and coalesced with entoconid. On the second lower molar (m2), the mesolophid is short and coalesced with entoconid; the anterolabial cingulum is small; the ectostolophid is developed and reaches perpendicularly the labial margin of the tooth. The third lower molar (m3) has a squarish occlusal shape; the hypoflexid is narrow and oriented perpendicularly; the hypoconulid is well-developed.

Mandible: The coronoid process of the mandible is narrow, slightly long, and falciform, resulting in a deep sigmoid notch. The angular process is slightly long and reaches the level of the condylar process. The capsular process of the lower incisor alveolus is absent or indistinct. The mental foramen is below the diastemal border on the lateral surface of the mandible.

Palatal rugae: This species has three diastema palatal rugae and five incomplete (interdental) transverse palatal ridges.

Stomach: The stomach is classified as unilocular-hemiglandular type (Carleton, 1973; Pacheco, 2003). It features an unequal distribution of cornified and glandular epithelia, with the cornified epithelium constituting almost one-third. The

incisura angularis is notably shallow. The thick bordering fold crosses the lesser curvature of the stomach slightly anterior to the incisura angularis.

Gall bladder: Absent.

Karyotype: Unknown.

Measurements of Holotype: GLS, 30.97; CIL, 26.9; CML, 17.08; LOF, 9.19; LN, 13.05; LD, 8.5; LIF, 5.71; LM, 4.98; BIF, 2.33; BR, 5.39; BPB, 3.25; BM1, 1.58; BN, 4.02; LIB, 5.74; ZB, 15.68; RL, 11.8; BB, 13.86; BZP, 2.8; DI, 1.32; HBC, 9.2; MFB, 2.86; MN, 5.3. Measurements of additional specimens are provided in table 4.

Distribution: "*Thomasomys*" sp. 4 "Satipo" sp. nov. is distributed in the montane forest of Pampa Hermosa in Satipo from 2330 to 2472 m elevation.

Taxonomic Comparisons: "*Thomasomys*" sp. 4 "Satipo" differs from "*Thomasomys*" sp. 4 "Oxapampa" by its tips on its ventral pelage yellowish (vs. light gray tips); tail faintly bicolored with 23 scales/cm and long whitish hair on the scales (vs. bicolored tail with 21 scales/cm and short, dark hair on the scales); pencil tail shorter; digital ungual tuft longer; thenar of the manus larger than hypothenar (vs. subequal than hypothenar); thenar and hypothenar pads of the hind foot widely separated (vs. closer pads); digital pads of the foot less swollen; supercilliary vibrissae absent; anterior border of nasals triangular (vs. rounded); infraorbital foramen narrower; zygomatic notch deeper; zygomatic plate broader; subsquamosal fenestra larger than postglenoid foramen (vs. subequal to postglenoid foramen); maxillo-palatal suture surpasses the M2 anterior border (vs. reaches the

M2 anterior border); manubrium of malleus thinner; occipital condyle less swollen; coronoid process shorter; anteromedian flexus deeper; M1 mesoloph, M2 anteroloph, M2 mesoloph, and M3 anteroloph longer; m1 metaconid more massive; and m2 anterocingulum shorter.

"*Thomasomys*" sp. 4 "Satipo" differs from "*Thomasomys*" sp. 4 "Tarma" by its tips on its ventral pelage yellowish (vs. light gray tips). Tail with 23 scales per cm while "Tarma" has 21 scales per cm; hair on the scales of the tail longer and whitish (vs. short and dark); pencil tail longer whitish (vs. short and dark); digital pads in the foot less swollen; plantar skin of hind foot paler; supercilliary vibrissae absent; zygomatic notch deeper; zygomatic plate broader; incisive foramen shorter; palatal slightly straight or with a small median process (vs. slightly rounded); paraoccipital process smaller and broader; jugal shorter; maxillo-palatal suture surpasses M2 anterior border (vs. reaches M2 anterior border); orbicular apophysis of malleus larger; manubrium of malleus thinner; squamosal ridge shallow (vs. conspicuous); mandible ramus broader; anteromedian flexus deeper; M1 mesoloph, M2 anteroloph, M2 mesoloph, and M3 anteroloph longer; m1 metaconid less massive; m2 anterocingulum shorter; m2 ectolophid present; m2 ectostylid and m3 ectolophid absent.

Natural history: "*Thomasomys*" sp. 4 "Satipo" is sympatric with the sigmodontines *Akodon aerosus*, *A. josemariarguedasi*, *Akodon* cf. *torques*, *Microryzomys minutus*, *Necromys amoenus*, *Nephelomys keaysi*, *Thomasomys* aff. *aureus*, *Thomasomys* sp. D (Ruelas et al. 2024).

DISCUSSION

Thomasomys *complexity shading* "Thomasomys" *sp. 4 boundaries*

The challenge of identifying a genus within a group characterized by diverse morphology, such as the Thomasomyini, is often compounded by the extensive diversity and spectrum of morphological traits and sizes within the genus itself. The significant intraspecific variation, as noticed by Pacheco (2003, 2015) for *Thomasomys*, poses challenges in distinguishing between ancestral traits (plesiomorphies) and evolved/specialized ones (apomorphies) essential for recognizing and differentiating the related genera such as *Aepeomys*, *Chilomys*, "*Thomasomys*" sp. 4, and *Rhipidomys*, found within the expansive *Thomasomys* clade in a morphological phylogeny (Pacheco, 2003). In this scenario where related genera exhibit less diversity like *Aepeomys* or *Chilomys* or "*Thomasomys*" sp. 4, their distinctive morphological traits risk being overshadowed or confused with the variable characteristics present in *Thomasomys*. The morphological convergence or similarity heightens the difficulty of establishing clear taxonomic boundaries (see Pacheco, 2015). Moreover, the wide array of morphological forms within a single genus may result in an undue emphasis on certain morphological characteristics, diminishing their diagnostic value at the intergeneric level. Consequently, the uniqueness of less diverse sister genera could be obscured, underlining the need for a refined taxonomic approach to accurately delineate genus and species relationships. For instance, the upper incisor in *Aepeomys* is slightly opisthodont, in *Chilomys* it is proodont or orthodont, and in *Rhipidomys*, it is opisthodont. In *Thomasomys*, all three states are present (orthodont, opisthodont, proodont).

Supraorbital ridges present in *Rhipidomys* are usually absent in *Thomasomys* but present in some species of the Aureus group. The rostrum of *Chilomys* is short, usually long in most *Thomasomys* species, but notably short in *T. andersoni*, *T. oreas,* and *T. notatus*. Genal vibrissae 1 is absent in *Aepeomys* and usually present in *Thomasomys* but absent in *T. macrotis*, *T. caudivarius*, *T. erro*, *T. incanus*, *T. laniger*, *T. paramorum*, and polymorphic (absent/present) in populations of *T. baeops*, *T. cinereus*, and *T. cinnameus* (Pacheco, 2003).

Being so morphologically diverse, *Thomasomys* was confirmed as monophyletic (fig. 2, appendix 5, appendix 6), consistent with prior research (e.g., Brito et al., 2019; Pacheco & Ruelas, 2023; Parada et al., 2013; Ruelas et al., 2024), and its major clades align with the findings of Ruelas et al. (2024), which categorize species into species groups (sensu Pacheco, 2015) such as Notatus (*T. notatus*), Gracilis (*T. oreas*, *Thomasomys* sp. 8 (sensu Pacheco, 2003)), Baeops (*T. taczanowskii*), Cinereus (*T. australis*, *T. daphne*, *T. cinereus*, *T. lojapiuranus*, *T. shallqukucha*), Aureus "Western" (*T. praetor*, *T. pyrrhonotus*, *T.* cf. *pyrrhonotus*), Aureus "Eastern" (*T.* cf. *apeco*, *T.* aff. *aures*, *Thomasomys* sp. 1 (sensu Pacheco, 2003), and Incanus (*T. ischyrus*, *Thomasomys* sp. 6 (sensu Pacheco, 2003), *T.* aff. *kalinowskii*, *T. incanus*, *Thomasomys* cf. *incanus*, *Thomasomys* sp. A (sensu Ruelas et al. 2024)). Ruelas et al. (2024) found Cinereus monophyletic but weakly supported. Here, the well-supported monophyly of this group might be influenced by limited sampling, with many species from Bolivia, Colombia, and Ecuador not represented. Furthermore, the Aureus "Eastern" and Aureus "Western" groups were found paraphyletic in all analyses. Yet, the relationships within the Incanus group remain unresolved, with some clades potentially being paraphyletic (figs. 2, 3). This

complexity underscores the need for further research within *Thomasomys*, leveraging both morphological and genetic data to refine our understanding of its taxonomy and diversity.

Pacheco (2003) identified "*Thomasomys*" sp. 4 as the sister of *Thomasomys* sp. 5 within a clade containing also *Aepeomys* and other members of the Incanus group. *Thomasomys* aff. *incanus* of Ruelas et al. (2024) is likely *Thomasomys* sp. 5, although it was not molecularly assessed here, turbinal morphology of this taxon is complex, yet not as complex and scrolled as that of "*Thomasomys*" sp. 4. This pattern is the same when comparing with the other members of the Incanus group (fig. 6; Ruelas et al., in prep.: figure 2). Our analyses confirm several morphological traits identified by Pacheco (2003) in "*Thomasomys*" sp. 4 that align with *Thomasomys* s.s. including a protuberant anus, genal 1 vibrissae absent, short palate, anterior process of ectotympanic small, carotid circulation pattern 2, hypoflexus of M1 narrow, protoflexus on M2 faint or absent. However, although scored by Pacheco (2003), penis' characters such as preputial glands absent, crater rim of glans penis multiply divided, and notch on midventral crater margin absent were not checked yet. Furthermore, Pacheco (2003) also identified unique traits for "*Thomasomys*" sp. 4, which allowed him to identify it as a candidate species. Notably, he observed a distinctly bicolored tail, with a dark dorsal surface contrasting sharply with a pale ventral surface, but our examination indicates this trait is specific to "Oxapampa" specimens, since "Tarma" and "Satipo" specimens exhibit only faintly bicolored tails. We agree with Pacheco's observation of the fifth digit's moderately elongated and the positioning of the claw of digit V, traits also found in *Aepeomys*, *Thomasomys dispar*, and *T. erro*. Furthermore, we confirm

Pacheco's finding of a broad zygomatic plate, exceeding the length of M1. The orbital branch of the internal carotid artery's exposure in the parapterygoid fossa, a trait shared with other thomasomyines like *Chilomys instans* and *T. incanus*. The distributional gastric epithelium intermediate I, particularly the fold crossing the lesser curvature between the pyloric sphincter and the incisura angularis, is also shared with *T. eleusis*, *T. kalinowskii*, and *Thomasomys* sp. 5 (sensu Pacheco, 2003) and *Thomasomys* sp. 7 (sensu Pacheco, 2003). However, we noted this character only in "Oxapampa" and "Tarma". Lastly, the absence of the gall bladder, consistent with *Rhipidomys*, *Rhagomys*, and most *Thomasomys* species but distinct from *T. oreas*, reaffirms the complex morphological spectrum within *Thomasomys* and its relatives.

The Thomasomyini tribe composition and taxonomic inflation

The delineation of tribes, particularly within the Sigmodontinae, could appear arbitrary and largely depends on the authors' discretion. Although there are no strict rules dictating the composition of a tribe in terms of its members and limits, pragmatically, tribes are expected to be monophyletic, exhibit a "barcoding gap" relative to other tribes, and be unified by a set of synapomorphies, which need not be exhaustive but can clearly define the group. Early taxonomists primarily relied on morphological similarities to group genera, leading to initial classifications and diversification hypotheses. These early classifications resulted in the formation of informal groups like the "thomasomyines," "phyllotines," "akodontines," and others, aiming to enhance the understanding of the interrelationships among these genera, albeit within the confines of morphological characteristics (e.g., Carleton,

1973; Hershkovitz, 1962, 1966). Many of these informal groups – better defined and properly named under the ICZN (1999) – are currently accepted as valid tribes and supported by both morphological and molecular evidence, resulting in monophyletic clades sharing morphological traits (e.g., Pardiñas et al., 2020; Smith & Patton, 1999).

The approach to group genera based on molecular monophyly is a more recent development in sigmodontines (e.g., D'Elía et al., 2006; Smith & Patton, 1991, 1993, 1999), yet it slightly retains the essence of simplifying classifications to better understand evolutionary processes and diversification, favoring coherent groupings over fragmentation. Genetic evidence is increasingly influential in taxonomic decisions, as numerous studies have shown (e.g., Gonçalves et al., 2020; Pardiñas et al., 2015). Morphological variability within a group should be understood as part of the lineage's success and can often be explained as an aspect of adaptation (e.g., Martinez et al., 2018, 2020; Schüßler et al., 2024; Sharov, 2014). Morphological disparities observed among genera or species in the same clade or cluster could represent evolutionary divergence due to adaptation to distinct ecological niches or geographical isolation (e.g., Pardiñas et al., 2022, Coelho et al., 2023). Conversely, similarities across genera in different groups may be attributed to morphological convergence where unrelated species evolve similar traits due to similar environmental pressures (e.g., Stayton, 2008; Losos, 2011; Martinez et al., 2018). The genetic perspective is crucial in contemporary taxonomy, providing insights that complement and sometimes challenge morphological assessments, thereby refining our understanding of the evolutionary relationships within the Sigmodontinae subfamily. However, there is a noticeable

trend in sigmodontinae taxonomy to limit morphological diversity at higher taxonomic levels such as tribes (e.g., Pardiñas et al., 2020, 2021, 2022). The evolutionary histories of each group or lineage vary, a fact that becomes evident in molecular analyses where mitochondrial genes mutate more rapidly than nuclear ones (Brown et al., 1979, 1982) showing usually different relationships at higher and lower levels (e.g., Parada et al., 2015; Steppan et al., 2005; Steppan & Schenk, 2017). Grouping genera implies not only the existence of synapomorphies but also a common evolutionary history.

Recognition of single-genus tribes in taxonomy, though accepted, is not inherently necessary or beneficial, and often leads to unwarranted taxonomic inflation, complicating mainly scientific communication and education. This inflation, driven by speculative ideas about past diversity or future diversification, disrupts traditional established tribes with solid molecular and morphological backing, creating monotypic tribes based on mere morphological distinctions, the same as those which define the genus. The artificial taxonomic boundaries and incomplete representation are two major problems with defining single-genus-based tribes. Phylogenetic inconsistencies, misleading synapomorphies, and decreased classification robustness might result from it. Such an approach also risks inaccurately defining the "barcoding gap" between tribes, leading to ambiguities in genetic markers. Overall, single-genus-based tribes undermine the accuracy and clarity of taxonomic classifications, misrepresenting evolutionary relationships and limiting the diversity within rodent groups. In contrast, a conservative taxonomic approach for these cases, which prioritizes stability, clarity, and biological significance, offers substantial benefits across scientific disciplines. It focuses on

meaningful biological differences and prevents the overemphasis on trivial differences, crucial for understanding evolutionary biology and phylogenetics. Such an approach ensures efficient resource allocation in research and better integration across various disciplines, accurately reflecting evolutionary relationships and supporting a comprehensive understanding of biodiversity and evolution.

The case of the Akodontini tribe – containing the monotypic and largest alive sigmodontine *Kunsia* and the third most diverse genus *Akodon* and widely distributed (Brandão et al., 2022; D'Elía & Pardiñas, 2015)– or Oryzomyini tribe – being the most diverse tribe with 31 genera (Brito et al., 2020; Weksler, 2006, 2015)–, with their wide morphological diversity and monophyly also supported by multiple morphological traits, exemplifies the effectiveness of a conservative approach. Akodontines and oryzomyines are two rich groups in general body morphology, dietary habits, and life habits (D'Elía & Pardiñas, 2015; Weksler, 2006, 2015). However, a possible fragmentation of the Akodontini has been recently in debate (e.g., Pardiñas et al., 2021). A conservative approach in mammalian taxonomy, particularly within sigmodontine radiation, is advocated by several studies, the challenges in classifying sigmodontine genera (D'Elía et al., 2006; Salazar-Bravo et al., 2013), and the call for a paradigm shift focusing on phylogenetic lineages (Padial & De la Riva, 2021). Such perspectives highlight the need for cautious and evidence-based taxonomy, especially in the complex sigmodontine realm. This approach also avoids the pitfalls of taxonomic inflation, which often leads to an excessive proliferation of taxonomic categories based on limited data, thus posing challenges in understanding evolutionary relationships and

in the scientific validation of classifications. On the other hand. while comparing the diversity of genera and tribes among subfamilies can be a fruitful exercise for a better understanding of taxonomic diversity (e.g., Pardiñas et al. 2021), it does not imply that a group with more species or genera is necessarily underestimated, or another is overestimated. For instance, comparing the diversity of *Thomasomys*, with 51 valid species, to that of *Aepeomys* or *Microryzomys*, each with just two valid species (Carleton, 2015; Carleton & Musser, 1989; Pacheco, 2015b; Pacheco & Ruelas, 2023), does not suggest an overestimation of *Thomasomys*. Or comparing the diversity in Oryzomyini versus Abrothrichini. Therefore, while taxonomic detailing is important for cataloging biodiversity, a more conservative and evidence-based approach is imperative for maintaining clarity and effectiveness in taxonomy. And most importantly, it allows us to understand the diversification and evolutive patterns of these groups in a wider sense.

The classification and composition of the Thomasomyini tribe, even before its formal establishment, have been subjects of ongoing debate and revision by several authors. Primarily, Hershkovitz (1962, 1966) informally grouped several pentalophodont taxa (including *Aepeomys*, *Chilomys*, *Delomys*, *Phaenomys*, *Rhagomys*, *Rhipidomys*, and *Thomasomys*) within the Oryzomyini tribe, characterizing them as "forest dwelling, broad footed, long tailed, 6-mammate, brachydont-pentalophodont mice with a wide-short palate and weakly projecting zygomatic plate." He noted, crucially, that these shared traits might be ancestral, rather than indicative of close evolutionary relationships. Then Steadman and Ray (1982) formally described the tribe, including *Megaoryzomys* – an extinct giant rat –, *Thomasomys*, and *Rhipidomys*, based on the combination of short palates and

medium to large pentalophodont molars. Subsequent studies, such as those by Cerqueira (1982), Eisenberg and Redford (1999), and McKenna and Bell (1997), added or removed genera from the tribe, reflecting the ongoing uncertainty in its composition. Voss (1993) further questioned the validity of the tribe as a natural group, suggesting the genera be recognized as an assemblage of "pleisiomorphic Neotropical muroids." Pacheco (2003), and later Pacheco et al. (2015), significantly influenced the understanding of the tribe. Through cladistic analysis, Pacheco (2003) identified a monophyletic Thomasomyini, comprising 11 genera, supported by ten distinct traits. He delineated an "Andean thomasomyine clade" (including *Aepeomys*, *Chilomys*, *Rhipidomys*, and *Thomasomys*) and linked six other genera from southeastern Brazil (*Abrawayaomys*, *Juliomys*, *Phaenomys*, *Rhagomys* – also Andean–, *Wiedomys*, and *Wilfredomys*) to this group. Pacheco et al. (2015) refined the tribe to include only the "Andean thomasomyine clade" plus *Rhagomys*, based on both morphological and molecular evidence that were available until that date (e.g., D'Elía et al., 2006; Smith & Patton, 1999). This redefinition left other previously included species as Sigmodontinae incertae sedis, such as *Abrawayaomys*, *Delomys*, and *Juliomys*, and found in recent revisions closer other tribes (e.g., Steppan & Schenk, 2017; Ventura et al., 2013). Early molecular studies have supported the "Andean thomasomyine clade." For instance, D'Elía (2006) found that *Rhagomys* and *Thomasomys* as sister clades within the Thomasomyini, placing *Rhipidomys* at the base. This finding was corroborated by Salazar-Bravo et al. (Parada et al., 2013) and Parada et al. (2015), who further confirmed the close relationship between *Rhagomys* and *Thomasomys*, still with *Rhipidomys* at the base. Steppan and Schenck et al. (2017) expanded on this, identifying Thomasomyini,

including *Rhagomys* with *Aepeomys* at the base, as one of the twelve major branches of the Sigmodontinae family, consolidating their placement. Recently, the tribe's composition faced further scrutiny. Pardiñas et al. (2022) described a new tribe exclusive for *Rhagomys* based on its morphological uniqueness, although the existing molecular evidence suggests *Rhagomys* closely related to the other genera included in the Thomasomyini. This proposition aimed to maintain the diagnostic clarity of Thomasomyini, arguing that including *Rhagomys* diluted the tribe's distinctiveness. However, this view contrasts with Ruelas et al. (2024), who, through unilocus analyses, found *Rhagomys* nested within the Thomasomyini clade and sister of "*Thomasomys*" sp. 4. Our results, although with different topologies, support the close phylogenetic relationship of *Rhagomys* and Thomasomyini and align with the findings of Ruelas et al. (2024) and Pardiñas et al. (2022).

In light of the evidence, this and previous studies showed that Rhagomyini is not always sister of Thomasomyini, but Thomasomyini containing *Rhagomys* – whether basal, sister to another genus, or unresolved (fig. 2, appendix 5, appendix 6)– is always monophyletic, thus supporting the initial proposal by D'Elía et al. (2006) and Pacheco et al. (2015). In consequence, we consider *Rhagomys* should be retained as part of the Thomasomyini tribe. Therefore, we propose retaining *Rhagomys* within the Thomasomyini tribe, acknowledging the complexities this entails for maintaining the tribe's prior composition. For instance, the relationship of *Rhagomys* within the tribe has been clouded by limited and poor-quality material (Pardiñas et al. 2022), a difficulty also encountered in *Aepeomys*, another tribe member. This scarcity of data may result in an incomplete phylogenetic tree. *Aepeomys*, represented in early molecular studies by only a single nuclear sequence

(D'Elía et al., 2006), often lacks presence in mitochondrial analyses but shows distinctive morphological features compared to other thomasomyines, like a rostral tube and a prominent masseteric tubercle (see figs. 3, 5, table 3). The basal position of *Aepeomys* within the Thomasomyini clade in the mitochondrial analyzes is essential in defining the tribe composition, affirming the inclusion of *Rhagomys*.

With the addition of *Rhagomys* to Thomasomyini, two options emerge for the detailed description made by Pardiñas et al. (2022) which support the *Rhagomys*' morphological differences respect to other genera of the tribe. The first, less parsimonious option, proposes two subtribes: Rhagomyina and Thomasomyina. Here, Pardiñas et al.'s (2022) description of the Rhagomini would form the basis for the new Rhagomina subtribe, while their Thomasomyini concept would define the Thomasomyina subtribe. However, the composition of Thomasomyina would not be completely clear. Considering monophyly and synapomorphies, this subtribe could include only *Thomasomys* and *Rhypidomys* or in the strictest case, only *Thomasomys*. This outlook could suggest that, in view of the unresolved relationships of the other members of the tribe, each genus could be included in a monotypic subtribe. However, as we explained before, it generates more unnecessary inflation in the taxonomical grouping. The second, more conservative option, advocates for interpreting Pardiñas et al.'s (2022) detailed account of *Rhagomys* not as the foundation for a new subtribe, but rather as a thorough redescription of the *Rhagomys* genus itself. This perspective avoids unnecessary expansion of taxonomic categories and maintains a streamlined classification system. Given the considerations of monophyly and synapomorphies,

this latter approach is deemed more suitable for integrating *Rhagomys* within the Thomasomyini without complicating the tribe's taxonomic structure unnecessarily.

Comments on biogeography in the Tropical Andes

The study of global and regional disparities in species diversity, especially the debate on the latitudinal gradient of diversity, is a cornerstone of evolutionary biology (Jablonski et al., 2006; Mittelbach et al., 2007). While the Andes are renowned as a center for biodiversity and endemism (Orme et al. 2005), yet the significance of the Tropical Andes or Moist north-central Andes (Josse et al., 2003; Kelt & Meserve, 2014), encompassing montane forests and páramo, is frequently overlooked in biogeographical studies. This region is even more diverse than the highest Andean habitats, in the Central and Southern Andes, like the dry puna (Chazot et al., 2016, 2018; Patterson et al., 2012). Montane forests and paramos, distributed in the Northern and northeastern Central Andes, play a critical role in the evolution of South American fauna, exhibiting a unique hump-shaped pattern of species richness along elevation and latitudinal gradients (Patterson et al., 2012; Young, 1992; Young & León, 1999). This pattern highlights the critical need to account for regional geographical and climatic differences when analyzing Andean biodiversity and ecosystems.

Through detailed morphological and molecular analyses, we have uncovered a new genus endemic to the Tropical Andes mainly distributed in the montane forests, introducing three novel species: "Oxapampa," "Satipo," and "Tarma." This discovery adds to the list of rodent genera endemic to the Tropical Andes, such as *Aepeomys*, *Anotomys*, *Chibchanomys*, *Chilomys*, *Eremoryzomys*,

Handleyomys, *Lenoxus*, *Microryzomys*, *Neomicroxus*, *Nephelomys*, *Oreoryzomys*, *Pattonimus*, *Tapecomys*, and *Thomasomys* (Alvarado- Serrano & D'Elía, 2015; Brito et al., 2020, 2022; Carleton, 2015; Gómez- Laverde et al., 2015; Pacheco, 2015b, 2015a; Pacheco & Ruelas, 2023; Patton, 2015; Percequillo, 2015a, 2015b; Ruelas et al., 2021; Salazar-Bravo, 2015; Uturunco & Pacheco, 2016; Voss, 2015). The significant presence of endemic genera and species in the Tropical Andes highlights their important role in determining sigmodontine rodents' biogeographical patterns. These kinds of habitats reach peak diversity at mid to high elevations due to their varied physiographic diversity, which fosters an environment conducive to hyper-diversification (Rickart et al., 2011; Vieu et al., 2022). This is particularly evident in the *Thomasomys* species, which exhibit their highest diversity between elevations of 2000 to 3500 m (Ruelas et al. 2024).

Between the Northern and Central Andes, the Huancabamba depression marks the limit between both sections (Duellman & Pramuk, 1999). This depression, alongside the Marañón zone (Marañón valley and river), plays a critical role in shaping the montane forests in the northwestern of Peru by facilitating the penetration of Amazonian moisture to the western slopes, supporting the presence of montane forest specialized species such as *Thomasomys taczanowskii*, *T. pyrrhonotus*, *T. pagaibambensis*, among others, in areas close to arid zones (Pacheco, 2015b). The combined influence of this distinct geography and the Marañón zone significantly drives biogeographical processes and species diversification within the region. Ruelas et al. (2024) and previous authors (e.g., Hurtado & Pacheco, 2017; Pacheco, 2015b; Ruelas et al., 2021) have highlighted the role in the diversification of this region for the *Thomasomys* groups and species

and some sigmodontines. Within the Thomasomyini tribe, *Aepeomys* and *Chilomys* occur in the Northern Andes. *Thomasomys*, on the other hand, occurs across the Northern and Central Andes. While *Rhipidomys* and *Rhagomys* have some species in both Andean sections. The geographical and environmental uniqueness of the Northern Andes, characterized by their youth, lower elevation, and narrowness, supports diverse montane forests and paramos along the cordillera. In contrast, the Central Andes, with montane forests, named also Yungas, predominantly on the eastern side and at higher elevations (Young, 1992; Young & León, 1999)are important for the diversity of the *Thomasomys* genus, particularly for species within the Incanus group (Pacheco, 2015c)). This region's unique environmental conditions are key in fostering distinctive species and morphological characteristics. The inclusion of "*Thomasomys*" sp. 4 as part of the Incanus group's clade (Pacheco, 2003) highlights shared evolutionary traits between them, pointing to significant synapomorphies. Intriguingly, the group also included *Aepeomys*, suggesting notable morphological convergence among these taxa. Such convergence might represent an adaptive morphological strategy developed to thrive in the cooler temperature characteristic of high-elevation habitats. This adaptation is notably evidenced in the more scrolled and complex structure of their turbinals (see fig. 6; Ruelas et al., in prep.). This underscores the Central Andes' important role in shaping the evolutionary paths of these sigmodontine rodents, further supporting the region's critical contribution to the speciation and morphological diversification of the Thomasomyini.

The representation of both sections of the Tropical Andes, Northern and Central, in biogeographical studies in small mammals tends to be minimal and often

overshadowed by more generalized, large-scale approaches. Typically, montane forests and paramos are included in broader regional analyses as part of the Northern and whole Central Andes, despite their extensive range. This approach, which treats these diverse areas as a singular large unit (e.g., Hurtado & D'Elía, 2022; Vallejos-Garrido et al., 2023), or in the division of the Northern and Central Andes and Altiplano (Schenk & Steppan, 2018), can lead to an underestimation of the unique biodiversity and ecological dynamics specific to both sections of the Tropical Andes and diminish its importance in the colonization process of the Andes. Our molecular analyses, though not explicitly focused on biogeographic analysis, allow us to draw inferences about the colonization history of the Andes by the Thomasomyini tribe. The divergent tree topologies from mitochondrial and nuclear phylogenies offer contrasting insights into the colonization history of the Andes by the Thomasomyini tribe (figs. 2, 3). The mitochondrial phylogeny positions the Andean genus *Aepeomys* as basal (fig. 2), suggesting it was the first thomasomyine to colonize the Andes, with subsequent dispersal and colonization of the Amazon basin by other genera. Conversely, the nuclear and concatenated phylogeny places *Rhagomys* at the base or unresolved, indicating a more complex colonization pattern. Given presence of *Rhagomys* in the Brazilian Atlantic Forest and the montane forests of Peru and Ecuador, this suggests a more complex series of dispersal and colonization events. The presence of *Rhagomys* in such geographically and ecologically diverse regions implies multiple colonization events or a broad ancestral range that has since fragmented. These contrasting phylogenetic insights highlight the complexity of evolutionary histories within the Thomasomyini tribe.

To understand Andean colonization fully, it is crucial to recognize both sections of the Tropical Andes as a key factor in assessing the Andes' impact on the Thomasomyini diversification. The diversity patterns across the Andes' elevational range are markedly varied, with puna-specialized rodents exhibiting lower diversity compared to their counterparts in montane forests and paramos, who often have more restricted ranges (Patton et al., 2015). High-elevation habitats drive speciation and endemism due to the Andes' complex topography and climate (Patterson et al., 1992; Voss, 2003). Montane forests harbor higher Thomasomyini diversity, providing microenvironments conducive to speciation (Brito et al., 2019; Pacheco & Ruelas, 2023). The Andes act as both barriers and corridors for gene flow, influencing genetic structure and diversification (Schenk & Steppan, 2018). Additionally, beta diversity patterns in Andean rodents, influenced by historical and current factors, drive turnover and nestedness (Novillo et al., 2024). Furthermore, the distribution of sigmodontines is also significantly shaped by deep rivers such as the Rio Marañón, Rio Apurimac, and Rio Huallaga (e.g., Hurtado & Pacheco, 2017; Pacheco, 2015b; Ruelas et al., 2024). Utilizing an expanded set of nuclear genes and refined regional categorization of the Tropical Andes will enhance our grasp of the biogeographical and evolutionary forces that have driven the current distribution and diversity of the Thomasomyini.

ACKNOWLEDGMENTS

We thank Maria Peralta, Elena Vivar, Sergio Solari, Carlos Jiménez, Betsy Inche, Elizabeth Escobar, Diego Marcelo, Andderson Solis, J. Sanchez, Anthony Almeyda, Jose L. Mena, Lucia Luna, and other colleagues for collecting the

specimens and tissues used here. We thank Rafael Lecaros for his help measuring specimens and taking photos. We also thank Rob Voss from the America Museum of Natural History (AMNH, New York), Adam Ferguson and Bruce Patterson from the Field Museum of Natural History (FMNH, Chicago), for facilitating DR access to the mammal collection; Roberto Portela Miguez for sharing with us the photographs of the holotypes of *Thomasomys* housed at The Natural History Museum (NHM, London) and for facilitating DR access to the mammal collection; and Marie-Ka Tilak (Université de Montpellier, France) for helping us in the obtention of the sequences. We thank the *platform GenSeq* from LabEx CeMEB (Montpellier) for DNA extraction facilities, and especially Erick Desmarais et Frédérique Cerqueira for their help and time. 3D-data acquisitions were performed using the µ-CT facilities of the MRI platform member of the national infrastructure France-BioImaging supported by the French National Research Agency (ANR-10-INBS-04, «Investments for the future»), and of the Labex CEMEB (ANR-10-LABX-0004) and NUMEV (ANR-10-LABX-0020). We would like to thank Frédéric Delsuc for his help and support concerning this project on *Thomasomys*. DR was supported by a scholarship of the Franco Peruvian School of Life Sciences. This study was partially funded by CONCYTEC through the PROCIENCIA program in the framework of the "Proyectos de Investigación Básica 2023-01" contest, according to the contract No. PE501078825; the 2022 Collection Study Grant given by AMNH to DR.

REFERENCES

Allio, R., Delsuc, F., Belkhir, K., Douzery, E. J. P., Ranwez, V., & Scornavacca, C. (2024). OrthoMaM v12: A database of curated single-copy ortholog alignments

and trees to study mammalian evolutionary genomics. *Nucleic Acids Research*, *52*(D1), D529–D535. https://doi.org/10.1093/nar/gkad834

Allio, R., Schomaker-Bastos, A., Romiguier, J., Prosdocimi, F., Nabholz, B., & Delsuc, F. (2020). MitoFinder: Efficient automated large-scale extraction of mitogenomic data in target enrichment phylogenomics. *Molecular Ecology Resources*, *20*(4), 892–905. https://doi.org/10.1111/1755-0998.13160

Alvarado- Serrano, D. F., & D'Elía, G. (2015). Genus *Neomicroxus* Alvarado-Serrano and D'Elía, 2013. In J. L. Patton, U. F. J. Pardiñas, & G. D'Elía (Eds.), *Mammals of South America. Volume 2, Rodents* (pp. 96–99). The University of Chicago Press.

Bivand, R., & Lewin-Koh, N. (2023). *Tools for Handling Spatial Objects*. http://maptools.r-forge.r-project.org/

Borisenko, A. V., Lim, B. K., Ivanova, N. V., Hanner, R. H., & Hebert, P. D. N. (2008). DNA barcoding in surveys of small mammal communities: A field study in Suriname. *Molecular Ecology Resources*, *8*(3), 471–479. https://doi.org/10.1111/j.1471-8286.2007.01998.x

Brack, A. (1987). *Plan Maestro del Parque Nacional Yanachaga-Chemillén* (p. 176). USAID/PEPP.

Brandão, M. V., Carmignotto, A. P., Percequillo, A. R., Christoff, A. U., Mendes-Oliveira, A. C., & Geise, L. (2022). A new species of *Akodon* Meyen, 1833 (Rodentia: Cricetidae) from dry forests of the Amazonia-Cerrado transition. *Zootaxa*, *5205*(5), Article 5. https://doi.org/10.11646/zootaxa.5205.5.1

Brito, J., Koch, C., Percequillo, A. R., Tinoco, N., Weksler, M., Pinto, C. M., & Pardiñas, U. F. J. (2020). A new genus of oryzomyine rodents (Cricetidae,

Sigmodontinae) with three new species from montane cloud forests, western Andean cordillera of Colombia and Ecuador. *PeerJ*, *8*, e10247. https://doi.org/10.7717/peerj.10247

Brito, J., Tinoco, N., Chávez, D., Moreno-Cárdenas, P., Batallas, D., & Ojala-Barbour, R. (2017). New species of arboreal rat of the genus *Rhipidomys* (Cricetidae, Sigmodontinae) from Sangay National Park, Ecuador. *Neotropical Biodiversity*, *3*(1), 65–79. https://doi.org/10.1080/23766808.2017.1292755

Brito, J., Tinoco, N., Curay, J., Vargas, R., Reyes-Puig, C., Romero, V., & Pardiñas, U. F. J. (2019). Diversidad insospechada en los Andes de Ecuador: Filogenia del grupo "cinereus" de *Thomasomys* y descripción de una nueva especie (Rodentia, Cricetidae). *Mastozoología Neotropical*, *26*(2), 308–330. https://doi.org/10.31687/saremMN.19.26.2.0.04

Brito, J., Tinoco, N., Pinto, C. M., García, R., Koch, C., Fernandez, V., Burneo, S., & Pardiñas, U. F. J. (2022). Unlocking Andean sigmodontine diversity: Five new species of *Chilomys* (Rodentia: Cricetidae) from the montane forests of Ecuador. *PeerJ*, *10*, e13211. https://doi.org/10.7717/peerj.13211

Brito, J., Vaca-Puente, S., Koch, C., & Tinoco, N. (2021). Discovery of the first Amazonian *Thomasomys* (Rodentia, Cricetidae, Sigmodontinae): A new species from the remote Cordilleras del Cóndor and Kutukú in Ecuador. *Journal of Mammalogy*, *102*(2), 615–635. https://doi.org/10.1093/jmammal/gyaa183

Brown, W. M., George, M., & Wilson, A. C. (1979). Rapid evolution of animal mitochondrial DNA. *Proceedings of the National Academy of Sciences*, *76*(4), 1967–1971. https://doi.org/10.1073/pnas.76.4.1967

Brown, W. M., Prager, E. M., Wang, A., & Wilson, A. C. (1982). Mitochondrial DNA sequences of primates: Tempo and mode of evolution. *Journal of Molecular Evolution*, *18*, 225–239.

Campos, B. A. T. P., Percequillo, A. R., Miranda, G., & Langguth, A. (2022). Two new species of *Rhipidomys* (Rodentia: Sigmodontinae) from eastern Brazil, with comments on the taxonomy of the genus. *Hystrix, the Italian Journal of Mammalogy*. https://doi.org/10.4404/hystrix-00443-2021

Carleton, M. D. (1973). A survey of gross stomach morphology in New World Cricetinae (Rodentia, Muroidea), with comments on functional interpretations. *Micellaneous Publications Museum of Zooology, University of Michigan*, *146*, 1–43.

Carleton, M. D. (1980). Phylogenetic relationships in neotomine-peromyscine rodents (Muroidea) and a reappraisal of the dichotomy within New World Cricetinae. *Miscellaneous Publications Museum of Zoology, University of Michigan*, *157*, 1–146.

Carleton, M. D. (2015). Genus *Microryzomys* Thomas, 1917. In J. L. Patton, U. F. J. Pardiñas, & G. D'Elia (Eds.), *Mammals of South America. Volume 2, Rodents* (pp. 355–359). The University of Chicago Press.

Carleton, M. D., & Musser, G. G. (1989). Systematic studies of oryzomyine rodents (Muridae, Sigmodontinae): A synopsis of *Microryzomys*. *Bulletin of the American Museum of Natural History*, *191*, 1–83.

Catchpole, D. (2012). *Orographic gradients in climate and forest cover at the Cordillera Yanachaga, Peru* [Ph.D. Thesis, University of Tasmania]. eprints.utas.edu.au/15897/

Cerqueira, R. (1982). South American landscapes and their mammals. In M. A. Mares & H. H. Genoways (Eds.), *Mammalian biology in South America. Pymatuning Laboratory of Ecology* (pp. 53–75).

Chazot, N., De-Silva, D. L., Willmott, K. R., Freitas, A. V. L., Lamas, G., Mallet, J., Giraldo, C. E., Uribe, S., & Elias, M. (2018). Contrasting patterns of Andean diversification among three diverse clades of Neotropical clearwing butterflies. *Ecology and Evolution*, *8*(8), 3965–3982. https://doi.org/10.1002/ece3.3622

Chazot, N., Willmott, K. R., Condamine, F. L., de-Silva, D. L., Freitas, A. V. L., Lamas, G., Morlon, H., Giraldo, C. E., Jiggins, C. D., Joron, M., Mallet, J., Uribe, S., & Elias, M. (2016). Into the Andes: Multiple independent colonizations drive montane diversity in the Neotropical clearwing butterflies *Godyridina*. *Molecular Ecology*, *25*(22), 5765–5784. https://doi.org/10.1111/mec.13773

Chen, S., Zhou, Y., Chen, Y., & Gu, J. (2018). fastp: An ultra-fast all-in-one FASTQ preprocessor. *Bioinformatics*, *34*(17), i884–i890. https://doi.org/10.1093/bioinformatics/bty560

Chernomor, O., von Haeseler, A., & Minh, B. Q. (2016). Terrace aware data structure for phylogenomic inference from supermatrices. *Systematic Biology*, *65*(6), 997–1008. https://doi.org/10.1093/sysbio/syw037

Coelho, F. E. A., Camurugi, F., & Garda, A. A. (2023). The roles of niche divergence, dispersal, and geology on the diversification of Neotropical true frogs from the *Rana palmipes* species group (Amphibia, Anura, Ranidae) during the Great American Biotic Interchange. *Organisms Diversity & Evolution*, *23*(4), 967–981. https://doi.org/10.1007/s13127-023-00619-6

D'Elía, G., Luna, L., González, E. M., & Patterson, B. D. (2006). On the Sigmodontinae radiation (Rodentia, Cricetidae): An appraisal of the phylogenetic position of *Rhagomys*. *Molecular Phylogenetics and Evolution*, *38*(2), 558–564. https://doi.org/10.1016/j.ympev.2005.08.011

D'Elía, G., & Pardiñas, U. F. J. (2015). Tribe Akodontini Vorontsov, 1959. In J. L. Patton, U. F. J. Pardiñas, & G. D'Elía (Eds.), *Mammals of South America. Volume 2, Rodents* (pp. 291–465). The University of Chicago Press.

Duellman, W. E., & Pramuk, J. B. (1999). Frogs of the genus *Eleutherodactylus* (Anura: Leptodactylidae) in the Andes of northern Peru. *Scientific Papers*, *13*, 1–78.

Edgar, R. C. (2004). MUSCLE: Multiple sequence alignment with high accuracy and high throughput. *Nucleic Acids Research*, *32*(5), 1792–1797. https://doi.org/10.1093/nar/gkh340

Eisenberg, J. F., & Redford, K. H. (1999). *Mammals of the Neotropics: Vol. Volume 3, the Central Neotropics: Ecuador, Perú, Bolivia, Brazil*. University of Chicago Press.

García, F. J., Almeida, T. G., Machado, M., Delgado-Jaramillo, M. I., Araujo-Reyes, D., Vásquez-Parra, O., & Flórez, G. (2020). Description of a new species of arboreal rat of the *Rhipidomys fulviventer* group, from Venezuela (Rodentia: Cricetidae). *Anartia*, *30*, Article 30.

Gómez- Laverde, M., Voss, R. S., & Pacheco, V. (2015). Genus *Handleyomys* Voss, Gómez- Laverde, and Pacheco, 2002. In J. L. Patton, U. F. J. Pardiñas, & G. D'Elía (Eds.), *Mammals of South America. Volume 2, Rodents* (pp. 321–323). The University of Chicago Press.

Gonçalves, P. R., Christoff, A. U., Machado, L. F., Bonvicino, C. R., Peters, F. B., & Percequillo, A. R. (2020). Unraveling deep branches of the sigmodontinae tree (Rodentia: Cricetidae) in eastern South America. *Journal of Mammalian Evolution*, *27*(1), 139–160. https://doi.org/10.1007/s10914-018-9444-y

Hershkovitz, P. (1962). Evolution of neotropical cricetine rodents (Muridae) with special reference to the phyllotine group. *Fieldiana: Zoology*, *46*, 1–524. https://doi.org/10.5962/bhl.title.2781

Hershkovitz, P. (1966). South American swamp and fossorial rats of the Scapteromyine group (Cricetinae, Muridae) with comments on the glans penis in murid taxonomy. *Zeitschrift Für Säugetierkunde*, *31*, 82–149.

Hershkovitz, P. (1994). The description of a new species of South American hocicudo, or long-nose mouse, genus Oxymycterus (Sigmodontinae, Muroidea), with a critical review of the generic content. *Fieldiana: Zoology. New Series*, *79*, 1–43.

Hurtado, N., & D'Elía, G. (2022). Historical biogeography of a rapid and geographically wide diversification in Neotropical mammals. *Journal of Biogeography*, *49*(5), 781–793. https://doi.org/10.1111/jbi.14352

Hurtado, N., & Pacheco, V. (2017). Revision of *Neacomys spinosus* (Thomas, 1882) (Rodentia: Cricetidae) with emphasis on Peruvian populations and the description of a new species. *Zootaxa*, *4242*(3), 401. https://doi.org/10.11646/zootaxa.4242.3.1

ICZN. (1999). *International code of zoological nomenclature* (4th ed., Vol. 1999, pp. 1–344). International Trust for Zoological Nomenclature, c/o Natural History Museum. https://doi.org/10.5962/bhl.title.50608

INRENA. (2006). *Parque Nacional Yanachaga-Chemillén. Plan de uso público* (p. 181). INRENA.

Jablonski, D., Roy, K., & Valentine, J. W. (2006). Out of the Tropics: Evolutionary Dynamics of the Latitudinal Diversity Gradient. *Science*, *314*(5796), 102–106. https://doi.org/10.1126/science.1130880

Johnson, M. G., Gardner, E. M., Liu, Y., Medina, R., Goffinet, B., Shaw, A. J., Zerega, N. J., & Wickett, N. J. (2016). HybPiper: Extracting coding sequence and introns for phylogenetics from high-throughput sequencing reads using target enrichment. *Applications in Plant Sciences*, *4*(7), Article 7.

Jolliffe, I. T., & Cadima, J. (2016). Principal component analysis: A review and recent developments. *Philosophical Transactions of the Royal Society A: Mathematical, Physical and Engineering Sciences*, *374*(2065), 20150202. https://doi.org/10.1098/rsta.2015.0202

Josse, C., Navarro, G., Comer, P., Evans, R., Faber-Langendoen, D., Fellows, M., Kittel, G., Menard, S., Pyne, M., Reid, M., Schulz, K., Snow, K., & Teague, J. (2003). *Ecological systems of latin America and the Caribbean: A working classification of terrestrial systems* (p. 47). NatureServe.

Kalyaanamoorthy, S., Minh, B. Q., Wong, T. K. F., von Haeseler, A., & Jermiin, L. S. (2017). ModelFinder: Fast model selection for accurate phylogenetic estimates. *Nature Methods*, *14*(6), Article 6. https://doi.org/10.1038/nmeth.4285

Kelt, D. A., & Meserve, P. L. (2014). Status and challenges for conservation of small mammal assemblages in South America. *Biological Reviews*, *89*(3), 705–722. https://doi.org/10.1111/brv.12080

Keselman, H. J., Murray, R., & Rogan, J. (1976). Effect of very unequal group sizes on Tukey's multiple comparison test. *Educational and Psychological Measurement*, *36*(2), 263–270. https://doi.org/10.1177/001316447603600203

Keselman, H. J., & Rogan, J. C. (1977). The Tukey multiple comparison test: 1953–1976. *Psychological Bulletin*, *84*(5), 1050–1056. https://doi.org/10.1037/0033-2909.84.5.1050

Korkmaz, S., Göksülük, D., & Zararsız, G. (2021). *MVN: an R package for assessing multivariate normality* (5.9) [Computer software]. https://cran.r-project.org/web/packages/MVN/vignettes/MVN.html

Kuhn, M., Wing, J., Weston, S., Williams, A., Keefer, C., Engelhardt, A., Cooper, T., Mayer, Z., Kenkel, B., R Core Team, Benesty, M., Lescarbeau, R., Ziem, A., Scrucca, L., Tang, Y., Candan, C., & Hunt, T. (2023). *caret: Classification and Regression Training* (6.0-94) [Computer software]. https://cran.r-project.org/web/packages/caret/index.html

Kumar, S., Stecher, G., & Tamura, K. (2016). MEGA7: Molecular evolutionary genetics analysis version 7.0 for bigger datasets. *Molecular Biology and Evolution*, *33*(7), 1870–1874. https://doi.org/10.1093/molbev/msw054

Lau, M. K. (2013). Dunnett-Tukey-Kramer pairwise multiple comparison test adjusted for unequal variances and unequal sample sizes. *R Package Version 3.5.*, Available from: https://cran.r-project.org/package=DTK.

Lee, T. E., Tinoco, N., & Brito, J. (2022). A new species of Andean mouse of the genus *Thomasomys* (Cricetidae, Sigmodontinae) from the eastern Andes of Ecuador. *Vertebrate Zoology*, *72*, 219–233. https://doi.org/10.3897/vz.72.e78219

Leo L, M., & Gardner, A. L. (1993). A new species of a giant *Thomasomys* (Mammalia: Muridae: Sigmodontinae) from the Andes of northcentral Peru. *Proceedings of the Biological Society of Washington*, *106*(3), 417–428.

Losos, J. B. (2011). Convergence, adaptation, and constraint. *Evolution*, *65*(7), 1827–1840. https://doi.org/10.1111/j.1558-5646.2011.01289.x

Luna, L., & Pacheco, V. (2002). A new species of *Thomasomys* (Muridae: Sigmodontinae) from the Andes of southeastern Peru. *Journal of Mammalogy*, *83*(3), 834–842.

Martinez Arbizu, P. (2020). *pairwiseAdonis: Pairwise multilevel comparison using adonis* (0.4) [R].

https://github.com/pmartinezarbizu/pairwiseAdonis/blob/master/pairwiseAdonis/R/pairwise.adonis.R

Martinez, Q., Clavel, J., Esselstyn, J. A., Achmadi, A. S., Grohé, C., Pirot, N., & Fabre, P.-H. (2020). Convergent evolution of olfactory and thermoregulatory capacities in small amphibious mammals. *Proceedings of the National Academy of Sciences*, *117*(16), 8958–8965. https://doi.org/10.1073/pnas.1917836117

Martinez, Q., Lebrun, R., Achmadi, A. S., Esselstyn, J. A., Evans, A. R., Heaney, L. R., Miguez, R. P., Rowe, K. C., & Fabre, P.-H. (2018). Convergent evolution of an extreme dietary specialisation, the olfactory system of worm-eating rodents. *Scientific Reports*, *8*(1), 17806. https://doi.org/10.1038/s41598-018-35827-0

McKenna, M., & Bell, S. K. (1997). *Classification of mammals: Above the species level*. Columbia University Press.

Melo-Dias, M., Huatuco, J. F. A., Arizapana-Almonacid, M. A., Castañeda-Tinco, M. I., Chanamé, F., Ninahuamán, J. U., & Passamani, M. (2022). Living at the top of the forest line: Medium and large mammals in a high-mountain ecotone in Peruvian Central Andes. *Biota Neotropica*, *22*, e20211307. https://doi.org/10.1590/1676-0611-BN-2021-1307

Meyer, M., & Kircher, M. (2010). Illumina sequencing library preparation for highly multiplexed target capture and sequencing. *Cold Spring Harbor Protocols*, *2010*(6), pdb.prot5448. https://doi.org/10.1101/pdb.prot5448

Mittelbach, G. G., Schemske, D. W., Cornell, H. V., Allen, A. P., Brown, J. M., Bush, M. B., Harrison, S. P., Hurlbert, A. H., Knowlton, N., Lessios, H. A., McCain, C. M., McCune, A. R., McDade, L. A., McPeek, M. A., Near, T. J., Price, T. D., Ricklefs, R. E., Roy, K., Sax, D. F., … Turelli, M. (2007). Evolution and the latitudinal diversity gradient: Speciation, extinction and biogeography. *Ecology Letters*, *10*(4), 315–331. https://doi.org/10.1111/j.1461-0248.2007.01020.x

Nguyen, L.-T., Schmidt, H. A., von Haeseler, A., & Minh, B. Q. (2015). IQ-TREE: A fast and effective stochastic algorithm for estimating maximum-likelihood phylogenies. *Molecular Biology and Evolution*, *32*(1), 268–274. https://doi.org/10.1093/molbev/msu300

Novillo, A., Lanzone, C., Jayat, J. P., Teta, P., Ojeda, A. A., Cristobal, L., & Ojeda, R. A. (2024). Beta diversity patterns in Andean rodents: Current and historical factors as drivers of turnover and nestedness. *Journal of Mammalogy*, *105*(2), 230–240. https://doi.org/10.1093/jmammal/gyad123

Oksanen, J., Simpson, G. L., Blanchet, F. G., Kindt, R., Legendre, P., Minchin, P. R., O'Hara, R. B., Solymos, P., Stevens, M. H. H., Szoecs, E., Wagner, H., Barbour, M., Bedward, M., Bolker, B., Borcard, D., Carvalho, G., Chirico, M., Caceres, M. D., Durand, S., … Weedon, J. (2022). *vegan: Community Ecology Package* (2.6-4) [Computer software]. https://cran.r-project.org/web/packages/vegan/index.html

Pacheco, V. (2003). *Phylogenetic analyses of the Thomasomyini (Muroidea: Sigmodontinae) based on morphological data* [Ph.D. dissertation]. The City University of New York.

Pacheco, V. (2015a). Genus *Aepeomys* Thomas, 1898. In J. L. Patton, U. F. J. Pardiñas, & G. D'Elía (Eds.), *Mammals of South America. Volume 2, Rodents* (pp. 574–577). The University of Chicago Press.

Pacheco, V. (2015b). Genus *Thomasomys* Coues, 1884. In J. L. Patton, U. F. J. Pardiñas, & G. D'Elia (Eds.), *Mammals of South America. Volume 2, Rodents* (pp. 617–682). The University of Chicago Press.

Pacheco, V., Córdova, J. H., & Velásquez, M. (2012). Karyotypes of *Akodon orophilus* Osgood 1913 and *Thomasomys* sp. (Rodentia: Sigmodontinae) from Huánuco, Peru. *Revista Peruana de Biología*, *19*(1), Article 1. https://doi.org/10.15381/rpb.v19i1.796

Pacheco, V., Patton, J. L., & D'Elía, G. (2015). Tribe Thomasomyini Steadman and Ray, 1982. In J. L. Patton, U. F. J. Pardiñas, & G. D'Elía (Eds.), *Mammals of South America. Volume 2, Rodents* (pp. 571–574). The University of Chicago Press.

Pacheco, V., & Ruelas, D. (2023). Systematic revision of *Thomasomys cinereus* (Rodentia: Cricetidae: Sigmodontinae) from northern Peru and southern Ecuador, with descriptions of three new species. *Bulletin of the American Museum of Natural History, 461*, 1–71.

Padial, J. M., & De la Riva, I. (2021). A paradigm shift in our view of species drives current trends in biological classification. *Biological Reviews*, *96*(2), 731–751. https://doi.org/10.1111/brv.12676

Parada, A., D'Elía, G., & Palma, R. E. (2015). The influence of ecological and geographical context in the radiation of Neotropical sigmodontine rodents. *BMC Evolutionary Biology*, *15*(1), 172. https://doi.org/10.1186/s12862-015-0440-z

Parada, A., Pardiñas, U. F. J., Salazar-Bravo, J., D'Elía, G., & Palma, R. E. (2013). Dating an impressive Neotropical radiation: Molecular time estimates for the Sigmodontinae (Rodentia) provide insights into its historical biogeography. *Molecular Phylogenetics and Evolution*, *66*(3), 960–968. https://doi.org/10.1016/j.ympev.2012.12.001

Pardiñas, U. F. J., Cañón, C., Galliari, C. A., Brito, J., Bernal Hoverud, N., Lessa, G., & de Oliveira, J. A. (2020). Gross stomach morphology in akodontine rodents (Cricetidae: Sigmodontinae: Akodontini): a reappraisal of its significance in a phylogenetic context. *Journal of Mammalogy*, *101*(3), 835–857. https://doi.org/10.1093/jmammal/gyaa023

Pardiñas, U. F. J., Curay, J., Brito, J., & Cañón, C. (2021). A unique cricetid experiment in the northern high-Andean Páramos deserves tribal recognition.

Journal of Mammalogy, 102(1), 155–172. https://doi.org/10.1093/jmammal/gyaa147

Pardiñas, U. F. J., Teta, P., & Salazar-Bravo, J. (2015). A new tribe of sigmodontinae rodents (Cricetidae). *Mastozoología Neotropical*, *22*(1), 171–186.

Pardiñas, U. F. J., Tinoco, N., Barbière, F., Ronez, C., Cañón, C., Lessa, G., Koch, C., & Brito, J. (2022). Morphological disparity in a hyperdiverse mammal clade: A new morphotype and tribe of Neotropical cricetids. *Zoological Journal of the Linnean Society,* zlac016. https://doi.org/10.1093/zoolinnean/zlac016

Patterson, B. D., Solari, S., & Velazco, P. M. (2012). The role of the Andes in the diversification and biogeography of Neotropical mammals. In B. D. Patterson & L. P. Costa (Eds.), *Bones, Clones, and Biomes* (pp. 351–378). The University of Chicago Press. https://doi.org/10.7208/chicago/9780226649214.001.0001

Patton, J. L. (2015). Genus *Lenoxus* Thomas, 1909. In J. L. Patton, U. F. J. Pardiñas, & G. D'Elia (Eds.), *Mammals of South America. Volume 2, Rodents* (pp. 231–232). The University of Chicago Press.

Patton, J. L., Pardiñas, U. F. J., & D'Elía, G. (Eds.). (2015). *Mammals of South America, Volume 2: Rodents*. University of Chicago Press.

Percequillo, A. R. (2015a). Genus *Nephelomys* Weksler, Percequillo, and Voss, 2006. In J. L. Patton, U. F. J. Pardiñas, & G. D'Elía (Eds.), *Mammals of South America. Volume 2, Rodents* (pp. 377–390). The University of Chicago Press.

Percequillo, A. R. (2015b). Genus *Oreoryzomys* Weksler, Percequillo, and Voss, 2006. In J. L. Patton, U. F. J. Pardiñas, & G. D'Elía (Eds.), *Mammals of South America. Volume 2, Rodents* (pp. 437–439). The University of Chicago Press.

R Core Team. (2022). *R: A language and environment for statistical computing* [R]. R Foundation for Statistical Computing. URL https://www.R-project.org/

Rambaut, A., Drummond, A. J., Xie, D., Baele, G., & Suchard, M. A. (2018). Posterior summarization in Bayesian phylogenetics using Tracer 1.7. *Systematic Biology*, *67*(5), 901–904. https://doi.org/10.1093/sysbio/syy032

Ranwez, V., Douzery, E. J., Cambon, C., Chantret, N., & Delsuc, F. (2018). MACSE v2: Toolkit for the alignment of coding sequences accounting for frameshifts and stop codons. *Molecular Biology and Evolution*, *35*(10), Article 10.

Reig, O. A. (1977). A proposed unified nomenclature for the enamelled components of the molar teeth of the Cricetidae (Rodentia). *Journal of Zoology*, *181*(2), 227–241. https://doi.org/10.1111/j.1469-7998.1977.tb03238.x

Rickart, E. A., Heaney, L. R., Balete, D. S., & Tabaranza, B. R. (2011). Small mammal diversity along an elevational gradient in northern Luzon, Philippines. *Mammalian Biology*, *76*(1), 12–21. https://doi.org/10.1016/j.mambio.2010.01.006

Ronquist, F., Teslenko, M., van der Mark, P., Ayres, D. L., Darling, A., Höhna, S., Larget, B., Liu, L., Suchard, M. A., & Huelsenbeck, J. P. (2012). MrBayes 3.2: Efficient Bayesian phylogenetic inference and model choice across a large model space. *Systematic Biology*, *61*(3), 539–542. https://doi.org/10.1093/sysbio/sys029

RStudio Team. (2023). *RStudio: Integrated Development Environment for R* [R]. R Core Team. www.rstudio.com/

Ruelas, D., Fabre, P.-H., Pacheco, V., & Martinez, Q. (in prep.). Introduction to the *Thomasomys* (Rodentia: Cricetidae) turbinal bone adaptations: Insights into elevation and environmental challenges. *Journal of Mammalogy*, *xx*, xx.

Ruelas, D., & Pacheco, V. (2021). A new species of *Thomasomys* Coues, 1884 (Rodentia: Sigmodontinae) from the montane forests of northern Peru with comments on the "aureus" group. *Revista Peruana de Biología*, *28*(3), e19912. https://doi.org/10.15381/rpb.v28i3.19912

Ruelas, D., Pacheco, V., Inche, B., & Tinoco, N. (2021). A preliminary review of *Nephelomys albigularis* (Tomes, 1860) (Rodentia: Cricetidae), with the description of a new species from the Peruvian montane forests. *Zootaxa*, *5027*(2), 175–210. https://doi.org/10.11646/zootaxa.5027.2.3

Ruelas, D., Pacheco, V., & Jiménez, C. F. (2020). Range extension and phylogenetic relationships of *Akodon josemariarguedasi* (Rodentia: Cricetidae) with comments on the aerosus species group. *Mammalia, 84*(2), 207–213. https://doi.org/10.1515/mammalia-2018-0209

Ruelas, D., Pacheco, V., Pérez, J., Diaz-Nieto, J., & Fabre, P.-H. (2024). Unilocus delimitation methods reveal the underestimated species diversity of *Thomasomys* (Rodentia, Cricetidae). *Zoologica Scripta*.

Salazar-Bravo, J. (2015). Genus *Tapecomys* S. Anderson and Yates, 2000. In J. L. Patton, U. F. J. Pardiñas, & G. D'Elía (Eds.), *Mammals of South America. Volume 2, Rodents* (pp. 556–559). The University of Chicago Press.

Salazar-Bravo, J., Pardiñas, U. F. J., & D'Elía, G. (2013). A phylogenetic appraisal of Sigmodontinae (Rodentia, Cricetidae) with emphasis on phyllotine genera:

Systematics and biogeography. *Zoologica Scripta*, *42*(3), 250–261. https://doi.org/10.1111/zsc.12008

Schenk, J. J., & Steppan, S. J. (2018). The role of geography in adaptive radiation. *The American Naturalist*, *192*(4), 415–431. https://doi.org/10.1086/699221

Schüßler, D., Blanco, M. B., Guthrie, N. K., Sgarlata, G. M., Dammhahn, M., Ernest, R., Evasoa, M. R., Hasiniaina, A., Hending, D., Jan, F., le Pors, B., Miller, A., Olivieri, G., Rakotonanahary, A. N., Rakotondranary, S. J., Rakotondravony, R., Ralantoharijaona, T., Ramananjato, V., Randrianambinina, B., … Radespiel, U. (2024). Morphological variability or inter-observer bias? A methodological toolkit to improve data quality of multi-researcher datasets for the analysis of morphological variation. *American Journal of Biological Anthropology*, *183*(1), 60–78. https://doi.org/10.1002/ajpa.24836

Schwarz, G. (1978). Estimating the dimension of a model. *The Annals of Statistics*, *6*(2), 461–464. https://doi.org/10.1214/aos/1176344136

SERNANP (Ed.). (2012). *Plan Maestro del Santuario Nacional Pampa Hermosa 2012-2017* (1st ed.).

Sharov, A. A. (2014). Evolutionary constraints or opportunities? *Bio Systems*, *0*, 21–30. https://doi.org/10.1016/j.biosystems.2014.04.005

Smith, M. F., & Patton, J. L. (1991). Variation in mitochondrial cytochrome b sequence in natural populations of South American akodontine rodents (Muridae: Sigmodontinae). *Molecular Biology and Evolution*, *8*(1), 85–103. https://doi.org/10.1093/oxfordjournals.molbev.a040638

Smith, M. F., & Patton, J. L. (1993). The diversification of South American murid rodents: Evidence from mitochondrial DNA sequence data for the akodontine tribe. *Biological Journal of the Linnean Society*, *50*(3), 149–177. https://doi.org/10.1006/bijl.1993.1052

Smith, M. F., & Patton, J. L. (1999). Phylogenetic relationships and the radiation of sigmodontine rodents in South America: Evidence from cytochrome b. *Journal of Mammalian Evolution*, *6*(2), 89–128.

Stayton, C. T. (2008). Is convergence surprising? An examination of the frequency of convergence in simulated datasets. *Journal of Theoretical Biology*, *252*(1), 1–14. https://doi.org/10.1016/j.jtbi.2008.01.008

Steadman, D. W., & Ray, C. E. (1982). Relationships of *Megaoryzomys curioi*, an extinct cricetine rodent (Muroidea: Muridae) from the Galápagos islands, Ecuador. *Smithsonian Contributions to Paleobiology*, *51*, 1–23. https://doi.org/10.5479/si.00810266.51.1

Steppan, S. J., Adkins, R. M., Spinks, P. Q., & Hale, C. (2005). Multigene phylogeny of the Old World mice, Murinae, reveals distinct geographic lineages and the declining utility of mitochondrial genes compared to nuclear genes. *Molecular Phylogenetics and Evolution*, *37*(2), 370–388. https://doi.org/10.1016/j.ympev.2005.04.016

Steppan, S. J., & Schenk, J. J. (2017). Muroid rodent phylogenetics: 900-species tree reveals increasing diversification rates. *PLOS ONE*, *12*(8), e0183070. https://doi.org/10.1371/journal.pone.0183070

Tilak, M.-K., Justy, F., Debiais-Thibaud, M., Botero-Castro, F., Delsuc, F., & Douzery, E. J. P. (2015). A cost-effective straightforward protocol for shotgun

Illumina libraries designed to assemble complete mitogenomes from non-model species. *Conservation Genetics Resources*, *7*(1), 37–40. https://doi.org/10.1007/s12686-014-0338-x

Tribe, C. J. (2015). Genus *Rhipidomys* Tschudi, 1845. In J. L. Patton, U. F. J. Pardiñas, & G. D'Elía (Eds.), *Mammals of South America. Volume 2, Rodents* (pp. 583–617). University of Chicago Press.

Uturunco, A. C. J., & Pacheco, V. (2016). Redescripción de *Eremoryzomys* polius (Rodentia: Cricetidae) y descripción de una nueva especie del género *Eremoryzomys*. *Mastozoología Neotropical*, *23*(2), 483–503.

Vallejos-Garrido, P., Pino, K., Espinoza-Aravena, N., Pari, A., Inostroza-Michael, O., Toledo-Muñoz, M., Castillo-Ravanal, B., Romero-Alarcón, V., Hernández, C. E., Palma, R. E., & Rodríguez-Serrano, E. (2023). The importance of the Andes in the evolutionary radiation of Sigmodontinae (Rodentia, Cricetidae), the most diverse group of mammals in the Neotropics. *Scientific Reports*, *13*(1), Article 1. https://doi.org/10.1038/s41598-023-28497-0

Ventura, K., Silva, M., Geise, L., Leite, Y. L., Pardiñas, U. F., Yonenaga-Yassuda, Y., & D'Elía, G. (2013). The phylogenetic position of the enigmatic Atlantic forest-endemic spiny mouse Abrawayaomys (Rodentia: Sigmodontinae). *Zoological Studies*, *52*(1), 55. https://doi.org/10.1186/1810-522X-52-55

Vieu, J. C., Hughes, C. E., Kissling, J., & Grant, J. R. (2022). Evolutionary diversification in the hyper-diverse montane forests of the tropical Andes: Radiation of Macrocarpaea (Gentianaceae) and the possible role of range expansion. *Botanical Journal of the Linnean Society*, *199*(1), 53–75. https://doi.org/10.1093/botlinnean/boab065

Vivar Pinares, S. E. (2006). *Análisis de distribución altitudinal de mamíferos pequeños en el Parque Nacional Yanachaga Chemillén, Pasco, Perú* [Tesis para optar al grado académico de Magíster en Zoología con mención en Sistemática y Evolución, Universidad Nacional Mayor de San Marcos, Facultad de Ciencias Biológicas].

Voss, R. S. (1988). Systematics and ecology of ichthyomyine rodents (Muroidea): Patterns of morphological evolution in a small adaptive radiation. *Bulletin of the American Museum of Natural History, 188*(2), 259–493.

Voss, R. S. (1993). A revision of the Brazilian muroid rodent genus *Delomys*: With remarks on "thomasomyine" characters. *American Museum Novitates*, *3073*, 1–44.

Voss, R. S. (2003). A new species of *Thomasomys* (Rodentia: Muridae) from eastern Ecuador, with remarks on mammalian diversity and biogeography in the Cordillera Oriental. *American Museum Novitates*, *3421*, 1–47.

Voss, R. S. (2015). Tribe Ichthyomyini Vorontsov, 1959. In J. L. Patton, U. F. J. Pardiñas, & G. D'Elia (Eds.), *Mammals of South America. Volume 2, Rodents* (pp. 279–291). The University of Chicago Press.

Weksler, M. (2006). Phylogenetic Relationships of Oryzomine Rodents (Muroidea: Sigmodontinae): Separate and Combined Analyses of Morphological and Molecular Data. *Bulletin of the American Museum of Natural History*, *296*, 1–149. https://doi.org/10.1206/0003-0090(2006)296[0001:PROORM]2.0.CO;2

Weksler, M. (2015). Tribe Oryzomyini Vorontsov, 1959. In J. L. Patton, U. F. J. Pardiñas, & G. D'Elía (Eds.), *Mammals of South America. Volume 2, Rodents* (pp. 291–465). The University of Chicago Press.

Wickham, H., Hester, J., Chang, W., Bryan, J., & RStudio. (2022). *devtools: Tools to Make Developing R Packages Easier* (2.4.5) [Computer software]. https://cran.r-project.org/web/packages/devtools/index.html

Young, K. R. (1992). Biogeography of the montane forest zone of the eastern slopes of Peru. *Memorias Del Museo de Historia Natural*, *21*, 119–154.

Young, K. R., & León, B. (1999). *Peru's humid Eastern montane forests: An overview of their physical settings, biological diversity, human use and settlement, and conservation needs* (DIVA, Technical Report 5; p. 97). Centre for Research on Cultural and Biological Diversity of Andean Rainforests (DIVA).

APPENDIX 1

List of specimens studied here and their collection localities. Locality numbers (in brackets) are those showed in fig. 1. Acronyms correspond to the Museo de Historia Natural de la Universidad Nacional Mayor de San Marcos (MUSM, Lima, Peru), Natural History Museum (NHMUK, London, UK), Field Museum of Natural History (FMNH, Chicago, USA), and American Museum of Natural History (AMNH, New York, USA). All specimens were used in qualitative analysis. Superscript q= specimens used in quantitative analyses. Asterisks indicate the holotype.

"*Thomasomys*" sp. 4 "Oxapampa" (n= 69): PERU: Huánuco, Pachitea, Chaglla, Palmapampa, a 2 hrs. carretera de Chaglla, -9.89° -75.89° (MUSM 17836^{q}, 17837^{q}) [1]. Pasco, Oxapampa, Huancabamba, Santa Barbara, -10.34° -75.64° (MUSM 24324^{q}, 24325^{q}, 46247, 46248^{q}) [2]; Oxapampa, San Alberto, 7 km al este de Oxapampa, limite este del Parque Nacional Yanachaga-Chemillen, -10.55° -75.4° (MUSM 10571, 14961, 14962, 14963, 14964^{q}, 14965, 14967-14969^{q}, 14971, 14973^{q}, 14975^{q}, 14976^{q}, 14977, 14979, 14980^{q}, 14981^{q}) [3]; Oxapampa, San Alberto, Abra Esperanza, -10.53° -75.35° (MUSM 24287^{q}, 24288, 24289-24291^{q}, 24292, 24293-24296^{q}, 24297, 24298-24304^{q}, 24305-24307, 24308^{q}, 24309^{q}, 24313^{q}, 24315-24317^{q}, 24320^{q}, 24323^{q}, 46233, 46234^{q}, 46236, 46237^{q}, 46239^{q}, 46241^{q}, 46242, 46245, 46246^{q}) [4]; Palcazú, Primera Estacion Biologica de San Alberto, Parque Nacional Yanachaga-Chemillen, 10 Km E de Oxapampa, -10.55° -75.33° (MUSM 11340, 11444, 11447^{q}, 11457, 11463, 11467^{q}, 11475, 11480^{q}) [5].

"*Thomasomys*" sp. 4 "Tarma" (n= 24): PERU: Junín, Tarma, Huasahuasi, San Pedro de Churco, margen izquierdo de Río Churco 1, -11.03° -75.54° (MUSM 42509[q], 42519[q], 42520[q], 42565[q], 42568, 52877, 52893, 52895[q], 52896, 52899, 52900) [6], San Pedro de Churco, margen izquierdo de Río Churco 2, -11.06° -75.61° (MUSM 42504[q], 42505[q],42507, 42508[q], 42511[q], 42512[q], 42515-42518[q], 42566, 42567[q], 42570) [7].

"*Thomasomys*" sp. 4 "Satipo" (n= 22): PERU: Junín, Satipo, Pampa Hermosa, Calabaza, -11.51° -74.85° (MUSM 40810, 40811-40813[q], 40820, 40823[q], 46089-46092[q], 46095[q], 46098- 46101[q]) [8]. Satipo, Pampa Hermosa, Carrizal, -11.50 -74.87 (MUSM 40830, 40832, 40834, 40850, 40851, 40854, 40855) [9].

Aepeomys lugens (n= 12): VENEZUELA: Mérida, La Loma del Morro (NHMUK 96.11.1.5 [q,]*, holotype of *Oryzomys lugens*); Mérida, Libertador, Sierra de Mérida (AMNH 143670[q], FMNH 22153[q], 22154[q], 22155[q]); Mérida, Mucujun River (AMNH 143669[q], FMNH 22149[q], 22150[q], 22152); Merida, Paramo Tambor (FMNH 22157[q], 22158); Mérida, Libertador, Paramo de Los Conejos (AMNH 96169[q,]*, holotype of *Thomasomys ottleyi*).

Chilomys fumeus (n= 4): COLOMBIA: Cundinamarca, Páramo de Tamá (FMNH 18689, 18690*, holotype of *Chilomys fumeus*). VENEZUELA: Mérida, R Mucujun (FMNH 22171); Mérida, Paramo Tambor (FMNH 22172).

Chilomys instans (n= 3): COLOMBIA: Cauca, Popayán, Cerro Munchique (AMNH 181477); Antioquia, Sonson, Paramo, 7 km E (FMNH 70343); Antioquia, Sonson, Las Frias, 10 km E (FMNH 70345).

Chilomys* cf. *weksleri (n= 10): ECUADOR: Pichincha, Saloya ("Galaya") West (FMNH 53403); Pichincha, Volcan Pichincha (FMNH 53405); Pichincha, Quito, San Rafael River (AMNH 64645, 64648); Pichincha, Quito, San Ignacio (AMNH 64640, 64644); Pichincha, Quito, Santa Rosa (AMNH 64647); Pichincha, Pita River canyon (AMNH 64649-64651).

***Chilomys* sp.** (n= 2): ECUADOR: Cañar, San Antonio (AMNH 62921); Cañar, Chical (AMNH 62922).

Rhipidomys couesi (n= 1): TRINIDAD: Princestown (AMNH 4685*, holotype of *Rhipidomys couesi*).

Rhipidomys fulviventer (n= 2): VENEZUELA: Tâchira, Pàramo de Tamà, head of Tachira River (AMNH 18691, holotype of *Rhipidomys fulviventer elatturus*); Sucre (AMNH 14737*, holotype of *Oryzomys tenuicauda*).

Rhipidomys latimanus (n= 3): COLOMBIA: Valle del Cauca, Miraflores, west slope of Central Andes, near Palmira (AMNH 32243*, holotype of *Rhipidomys mollisimus*); Cauca, Cocal (AMNH 32376*, holotype of *Rhipidomys cocalensis*); Quindío, Central Andes, El Roble (AMNH 32970*, holotype of *Rhipidomys quindianus*).

Rhipidomys macconnelli (n= 1): VENEZUELA: Bolívar, South slope Mt. Auyan-tepui (AMNH 131154*, holotype of *Thomasomys macconnelli subnubis*).

Rhipidomys nitela (n= 3): VENEZUELA: Bolivar, Rio Yuruan (AMNH 30735*, holotype of *Rhipidomys venezuelae yuruanus*); BRITISH GUIANA: Minehaha Creek, Lower Essequibo River (AMNH 36332*, holotype of *Rhipidomys milleri*);

TRINIDAD AND TOBAGO: Little Tobago Island (AMNH 184555*, holotype of *Rhipidomys nitela tobagi*).

Thomasomys andersoni (n= 1): BOLIVIA: Cochabamba, "an elfin forest near the headquarters of the Corani hydroelectric plant" (AMNH 268734*, holotype of *Thomasomys andersoni*).

Thomasomys aureus (n= 2): ECUADOR: Pallatanga (sensu Pacheco, 2015) (NHMUK 7.1.1.104*, holotype of *Hesperomys aureus*); Pichincha, Mt. Pichincha (AMNH 36280*, holotype of *Thomasomys aureus altorum*).

Thomasomys auricularis (n= 1): ECUADOR: El Oro, Cordillera de Chilla, Taraguacocha, on trail from Zaruma to Zaraguro (AMNH 47697*, holotype of *Thomasomys aureus*).

Thomasomys australis (n= 1): BOLIVIA: Cochabamba, Incachaca (AMNH 38550*, holotype of *Thomasomys daphne australis*).

Thomasomys baeops (n= 1): ECUADOR: Pichincha, Río Pita, above the Chillo Valley (NHMUK 98.8.1.7*, holotype of *Oryzomys baeops*).

Thomasomys bombycinus (n= 1): COLOMBIA: Antioquia, Paramillo, western Andes (AMNH 37740*, holotype of *Thomasomys bombycinus*).

Thomasomys caudivarius (n= 1): ECUADOR: El Oro, Taraguacocha, Cordillera de Chilla (AMNH 47668*, holotype of *Thomasomys caudivarius*).

Thomasomys cinereiventer (n= 1): COLOMBIA: Cauca, crest of western Andes, 40 miles [64 km] west of Popayán (AMNH 32436*, holotype of *Thomasomys cinereiventer*).

Thomasomys cinereus (n= 9): PERU: Cajamarca, Cutervo (NHMUK 81.9.7.29*, holotype of *Hesperomys* (*Rhipidomys*) *cinereus*); Cajamarca, 3.81 km NE from Monteseco (MUSM 46759[q]); Cajamarca, Quengorrio (MUSM 38350[q]); Cajamarca, Porvenir (MUSM 38496[q]); La Libertad, El Fundo-Río Chuyuhual (MUSM 41103[q]); La Libertad, La Arena (MUSM 24138[q], 24139[q], 24172[q]); La Libertad, Lagunas Norte, río Chuyuhual (MUSM 24928[q]).

Thomasomys cinnameus (n= 1): ECUADOR: Tungurahua, Hacienda San Francisco, east of Ambato (AMNH 67401*, holotype of *Thomasomys cinnameus*).

Thomasomys contradictus (n= 1): COLOMBIA: Quindío, Santa Isabel (AMNH 32955*, holotype of *Thomasomys contradictus*).

Thomasomys dispar (n= 1): COLOMBIA: Huila, Andalucía, Eastern Andes (AMNH 33761*, holotype of *Thomasomys dispar*).

Thomasomys eleusis (n= 4): PERU: Amazonas, Tambo Jenes (NHMUK 1926.4.1.48[q,]*, holotype of *Thomasomys eleusis*); Amazonas, mountains E of Balsas (FMNH 19813[q]); Amazonas, San Pedro (AMNH 72103[q], 72105[q]).

Thomasomys emeritus (n= 1): VENEZUELA: Mérida, Montes de Escagüey (NHMUK 5.1.1.4*, holotype of *Thomasomys emeritus*).

Thomasomys erro (n= 1): ECUADOR: Napo, "upper slopes of Mt. Sumaco, exact altitude unknown, but probably 8000– 9000 feet [approx. 2438– 2743 m] at head of the Rio Suno [= Río Suno], a tributary of the Rio Napo [= Río Napo]" (AMNH 68195*, holotype of *Thomasomys erro*).

Thomasomys fumeus (n= 1): ECUADOR: Tungurahua, Hacienda San Francisco, east of Ambato (AMNH 67537*, holotype of *Thomasomys rhoadsi fumeus*).

Thomasomys hudsoni (n= 1): ECUADOR: Azuay, Bestión (AMNH 47690*, holotype of *Thomasomys hudsoni*).

Thomasomys incanus (n= 8): PERU: Junín, Valley of Vitoc [= Río Tulumayo] (NHMUK 94.10.1.4[q,]*, holotype of *Oryzomys incanus*); Junín, Alcas, 25 miles NE of Cerro (NHMUK 1927.11.1.172 [q]); Junín, Alcas, 25 miles 5 NE of Cerro Junín (NHMUK 27.11.1.169*, holotype of *Thomasomys fraternus*); Huánuco, mountains 15 miles NE Huánuco (FMNH 23725[q], 23728[q], 23730[q], 23731[q], 23734[q]).

Thomasomys ischyrus (n= 15): PERU: Amazonas, Uscho (FMNH 19803[q,]*, holotype of *Thomasomys cinereus ischyrus*); Amazonas, La Lejía (AMNH 72106[q] 72107[q] 72108[q], 72109); Amazonas, Leimabamba (NHMUK 26.4.1.38[q], 26.4.1.44[q]); Amazonas, Celendin (NHMUK 26.5.3.80[q], 26.5.3.82[q]); Amazonas, Goncha (NHMUK 26.8.6.35[q], 26.8.6.36[q], 26.8.6.38[q], 26.8.6.41[q]); Amazonas, Corosha (NHMUK 26.8.6.40[q], 26.8.6.42[q]).

Thomasomys kalinowskii (n= 7): PERU: Junín, Valley of Vitoc NHMUK94.10.1.2[q,]*, holotype of *Oryzomys kalinowskii*); Junín, San Pedro de Churco (MUSM 42502[q], 42503[q], 52892[q], DMC37[q], DMC41[q], DMC68[q]).

Thomasomys ladewi (n= 5): BOLIVIA: La Paz, Aceramarca River (AMNH 72113[q,]*, holotype of *Thomasomys ladewi*); La Paz, Aceramarca River (AMNH 72114[q], 264778[q], 264780[q], 264781[q]).

Thomasomys laniger (n= 1): COLOMBIA: Cundinamarca, Bogota Region (NHMUK 95.8.1.39*, holotype of *Oryzomys laniger*).

Thomasomys nicefori (n= 1): COLOMBIA: Antioquia, San Pedro, north of Medellín (NHMUK 21.7.1.20*, holotype of *Thomasomys nicefori*).

Thomasomys niveipes (n= 1): COLOMBIA: Cundinamarca, La Hoya del Barro Blanco at the head of the Río Teusacá and includes the Laguna El Verjón (sensu Gómez-Laverde et al. 1997) (NHMUK 96.11.1.4*, holotype of *Oryzomys niveipes*)

Thomasomys oreas (n= 1): BOLIVIA: Cocapunco, about 80 miles north of La Paz (AMNH 72130*, holotype of *Thomasomys oreas*).

Thomasomys paramorum (n= 1): ECUADOR: Chimborazo, Páramo south of Mt Chimborazo, "Urbina just a few kilometers SE of Chimborazo" (sensu Voss, 2007) (NHMUK 97.11.7.82*, holotype of *Thomasomys paramorum*).

Thomasomys popayanus (n= 1): COLOMBIA: Cauca, crest of western Andes, 40 miles [64 km] west of Popayán (AMNH 32371*, holotype of *Thomasomys popayanus*).

Thomasomys praetor (n= 1): PERU: Cajamarca, eastern slope of Páramo between San Pablo and Cajamarca (NHMUK 0.3.15.3*, holotype of *Oryzomys praetor*).

Thomasomys princeps (n= 1): COLOMBIA: Cundinamarca, Bogotá region (NHMUK 95.8.1.37*, holotype of *Oryzomys princeps*).

Thomasomys pyrrhonotus (n= 1): PERU: Cajamarca, Tambillo, Río Malleta (NHMUK 81.9.7.24*, holotype of *Hesperomys pyrrhonotus*).

Thomasomys* cf. *pyrrhonotus (n= 1): PERU: Piura, Huancabamba, El Carmen de la Frontera, Habas Pite (MUSM 55555).

Thomasomys rosalinda (n= 1): PERU: Amazonas, Goncha (NHMUK 26.8.6.31*, holotype of *Thomasomys rosalinda*).

Thomasomys silvestris (n= 1): ECUADOR: Pichincha, Las Máquinas, on Santo Domingo trail, west of Corazón (AMNH 66288*, holotype of *Thomasomys silvestris*).

Thomasomys *shallqukucha* (n= 9): PERU: Lambayeque, Geomarca (MUSM 46870[q], 46871[q], 46874[q], 46878[q], 46880[q], 46885[q], 46887[q], 46889[q]); Lambayeque, Palomapampa (MUSM47229[q]).

Thomasomys taczanowskii (n= 1): PERU: Cajamarca, Tambillo, Río Malleta (NHMUK 81.9.7.23*, holotype of *Hesperomys* (*Rhipidomys*) *taczanowskii*).

Thomasomys vestitus (n= 1): VENEZUELA: Mérida, Río Milla (NHMUK 98.5.15.3*, holotype of *Oryzomys vestitus*).

Thomasomys vulcani (n= 1): ECUADOR: Pichincha, mount volcán Pichincha (NHMUK 98.5.1.10*, holotype of *Aepeomys vulcani*).

APPENDIX 2

Specimens used in molecular analyses.

Species	Mitochondrial genes	Nuclear genes
"*Thomasomys*" sp. 4 "Oxapampa" MUSM 11463	13 (ND1, ND2, COX1, COX2, ATP8, ATP6, COX3, ND3, ND4, ND4L, ND5, ND6, CYTB)	5 (BRCA1, RBP3, RAG1, ACP5, GHR)
"*Thomasomys*" sp. 4 "Oxapampa"	1 (CYTB)	
"*Thomasomys*" sp. 4 "Oxapampa"	1 (CYTB)	
"*Thomasomys*" sp. 4 "Oxapampa"	1 (CYTB)	
"*Thomasomys*" sp. 4 "Oxapampa" MUSM 24288	13 (ND1, ND2, COX1, COX2, ATP8, ATP6, COX3, ND3, ND4, ND4L, ND5, ND6, CYTB)	5 (BRCA1, RBP3, RAG1, ACP5, GHR)
"*Thomasomys*" sp. 4 "Oxapampa" MUSM 24297	1 (CYTB)	
"*Thomasomys*" sp. 4 "Oxapampa" MUSM 24300	10 (ND2, COX1, COX2, ATP6, COX3, ND3, ND4, ND5, ND6, CYTB)	5 (BRCA1, RBP3, RAG1, ACP5, GHR)

"*Thomasomys*" sp. 4 "Tarma"	1 (CYTB)	
"*Thomasomys*" sp. 4 "Tarma"	1 (CYTB)	
"*Thomasomys*" sp. 4 "Tarma"	1 (CYTB)	
"*Thomasomys*" sp. 4 "Tarma" MUSM 52877	4 (COX3, ND3, ND4, ND4L)	5 (BRCA1, RBP3, RAG1, ACP5, GHR)
"*Thomasomys*" sp. 4 "Tarma" MUSM 52895	12 (ND1, ND2, COX1, ATP8, ATP6, COX3, ND3, ND4, ND4L, ND5, ND6, CYTB)	5 (BRCA1, RBP3, RAG1, ACP5, GHR)
"*Thomasomys*" sp. 4 "Tarma" MUSM52896	13 (ND1, ND2, COX1, COX2, ATP8, ATP6, COX3, ND3, ND4, ND4L, ND5, ND6, CYTB)	5 (BRCA1, RBP3, RAG1, ACP5, GHR)
"*Thomasomys*" sp. 4 "Satipo" MUSM 40810	13 (ND1, ND2, COX1, COX2, ATP8, ATP6, COX3, ND3, ND4, ND4L, ND5, ND6, CYTB)	5 (BRCA1, RBP3, RAG1, ACP5, GHR)
Abrawayaomys ruschii		3 (BRCA1, RBP3, RAG1)
Abrothrix andina	3 (ND3, ND4, ND4L)	4 (BRCA1, RBP3, RAG1, GHR)

Aepeomys lugens AMNH 143669	12 (ND1, ND2, COX1, COX2, ATP8, ATP6, COX3, ND3, ND4, ND4L, ND5, CYTB)	3 (RBP3, RAG1, GHR)
Aepeomys lugens AMNH 143670	1 (CYTB)	5 (BRCA1, RBP3, RAG1, ACP5, GHR)
Akodon josemariarguedasi MUSM 44705	13 (ND1, ND2, COX1, COX2, ATP8, ATP6, COX3, ND3, ND4, ND4L, ND5, ND6, CYTB)	
Akodon montensis	13 (ND1, ND2, COX1, COX2, ATP8, ATP6, COX3, ND3, ND4, ND4L, ND5, ND6, CYTB)	1 (RBP3)
Akodon torques	1 (CYTB)	5 (BRCA1, RBP3, RAG1, ACP5, GHR)
Andinomys edax	2 (COX1, CYTB)	4 (BRCA1, RBP3, RAG1, GHR)
Brucepattersonius soricinus		4 (BRCA1, RBP3, RAG1, GHR)
Calomys musculinus	4 (ND3, ND4, ND4L, CYTB)	2 (RBP3, RAG1)
Calomys venustus		3 (RBP3, RAG1, GHR)
Chilomys instans	1 (CYTB)	
Chilomys instans AMNH 181477	3 (ND1, ND6, CYTB)	5 (BRCA1, RBP3, RAG1, ACP5, GHR)

Chilomys instans AMNH 66849	1 (ND6)	5 (BRCA1, RBP3, RAG1, ACP5, GHR)
Chilomys percequilloi	2 (COX1, CYTB)	
Eligmodontia moreni		4 (RBP3, RAG1, ACP5, GHR)
Eligmodontia typus	3 (ND3, ND4, ND4L)	1 (RBP3)
Euneomys chinchilloides		5 (BRCA1, RBP3, RAG1, ACP5, GHR)
Holochilus sciureus	12 (ND1, ND2, COX1, COX2, ATP8, ATP6, COX3, ND3, ND4, ND4L, ND6, CYTB)	1 (RBP3)
Irenomys tarsalis		4 (BRCA1, RBP3, RAG1, GHR)
Juliomys pictipes	2 (COX1, CYTB)	5 (BRCA1, RBP3, RAG1, ACP5, GHR)
Lenoxus apicalis		5 (BRCA1, RBP3, RAG1, ACP5, GHR)
Melanomys caliginosus	12 (ND1, ND2, COX1, COX2, ATP8, ATP6, COX3, ND3, ND4, ND4L, ND6, CYTB)	1 (RBP3)
Necromys amoenus	1 (CYTB)	5 (BRCA1, RBP3, RAG1, ACP5, GHR)
Necromys lactens	3 (ND3, ND4, ND4L)	

Neomicroxus bogotensis		1 (RBP3)
Nephelomys albigularis	3 (ND3, ND4, ND4L)	
Nephelomys keaysi		2 (RBP3, GHR)
Notiomys edwardsii		5 (BRCA1, RBP3, RAG1, ACP5, GHR)
Oligoryzomys stramineus	12 (ND1, ND2, COX1, COX2, ATP8, ATP6, COX3, ND3, ND4, ND4L, ND6, CYTB)	1 (RBP3)
Oryzomys palustris	3 (ND3, ND4, ND4L)	1 (RBP3)
Oxymycterus nasutus		5 (BRCA1, RBP3, RAG1, ACP5, GHR)
Oxymycterus rufus	4 (COX1, ND3, ND4, ND4L)	2 (RBP3, ACP5)
Phyllotis darwini	3 (ND3, ND4, ND4L)	
Phyllotis haggardi		3 (RBP3, RAG1, GHR)
Punomys kofordi		5 (BRCA1, RBP3, RAG1, ACP5, GHR)
Reithrodon auritus	3 (ND3, ND4, ND4L)	5 (BRCA1, RBP3, RAG1, ACP5, GHR)
Rhagomys longilingua	2 (COX1, CYTB)	3 (RBP3, ACP5, GHR)

Rhagomys rufescens		2 (RBP3, RAG1)
Rhagomys septentrionalis	2 (COX1, CYTB)	1 (RBP3)
Rheomys raptor		3 (RBP3, RAG1, ACP5)
Rhipidomys gardneri MUSM 36654	13 (ND1, ND2, COX1, COX2, ATP8, ATP6, COX3, ND3, ND4, ND4L, ND5, ND6, CYTB)	
Rhipidomys gardneri MUSM 41308		5 (BRCA1, RBP3, RAG1, ACP5, GHR)
Rhipidomys macconnelli	1 (CYTB)	4 (BRCA1, RAG1, ACP5, GHR)
Rhipidomys mastacalis	1 (CYTB)	5 (BRCA1, RBP3, RAG1, ACP5, GHR)
Rhipidomys nitela	2 (COX1, CYTB)	1 (ACP5)
Rhipidomys venezuelae	1 (CYTB)	2 (RAG1, ACP5)
Rhipidomys venustus	1 (CYTB)	2 (RBP3, RAG1)
Rhipidomys wetzeli	2 (COX1, CYTB)	

Rhipidomys sp.	13 (ND1, ND2, COX1, COX2, ATP8, ATP6, COX3, ND3, ND4, ND4L, ND5, ND6, CYTB)	
Sigmodon hispidus	13 (ND1, ND2, COX1, COX2, ATP8, ATP6, COX3, ND3, ND4, ND4L, ND5, ND6, CYTB)	5 (BRCA1, RBP3, RAG1, ACP5, GHR)
Thomasomys cf. *apeco* MUSM 52644	13 (ND1, ND2, COX1, COX2, ATP8, ATP6, COX3, ND3, ND4, ND4L, ND5, ND6, CYTB)	5 (BRCA1, RBP3, RAG1, ACP5, GHR)
Thomasomys aff. *aureus* MUSM 47039	10 (ND2, COX1, ATP6, COX3, ND3, ND4, ND4L, ND5, ND6, CYTB)	5 (BRCA1, RBP3, RAG1, ACP5, GHR)
Thomasomys australis MSB 70447	7 (ND1, ND2, COX1, COX2, ATP6, COX3, ND3)	5 (BRCA1, RBP3, RAG1, ACP5, GHR)
Thomasomys cinereus MUSM 41103	13 (ND1, ND2, COX1, COX2, ATP8, ATP6, COX3, ND3, ND4, ND4L, ND5, ND6, CYTB)	5 (BRCA1, RBP3, RAG1, ACP5, GHR)
Thomasomys cinereus MUSM 51109	13 (ND1, ND2, COX1, COX2, ATP8, ATP6, COX3, ND3, ND4, ND4L, ND5, ND6, CYTB)	5 (BRCA1, RBP3, RAG1, ACP5, GHR)

Thomasomys daphne FMNH 175228	6 (COX1, COX2, ATP8, COX3, ND3, ND4L)	5 (BRCA1, RBP3, RAG1, ACP5, GHR)
Thomasomys daphne MSB 236318	3 (COX3, ND3, ND4L)	5 (BRCA1, RBP3, RAG1, ACP5, GHR)
Thomasomys incanus MUSM 46190	13 (ND1, ND2, COX1, COX2, ATP8, ATP6, COX3, ND3, ND4, ND4L, ND5, ND6, CYTB)	5 (BRCA1, RBP3, RAG1, ACP5, GHR)
Thomasomys incanus MUSM 52866	3 (COX3, ND3, ND4L)	5 (BRCA1, RBP3, RAG1, ACP5, GHR)
Thomasomys cf. *incanus* MUSM 40805	2 (ND3, ND4L)	5 (BRCA1, RBP3, RAG1, ACP5, GHR)
Thomasomys ischyrus MUSM 14984		5 (BRCA1, RBP3, RAG1, ACP5, GHR)
Thomasomys ischyrus MUSM 18741	13 (ND1, ND2, COX1, COX2, ATP8, ATP6, COX3, ND3, ND4, ND4L, ND5, ND6, CYTB)	

Thomasomys ischyrus MUSM 24406	13 (ND1, ND2, COX1, COX2, ATP8, ATP6, COX3, ND3, ND4, ND4L, ND5, ND6, CYTB)	5 (BRCA1, RBP3, RAG1, ACP5, GHR)
Thomasomys ischyrus MUSM 36991	6 (ND1, COX1, ND3, ND4, ND4L, ND6)	5 (BRCA1, RBP3, RAG1, ACP5, GHR)
Thomasomys ischyrus MUSM48102	1 (CYTB)	
Thomasomys ischyrus MUSM 50731	8 (ND1, COX1, ATP8, ATP6, ND3, ND4L, ND6, CYTB)	5 (BRCA1, RBP3, RAG1, ACP5, GHR)
Thomasomys aff. *ischyrus* MUSM 18741		5 (BRCA1, RBP3, RAG1, ACP5, GHR)
Thomasomys aff. *ischyrus* MUSM 48102		5 (BRCA1, RBP3, RAG1, ACP5, GHR)
Thomasomys aff. *ischyrus* MUSM 52650	13 (ND1, ND2, COX1, COX2, ATP8, ATP6, COX3, ND3, ND4, ND4L, ND5, ND6, CYTB)	5 (BRCA1, RBP3, RAG1, ACP5, GHR)

Thomasomys kalinowskii MUSM 24282	10 (COX1, COX2, ATP8, ATP6, COX3, ND3, ND4, ND4L, ND5, ND6)	5 (BRCA1, RBP3, RAG1, ACP5, GHR)
Thomasomys kalinowskii MUSM 52878	2 (ND1, COX1)	5 (BRCA1, RBP3, RAG1, ACP5, GHR)
Thomasomys aff. *kalinowskii* MUSM 14984	8 (COX2, ATP8, ATP6, ND3, ND4L, ND5, ND6, CYTB)	
Thomasomys lojapiuranus MUSM 56159	13 (ND1, ND2, COX1, COX2, ATP8, ATP6, COX3, ND3, ND4, ND4L, ND5, ND6, CYTB)	5 (BRCA1, RBP3, RAG1, ACP5, GHR)
Thomasomys notatus FMNH 170701	12 (ND1, ND2, COX1, COX2, ATP8, ATP6, COX3, ND3, ND4, ND5, ND6, CYTB)	2 (RBP3, GHR)
Thomasomys notatus MUSM 47044	4 (COX1, ND5, ND6, CYTB)	5 (BRCA1, RBP3, RAG1, ACP5, GHR)
Thomasomys oreas MSB 87126	2 (ATP6, COX3)	5 (BRCA1, RBP3, RAG1, ACP5, GHR)

Thomasomys praetor MUSM 40209	11 (ND1, ND2, COX1, ATP6, COX3, ND3, ND4, ND4L, ND5, ND6, CYTB)	5 (BRCA1, RBP3, RAG1, ACP5, GHR)
Thomasomys pyrrhonotus MUSM 47234	5 (COX1, COX3, ND3, ND6, CYTB)	5 (BRCA1, RBP3, RAG1, ACP5, GHR)
Thomasomys pyrrhonotus MUSM 52408	13 (ND1, ND2, COX1, COX2, ATP8, ATP6, COX3, ND3, ND4, ND4L, ND5, ND6, CYTB)	5 (BRCA1, RBP3, RAG1, ACP5, GHR)
Thomasomys aff. *pyrrhonotus* MUSM 55555	3 (COX3, ND3, ND4L)	5 (BRCA1, RBP3, RAG1, ACP5, GHR)
Thomasomys shallqukucha MUSM 46881	12 (ND1, ND2, COX1, COX2, ATP8, ATP6, COX3, ND3, ND4, ND4L, ND5, ND6)	5 (BRCA1, RBP3, RAG1, ACP5, GHR)
Thomasomys shallqukucha MUSM 47230	13 (ND1, ND2, COX1, COX2, ATP8, ATP6, COX3, ND3, ND4, ND4L, ND5, ND6, CYTB)	5 (BRCA1, RBP3, RAG1, ACP5, GHR)
Thomasomys taczanowskii MUSM 46894	13 (ND1, ND2, COX1, COX2, ATP8, ATP6, COX3, ND3, ND4, ND4L, ND5, ND6, CYTB)	5 (BRCA1, RBP3, RAG1, ACP5, GHR)

Thomasomys taczanowskii MUSM 47235	13 (ND1, ND2, COX1, COX2, ATP8, ATP6, COX3, ND3, ND4, ND4L, ND5, ND6, CYTB)	5 (BRCA1, RBP3, RAG1, ACP5, GHR)
Thomasomys taczanowskii MUSM 47236	13 (ND1, ND2, COX1, COX2, ATP8, ATP6, COX3, ND3, ND4, ND4L, ND5, ND6, CYTB)	5 (BRCA1, RBP3, RAG1, ACP5, GHR)
Thomasomys taczanowskii MUSM 56170	13 (ND1, ND2, COX1, COX2, ATP8, ATP6, COX3, ND3, ND4, ND4L, ND5, ND6, CYTB)	5 (BRCA1, RBP3, RAG1, ACP5, GHR)
Thomasomys sp. 1 AMNH 72132	12 (ND1, ND2, COX1, COX2, ATP6, COX3, ND3, ND4, ND4L, ND5, ND6, CYTB)	3 (BRCA1, RBP3, ACP5)
Thomasomys sp. 1 MUSM 12000	6 (COX1, ATP6, COX3, ND3, ND4L, CYTB)	5 (BRCA1, RBP3, RAG1, ACP5, GHR)
Thomasomys sp. 6 MUSM 46254	13 (ND1, ND2, COX1, COX2, ATP8, ATP6, COX3, ND3, ND4, ND4L, ND5, ND6, CYTB)	4 (BRCA1, RAG1, ACP5, GHR)
Thomasomys sp. 8 MUSM 34881	13 (ND1, ND2, COX1, COX2, ATP8, ATP6, COX3, ND3, ND4, ND4L, ND5, ND6, CYTB)	5 (BRCA1, RBP3, RAG1, ACP5, GHR)

Thomasomys sp. A MUSM 42490	13 (ND1, ND2, COX1, COX2, ATP8, ATP6, COX3, ND3, ND4, ND4L, ND5, ND6, CYTB)	5 (BRCA1, RBP3, RAG1, ACP5, GHR)
Thomasomys sp. A MUSM 52861	13 (ND1, ND2, COX1, COX2, ATP8, ATP6, COX3, ND3, ND4, ND4L, ND5, ND6, CYTB)	5 (BRCA1, RBP3, RAG1, ACP5, GHR)
Wiedomys cerradensis	13 (ND1, ND2, COX1, COX2, ATP8, ATP6, COX3, ND3, ND4, ND4L, ND5, ND6, CYTB)	4 (BRCA1, RBP3, RAG1, GHR)
Wilfredomys oenax	1 (CYTB)	4 (BRCA1, RBP3, RAG1, GHR)

APPENDIX 3

DNA substitution rates among 13 mitochondrial and 5 nuclear partitions. Abbreviations: N – number of sequences; Site – number of positions; Unique – number of unique site patterns; Infor – number of parsimony-informative sites; Invar – number of invariant sites; Const – number of constant sites. Superscript: mt – mitochondrial, n – nuclear

#	Gene	N	Site	Unique	Infor	Invar	Const
1	ND1^{m}	40	957	494	396	480	479
2	ND2^{m}	38	978	615	492	387	387
3	COX1^{m}	53	1545	686	531	942	942
4	COX2^{m}	38	684	322	248	398	398
5	ATP8^{m}	37	204	143	113	71	71
6	ATP6^{m}	43	681	379	285	330	330
7	COX3^{m}	47	783	397	309	432	432
8	ND3^{m}	58	348	227	193	131	131
9	ND4L^{m}	54	297	199	158	110	110
10	ND4^{m}	48	1377	780	615	639	639
11	ND5^{m}	37	1812	1015	807	839	839
12	ND6^{m}	44	528	322	255	227	227
13	CYTB^{m}	64	1140	651	487	567	567
14	GHR^{n}	73	934	396	128	662	662
15	ACP5^{n}	66	277	103	33	227	227
16	RAG1^{n}	75	2050	790	286	1473	1473

17	RBP3[n]	85	1338	574	238	905	905
18	BRCA1[n]	68	1549	751	457	764	764

APPENDIX 4

Best-fit model according to BIC

Edge-unlinked partition model and separate models between partitions. Superscript: m – mitochondrial, n – nuclear

#	Gene	Model	Parameters
1	ND1^{m}	TIM2+I+G4	TIM2{8.02434,35.3224,70.1985}+F{0.302971,0.294707,0.112656,0.289667}+I{0.451504}+G4{1.09835}
2	ND2^{m}	GTR+I+G4	GTR{1.79237,7.55682,0.89807,0.100339,11.3718}+F{0.346794,0.289088,0.0809787,0.283139}+I{0.304543}+G4{0.950777}
3	COX1^{m}	TIM2+I+G4	TIM2{5.09138,17.6412,51.0109}+F{0.285557,0.257317,0.158773,0.298353}+I{0.583919}+G4{1.36236}
4	COX2^{m}	TIM2+I+G4	TIM2{6.8509,37.4904,100}+F{0.333003,0.266771,0.130935,0.26929}+I{0.545947}+G4{1.30459}
5	ATP8^{m}	TN+I+G4	TN{10.9962,7.00215}+F{0.380692,0.289576,0.0647607,0.264972}+I{0.297936}+G4{1.75577}

6	ATP6^{m}	TIM2+I+G4	TIM2{4.26808,27.4924,38.9876}+F{0.317666,0.290331,0.0980741,0.293929}+I{0.40435}+G4{0.842187}
7	COX3^{m}	TIM2+I+G4	TIM2{9.17108,39.6924,100}+F{0.296715,0.283635,0.139431,0.280218}+I{0.518265}+G4{1.39384}
8	ND3^{mt}	TIM2+I+G4	TIM2{2.86805,13.6212,24.6991}+F{0.308149,0.278301,0.11209,0.30146}+I{0.349391}+G4{1.2968}
9	ND4L^{m}	TIM2+I+G4	TIM2{5.50395,25.7661,51.9064}+F{0.307461,0.273387,0.110749,0.308404}+I{0.323088}+G4{0.954276}
10	ND4^{mt}	TIM2+I+G4	TIM2{4.32062,24.2242,43.8144}+F{0.33332,0.282429,0.0963,0.287951}+I{0.410063}+G4{0.98891}
11	ND5^{m}	TIM2+I+G4	TIM2{4.501,30.6455,48.0838}+F{0.321826,0.294668,0.101072,0.282434}+I{0.409206}+G4{1.33694}
12	ND6^{m}	TPM3u+I+G4	TPM3u{0.331751,12.686}+F{0.195578,0.0752935,0.322002,0.407126}+I{0.335392}+G4{0.795359}

13	CYTB[m]	GTR+I+G4	GTR{2.79096,10.2546,1.93235,0.181976,22.2618}+F{0.295449,0.288843,0.123484,0.292224}+I{0.453966}+G4{0.904439}
14	GHR[n]	HKY+G4	HKY{5.60311}+F{0.288937,0.267339,0.229983,0.213741}+G4{0.388616}
15	ACP5[n]	K2P+G4	K2P{7.19023}+G4{0.136684}
16	RAG1[n]	TNe+G4	TNe{5.22145,6.38242}+G4{0.400483}
17	RBP3[n]	TIMe+G4	TIMe{6.40046,0.587953,5.28937}+G4{0.397627}
18	BRCA1[n]	TIM2+G4	TIM2{0.702612,2.61511,3.20427}+F{0.372635,0.195458,0.222359,0.209549}+G4{1.86784}

APPENDIX 5

Phylogenetic trees based on maximum likelihood (ML, left) and Bayesian inference (BI, right) using 13 mitochondrial genes. The values above the branches represent bootstrap support values for ML and posterior probabilities for BI. Lineages of "*Thomasomys*" sp. 4 are in bold. Numbers in the brackets are keyed in appendix 1 and mapped in figure 1.

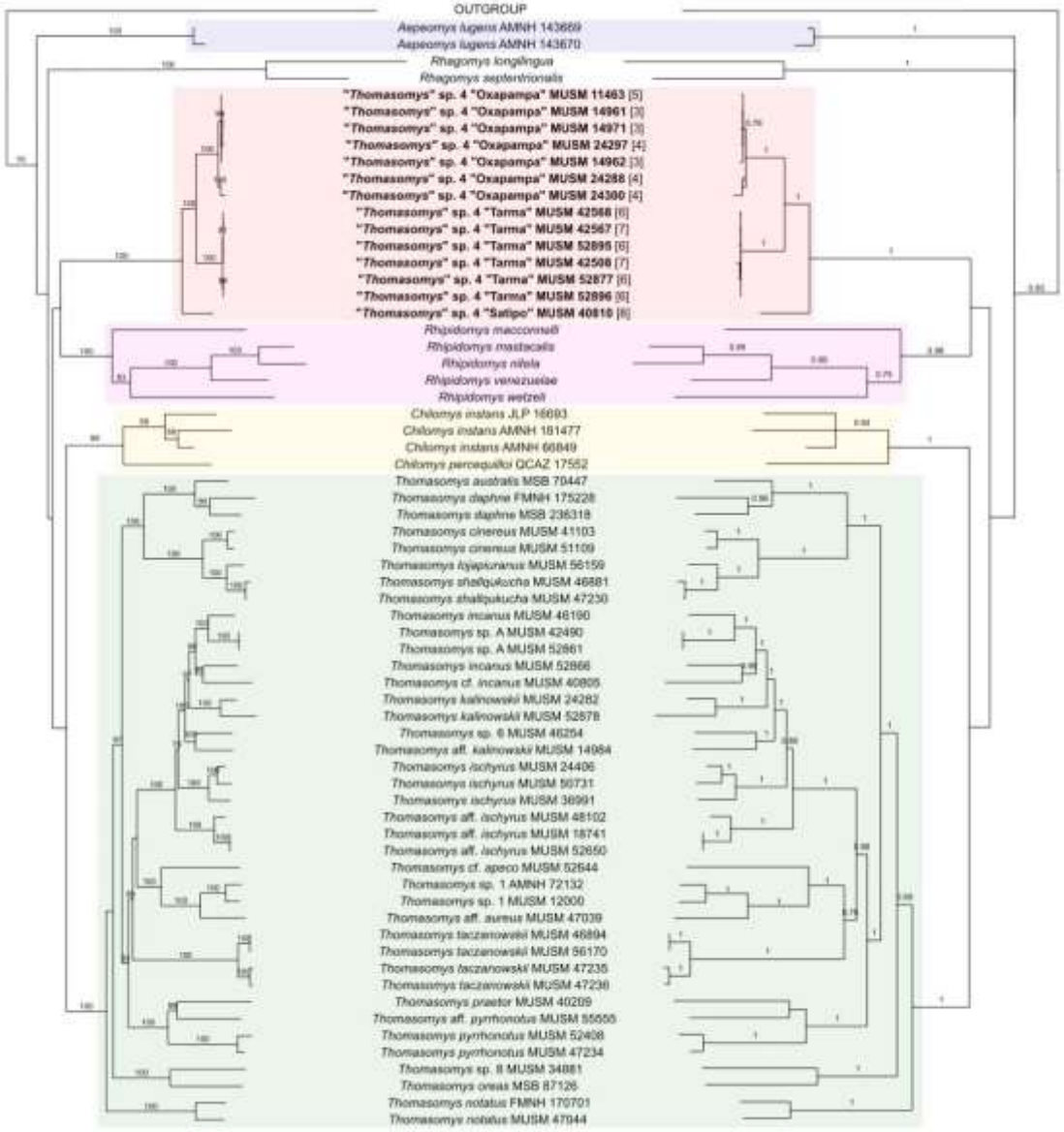

APPENDIX 6

Phylogenetic trees based on maximum likelihood (ML, left) and Bayesian inference (BI, right) using 5 nuclear genes. The values above the branches represent bootstrap support values for ML and posterior probabilities for BI. Lineages of "*Thomasomys*" sp. 4 are in bold. Numbers in brackets are keyed in appendix 1 and mapped in figure 1.

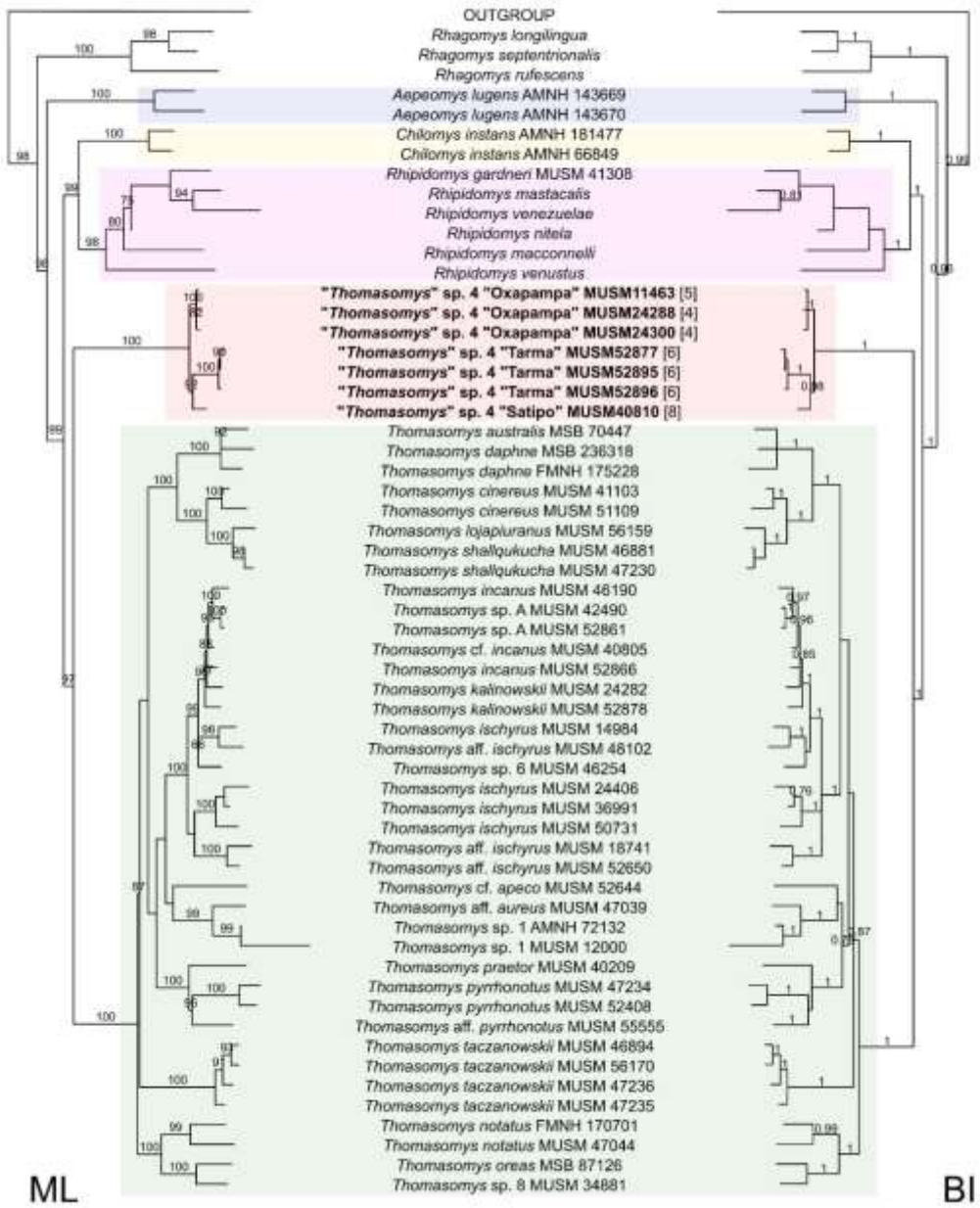

APPENDIX 7

Craniodental measurements (in mm) of *Aepeomys lugens*, *Thomasomys cinereus*, *T eleusis*, *T. incanus*, *T. ischyrus*, *T. kalinowskii*, *T. ladewi*, and *T. shallqukucha*. Table entries include the sample mean, standard deviation, observed range (in parentheses), and sample size. Abbreviations are explained in Material and Methods. Asterisks show species that include measurements of the holotype.

Variables	***Aepeomys lugens****	***Thomasomys cinereus***	***Thomasomys eleusis****	***Thomasomys incanus****	***Thomasomys ischyrus****	***Thomasomys kalinowskii****	***Thomasomys ladewi****	***Thomasomys shallqukucha***
GLS	30.71±0.88	32.64±0.52	33.14±0.35	29.95±0.5	33.42±0.53	34.75±0.83	33.31±0.28	33.8±0.72
	(29.59-32.61)	(31.86-33.25)	(32.68-33.65)	(28.89-30.54)	(32.5-34.4)	(33.3-35.93)	(32.96-33.73)	(32.87-34.76)
	11	8	4	7	13	7	4	9
CIL	27.16±0.89	30.13±0.63	29.74±0.62	26.93±0.36	30.19±0.59	32.14±0.6	31.08±0.41	31.28±0.61
	(26.18-29.17)	(29.12-30.98)	(28.83-30.5)	(26.31-27.42)	(29.07-31.42)	(31.28-32.96)	(30.55-31.79)	(30.41-32.47)
	11	8	4	7	14	7	5	9

CML	17.75±0.5 (17.14-18.72) 11	19.71±0.46 (18.87-20.37) 8	19.4±0.43 (18.81-19.91) 4	17.5±0.27 (17.21-17.89) 7	19.74±0.34 (19.4-20.48) 14	20.61±0.59 (19.71-21.37) 7	20.2±0.28 (19.72-20.55) 5	20.11±0.39 (19.49-20.75) 9
LOF	8.46±0.19 (8.16-8.76) 11	11.12±0.37 (10.59-11.78) 8	9.79±0.36 (9.52-10.4) 4	8.71±0.24 (8.29-8.99) 7	9.74±0.21 (9.37-10.1) 14	10.9±0.33 (10.51-11.37) 7	10.76±0.17 (10.46-10.9) 5	10.84±0.32 (10.22-11.31) 9
LN	11.89±0.66 (11.28-13.42) 11	12.81±0.56 (12.14-13.49) 8	13.22±0.38 (12.72-13.78) 4	11.79±0.42 (11.15-12.32) 7	13.48±0.38 (13.1-14.5) 13	13.79±0.44 (13.16-14.3) 7	12.21±0.19 (11.89-12.39) 4	12.86±0.41 (12.33-13.4) 9
LD	8.23±0.4 (7.71-9.07) 11	8.85±0.25 (8.36-9.16) 8	8.78±0.21 (8.45-9.03) 4	8.23±0.23 (7.82-8.48) 7	8.92±0.3 (8.29-9.45) 14	9.77±0.18 (9.45-10.04) 7	9.34±0.2 (8.98-9.54) 5	9.54±0.25 (9.2-10.14) 9

LIF	5.4±0.45 (4.74-6.3) 11	6.81±0.2 (6.44-7.07) 8	6.45±0.32 (6.06-6.84) 4	5.94±0.23 (5.66-6.4) 7	6.76±0.32 (6.26-7.43) 14	7.4±0.18 (7.04-7.57) 7	6.72±0.36 (6.14-7.09) 5	6.58±0.18 (6.38-6.85) 9
LM	4.42±0.13 (4.2-4.6) 11	5.33±0.16 (5.01-5.57) 8	5.33±0.23 (5-5.62) 4	4.58±0.13 (4.35-4.75) 7	5.37±0.18 (4.91-5.68) 14	5.78±0.13 (5.54-5.96) 7	5.95±0.17 (5.67-6.21) 5	5.21±0.11 (5.05-5.41) 9
BIF	2.16±0.17 (1.87-2.45) 11	2.43±0.1 (2.27-2.61) 8	2.06±0.18 (1.89-2.35) 4	2.06±0.06 (1.97-2.17) 7	2.22±0.23 (1.86-2.54) 14	2.17±0.09 (2.04-2.31) 7	2.34±0.1 (2.19-2.46) 5	2.37±0.1 (2.22-2.54) 9
BR	4.87±0.18 (4.6-5.21) 11	5.52±0.19 (5.31-5.94) 8	5.32±0.3 (4.88-5.73) 4	5.04±0.23 (4.7-5.37) 5	5.36±0.26 (4.83-5.75) 14	5.73±0.11 (5.57-5.89) 7	5.85±0.23 (5.63-6.14) 5	5.41±0.18 (5.05-5.59) 9

BPB	3.4±0.16 (3.01-3.68) 11	3.52±0.23 (3.1-3.87) 8	3.34±0.15 (3.17-3.58) 4	2.94±0.13 (2.72-3.16) 7	3.55±0.28 (3.01-3.92) 13	3.64±0.15 (3.47-3.91) 7	3.36±0.27 (3.04-3.72) 5	3.58±0.18 (3.21-3.75) 9
BM1	1.45±0.04 (1.39-1.52) 11	1.67±0.07 (1.57-1.77) 8	1.72±0.11 (1.59-1.89) 4	1.46±0.07 (1.35-1.53) 7	1.75±0.09 (1.6-1.92) 14	1.87±0.04 (1.8-1.93) 7	2±0.1 (1.91-2.17) 5	1.74±0.1 (1.59-1.95) 9
BN	3.58±0.22 (3.25-3.98) 11	4.14±0.2 (3.84-4.46) 8	3.85±0.21 (3.64-4.09) 4	3.65±0.2 (3.36-3.93) 7	3.76±0.28 (3.4-4.21) 14	4.36±0.15 (4.12-4.58) 7	4.46±0.1 (4.35-4.61) 4	4.3±0.18 (3.98-4.52) 9
LIB	5.98±0.15 (5.8-6.2) 11	5.02±0.21 (4.7-5.35) 8	5.45±0.07 (5.34-5.55) 4	5.09±0.28 (4.64-5.46) 7	5.88±0.4 (5.38-6.67) 14	5.51±0.15 (5.2-5.71) 7	5.39±0.14 (5.16-5.55) 5	5.3±0.16 (5.05-5.53) 9

ZB	14±0.42 (13.57-14.8) 10	17.39±0.61 (16.32-18.29) 8	15.81±0.5 (15.28-16.61) 4	14.42±0.24 (14.08-14.64) 3	16.3±0.51 (15.48-16.93) 10	18.2±0.4 (17.49-18.98) 7	18.24±0.15 (18.05-18.48) 5	17.46±0.52 (16.63-18.42) 9
RL	11.79±0.47 (11.15-12.79) 11	11.24±0.26 (10.67-11.56) 8	11.96±0.28 (11.49-12.18) 4	11.05±0.29 (10.55-11.4) 7	12.37±0.4 (11.85-13.17) 13	12.49±0.48 (11.95-13.47) 7	11.2±0.28 (10.85-11.54) 4	12.3±0.31 (11.82-12.62) 9
BB	13.06±0.24 (12.63-13.56) 11	14.15±0.41 (13.47-14.74) 8	14.24±0.14 (14-14.36) 4	13.51±0.34 (13.02-13.89) 7	14.68±0.45 (13.84-15.35) 11	15.52±0.3 (15.3-16.23) 7	15.76±0.08 (15.61-15.84) 5	14.14±0.24 (13.59-14.4) 9
BZP	1.8±0.17 (1.46-1.97) 11	2.59±0.12 (2.38-2.8) 8	2.79±0.05 (2.72-2.85) 4	2.15±0.13 (1.97-2.37) 7	2.53±0.17 (2.29-2.89) 14	3.18±0.16 (2.93-3.47) 7	3.19±0.16 (2.87-3.31) 5	2.74±0.18 (2.47-3.06) 9

DI	1.27±0.06 (1.19-1.36) 11	1.61±0.09 (1.47-1.71) 8	1.54±0.09 (1.43-1.64) 4	1.32±0.09 (1.17-1.42) 7	1.57±0.13 (1.4-1.85) 14	1.83±0.1 (1.7-2.02) 7	1.74±0.13 (1.55-1.97) 5	1.71±0.05 (1.65-1.81) 9
HBC	9.1±0.2 (8.75-9.51) 11	9.36±0.21 (9.06-9.64) 8	9.61±0.28 (9.31-10.05) 4	9.15±0.56 (8.33-9.87) 7	9.76±0.41 (9.17-10.81) 14	10.21±0.23 (9.8-10.56) 7	10.34±0.2 (10.01-10.58) 5	9.38±0.22 (9.06-9.68) 9
MFB	2.21±0.17 (1.95-2.4) 11	2.03±0.13 (1.83-2.23) 8	2.38±0.18 (2.07-2.51) 4	2.03±0.12 (1.81-2.14) 5	2.63±0.14 (2.38-2.92) 13	2.53±0.2 (2.17-2.8) 7	2.32±0.15 (2.11-2.49) 5	2.48±0.17 (2.27-2.77) 9
MN	4.64±0.11 (4.49-4.87) 11	5.65±0.21 (5.19-5.8) 8	5.6±0.21 (5.35-5.93) 4	4.8±0.17 (4.58-5.02) 7	5.66±0.22 (5.36-6.08) 14	6.03±0.09 (5.85-6.11) 7	6.46±0.19 (6.21-6.75) 5	5.37±0.14 (5.11-5.54) 9

APPENDIX 8

Normality Assessment for individual variables for genus-level and species-level matrixes.

#	Variable	Genus-level matrix			Species-level matrix		
		Statistic	P-value	Normality	Statistic	P-value	Normality
1	GLS	2.1199	<0.001	No	0.5416	0.1565	Yes
2	CIL	5.2556	<0.001	No	0.7009	0.0632	Yes
3	CML	6.0478	<0.001	No	0.5133	0.1847	Yes
4	LOF	3.7359	<0.001	No	0.5318	0.1658	Yes
5	LN	0.9095	0.0199	No	0.2593	0.6998	Yes
6	LD	0.6708	0.0779	Yes	0.2756	0.6445	Yes
7	LIF	0.345	0.4797	Yes	0.6805	0.0711	Yes
8	LM	0.8092	0.0353	No	0.2656	0.6784	Yes
9	BIF	0.7298	0.0556	Yes	0.2482	0.7375	Yes
10	BR	0.1919	0.8943	Yes	0.3844	0.3814	Yes
11	BPB	0.4993	0.2056	Yes	0.2821	0.6232	Yes
12	BM1	0.6008	0.1162	Yes	0.2066	0.8614	Yes
13	BN	1.3585	0.0015	No	0.6361	0.0918	Yes
14	LIB	1.6723	3.00E-04	No	0.3744	0.4027	Yes
15	ZB	1.3197	0.0019	No	0.2164	0.8357	Yes
16	RL	0.2932	0.5968	Yes	0.1713	0.9266	Yes
17	BB	0.7635	0.0458	No	0.4883	0.2135	Yes
18	BZP	2.8045	<0.001	No	0.3973	0.3555	Yes
19	DI	2.483	<0.001	No	0.5247	0.1728	Yes

20	HBC	2.2431	<0.001	No	0.3261	0.5125	Yes
21	MFB	1.8536	1.00E-04	No	0.4613	0.249	Yes
22	MN	1.4247	0.0011	No	0.3865	0.3771	Yes

APPENDIX 9

Correlation analysis using the Spearman's coefficient for (A) genus-level matrix and (B) species-level matrix.

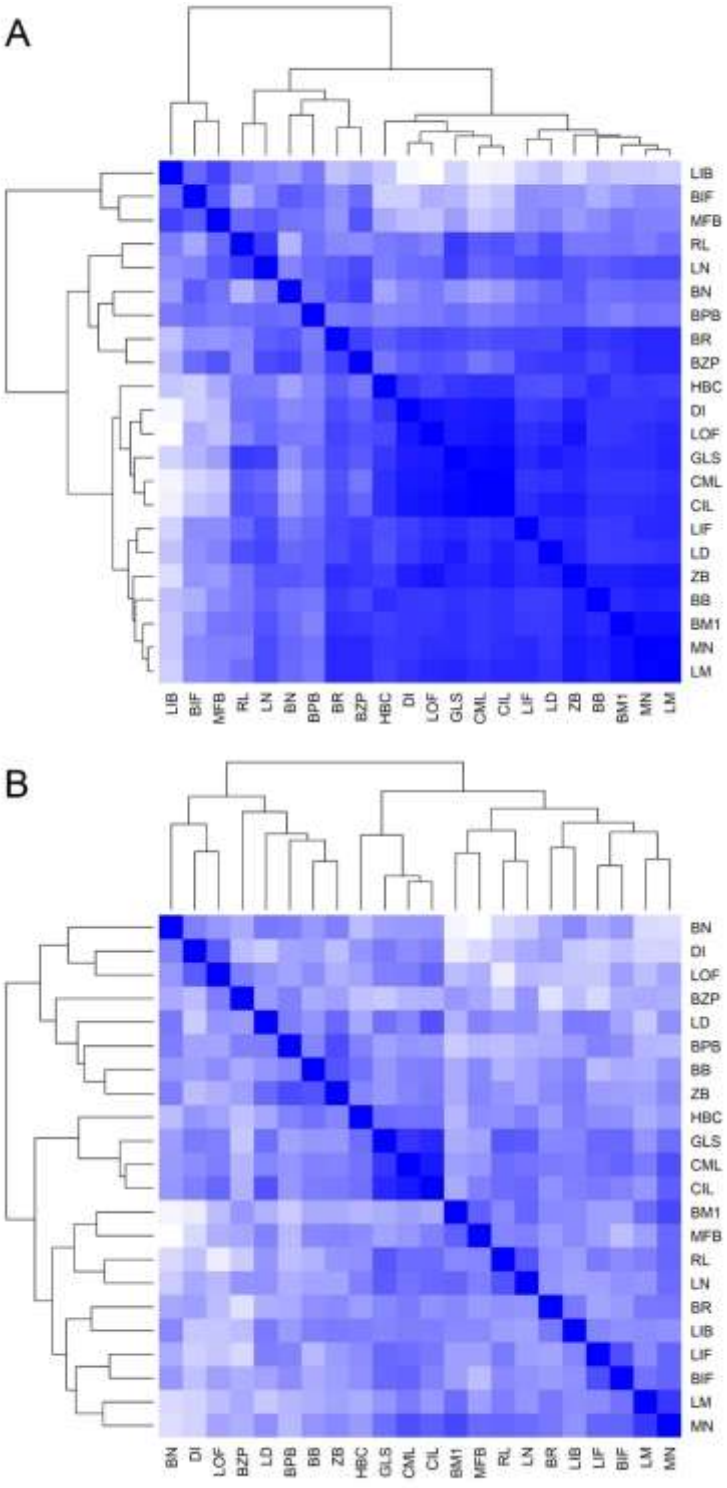

FIGURES

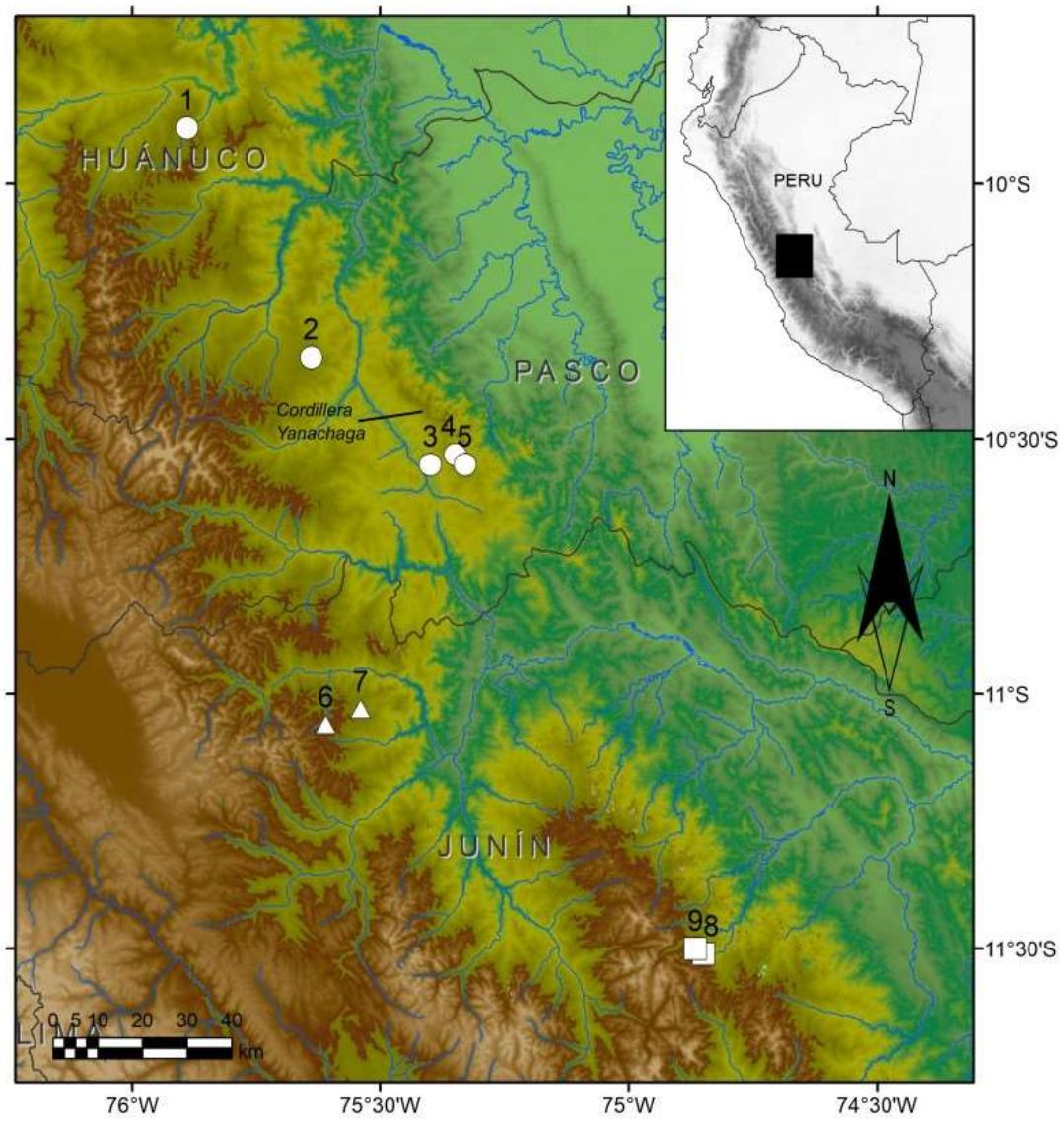

Figure 1. Collecting localities for examined specimens of the "*Thomasomys*" sp. 4 from central Peru: "Oxapampa" (circles), "Tarma" (squares), and "Satipo" (triangles). Numbers are keyed in appendix 1. Outline map of Peru, indicating the boundaries (black square) of the area shown.

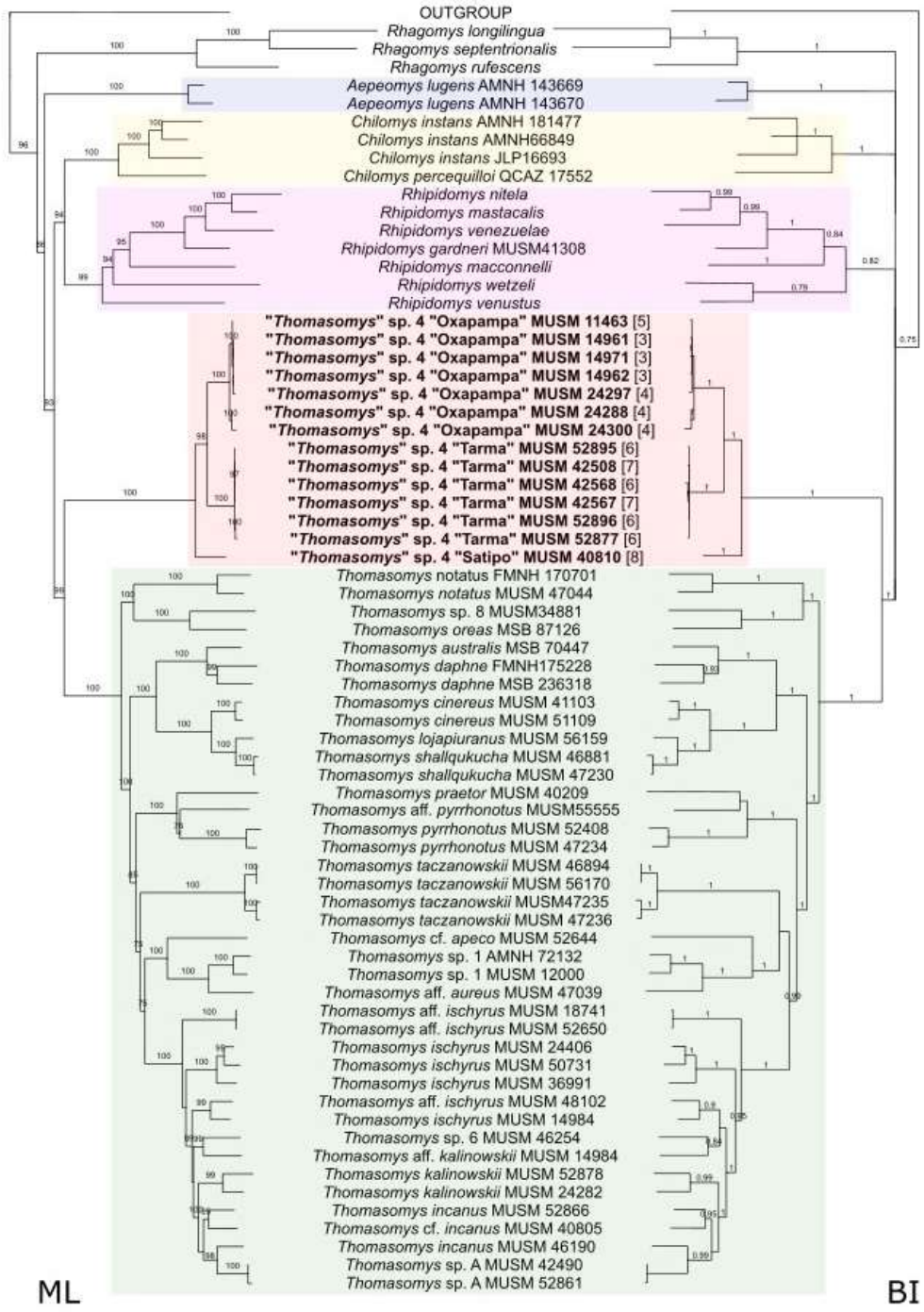

Figure 2. Phylogenetic trees based on maximum likelihood (ML, left) and Bayesian inference (BI, right) using 13 mitochondrial genes and five nuclear genes. The values above the branches represent bootstrap support values for ML and posterior probabilities for BI. Lineages of "*Thomasomys*" sp. 4 are in bold. Numbers in the brackets are keyed in appendix 1 and mapped in figure 1.

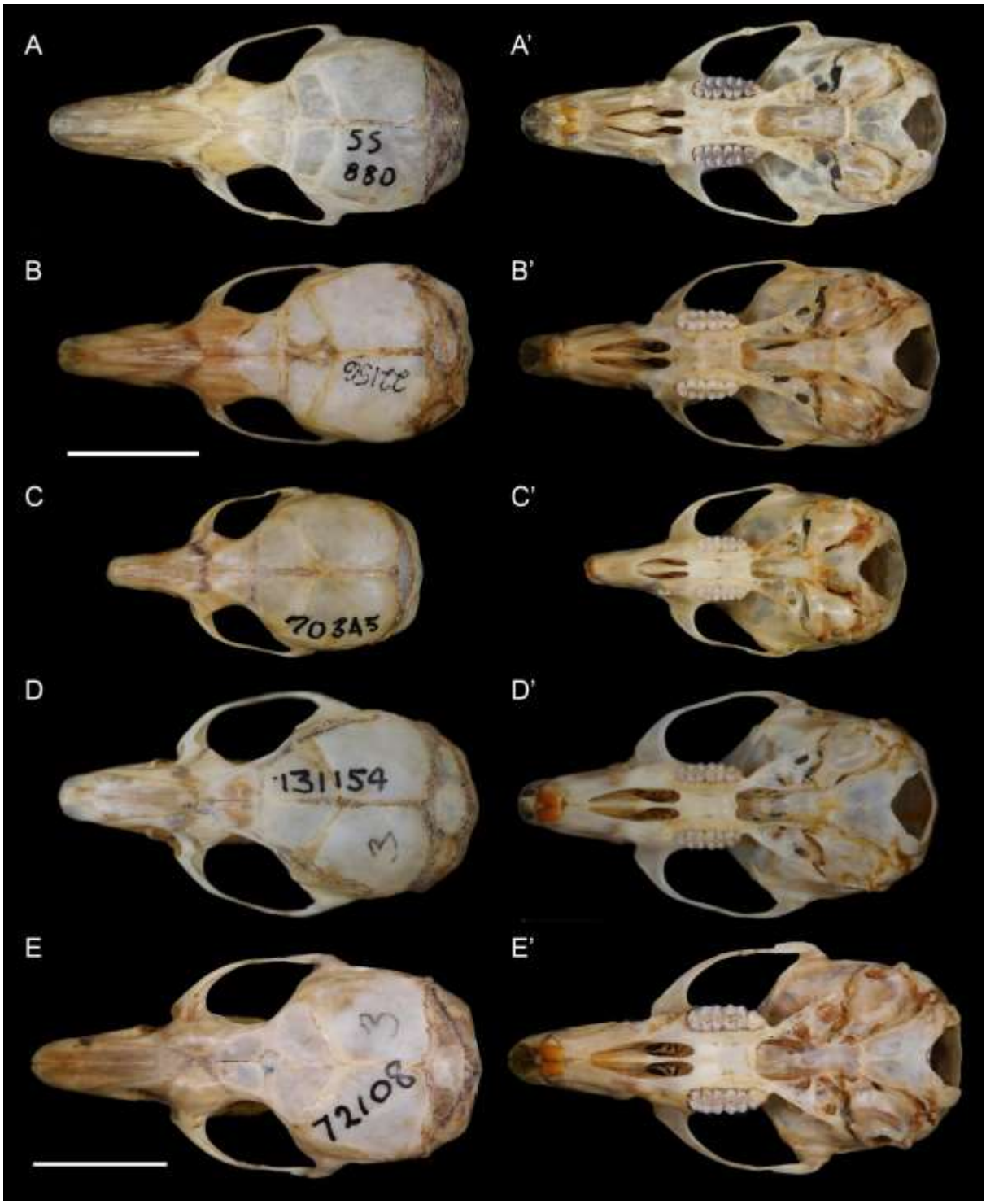

Figure 3. Dorsal and ventral view of the skulls of "*Thomasomys*" sp. 4 "Oxapampa" (A, A': MUSM 10571), *Aepeomys lugens* (B, B': AMNH 143670), *Chilomys instans* (C, C': FMNH 70345), *Rhipidomys macconnelli* (D. D': AMNH 131154), *Thomasomys ischyrus* (E, E': AMNH 72108). Scale bar: 10 mm.

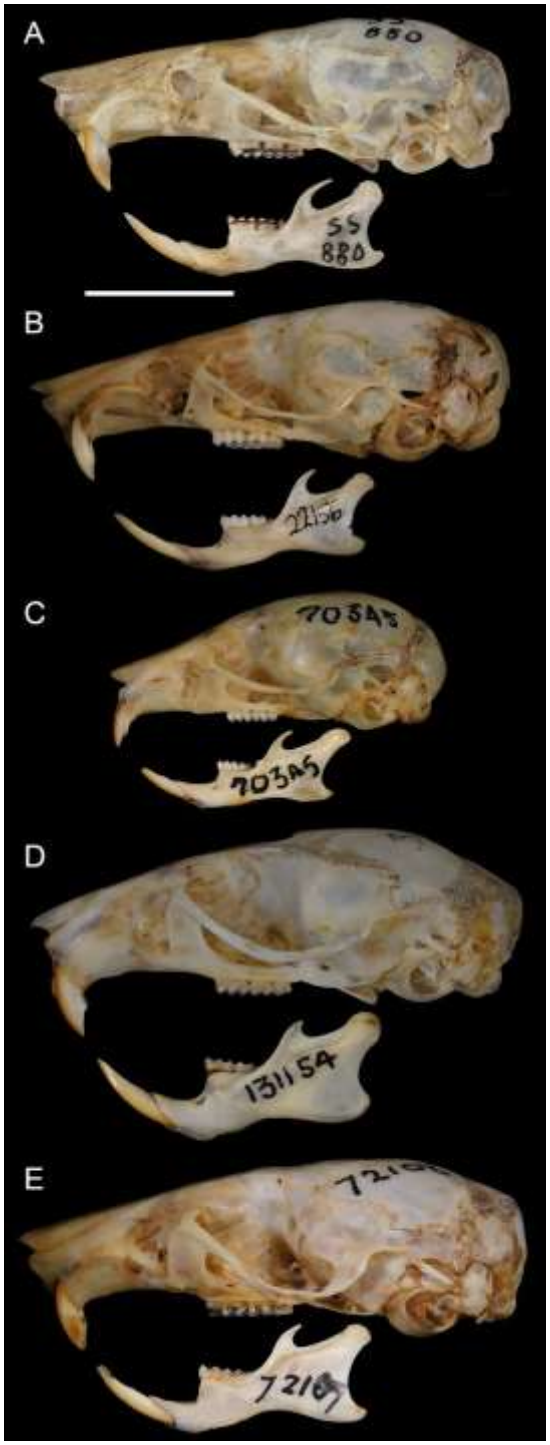

Figure 4. Lateral view of the skull and mandibular view of "*Thomasomys*" sp. 4 "Oxapampa" (A: MUSM 10571), *Aepeomys lugens* (B: AMNH 143670), *Chilomys instans* (C: FMNH 70345), *Rhipidomys macconnelli* (D: AMNH 131154), *Thomasomys ischyrus* (E: skull: AMNH 72108, mandible: AMNH 72109). Scale bar: 10 mm.

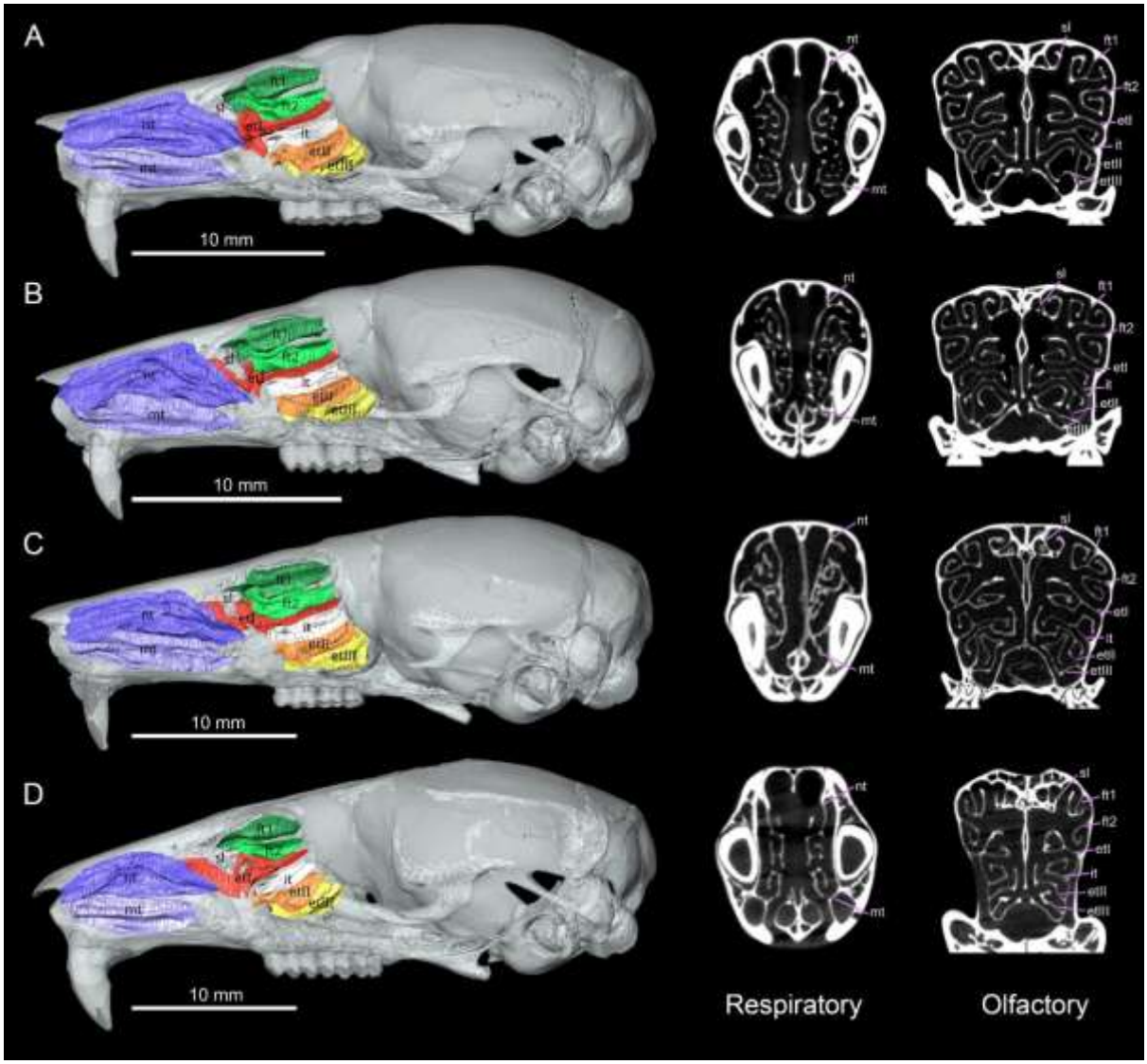

Figure 5. Respiratory and olfactory turbinals of A: "*Thomasomys*" sp. 4 "Oxapampa" (MUSM 11340), B: "*Thomasomys*" sp. 4 "Satipo" (MUSM 40820), C: *Aepeomys lugens* (NHMUK 1905.2.5.15), D: *Thomasomys* cf. *pyrrhonotus* (MUSM 55555). Abbreviations: nt – nasoturbinal, mt – maxilloturbinal, sl – semicircular lamina, ft1 – frontoturbinal 1, ft2 – frontoturbinal 2, it – interturbinal, etI – ethmoturbinal I, etII – ethmoturbinal II, etIII – ethmoturbinal III.



Figure 6. Dorsal, lateral, and ventral pelage of "*Thomasomys*" sp. 4 "Oxapampa" (MUSM 24325). Scale bar = 5 cm.



Figure 7. Dorsal, lateral, and ventral pelage of "*Thomasomys*" sp. 4 "Tarma" (MUSM 42508, paratype). Scale bar = 5 cm.



Figure 8. Dorsal, lateral, and ventral pelage of "*Thomasomys*" sp. 4 "Satipo" (MUSM 40811, paratype). Scale bar = 5 cm.

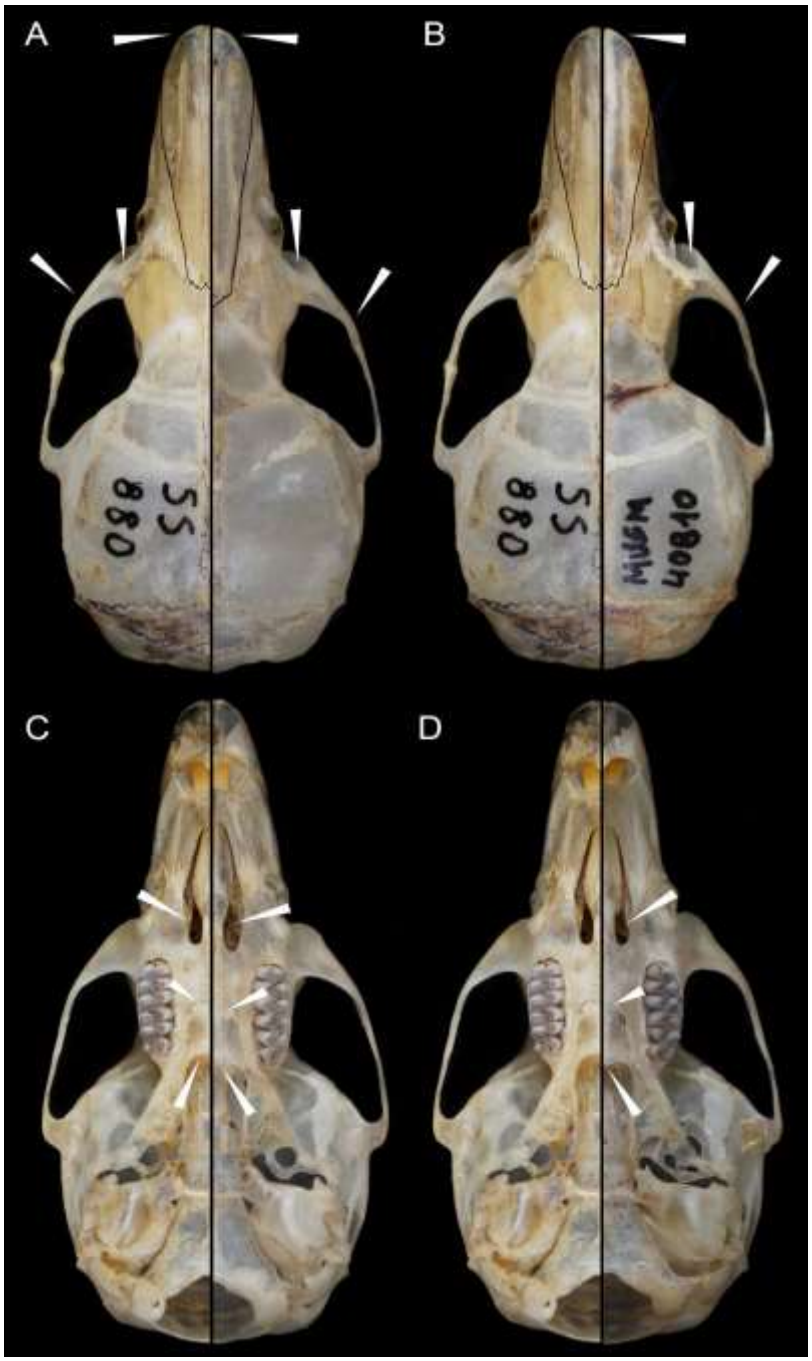

Figure 9. Selected characters of the skulls in dorsal view of: A, “Oxapampa” vs. “Tarma”; B, “Oxapampa” vs “Satipo”, and ventral view: C, “Oxapampa” vs. “Tarma”; D, “Oxapampa” vs “Satipo”. Not scaled. The figure shows differences between several characteristics emphasized by pointers. Shown above are the border of the nasals, zygomatic notch, and zygomatic arch. At the bottom, incisive foramen, maxillo-palatal suture, and border of palate.



Figure 10. Left auditory region in lateral view of "*Thomasomys*" sp. 4 "Oxapampa" (A, MUSM 46245), "*Thomasomys*" sp. 4 "Tarma" (B, MUSM 42509), and "*Thomasomys*" sp. 4 "Satipo" (C, MUSM 46089). Abbreviations: ab, auditory bulla; oa, orbicular apophysis of the malleus.

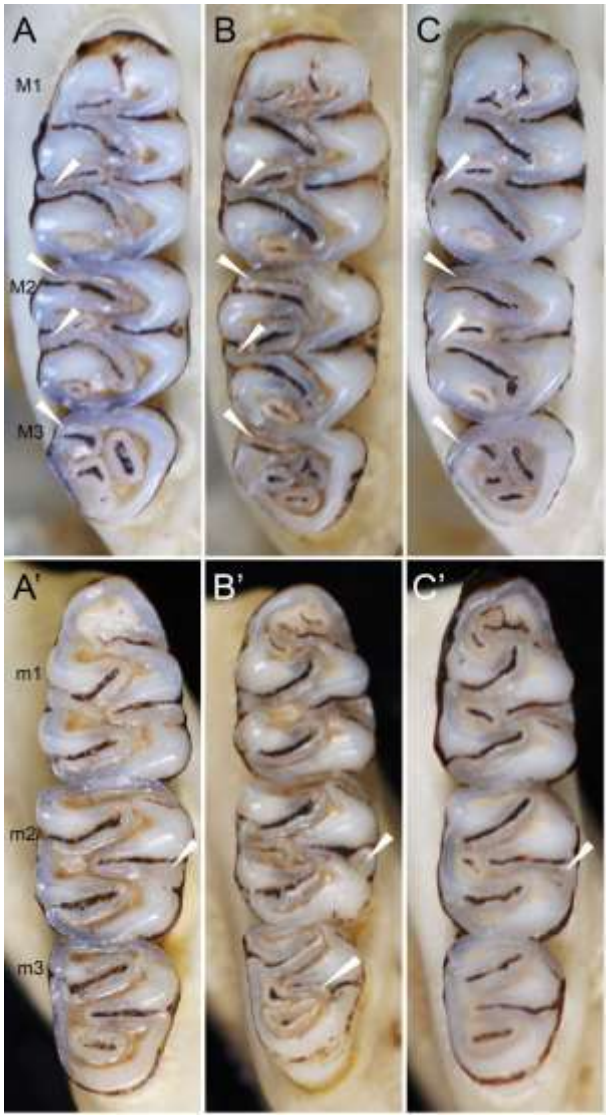

Figure 11. Upper and lower right toothrows. Morphological comparisons of (A, B, and C) upper and (A', B', and C') lower right toothrows in occlusal view of "*Thomasomys*" sp. 4 "Oxapampa" (A and A'; MUSM 10571, holotype), "*Thomasomys*" sp. 4 "Tarma" (B and B'; MUSM 52895, holotype), and "*Thomasomys*" sp. 4 "Satipo" (C and C'; MUSM 40810, holotype). Shown above are M1 mesoloph, M2 anteroloph, M2 mesoploph, M3 anteroloph. At the bottom, m2 ectolophid in A' and C', m2 ectostylid only in B', m3 ectolophid only in B'.

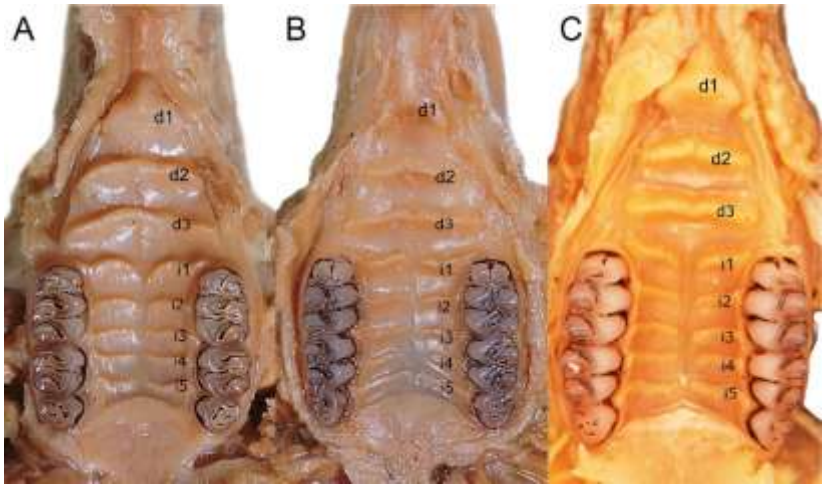

Figure 12. Soft palate of "*Thomasomys*" sp. 4 "Oxapampa" (MUSM 11471), "Tarma" (MUSM 42514), and "Satipo" (MUSM 40832) showing differences in the palatal rugae. Abbreviations: d1–d3, diastemal palatal rugae; i1–i5, interdental rugae.

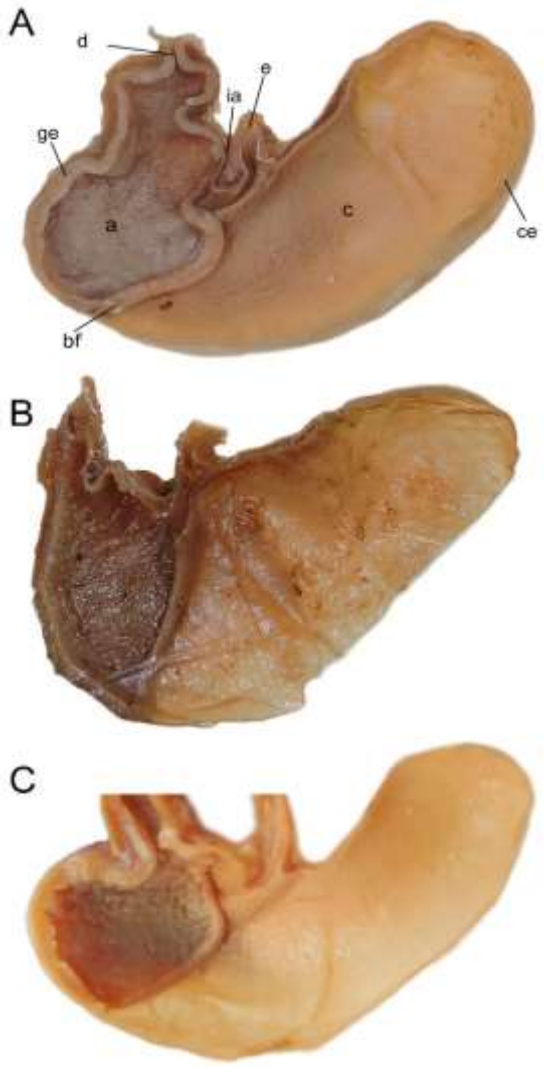

Figure 13. Stomach morphology in three species of "*Thomasomys*" sp. 4: A, Oxapampa (MUSM 11471); B, Tarma (MUSM 42514); C, Satipo (MUSM 40854). Abbreviations: a, antrum; bf, bordering fold; c, corpus; ce, cornified epithelium; d, duodenum; e, esophagum, ge, glandular epithelium; ia, incisura angularis.

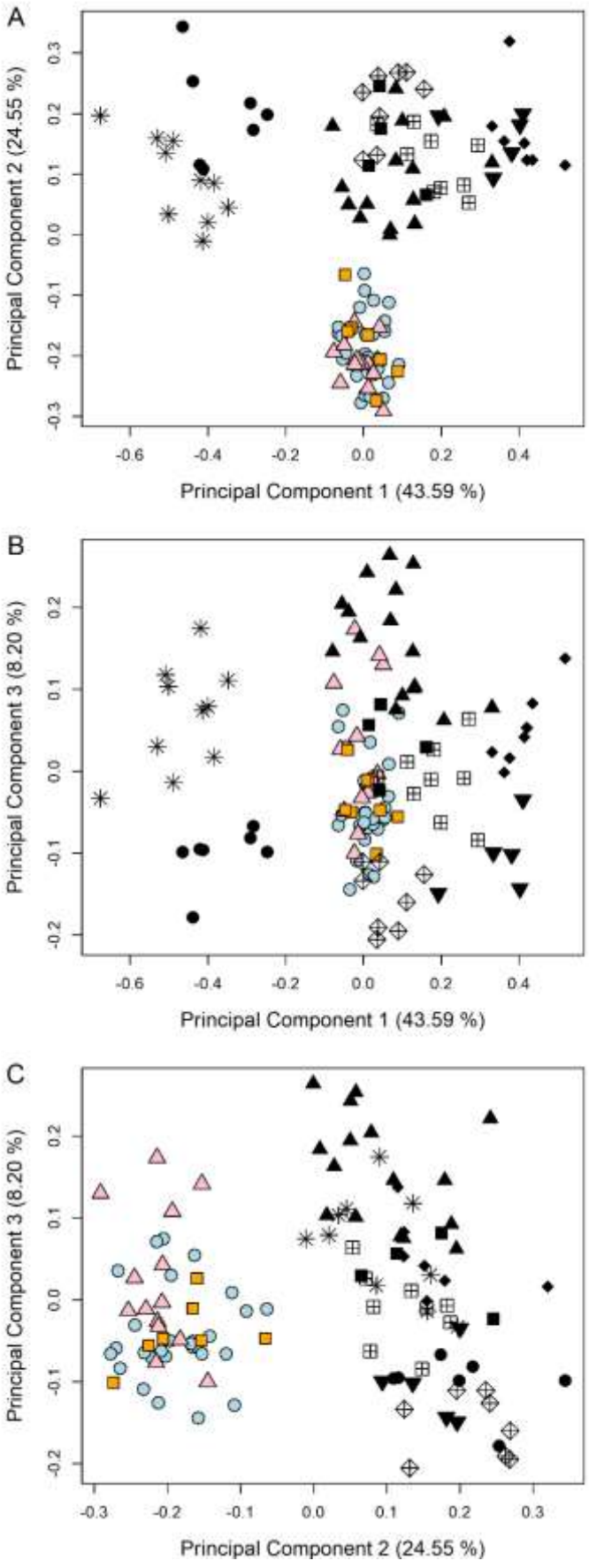
A
Principal Component 2 (24.55 %)
Principal Component 1 (43.59 %)
B
Principal Component 3 (8.20 %)
Principal Component 1 (43.59 %)
C
Principal Component 3 (8.20 %)
Principal Component 2 (24.55 %)

Figure 14. Principal Component Analysis (PCA) plot of morphological variables among "*Thomasomys*" sp. 4, *Aepeomys*, and *Thomasomys*, depicting (A) PC1 vs. PC2, (B) PC1 PC3, and (C) PC2 vs. PC3. Symbols represent: "*Thomasomys*" sp. 4 "Oxapampa" (light blue circles), "*Thomasomys*" sp. 4 "Satipo" (orange squares), "*Thomasomys*" sp. 4 "Tarma" (pink triangles), *Aepeomys lugens* (asterisks), *Thomasomys cinereus* (diamond plus), *T. eleusis* (black squares), *T. incanus* (black circles), *T. ischyrus* (black triangles), *T. kalinowskii* (black diamonds), *T. ladewi* (black inverted triangles), and *T. shallqukucha* (square plus).

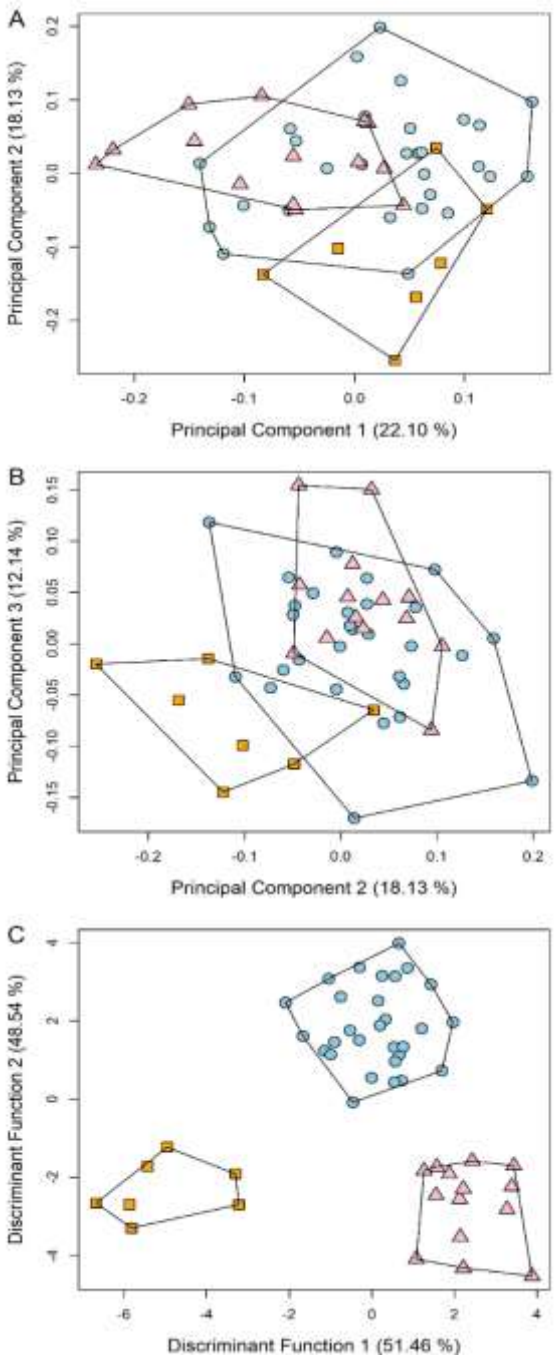

Figure 15. Multivariate analysis of craniodental variables among "*Thomasomys*" sp. 4 “Oxapampa” (circles), “Satipo” (squares), and “Tarma” (triangles). Principal component analysis plots: (A) PC1 vs. PC2 and (B) PC2 vs. PC3. Discriminant function plot: (C) DF1 and DF2.



Figure 16. Dorsal, ventral, and lateral views of the skull and mandible of "*Thomasomys*" sp. 4 "Oxapampa" (MUSM 10571, holotype), an adult male from San Alberto, Oxapampa province, Pasco department, Peru. Scale bar = 10 mm.



Figure 17. Dorsal, ventral, and lateral views of the skull and mandible of "*Thomasomys*" sp. 4 "Tarma" (MUSM 52895, holotype), an adult male from San Pedro de Churco, Tarma province, Junín department, Peru. Scale bar = 10 mm.



Figure 18. Dorsal, ventral, and lateral views of the skull and mandible of "*Thomasomys*" sp. 4 "Satipo" (MUSM 40810, holotype), an adult male from Calabaza, Satipo province, Junín department, Peru. Scale bar = 10 mm.

TABLES

TABLE 1

Ingroup taxa sequenced for mitochondrial and nuclear genes used in phylogenetic tree reconstruction.

Species include new taxa (marked with an asterisk) described in this study. Voucher provides the museum catalog number. Locality numbers in brackets (for "*Thomasomys*" sp. 4) are mapped in figure 1. Abbreviations: AMNH, American Museum of Natural History, United States; FMNH, Field Museum of Natural History, Chicago, United States; MBUCV, Museo de Biología de la Universidad Central de Venezuela, Caracas, Venezuela; MEPN, Museo de la Escuela Politécnica Nacional, Quito, Ecuador; MSB, Museum of Southwestern Biology, University of New Mexico, United States; MUSM: Museo de Historia Natural, Universidad Nacional Mayor de San Marcos, Lima, Peru; MZUSP: Museu de Zoologia da Universidade de São Paulo, São Paulo ,Brazil,; QCAZ, Museo de Zoología de la Pontificia Universidad Católica del Ecuador, Quito, Ecuador; USNM, National Museum of Natural History, Smithsonian Institution, Washington D.C., United States; JLP, James L. Patton (field number).

Species	Voucher	Locality	Source
"*Thomasomys*" sp. 4 "Oxapampa"*	MUSM 11463	Peru: Pasco, Oxapampa, Palcazú [5]	This study
"*Thomasomys*" sp. 4 "Oxapampa"*	MUSM 24288	Peru: Pasco, Oxapampa, San Alberto [4]	This study

"*Thomasomys*" sp. 4 “Oxapampa”*	MUSM 24300	Peru: Pasco, Oxapampa, San Alberto [4]	This study
"*Thomasomys*" sp. 4 “Oxapampa”*	MUSM 14971	Peru: Pasco, Oxapampa San Alberto [3]	Ruelas et al. (2024)
"*Thomasomys*" sp. 4 “Oxapampa”*	MUSM 14961	Peru: Pasco, Oxapampa, San Alberto [3]	Ruelas et al. (2024)
"*Thomasomys*" sp. 4 “Oxapampa”*	MUSM 14962	Peru: Pasco, Oxapampa, San Alberto [3]	Ruelas et al. (2024)
"*Thomasomys*" sp. 4 “Oxapampa”*	MUSM 24297	Peru: Pasco, Oxapampa, San Alberto [4]	Ruelas et al. (2024)
"*Thomasomys*" sp. 4 “Tarma”*	MUSM 52877	Peru: Junín, Tarma, San Pedro de Churco [6]	This study
"*Thomasomys*" sp. 4 “Tarma”*	MUSM 52895	Peru: Junín, Tarma, San Pedro de Churco [6]	This study
"*Thomasomys*" sp. 4 “Tarma”*	MUSM 52896	Peru: Junín, Tarma, San Pedro de Churco [6]	This study
"*Thomasomys*" sp. 4 “Tarma”*	MUSM42508	Peru: Junín, Tarma, San Pedro de Churco [7]	Ruelas et al. (2024)
"*Thomasomys*" sp. 4 “Tarma”*	MUSM 42568	Peru: Junín, Tarma, San Pedro de Churco [6]	Ruelas et al. (2024)
"*Thomasomys*" sp. 4 “Tarma”*	MUSM 42567	Peru: Junín, Tarma, San Pedro de Churco [7]	Ruelas et al. (2024)
"*Thomasomys*" sp. 4 “Satipo”*	MUSM 40810	Peru: Junín, Satipo, Pampa Hermosa [8]	This study
Aepeomys lugens	AMNH 143669	Colombia: Mérida	This study
Aepeomys lugens	AMNH 143670	Colombia: Mérida	This study

Chilomys instans	JLP 16693	Colombia: Risaralda, La Pastora, Reserva Ucumari	Smith and Patton (1999)
Chilomys instans	AMNH 181477	Colombia: Cauca	This study
Chilomys instans	AMNH 66849	Colombia: Bolivar	This study
Chilomys percequilloi	QCAZ 17552	Ecuador: Morona Santiago, Cantón Méndez, Parroquia Patuca, Cordillera de Kutukú	Brito et al. (2022)
Rhagomys longilingua	MUSM 20009 (FMNH 175218)	Peru, Madre de Dios, Maskoitania, 13.4 km NNW Atalaya	Pardiñas et al. (2022)
Rhagomys rufescens	MN 66056	Brazil: Mata do Paraiso, Vicosa, Minas Gerais state	Gonçalves et al. (2018)
Rhagomys septentrionalis	MEPN 10898	Ecuador: Zamora Chinchipe, Refugio de Vida Silvestre “El Zarza”	Pardiñas et al. (2022)
Rhipidomys gardneri	MUSM 36654	Peru: Cusco	This study
Rhipidomys macconnelli	MBUCV	Venezuela: Amazonas, Cerro Neblina	Smith and Patton (1999)

	ALG14063		
Rhipidomys mastacalis	MZUSP MAM196	Brazil: Espirito Santo, Reserva Florestal Cia, Vale do Rio Doce, 30 km N (by road) from Linhares	Smith and Patton (1999)
Rhipidomys nitela	MZUSP 21316	Brazil: Para, [97] Rio Xingu	Smith and Patton (1999)
Rhipidomys nitela	ROM 114147	Suriname: Brokopondo	Borisenko et al. (2008)
Rhipidomys venezuelae	AMNH 24857	Venezuela: Falcon, Serrana de San Luis; Parque Nacional J. C. Falcon; ca. 8 km W + 1 km N Cabure; Sector El Haiton	Steppan and Schenk (2017)
Rhipidomys venustus	AMNH 24865	Venezuela: Falcon, Serrana de San Luis; Parque Nacional J. C. Falcon; Sector Cumbres de Uria; ca. 9 km N Cabure	Steppan and Schenk (2017)
Rhipidomys wetzeli	USNM 560658	Venezuela: Amazonas, Cerro Neblina	Smith and Patton (1999)
Rhipidomys wetzeli	ROM 115360	Guyana: Cuyuni-Mazaruni	Borisenko et al. (2008)

Thomasomys australis	MSB 70447	Bolivia: Cochabamba	This study
Thomasomys cf. *apeco*	MUSM 52644	Peru: Huánuco	This study
Thomasomys aff. *aureus*	MUSM 47039	Peru: Amazonas	This study
Thomasomys cinereus	MUSM 41103	Peru: La Libertad	This study
Thomasomys cinereus	MUSM 51109	Peru: Cajamarca	This study
Thomasomys daphne	FMNH 175228	Peru: Cusco	This study
Thomasomys daphne	MSB 236318	Bolivia: La Paz	This study
Thomasomys incanus	MUSM 46190	Peru: Pasco	This study
Thomasomys incanus	MUSM 52866	Peru: Junín	This study
Thomasomys cf. *incanus*	MUSM 40805	Peru: Junín	This study
Thomasomys ischyrus	MUSM 14984	Peru: Pasco	This study
Thomasomys ischyrus	MUSM 18741	Peru: Huánuco	This study
Thomasomys ischyrus	MUSM 24406	Peru: San Martin	This study
Thomasomys ischyrus	MUSM 36991	Peru: Amazonas	This study

Thomasomys ischyrus	MUSM 48102	Peru: Huánuco	This study
Thomasomys ischyrus	MUSM 50731	Peru: Amazonas	This study
Thomasomys ischyrus	MUSM 52650	Peru: Huánuco	This study
Thomasomys kalinowskii	MUSM 24282	Peru: Pasco	This study
Thomasomys kalinowskii	MUSM 52878	Peru: Junín	This study
Thomasomys lojapiuranus	MUSM 56159	Peru: Piura	This study
Thomasomys notatus	FMNH 170701	Peru: Cusco	This study
Thomasomys notatus	MUSM 47044	Peru: Amazonas	This study
Thomasomys oreas	MSB 87126	Bolivia: Cochabamba	This study
Thomasomys praetor	MUSM 40209	Peru: Ancash	This study
Thomasomys pyrrhonotus	MUSM 47234	Peru: Lambayeque	This study
Thomasomys pyrrhonotus	MUSM 52408	Peru: Cajamarca	This study
Thomasomys aff. *pyrrhonotus*	MUSM 55555	Peru: Piura	This study
Thomasomys shallqukucha	MUSM 46881	Peru: Lambayeque	This study

Thomasomys shallqukucha	MUSM 47230	Peru: Lambayeque	This study
Thomasomys taczanowskii	MUSM 46894	Peru: Lambayeque	This study
Thomasomys taczanowskii	MUSM 47235	Peru: Lambayeque	This study
Thomasomys taczanowskii	MUSM 47236	Peru: Lambayeque	This study
Thomasomys taczanowskii	MUSM 56170	Peru: Piura	This study
Thomasomys sp. 1 (sensu Pacheco, 2003)	AMNH 72132	Bolivia: La Paz	This study
Thomasomys sp. 1 (sensu Pacheco, 2003)	MUSM 12000	Peru: Cusco	This study
Thomasomys sp. 6 (sensu Pacheco, 2003)	MUSM 46254	Peru: Pasco	This study
Thomasomys sp. 8 (sensu Pacheco, 2003)	MUSM 34881	Peru: Ayacucho	This study
Thomasomys sp. A (sensu Ruelas et	MUSM 42490	Peru: Junín	This study

al. 2024)			
Thomasomys sp. A (sensu Ruelas et al., 2024)	MUSM 52861	Peru: Junín	This study

TABLE 2

Selected morphological comparisons among "*Thomasomys*" sp. 4 (this study, Pacheco 2003), *Aepeomys* (Pacheco 2015, Pacheco et al. 2015), *Chilomys* (Pacheco 2015, Brito et al. 2022), *Rhipidomys* (Pacheco et al. 2015, Tribe 2015, Campos et al. 2021), and *Thomasomys* (Pacheco 2015, Pacheco et al. 2015) based on bibliography and our observations.

Characters	**"*Thomasomys*" sp. 4**	***Aepeomys***	***Chilomys***	***Rhipidomys***	***Thomasomys***
Body pelage	Slightly countershaded	Slightly countershaded	Slightly to moderate countershaded	Moderately to distinctly countershaded	Moderately to distinctly countershaded
Mystacial vibrissae	Short	Short	Long	Very long	Long or very long
Genal I vibrissae	Present	Absent	Present	Usually absent	Variably present
Claw of hallux	Long	Short	Long	Long	Variable
Dark metatarsal patches	Absent	Absent	Present	Present	Usually present
Gap between	Present	Present	Present	Absent	Usually present

hypothenar and thenar pads of hindfeet					
Relative size of fifth digit (dV) of pes	Moderately long	Moderately long	Long of very long	Very long	Long or very long
Ungual tuft	Dense	Very dense	Less dense	Variable	Variable
Pencil tail	Short pencil	Short pencil	Short pencil	Long pencil	Typically short
Countershading tail	Bicolored	Monocolored	Monocolored	Typically monocolored	Monocolored
Tail length respect to the body size	Slightly short	Long	Long	Long	Usually long
Nasals	Broad, cuminate or rouded, extended beyond the	Narrow, cuminate, extended beyond the premaxillae	Narrow, rounded, smaller, equal or slightly longer than	Narrow or broad, cuminate or rounded, extended beyond the	Narrow or broad, cuminate or rounded, usually extended

	premaxillae		premaxillae	premaxillae	beyond the premaxillae
Rostral tube	Present	Present	Absent	Absent	Usually absent
Rostrum	Long	Long	Short	Variable	Variable
Lacrimal bone	Small	Very small	Small	Small	Usually small
Turbinal bones	Very complex	Complex	Simple	Simple	Complex
Anterodorsal frontal sinuses	Slightly inflated	Slightly inflated or flat	Slightly inflated	Usually flat	Usually flat
Supraorbital ridges	Absent	Absent	Present (slightly developed)	Present	Typically absent
Masseteric tubercle	Reduced	Prominent	Reduced	Reduced or absent	Typically absent, or reduced
Incisive foramina	Short, do not reach the anterior roots of	Short, do not reach the anterior roots of	Short, do not reach the anterior roots of	Usually pass the anterior roots of M1	Long, typically reach the anterior roots of

	M1	M1	M1		M1
Palate	Moderately long	Moderately long	Usually long	Variable but typically short	Short
Posterolateral palatal pits	Simple and small	Simple and very small	Simple and small	Absent or simple and small	Simple and small
Sphenopalatine vacuities	Absent or barely as narrow slits	Moderately elongated perforations	Absent	Absent	Typically with moderate elongated perforations
Mesopterygoid fossa	Wide and typically sided	Wide and typically sided	Narrow and typically parallel sided	Narrow and convergent anteriorly	Variable and typically parallel sided
Zygomatic arches	Converge anteriorly to slightly subparallel	Converge anteriorly	Subparallel	Typically subparallel	Typically converge anteriorly
Zygomatic plate	Slightly broad	Slightly broad	Slightly broad	Slightly narrow	Slightly narrow

breadth					
Zygomatic plate slope	Slanted backward from the base	Slanted backward from the base	Vertical	Vertical	Typically vertical
Upper incisor orientation	Orthodont or slightly opisthodont	Slightly opisthodont	Proodont or orthodont	Opisthodont	Orthodont or opisthodont
Capsular process	Absent	Absent	Present	Present	Present or absent
Malleus lamina	Rectancular shape	Square shape	Rectancular shape	Rectancular shape	Usually square shape
Gall bladder	Absent	Present	Present	Absent	Present

TABLE 3

Morphological comparisons of selected characters among the "*Thomasomys*" sp. 4 lineages (“Oxapampa” (n= 69), “Tarma” (n= 24), and “Satipo” (n= 22)).

Characters	**"Oxapampa"**	**"Tarma"**	**"Satipo"**
Ventral pelage	Light gray tips	Light gray tips	Whitish or yellowish tips
Scales (tail)	21/cm	21/cm	23/cm
Tail coloration	Bicolored	Faintly bicolored	Faintly bicolored
Hair on the scales	Short and dark	Short and dark	Long and whitish
Pencil tail	Short and whitish	Short and dark	Long and whitish
Digital ungual tuft	Short	Long	Long
Thenar of the manus	Subequal than hypothenar	Larger than hypothenar	Larger than hypothenar
Thenar and hypothenar pads of hind foot	Closely approximated	Widely separated	Widely separated
Digital pads (foot)	Very swollen	Very swollen	Swollen
Plantar skin of hind foot	Pale	Dark	Pale
Supercilliary vibrissae	Present	Present	Absent
Anterior border of nasals	Rounded	Triangular	Triangular

Infraorbital foramen (frontal view)	Slightly wide	Narrow	Narrow
Zygomatic notch	Shallow	Shallow	Deep
Zygomatic plate	Moderate	Moderate	Broad
Incisive foramen	Very short	Short	Very short
Palatal posterior border	Slightly straight or with a small median process	Slightly rounded	Slightly straight or with a small median process
Subsquamosal fenestra	Subequal to postglenoid foramen	Larger than postglenoid foramen	Larger than postglenoid foramen
Paraoccipital process	Small and broad	Long and thin	Small and broad
Jugal	Long	Very long	Long
Maxillo-palatal suture	Reach M2 anterior border	Reach M2 anterior border	Surpass M2 anterior border
Orbicular apophysis of malleus	Large	Small	Large
Manubrium of malleus	Thin	Thin	Very thin
Squamosal ridge	Shallow	Conspicuous	Shallow
Occipital condyle	Very swollen	Swollen	Swollen

Mandible ramus	Broad	Narrow	Broad
Coronoid process	Long	Short	Short
Anteromedian flexus	Deep	Deep	Very deep
M1 mesoloph	Long	Long	Very long
M2 anteroloph	Long	Long	Very long
M2 mesoloph	Long	Long	Very long
M3 anteroloph	Long	Long	Very long
m1 metaconid	Massive	Massive	Very massive
m2 anterocingulum	Long	Long	Short
m2 ectolophid	Present	Absent	Present
m2 ectostylid	Absent	Present	Absent
m3 ectolophid	Absent	Present	Absent

TABLE 4

Body mass (in grams) and external and craniodental measurements (in mm) for the lineages of "*Thomasomys*" sp. 4. "Oxapampa," "Tarma," and "Satipo." Table entries include the sample mean, standard deviation, observed range (in parentheses), and sample size. CIL (marked with an asterisk) was not used in multivariate analyses to reduce the number of highly correlated variables.

Measurements	**"Oxapampa"**	**"Tarma"**	**"Satipo"**
W	41.8 ± 5.44 (34–50) 20	38.42 ± 4.68 (30–44.5) 12	34.93 ± 4.25 (29–40) 7
TL	230 ± 9.28 (213–247) 22	231.58 ± 7.4 (220–244) 12	239.57 ± 13.86 (220–260) 7
T	118.62 ± 7.68 (110–140) 21	118.83 ± 3.49 (114–126) 12	123.57 ± 11 (111–140) 7
F	27.6 ± 1.39 (26–32) 20	27.35 ± 1.14 (26–30) 13	26.57 ± 2.17 (22–28.5) 7
E	20.2 ± 0.95 (18.5–22) 22	20.04 ± 1.28 (17–22) 13	20.57 ± 0.89 (19.5–22) 7
Tail %	51.46 ± 2.28 (48.5–56.68) 21	51.35 ± 1.87 (48.77–54.55) 12	51.51 ± 1.99 (49.17–53.85) 7
GLS	31.14 ± 0.56 (29.9–32.12) 25	31.2 ± 0.28 (30.9–31.55) 8	30.58 ± 0.27 (30.28–30.79) 3
CIL*	27.15 ± 0.57 (26.18–28.26) 23	27.33 ± 0.34 (26.72–27.79) 14	26.8 ± 0.13 (26.64–26.94) 4
CML	17.36 ± 0.35 (16.69–17.96) 28	17.4 ± 0.28 (17–17.82) 14	16.95 ± 0.14 (16.8–17.11) 5

LOF	9.07 ± 0.34 (8.48–9.72) 29	8.85 ± 0.14 (8.62–9.06) 14	9.1 ± 0.1 (8.98–9.25) 7
LN	12.83 ± 0.57 (12.02–14.19) 27	13.22 ± 0.33 (12.74–13.78) 13	12.85 ± 0.41 (12.44–13.56) 6
LD	8.64 ± 0.25 (8.21–9.2) 29	8.75 ± 0.21 (8.35–9.11) 14	8.71 ± 0.24 (8.5–9.08) 7
LIF	6.27 ± 0.27 (5.74–6.77) 28	6.23 ± 0.16 (5.93–6.54) 14	5.63 ± 0.34 (5.12–6.01) 7
LM	5.01 ± 0.12 (4.78–5.28) 29	5.07 ± 0.08 (4.92–5.26) 14	4.92 ± 0.06 (4.81–4.98) 7
BIF	2.61 ± 0.15 (2.38–3) 29	2.59 ± 0.09 (2.46–2.74) 14	2.34 ± 0.15 (2.2–2.64) 7
BR	5.26 ± 0.21 (4.88–5.73) 26	5.38 ± 0.23 (4.93–5.93) 14	5.36 ± 0.13 (5.15–5.56) 7
BPB	3.57 ± 0.21 (3.24–3.98) 29	3.37 ± 0.21 (3.09–3.75) 14	3.54 ± 0.22 (3.23–3.81) 7
BM1	1.59 ± 0.06 (1.47–1.71) 28	1.68 ± 0.05 (1.6–1.78) 14	1.62 ± 0.04 (1.57–1.69) 7
BN	4.33 ± 0.28 (3.73–4.68) 29	4.23 ± 0.35 (3.72–4.75) 14	4.44 ± 0.35 (4.02–4.95) 7
LIB	6.01 ± 0.13 (5.74–6.32) 28	6.12 ± 0.19 (5.85–6.51) 14	5.98 ± 0.24 (5.74–6.31) 6
ZB	15.53 ± 0.4 (14.89–16.28) 28	15.59 ± 0.27 (15.18–16.1) 14	15.8 ± 0.2 (15.43–16.04) 7
RL	11.62 ± 0.29 (11.09–12.36) 29	11.96 ± 0.19 (11.69–12.31) 13	11.4 ± 0.3 (11.01–11.8) 7
BB	13.82 ± 0.5 (13.12–14.71) 29	13.84 ± 0.39 (13.31–14.52) 14	14 ± 0.54 (13.09–14.77) 7

BZP	2.8 ± 0.17 (2.53–3.36) 29	2.68 ± 0.14 (2.41–2.95) 14	2.88 ± 0.06 (2.8–2.96) 7
DI	1.34 ± 0.1 (1.15–1.57) 29	1.28 ± 0.06 (1.18–1.4) 14	1.35 ± 0.06 (1.27–1.43) 7
HBC	9.09 ± 0.25 (8.63–9.46) 28	9.16 ± 0.19 (8.84–9.47) 13	9 ± 0.16 (8.82–9.2) 6
MFB	2.69 ± 0.13 (2.36–2.96) 28	2.82 ± 0.16 (2.58–3.12) 14	2.75 ± 0.12 (2.54–2.9) 7
MN	5.29 ± 0.11 (5.06–5.6) 27	5.38 ± 0.05 (5.33–5.48) 9	5.18 ± 0.08 (5.07–5.3) 7

TABLE 5

Eigenvalues values for the first three components of the PCA of craniodental variables among the "*Thomasomys*" sp. 4 lineages, *Aepeomys lugens*, and some *Thomasomys* species. The eigenvalues of the variables that explain most of the variance for each component are indicated by the bold numbers.

Variables	**PC1**	**PC2**	**PC3**
% variance	43.59	24.55	8.20
CML	0.180	0.273	0.152
LN	0.146	-0.048	0.206
LD	0.187	0.047	0.059
LIF	0.303	0.099	0.066
BIF	0.102	-0.412	-0.253
BR	0.174	0.039	-0.077
BPB	0.132	-0.086	0.116
BM1	0.318	0.081	0.120
BN	0.230	-0.204	**-0.515**
LIB	-0.054	-0.308	0.305
RL	0.063	0.004	0.292
BB	0.173	0.077	0.081
BZP	**0.602**	-0.242	-0.255
DI	**0.397**	**0.480**	0.082
HBC	0.113	0.132	0.146
MFB	0.196	**-0.526**	**0.535**

TABLE 6

Eigenvalues values for the first three components of the PCA and two linear discriminants of the LDA of craniodental variables among the "*Thomasomys*" sp. 4 lineages ("Oxapampa," "Tarma," and "Satipo"). The eigenvalues of the variables that explain most of the variance for each component are indicated by the bold numbers.

Variables	**PC1**	**PC2**	**PC3**	**LD1**	**LD2**
% variance	22.10	18.13	12.14	51.46	48.54
GLS	0.015	0.073	0.065	-9.779	-9.065
CML	0.016	0.106	0.045	30.739	54.275
LOF	0.096	-0.048	-0.055	-12.487	6.934
LN	-0.114	0.101	-0.033	-3.130	-8.364
LD	0.039	0.110	-0.100	3.760	-18.450
LIF	-0.036	**0.512**	0.222	5.502	28.226
LM	-0.081	0.089	0.034	5.623	16.558
BIF	0.058	**0.613**	0.231	7.579	4.685
BR	-0.021	0.077	0.153	-20.937	-5.947
BPB	0.303	0.374	**-0.530**	-0.165	7.932
BM1	-0.302	0.100	-0.074	1.137	-9.887
BN	**0.690**	0.097	0.044	0.221	-10.253
LIB	0.004	0.120	0.011	10.958	-7.761
ZB	0.046	0.099	-0.119	-43.175	-18.937
RL	-0.102	0.099	0.089	21.022	-13.274

BB	0.038	0.048	-0.097	3.303	10.178
BZP	0.029	-0.014	**-0.667**	-15.600	12.409
DI	**0.373**	-0.276	0.232	-3.110	4.133
HBC	0.001	0.081	0.004	3.014	-11.829
MFB	**-0.371**	0.068	-0.179	-1.878	-6.827
MN	-0.116	0.151	0.040	41.454	-55.845

GENERAL DISCUSSION

In this study, Ruelas et al. (2024: Chapter 1; in prep.: Chapter 3) found the monophyly of *Thomasomys*, contingent upon the exclusion of "*Thomasomys*" sp. 4 which was found either related to *Thomasomys* or to *Rhagomys* using different molecular datasets. Furthermore, Ruelas et al. (2024: Chapter 1) corroborated the monophyly of the Baeops, Cinereus, and Notatus groups represented by major clades in phylogeny. In contrast, the Gracilis and Aureus groups as paraphyletic in agreement with early studies (e.g., Salazar-Bravo & Yates, 2007; Lee et al., 2015, 2018; Brito et al., 2019; Pacheco & Ruelas, 2023). Interestingly, the inclusion of *Thomasomys macrotis* into the Incanus group resulted in the latter being recognized as monophyletic, thus clarifying the taxonomic relationships within these groups early discussed by Leo and Gardner (1993) and Pacheco (2003, 2015c). As well as Ruelas et al. (2024; as discussed in Chapter 1) found that the major clades within the Cinereus and Aureus groups are geographically segregated, with distributions either west or east of the Marañón River. Despite these advancements, our knowledge remains incomplete, particularly due to the absence of molecular data on several species.

Ruelas et al. (2024: Chapter 1) also found that *T. aureus* s.l. is paraphyletic, comprising at least five candidate species, each with a small distribution range. This finding is consistent with the pattern of limited distribution ranges typically seen in this genus. The careful delimitation of *T. aureus* s.s. provides crucial insights into the species' diversity. It suggests that other populations previously categorized under *aureus* epithet should merit species distinction and be understood as part of

a likely case of morphological convergence. This is particularly intriguing because species within the *T. aureus* complex, despite their external similarity, are related to distinctly different species, for instance, *T.* aff. *aureus* "Lambayeque-Cajamarca S" and *T. praetor*. Such findings demonstrate that morphological similarities within the *T. aureus* complex mask profound phylogenetic differences, proving that these visually similar species have evolved independently. This situation in the *T. aureus* complex mirrors a scenario observed in the *Akodon orophilus* species complex, initially seen as a single species. Karyological and morphological studies (Jiménez et al., 2013; Jiménez & Pacheco, 2016) revealed it as three morphologically similar species: *A. orophilus*, *A. josemariarguedasi,* and *A. kotosh*. Subsequently, a molecular study (Ruelas et al., 2020) found them not closely related, highlighting the limitations of using only morphology for small rodent classification.

Despite the inherent limitations, Ruelas et al. (2024: Chapter 1) made significant progress in species identification within the genus and not only identified several cryptic species but also provided molecular support for some candidate species previously reported by Pacheco (2003, 2015c) and other authors (e.g., Brito et al., 2019, 2021; Lee et al., 2018, 2022; Pacheco & Ruelas, 2023). This hidden diversity could be doubling the number of known *Thomasomys* species, enhancing the understanding of the genus's diversity and aiding in the more accurate classification of its species.

Furthermore, the discovery of a new genus within the Thomasomyini, "*Thomasomys*" sp. 4, comprising three species ("Oxapampa," "Tarma," "Satipo"), is an important development in the field of sigmodontine taxonomy (Ruelas et al.

in prep.: Chapter 3). Its phylogenetic relationships in a multilocus approach, however, remain ambiguous, as they vary according to the dataset and analysis used. Depending on the method, it is either weakly supported as a sister group to *Rhagomys* using mitochondrial genes in Maximum Likelihood (ML) analysis, to *Chilomys* in Bayesian Inference (BI), or to *Thomasomys* with nuclear genes (Ruelas in prep.: Chapter 3). These findings could demonstrate that the extensive morphological diversity found in *Thomasomys* has overshadowed the unique morphological characteristics of other Thomasomyini genera, such as *Aepeomys*, *Chilomys*, *Rhipidomys*, and "*Thomasomys*" sp. 4. Ruelas et al. (in prep.: Chapter 3) emphasizes the significant challenges in accurately defining species and genus boundaries within the *Thomasomys* clade sensu Pacheco (2003). They observed that "*Thomasomys*" sp. 4 and species within the Incanus group and *Aepeomys*, which share complex and scrolled turbinals, might exhibit convergent evolution due to inhabiting similar elevations but different distribution. Specifically, the variation in morphological traits and the constraints posed by limited sample characteristics have led to an underestimation of the distinct identities of species within this complex. This raises the possibility of two distinct morphological diversification paths within the group, one for *Rhagomys* and another for *Aepeomys*, *Chilomys*, *Rhipidomys*, *Thomasomys*, and "*Thomasomys*" sp. 4. The significant morphological disparity between these two groups has been noted by various authors (e.g., Luna, 2015; Pardiñas et al., 2022) and is attributed to the specialization of *Rhagomys* in dense understory habitats, such as reeds, bamboos, and similar vegetation. This marked morphological divergence has been a key factor in the decision to establish Rhagomyini as a separate tribe only for *Rhagomys*.

However, Ruelas et al. (in prep.: Chapter 3) challenge this decision, through a more comprehensive gene sampling (13 mitochondrial and 5 nuclear genes), advocating for the reclassification of *Rhagomys* within Thomasomyini. Phylogenetic evidence suggests that Thomasomyini, including *Rhagomys*—whether positioned as basal, sister to another thomasomyine genus, or with unresolved relationships—consistently forms a well-supported lineage. This perspective aligns with the initial proposal by D'Elía et al. (2006) and Pacheco et al. (2015), and advocates for a conservative taxonomic approach emphasizing stability, clarity, and biological significance. Integrating ecological data into discussions enhances understanding of the evolutionary and adaptive significance of these taxonomic groupings, ensuring taxonomic decisions reflect both genetic relationships and ecological adaptations. This holistic approach provides a comprehensive framework for studying the diverse and complex Thomasomyini tribe. By minimizing abrupt taxonomic changes, this approach highlights meaningful biological differences and evolutionary relationships across the tribe, thereby facilitating a more refined understanding of evolutionary dynamics within Thomasomyini and contributing towards a refined and accurate taxonomy. This conservative strategy ensures that taxonomic classifications are reflective of evolutionary histories, thereby enhancing research across various scientific fields.

All genera within the Thomasomyini tribe, including *Aepeomys*, *Chilomys*, *Thomasomys*, and "*Thomasomys*" sp. 4, are endemic to montane forests and paramos, with some species of *Rhipidomys* and *Rhagomys* also being endemic to these high-elevation habitats. This distribution has led to the informal designation of the tribe as "Andean thomasomines" (Pacheco, 2003). These species, particularly

those in the genus *Thomasomys,* are highly specialized for survival in cooler, high-elevation environments, typically most of them inhabiting between 2000 to 3500 meters (Ruelas et al. 2024: Chapter 1).

Thomasomys, noted for its diversity within the Sigmodontinae subfamily, exhibits significant adaptability in these habitats. Ruelas (in rev.: Chapter 2) focuses on their high-elevation adaptations, especially examining the role of size of turbinal surface areas, reveals a strong correlation between turbinal surface areas (when sized by skull length), elevation, and annual precipitation, suggesting adaptations for efficient respiratory function in high-elevation environments. This aligns with studies on other small mammals in high-altitude environments, which focus on adaptations in metabolic rate, respiration, blood oxygen capacity, and moisture retention (e.g., Arias-Reyes et al., 2021; Martinez et al., 2020; Schippers et al., 2012; Withers et al., 2016a). Larger *Thomasomys* species are noted to have less respiratory surface area relative to their size (e.i., species of the Aureus group), a trend consistent with larger caniform species (Green et al., 2012). The study also underscores the potential influences of diet, habitat, and age on turbinal morphology, highlighting areas for further research. However, there is a minimal correlation between turbinal areas and bioclimatic variables, pointing to the influence of diet and habitat (e.g., type of forest). On the other hand, Ruelas (in rev.: Chapter 2) identified a correlation between OTSA (sized by TTSA) and bioclimatic variables, suggesting an evolutionary adaptation of olfactory proportion to environmental pressures, crucial for survival in varied montane ecosystems. This underscores the critical role of olfaction in *Thomasomys*' ecological success, highlighting its evolutionary adaptations to high-elevation habitats. Continued

research into their morphological and physiological traits is essential to understanding the mechanisms behind its success.

The significant correlation observed between respiratory and olfactory turbinals challenges the traditional view of a trade-off between these structures, suggesting a potential co-dependence (Green et al., 2012; Martinez et al., 2018, 2020; Van Valkenburgh et al., 2011). Furthermore Ruelas et al. (in rev.: Chapter 2) emphasizes the importance of sizing turbinals, particularly by skull length (SL) and total turbinal surface area (TTSA), for precise assessments and insights into evolutionary patterns. This approach is fundamental for distinguishing species and deciphering their evolutionary and ecological adaptations. Ruelas et al. (in rev.: Chapter 2) showed that scaling by SL highlights how elevation influences turbinal development, linking turbinal structures to body size and potential allometric changes. In contrast, scaling by TTSA emphasizes functional adaptations to environmental factors explained, underlining the notable impact of bioclimatic variables on turbinal proportions (e.g., Green et al., 2012; Martinez et al., 2018, 2020; Mitchell et al., 2023; Porto et al., 2013; Weaver & Grossnickle, 2020).

Finally, Ruelas et al. (in rev.: Chapter 2) proposes that the adaptive radiation and success of *Thomasomys* in challenging, high-elevation habitats may be a significant evolutionary response to new environments. Further comprehensive molecular studies and comparative research with other high-altitude mammals are needed to fully substantiate this hypothesis.

Future research on *Thomasomys* must prioritize the inclusion of holotypes to elucidate or clarify the status of candidate species identified in this work and by

other authors (Ruelas et al., in prog.). This approach is crucial for *Thomasomys*, where species are often hypothesized to occupy very limited distribution ranges, and specimens from neighboring localities are scarce. Moreover, the extensive morphological diversity within the genus complicates taxonomic efforts, rendering it challenging to verify the accuracy of species identification in recent collections or specimens used for comparisons from scientific collections. For example, the classification of species and candidate species within the Aureus group previously identified as *T. aureus* from Ecuador needs reevaluation to determine if they represent distinct valid species or candidates, or if they are part of *T. aureus* s.s., which is known only from a skin without a skull. Although other specimens have been used to represent *T. aureus* s.s. in molecular and morphological phylogenies, with their locality posited as the likely type locality, the true type locality remains uncertain. Similarly, the validity of *T. nicefori*, debated by some as synonymous with *T. popayanus* (e.g., Voss 2003, Pacheco 2015c), requires clarification.

The discovery of multiple clades for *T. kalinowskii* or *T. ischyrus* by Ruelas et al. (2024: Chapter 1; in prep.: Chapter 3) further underscores the need for detailed examination. However, obtaining sequences from holotypes, many of which were collected and described over a century ago (Table 1), presents a significant challenge. The preparation methods and storage conditions of these specimens will significantly influence the feasibility of extracting viable DNA for molecular analyses. Additionally, all candidate species warrant thorough taxonomic revision to ascertain their status as distinct valid species. For species and candidates previously characterized by Pacheco (2003, 2015c), this process is facilitated by existing morphological data. This strategic focus on holotype integration and

comprehensive taxonomic review is essential for advancing our understanding of *Thomasomys* diversity and ensuring accurate species delineation within this complex genus.

In addition, comprehensive biogeographical analyses are imperative to understand the dynamics of Andean colonization and diversification of *Thomasomys* (Ruelas et al. in progress). Highlighting the critical influence of montane forests on species distribution, forthcoming research should meticulously explore the historical and ecological drivers that have driven exceptional endemism and diversity. Using advanced molecular methodologies and precise regional classification of the Tropical Andes will be essential for clarifying the complex evolutionary histories of the Thomasomyini members, but particularly *Thomasomys* given its success in a long but narrow strip of high forest like the montane forests. As well as turbinals should be assessed in a phylogenetic approach to enhance our understanding about their role in the evolutionary process. Moreover, investigations should test the role of geographical barriers, like rivers and elevation gradients, in influencing *Thomasomys* species dispersal and the processes of speciation. A deeper understanding of these biogeographical determinants will not only shed light on the *Thomasomys*' adaptive strategies across the varied Andean landscapes but also guide targeted conservation efforts to conserve their distinctive habitats. Adopting this multidimensional research approach will enhance our understanding of the Andes as an important evolutionary arena, emphasizing the significance of regional ecological factors in shaping biodiversity.

CONCLUSIONS

This study reveals *Thomasomys*' monophyly in a unilocus and multilocus approach, contingent on excluding "*Thomasomys*" sp. 4, suggesting a new genus. Major clades within *Thomasomys*, such as Baeops, Cinereus, and Notatus, are confirmed as monophyletic, while Gracilis and Aureus groups appear paraphyletic. The inclusion of *T. macrotis* in the Incanus group clarifies its monophyly, addressing previous taxonomic ambiguities. The geographical segregation of the Cinereus and Aureus groups by the Marañón River highlights the complexity of *Thomasomys*' speciation. The paraphyly of *T. aureus* s.l., revealing five candidate species, underscores the genus's diverse yet limited distribution ranges, suggesting a need for careful species delimitation and consideration of morphological convergence.

This study also marks a significant advancement in our comprehension of the *Thomasomys* genus, revealing a hidden diversity that could potentially double the number of recognized species within this genus. These findings emphasize the importance of molecular and morphological analyses in understanding species diversity, particularly in genera with complex taxonomic histories like *Thomasomys*.

The discovery of the new genus "*Thomasomys*" sp. 4 in the Peruvian Yungas and the detailed examination of turbinal bones in *Thomasomys* and related genera suggest evolutionary adaptations in response to Andean environmental pressures for the Andean members of the Thomasomyini. The study's findings on the turbinal bone structures of *Thomasomys* suggest evolutionary adaptations for efficient respiratory function in high-elevation environments, with implications for

understanding the ecological success of *Thomasomys* across varied montane ecosystems.

Future research should focus on incorporating holotypes for clarifying candidate species statuses, comprehensive biogeographical analyses to understand Andean diversification, and the examination of geographical barriers in speciation. This integrative approach will enhance our understanding of Andean biodiversity and the evolutionary success of *Thomasomys* in high-elevation habitats.

REFERENCES

Alva, W. (2009). *Geografía general del Perú*. Ed. San Marcos.

Alvarado- Serrano, D. F., & D'Elía, G. (2015). Genus *Neomicroxus* Alvarado-Serrano and D'Elía, 2013. In J. L. Patton, U. F. J. Pardiñas, & G. D'Elía (Eds.), *Mammals of South America. Volume 2, Rodents* (pp. 96–99). The University of Chicago Press.

Antonelli, A., & Sanmartín, I. (2011). Why are there so many plant species in the Neotropics? *TAXON*, *60*(2), 403–414. https://doi.org/10.1002/tax.602010

Aparecido, L. M. T., Teodoro, G. S., Mosquera, G., Brum, M., Barros, F. de V., Pompeu, P. V., Rodas, M., Lazo, P., Müller, C. S., Mulligan, M., Asbjornsen, H., Moore, G. W., & Oliveira, R. S. (2018). Ecohydrological drivers of Neotropical vegetation in montane ecosystems. *Ecohydrology*, *11*(3), e1932. https://doi.org/10.1002/eco.1932

Arias-Reyes, C., Soliz, J., & Joseph, V. (2021). Mice and rats display different ventilatory, hematological, and metabolic features of acclimatization to hypoxia. *Frontiers in Physiology*, *12*, 647822. https://doi.org/10.3389/fphys.2021.647822

Brito, J., Koch, C., Percequillo, A. R., Tinoco, N., Weksler, M., Pinto, C. M., & Pardiñas, U. F. J. (2020). A new genus of oryzomyine rodents (Cricetidae, Sigmodontinae) with three new species from montane cloud forests, western Andean cordillera of Colombia and Ecuador. *PeerJ*, *8*, e10247. https://doi.org/10.7717/peerj.10247

Brito, J., Tinoco, N., Curay, J., Vargas, R., Reyes-Puig, C., Romero, V., & Pardiñas, U. F. J. (2019). Diversidad insospechada en los Andes de Ecuador:

Filogenia del grupo “cinereus” de *Thomasomys* y descripción de una nueva especie (Rodentia, Cricetidae). *Mastozoología Neotropical*, *26*(2), 308–330. https://doi.org/10.31687/saremMN.19.26.2.0.04

Brito, J., Tinoco, N., Pinto, C. M., García, R., Koch, C., Fernandez, V., Burneo, S., & Pardiñas, U. F. J. (2022). Unlocking Andean sigmodontine diversity: Five new species of *Chilomys* (Rodentia: Cricetidae) from the montane forests of Ecuador. *PeerJ*, *10*, e13211. https://doi.org/10.7717/peerj.13211

Brito, J., Vaca-Puente, S., Koch, C., & Tinoco, N. (2021). Discovery of the first Amazonian *Thomasomys* (Rodentia, Cricetidae, Sigmodontinae): A new species from the remote Cordilleras del Cóndor and Kutukú in Ecuador. *Journal of Mammalogy*, *102*(2), 615–635. https://doi.org/10.1093/jmammal/gyaa183

Cabrera, A. (1961). Catálogo de los mamíferos de América del Sur. II (Sirenia—Perissodactyla—Artiodactyla—Lagomorpha—Rodentia—Cetacea). *Revista del Museo Argentino de Ciencias Naturales “Bernardino Rivadavia,” 4*, 309–732.

Carleton, M. D. (2015). Genus *Microryzomys* Thomas, 1917. In J. L. Patton, U. F. J. Pardiñas, & G. D’Elia (Eds.), *Mammals of South America. Volume 2, Rodents* (pp. 355–359). The University of Chicago Press.

Cavelier, J. (1996). Environmental Factors and Ecophysiological Processes along Altitudinal Gradients in Wet Tropical Mountains. In S. S. Mulkey, R. L. Chazdon, & A. P. Smith (Eds.), *Tropical Forest Plant Ecophysiology* (pp. 399–439). Springer US. https://doi.org/10.1007/978-1-4613-1163-8_14

Cazalis, V., Princé, K., Mihoub, J.-B., Kelly, J., Butchart, S. H. M., & Rodrigues, A. S. L. (2020). Effectiveness of protected areas in conserving tropical forest birds. *Nature Communications*, *11*(4461), Article 1. https://doi.org/10.1038/s41467-020-18230-0

Ceballos, G., & Ehrlich, P. R. (2006). Global mammal distributions, biodiversity hotspots, and conservation. *Proceedings of the National Academy of Sciences*, *103*(51), 19374–19379. https://doi.org/10.1073/pnas.0609334103

Cerqueira, R. (1982). South American landscapes and their mammals. In M. A. Mares & H. H. Genoways (Eds.), *Mammalian biology in South America. Pymatuning Laboratory of Ecology* (pp. 53–75).

Chapman, F. M. (1926). The distribution of bird-life in Ecuador: A contribution to a study of the origin of Andean bird-life. *Bulletin of the American Museum of Natural History*, *55*, 1–784.

D'Elía, G., Luna, L., González, E. M., & Patterson, B. D. (2006). On the Sigmodontinae radiation (Rodentia, Cricetidae): An appraisal of the phylogenetic position of *Rhagomys*. *Molecular Phylogenetics and Evolution*, *38*(2), 558–564. https://doi.org/10.1016/j.ympev.2005.08.011

Duellman, W. E., & Pramuk, J. B. (1999). Frogs of the genus *Eleutherodactylus* (Anura: Leptodactylidae) in the Andes of northern Peru. *Scientific Papers*, *13*, 1–78.

Eisenberg, J. F., & Redford, K. H. (1999). *Mammals of the Neotropics: Vol. Volume 3, the Central Neotropics: Ecuador, Perú, Bolivia, Brazil*. University of Chicago Press.

Ellerman, J. R. (1941). *The families and genera of living rodents: Vol. 2 Family Muridae* (pp. 1–712). British Museum. https://www.biodiversitylibrary.org/item/34532

Gansser, A. (1973). Facts and theories on the Andes: Twenty-sixth William Smith lecture. *Journal of the Geological Society*, *129*(2), 93–131. https://doi.org/10.1144/gsjgs.129.2.0093

Gardner, A. L., & Romo, M. R. (1993). A new *Thomasomys* (Mammalia: Rodentia) from the Peruvian Andes. *Proceedings of the Biological Society of Washington*, *106*(4), 762–774. https://doi.org/10.4135/9781412994064.n303

Gómez- Laverde, M., Voss, R. S., & Pacheco, V. (2015). Genus *Handleyomys* Voss, Gómez- Laverde, and Pacheco, 2002. In J. L. Patton, U. F. J. Pardiñas, & G. D'Elía (Eds.), *Mammals of South America. Volume 2, Rodents* (pp. 321–323). The University of Chicago Press.

Gonçalves, P. R., Christoff, A. U., Machado, L. F., Bonvicino, C. R., Peters, F. B., & Percequillo, A. R. (2020). Unraveling deep branches of the Sigmodontinae tree (Rodentia: Cricetidae) in eastern South America. *Journal of Mammalian Evolution*, *27*(1), 139–160. https://doi.org/10.1007/s10914-018-9444-y

Graham, A. (2009). The Andes: A geological overview from a biological perspective. *Annals of the Missouri Botanical Garden*, *96*(3), 371–385. https://doi.org/10.3417/2007146

Green, P. A., Van Valkenburgh, B., Pang, B., Bird, D., Rowe, T., & Curtis, A. (2012). Respiratory and olfactory turbinal size in canid and arctoid

carnivorans. *Journal of Anatomy*, *221*(6), 609–621. https://doi.org/10.1111/j.1469-7580.2012.01570.x

Gutiérrez, E. E., Maldonado, J. E., Radosavljevic, A., Molinari, J., Patterson, B. D., Martínez-C, J. M., Rutter, A. R., Hawkins, M. T. R., Garcia, F. J., & Helgen, K. M. (2015). The Taxonomic Status of Mazama bricenii and the Significance of the Táchira Depression for Mammalian Endemism in the Cordillera de Mérida, Venezuela. *PLOS ONE*, *10*(6), e0129113. https://doi.org/10.1371/journal.pone.0129113

Hazzi, N. A., Moreno, J. S., Ortiz-Movliav, C., & Palacio, R. D. (2018). Biogeographic regions and events of isolation and diversification of the endemic biota of the tropical Andes. *Proceedings of the National Academy of Sciences of the United States of America*, *115*(31), 7985–7990. https://doi.org/10.1073/pnas.1803908115

Hershkovitz, P. (1962). Evolution of neotropical cricetine rodents (Muridae) with special reference to the phyllotine group. *Fieldiana: Zoology*, *46*, 1–524. https://doi.org/10.5962/bhl.title.2781

Hershkovitz, P. (1966). South American swamp and fossorial rats of the Scapteromyine group (Cricetinae, Muridae) with comments on the glans penis in murid taxonomy. *Zeitschrift Für Säugetierkunde*, *31*, 82–149.

Hoorn, C., Wesselingh, F. P., ter Steege, H., Bermudez, M. A., Mora, A., Sevink, J., Sanmartin, I., Sanchez-Meseguer, A., Anderson, C. L., Figueiredo, J. P., Jaramillo, C., Riff, D., Negri, F. R., Hooghiemstra, H., Lundberg, J., Stadler, T., Sarkinen, T., & Antonelli, A. (2010). Amazonia through time: Andean

uplift, climate change, landscape evolution, and biodiversity. *Science*, *330*(6006), 927–931. https://doi.org/10.1126/science.1194585

Hurtado, N., & D'Elía, G. (2019). An assessment of species limits of the South American mouse genus *Oligoryzomys* (Rodentia, Cricetidae) using unilocus delimitation methods. *Zoologica Scripta*, *48*(5), 557–570. https://doi.org/10.1111/zsc.12365

Hurtado, N., & D'Elía, G. (2022). Historical biogeography of a rapid and geographically wide diversification in Neotropical mammals. *Journal of Biogeography*, *49*(5), 781–793. https://doi.org/10.1111/jbi.14352

Hurtado, N., & Pacheco, V. (2017). Revision of *Neacomys spinosus* (Thomas, 1882) (Rodentia: Cricetidae) with emphasis on Peruvian populations and the description of a new species. *Zootaxa*, *4242*(3), 401. https://doi.org/10.11646/zootaxa.4242.3.1

Jiménez, C. F., & Pacheco, V. (2016). A new species of grass mouse, genus *Akodon* Meyen, 1833 (Rodentia, Sigmodontinae), from the central Peruvian Yungas. *Therya*, *7*(3), 449–464. https://doi.org/10.12933/therya-16-336

Jiménez, C. F., Pacheco, V., & Vivas, D. (2013). An introduction to the systematics of *Akodon orophilus* Osgood, 1913 (Rodentia: Cricetidae) with the description of a new species. *Zootaxa*, *3669*(3), Article 3. https://doi.org/10.11646/zootaxa.3669.3.2

Josse, C., Navarro, G., Comer, P., Evans, R., Faber-Langendoen, D., Fellows, M., Kittel, G., Menard, S., Pyne, M., Reid, M., Schulz, K., Snow, K., & Teague, J. (2003). *Ecological systems of latin America and the Caribbean: A working classification of terrestrial systems* (p. 47). NatureServe.

Kelt, D. A., & Meserve, P. L. (2014). Status and challenges for conservation of small mammal assemblages in South America. *Biological Reviews*, *89*(3), 705–722. https://doi.org/10.1111/brv.12080

Lee, T. E., Tinoco, N., & Brito, J. (2022). A new species of Andean mouse of the genus *Thomasomys* (Cricetidae, Sigmodontinae) from the eastern Andes of Ecuador. *Vertebrate Zoology*, *72*, 219–233. https://doi.org/10.3897/vz.72.e78219

Luna, L. (2015). Genus *Rhagomys* Thomas, 1886. In J. L. Patton, U. F. J. Pardiñas, & G. D'Elía (Eds.), *Mammals of South America. Volume 2, Rodents* (pp. 580–583). The University of Chicago Press.

Luna, L., & Pacheco, V. (2002). A new species of *Thomasomys* (Muridae: Sigmodontinae) from the Andes of southeastern Peru. *Journal of Mammalogy*, *83*(3), 834–842.

Maestri, R., & Patterson, B. D. (2016). Patterns of Species Richness and Turnover for the South American Rodent Fauna. *PLOS ONE*, *11*(3), e0151895. https://doi.org/10.1371/journal.pone.0151895

Martinez, Q., Amson, E., Ruf, I., Smith, T. D., Pirot, N., Broyon, M., Lebrun, R., Captier, G., Martín, C. G., Ferreira, G. S., & Fabre, P.-H. (2023). *Turbinal bones are still one of the last frontiers of the tetrapod skull: Hypotheses, challenges and perspectives*. PaleorXiv. https://doi.org/10.31233/osf.io/2gm95

Martinez, Q., Clavel, J., Esselstyn, J. A., Achmadi, A. S., Grohé, C., Pirot, N., & Fabre, P.-H. (2020). Convergent evolution of olfactory and thermoregulatory capacities in small amphibious mammals. *Proceedings of*

the National Academy of Sciences, *117*(16), 8958–8965. https://doi.org/10.1073/pnas.1917836117

Martinez, Q., Lebrun, R., Achmadi, A. S., Esselstyn, J. A., Evans, A. R., Heaney, L. R., Miguez, R. P., Rowe, K. C., & Fabre, P.-H. (2018). Convergent evolution of an extreme dietary specialisation, the olfactory system of worm-eating rodents. *Scientific Reports*, *8*(1), 17806. https://doi.org/10.1038/s41598-018-35827-0

McKenna, M., & Bell, S. K. (1997). *Classification of mammals: Above the species level*. Columbia University Press.

Mitchell, D. R., Sherratt, E., & Weisbecker, V. (2023). Facing the facts: Adaptive trade-offs along body size ranges determine mammalian craniofacial scaling. *Biological Reviews*, 1–29. https://doi.org/10.1111/brv.13032

Mittermeier, R. A., Myers, N., Thomsen, J. B., Da Fonseca, G. A. B., & Olivieri, S. (1998). Biodiversity hotspots and major tropical wilderness areas: Approaches to setting conservation priorities. *Conservation Biology*, *12*(3), 516–520. https://doi.org/10.1046/j.1523-1739.1998.012003516.x

Moreno Cárdenas, P. A., & Novillo-Gonzalez, M. (2020). First record of *Thomasomys cinereus* Thomas, 1882 (Rodentia, Cricetidae, Sigmodontinae) in Ecuador. *Therya*, *11*(1), 41–45. https://doi.org/10.12933/therya-20-640

Myers, N., Mittermeier, R. A., Mittermeier, C. G., da Fonseca, G. A. B., & Kent, J. (2000). Biodiversity hotspots for conservation priorities. *Nature*, *403*(6772), Article 6772. https://doi.org/10.1038/35002501

Navas, C. A. (2002). Herpetological diversity along Andean elevational gradients: Links with physiological ecology and evolutionary physiology. *Comparative Biochemistry and Physiology Part A: Molecular & Integrative Physiology*, *133*(3), 469–485. https://doi.org/10.1016/S1095-6433(02)00207-6

Noblecilla, M. C., & Pacheco, V. (2013). Dieta de roedores sigmodontinos (Cricetidae) en los bosques montanos tropicales de Huánuco, Perú. *Revista Peruana de Biología*, *19*(3), 317–322. https://doi.org/10.15381/rpb.v19i3.1046

Ojeda, R. A., & Novillo, A. (2013). Diversity and conservation of neotropical mammals. In S. A. Levin (Ed.), *Encyclopedia of Biodiversity* (Second, pp. 582–594). Academic Press. https://doi.org/10.1016/B978-0-12-384719-5.00353-1

Pacheco, V. (2003). *Phylogenetic analyses of the Thomasomyini (Muroidea: Sigmodontinae) based on morphological data* [Ph.D. dissertation]. The City University of New York.

Pacheco, V. (2015a). Genus *Aepeomys* Thomas, 1898. In J. L. Patton, U. F. J. Pardiñas, & G. D'Elía (Eds.), *Mammals of South America. Volume 2, Rodents* (pp. 574–577). The University of Chicago Press.

Pacheco, V. (2015b). Genus *Chilomys* Thomas, 1897. In J. L. Patton, U. F. J. Pardiñas, & G. D'Elía (Eds.), *Mammals of South America. Volume 2, Rodents* (pp. 577–580). The University of Chicago Press.

Pacheco, V. (2015c). Genus *Thomasomys* Coues, 1884. In J. L. Patton, U. F. J. Pardiñas, & G. D'Elia (Eds.), *Mammals of South America. Volume 2, Rodents* (pp. 617–682). The University of Chicago Press.

Pacheco, V., Córdova, J. H., & Velásquez, M. (2012). Karyotypes of *Akodon orophilus* Osgood 1913 and *Thomasomys* sp. (Rodentia: Sigmodontinae) from Huánuco, Peru. *Revista Peruana de Biología*, *19*(1), Article 1. https://doi.org/10.15381/rpb.v19i1.796

Pacheco, V., Patton, J. L., & D'Elía, G. (2015). Tribe Thomasomyini Steadman and Ray, 1982. In J. L. Patton, U. F. J. Pardiñas, & G. D'Elía (Eds.), *Mammals of South America. Volume 2, Rodents* (pp. 571–574). The University of Chicago Press.

Pacheco, V., & Ruelas, D. (2023). Systematic revision of *Thomasomys cinereus* (Rodentia: Cricetidae: Sigmodontinae) from northern Peru and southern Ecuador, with descriptions of three new species. *Bulletin of the American Museum of Natural History*, *461*, 1–71.

Pacheco, V., Salas, E., Cairampoma, L., Noblecilla, M., Quintana, H., Ortiz, F., Palermo, P., & Ledesma, R. (2007). Contribución al conocimiento de la diversidad y conservación de los mamíferos en la cuenca del río Apurímac, Perú. *Revista Peruana de Biología*, *14*(2), 169–180. https://doi.org/10.15381/rpb.v14i2.1722

Parada, A., D'Elía, G., & Palma, R. E. (2015). The influence of ecological and geographical context in the radiation of Neotropical sigmodontine rodents. *BMC Evolutionary Biology*, *15*(172), 1–17. https://doi.org/10.1186/s12862-015-0440-z

Pardiñas, U. F. J., Tinoco, N., Barbière, F., Ronez, C., Cañón, C., Lessa, G., Koch, C., & Brito, J. (2022). Morphological disparity in a hyperdiverse mammal clade: A new morphotype and tribe of Neotropical cricetids. *Zoological Journal of the Linnean Society*, zlac016. https://doi.org/10.1093/zoolinnean/zlac016

Parsons, T. S. (1967). Evolution of the nasal structure in the lower tetrapods. *American Zoologist*, *7*(3), 397–413. https://doi.org/10.1093/icb/7.3.397

Patterson, B. D., Pacheco, V., & Ashley, M. V. (1992). On the origins of the western slope region of endemism: Systematics of fig-eating bats, genus Artibeus. *Memorias Del Museo de Historia Natural, UNMSM*, *21*, 189–205.

Patterson, B. D., Solari, S., & Velazco, P. M. (2012). The role of the Andes in the diversification and biogeography of Neotropical mammals. In B. D. Patterson & L. P. Costa (Eds.), *Bones, Clones, and Biomes* (pp. 351–378). The University of Chicago Press. https://doi.org/10.7208/chicago/9780226649214.001.0001

Patton, J. L. (2015). Genus *Lenoxus* Thomas, 1909. In J. L. Patton, U. F. J. Pardiñas, & G. D'Elia (Eds.), *Mammals of South America. Volume 2, Rodents* (pp. 231–232). The University of Chicago Press.

Percequillo, A. R. (2015a). Genus *Nephelomys* Weksler, Percequillo, and Voss, 2006. In J. L. Patton, U. F. J. Pardiñas, & G. D'Elía (Eds.), *Mammals of South America. Volume 2, Rodents* (pp. 377–390). The University of Chicago Press.

Percequillo, A. R. (2015b). Genus *Oreoryzomys* Weksler, Percequillo, and Voss, 2006. In J. L. Patton, U. F. J. Pardiñas, & G. D'Elía (Eds.), *Mammals of*

South America. Volume 2, Rodents (pp. 437–439). The University of Chicago Press.

Percequillo, A. R., Prado, J. R. do, Abreu, E. F., Dalapicolla, J., Pavan, A. C., de Almeida Chiquito, E., Brennand, P., Steppan, S. J., Lemmon, A. R., Lemmon, E. M., & Wilkinson, M. (2021). Tempo and mode of evolution of oryzomyine rodents (Rodentia, Cricetidae, Sigmodontinae): A phylogenomic approach. *Molecular Phylogenetics and Evolution*, *159*, 107120. https://doi.org/10.1016/j.ympev.2021.107120

Pine, R. H. (1980). Notes on rodents of the genera Wiedomys and Thomasomys (including Wilfredomys). *Mammalia*, *44*(2), 195–202. https://doi.org/10.1515/mamm.1980.44.2.195

Porto, A., Shirai, L. T., de Oliveira, F. B., & Marroig, G. (2013). Size variation, growth strategies, and the evolution of modularity in the mammalian skull. *Evolution*, *67*(11), 3305–3322. https://doi.org/10.1111/evo.12177

Reig, O. A. (1986). Diversity patterns and differentiation of high Andean rodents. In F. Vuilleumier & M. Monasterio (Eds.), *High Altitude Tropical Biogeography* (pp. 404–438). Oxford University Press.

Ruelas, D., Fabre, P.-H., Pacheco, V., & Martinez, Q. (in rev.). Introduction to the *Thomasomys* (Rodentia: Cricetidae) turbinal bone adaptations: Insights into elevation and environmental challenges. *Journal of Mammalogy*.

Ruelas, D., & Pacheco, V. (2021). Small mammals from the Seasonally Dry Tropical Forests of the Huallaga river basin and new records for San Martín department, Peru. *Check List*, *17*(3), 877–894. https://doi.org/10.15560/17.3.877

Ruelas, D., & Pacheco, V. (2022). Taxonomic status and phylogenetic position of *Oxymycterus juliacae* Allen 1900 (Rodentia: Cricetidae). *Mammalia*, *86*(2), 196–214. https://doi.org/10.1515/mammalia-2021-0028

Ruelas, D., Pacheco, V., Inche, B., & Tinoco, N. (2021). A preliminary review of *Nephelomys albigularis* (Tomes, 1860) (Rodentia: Cricetidae), with the description of a new species from the Peruvian montane forests. *Zootaxa*, *5027*(2), 175–210. https://doi.org/10.11646/zootaxa.5027.2.3

Ruelas, D., Pacheco, V., & Jiménez, C. F. (2020). Range extension and phylogenetic relationships of *Akodon josemariarguedasi* (Rodentia: Cricetidae) with comments on the aerosus species group. *Mammalia*, *84*(2), 207–213. https://doi.org/10.1515/mammalia-2018-0209

Ruelas, D., Pacheco, V., Pérez, J., Diaz-Nieto, J., & Fabre, P.-H. (2024). Unilocus delimitation methods reveal the underestimated species diversity of *Thomasomys* (Rodentia, Cricetidae). *Zoologica Scripta*.

Sahley, C. T., Cervantes, K., Pacheco, V., Salas, E., Paredes, D., & Alonso, A. (2015). Diet of a sigmodontine rodent assemblage in a Peruvian montane forest. *Journal of Mammalogy*, *96*(5), 1071–1080. https://doi.org/10.1093/jmammal/gyv112

Sahley, C. T., Cervantes, K., Salas, E., Paredes, D., Pacheco, V., & Alonso, A. (2016). Primary seed dispersal by a sigmodontine rodent assemblage in a Peruvian montane forest. *Journal of Tropical Ecology*, *32*(2), 125–134. https://doi.org/10.1017/S0266467416000043

Salazar-Bravo, J. (2015). Genus *Tapecomys* S. Anderson and Yates, 2000. In J. L. Patton, U. F. J. Pardiñas, & G. D'Elía (Eds.), *Mammals of South America. Volume 2, Rodents* (pp. 556–559). The University of Chicago Press.

Salazar-Bravo, J., & Yates, T. L. (2007). A new species of *Thomasomys* (Cricetidae: Sigmodontinae) from central Bolivia. In D. A. Kelt, E. P. Lessa, J. Salazar-Bravo, & J. L. Patton (Eds.), *The quintessential naturalist honoring the life and legacy of Oliver P. Pearson* (pp. 747–774). University of California Press.

Schenk, J. J., & Steppan, S. J. (2018). The role of geography in adaptive radiation. *The American Naturalist*, *192*(4), 415–431. https://doi.org/10.1086/699221

Schippers, M.-P., Ramirez, O., Arana, M., Pinedo-Bernal, P., & McClelland, G. B. (2012). Increase in Carbohydrate Utilization in High-Altitude Andean Mice. *Current Biology*, *22*(24), 2350–2354. https://doi.org/10.1016/j.cub.2012.10.043

Schmidt-Nielsen, K., Hainsworth, F. R., & Murrish, D. E. (1970). Counter-current heat exchange in the respiratory passages: Effect on water and heat balance. *Respiration Physiology*, *9*(2), 263–276. https://doi.org/10.1016/0034-5687(70)90075-7

Smith, M. F., & Patton, J. L. (1999). Phylogenetic relationships and the radiation of sigmodontine rodents in South America: Evidence from cytochrome b. *Journal of Mammalian Evolution*, *6*(2), 89–128.

Steadman, D. W., & Ray, C. E. (1982). Relationships of *Megaoryzomys curioi*, an extinct cricetine rodent (Muroidea: Muridae) from the Galápagos islands,

Ecuador. *Smithsonian Contributions to Paleobiology*, *51*, 1–23. https://doi.org/10.5479/si.00810266.51.1

Steppan, S. J., & Schenk, J. J. (2017). Muroid rodent phylogenetics: 900-species tree reveals increasing diversification rates. *PLOS ONE*, *12*(8), e0183070. https://doi.org/10.1371/journal.pone.0183070

Tejedor Garavito, N., Álvarez, E., Caro, S. A., Murakami, A. A., Blundo, C., Espinoza, T. E. B., Cuadros, M. A. L. T., Gaviria, J., Gutíerrez, N., Jørgensen, P. M., León, B., Camacho, R. L., Malizia, L., Millán, B. B., Moraes, M., Pacheco, S., Benayas, J. M. R., Reynel, C., Flor, M. T. de la, … Newton, A. C. (2012). Evaluación del estado de conservación de los bosques montanos en los Andes tropicales: *Ecosistemas*, *21*(1–2), Article 1–2.

Thomas, O. (1882). On a collection of rodents from north Peru. *Proceedings of The Zoological Society of London, 1882 (part I)*, 98–111.

Thomas, O. (1906). LXVIII.- Notes on South-American rodents. *Annals and Magazine of Natural History*, *18*(7), 442–448. https://doi.org/10.1080/00222930608562646

Upham, N. S., Ojala-Barbour, R., Brito M, J., Velazco, P. M., & Patterson, B. D. (2013). Transitions between Andean and Amazonian centers of endemism in the radiation of some arboreal rodents. *BMC Evolutionary Biology*, *13*(1), 191. https://doi.org/10.1186/1471-2148-13-191

Vallejos-Garrido, P., Pino, K., Espinoza-Aravena, N., Pari, A., Inostroza-Michael, O., Toledo-Muñoz, M., Castillo-Ravanal, B., Romero-Alarcón, V., Hernández, C. E., Palma, R. E., & Rodríguez-Serrano, E. (2023). The

importance of the Andes in the evolutionary radiation of Sigmodontinae (Rodentia, Cricetidae), the most diverse group of mammals in the Neotropics. *Scientific Reports*, *13*(1), Article 1. https://doi.org/10.1038/s41598-023-28497-0

Van Valkenburgh, B., Curtis, A., Samuels, J. X., Bird, D., Fulkerson, B., Meachen-Samuels, J., & Slater, G. J. (2011). Aquatic adaptations in the nose of carnivorans: Evidence from the turbinates: Aquatic adaptations in the nose of carnivorans. *Journal of Anatomy*, *218*(3), 298–310. https://doi.org/10.1111/j.1469-7580.2010.01329.x

Villarreal, A., Zambrano-Cevallos, R., Brito, J., & Burneo, S. F. (2022). Movement and habitat use of three high Andean rodent species (Cricetidae: Sigmodontinae) in Andean páramos of Ecuador. *Neotropical Biodiversity*, *8*(1), 343–358. https://doi.org/10.1080/23766808.2022.2132023

Voss, R. S. (1993). A revision of the Brazilian muroid rodent genus *Delomys*: With remarks on "thomasomyine" characters. *American Museum Novitates*, *3073*, 1–44.

Voss, R. S. (2015). Tribe Ichthyomyini Vorontsov, 1959. In J. L. Patton, U. F. J. Pardiñas, & G. D'Elia (Eds.), *Mammals of South America. Volume 2, Rodents* (pp. 279–291). The University of Chicago Press.

Weaver, L. N., & Grossnickle, D. M. (2020). Functional diversity of small-mammal postcrania is linked to both substrate preference and body size. *Current Zoology*, *66*(5), 539–553. https://doi.org/10.1093/cz/zoaa057

Weir, J. T. (2006). Divergent timing and patterns of species accumulation in lowland and highland neotropical birds. *Evolution*, *60*(4), 842–855. https://doi.org/10.1111/j.0014-3820.2006.tb01161.x

Withers, P., Cooper, C. E., Maloney, S. K., Bozinovic, F., & Cruz-Neto, A. P. (2016a). Physiological adaptations to extreme environments. In P. Withers, C. E. Cooper, S. K. Maloney, F. Bozinovic, & A. P. Cruz-Neto (Eds.), *Ecological and environmental physiology of mammals* (pp. 290–392). Oxford Academic.

Withers, P., Cooper, C. E., Maloney, S. K., Bozinovic, F., & Cruz-Neto, A. P. (2016b). Physiological characteristics of mammals. In P. Withers, C. E. Cooper, S. K. Maloney, F. Bozinovic, & A. P. Cruz-Neto (Eds.), *Ecological and environmental physiology of mammals* (pp. 146–289). Oxford Academic.

SUPPLEMENTARY INFORMATION



Supplementary information - Article 1

"Unilocus delimitation methods reveal the underestimated species diversity of *Thomasomys* (Rodentia, Cricetidae)"

Zoologica Scripta

Unilocus delimitation methods reveal the underestimated species diversity of Thomasomys (Rodentia, Cricetidae)

Journal:	*Zoologica Scripta*
Manuscript ID	ZSC-08-2023-0109
Wiley - Manuscript type:	Original Article
Date Submitted by the Author:	15-Aug-2023
Complete List of Authors:	Ruelas, Dennisse; Universidad Nacional Mayor de San Marcos, ; ISEM, Pacheco, Victor; Universidad Nacional Mayor de San Marcos, Museo de Historia Natural Perez, Jose; Universidad Peruana Cayetano Heredia Diaz-Nieto , Juan; EAFIT University Fabre, Pierre-Henri; ISEM
Keywords:	Andes, Thomasomyini, species groups, Marañón

SCHOLARONE™
Manuscripts

Figure S1. Phylogenetic tree of *Thomasomys* based on Cytb mitochondrial gene and Maximum likelihood. Bootstrap supports are shown at branch nodes.

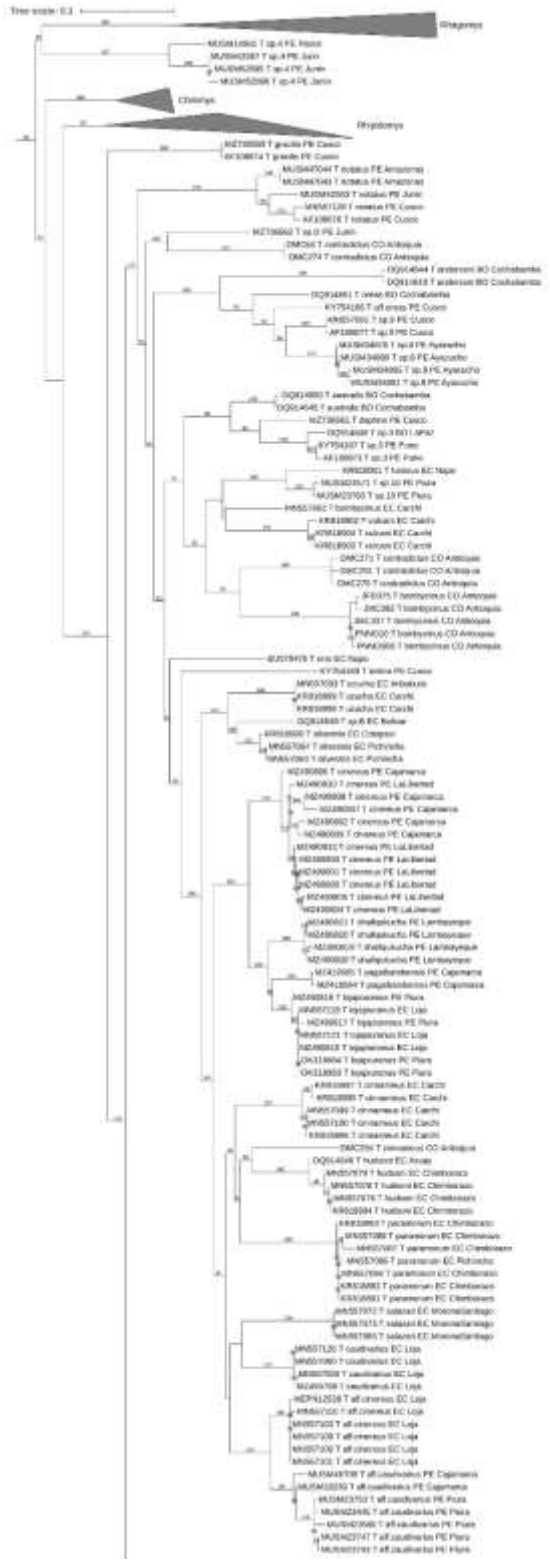

(part 1)

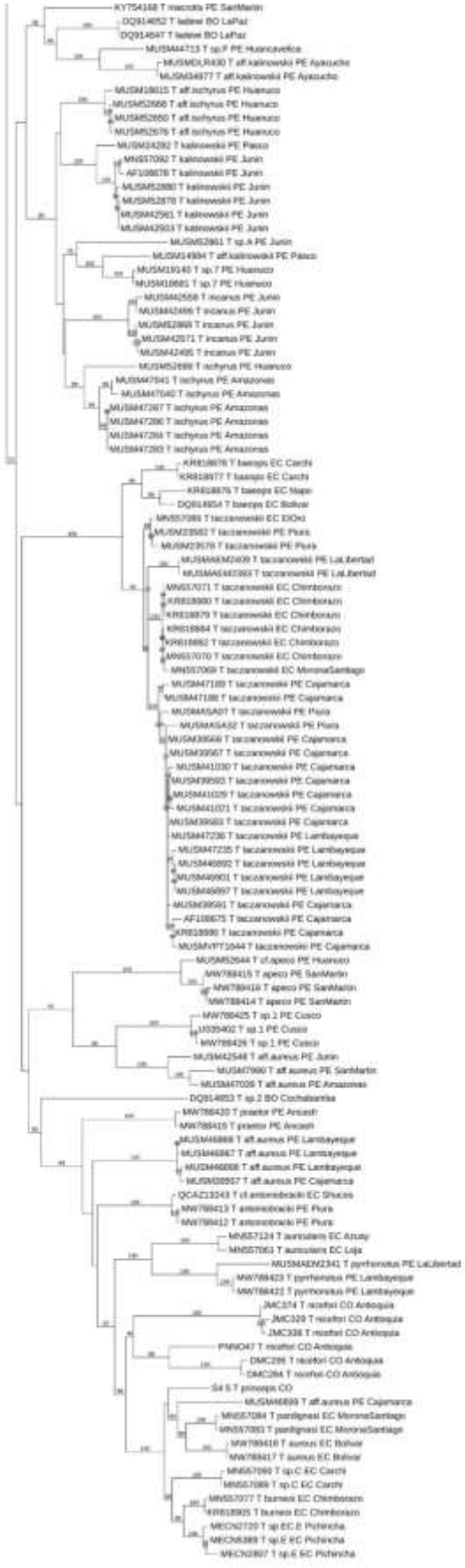
KY754168 T macrotis PE SanMartin
DQ914652 T ladewi BO LaPaz
DQ914647 T ladewi BO LaPaz
MUSM44713 T sp.F PE Huancavelica
MUSMDUR430 T aff.kalinowskii PE Ayacucho
MUSM34977 T aff.kalinowskii PE Ayacucho
MUSM19615 T aff.ischyrus PE Huanuco
MUSM52668 T aff.ischyrus PE Huanuco
MUSM52650 T aff.ischyrus PE Huanuco
MUSM52676 T aff.ischyrus PE Huanuco
MUSM34282 T kalinowskii PE Pasco
MNS57092 T kalinowskii PE Junin
AF108678 T kalinowskii PE Junin
MUSM52880 T kalinowskii PE Junin
MUSM52878 T kalinowskii PE Junin
MUSM42561 T kalinowskii PE Junin
MUSM42503 T kalinowskii PE Junin
MUSM52861 T sp.A PE Junin
MUSM14984 T aff.kalinowskii PE Pasco
MUSM19140 T sp.7 PE Huanuco
MUSM19681 T sp.7 PE Huanuco
MUSM42568 T incanus PE Junin
MUSM42466 T incanus PE Junin
MUSM52868 T incanus PE Junin
MUSM42571 T incanus PE Junin
MUSM42495 T incanus PE Junin
MUSM52899 T ischyrus PE Huanuco
MUSM47041 T ischyrus PE Amazonas
MUSM47040 T ischyrus PE Amazonas
MUSM47287 T ischyrus PE Amazonas
MUSM47286 T ischyrus PE Amazonas
MUSM47284 T ischyrus PE Amazonas
MUSM47283 T ischyrus PE Amazonas
KR618878 T baeops EC Carchi
KR618877 T baeops EC Carchi
KR618876 T baeops EC Napo
DQ914654 T baeops EC Bolivar
MNS57089 T taczanowskii EC ElOro
MUSM23582 T taczanowskii PE Piura
MUSM23578 T taczanowskii PE Piura
MUSMAEM2409 T taczanowskii PE LaLibertad
MUSMAEM2393 T taczanowskii PE LaLibertad
MNS57071 T taczanowskii EC Chimborazo
KR618880 T taczanowskii EC Chimborazo
KR618879 T taczanowskii EC Chimborazo
KR618884 T taczanowskii EC Chimborazo
KR618882 T taczanowskii EC Chimborazo
MNS57070 T taczanowskii EC Chimborazo
MNS57069 T taczanowskii EC MoronaSantiago
MUSM47189 T taczanowskii PE Cajamarca
MUSM47188 T taczanowskii PE Cajamarca
MUSMASA01 T taczanowskii PE Piura
MUSMASA32 T taczanowskii PE Piura
MUSM39568 T taczanowskii PE Cajamarca
MUSM39567 T taczanowskii PE Cajamarca
MUSM41030 T taczanowskii PE Cajamarca
MUSM39593 T taczanowskii PE Cajamarca
MUSM41029 T taczanowskii PE Cajamarca
MUSM41021 T taczanowskii PE Cajamarca
MUSM39583 T taczanowskii PE Cajamarca
MUSM47236 T taczanowskii PE Lambayeque
MUSM47235 T taczanowskii PE Lambayeque
MUSM46892 T taczanowskii PE Lambayeque
MUSM46901 T taczanowskii PE Lambayeque
MUSM46897 T taczanowskii PE Lambayeque
MUSM39581 T taczanowskii PE Cajamarca
AF108675 T taczanowskii PE Cajamarca
KR618890 T taczanowskii PE Cajamarca
MUSMVPT1644 T taczanowskii PE Cajamarca
MUSM52644 T cf.apeco PE Huanuco
MW788415 T apeco PE SanMartin
MW788416 T apeco PE SanMartin
MW788414 T apeco PE SanMartin
MW788425 T sp.1 PE Cusco
U035402 T sp.1 PE Cusco
MW788426 T sp.1 PE Cusco
MUSM42546 T aff.aureus PE Junin
MUSM47990 T aff.aureus PE SanMartin
MUSM47026 T aff.aureus PE Amazonas
DQ914653 T sp.2 BO Cochabamba
MW788420 T praetor PE Ancash
MW788419 T praetor PE Ancash
MUSM46868 T aff.aureus PE Lambayeque
MUSM46867 T aff.aureus PE Lambayeque
MUSM46898 T aff.aureus PE Lambayeque
MUSM39557 T aff.aureus PE Cajamarca
QCAZ13343 T cf.antomolinai EC Shuaras
MW788413 T antomolinai PE Piura
MW788412 T antomolinai PE Piura
MNS57124 T aureolaris EC Azuay
MNS57063 T aureolaris EC Loja
MUSMAEM2341 T pyrrhonotus PE LaLibertad
MW788423 T pyrrhonotus PE Lambayeque
MW788421 T pyrrhonotus PE Lambayeque
JMC374 T nicefori CO Antioquia
JMC329 T nicefori CO Antioquia
JMC308 T nicefori CO Antioquia
PNNO47 T nicefori CO Antioquia
DMC286 T nicefori CO Antioquia
DMC284 T nicefori CO Antioquia
S4 6 T pinnapa CO
MUSM46899 T aff.aureus PE Cajamarca
MNS57084 T pardignasi EC MoronaSantiago
MNS57083 T pardignasi EC MoronaSantiago
MW788418 T aureus EC Bolivar
MW788417 T aureus EC Bolivar
MNS57090 T sp.C EC Carchi
MNS57089 T sp.C EC Carchi
MNS57077 T bureau EC Chimborazo
KR618905 T bureau EC Chimborazo
MECN2720 T sp.E.6 EC Pichincha
MECN5389 T sp.E.6 EC Pichincha
MECN2807 T sp.6 EC Pichincha

(part2)

Figure S2. Collecting localities of the taxa contained into the clade A of *Thomasomys*.

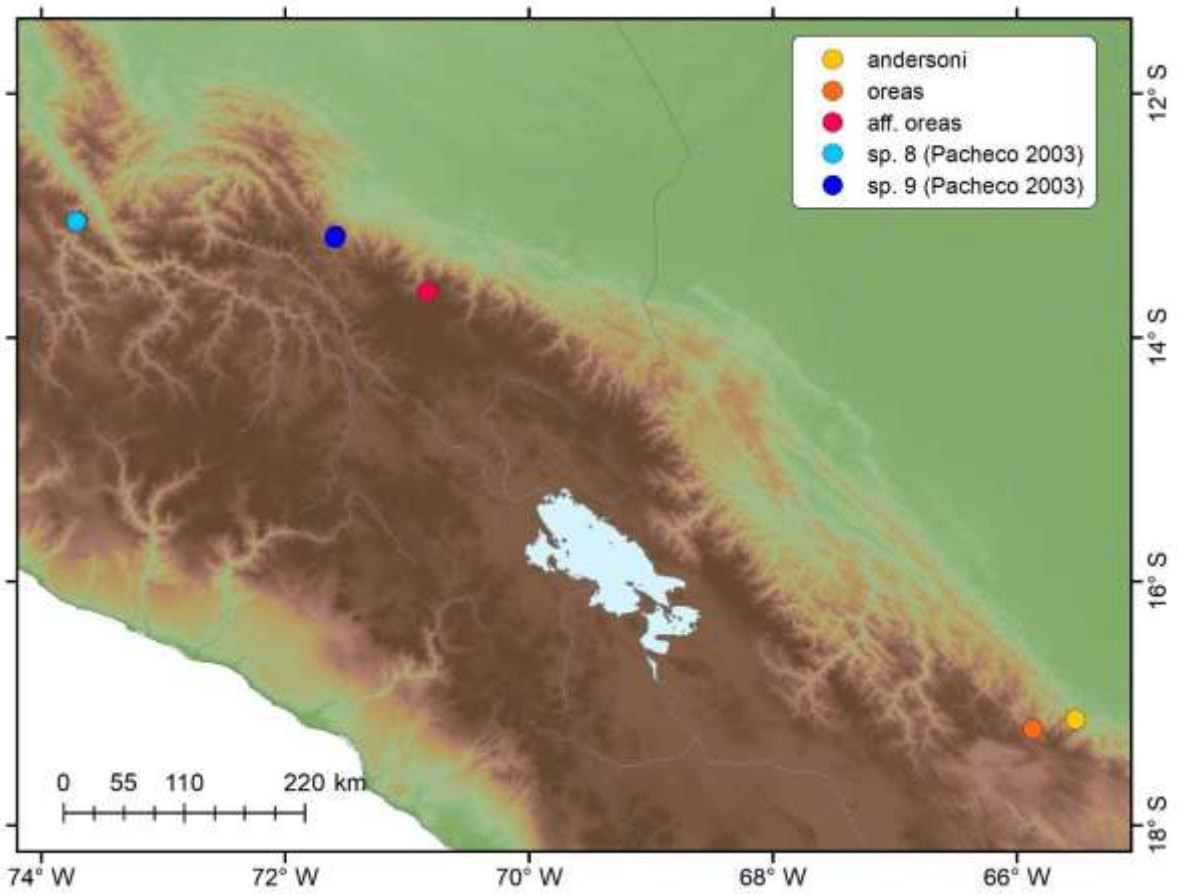

Figure S3. Collecting localities of the taxa contained into the clade B of *Thomasomys*.

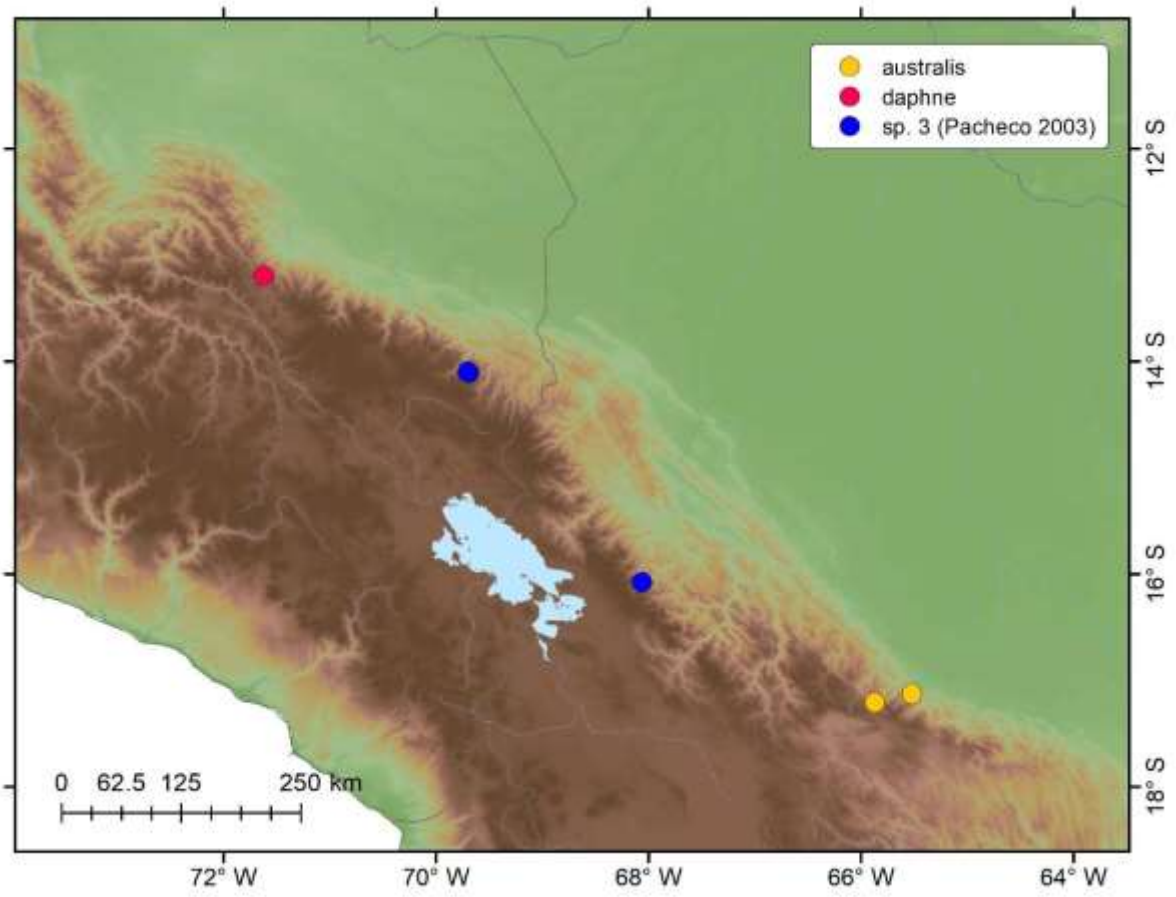

Figure S4. Collecting localities of the taxa contained into the clade C of *Thomasomys*.

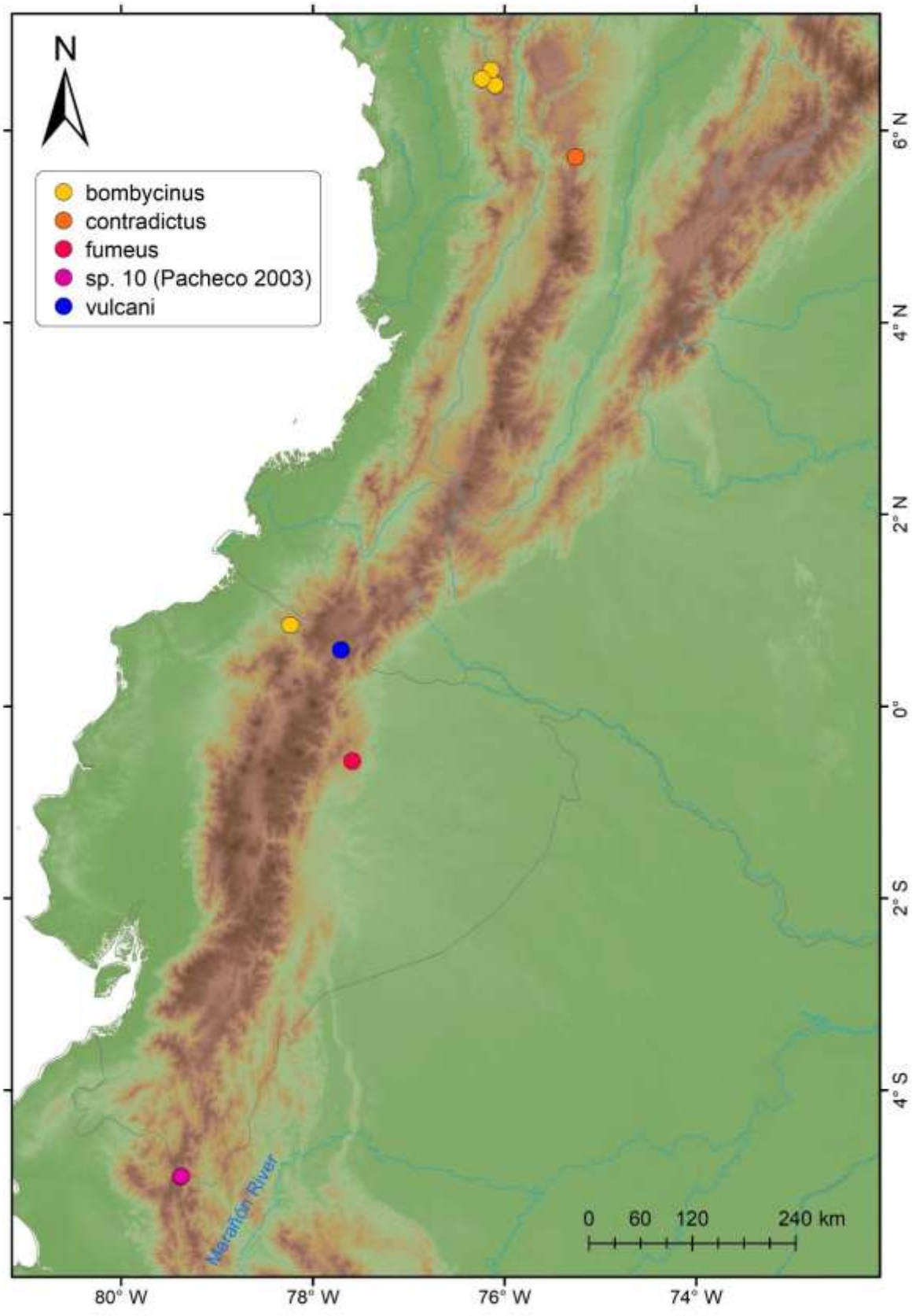

Figure S5. Collecting localities of the taxa contained into the clade D of *Thomasomys*.

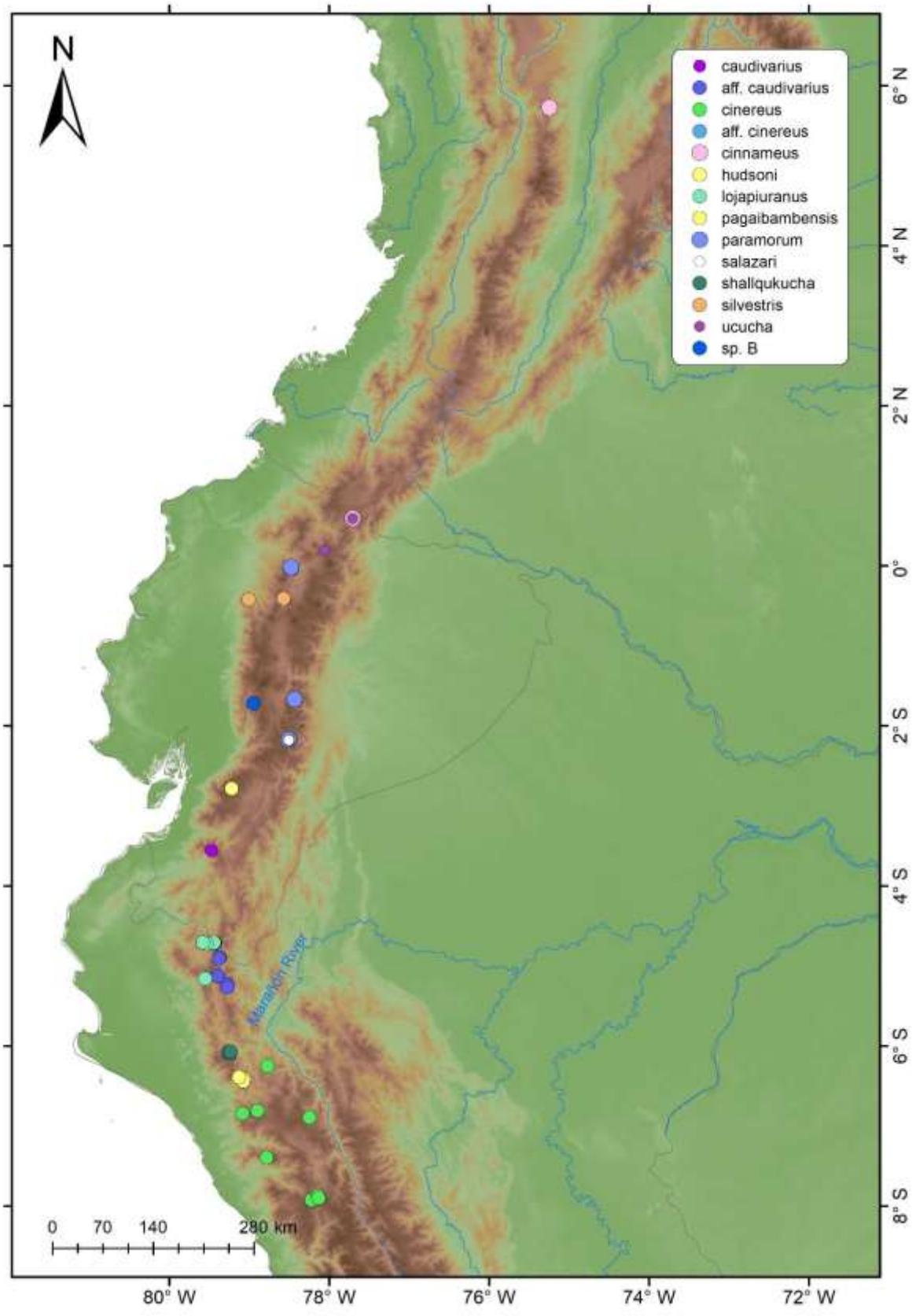

Figure S6. Collecting localities of the taxa contained into the clade E (square) and H (circles) of *Thomasomys*.

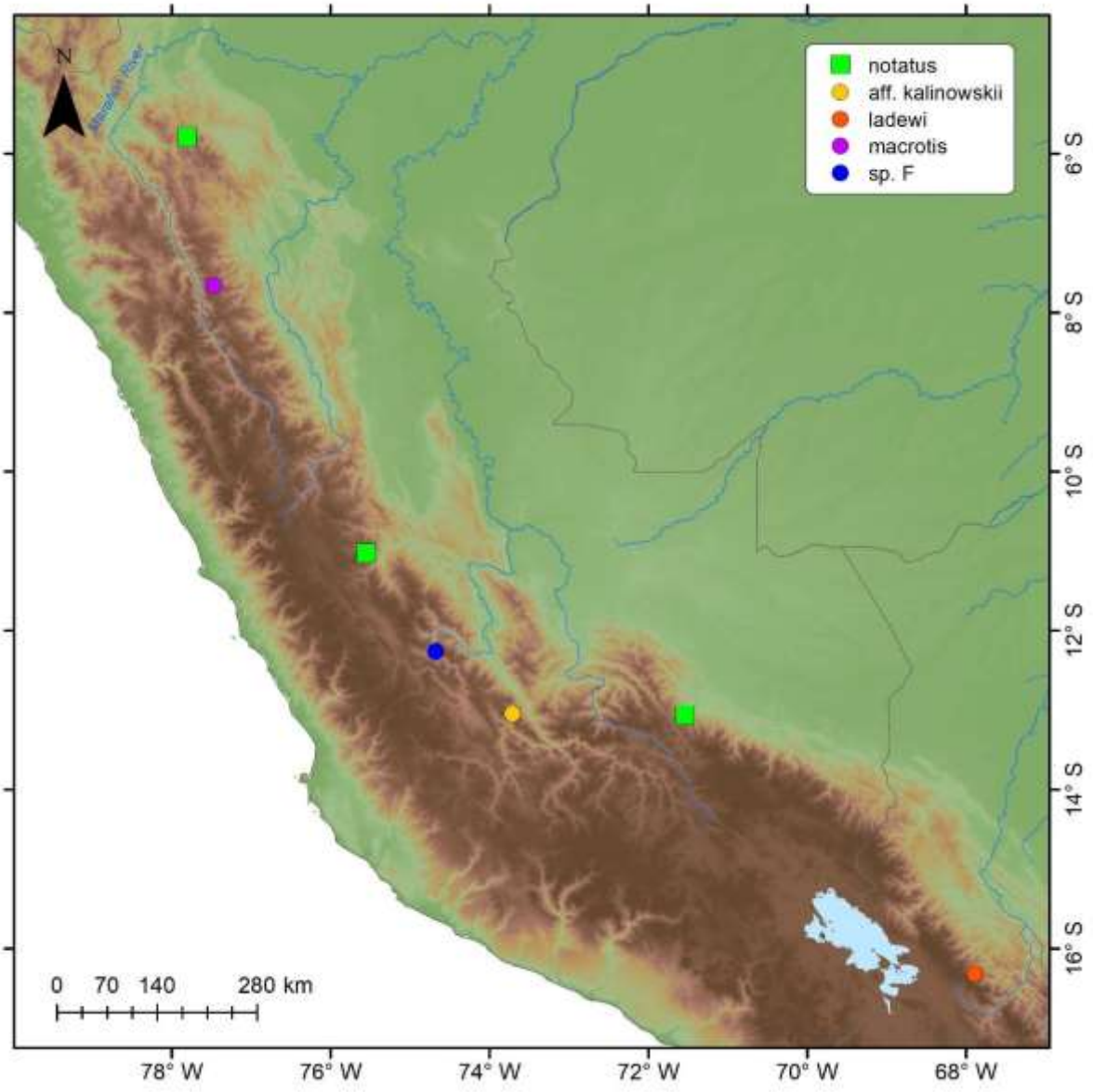

Figure S7. Collecting localities of the taxa contained into the clade F of *Thomasomys*.

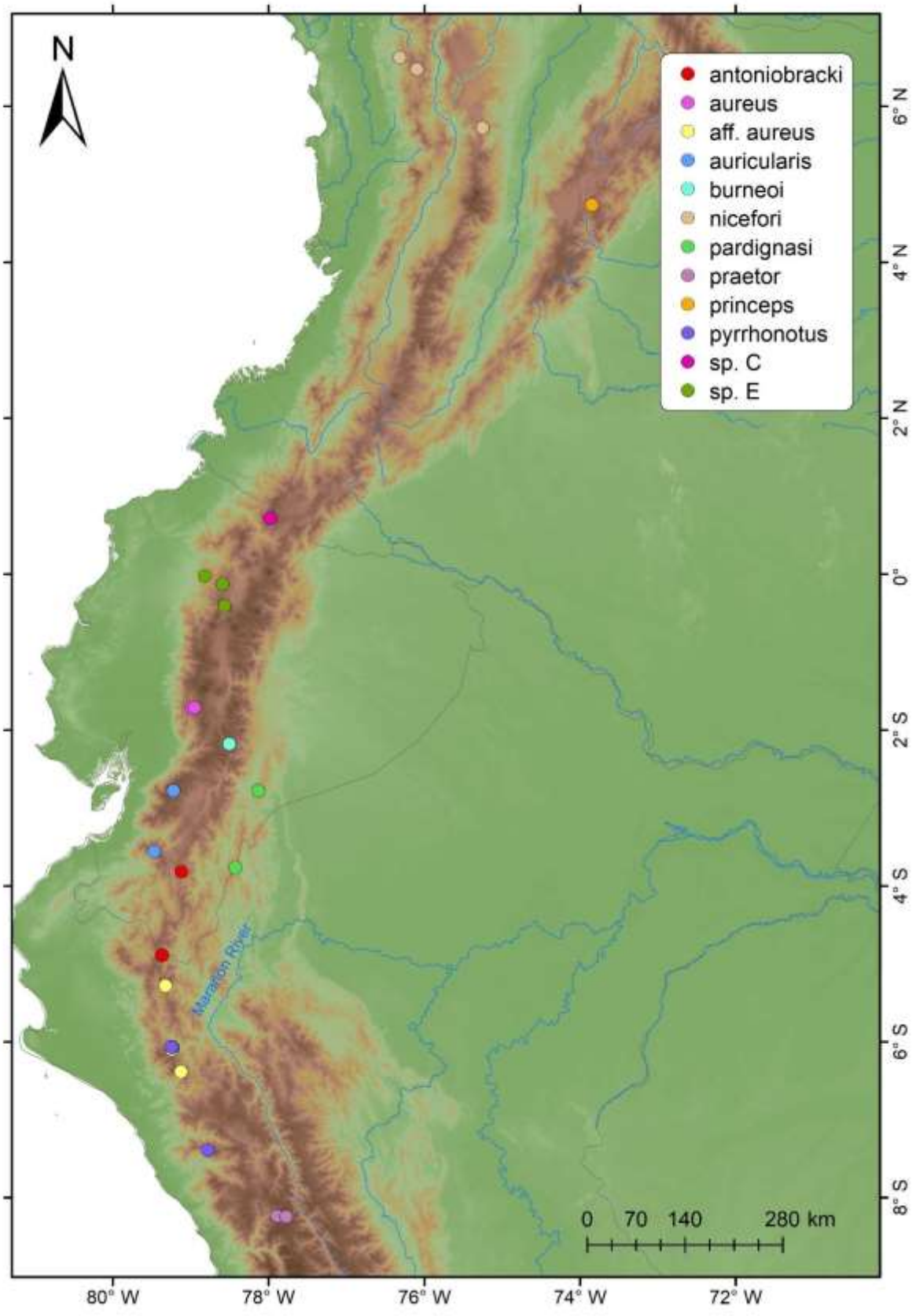

Figure S8. Collecting localities of the taxa contained into the clade G of *Thomasomys*.

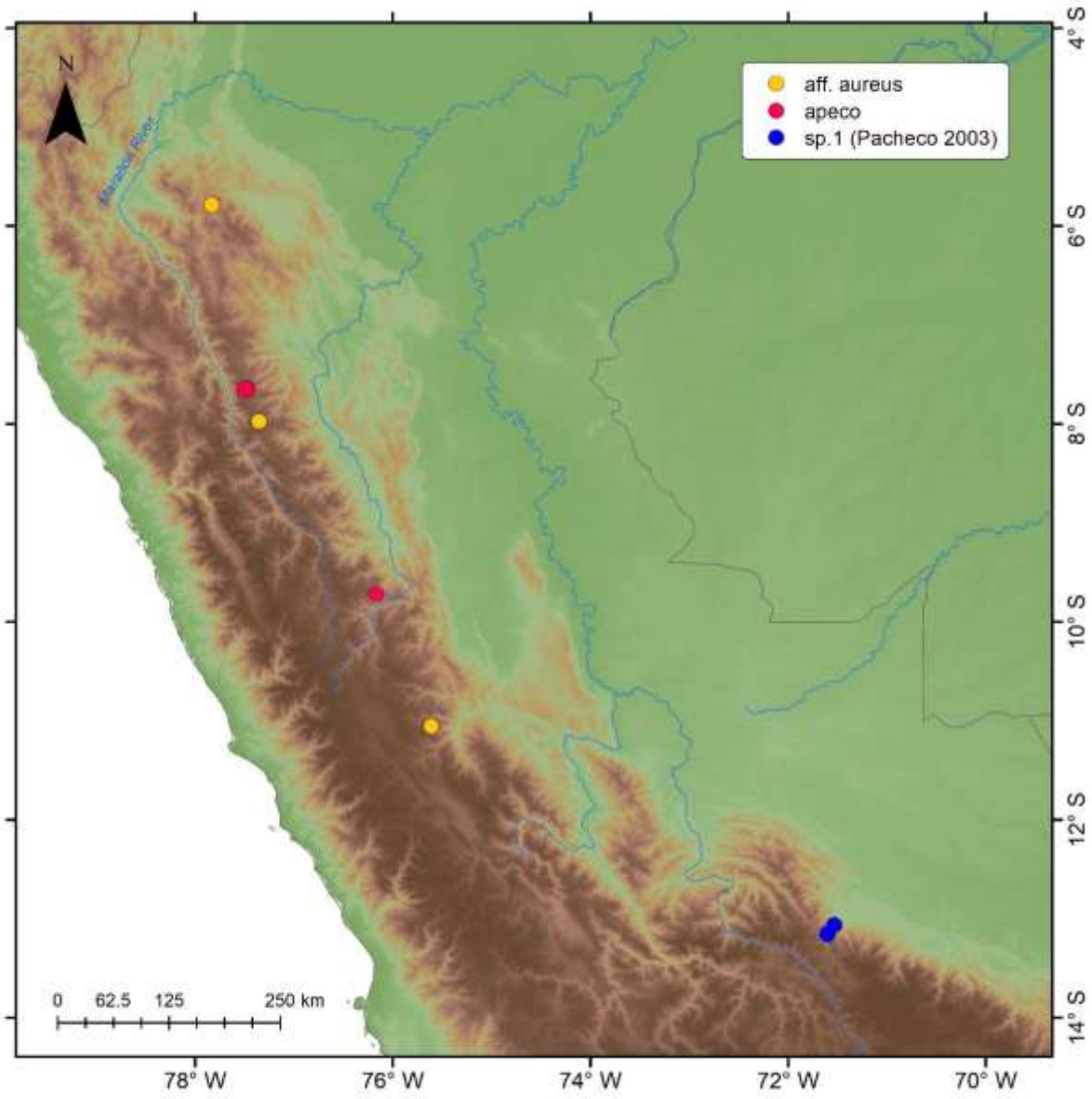

Figure S9. Collecting localities of the taxa contained into the clade I of *Thomasomys*.

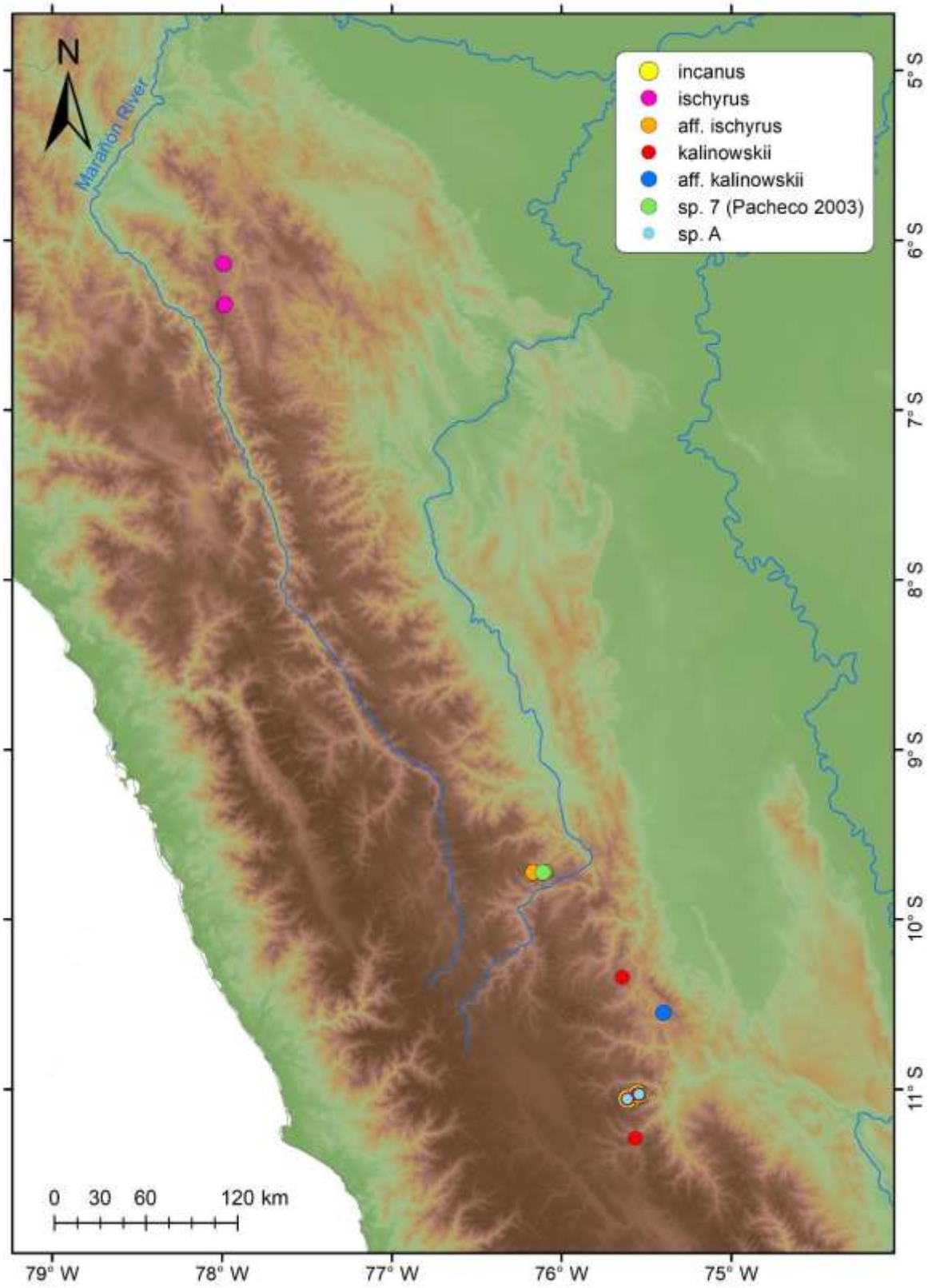

Figure S10. Collecting localities of the taxa contained into the clade J of *Thomasomys*.

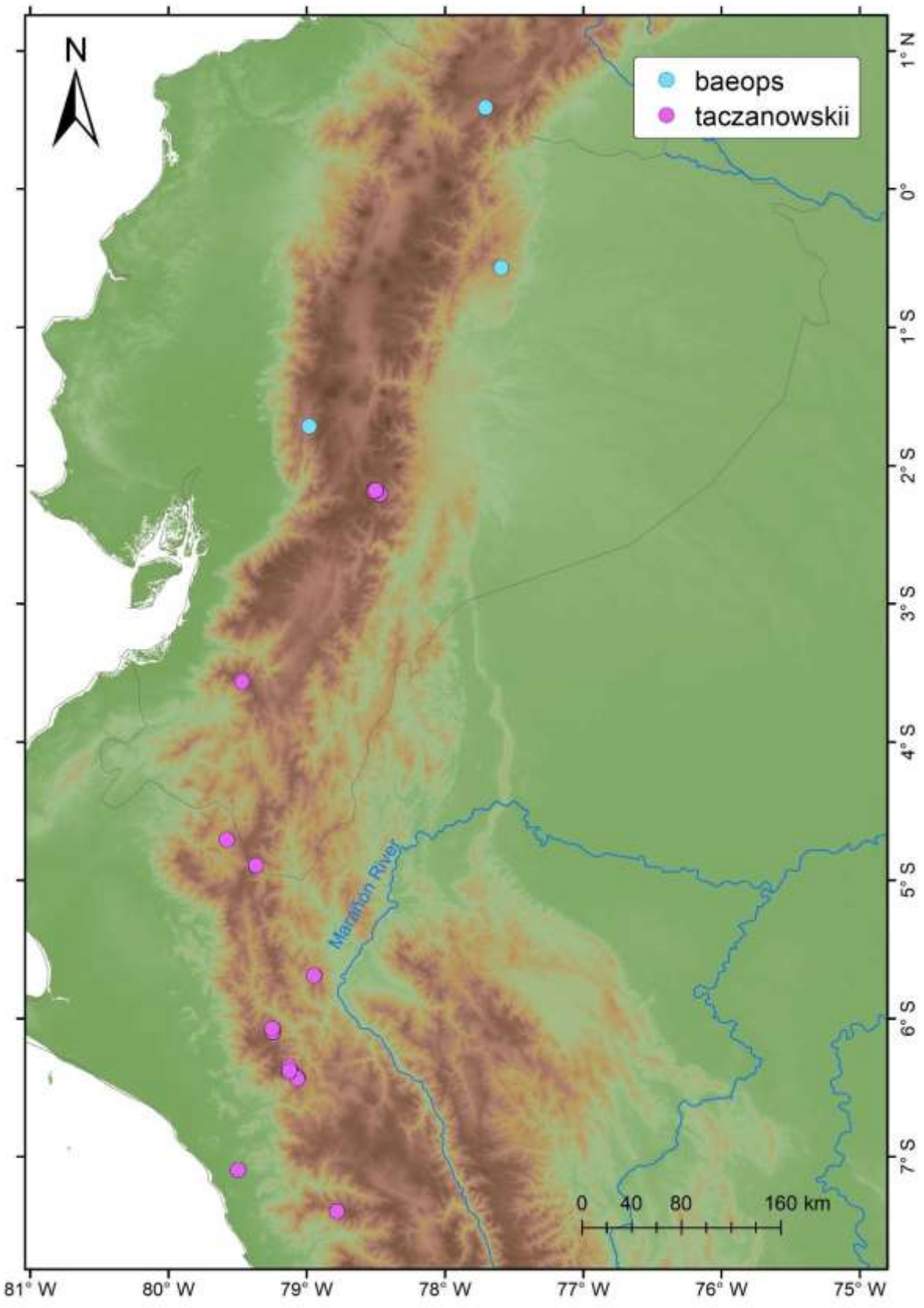

Figure S11. Collecting localities of unresolved taxa of *Thomasomys* (circles) and "*Thomasomys*" sp. 4 (triangles).

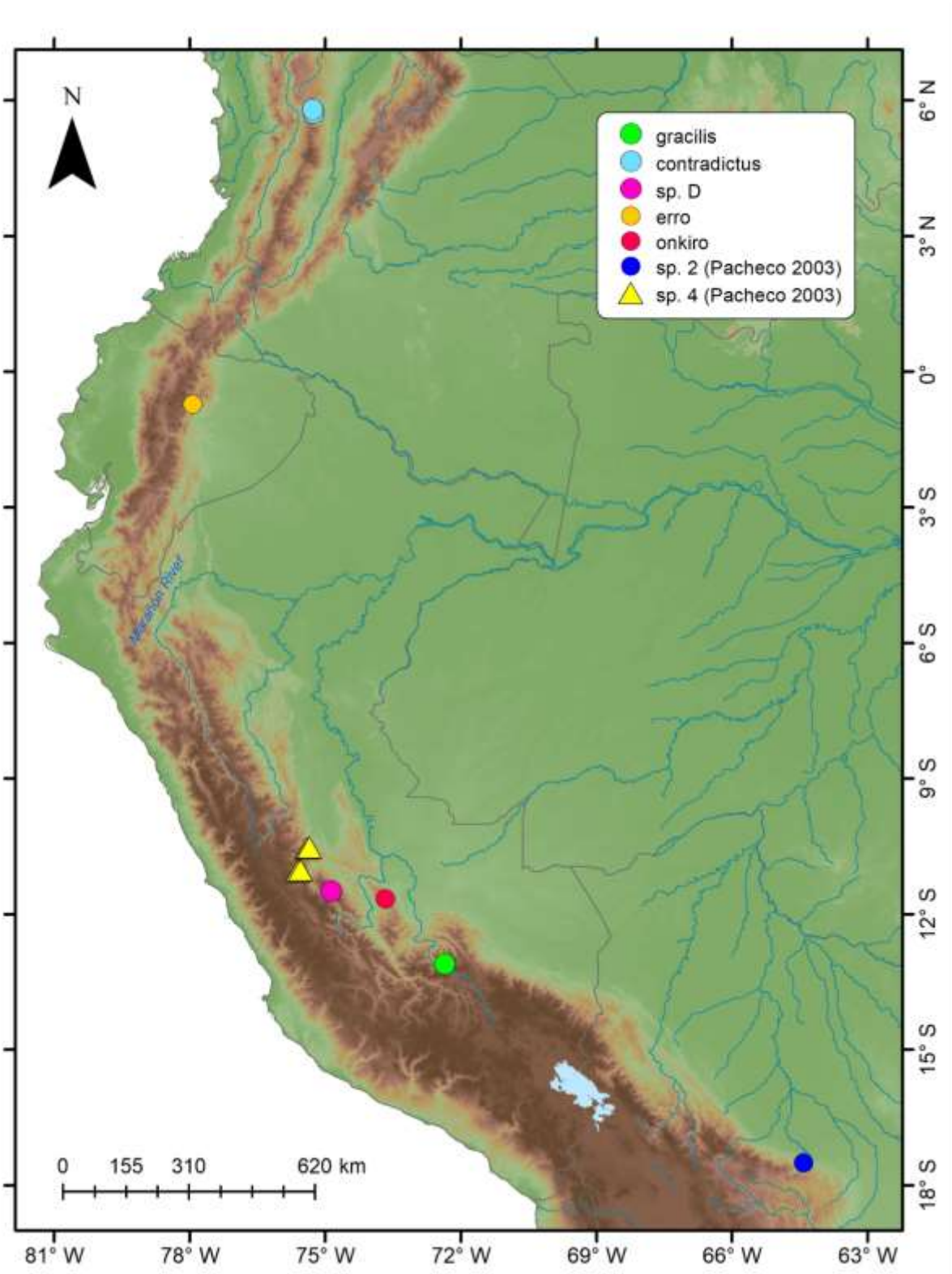

Table S1. Informal species groups based on morphological characters suggested by Pacheco (2015) with modifications of (a) Brito et al. (2019), (b) Ruelas and Pacheco (2021), (c) Brito et al. (2021), (d) Lee et al. (2022), and (e) Pacheco and Ruelas (2023).

Cinereus	**Incanus**	**Aureus**	**Baeops**	**Gracilis**	**Macrotis**	**Notatus**
australis	*eleusis*	*antoniobracki*[b]	*baeops*	*andersoni*	*macrotis*	*notatus*
bombycinus	*incanus* (includes *Thomasomys* sp. 5 and *Thomasomys* sp. 6)	*apeco*	*taczanowskii*	*gracilis*		
caudivarius	*ischyrus*	*aureus* (includes *Thomasomys* sp. 1 and *Thomasomys* sp. 2)		*oreas* (includes *Thomasomys* sp. 8 and *Thomasomys* sp. 9)		
cinereiventer	*kalinowskii* (includes *Thomasomys* sp. 7)	*auricularis*				
cinereus	*ladewi*	*burneoi*[d]				

cinnameus		*nicefori*				
contradictus		*pardignasi*[c]				
daphne (includes *Thomasomys* sp. 3)		*popayanus*				
dispar		*praetor*				
erro		*princeps*				
emeritus		*pyrrhonotus*				
fumeus		*rosalinda*				
hudsoni						
hylophilus						
laniger						
lojapiuranus[e]						
monochromos						
niveipes						
onkiro						
pagaibambensis[e]						

paramorum						
salazari[a]						
shallqukucha[e]						
silvestris						
ucucha						
vestitus						
vulcani (includes *Thomasomys* sp. 10)						

* *Thomasomys* sp. 4 has not been assigned to any species group.

References

Brito, J., Tinoco, N., Curay, J., Vargas, R., Reyes-Puig, C., Romero, V., & Pardiñas, U. F. J. (2019). Diversidad insospechada en los Andes de Ecuador: Filogenia del grupo "cinereus" de *Thomasomys* y descripción de una nueva especie (Rodentia, Cricetidae). *Mastozoología Neotropical*, *26*(2), 308–330. https://doi.org/10.31687/saremMN.19.26.2.0.04

Brito, J., Vaca-Puente, S., Koch, C., & Tinoco, N. (2021). Discovery of the first Amazonian *Thomasomys* (Rodentia, Cricetidae, Sigmodontinae): A new species from the remote Cordilleras del Cóndor and Kutukú in Ecuador. *Journal of Mammalogy*, *102*(2), 615–635. https://doi.org/10.1093/jmammal/gyaa183

Lee, T. E., Tinoco, N., & Brito, J. (2022). A new species of Andean mouse of the genus *Thomasomys* (Cricetidae, Sigmodontinae) from the eastern Andes of Ecuador. *Vertebrate Zoology*, *72*, 219–233. https://doi.org/10.3897/vz.72.e78219

Pacheco, V. (2015). Genus *Thomasomys* Coues, 1884. In J. L. Patton, U. F. J. Pardiñas, & G. D'Elia (Eds.), *Mammals of South America. Vol. 2, Rodents* (Vol. 2, pp. 617–682). The University of Chicago Press.

Pacheco, V., & Ruelas, D. (2023). Systematic revision of *Thomasomys cinereus* (Rodentia: Cricetidae: Sigmodontinae) from northern Peru and southern Ecuador, with descriptions of three new species. *Bulletin of the American Museum of Natural History*, *461*, 71.

Ruelas, D., & Pacheco, V. (2021). A new species of *Thomasomys* Coues, 1884 (Rodentia: Sigmodontinae) from the montane forests of northern Peru with comments on the "aureus" group. *Revista Peruana de Biología*, *28*(3), e19912. https://doi.org/10.15381/rpb.v28i3.19912

Table S2. List of specimens included in this study. GenBank accession and collection numbers, locality, and bibliographic source are provided for each terminal species. Asterisks show the material type (holotype or paratype). Collection/Collector number: AMNH and AMCC – American Museum of Natural History; CBF – Colección Boliviana de Fauna; CIT – Laboratorio de Citogenética de Vertebrados, Instituto de Biociencias, Universidade de São Paulo; FMNH – Field Museum of Natural History; LCM – Laboratorio de Citogenética de Mamíferos, Universidad de Chile; LSUMZ – Museum of Natural Science, Louisiana State University; MBUCV – Museo de Biología de la Universidad Central de Venezuela; MECN – Museo Ecuatoriano de Ciencias Naturales; MEPN – Museo de Historia Natural Gustavo Orcés V, Escuela Politécnica Nacional; MN – Museu Nacional, Universidade Federal do Rio de Janeiro; MNHN – Museo Nacional de Historia Natural, Uruguay; MNK – Museo de Historia Natural "Noel Kempff Mercado"; MSB –Museum of Southwestern Biology, University of New Mexico; MUSM – Museo de Historia Natural, Universidad Nacional Mayor de San Marcos; MVZ – Museum of Vertebrate Zoology, University of California; MZUSP – Museu de Zoologia Universidade de São Paulo; OK – Collection of Vertebrates, Oklahoma State University; QCAZ – Museo de Zoología de la Pontificia Universidad Católica del Ecuador; TK and TTU – Museum of Texas Tech University; UFES – Tissue collections at Universidade Federal do Espírito Santo; UFMG – Collection at Universidade Federal de Minas Gerais; UMMZ – Collection at University of Michigan Museum of Zoology; USNM – National Museum of Natural History, United States; CRB – Cibele R. Bonvicino (field number); DMC – David Marín Cardona (field number); JFD – Juan F. Díaz-Nieto (field number); JLP – James L. Patton (field number); JMC – Juan M. Martinez-Cerón (field number); LHE – Louise H. Emmons (field number); MNFS – M. N. F da Silva (field number); PNNO – Parque Nacional Las Orquídeas (field number); RCD – Robert C. Dowler (field

number); RGR – Rita Gomes Rocha (field number); RM – Raquel T. Moura (field number); TEL – Tom Lee (field number); UP – Ulyses Pardiñas (field number).

Genbank accession	**Species**	**Collection/ Collector number**	**Locality**	**Source**
AF297892	*Abrothrix olivaceus*	FMNH 129876	Chile: Aysen, General Carrera, Balmaceda, 8 km W, Fundo Esmerelda	Smith et al. (2001)
M35703	*Akodon aerosus*	MVZ 171679	Peru: Cusco, 72 km NE Paucartambo	Smith and Patton (1999)
M35691	*Akodon boliviensis*	MVZ 171607	Peru: Puno, 12 km S Santa Rosa	Smith and Patton (1999)
M35700	*Akodon torques*	MVZ 17120	Peru: Cusco, 32 km NE Paucartambo	Smith and Patton (1999)
AF159284	*Andinomys edax*	-	Bolivia: Tarija, Oconnor, 61 kilometers by road east of Tarija, Rancho Tambo	Anderson and Yates (2000)
AF108690	*Auliscomys micropus*	MVZ 182661	Argentina: Rio Negro, Pampa Quemada, 12 km W Bariloche	Smith and Patton (1999)
AY275112	*Blarinomys breviceps*	CIT 1391	Brazil: São Paulo, Serra da Cantareira	D'Elía (2003)

AY277486	*Brucepattersonius soricinus*	MVZ 183036	Brazil: São Paulo, Estacao Biologica de Boraceia, 3 km E, 28 km SE Biritiba-Mirim, Municipio de Salesopolis	D'Elía (2003)
AF108679	*Chilomys instans*	MVZ JLP16693	Colombia: Risaralda, Pereira, Reserva Ucumari	Smith and Patton (1999)
KR818906	*Chilomys instans*	TEL 2775	Ecuador: Carchi, San Pedro de Huaca, Páramo de la Estación Guandera	Lee et al. (2015)
AY195862	*Deltamys kempi*	MNHN 4151	Uruguay: San José, Ruta 1 sobre Arroyo Cufre	D'Elía et al. (2003)
AF159290	*Graomys griseoflavus*	MSB 232411	Bolivia: Santa Cruz, 53 km E of Boyuibe	Anderson and Yates (2000)
AF108697	*Holochilus sciureus*	JLP 15199	Brazil: Amazonas, Eirunepe, Rio Jurua	Smith and Patton (1999)
AF133667	*Juscelinomys huanchacae*	MNK 2632	Bolivia: Santa Cruz, Parque Nacional Noel Kempff Mercado, Huanchaca II	Emmons (1999)
AY275120	*Kunsia tomentosus*	LHE 1619	Bolivia: Santa Cruz, Margabalito	D'Elía (2003)
AF108698	*Microryzomys minutus*	MVZ 173975	Peru: Cusco, 3 km E Amaybamba	Smith and Patton (1999)
AY273912	*Necromys lasiurus*	TK 64302	Paraguay: Concepción, Parque Nacional Serranía de San Luis	D'Elía (2003)

AF181283	*Nectomys squamipes*	MN 42685	Brazil: Mato Grosso do Sul, Maracaju, Fazenda da Mata	Bonvicino and Moreira (2001)
AF108700	*Nesoryzomys fernandinae*	RCD 3392	Ecuador: Galapagos Archipelago, Fernandina Island	Smith and Patton (1999)
U58382	*Oecomys bicolor*	MNFS 1499	Brazil: Acre, Sobral	Patton and da Silva (1995)
U03535	*Oligoryzomys longicaudus*	MVZ 155842	Argentina: Rio Negro, 12 km W Bariloche	Smith and Patton (1999)
AY275126	*Oxymycterus rufus*	UP AC004	Argentina	D'Elía (2003)
AF484213	*Phyllotis magister*	LCM 1817	Chile: Antofagasta, Calama	Kuch et al. (2002)
KX423691	*Rhagomys longilingua*	CBF 7620	Bolivia: Bajo Hornun, Parque Nacional and Area Natural de Manejo Integrado Cotapata	Salazar-Bravo et al. (2016)
AY206770	*Rhagomys rufescens*	MN 66056	Brazil: Minas Gerais	Percequillo et al. (2004)
KY366342	*Rhipidomys albujai*	MECN 3790	Ecuador: Parque Nacional Sangay, Sardinayacu	Brito et al. (2017)
KY366344	*Rhipidomys albujai*	MEPN 12196	Ecuador: Parque Nacional Sangay, Sardinayacu	Brito et al. (2017)
HM594636	*Rhipidomys emiliae*	UFES BAC305	Brazil: Para, Carajas	Rocha et al. (2011)

HM594628	*Rhipidomys ipukensis*	RGR 425	Brazil: Tocantins, Lagoa da Confusão	Rocha et al. (2011)
KY366338	*Rhipidomys latimanus*	QCAZ 4784	Ecuador: Cotopaxi, Sigchos, San Francisco de las Pampas	Brito et al. (2017)
HM594659	*Rhipidomys leucodactylus*	MZUSP APC260	Brazil: Mato Grosso, Aripuanã	Rocha et al. (2011)
HM594646	*Rhipidomys macrurus*	UFMG 2944	Brazil: Minas Gerais, Nova Ponte, 12 km W Nova Ponte	Rocha et al. (2011)
HM594643	*Rhipidomys mastacalis*	UFMG 2925	Brazil: Minas Gerais, São Gonçalo do Rio Preto, 15 km S São Gonçalo do Rio Preto	Rocha et al. (2011)
KY366335	*Rhipidomys masticalis*	RM 117	Brazil: Fazenda Caititu	Brito et al. (2017)
HQ634184	*Rhipidomys wetzeli*	MBUCV 3311	Venezuela: Amazonas, 2.5 km NE del Pico Phelps, Cerro Neblina	de la Sancha et al. (2007)
AY275131	*Scapteromys aquaticus*	UP BAL509	Argentina: La Balandra	D'Elía (2003)
KY754152	*Sigmodon alstoni*	AMCC 112960	Venezuela: Apure, Hato el Frio, Saman de Apure	Steppan and Schenk (2017)
KY754153	*Sigmodon arizonae*	MSB 54086		Steppan and Schenk (2017)

KX866980	*Sigmodon hispidus*	TTU-M 80670	United States: Texas, Morris CO, White Oak Creek Wma (Wocwma-2)	Milazzo et al. (2017)
HQ290330	*Sigmodon hispidus*	OK5834	United States: Kansas, Ellis County, 1.6 km S, 3.2 km W Hays	Bradley et al. (2012)
KY754165	*Thaptomys nigrita*	MVZ 183040	Brazil: São Paulo, Base do Carmo, Fazenda Intervales, Município de Capão Bonito	Steppan and Schenk (2017)
DQ914643	*Thomasomys andersoni*	MSB 146437	Bolivia: Cochabamba, Chapare, Colomi	Salazar-Bravo and Yates (2007)
DQ914644	*Thomasomys andersoni*	AMNH 268734*	Bolivia: Cochabamba, Capinota, Corani	Salazar-Bravo and Yates (2007)
MW788412	*Thomasomys antoniobracki*	MUSM 23756*	Peru: Piura, Huancabamba, Minera Majaz, Campamento Alto Parramata	Ruelas and Pacheco (2021)
MW788413	*Thomasomys antoniobracki*	MUSM 23757*	Peru: Piura, Huancabamba, Minera Majaz, Campamento Alto Parramata	Ruelas and Pacheco (2021)
MW788414	*Thomasomys apeco*	MUSM 7199*	Peru: San Martín, Mariscal Cáceres, P.N. Río Abiseo, Los Chochos	Ruelas and Pacheco (2021)

MW788415	*Thomasomys apeco*	MUSM 7200*	Peru: San Martín, Mariscal Cáceres, P.N. Río Abiseo, Puerta de Monte	Ruelas and Pacheco (2021)
MW788416	*Thomasomys apeco*	MUSM 7201*	Peru: San Martín, Mariscal Cáceres, P.N. Río Abiseo, Pampa de Cuy	Ruelas and Pacheco (2021)
OP978392	*Thomasomys apeco*	MUSM 52644	Peru: Huánuco, Huánuco, Bosque Unchog	This study
MW788417	*Thomasomys aureus*	MSB 70707	Ecuador: Bolivar, Rio Tatahuazo, 2.5 km E of Cruz de Lizo	Ruelas and Pacheco (2021)
MW788418	*Thomasomys aureus*	MSB 70708	Ecuador: Bolivar, Rio Tatahuazo, 4 km E of Cruz de Lizo	Ruelas and Pacheco (2021)
GB	*Thomasomys* aff. *aureus*	QCAZ 13243	Ecuador: Zamora Chinchipe, Shucos	Brito et al. (2021)
OP978395	*Thomasomys* aff. *aureus*	MUSM 46699	Peru: Cajamarca, San Ignacio, Cerro La Viuda (Tabaconas-Namballe National Sanctuary)	This study
OP978396	*Thomasomys* aff. *aureus*	MUSM 42548	Peru: Junín, Tarma, San Pedro de Churco, margen izquierdo de río Churco	This study
OP978393	*Thomasomys* aff. *aureus*	MUSM 47039	Peru: Amazonas, Bongará, Copal	This study

OP978400	*Thomasomys* aff. *aureus*	MUSM 7990	Peru: San Martín, Mariscal Cáceres, P.N. Río Abiseo, Las Palmas	This study
OP978394	*Thomasomys* aff. *aureus*	MUSM 39557	Peru: Cajamarca, Chota, Paja Blanca	This study
OP978397	*Thomasomys* aff. *aureus*	MUSM 46867	Peru: Lambayeque, Ferreñafe, Geomarca	This study
OP978398	*Thomasomys* aff. *aureus*	MUSM 46868	Peru: Lambayeque, Ferreñafe, Geomarca	This study
OP978399	*Thomasomys* aff. *aureus*	MUSM 46869	Peru: Lambayeque, Ferreñafe, Geomarca	This study
MN557061	*Thomasomys auricularis*	MECN 4695	Ecuador: Loja, Saraguro, Cerro de Arcos	Brito et al. (2019)
MN557124	*Thomasomys auricularis*	QCAZ 6011	Ecuador: Azuay, Cuenca, Parque Nacional El Cajas, Laguna La Toreadora	Brito et al. (2019)
MN557125	*Thomasomys auricularis*	QCAZ 6015	Ecuador: Azuay, Cuenca, Parque Nacional El Cajas, Laguna La Toreadora	Brito et al. (2019)
DQ914645	*Thomasomys australis*	AMNH 268736	Bolivia: Cochabamba, Capinota, Corani	Salazar-Bravo and Yates (2007)
DQ914650	*Thomasomys australis*	MSB 70447	Bolivia: Cochabamba, Chapare, Colomi	Salazar-Bravo and Yates (2007)

DQ914654	*Thomasomys baeops*	MSB 70704	Ecuador: Bolivar, Rio Tatahuazo, 4 km E Cruz de Lizo	Salazar-Bravo and Yates (2007)
KR818876	*Thomasomys baeops*	TEL 1960	Ecuador: Napo, Parque Nacional Sumaco Napo-Galeras, Volcán Sumaco, Segundo refugio, Refugio Laguna, Entrada desde Pacto Sumaco, 16 km NE Wawa Sumaco	Lee et al. (2015)
KR818877	*Thomasomys baeops*	TEL 2699	Ecuador: Carchi, San Pedro de Huaca, Páramo de la Estación Guandera	Lee et al. (2015)
KR818878	*Thomasomys baeops*	TEL 2791	Ecuador: Carchi, San Pedro de Huaca, Páramo de la Estación Guandera	Lee et al. (2015)
MN557062	*Thomasomys bombycinus*	MECN 4957	Ecuador: Carchi, Reserva Drácula	Brito et al. (2019)
OP978403	*Thomasomys bombycinus*	JMC 382	Colombia: Antioquia, Páramo del Sol, Campamento Llano Grande, quebrada La Encarnación	This study
OP991879	*Thomasomys bombycinus*	PNNO 8	Colombia: Antioquia, Vereda Piedras, Quebrada La Mina	This study

OP978402	*Thomasomys bombycinus*	JMC 337	Colombia: Antioquia, Páramo del Sol, Campamento Llano Grande, quebrada La Encarnación	This study
OP991880	*Thomasomys bombycinus*	PNNO 10	Colombia: Antioquia, Vereda Piedras, Quebrada La Mina	This study
OP978401	*Thomasomys bombycinus*	JFD 375	Colombia: Antioquia, Vereda Calles, Sitio el Macho	This study
KR818905	*Thomasomys burneoi*	TEL 2878[p]	Ecuador: Chimborazo, Guamote, Parque Nacional Sangay, Lagunas de Atillo, Punto de Muestreo 3	Lee et al. (2015)
MN557077	*Thomasomys burneoi*	MECN 5666[p]	Ecuador: Chimborazo, Guamote, Parque Nacional Sangay - Laguna Negra	Brito et al. (2019)
MZ490799	*Thomasomys caudivarius*	MEPN 12491	Ecuador: Loja, Saraguro, Manu, Cerro de Arcos	Pacheco and Ruelas (2023)
MN557059	*Thomasomys caudivarius*	MECN 4687/ QCAZ17505	Ecuador: Loja, Saraguro, Cerro de Arcos	Brito et al. (2019)
MN557060	*Thomasomys caudivarius*	MECN 4692/ QCAZ17506	Ecuador: Loja, Saraguro, Cerro de Arcos	Brito et al. (2019)

MN557126	*Thomasomys caudivarius*	MECN 4699/ QCAZ17508	Ecuador: Loja, Saraguro, Cerro de Arcos	Brito et al. (2019)
OP978406	*Thomasomys* aff. *caudivarius*	MUSM 23445	Peru: Piura, Huancabamba, Minera Majaz, Campamento Nueva York	This study
OP978407	*Thomasomys* aff. *caudivarius*	MUSM 23580	Peru: Piura, Huancabamba, Minera Majaz, Campamento Alto Parramata	This study
OP978404	*Thomasomys* aff. *caudivarius*	MUSM 18239	Peru: Cajamarca, San Ignacio, Tabaconas, Lagunas Arreviatadas	This study
OP978408	*Thomasomys* aff. *caudivarius*	MUSM 23743	Peru: Piura, Huancabamba, Cerro Chinguela	This study
OP978409	*Thomasomys* aff. *caudivarius*	MUSM 23747	Peru: Piura, Huancabamba, Cerro Chinguela	This study
OP978410	*Thomasomys* aff. *caudivarius*	MUSM 23753	Peru: Piura, Huancabamba, Minera Majaz, Campamento Nueva York	This study

OP978405	*Thomasomys* aff. *caudivarius*	MUSM 46709	Peru: Cajamarca, San Ignacio, Piedra Cueva in Cerro Coyona (Tabaconas-Namballe National Sanctuary)	This study
MZ490809	*Thomasomys cinereus*	MUSM 46909	Peru: Cajamarca, Santa Cruz, Bosque San Pedro	Pacheco and Ruelas (2023)
MZ490803	*Thomasomys cinereus*	MUSM 41103	Peru: La Libertad, Santiago de Chuco, El Fundo-Río Chuyuhual	Pacheco and Ruelas (2023)
MZ490804	*Thomasomys cinereus*	MUSM 42010	Peru: La Libertad, Santiago de Chuco, El Fundo-Río Chuyuhual	Pacheco and Ruelas (2023)
MZ490805	*Thomasomys cinereus*	MUSM 42011	Peru: La Libertad, Santiago de Chuco, El Fundo-Río Chuyuhual	Pacheco and Ruelas (2023)
MZ490806	*Thomasomys cinereus*	MUSM 46716	Peru: Cajamarca, San Ignacio, Parque Nacional Cutervo, 100 m over Tragadero	Pacheco and Ruelas (2023)
MZ490807	*Thomasomys cinereus*	MUSM 46756	Peru: Cajamarca, Santa Cruz, 3.81 km NE from Monteseco	Pacheco and Ruelas (2023)
MZ490808	*Thomasomys cinereus*	MUSM 46757	Peru: Cajamarca, Santa Cruz, 3.81 km NE from Monteseco	Pacheco and Ruelas (2023)

MZ490800	*Thomasomys cinereus*	MUSM 24169	Peru: La Libertad, Daniel A. Carrión, La Arena	Pacheco and Ruelas (2023)
MZ490801	*Thomasomys cinereus*	MUSM 24172	Peru: La Libertad, Daniel A. Carrión, La Arena	Pacheco and Ruelas (2023)
MZ490802	*Thomasomys cinereus*	MUSM 38007	Peru: Cajamarca, Celendín, CC.PP. Sorochuco	Pacheco and Ruelas (2023)
MZ490810	*Thomasomys cinereus*	MUSM 51110	Peru: La Libertad, Contumazá, Bosque Cachil	Pacheco and Ruelas (2023)
MZ490811	*Thomasomys cinereus*	MUSM 51115	Peru: La Libertad, Contumazá, Bosque Cachil	Pacheco and Ruelas (2023)
MZ490812	*Thomasomys cinereus*	MUSM 51117	Peru: La Libertad, Contumazá, Bosque Cachil	Pacheco and Ruelas (2023)
MZ490813	*Thomasomys cinereus*	MUSM EV1626	Peru: La Libertad, La Clambay	Pacheco and Ruelas (2023)
OP978411	*Thomasomys* aff. *cinereus*	MEPN 12538	Ecuador: Loja, Espíndola, Parque Nacional Yacuri	This study

MN557101	*Thomasomys* aff. *cinereus*	QCAZ 15612	Ecuador: Loja, Espíndola, Parque Nacional Yacuri	Brito et al. (2019)
MN557102	*Thomasomys* aff. *cinereus*	QCAZ 15613	Ecuador: Loja, Espíndola, Parque Nacional Yacuri	Brito et al. (2019)
MN557103	*Thomasomys* aff. *cinereus*	QCAZ 15614	Ecuador: Loja, Espíndola, Parque Nacional Yacuri	Brito et al. (2019)
MN557104	*Thomasomys* aff. *cinereus*	QCAZ 15615	Ecuador: Loja, Espíndola, Parque Nacional Yacuri	Brito et al. (2019)
MN557105	*Thomasomys* aff. *cinereus*	QCAZ 15616	Ecuador: Loja, Espíndola, Parque Nacional Yacuri	Brito et al. (2019)
MN557106	*Thomasomys* aff. *cinereus*	QCAZ 15617	Ecuador: Loja, Espíndola, Parque Nacional Yacuri	Brito et al. (2019)
MN557107	*Thomasomys* aff. *cinereus*	QCAZ 15618	Ecuador: Loja, Espíndola, Parque Nacional Yacuri	Brito et al. (2019)
MN557108	*Thomasomys* aff. *cinereus*	QCAZ 15619	Ecuador: Loja, Espíndola, Parque Nacional Yacuri	Brito et al. (2019)

MN557109	*Thomasomys* aff. *cinereus*	QCAZ 15620	Ecuador: Loja, Espíndola, Parque Nacional Yacuri	Brito et al. (2019)
MN557110	*Thomasomys* aff. *cinereus*	QCAZ 15621	Ecuador: Loja, Espíndola, Parque Nacional Yacuri	Brito et al. (2019)
MN557111	*Thomasomys* aff. *cinereus*	QCAZ 15622	Ecuador: Loja, Espíndola, Parque Nacional Yacuri	Brito et al. (2019)
MN557112	*Thomasomys* aff. *cinereus*	QCAZ 15623	Ecuador: Loja, Espíndola, Parque Nacional Yacuri	Brito et al. (2019)
MN557113	*Thomasomys* aff. *cinereus*	QCAZ 15624	Ecuador: Loja, Espíndola, Parque Nacional Yacuri	Brito et al. (2019)
MN557114	*Thomasomys* aff. *cinereus*	QCAZ 15626	Ecuador: Loja, Espíndola, Parque Nacional Yacuri	Brito et al. (2019)
MN557115	*Thomasomys* aff. *cinereus*	QCAZ 15627	Ecuador: Loja, Espíndola, Parque Nacional Yacuri	Brito et al. (2019)
MN557116	*Thomasomys* aff. *cinereus*	QCAZ 15628	Ecuador: Loja, Espíndola, Parque Nacional Yacuri	Brito et al. (2019)

MN557117	*Thomasomys* aff. *cinereus*	QCAZ 15629	Ecuador: Loja, Espíndola, Parque Nacional Yacuri	Brito et al. (2019)
MN557118	*Thomasomys* aff. *cinereus*	QCAZ 15630	Ecuador: Loja, Espíndola, Parque Nacional Yacuri	Brito et al. (2019)
KR818895	*Thomasomys cinnameus*	TEL 2806	Ecuador: Carchi, San Pedro de Huaca, Páramo de la Estación Guandera	Lee et al. (2015)
KR818896	*Thomasomys cinnameus*	TEL 2811	Ecuador: Carchi, San Pedro de Huaca, Páramo de la Estación Guandera	Lee et al. (2015)
KR818897	*Thomasomys cinnameus*	TEL 2690	Ecuador: Carchi, San Pedro de Huaca, Páramo de la Estación Guandera	Lee et al. (2015)
MN557099	*Thomasomys cinnameus*	QCAZ 14919	Ecuador: Carchi, San Pedro de Huaca, Páramo de la Estación Guandera	Brito et al. (2019)
MN557100	*Thomasomys cinnameus*	QCAZ 14920	Ecuador: Carchi, San Pedro de Huaca, Páramo de la Estación Guandera	Brito et al. (2019)
OP978412	*Thomasomys cinnameus*	DMC 294	Colombia: Antioquia, Sonson, Vereda las Palomas, Páramo Las Palomas	This study

OP978414	*Thomasomys contradictus*	DMC 274	Colombia: Antioquia, Sonson, Vereda las Palomas, Páramo Las Palomas	This study
OP978417	*Thomasomys contradictus*	DMC 64	Colombia: Antioquia, Sonson, Vereda Norí, Finca Alejandría	This study
OP978413	*Thomasomys contradictus*	DMC 271	Colombia: Antioquia, Sonson, Vereda las Palomas, Páramo Las Palomas	This study
OP978415	*Thomasomys contradictus*	DMC 275	Colombia: Antioquia, Sonson, Vereda las Palomas, Páramo Las Palomas	This study
OP978416	*Thomasomys contradictus*	DMC 291	Colombia: Antioquia, Sonson, Vereda las Palomas, Páramo Las Palomas	This study
MZ736561	*Thomasomys daphne*	MUSM 9369	Peru: Cusco, Paucartambo, Paucartambo, Challabamba, P.V. Acjanaco	Pacheco and Ruelas (2023)
EU579476	*Thomasomys erro*	TEL 1663	Ecuador: Napo, Archidona, Archidona, Sierra Azul, Cloud Forest Reserve	Hanson (2008)

KR818901	*Thomasomys fumeus*	TEL 1894	Ecuador: Napo, Parque Nacional Sumaco Napo-Galeras, Volcán Sumaco, Segundo refugio, Refugio Laguna, Entrada desde Pacto Sumaco, 16 km NE Wawa Sumac	Lee et al. (2015)
AF108674	*Thomasomys gracilis*	MVZ 166668	Peru: Cusco, 90 km SE Quillabamba	Smith and Patton (1999)
MZ736560	*Thomasomys gracilis*	MVZ 166669	Peru: Cusco, 90 km SE Quillabamba	Smith and Patton (1999)
DQ914646	*Thomasomys hudsoni*	MSB 140583	Ecuador: Azuay, Cajas, Cuenca, Sayausi	Salazar-Bravo and Yates (2007)
KR818894	*Thomasomys hudsoni*	TEL 2243	Ecuador: Chimborazo, Guamote, Parque Nacional Sangay, Lagunas de Atillo	Lee et al. (2015)
MN557076	*Thomasomys hudsoni*	MECN 5664	Ecuador: Chimborazo, Guamote, Parque Nacional Sangay - Laguna Negra	Brito et al. (2019)
MN557078	*Thomasomys hudsoni*	MECN 5667	Ecuador: Chimborazo, Guamote, Parque Nacional Sangay - Bosque de Polilepys	Brito et al. (2019)
MN557079	*Thomasomys hudsoni*	MECN 5668	Ecuador: Chimborazo, Guamote, Parque Nacional Sangay - Bosque de Polilepys	Brito et al. (2019)

OP978418	*Thomasomys incanus*	MUSM 42495	Peru: Junín, Tarma, San Pedro de Churco	This study
OP978419	*Thomasomys incanus*	MUSM 42499	Peru: Junín, Tarma, San Pedro de Churco	This study
OP978420	*Thomasomys incanus*	MUSM 42558	Peru: Junín, Tarma, San Pedro de Churco	This study
OP978422	*Thomasomys incanus*	MUSM 52868	Peru: Junín, Tarma, San Pedro de Churco	This study
OP978423	*Thomasomys incanus*	MUSM 52870	Peru: Junín, Tarma, San Pedro de Churco	This study
OP978421	*Thomasomys incanus*	MUSM 42571	Peru: Junín, Tarma, San Pedro de Churco	This study
OP978424	*Thomasomys ischyrus*	MUSM 47040	Peru: Amazonas, Luya, ACP Huiquilla	This study
OP978425	*Thomasomys ischyrus*	MUSM 47041	Peru: Amazonas, Luya, ACP Huiquilla	This study
OP978426	*Thomasomys ischyrus*	MUSM 47283	Peru: Amazonas, Luya, a 100 m aprox. de la caverna Quiocta	This study
OP978427	*Thomasomys ischyrus*	MUSM 47284	Peru: Amazonas, Luya, a 100 m aprox. de la caverna Quiocta	This study
OP978428	*Thomasomys ischyrus*	MUSM 47286	Peru: Amazonas, Luya, a 80 m aprox. de la caverna Quiocta	This study
OP978429	*Thomasomys ischyrus*	MUSM 47287	Peru: Amazonas, Luya, a 80 m aprox. de la caverna Quiocta	This study

OP978430	*Thomasomys ischyrus*	MUSM 52699	Peru: Huánuco, Huánuco, Bosque Unchog	This study
OP978434	*Thomasomys* aff. *ischyrus*	MUSM 52676	Peru: Huánuco, Huánuco, Bosque Unchog	This study
OP978432	*Thomasomys* aff. *ischyrus*	MUSM 52650	Peru: Huánuco, Huánuco, Bosque Unchog	This study
OP978433	*Thomasomys* aff. *ischyrus*	MUSM 52668	Peru: Huánuco, Huánuco, Bosque Unchog	This study
OP978431	*Thomasomys* aff. *ischyrus*	MUSM 18615	Peru: Huánuco, Huánuco, Bosque de Carpish	This study
AF108678	*Thomasomys kalinowskii*	MVZ 172598	Peru: Junín, 16 km NNE Palca	Smith and Patton (1999)
MN557092	*Thomasomys kalinowskii*	MVZ 172599	Peru: Junín, 16 km NNE (by road) Palca	Brito et al. (2019)
OP978435	*Thomasomys kalinowskii*	MUSM 42503	Peru: Junín, Tarma, San Pedro de Churco	This study
OP978441	*Thomasomys kalinowskii*	MUSM 42560	Peru: Junín, Tarma, San Pedro de Churco	This study
OP978436	*Thomasomys kalinowskii*	MUSM 42561	Peru: Junín, Tarma, San Pedro de Churco	This study
OP978439	*Thomasomys kalinowskii*	MUSM 24282	Peru: Pasco, Oxapampa, Santa Barbara	This study
OP978440	*Thomasomys kalinowskii*	MUSM 24283	Peru: Pasco, Oxapampa, Santa Barbara	This study

OP978442	*Thomasomys kalinowskii*	MUSM 42564	Peru: Junín, Tarma, San Pedro de Churco, margen izquierdo de río Churco	This study
OP978437	*Thomasomys kalinowskii*	MUSM 52878	Peru: Junín, Tarma, San Pedro de Churco	This study
OP978438	*Thomasomys kalinowskii*	MUSM 52880	Peru: Junín, Tarma, San Pedro de Churco	This study
OP978445	*Thomasomys* aff. *kalinowskii*	MUSM 14984	Peru: Pasco, Oxapampa, San Alberto, 7 Km al este de Oxapampa, limite este del P.N. Yanachaga Chemillen	This study
OP978443	*Thomasomys* aff. *kalinowskii*	MUSM 34877	Peru: Ayacucho, La Mar, Chiquintirca, Modelo 6	This study
OP978444	*Thomasomys* aff. *kalinowskii*	MUSM DLR430	Peru: Ayacucho	This study
DQ914647	*Thomasomys ladewi*	MSB 68484	Bolivia: La Paz, Rio Aceromarca	Salazar-Bravo and Yates (2007)
DQ914652	*Thomasomys ladewi*	MSB 68483	Bolivia: La Paz, Rio Aceromarca	Salazar-Bravo and Yates (2007)
MZ490815	*Thomasomys lojapiuranus*	MEPN 12549	Ecuador: Loja, Parque Nacional Yacuri	Pacheco and Ruelas (2023)

MN557119	*Thomasomys lojapiuranus*	QCAZ 16230	Ecuador: Loja, Amaluza, Jimbura, Parque Nacional Yacuri	Brito et al. (2019)
MN557120	*Thomasomys lojapiuranus*	QCAZ 16231	Ecuador: Loja, Amaluza, Jimbura, Parque Nacional Yacuri	Brito et al. (2019)
MN557121	*Thomasomys lojapiuranus*	QCAZ 16328	Ecuador: Loja, Amaluza, Jimbura, Parque Nacional Yacuri	Brito et al. (2019)
MN557122	*Thomasomys lojapiuranus*	QCAZ 16329	Ecuador: Loja, Amaluza, Jimbura, Parque Nacional Yacuri	Brito et al. (2019)
MN557123	*Thomasomys lojapiuranus*	QCAZ 16330	Ecuador: Loja, Amaluza, Jimbura, Parque Nacional Yacuri	Brito et al. (2019)
MZ490816	*Thomasomys lojapiuranus*	MUSM 23758*	Peru: Piura, Huancabamba, Pariamarca Alto	Pacheco and Ruelas (2023)
MZ490817	*Thomasomys lojapiuranus*	MUSM 511	Peru: Piura, Ayabaca, bosque de Huamba, 44 km E- de Ayabaca	Pacheco and Ruelas (2023)
OK318983	*Thomasomys lojapiuranus*	MUSM ASA11	Peru: Piura, Ayabaca, Aypate	Pacheco and Ruelas (2023)

OK318984	*Thomasomys lojapiuranus*	MUSM ASA12	Peru: Piura, Ayabaca, Aypate	Pacheco and Ruelas (2023)
OK318985	*Thomasomys lojapiuranus*	MUSM ASA16	Peru: Piura, Ayabaca, Aypate	Pacheco and Ruelas (2023)
KY754168	*Thomasomys macrotis*	LSUMZ 27287*	Peru: San Martín, Puerta del Monte, ca 30 km NE Los Alisos	Steppan and Schenk (2017)
OP991881	*Thomasomys nicefori*	PNNO 47	Colombia: Antioquia, Vereda la Clara, Quebrada Santiago	This study
OP978446	*Thomasomys nicefori*	DMC 284	Colombia: Antioquia, Vereda las Palomas, Páramo Las Palomas	This study
OP978447	*Thomasomys nicefori*	DMC 295	Colombia: Antioquia, Vereda las Palomas, Páramo Las Palomas	This study
OP978450	*Thomasomys nicefori*	JMC 374	Colombia: Antioquia, Páramo del Sol, Campamento Llano Grande, quebrada La Encarnación	This study
OP978449	*Thomasomys nicefori*	JMC 339	Colombia: Antioquia, Páramo del Sol, Campamento Llano Grande, quebrada La Encarnación	This study

OP978448	*Thomasomys nicefori*	JMC 329	Colombia: Antioquia, Páramo del Sol, Campamento Llano Grande, quebrada La Encarnación	This study
AF108676	*Thomasomys notatus*	MVZ 166706	Peru: Cusco, 72 km NE Paucartambo (by rd.)	Smith and Patton (1999)
MN557128	*Thomasomys notatus*	UMMZ 160588	Peru: Cusco, 72 km NE Paucartambo (by rd.)	Brito et al. (2019)
OP978453	*Thomasomys notatus*	MUSM 42563	Peru: Junín, Tarma, San Pedro de Churco, margen izquierdo del río Churco	This study
OP978451	*Thomasomys notatus*	MUSM 47043	Peru: Amazonas, Bongará, Yerbabuena	This study
OP978452	*Thomasomys notatus*	MUSM 47044	Peru: Amazonas, Bongará, Yerbabuena	This study
KY754169	*Thomasomys onkiro*	USNM 582124	Peru: Cusco, La Convención, Cordillera de Vilcabamba N, Camp One	Steppan and Schenk (2017)
DQ914651	*Thomasomys oreas*	MSB 87126	Bolivia: Cochabamba, Corani, Quchapampa Jach'a Suyu	Salazar-Bravo and Yates (2007)
KY754166	*Thomasomys* aff. *oreas*	MUSM 17457	Peru: Cusco, Quispicanchi, Chacarara, Hatunpampa	Steppan and Schenk (2017)
MZ490823	*Thomasomys pagaibambensis*	MUSM 39526	Peru: Cajamarca, Chota, Pagaibamba Alto	Pacheco and Ruelas (2023)

MZ490824	*Thomasomys pagaibambensis*	MUSM 39529	Peru: Cajamarca, Chota, Pagaibamba Bajo	Pacheco and Ruelas (2023)
MZ419564	*Thomasomys pagaibambensis*	MUSM 40973*	Peru: Cajamarca, Chota, Pagaibamba	Pacheco and Ruelas (2023)
MZ419565	*Thomasomys pagaibambensis*	MUSM 41009	Peru: Cajamarca, Chota, Paja Blanca	Pacheco and Ruelas (2023)
KR818891	*Thomasomys paramorum*	TEL 2244	Ecuador: Chimborazo, Guamote, Parque Nacional Sangay, Lagunas de Atillo, Punto de Muestreo 4	Lee et al. (2015)
KR818892	*Thomasomys paramorum*	TEL 2247	Ecuador: Chimborazo, Guamote, Parque Nacional Sangay, Lagunas de Atillo, Punto de Muestreo 4	Lee et al. (2015)
KR818893	*Thomasomys paramorum*	TEL 2380	Ecuador: Chimborazo, Guamote, Parque Nacional Sangay, Lagunas de Atillo, Punto de Muestreo 4	Lee et al. (2015)
MN557087	*Thomasomys paramorum*	MEPN 12631	Ecuador: Chimborazo, Riobamba, Parque Nacional Sangay - Paramo	Brito et al. (2019)
MN557088	*Thomasomys paramorum*	MEPN 12634	Ecuador: Chimborazo, Riobamba, Parque Nacional Sangay - Paramo	Brito et al. (2019)

MN557094	*Thomasomys paramorum*	QCAZ 11986	Ecuador: Chimborazo, Guamote, Parque Nacional Sangay, Lagunas de Atillo, Punto de Muestreo 4	Brito et al. (2019)
MN557095	*Thomasomys paramorum*	QCAZ 11987	Ecuador: Chimborazo, Guamote, Parque Nacional Sangay, Lagunas de Atillo, Punto de Muestreo 4	Brito et al. (2019)
MN557096	*Thomasomys paramorum*	QCAZ 12602	Ecuador: Pichincha, Quito, San Antonio de Pichincha, Monte Casitahua	Brito et al. (2019)
MN557097	*Thomasomys paramorum*	QCAZ 12610	Ecuador: Pichincha, Quito, San Antonio de Pichincha, Monte Casitahua	Brito et al. (2019)
MN557098	*Thomasomys paramorum*	QCAZ 12624	Ecuador: Pichincha, Quito, San Antonio de Pichincha, Monte Casitahua	Brito et al. (2019)
MN557083	*Thomasomys pardignasi*	QCAZ 17489/ MECN 5852*	Ecuador: Morona Santiago, Santiago, Cordillera de Kutukú 2	Brito et al. (2019)
MN557084	*Thomasomys pardignasi*	QCAZ 17490/ MECN 5853*	Ecuador: Morona Santiago, Santiago, Cordillera de Kutukú 2	Brito et al. (2019)
MN557085	*Thomasomys pardignasi*	QCAZ 17493/ MEPN 12053	Ecuador: Zamora Chinchipe, Yantzaza, Cordillera de Cóndor, Alto Machinaza	Brito et al. (2019)

MW788419	*Thomasomys praetor*	MUSM 40080	Peru: Áncash, Pallasca, Quebrada Challhuacocha Baja	Ruelas and Pacheco (2021)
MW788420	*Thomasomys praetor*	MUSM 40209	Peru: Áncash, Pallasca, Cochaconchucos	Ruelas and Pacheco (2021)
MW788421	*Thomasomys praetor*	MUSM 40211	Peru: Áncash, Pallasca, Quebrada Challhuacocha Baja	Ruelas and Pacheco (2021)
OP978501	*Thomasomys princeps*		Colombia: Cundinamarca, Páramo de Chingaza	García Loaiza (2015)
MW788422	*Thomasomys pyrrhonotus*	MUSM 47232	Peru: Lambayeque, Ferreñafe, Palomapampa	Ruelas and Pacheco (2021)
MW788423	*Thomasomys pyrrhonotus*	MUSM 47233	Peru: Lambayeque, Ferreñafe, Palomapampa	Ruelas and Pacheco (2021)
MW788424	*Thomasomys pyrrhonotus*	MUSM 47234	Peru: Lambayeque, Ferreñafe, Palomapampa	Ruelas and Pacheco (2021)
OP978454	*Thomasomys pyrrhonotus*	MUSM 51119	Peru: La Libertad, Contumazá, Bosque Cachil	This study

KR818888	*Thomasomys salazari*	TEL 2271	Ecuador: Chimborazo, Guamote, Parque Nacional Sangay, Lagunas de Atillo	Lee et al. (2015)
KR818889	*Thomasomys salazari*	TEL 2293	Ecuador: Ecuador: Chimborazo, Guamote, Parque Nacional Sangay, Lagunas de Atillo	Lee et al. (2015)
KR818890	*Thomasomys salazari*	TEL 2354	Ecuador: Chimborazo, Guamote, Parque Nacional Sangay, Lagunas de Atillo	Lee et al. (2015)
MN557065	*Thomasomys salazari*	MECN 5634	Ecuador: Morona Santiago, Morona, Parque Nacional Sangay - Guardianía de Atillo	Brito et al. (2019)
MN557066	*Thomasomys salazari*	MECN 5636	Ecuador: Morona Santiago, Morona, Parque Nacional Sangay - Guardianía de Atillo	Brito et al. (2019)
MN557067	*Thomasomys salazari*	MECN 5637	Ecuador: Morona Santiago, Morona, Parque Nacional Sangay - Sisñan	Brito et al. (2019)
MN557068	*Thomasomys salazari*	MECN 5638	Ecuador: Morona Santiago, Morona, Parque Nacional Sangay - Sisñan	Brito et al. (2019)
MN557072	*Thomasomys salazari*	MECN 5649*	Ecuador: Morona Santiago, Morona, Parque Nacional Sangay - Guardianía de Atillo	Brito et al. (2019)

MN557073	*Thomasomys salazari*	MECN 5653	Ecuador: Morona Santiago, Morona, Parque Nacional Sangay - Guardianía de Atillo	Brito et al. (2019)
MN557074	*Thomasomys salazari*	MECN 5654	Ecuador: Morona Santiago, Morona, Parque Nacional Sangay - Guardianía de Atillo	Brito et al. (2019)
MN557080	*Thomasomys salazari*	MECN 5671	Ecuador: Morona Santiago, Morona, Parque Nacional Sangay - Guardianía de Atillo	Brito et al. (2019)
MN557081	*Thomasomys salazari*	MECN 5674	Ecuador: Chimborazo, Guamote, Parque Nacional Sangay - Laguna Negra	Brito et al. (2019)
MN557082	*Thomasomys salazari*	MECN 5675	Ecuador: Chimborazo, Guamote, Parque Nacional Sangay - Laguna Negra	Brito et al. (2019)
MZ490818	*Thomasomys shallqukucha*	MUSM 46883*	Peru: Lambayeque, Ferreñafe, Geomarca	Pacheco and Ruelas (2023)
MZ490819	*Thomasomys shallqukucha*	MUSM 46886*	Peru: Lambayeque, Ferreñafe, Geomarca	Pacheco and Ruelas (2023)
MZ490820	*Thomasomys shallqukucha*	MUSM 47227	Peru: Lambayeque, Ferreñafe, Palomapampa	Pacheco and Ruelas (2023)

MZ490821	*Thomasomys shallqukucha*	MUSM 47228	Peru: Lambayeque, Ferreñafe, Palomapampa	Pacheco and Ruelas (2023)
MZ490822	*Thomasomys shallqukucha*	MUSM 47229	Peru: Lambayeque, Ferreñafe, Palomapampa	Pacheco and Ruelas (2023)
KR818900	*Thomasomys silvestris*	TEL 2488	Ecuador: Cotopaxi, Sigchos, Reserva Integral Otonga	Lee et al. (2015)
MN557063	*Thomasomys silvestris*	MECN 5238	Ecuador: Pichincha, Mejía, Tambillo	Brito et al. (2019)
MN557064	*Thomasomys silvestris*	MECN 5394	Ecuador: Pichincha	Brito et al. (2019)
OP978476	*Thomasomys taczanowskii*	MUSM ASA32	Peru: Piura, Ayabaca, Aypate	This study
OP978473	*Thomasomys taczanowskii*	MUSM 23578	Peru: Piura, Huancabamba, Minera Majaz, Campamento Alto Parramata	This study
OP978474	*Thomasomys taczanowskii*	MUSM 23582	Peru: Piura, Huancabamba, Minera Majaz, Campamento Alto Parramata	This study
OP978475	*Thomasomys taczanowskii*	MUSM ASA07	Peru: Piura, Ayabaca, Aypate	This study

OP978455	*Thomasomys taczanowskii*	MUSM 39567	Peru: Cajamarca, Chota, Pagaibamba Medio	This study
OP978456	*Thomasomys taczanowskii*	MUSM 39568	Peru: Cajamarca, Chota, Pagaibamba Medio	This study
OP978457	*Thomasomys taczanowskii*	MUSM 39583	Peru: Cajamarca, Chota, Plataforma 5	This study
OP978458	*Thomasomys taczanowskii*	MUSM 39591	Peru: Cajamarca, Chota, Quebrada Honda	This study
OP978459	*Thomasomys taczanowskii*	MUSM 39593	Peru: Cajamarca, Chota, Quebrada Honda	This study
OP978460	*Thomasomys taczanowskii*	MUSM 41021	Peru: Cajamarca, Chota, Pagaibamba	This study
OP978461	*Thomasomys taczanowskii*	MUSM 41029	Peru: Cajamarca, Chota, Paja Blanca	This study
OP978462	*Thomasomys taczanowskii*	MUSM 41030	Peru: Cajamarca, Chota, Paja Blanca	This study

OP978468	*Thomasomys taczanowskii*	MUSM 46892	Peru: Lambayeque, Ferreñafe, Geomarca	This study
OP978469	*Thomasomys taczanowskii*	MUSM 46897	Peru: Lambayeque, Ferreñafe, Geomarca	This study
OP978470	*Thomasomys taczanowskii*	MUSM 46901	Peru: Lambayeque, Ferreñafe, Geomarca	This study
OP978463	*Thomasomys taczanowskii*	MUSM 47188	Peru: Cajamarca, Jaén, ACR Bosque de Huamantanga	This study
OP978464	*Thomasomys taczanowskii*	MUSM 47189	Peru: Cajamarca, Jaén, ACR Bosque de Huamantanga	This study
OP978471	*Thomasomys taczanowskii*	MUSM 47235	Peru: Lambayeque, Ferreñafe, Palomapampa	This study
OP978472	*Thomasomys taczanowskii*	MUSM 47236	Peru: Lambayeque, Ferreñafe, Palomapampa	This study
OP978465	*Thomasomys taczanowskii*	MUSM VPT1644	Peru: Cajamarca, Santa Cruz, 2 km E Monteseco	This study

AF108675	*Thomasomys taczanowskii*	MVZ 181999	Peru: Cajamarca, 2.5 km NE Monte Seco on trail to Chorro Blanco, Rio Zana	Smith and Patton (1999)
KR818879	*Thomasomys taczanowskii*	TEL 2254	Ecuador: Chimborazo, Guamote, Parque Nacional Sangay, Lagunas de Atillo	Lee et al. (2015)
KR818880	*Thomasomys taczanowskii*	TEL 2261	Ecuador: Chimborazo, Guamote, Parque Nacional Sangay, Lagunas de Atillo	Lee et al. (2015)
KR818881	*Thomasomys taczanowskii*	TEL 2290	Ecuador: Chimborazo, Guamote, Parque Nacional Sangay, Lagunas de Atillo	Lee et al. (2015)
KR818882	*Thomasomys taczanowskii*	TEL 2306	Ecuador: Chimborazo, Guamote, Parque Nacional Sangay, Lagunas de Atillo	Lee et al. (2015)
KR818883	*Thomasomys taczanowskii*	TEL 2331	Ecuador: Chimborazo, Guamote, Parque Nacional Sangay, Lagunas de Atillo	Lee et al. (2015)
KR818884	*Thomasomys taczanowskii*	TEL 2386	Ecuador: Chimborazo, Guamote, Parque Nacional Sangay, Lagunas de Atillo	Lee et al. (2015)
KR818885	*Thomasomys taczanowskii*	QCAZ 11947	Ecuador: Chimborazo, Guamote, Parque Nacional Sangay, Lagunas de Atillo	Lee et al. (2015)

KR818886	*Thomasomys taczanowskii*	MVZ 181999	Peru: Cajamarca, Rio Zaña, 2.5 km NE Monte Seco on trail to Chorro Blanco	Lee et al. (2015)
KR818887	*Thomasomys taczanowskii*	MVZ 182003	Peru: Cajamarca, Rio Zaña, 2.5 km NE Monte Seco on trail to Chorro Blanco	Smith and Patton (1999)
MN557069	*Thomasomys taczanowskii*	MECN 5640/ QCAZ17515	Ecuador: Morona Santiago, Morona, Parque Nacional Sangay - Sisñan	Brito et al. (2019)
MN557070	*Thomasomys taczanowskii*	MECN 5641/ QCAZ17503	Ecuador: Chimborazo, Guamote, Parque Nacional Sangay - Bosque de Polilepys	Brito et al. (2019)
MN557071	*Thomasomys taczanowskii*	MECN 5642/ QCAZ17502	Ecuador: Chimborazo, Guamote, Parque Nacional Sangay - Laguna Negra	Brito et al. (2019)
MN557086	*Thomasomys taczanowskii*	MEPN 12500/ QCAZ17517	Ecuador: El Oro, Zaruma: Cerro de Arcos	Brito et al. (2019)
OP978466	*Thomasomys taczanowskii*	MUSM 51118	Peru: La Libertad, Contumazá, Bosque Cachil	This study
OP978467	*Thomasomys taczanowskii*	MUSM 51124	Peru: La Libertad, Contumazá, Bosque Cachil	This study

OP978480	*Thomasomys taczanowskii*	MUSM 51130	Peru: La Libertad, Contumazá, Bosque Cachil	This study
OP978477	*Thomasomys taczanowskii*	MUSM 51140	Peru: La Libertad, Contumazá, Bosque Cachil	This study
OP978478	*Thomasomys taczanowskii*	MUSM 51146	Peru: La Libertad, Contumazá, Bosque Cachil	This study
OP978479	*Thomasomys taczanowskii*	MUSM 51147	Peru: La Libertad, Contumazá, Bosque Cachil	This study
KR818898	*Thomasomys ucucha*	TEL 2692	Ecuador: Carchi, San Pedro de Huaca, Páramo de la Estación Guandera	Lee et al. (2015)
KR818899	*Thomasomys ucucha*	TEL 2800	Ecuador: Carchi, San Pedro de Huaca, Páramo de la Estación Guandera	Lee et al. (2015)
MN557093	*Thomasomys ucucha*	QCAZ 11707	Ecuador: Imbabura, Ibarra, Comunidad de Zuleta, Hacienda San Pedro, Sector la Rinconada	Brito et al. (2019)
KR818902	*Thomasomys vulcani*	TEL 2703	Ecuador: Carchi, San Pedro de Huaca, Páramo de la Estación Guandera	Lee et al. (2015)

KR818903	*Thomasomys vulcani*	TEL 2728	Ecuador: Carchi, San Pedro de Huaca, Páramo de la Estación Guandera	Lee et al. (2015)
KR818904	*Thomasomys vulcani*	TEL 2746	Ecuador: Carchi, San Pedro de Huaca, Páramo de la Estación Guandera	Lee et al. (2015)
MW788425	*Thomasomys* sp. 1 (Pacheco 2003)	MUSM 11999	Peru: Cusco, Paucartambo, Paucartambo, Pillahuata	Ruelas and Pacheco (2021)
MW788426	*Thomasomys* sp. 1 (Pacheco 2003)	MUSM 12000	Peru: Cusco, Paucartambo, Paucartambo, Pillahuata	Ruelas and Pacheco (2021)
U035402	*Thomasomys* sp. 1 (Pacheco 2003)	MVZ 170076	Peru: Cusco, Paucartambo, 72 km NE Paucartambo (by rd.)	Smith and Patton (1999)
DQ914653	*Thomasomys* sp. 2 (Pacheco 2003)	AMNH 260422	Bolivia: Cochabamba, Campero, ca. 28 kilometers by road west of Comarapa	Salazar-Bravo and Yates (2007)
AF108673	*Thomasomys* sp. 3 (Pacheco 2003)	MVZ 171502	Peru: Puno, Agualani, 9 km N Limbani	Smith and Patton (1999)
DQ914649	*Thomasomys* sp. 3 (Pacheco 2003)	AMNH 268737	Bolivia: La Paz, Larecaja, Sayani	Salazar-Bravo and Yates (2007)

KY754167	*Thomasomys* sp. 3 (Pacheco 2003)	MVZ 171501	Peru: Puno, Agualani, 9 km N Limbani	Steppan and Schenk (2017)
OP978484	*Thomasomys* sp. 4 (Pacheco 2003)	MUSM 14961	Peru: Pasco, Oxapampa, San Alberto, 7 km al este de Oxapampa, limite este del P.N. Yanachaga Chemillen	This study
OP978485	*Thomasomys* sp. 4 (Pacheco 2003)	MUSM 14962	Peru: Pasco, Oxapampa, San Alberto, 7 km al este de Oxapampa, limite este del P.N. Yanachaga Chemillen	This study
OP978486	*Thomasomys* sp. 4 (Pacheco 2003)	MUSM 14971	Peru: Pasco, Oxapampa, San Alberto, 7 km al este de Oxapampa, limite este del P.N. Yanachaga Chemillen	This study
OP978487	*Thomasomys* sp. 4 (Pacheco 2003)	MUSM 24297	Peru: Pasco, Oxapampa, San Alberto, Abra Esperanza	This study
OP978483	*Thomasomys* sp. 4 (Pacheco 2003)	MUSM 42567	Peru: Junín, Tarma, San Pedro de Churco	This study
OP978489	*Thomasomys* sp. 4 (Pacheco 2003)	MUSM 42568	Peru: Junín, Tarma, San Pedro de Churco	This study
OP978482	*Thomasomys* sp. 4 (Pacheco 2003)	MUSM 52896	Peru: Junín, Tarma, San Pedro de Churco	This study

OP978488	*Thomasomys* sp. 4 (Pacheco 2003)	MUSM 42508	Peru: Junín, Tarma, San Pedro de Churco	This study
OP978481	*Thomasomys* sp. 4 (Pacheco 2003)	MUSM 52895	Peru: Junín, Tarma, San Pedro de Churco	This study
OP978490	*Thomasomys* sp. 7 (Pacheco 2003)	MUSM 18681	Peru: Huánuco, Huánuco, Bosque de Carpish	This study
OP978491	*Thomasomys* sp. 7 (Pacheco 2003)	MUSM 19140	Peru: Huánuco, Huánuco, Caserío de San Pedro de Carpish	This study
OP978492	*Thomasomys* sp. 8 (Pacheco 2003)	MUSM 34878	Peru: Ayacucho, La Mar, Chiquintirca	This study
OP978493	*Thomasomys* sp. 8 (Pacheco 2003)	MUSM 34880	Peru: Ayacucho, La Mar, Chiquintirca	This study
OP978494	*Thomasomys* sp. 8 (Pacheco 2003)	MUSM 34881	Peru: Ayacucho, La Mar, Chiquintirca	This study
OP978495	*Thomasomys* sp. 8 (Pacheco 2003)	MUSM 34885	Peru: Ayacucho, La Mar, Chiquintirca	This study

AF108677	*Thomasomys* sp. 9 (Pacheco 2003)	MVZ 166703	Peru: Cusco, 32 km NE Paucartambo	Smith and Patton (1999)
MN557091	*Thomasomys* sp. 9 (Pacheco 2003)	MVZ 166704	Peru: Cusco, 32 km NE (by road) Paucartambo, km 112	Brito et al. (2019)
OP978497	*Thomasomys* sp. 10 (Pacheco 2003)	MUSM 23765	Peru: Piura, Huancabamba, Minera Majaz, Campamento Nueva York	This study
OP978496	*Thomasomys* sp. 10 (Pacheco 2003)	MUSM 23571	Peru: Piura, Huancabamba, Quebrada El Gallo	This study
OP978498	*Thomasomys* sp. A	MUSM 52861	Peru: Junín, Tarma, San Pedro de Churco	This study
OP978500	*Thomasomys* sp. A	MUSM 42490	Peru: Junín, Tarma, San Pedro de Churco	This study
DQ914648	*Thomasomys* sp. B	MSB 70714	Ecuador: Bolivar, Rio Tatahuazo, 4 km E of Cruz de Lizo	Salazar-Bravo and Yates (2007)
MN557089	*Thomasomys* sp. C	MEPN 12722	Ecuador: Carchi, El Angel, Bosque de Polylepis	Brito et al. (2019)
MN557090	*Thomasomys* sp. C	MEPN 12742	Ecuador: Carchi, El Angel, Bosque de Polylepis	Brito et al. (2019)
MZ736562	*Thomasomys* sp. D	MUSM 40809	Peru: Junín, Satipo, Carrizal	Pacheco and Ruelas (2023)

GB	*Thomasomys* sp. E	MECN 2720	Ecuador: Pichincha, Solaya Rive	Brito et al. (2021)
GB	*Thomasomys* sp. E	MECN 2807	Ecuador: Pichincha, Nono, Río Verde Cocha	Brito et al. (2021)
GB	*Thomasomys* sp. E	MECN 5389	Ecuador: Pichincha, Mejía, Tambillo Alto	Brito et al. (2021)
OP978499	*Thomasomys* sp. F	MUSM 44713	Peru: Huancavelica, Tayacaja, Quintao	This study
AF108685	*Wiedomys pyrrhorhinos*	UFMG LC43	Brazil: Bahía, Toca Velha, 7 km SE Canudos	Smith and Patton (1999)

References

Anderson, S., & Yates, T. L. (2000). A new genus and species of phyllotine rodent from Bolivia. Journal of Mammalogy, 81(1), 18–36. https://doi.org/10.1644/1545-1542(2000)081<0018:ANGASO>2.0.CO;2

Bonvicino, C. R., & Moreira, M. A. (2001). Molecular phylogeny of the genus *Oryzomys* (Rodentia: Sigmodontinae) based on cytochrome b DNA sequences. Molecular Phylogenetics and Evolution, 18(2), 282–292. https://doi.org/10.1006/mpev.2000.0878

Bradley, R. D., Lack, J. B., Pfau, R. S., Peppers, L. L., Henson, D. D., Stallings, A. O., Hoang, C. N., & Bussche, R. A. V. D. (2012). Genetic and conservation status of a relictual population of the hispid cotton rat (*Sigmodon hispidus eremicus*). The Southwestern Naturalist, 57(3), 231–239. https://doi.org/10.1894/0038-4909-57.3.231

Brito, J., Tinoco, N., Curay, J., Vargas, R., Reyes-Puig, C., Romero, V., & Pardiñas, U. F. J. (2019). Diversidad insospechada en los Andes de ecuador: filogenia del grupo “cinereus” de *Thomasomys* y descripción de una nueva especie (Rodentia, Cricetidae). Mastozoología Neotropical, 26, 308–330. https://doi.org/10.31687/saremMN.19.26.2.0.04

Brito, J., Vaca-Puente, S., Koch, C., & Tinoco, N. (2021). Discovery of the first Amazonian *Thomasomys* (Rodentia, Cricetidae, Sigmodontinae): a new species from the remote Cordilleras del Cóndor and Kutukú in Ecuador. Journal of Mammalogy, 102, 615–635. https://doi.org/10.1093/jmammal/gyaa183

Brito, J. M., Tinoco, N., Chávez, D., Moreno-Cárdenas, P., Batallas, D., & Ojala-Barbour, R. (2017). New species of arboreal rat of the genus *Rhipidomys* (Cricetidae, Sigmodontinae) from Sangay National Park, Ecuador. Neotropical Biodiversity, 3, 65–79. https://doi.org/10.1080/23766808.2017.1292755

de la Sacha, N., Solari, S., & Owen, R. D. (2007). First records of *Monodelphis kunsi* Pine (Didelphimorphia, Didelphidae) from Paraguay, with an evaluation of its distribution. Mastozoología Neotropical, 14, 241–247.

D’Elía, G. (2003). Phylogenetics of Sigmodontinae (Rodentia, Muroidea, Cricetidae), with special reference to the akodont group, and with additional comments on historical biogeography. Cladistics, 19, 307–323. https://doi.org/10.1111/j.1096-0031.2003.tb00375.x

Emmons, L. (1999). Two new species of *Juscelinomys* (Rodentia, Muridae) from Bolivia. American Museum Novitates 3280, 1–15.

García Loaiza, L. M. (2015). Variabilidad genética y estatus taxonómico de especies de *Thomasomys* (Rodentia: Cricetidae) en el páramo de Chingaza, Colombia (Master dissertation). Universidad Nacional de Colombia, Bogotá.

Hanson, J.D. (2008). Molecular phylogenetics of Oryzomyini: does a multigene approach help resolve a systematic conundrum? (Ph.D. dissertation). Texas Tech University.

Kuch, M., Rohland, N., Betancourt, J. L., Latorre, C., Steppan, S., & Poinar, H. N. (2002). Molecular analysis of an 11,700-year-old rodent midden from the Atacama Desert, Chile. Molecular Ecology, 11, 913–924. https://doi.org/10.1046/j.1365-294x.2002.01492.x

Lee, T. E., Ritchie, A. R., Vaca-Puente, S., Brokaw, J. M., Camacho, M. A., & Burneo, S. F. (2015). Small mammals of Guandera Biological Reserve, Carchi Province, Ecuador and comparative Andean small mammal ecology. Occasional papers, Museum of Texas Tech University, 334, 1–17.

Milazzo, M. L., Cajimat, M. N. B., Richter, M. H., Bradley, R. D., & Fulhorst, C. F. (2017). Muleshoe virus and other hantaviruses associated with neotomine or sigmodontine rodents in Texas. Vector Borne Zoonotic Diseases, 17, 720–729. https://doi.org/10.1089/vbz.2017.2108

Pacheco, V., & Ruelas, D. (2023). Systematic revision of *Thomasomys cinereus* (Rodentia: Cricetidae: Sigmodontinae) from northern Peru and southern Ecuador, with descriptions of three new species. Bulletin of the American Museum of Natural History, 461, 71.

Patton, J., & Silva, M. N. F. (1995). A review of the spiny mouse genus *Scolomys* (Rodentia: Muridae: Sigmodontinae) with the description of a new species from the western Amazon of Brazil. Proceedings of the Biological Society of Washington, 108, 319–337.

Percequillo, A. R., Gonçalves, P. R., & de Oliveira, J. A. (2004). The rediscovery of *Rhagomys rufescens* (Thomas, 1886), with a morphological redescription and comments on its systematic relationships based on morphological and molecular (Cytochrome b) characters. Mammalian Biology, 69, 238–257. https://doi.org/10.1078/1616-5047-00140

Rinehart, T. A., Grahn, R. A., & Wichman, H. A. (2005). SINE extinction preceded LINE extinction in sigmodontine rodents: implications for retrotranspositional dynamics and mechanisms. Cytogenet. Genome Research, 110, 416–425. https://doi.org/10.1159/000084974

Rocha, R. G., Ferreira, E., Costa, B. M. A., Martins, I. C. M., Leite, Y. L. R., Costa, L. P., & Fonseca, C. (2011). Small mammals of the mid-Araguaia River in central Brazil, with the description of a new species of climbing rat. Zootaxa, 2789, 1–34. https://doi.org/10.11646/zootaxa.2789.1.1

Ruelas, D., & Pacheco, V. (2021). A new species of *Thomasomys* Coues, 1884 (Rodentia: Sigmodontinae) from the montane forests of northern Peru with comments on the "aureus" group. Revista Peruana de Biologia, 28, e19912. https://doi.org/10.15381/rpb.v28i3.19912

Salazar Bravo, J., Pardiñas, U. F. J., Zeballos, H., & Teta, P. V. (2016). Description of a new tribe of sigmodontine rodents (Cricetidae: Sigmodontinae) with an updated summary of valid tribes and their generic contents. Occasional papers, Museum of Texas Tech University, 338, 1–23.

Salazar-Bravo, J., & Yates, T. L. (2007). A new species of Thomasomys (Cricetidae: Sigmodontinae) from central Bolivia. In D. Kelt, E. P. Lessa, J. Salazar-Bravo, & J. L. Patton (Eds.), The quintessential naturalist honoring the life and legacy of Oliver P. Pearson (pp. 747–774). University of California Press.

Smith, M. F., Kelt, D. A., & Patton, J. L. (2001). Testing models of diversification in mice in the *Abrothrix olivaceus/xanthorhinus* complex in Chile and Argentina. Molecular Ecology, 10, 397–405. https://doi.org/10.1046/j.1365-294X.2001.01183.x

Smith, M. F., & Patton, J. L. (1999). Phylogenetic relationships and the radiation of sigmodontine rodents in South America: evidence from cytochrome b. Journal of Mammalian Evololution, 6, 89–128.

Steppan, S. J., & Schenk, J. J. (2017). Muroid rodent phylogenetics: 900-species tree reveals increasing diversification rates. PLOS ONE, 12, e0183070. https://doi.org/10.1371/journal.pone.0183070

Table S3. Summary of major clades based on the phylogenetic topology from Figure 2, species groups of Pacheco (2015), species of *Thomasomys* included each, and geographic distribution.

Major clades	**Pacheco's (2015) species groups**	**Species included**	**Distribution**
A	Gracilis (part)	*andersoni*, *oreas*, aff. *oreas*, *Thomasomys* sp. 8, *Thomasomys* sp. 9	S Peru, N Bolivia
B	Cinereus (part)	*australis*, *daphne*, *Thomasomys* sp. 3	S Peru, Bolivia
C	Cinereus (part)	*fumeus*, *bombycinus* "Ecuador," *bombycinus* "Colombia," *contradictus* 2, *vulcani*, *Thomasomys* sp. 10	Colombia, Ecuador, N Peru (W Marañón river)
D	Cinereus (part)	*caudivarius*, aff. *caudivarius*, *cinereus*, aff. *cinereus*, *cinnameus* "Ecuador", *cinnameus* "Colombia", *hudsoni*, *lojapiuranus*, *pagaibambensis*, *paramurum*,	Ecuador, N Peru (W Marañón river)

		salazari, *shallqukucha*, *silvestris*, *ucucha*, *Thomasomys* sp. B	
E	Notatus	*notatus*	C Peru (W Marañón river)
F	Aureus (part)	*antoniobracki*, *aureus*, aff. *aureus* "Cajamarca N", aff. *aureus* "Lambayeque-Cajamarca S", *auricularis*, *burneoi*, *nicefori*, *pardignasi*, *praetor*, *princeps*, *pyrrhonotus*, *Thomasomys* sp. C, *Thomasomys* sp. E	Colombia, Ecuador, N Peru (W Marañón river)
G	Aureus (part)	*apeco*, aff. *aureus* "Central" *Thomasomys* sp. 1	Bolivia, C and S Peru (E Marañón river)
H	Macrotis, Incanus (part)	*ladewi*, *macrotis*, aff. *kalinowskii* "Ayacucho", *Thomasomys* sp. F	C Peru (E Marañón river)
I	Incanus (part)	*incanus*, *ischyrus*, aff. *ischyrus*, *kalinowskii*, aff. *kalinowskii* "Pasco", *Thomasomys* sp. 7, *Thomasomys* sp. A	C Peru

J	Baeops	*baeops*, *taczanowskii*	Ecuador, N Peru (W Marañón river)
Unresolved	Gracilis (part), Cinereus (part), Aureus (part)	*gracilis*, *contradictus* 1, *erro*, *onkiro*, *Thomasomys* sp. D, *Thomasomys* sp. 2	

Table S4. Average genetic distance within and among the *Thomasomys* species based on Cytb gene. The percentage of genetic p-distance (below diagonal), along with its standard error (above diagonal), represents the value of base substitutions per site obtained by averaging over all sequence pairs. Abbreviations: In - intraspecific genetic distances. n/c - Not calculated

Taxa	In	1	2	3	4	5	6	7	8	9	10	11	12	13	14	15	16
1. *andersoni*	0.25		1.77	1.76	1.61	1.36	1.73	1.55	1.69	1.67	1.62	1.5	1.58	1.5	1.51	1.55	1.55
2. *antoniobraci*	0.25	17.67		1.29	1.29	0.99	1.01	1.46	1.33	1.57	1.26	1.21	1.37	1.37	1.38	1.3	1.51
3. *apeco*	1.57	18.6	12.91		1.43	1.07	1.46	1.43	1.32	1.43	1.36	1.52	1.4	1.51	1.49	1.47	1.48
4. *aureus*	0.13	15.99	10.96	13.74		1.02	1.35	1.41	1.47	1.65	0.92	1.48	1.48	1.34	1.47	1.38	1.54
5. *aff. aureus*	9.27	15.34	10.28	12.65	11.26		1.08	1.12	1.17	1.42	0.96	1.22	1.25	1.14	1.25	1.28	1.26
6. *auricularis*	1.17	16.03	7.5	13.36	10.03	10.93		1.54	1.63	1.75	1.49	1.34	1.52	1.72	1.57	1.41	1.94
7. *australis*	0.39	15.36	14.02	14.04	13.73	12.61	14.17		1.34	1.51	1.38	1.29	1.46	1.36	1.47	1.35	1.43
8. *baeops*	3.56	18.27	13.16	13.27	14.35	13.52	15.11	12.65		1.46	1.38	1.39	1.5	1.43	1.43	1.32	1.49
9. *bombycinus*	4.72	16.89	15.97	14.69	16.51	17.47	15.79	14.77	15.34		1.59	1.31	1.46	1.42	1.37	1.28	1.25
10. *burneoi*	0.13	15.67	11.06	13.03	6.31	10.61	11.96	13.41	13.78	16.72		1.48	1.44	1.35	1.43	1.39	1.44
11. *caudivarius*	0.15	14.32	11.19	15.63	14.32	13.99	11.66	10.82	14.07	12.61	13.72		1.32	1.2	1.09	1.04	1.41
12. *aff. caudivarius*	1.57	16.01	12.83	14.52	14.34	14.84	13.51	13.95	15.7	14.64	13.64	9.39		1.13	0.66	1.14	1.44
13. *cinereus*	1.48	15.01	12.71	15.39	13	12.8	15.43	13.08	14.44	14.49	12.78	10.83	9.89		1.16	1.11	1.2
14. *aff. cinereus*	0.18	14.71	12.79	14.32	13.97	14.17	13.16	13.49	14.39	13.45	13.17	8.92	4.06	9.35		1.07	1.36
15. *cinnameus*	3.9	16.81	13.16	15.23	13.75	14.72	12.93	13.39	13.73	13.36	14.17	9.37	10.66	10.62	9.99		1.28
16. *contradictus*	8.6	15.91	15.46	15.67	15.97	15.46	17.09	13.85	15.47	12.59	14.01	14.26	14.86	12.41	13.48	14.03	
17. *daphne*	n/c	12.82	12.02	14.01	11.86	11.21	13.19	8.28	12.07	13.23	11.09	11.09	14.66	12.04	12.28	12.13	12.93
18. *erro*	n/c	13.62	13.66	14.72	13.54	13.02	14.6	11.37	14.01	14.79	13.09	10.96	12.9	11	11.75	13.58	13.66
19. *fumeus*	n/c	15.62	14.48	14.93	15.56	14.65	14.76	11.57	16.28	14.2	14.9	12.15	15.25	12.74	13.87	13.82	13.55
20. *gracilis*	0.25	17.31	12.52	16.45	13.73	14.04	14.27	14.19	14.76	15.41	12.58	13.39	14.57	12.88	13.76	14.33	15.76
21. *hudsoni*	0.81	16.39	11.85	13.53	14.96	13.54	12.47	13.81	13.61	14.37	14.36	10.53	11.12	10.1	9.88	10.24	13.74
22. *incanus*	0.93	15.22	12.13	13.16	13.75	13.27	13.02	11.35	11.65	13.47	13.13	10.53	11.8	11.53	11.16	11.65	13.84
23. *ischyrus*	2.22	15.66	11.58	11.98	13.54	12.01	13.71	11.24	11.64	12.63	11.82	9.74	12.95	11.26	11.56	11.49	13.08
24. *aff. ischyrus*	0.54	16.26	12.71	11.95	12.61	12.18	14.39	13.51	11.98	14.62	11.76	11.88	13.47	11.66	12.19	12.34	14.76
25. *katinawskii*	1.22	14	12.43	12.4	13.85	12.41	13.91	11.43	12.4	14.54	12.53	11.73	12.77	11.97	11.53	11.52	13.93
26. *aff. katinawskii*	9.05	16.35	13.44	12.92	14.04	13.17	14.32	13.63	13.25	12.91	13.34	13.26	13.71	12.07	13.16	14.19	13.85
27. *laniger*	0.14	14.94	13.33	13.18	14.6	11.97	14.18	12.54	13.08	13.44	13.71	11.61	12.42	10.8	12.25	12.63	12.29
28. *laniger/urosus*	0.34	15.63	11.09	14.31	13.69	13.69	12.77	13.72	13.85	13.61	13.72	8.54	9.46	6.63	8.41	9.85	13.18
29. *macrotis*	n/c	15.85	13.11	13.85	16.9	12.37	10.96	11.5	14.47	13.21	13.01	13.09	11.42	9.93	12.14	13.11	11.97
30. *maculiger*	8.05	16.76	11.68	14.43	11.62	13.05	11.92	14.99	14.84	17.42	11.06	15.05	15.14	13.83	14.92	14.97	15.16
31. *notatus*	3.8	15.04	14.27	15.66	13.81	14.37	13	15.61	14.61	15.27	13.18	14.3	16.02	15.18	15.03	14.91	16.47
32. *oniscus*	n/c	17.94	15.74	14.65	14.26	14.86	14.87	14.52	15.52	14.71	13.78	12.16	12.61	13.47	12.45	13.11	14.93
33. *orcus*	n/c	14.14	16.59	16.9	16.27	14.32	10.77	14.07	15.6	14.69	14.17	15.29	13.96	12.91	14.11	17.14	13.95
34. *aff. orcus*	n/c	11.96	16.65	17.2	16.32	14.46	11.11	15.75	16.19	15	14.41	14.97	16.22	13.75	15.74	15.03	14.65
35. *pagabambaensis*	0.38	15.82	13.82	15.25	13.81	13.78	15.04	13.98	14.57	15.16	13.84	11.53	11.34	6.9	9.82	12	14.22
36. *paramorum*	0.67	18.46	14.83	15.86	15.12	15.17	14.92	14	17.29	14.72	14.83	10.08	10.98	10.71	10.67	11.61	14
37. *pardignoni*	0.38	15.17	9.7	13.62	5.06	10.61	10.11	13.49	13.65	15.21	5.52	13.08	13.49	12.15	13.09	13.37	15.16
38. *praetor*	0.5	15.83	9.69	13.17	11.23	11.34	10.23	13.08	13.68	15.86	12.65	12.72	15.17	12.54	15.09	13.45	14.88
39. *princeps*	n/c	15.3	10.95	13.36	5.81	11.54	10.07	14.39	14.32	16.96	5.23	13.19	13.5	13.11	13.32	14.25	15.14
40. *pyrrhonotus*	3.17	17.47	11.53	13.73	11.66	13.21	9.79	14.65	15.19	15.14	11.87	14.6	14.9	13.97	14.16	14.46	15.65
41. *salazari*	0	17.06	13.46	13.16	14.11	15.08	14.22	13.33	13.38	13.15	14.01	9.01	11.26	11.39	10.28	11.62	14.5
42. *shallquicha*	0.46	15.41	13.43	15.62	14.64	14.5	14.89	13.77	14.29	14.82	14.27	10.11	11.11	7.67	10.2	11.71	14.31
43. *silvestris*	0.52	14.5	13.37	14.89	14.23	13.94	13.83	11.23	13.87	12.4	13.55	9.01	11.24	9.18	9.4	9.37	13.93
44. *taczanowskii*	2.05	17.14	14.2	13.2	13.6	12.86	14.27	12.69	6.33	17.51	12.4	14.73	15.6	14.58	15.01	14.97	16.35
45. *ucucha*	0	16.29	12.91	14.2	11.1	13.94	12.9	12.57	14.34	11.37	11.39	9.23	11.09	9.54	10.51	9.29	13.11
46. *vulcani*	0.79	16.78	12.55	14.79	15.03	14.34	13.12	13.11	14.51	11.39	15.29	11.17	12.69	11.8	11.91	12.75	11.59
47. sp. 1	0.76	16.48	12.98	12.56	14.09	11.9	14.28	13.24	13.13	15.81	15.33	14.3	16.44	13.83	15.15	14.88	15.8
48. sp. 2	n/c	17.03	13.54	13.98	13.49	13.33	11.13	12.67	14.17	14.92	13.32	14.8	15.2	15.01	13.91	13.57	14.8
49. sp. 3	1.66	15.74	13.94	15.29	13.62	13.57	14.72	8.14	14.06	16.5	13.09	12.62	15.4	14.57	14.28	13.89	14.14
50. sp. 4	3.16	17.53	17.14	17.11	17.62	17.26	16.42	15.77	16.52	17.61	18.14	16.32	18.92	17.58	17.86	18.12	17.21
51. sp. 7	0.12	15.59	12.59	11.78	12.89	12.64	14.44	12.15	11.73	12.94	11.77	12.32	12.69	12.12	12.36	12.55	13.79
52. sp. 8	0.71	13.36	13.03	17.28	13.96	13.65	14.83	15.06	14.88	16	13.22	14.43	15.56	13.83	14.59	14.82	16.39
53. sp. 9	0.13	13.64	14.86	17.29	15.02	14.35	15.7	15.4	14.18	16.1	13.59	14.15	15.04	12.54	14.37	14.26	15.93
54. sp. 10	0.38	17.41	13.83	14.72	14.26	14.88	13.62	10.75	15.32	12.55	14.22	10.88	15.29	14.14	13.7	13.41	13.9
55. sp. A	n/c	15.92	13.07	14.21	13.81	12.95	14.73	12.78	13.09	14.79	13.51	13.34	13.6	12.63	13.75	13.3	14.71
56. sp. B	n/c	17.27	15.41	17.81	16.84	15.87	14.78	14.05	15.65	14.03	16.78	11.23	13.23	10.82	13.03	11.42	15.92
57. sp. C	0.25	16.17	13.37	15.72	8.58	11.82	7.46	15.65	13.07	17.28	5.47	16.2	14.85	14.93	15.11	18.27	16.23
58. sp. D	n/c	15.92	13.36	14.43	14	13.65	13.32	11.95	12.73	14.34	12.59	12.27	14.02	10.02	12.41	11.89	13.15
59. sp. E	1.11	15.58	10.53	12.96	6.78	10.46	10.63	13.67	13.39	15.48	3.31	12.21	13.39	12.7	13.36	14.5	14.09
60. sp. F	n/c	17.13	11.62	12.82	13.33	11.97	11.96	13.05	12.37	13.37	12.54	11.26	12.02	11.15	10.32	11.32	13.59

Taxa	17	18	19	20	21	22	23	24	25	26	27	28	29	30	31	32	33
1. *andersoni*	1.43	1.46	1.57	1.67	1.66	1.5	1.5	1.61	1.42	1.54	1.57	1.57	2.15	1.46	1.42	1.73	2.03
2. *antoniabrachi*	1.29	1.59	1.49	1.33	1.31	1.24	1.17	1.36	1.33	1.32	1.42	1.25	1.88	1.01	1.33	1.56	2.25
3. *apeco*	1.4	1.52	1.6	1.63	1.43	1.37	1.22	1.26	1.29	1.22	1.38	1.43	1.86	1.26	1.44	1.46	2.24
4. *aureus*	1.34	1.39	1.54	1.42	1.57	1.43	1.38	1.39	1.45	1.32	1.52	1.47	2.31	1.02	1.43	1.45	2.35
5. *aff. aureus*	1.04	1.17	1.26	1.23	1.24	1.15	1.01	1.06	1.13	1.07	1.05	1.21	1.43	0.95	1.15	1.25	1.69
6. *auriculatus*	1.53	1.65	1.65	1.71	1.49	1.53	1.48	1.62	1.59	1.53	1.68	1.5	2.34	1.23	1.39	1.6	2.61
7. *australis*	1.13	1.29	1.31	1.45	1.46	1.27	1.18	1.42	1.22	1.32	1.39	1.46	1.8	1.34	1.49	1.51	1.99
8. *bangs*	1.27	1.46	1.56	1.52	1.38	1.23	1.14	1.26	1.27	1.27	1.37	1.38	2.01	1.25	1.38	1.5	2.16
9. *bombycinus*	1.4	1.54	1.49	1.51	1.46	1.38	1.24	1.42	1.41	1.17	1.42	1.39	1.73	1.48	1.4	1.51	1.99
10. *burmai*	1.25	1.38	1.51	1.33	1.52	1.37	1.26	1.26	1.27	1.3	1.44	1.43	2.03	1.03	1.3	1.45	2.18
11. *cauthuriu*	1.28	1.28	1.36	1.38	1.2	1.19	1.11	1.28	1.28	1.28	1.33	1.03	1.96	1.32	1.36	1.32	2.17
12. *aff. cauthuriu*	1.47	1.43	1.52	1.4	1.24	1.3	1.35	1.4	1.29	1.29	1.36	1.14	1.66	1.32	1.48	1.36	2.04
13. *cinereus*	1.3	1.21	1.32	1.33	1.12	1.22	1.17	1.23	1.27	1.19	1.29	0.85	1.53	1.19	1.47	1.41	1.85
14. *aff. cinereus*	1.37	1.35	1.48	1.42	1.21	1.3	1.32	1.37	1.31	1.35	1.47	1.05	1.87	1.35	1.43	1.42	2.16
15. *cinnameus*	1.28	1.43	1.4	1.38	1.09	1.23	1.16	1.25	1.24	1.31	1.4	1.03	1.76	1.26	1.44	1.42	2.27
16. *contradictus*	1.37	1.4	1.38	1.55	1.35	1.33	1.23	1.43	1.36	1.24	1.24	1.32	1.55	1.24	1.52	1.46	1.79
17. *daphne*		1.31	1.21	1.27	1.37	1.11	1.12	1.19	1.18	1.22	1.32	1.29	1.69	1.12	1.22	1.35	1.69
18. *erro*	11.32		1.48	1.39	1.41	1.28	1.27	1.34	1.24	1.23	1.39	1.37	1.76	1.32	1.45	1.41	1.86
19. *fumeus*	10.52	13.28		1.5	1.46	1.48	1.33	1.53	1.38	1.45	1.53	1.45	1.84	1.29	1.56	1.71	2.15
20. *gracilis*	12.44	13.35	15.22		1.4	1.3	1.21	1.27	1.19	1.25	1.4	1.4	1.76	1.34	1.29	1.51	1.96
21. *hudsoni*	12.43	12.03	13.08	13.28		1.3	1.14	1.29	1.27	1.29	1.43	0.98	1.88	1.28	1.4	1.46	2
22. *incanus*	9.56	11.62	13.83	12.51	11.45		0.88	0.95	0.96	1.09	1.15	1.17	1.46	1.18	1.29	1.42	1.94
23. *izshyra*	9.63	11.63	12.47	12.28	10.79	7.57		0.84	0.85	1.04	1.03	1.19	1.45	1.12	1.18	1.29	1.79
24. *aff. izshyra*	10.41	12.64	14.64	12.75	11.45	7.97	6.25		0.89	1.15	1.17	1.25	1.62	1.16	1.28	1.39	2.11
25. *kalmanzhi*	10.56	11.31	13.43	11.45	11.44	7.69	6.88	6.76		1.12	1.21	1.19	1.49	1.17	1.25	1.34	1.94
26. *aff. kalmanzhi*	12.18	12.12	14.81	13.16	13.07	10.93	10.52	11.53	11.29		0.95	1.29	1.45	1.14	1.33	1.33	1.77
27. *ladeni*	11.79	12.04	13.31	13.49	11.97	9.82	8.67	9.93	10.69	9.43		1.41	1.35	1.21	1.32	1.41	1.81
28. *lagapurana*	11.76	12.48	13.49	13.98	8.24	11.42	11.87	12.33	11.4	13.65	12.57		1.79	1.21	1.37	1.38	2.33
29. *macroris*	9.42	11.4	11.77	12.25	13.05	8.81	8.65	9.75	9.74	11.33	7.12	12.19		1.4	1.89	1.88	2.03
30. *nicefori*	12.25	14.85	14.21	15.32	14.88	13.26	12.92	13.08	13.34	14.24	13.27	14.66	11.47		1.24	1.37	1.8
31. *notatus*	11.85	14.67	15.97	13.53	14.3	12.8	12.64	13.27	12.78	15.35	12.87	14.6	14.5	15.03		1.28	1.93
32. *ontiro*	12.39	12.75	16.39	15.81	13.28	12.61	11.82	12.93	12.86	14.11	12.06	12.96	12.51	16.38	13.26		2.06
33. *oreas*	10.01	12.34	14.83	13.9	13.45	13.38	12.25	14.45	13.64	13.88	11.6	17.01	14.33	15.88	14.02	14.46	
34. *aff. oreas*	7.34	12.36	15.04	15.22	14.56	15.11	13.48	14.51	14.24	14.67	13.44	15.5	16.45	16.48	13.57	13.86	8.83
35. *pagatbambanzis*	12.19	12.53	14.2	15.17	10.56	12.55	12.48	12.72	13.21	14.03	14.4	5	13.39	14.95	14.95	12.81	15.4
36. *paramorsus*	13.48	13.8	13.66	15.06	11.63	13.85	13.09	13.97	13.39	14.1	13.99	9.69	13.49	16.85	17.31	15.64	15.88
37. *pardignasi*	12.3	12.85	15.75	13.22	13.83	14.53	11.67	12.49	13.27	13.46	12.6	13.01	14.4	11.06	13.65	13.55	13.95
38. *pinetar*	11.75	14.35	15.19	13.86	13.75	13.04	12.06	12.38	13.26	13.07	11.25	13.72	12.38	13.13	14.84	15.72	16.33
39. *princeps*	11.64	13.48	14.29	13.81	14.52	14.26	13.07	13.11	13.5	14.14	13.2	14.53	13.95	10.32	13.24	14.33	14.77
40. *pyrrhonota*	12.16	14.31	15.39	14.38	13.3	13.08	12.29	13.26	14.15	13.51	12.78	14.09	11.38	12.62	12.74	14.08	14.48
41. *salacan*	13.78	13.13	12.06	13.95	10.25	12.68	11.63	13.28	12.14	13.66	13.81	8.95	12.55	16.2	16.02	13.91	15.21
42. *shallgukucha*	12.79	12.13	13.62	15.39	10.24	13.8	12.94	13.57	12.46	14.57	13.38	5.1	12.34	15.36	15.86	13.5	17.21
43. *sihezrus*	10.53	10.68	12.78	13.88	10.51	11.32	10.35	12.47	11.96	13.61	12.54	9.58	10.34	14.28	14.88	10.69	15.91
44. *taczanowzki*	12.44	13.16	15.34	14.58	14.96	12.5	11.24	11.68	11.51	13.25	13.18	16.02	14.41	14.15	14.33	15.95	14.41
45. *vaucha*	11.12	11.39	12.77	13.28	11.66	11.72	11.79	11.98	12.53	13.98	12.35	9.06	10.82	13.86	13.42	11.21	14.89
46. *volcomi*	10.61	14	10.78	13.51	11.93	12.31	12	12.87	12.6	12.47	12.19	10.26	11.77	14.33	14.33	14.69	14.72
47. sp. 1	12.57	13.95	13.13	13.76	15.68	13.5	12.88	13.06	12.77	13.58	12.96	14.56	13.25	16.16	12.82	13.59	14.91
48. sp. 2	12.56	14.93	12.2	16.29	15.11	13.57	13.44	14.96	12.46	13.1	12.16	14.68	13.09	14.85	14.25	15.17	16.13
49. sp. 3	6.5	12.96	13.89	14.67	14.29	12.38	12.37	13.82	13.17	15.43	14.55	14.59	13.63	14.49	15.4	14.64	16.33
50. sp. 4	14.58	17.26	16.95	17	17.25	17.14	16.24	16.88	16.18	16.45	16.51	17.15	17.47	18.47	17.81	18.08	19.83
51. sp. 7	9.96	11.59	14.85	12.07	12.59	8.69	7.72	7.85	7.14	10.72	10.99	12.19	10.37	13.73	13.17	12.96	15.29
52. sp. 8	7.56	14.64	14.21	13.89	13.66	14.08	13.92	14.33	14.13	15.34	15.36	13.71	13.2	15.97	13.44	16.01	9.82
53. sp. 9	9.67	12.94	14.25	13.96	14.15	13.64	13.31	14.1	13.35	14.54	13.48	13.6	14.68	16.06	13.39	15.1	8.04
54. sp. 10	11.37	14.73	6.04	13.26	13.37	13.29	12.03	12.59	13.72	13.66	14.57	12.63	14.55	15.81	15.46	13.99	15.34
55. sp. A	11.37	12.84	14.44	12.72	12.6	9.57	8.73	9.19	8.96	12.29	10.14	13.71	10.59	13.9	14.23	14.4	13.62
56. sp. B	13.19	12.53	13.98	13.76	12.59	12.67	12.05	13.68	13.27	15.49	13.26	12	11.85	15.81	16.46	14.22	15.32
57. sp. C	10.79	13.56	15.94	13.4	17.02	15.34	14.47	15.04	16.02	14.17	13.31	16.87	14.45	11.06	15.22	15.78	14.71
58. sp. D	10.52	12.98	12.72	13.74	12.8	12.64	11.79	13.22	11.16	13.77	13.13	11.43	10.56	14.57	13.45	12.88	12.39
59. sp. E	11.72	12.77	14.25	11.8	13.64	12.43	11.55	11.49	11.56	12.66	12.15	13.34	10.96	10.52	12.45	14	13.72
60. sp. F	11.99	11.15	13.82	11.62	10.87	10.09	9.1	9.9	10.66	8.55	8.78	12.14	9.63	13.06	13.72	13.29	14.17

Taxa	34	35	36	37	38	39	40	41	42	43	44	45	46	47	48	49	50
1. *anderzoni*	1.83	1.6	1.81	1.54	1.61	1.56	1.67	1.68	1.63	1.54	1.66	1.71	1.71	1.67	1.59	1.55	1.67
2. *antoniobrachi*	2.16	1.5	1.46	1.21	1.21	1.28	1.21	1.43	1.54	1.38	1.47	1.38	1.33	1.4	1.42	1.39	1.65
3. *apaco*	2.17	1.56	1.54	1.4	1.33	1.36	1.34	1.43	1.6	1.41	1.28	1.42	1.47	1.36	1.42	1.51	1.61
4. *aureus*	2.24	1.48	1.48	0.82	1.29	0.88	1.18	1.55	1.58	1.45	1.41	1.3	1.53	1.48	1.44	1.38	1.72
5. *aff. aureus*	1.69	1.23	1.29	0.97	1.01	1.04	1.1	1.37	1.32	1.23	1.11	1.2	1.21	1.05	1.13	1.21	1.47
6. *auriculatis*	2.02	1.76	1.57	1.35	1.28	1.3	1.21	1.63	1.75	1.6	1.55	1.46	1.45	1.6	1.33	1.64	1.76
7. *australis*	2.1	1.45	1.54	1.33	1.44	1.31	1.48	1.44	1.47	1.32	1.3	1.39	1.45	1.4	1.3	1.04	1.58
8. *bosqui*	2.15	1.43	1.71	1.41	1.42	1.5	1.43	1.34	1.46	1.38	0.78	1.4	1.4	1.39	1.41	1.41	1.56
9. *bombycinus*	1.94	1.51	1.48	1.45	1.61	1.64	1.47	1.4	1.52	1.3	1.56	1.29	1.28	1.53	1.5	1.56	1.61
10. *burmei*	2.17	1.47	1.48	0.83	1.39	0.82	1.23	1.51	1.48	1.39	1.29	1.28	1.54	1.54	1.45	1.37	1.71
11. *cavifrons*	2.05	1.27	1.16	1.39	1.42	1.47	1.45	1.16	1.21	1.18	1.5	1.15	1.23	1.49	1.53	1.36	1.55
12. *aff. cavifrons*	2.29	1.28	1.27	1.41	1.58	1.37	1.42	1.24	1.31	1.27	1.53	1.26	1.38	1.55	1.53	1.55	1.79
13. *cinereus*	1.92	0.93	1.21	1.31	1.32	1.39	1.36	1.31	1	1.12	1.47	1.18	1.32	1.45	1.56	1.45	1.73
14. *aff. cinereus*	2.34	1.21	1.27	1.44	1.61	1.39	1.41	1.19	1.25	1.14	1.52	1.22	1.4	1.52	1.42	1.47	1.75
15. *cinnameus*	1.96	1.24	1.16	1.35	1.38	1.42	1.39	1.2	1.22	1.02	1.46	1.01	1.31	1.48	1.41	1.35	1.69
16. *contradictus*	1.76	1.39	1.44	1.46	1.43	1.52	1.46	1.43	1.43	1.39	1.54	1.39	1.21	1.52	1.42	1.41	1.54
17. *daphne*	1.41	1.41	1.5	1.31	1.28	1.29	1.25	1.46	1.44	1.23	1.28	1.33	1.34	1.38	1.39	0.88	1.47
18. *erro*	1.97	1.4	1.45	1.39	1.52	1.46	1.41	1.49	1.39	1.28	1.41	1.27	1.49	1.45	1.52	1.44	1.71
19. *fumeus*	2.09	1.53	1.41	1.5	1.52	1.48	1.5	1.39	1.5	1.41	1.5	1.41	1.28	1.38	1.41	1.43	1.63
20. *gracilis*	2.09	1.5	1.43	1.35	1.42	1.4	1.4	1.46	1.58	1.4	1.48	1.38	1.4	1.41	1.61	1.51	1.74
21. *hidcoti*	1.99	1.24	1.3	1.44	1.51	1.54	1.35	1.17	1.2	1.26	1.55	1.3	1.3	1.62	1.59	1.51	1.63
22. *incanus*	2.05	1.3	1.45	1.44	1.41	1.46	1.32	1.37	1.4	1.25	1.36	1.29	1.29	1.39	1.47	1.29	1.6
23. *izabyria*	1.87	1.29	1.39	1.24	1.28	1.37	1.19	1.25	1.34	1.16	1.17	1.26	1.28	1.32	1.36	1.29	1.52
24. *aff. izabyria*	2.08	1.35	1.47	1.34	1.36	1.44	1.27	1.39	1.47	1.31	1.22	1.31	1.37	1.38	1.54	1.39	1.63
25. *kalinowskii*	1.99	1.35	1.39	1.4	1.42	1.37	1.34	1.29	1.32	1.26	1.26	1.32	1.33	1.38	1.35	1.35	1.54
26. *aff. kalinowskii*	1.76	1.39	1.31	1.31	1.26	1.33	1.26	1.38	1.45	1.34	1.27	1.36	1.18	1.26	1.31	1.45	1.5
27. *ladew*	1.99	1.67	1.54	1.4	1.26	1.39	1.33	1.53	1.53	1.41	1.37	1.38	1.36	1.36	1.4	1.52	1.65
28. *lagopiranus*	2.07	0.74	1.15	1.38	1.41	1.55	1.38	1.13	0.81	1.12	1.37	1.18	1.2	1.48	1.54	1.43	1.62
29. *macrotis*	2.24	1.95	1.98	2.05	1.77	1.99	1.63	1.82	1.8	1.67	1.96	1.77	1.75	1.83	1.92	1.93	2.05
30. *nicefori*	1.84	1.32	1.45	0.94	1.2	0.93	1.04	1.4	1.36	1.22	1.22	1.23	1.26	1.39	1.32	1.27	1.56
31. *notatus*	1.8	1.47	1.58	1.35	1.42	1.31	1.22	1.53	1.51	1.41	1.4	1.31	1.37	1.28	1.39	1.43	1.61
32. *oaxacae*	1.98	1.4	1.62	1.39	1.58	1.5	1.39	1.47	1.45	1.27	1.53	1.29	1.58	1.4	1.57	1.48	1.7
33. *oreas*	1.58	2.17	2.26	2.04	2.3	2.15	1.9	2.13	2.31	2.17	2.04	2.16	2.25	2.11	2.13	2.14	2.44
34. *aff. oreas*		1.89	2.33	2.09	2.14	2.02	1.9	2.34	2.06	1.97	2.05	2.12	2.24	2.01	1.98	2.14	1.94
35. *paganibenitus*	13.26		1.35	1.38	1.5	1.61	1.53	1.25	0.9	1.18	1.52	1.24	1.4	1.57	1.62	1.51	1.61
36. *paramorum*	16.84	12.34		1.42	1.58	1.53	1.48	1.28	1.28	1.3	1.73	1.21	1.35	1.55	1.49	1.57	1.85
37. *pardignasi*	14.49	12.42	15.1		1.32	0.87	1.14	1.47	1.41	1.36	1.33	1.2	1.42	1.47	1.46	1.39	1.67
38. *praetor*	14.94	14.65	15.83	11.59		1.41	1.22	1.57	1.6	1.41	1.36	1.3	1.43	1.36	1.43	1.42	1.59
39. *princeps*	14.35	15.38	15.12	5.62	11.85		1.18	1.63	1.55	1.44	1.38	1.3	1.46	1.5	1.46	1.48	1.68
40. *pyrrhonotus*	14.83	15.21	15.88	11.14	12.17	11.43		1.44	1.51	1.36	1.48	1.29	1.51	1.43	1.3	1.51	1.69
41. *salazari*	18.06	10.57	11.75	13.33	15	14.52	14.62		1.16	1.3	1.45	1.22	1.46	1.49	1.48	1.6	1.59
42. *shallqahuacha*	14.9	6.26	11.02	12.94	15.44	14.42	15.14	9.19		1.24	1.59	1.24	1.35	1.59	1.55	1.62	1.63
43. *silvestris*	13.64	10.01	11.4	12.88	12.85	13.65	13.39	11.22	10.19		1.43	0.91	1.43	1.41	1.46	1.26	1.61
44. *tacazanowskii*	15.21	15.38	17.59	12.88	13.35	13.34	16.35	14.8	15.79	13.75		1.42	1.47	1.35	1.35	1.39	1.41
45. *venefica*	15.12	10.01	11.13	10.15	12.11	11.11	13.11	9.88	9.58	6.69	14.27		1.34	1.42	1.39	1.33	1.63
46. *vulcani*	15.92	12.05	12.32	13.98	13.45	13.98	15.97	13.36	11.93	12.97	15.18	12.18		1.52	1.48	1.34	1.64
47. sp. 1	14.34	15.46	15.04	14.36	12.85	14.63	14.83	14.18	15.06	13.45	12.52	13.41	14.4		1.38	1.54	1.71
48. sp. 2	15.01	15.55	14.53	14.43	14.08	14.42	13.34	13.45	14.63	13.75	14.09	13.28	14.03	13.67		1.47	1.65
49. sp. 3	17.01	14.95	15.91	13.57	13.12	14.65	16.13	15.41	15.61	12.33	14.17	12.71	12.87	15.15	14.86		1.6
50. sp. 4	15.2	16.57	18.92	17.64	16.11	17.97	18.33	16.63	16.18	15.8	15.34	15.89	15.57	17.65	17.07	16.51	
51. sp. 7	14.59	12.44	13.24	12.91	13.04	12.55	13.38	12.56	12.8	11.87	11.26	12.2	11.91	12.59	14.23	13.82	17.32
52. sp. 8	6.74	13.94	16.21	14.17	14.24	13.2	13.45	16.6	14.78	14.28	15.03	13.64	14.54	15.84	15.91	16.27	16.77
53. sp. 9	6.82	13.79	14.79	14.26	14.48	13.48	14.17	15.17	13.73	13.14	14.19	11.99	14.33	14.19	15.33	16.85	18.03
54. sp. 10	17.11	13.7	13.12	14.91	14.75	14.27	15.51	11.28	14.02	12.47	16.39	11.89	10.59	13.48	13.2	13.46	15.27
55. sp. A	12.99	12.35	14.61	12.98	11.89	13.77	15.26	15.03	14.25	11.98	11.9	12.3	12.16	14.79	14.92	13.52	15.55
56. sp. B	14.08	12.31	14.39	14.81	13.97	15.19	15.94	12.34	12.91	6.49	15.9	8.47	13.66	17.78	14.82	14.55	16.67
57. sp. C	15.21	16.84	16.81	6.95	12.19	5.25	12.34	14.9	17.32	15.15	12.47	14.13	15.94	14.85	13.67	15.3	18.91
58. sp. D	14.21	13.29	14.01	13.62	13.55	12.19	15.02	12.25	13.28	12.64	12.86	12	12.49	13.07	13.43	14.15	17.28
59. sp. E	14.28	13.67	13.95	6.2	11.96	5.94	11.36	12.75	13.7	13.56	11.74	10.9	15.05	14.11	12.68	13.99	17.11
60. sp. F	15.08	11.84	14	11.39	11.42	13	12.45	11.27	12.15	12.77	12.14	11.35	11.9	12.83	12.59	15.37	15.51

Taxa	51	52	53	54	55	56	57	58	59	60
1. *andersoni*	1.59	1.46	1.48	1.69	1.57	1.77	2.14	1.61	1.58	1.72
2. *antoniobraccii*	1.41	1.36	1.49	1.44	1.35	1.53	2.02	1.39	1.21	1.27
3. *apeco*	1.28	1.58	1.62	1.5	1.42	1.67	2.12	1.51	1.32	1.31
4. *aurea*	1.38	1.48	1.56	1.45	1.46	1.69	1.49	1.44	0.91	1.48
5. *aff. aurea*	1.13	1.2	1.24	1.27	1.14	1.32	1.42	1.21	0.9	1.07
6. *auricularis*	1.62	1.67	1.7	1.5	1.65	1.77	1.72	1.68	1.35	1.47
7. *australis*	1.36	1.53	1.57	1.23	1.4	1.58	2.15	1.44	1.34	1.37
8. *bicaps*	1.25	1.45	1.35	1.46	1.36	1.55	1.91	1.32	1.35	1.27
9. *bombycina*	1.39	1.59	1.64	1.35	1.47	1.42	2.11	1.45	1.51	1.38
10. *bornaui*	1.3	1.39	1.45	1.52	1.43	1.69	1.23	1.35	0.6	1.35
11. *cavalvaria*	1.41	1.49	1.46	1.23	1.43	1.48	2.36	1.34	1.35	1.29
12. *aff. cavalvaria*	1.32	1.55	1.53	1.57	1.46	1.55	2.02	1.45	1.41	1.32
13. *cinerea*	1.33	1.36	1.32	1.41	1.33	1.25	2.08	1.17	1.31	1.29
14. *aff. cinerea*	1.42	1.43	1.48	1.44	1.54	1.54	2.2	1.36	1.4	1.29
15. *cinnamea*	1.33	1.45	1.41	1.35	1.36	1.29	2.23	1.23	1.42	1.25
16. *contradicta*	1.43	1.6	1.59	1.42	1.46	1.49	1.97	1.32	1.45	1.37
17. *daphne*	1.25	1.03	1.17	1.28	1.33	1.49	1.74	1.25	1.25	1.32
18. *erio*	1.29	1.47	1.38	1.51	1.41	1.46	1.97	1.45	1.3	1.3
19. *fumea*	1.53	1.55	1.55	0.89	1.48	1.61	2.24	1.39	1.42	1.48
20. *gracilis*	1.3	1.38	1.35	1.39	1.29	1.45	1.94	1.41	1.25	1.28
21. *hudsoni*	1.41	1.39	1.39	1.43	1.39	1.42	2.33	1.44	1.43	1.23
22. *incana*	1.07	1.39	1.38	1.39	1.18	1.42	2.12	1.34	1.29	1.15
23. *ischyra*	0.98	1.31	1.31	1.31	1.03	1.29	2.04	1.23	1.19	1.11
24. *aff. ischyra*	1	1.4	1.42	1.4	1.1	1.48	2.14	1.39	1.25	1.2
25. *kalinowskii*	0.88	1.39	1.37	1.41	1.06	1.33	2.17	1.24	1.17	1.24
26. *aff. kalinowskii*	1.05	1.38	1.34	1.33	1.23	1.43	1.75	1.31	1.17	0.92
27. *ladewi*	1.22	1.58	1.47	1.6	1.2	1.52	2.01	1.44	1.33	1.16
28. *lojaptorima*	1.27	1.4	1.45	1.31	1.41	1.37	2.31	1.31	1.37	1.37
29. *macrotis*	1.62	1.93	2.04	2.01	1.68	1.79	2.09	1.72	1.64	1.57
30. *nicefori*	1.2	1.33	1.33	1.36	1.22	1.35	1.37	1.28	0.94	1.21
31. *nitidus*	1.31	1.32	1.34	1.48	1.38	1.64	2.01	1.31	1.23	1.36
32. *ontiveros*	1.42	1.6	1.58	1.5	1.57	1.58	2.25	1.37	1.4	1.45
33. *orea*	2.15	1.67	1.48	2.2	1.98	2.03	2.13	1.96	1.98	2.12
34. *aff. orea*	2.04	1.28	1.32	2.21	1.96	2	2.15	2.04	2.05	2.13
35. *pagambambaea*	1.4	1.45	1.46	1.4	1.37	1.41	2.34	1.43	1.44	1.4
36. *parmorum*	1.47	1.66	1.59	1.35	1.56	1.6	2.29	1.5	1.4	1.5
37. *pardinasi*	1.33	1.45	1.45	1.51	1.35	1.56	1.4	1.42	0.85	1.28
38. *pinetor*	1.45	1.44	1.5	1.5	1.3	1.59	1.87	1.45	1.3	1.24
39. *principe*	1.37	1.39	1.44	1.53	1.43	1.58	1.16	1.31	0.83	1.43
40. *pyrrhonota*	1.32	1.34	1.42	1.48	1.46	1.54	1.69	1.44	1.12	1.28
41. *salazari*	1.33	1.58	1.47	1.3	1.51	1.45	2.08	1.33	1.35	1.37
42. *shallqukucha*	1.39	1.5	1.46	1.5	1.49	1.54	2.3	1.5	1.44	1.38
43. *silvatris*	1.3	1.49	1.4	1.39	1.34	0.97	2.15	1.38	1.38	1.42
44. *taczanowskii*	1.24	1.45	1.4	1.57	1.28	1.57	1.73	1.38	1.19	1.26
45. *ucucha*	1.36	1.43	1.34	1.34	1.31	1.13	2.08	1.31	1.21	1.27
46. *vulcani*	1.32	1.55	1.56	1.29	1.32	1.55	2.25	1.42	1.45	1.34
47. sp. 1	1.37	1.58	1.5	1.4	1.55	1.77	2.13	1.4	1.4	1.39
48. sp. 2	1.5	1.59	1.52	1.47	1.5	1.53	2.01	1.38	1.4	1.39
49. sp. 3	1.46	1.56	1.63	1.4	1.41	1.47	2.1	1.48	1.41	1.56
50. sp. 4	1.66	1.58	1.66	1.47	1.5	1.74	2.23	1.62	1.56	1.56
51. sp. 7		1.4	1.36	1.55	1.11	1.51	2.01	1.44	1.23	1.28
52. sp. 8	13.27		0.9	1.58	1.41	1.64	1.88	1.41	1.34	1.38
53. sp. 9	12.94	6.42		1.54	1.33	1.6	1.98	1.48	1.43	1.44
54. sp. 10	14.54	15.16	15.1		1.53	1.51	2.14	1.46	1.4	1.49
55. sp. A	8.76	13.46	12.68	15.06		1.46	1.97	1.45	1.26	1.28
56. sp. B	14.56	15.81	14.86	13.52	12.61		2.07	1.53	1.57	1.57
57. sp. C	14.49	12.59	14.33	15.69	12.9	15.47		1.97	1.15	1.88
58. sp. D	12.86	13.23	13.43	13.87	13.53	14.16	14.04		1.33	1.31
59. sp. E	11.28	12.94	13.81	13.75	12.04	15.71	5.66	13.18		1.28
60. sp. F	11.46	13.97	14.1	13.84	11.61	14.11	12.79	11.77	12.04	

Table S5. Summary of the results of species delimitation methods used in this study.

Taxa	ABGD	ASAP	PTP	sGMYC	mGMYC
Thomasomys andersoni	1	1	1	1	1
Thomasomys antoniobracki	1	1	1	1	1
Thomasomys apeco	2	2	2	2	2
Thomasomys aureus	1	1	1	1	1
Thomasomys aff. *aureus*	5	5	5	5	5
Thomasomys auricularis	1	1	1	1	1
Thomasomys australis	1	1	1	1	1
Thomasomys baeops	3	3	3	3	3
Thomasomys bombycinus	2	2	2	2	2
Thomasomys burneoi	1	1	1	1	1
Thomasomys caudivarius	1	1	1	1	1
Thomasomys aff. *caudivarius*	1	1	2	2	2
Thomasomys cinereus	1	1	1	5	6
Thomasomys aff. *cinereus*	1	1	1	1	1
Thomasomys cinnameus	2	2	2	2	2
Thomasomys contradictus	2	2	2	2	2
Thomasomys daphne	1	1	1	1	1
Thomasomys erro	1	1	1	1	1
Thomasomys fumeus	1	1	1	1	1
Thomasomys gracilis	1	1	1	1	1
Thomasomys hudsoni	1	1	1	2	2

Thomasomys incanus	1	1	1	1	1
Thomasomys ischyrus	2	3	3	3	3
Thomasomys aff. *ischyrus*	1	1	1	1	1
Thomasomys kalinowskii	2	2	2	2	3
Thomasomys aff. *kalinowskii*	2	2	2	2	2
Thomasomys ladewi	1	1	1	1	1
Thomasomys lojapiuranus	1	1	1	1	1
Thomasomys macrotis	1	1	1	1	1
Thomasomys nicefori	3	3	3	3	3
Thomasomys notatus	3	3	3	3	3
Thomasomys onkiro	1	1	1	1	1
Thomasomys oreas	1	1	1	1	1
Thomasomys aff. *oreas*	1	1	1	1	1
Thomasomys pagaibambensis	1	1	1	1	1
Thomasomys paramorum	1	1	1	1	1
Thomasomys pardignasi	1	1	1	1	1
Thomasomys praetor	1	1	1	1	1
Thomasomys princeps	1	1	1	1	1
Thomasomys pyrrhonotus	2	2	2	2	2
Thomasomys salazari	1	1	1	1	1
Thomasomys shallqukucha	1	1	1	1	1
Thomasomys silvestris	1	1	1	1	1
Thomasomys taczanowskii	4	4	4	6	7
Thomasomys ucucha	1	1	1	1	1

Thomasomys vulcani	1	1	1	1	1
Thomasomys sp. 1 (Pacheco 2003)	1	1	1	1	1
Thomasomys sp. 2 (Pacheco 2003)	1	1	1	1	1
Thomasomys sp. 3 (Pacheco 2003)	2	2	2	2	2
"Thomasomys" sp. 4 (Pacheco 2003)	2	2	2	2	3
Thomasomys sp. 7 (Pacheco 2003)	1	1	1	1	1
Thomasomys sp. 8 (Pacheco 2003)	1	1	1	1	1
Thomasomys sp. 9 (Pacheco 2003)	1	1	1	1	1
Thomasomys sp. 10 (Pacheco 2003)	1	1	1	1	1
Thomasomys sp. A	1	1	1	1	1
Thomasomys sp. B	1	1	1	1	1
Thomasomys sp. C	1	1	1	1	1
Thomasomys sp. D	1	1	1	1	1
Thomasomys sp. E	1	1	1	1	1
Thomasomys sp. F	1	1	1	1	1
Total	**83**	**84**	**85**	**92**	**96**
Total *Thomasomys*	**81**	**82**	**83**	**90**	**94**

Table S6. List of endangered species of *Thomasomys* in Venezuela (Romero & Pacheco, 2015), Ecuador (Tirira, 2021), Peru (MINAGRI, 2014), and Bolivia (MMAyA, 2009) and globally assessed (IUCN, 2023).

Species	Venezuela	Ecuador	Peru	Bolivia	IUCN
Thomasomys andersoni				vulnerable	
Thomasomys apeco			vulnerable		
Thomasomys auricularis		vulnerable			
Thomasomys bombycinus		endangered			vulnerable
Thomasomys caudivarius		vulnerable	vulnerable		
Thomasomys cinereus		near threatened	near threatened		
Thomasomys cinnameus		near threatened			
Thomasomys daphne			near threatened		
Thomasomys eleusis			vulnerable		vulnerable
Thomasomys erro		near threatened			

Thomasomys fumeus		near threatened			
Thomasomys gracilis			near threatened		near threatened
Thomasomys hudsoni					vulnerable
Thomasomys hylophilus	endangered				vulnerable
Thomasomys incanus			vulnerable		
Thomasomys ischyrus			vulnerable		
Thomasomys kalinowskii			vulnerable		
Thomasomys ladewi				near threatened	
Thomasomys macrotis			vulnerable		
Thomasomys monochromos					vulnerable
Thomasomys onkiro			vulnerable		
Thomasomys pardignasi		endangered			

Thomasomys praetor			vulnerable		near threatened
Thomasomys pyrrhonotus			vulnerable		
Thomasomys rosalinda			endangered		endangered
Thomasomys salazari		near threatened			
Thomasomys silvestris		near threatened			
Thomasomys taczanowskii		near threatened	near threatened		
Thomasomys ucucha		vulnerable			vulnerable
Thomasomys vulcani		vulnerable			
Total categorized species	1	13	15	2	9
Total species recorded	4	18	22	6	44

References

IUCN (2023). *The IUCN Red List of Threatened Species*. Version 2022-2. <https://www.iucnredlist.org> ISSN 2307-8235

MINAGRI - Ministerio de Agricultura y Riego (2014). Decreto Supremo que aprueba la actualización de la lista de clasificación y categorización de las especies amenazadas de fauna silvestre legalmente protegidas. *El Peruano,* 520497–520504.

MMAyA - Ministerio de Medio Ambiente y Agua (2009). *Libro rojo de la fauna silvestre de vertebrados de Bolivia*. Ministerio de Medio Ambiente y Agua. La Paz, Bolivia. 571 pp.

Romero, V. & Pacheco, V. (2015). Rata andina olivácea, Thomasomys hylophilus, in: J.P. Rodríguez, A. García-Rawlins y F. Rojas-Suárez (eds.) Libro Rojo de la Fauna Venezolana. Cuarta edición. Provita y Fundación Empresas Polar, Caracas, Venezuela.

Tirira, D. G. (2021). *Lista Roja de los mamíferos del Ecuador* (3rd ed.). Quito, Ecuador: Asociación Ecuatoriana de Mastozoología, Fundación Mamíferos y Conservación, Pontificia Universidad Católica del Ecuador y Ministerio del Ambiente, Agua y Transición Ecológica del Ecuador.

Supplementary information - Article 2

"Introduction to the *Thomasomys* (Rodentia: Cricetidae) turbinal bone adaptations: Insights into elevation and environmental challenges"

OXFORD UNIVERSITY PRESS | Journal of Mammalogy

Introduction to the Thomasomys (Rodentia: Cricetidae) turbinal adaptations: Insights into elevation and environmental challenges

Journal:	*Journal of Mammalogy*
Manuscript ID	JMAMM-2024-036
Manuscript Type:	Research Article
Date Submitted by the Author:	27-Feb-2024
Complete List of Authors:	Ruelas, Dennisse; Universidad Nacional Mayor de San Marcos, Facultad de Ciencias Biologicas; Institut des Sciences de l'Evolution de Montpellier, PEM; Universidad Peruana Cayetano Heredia, Doctorado en Ciencias de la Vida Fabre, Pierre-Henri; Universite de Montpellier, Institut des Sciences de l'Evolution de Montpellier (ISEM) Pacheco, Víctor; Universidad Nacional Mayor de San Marcos Museo de Historia Natural, Departamento de Mastozoologia; Universidad Nacional Mayor de San Marcos, Facultad de Ciencias Biológicas Martinez, Quentin; Universite de Montpellier, Institut des Sciences de l'Evolution de Montpellier (ISEM); Staatliches Museum für Naturkunde Stuttgart, .
Keywords:	Andes, heat and moisture conservation, montane forest, olfaction, Sigmodontinae

Note: The following files were submitted by the author for peer review, but cannot be converted to PDF. You must view these files (e.g. movies) online.

SuppData10_BioClim_analyses.tar
SuppData12_BioClim_TTSA.tar

SCHOLARONE™ Manuscripts

Supplementary Data SD1.— Altitudinal distribution of the *Thomasomys* species based on Pacheco (2015), Brito et al. (2019, 2021), Ruelas and Pacheco (2021), Lee et al. (2022), and Pacheco and Ruelas (2023).



Literature cited

Brito, J. et al. 2019. Diversidad insospechada en los Andes de Ecuador: filogenia del grupo "cinereus" de *Thomasomys* y descripción de una nueva especie (Rodentia, Cricetidae). Mastozoología Neotropical 26:308–330.

Brito, J., S. Vaca-Puente, C. Koch, and N. Tinoco. 2021. Discovery of the first Amazonian *Thomasomys* (Rodentia, Cricetidae, Sigmodontinae): a new species from the remote Cordilleras del Cóndor and Kutukú in Ecuador. Journal of Mammalogy 102:615–635.

Lee, T. E., N. Tinoco, and J. Brito. 2022. A new species of Andean mouse of the genus *Thomasomys* (Cricetidae, Sigmodontinae) from the eastern Andes of Ecuador. Vertebrate Zoology 72:219–233.

Pacheco, V. 2015. Genus *Thomasomys* Coues, 1884. Pp. 617–682 in Mammals of South America. Vol. 2, Rodents (J. L. Patton, U. F. J. Pardiñas & G. D'Elia, eds.). The University of Chicago Press, Chicago.

Pacheco, V., and D. Ruelas. 2023. Systematic revision of *Thomasomys cinereus* (Rodentia: Cricetidae: Sigmodontinae) from northern Peru and southern Ecuador, with descriptions of three new species. Bulletin of the American Museum of Natural History 461:71.

Ruelas, D., and V. Pacheco. 2021. A new species of *Thomasomys* Coues, 1884 (Rodentia: Sigmodontinae) from the montane forests of northern Peru with comments on the "aureus" group. Revista peruana de biología 28:e19912.

Supplementary Data SD2.— Map of the collection localities of the *Thomasomys* specimens used in this study. Samples are grouped based on the species groups sensu Pacheco (2015): Aureus, Baeops, Cinereus, Gracilis, Incanus, and Notatus. Localities are shown in Appendix 1.

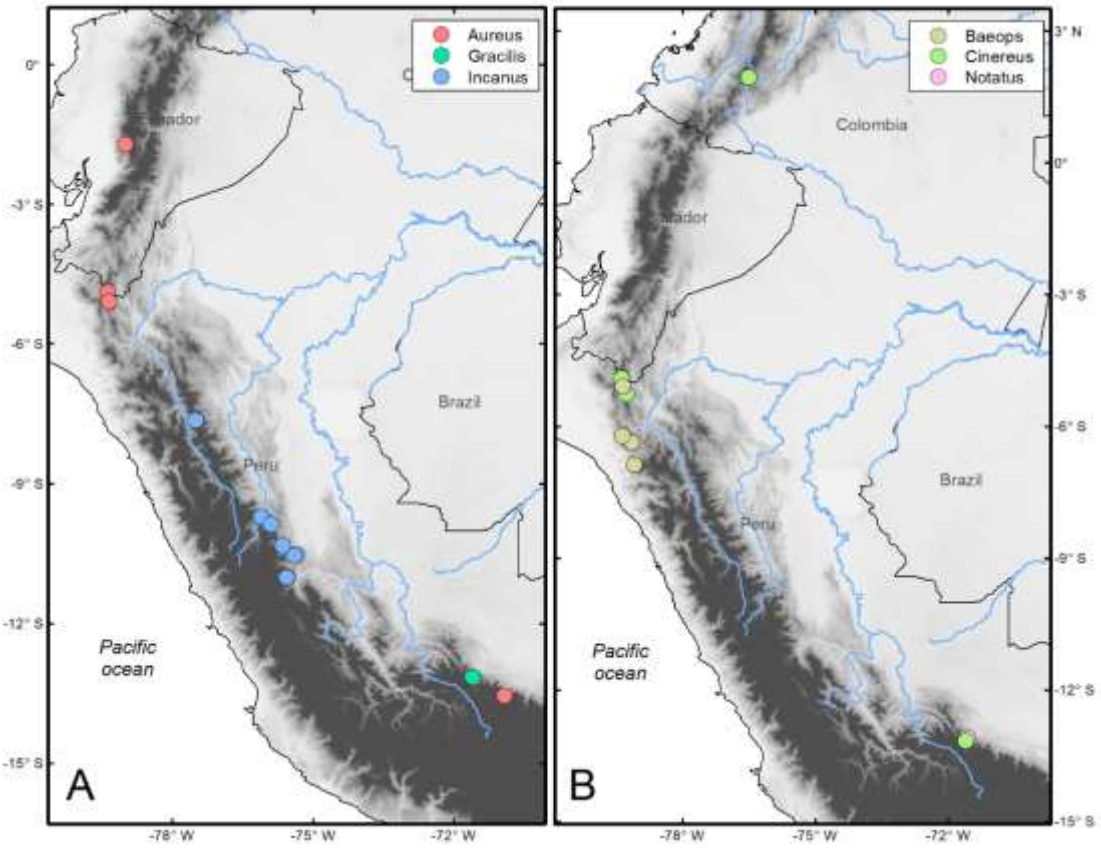

Supplementary Data SD3.— Dataset used for quantitative analyses. Species and vouchers used, species groups based on Pacheco (2015), total respiratory surface area (mm^2), total olfactory surface area (mm^2), skull length (mm), nasal length (mm), elevation (m a.s.l.), and bioclimatic variables (BIO). Abbreviations: MUSM – Museo de Historia Natural de la Universidad Nacional Mayor de San Marcos (Lima, Peru), FMNH – Field Museum of Natural History (Chicago, United States), MEPN – Museo de Historia Natural "Gustavo Orcés V." de la Escuela Politécnica Nacional (Quito, Ecuador).

Species	**Voucher**	**Group**	**Abbreviation**	**Respi**	**Olfa**	**Skull**	**Elevation**	**BIO01**	**BIO02**	**BIO03**	**BIO04**	**BIO05**	**BIO06**	**BIO07**	**BIO08**	**BIO09**	**BIO10**	**BIO11**	**BIO12**	**BIO13**	**BIO14**	**BIO15**	**BIO16**	**BIO17**	**BIO18**	**BIO19**
Thomasomys antoniobracki	MUSM 23754	Aureus	anto	171.72	257.26	44.76	2630	14.368	10.416	87.263	22.644	20.624	8.688	11.936	14.445	14.255	14.553	14.068	1342	223	41	54.139	598	173	332	205
Thomasomys antoniobracki	MUSM 23755	Aureus	anto	193.41	300.70	43.86	2720	14.368	10.416	87.263	22.644	20.624	8.688	11.936	14.445	14.255	14.553	14.068	1342	223	41	54.139	598	173	332	205
Thomasomys aureus	MEPN 6144	Aureus	aure	102.68	182.96	36.1	2600	12.010	10.256	87.181	25.773	18.008	6.244	11.764	12.219	11.679	12.295	11.665	673	116	9	65.957	334	45	279	53
Thomasomys aff. *aureus*	MUSM 52859	Aureus	afau	144.87	280.76	40.58	3217	9.731	12.425	77.499	71.216	16.608	0.576	16.032	10.101	8.672	10.380	8.672	863	151	16	67.707	418	50	238	50
Thomasomys aff. *aureus*	MUSM 52860	Aureus	afau	129.01	243.21	40.85	3217	9.731	12.425	77.499	71.216	16.608	0.576	16.032	10.101	8.672	10.380	8.672	863	151	16	67.707	418	50	238	50
Thomasomys aff. *caudivarius*	MUSM 46711	Cinereus	caud	143.91	262.45	33.35	3290	12.791	10.347	85.626	27.527	19.024	6.940	12.084	12.935	12.487	13.028	12.410	1193	191	57	40.896	473	191	282	216

Thomasomys aff. *caudivarius*	MUSM 23562	Cinereus	caud	119.75	156.77	30.58	2762	14.368	10.416	87.263	22.644	20.624	8.688	11.936	14.445	14.255	14.553	14.068	1342	223	41	54.139	598	173	332	205
Thomasomys aff. *caudivarius*	MUSM 23750	Cinereus	caud	115.76	180.61	30.46	2780	14.368	10.416	87.263	22.644	20.624	8.688	11.936	14.445	14.255	14.553	14.068	1342	223	41	54.139	598	173	332	205
Thomasomys daphne	MUSM 20014	Cinereus	daph	67.66	110.12	27.32	2880	12.087	13.651	73.485	116.486	20.072	1.496	18.576	12.807	10.537	13.163	10.379	456	76	9	63.385	212	37	131	41
Thomasomys daphne	MUSM 20017	Cinereus	daph	51.88	116.96	26.65	2880	12.087	13.651	73.485	116.486	20.072	1.496	18.576	12.807	10.537	13.163	10.379	456	76	9	63.385	212	37	131	41
Thomasomys daphne	FMNH 175229	Cinereus	daph	54.33	126.61	25.39	2880	12.087	13.651	73.485	116.486	20.072	1.496	18.576	12.807	10.537	13.163	10.379	456	76	9	63.385	212	37	131	41
Thomasomys cf. *dispar*	FMNH 72397	Cinereus	disp	142.64	176.98	31.97	2200	13.519	9.690	91.622	28.025	18.768	8.192	10.576	13.511	13.163	13.875	13.163	1880	202	110	20.250	569	394	519	394
Thomasomys cf. *dispar*	FMNH 72400	Cinereus	disp	163.45	200.96	31.94	2200	13.519	9.690	91.622	28.025	18.768	8.192	10.576	13.511	13.163	13.875	13.163	1880	202	110	20.250	569	394	519	394
Thomasomys incanus	MUSM 46187	Incanus	inca	119.67	210.01	29.55	2788	15.566	12.137	79.283	63.067	22.460	7.152	15.308	15.625	14.684	16.266	14.684	1007	152	27	55.949	437	91	302	91
Thomasomys incanus	MUSM 52873	Incanus	inca	96.24	190.75	29.43	3309	9.731	12.425	77.499	71.216	16.608	0.576	16.032	10.101	8.672	10.380	8.672	863	151	16	67.707	418	50	238	50
Thomasomys aff. *incanus*	MUSM 7985	Incanus	afin	143.19	224.57	31.31	2650	10.415	12.248	83.299	45.371	17.348	2.644	14.704	10.591	9.769	10.936	9.769	1235	188	28	55.156	483	94	417	94
Thomasomys aff. *incanus*	MUSM 8002	Incanus	afin	120.40	227.02	31.28	3380	10.415	12.248	83.299	45.371	17.348	2.644	14.704	10.591	9.769	10.936	9.769	1235	188	28	55.156	483	94	417	94
Thomasomys ischyrus	MUSM 18346	Incanus	isch	126.68	212.07	31.09	2757	15.685	12.616	81.965	47.657	22.796	7.404	15.392	15.594	15.079	16.251	15.079	786	117	19	56.537	328	65	198	65

Thomasomys ischyrus	MUSM 18347	Incanus	isch	157.97	258.17	32.5	2757	15.685	12.616	81.965	47.657	22.796	7.404	15.392	15.594	15.079	16.251	15.079	786	117	19	56.537	328	65	198	65
Thomasomys ischyrus	MUSM 17848	Incanus	isch	110.79	189.14	31.94	2900	12.539	13.523	81.052	53.928	20.024	3.340	16.684	12.613	11.777	13.144	11.777	1013	141	22	53.688	409	82	336	82
Thomasomys kalinowskii	MUSM 18381	Incanus	kali	117.55	187.98	30.47	2757	15.685	12.616	81.965	47.657	22.796	7.404	15.392	15.594	15.079	16.251	15.079	786	117	19	56.537	328	65	198	65
Thomasomys kalinowskii	MUSM 18374	Incanus	kali	160.70	212.55	33.25	2757	15.685	12.616	81.965	47.657	22.796	7.404	15.392	15.594	15.079	16.251	15.079	786	117	19	56.537	328	65	198	65
Thomasomys aff. *kalinowskii*	MUSM 14993	Incanus	afka	141.79	259.60	32.88	2200	18.333	12.806	80.807	63.279	25.544	9.696	15.848	18.450	17.433	18.995	17.433	1219	184	27	56.758	523	95	375	95
Thomasomys notatus	MUSM 17021	Notatus	nota	60.80	117.49	29.7	1900	16.680	12.709	77.343	89.810	24.304	7.872	16.432	17.108	15.441	17.553	15.405	1036	147	38	45.706	420	134	278	135
Thomasomys notatus	FMNH 170690	Notatus	nota	86.13	164.93	32.07	1920	16.680	12.709	77.343	89.810	24.304	7.872	16.432	17.108	15.441	17.553	15.405	1036	147	38	45.706	420	134	278	135
Thomasomys pagaibambensis	MUSM 39737	Cinereus	paga	162.47	257.66	33.43	2946	14.137	12.011	86.660	45.220	20.840	6.980	13.860	14.549	13.509	14.563	13.509	938	162	44	45.393	390	141	351	141
Thomasomys cf. *pyrrhonotus*	MUSM 55555	Aureus	pyrr	120.91	178.70	37.4	2117	14.839	10.840	87.113	25.398	21.244	8.800	12.444	14.982	14.604	15.026	14.505	1304	201	49	45.631	539	191	317	224
Thomasomys cf. *pyrrhonotus*	MUSM 55553	Aureus	pyrr	131.24	230.79	38.8	2169	14.839	10.840	87.113	25.398	21.244	8.800	12.444	14.982	14.604	15.026	14.505	1304	201	49	45.631	539	191	317	224
Thomasomys taczanowskii	MUSM 15066	Baeops	tacz	65.86	123.13	29.63	1500	16.085	12.392	87.961	57.666	22.736	8.648	14.088	16.791	15.448	16.791	15.448	726	167	10	75.365	379	50	379	50
Thomasomys taczanowskii	MUSM 15067	Baeops	tacz	64.10	105.88	27.95	1500	16.085	12.392	87.961	57.666	22.736	8.648	14.088	16.791	15.448	16.791	15.448	726	167	10	75.365	379	50	379	50

Thomasomys taczanowskii	MUSM 39741	Baeops	tacz	65.10	107.25	27.61	2265	14.137	12.011	86.660	45.220	20.840	6.980	13.860	14.549	13.509	14.563	13.509	938	162	44	45.393	390	141	351	141
Thomasomys taczanowskii	MUSM 39735	Baeops	tacz	61.01	95.73	27.61	2933	14.137	12.011	86.660	45.220	20.840	6.980	13.860	14.549	13.509	14.563	13.509	938	162	44	45.393	390	141	351	141
Thomasomys taczanowskii	MUSM 39738	Baeops	tacz	67.33	100.44	28.5	2950	14.137	12.011	86.660	45.220	20.840	6.980	13.860	14.549	13.509	14.563	13.509	938	162	44	45.393	390	141	351	141
Thomasomys taczanowskii	MUSM 21802	Baeops	tacz	65.26	103.09	27.78	2827	13.795	12.490	87.465	38.398	20.828	6.548	14.280	14.073	13.275	14.181	13.275	710	158	13	69.924	353	55	219	55
Thomasomys taczanowskii	MUSM 55562	Baeops	tacz	67.99	108.59	28.53	2117	14.839	10.840	87.113	25.398	21.244	8.800	12.444	14.982	14.604	15.026	14.505	1304	201	49	45.631	539	191	317	224
Thomasomys taczanowskii	MUSM 55567	Baeops	tacz	49.83	97.76	26.94	2117	14.839	10.840	87.113	25.398	21.244	8.800	12.444	14.982	14.604	15.026	14.505	1304	201	49	45.631	539	191	317	224
Thomasomys taczanowskii	MUSM 55558	Baeops	tacz	56.76	106.86	28.53	2117	14.839	10.840	87.113	25.398	21.244	8.800	12.444	14.982	14.604	15.026	14.505	1304	201	49	45.631	539	191	317	224
Thomasomys taczanowskii	MUSM 55583	Baeops	tacz	68.72	104.79	28.97	2169	14.839	10.840	87.113	25.398	21.244	8.800	12.444	14.982	14.604	15.026	14.505	1304	201	49	45.631	539	191	317	224
Thomasomys sp. 1	MUSM 9349	Aureus	sp01	157.50	241.33	38.97	2250	12.065	13.314	73.236	116.285	19.856	1.676	18.180	12.808	10.521	13.111	10.351	469	78	9	64.449	220	37	135	39
Thomasomys sp. 1	MUSM 19581	Aureus	sp01	108.10	223.83	37.05	2460	13.432	13.218	74.495	108.420	21.232	3.488	17.744	14.065	11.975	14.454	11.852	485	73	12	53.699	210	49	134	54
Thomasomys sp. 1	FMNH 75588	Aureus	sp01	157.26	274.73	40.78	2750	10.224	14.370	70.986	148.336	18.624	0.100	20.244	11.385	8.020	11.434	8.020	783	142	8	71.850	384	46	242	46
Thomasomys sp. 6	MUSM 46249	Incanus	sp06	119.38	267.41	32.33	3368	11.954	12.413	79.426	63.073	18.864	3.236	15.628	12.124	11.029	12.617	11.029	990	148	20	56.951	427	76	306	76

Thomasomys sp. 9	MUSM 20023	Gracilis	sp09	65.41	129.22	27.47	2880	12.087	13.651	73.485	116.486	20.072	1.496	18.576	12.807	10.537	13.163	10.379	456	76	9	63.385	212	37	131	41
Thomasomys sp. 10	MUSM 23763	Cinereus	sp10	183.51	256.21	32.85	2630	14.368	10.416	87.263	22.644	20.624	8.688	11.936	14.445	14.255	14.553	14.068	1342	223	41	54.139	598	173	332	205
Thomasomys sp. 10	MUSM 23764	Cinereus	sp10	165.81	261.01	32.85	2780	14.368	10.416	87.263	22.644	20.624	8.688	11.936	14.445	14.255	14.553	14.068	1342	223	41	54.139	598	173	332	205

Supplementary Data SD4.— Morphological variability of the nasoturbinals (nt) and maxilloturbinals (mt) of *Thomasomys* species groups sensu Pacheco (2015).

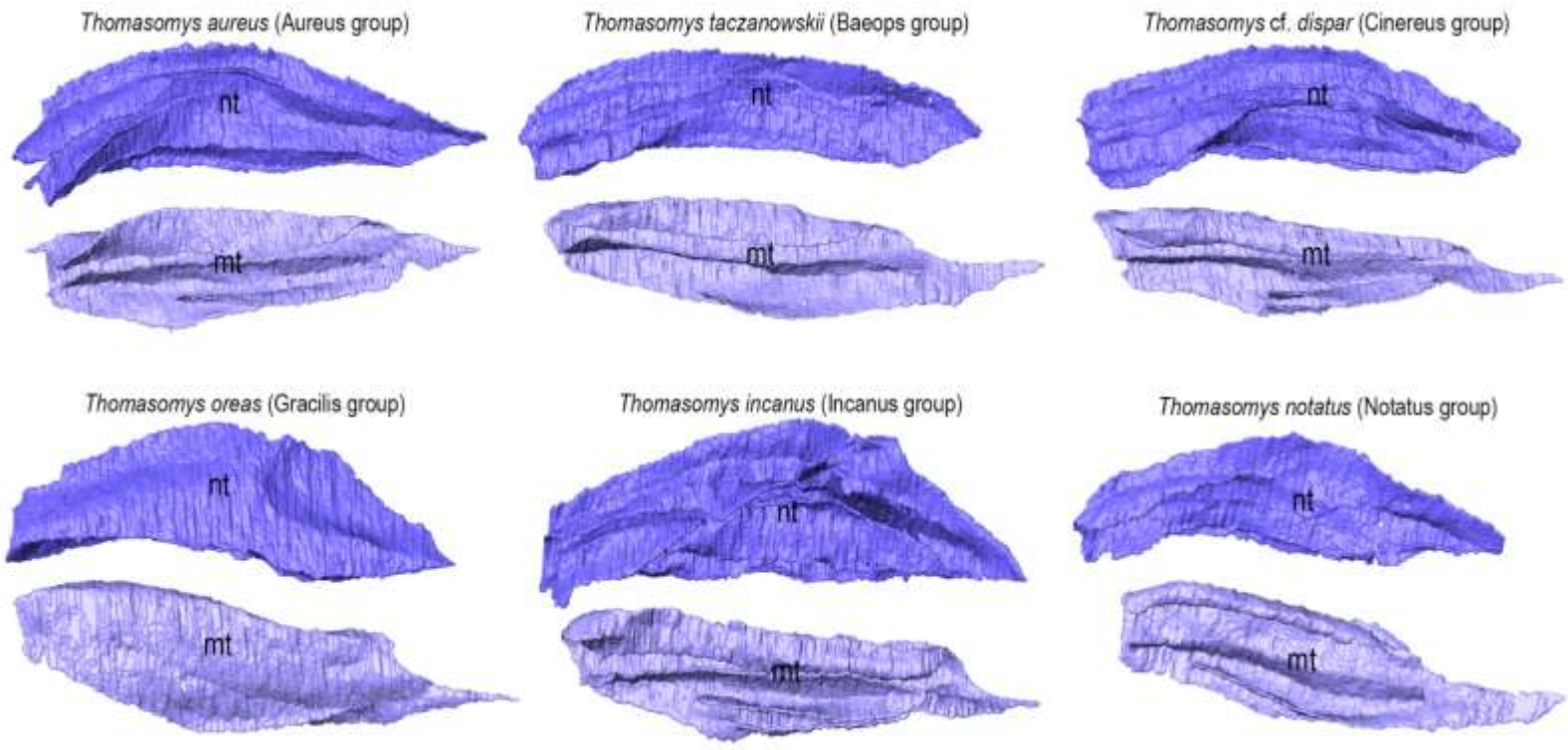

Supplementary Data SD5.— (A) Boxplot of the non-corrected RTSA and OTSA. (B) Boxplot of the relative RTSA and relative OTSA (corrected by skull length). Colors represent the species groups of *Thomasomys* sensu Pacheco (2015).

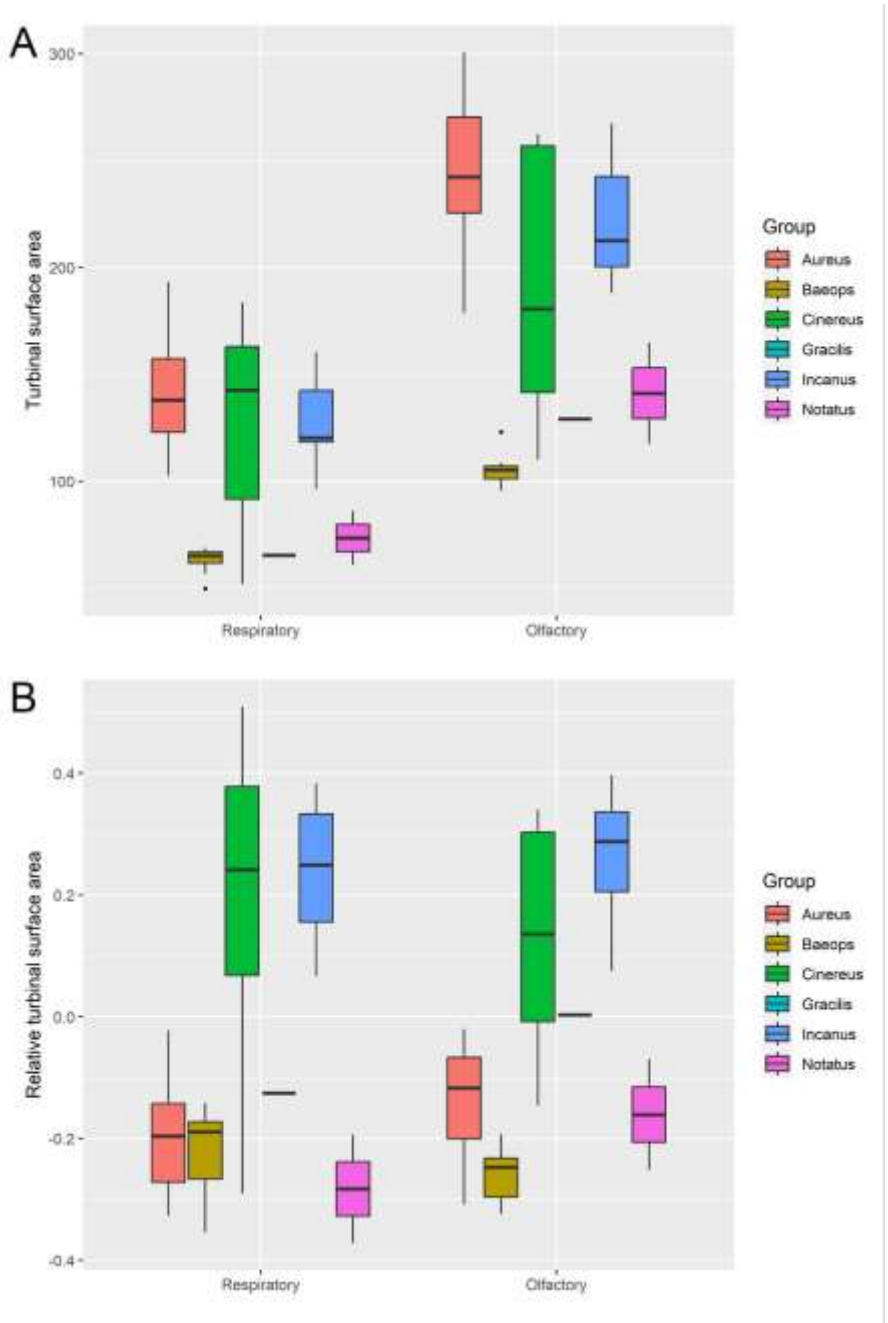

Supplementary Data SD6.— 3D representations of turbinal bones that suggest that altitude is an driver of the evolution of the size of respiratory and olfactory turbinals. Color of turbinals is explained in Fig. 1.

important

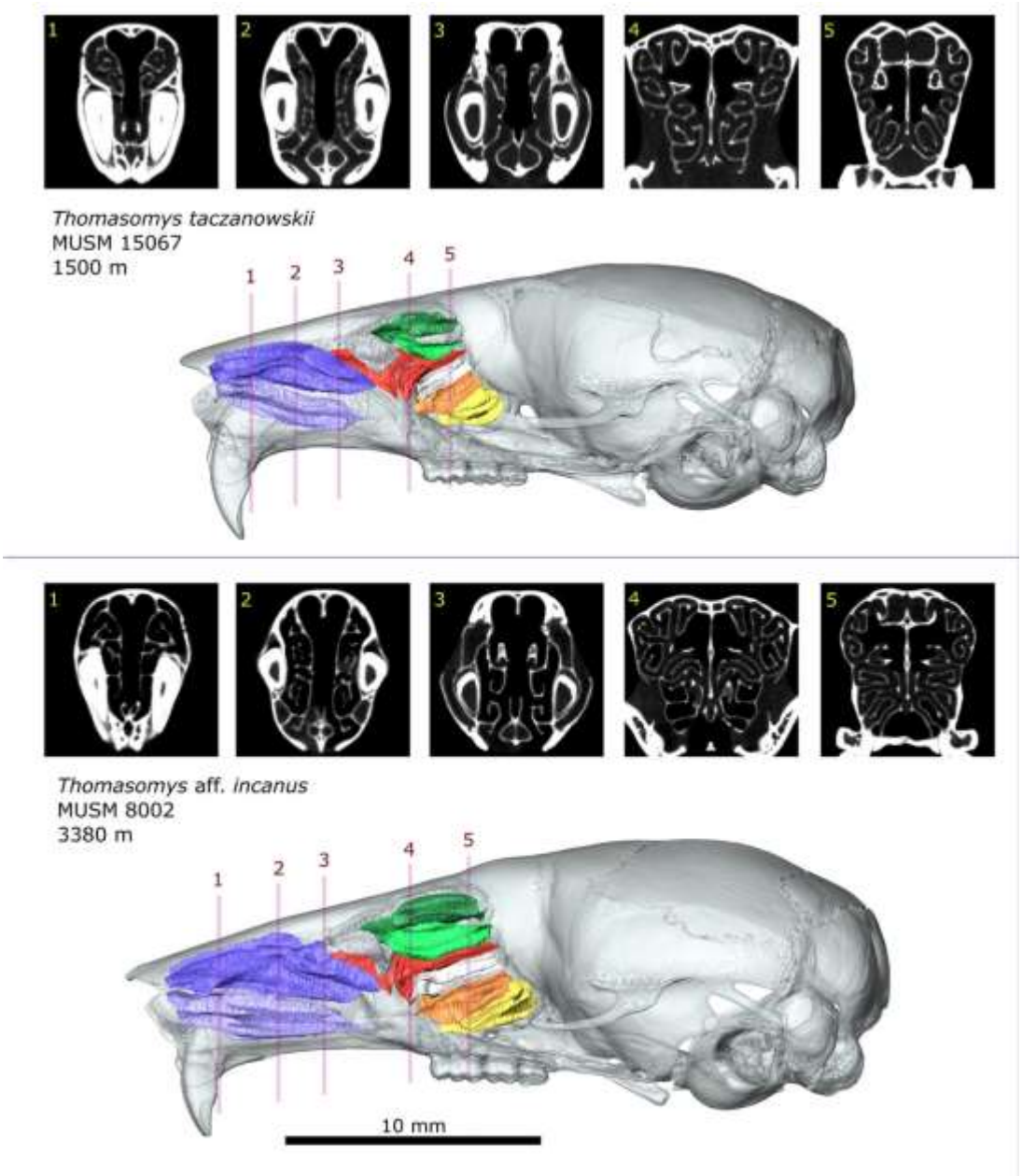

Supplementary Data SD7.— Linear regression between elevation (in m) and skull length of *Thomasomys* (in mm). Abbreviations for species are shown in Supplementary Data SD3.

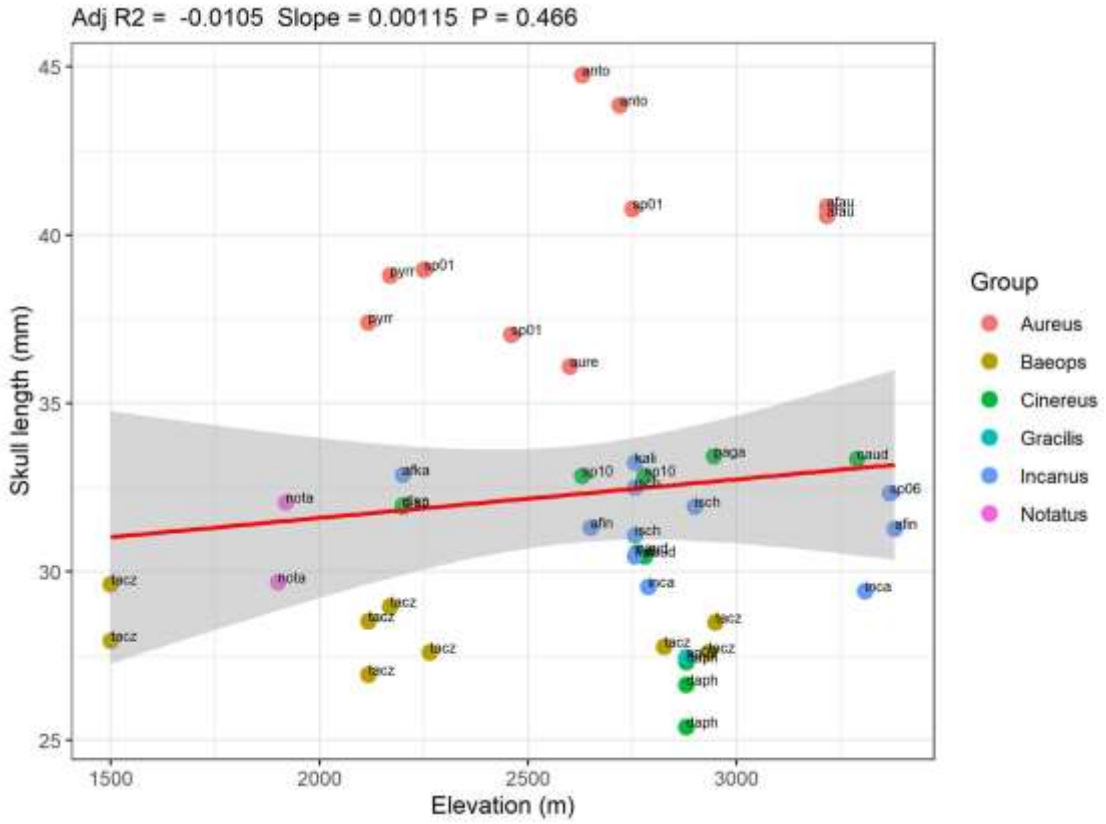

Supplementary Data SD8.— PCA plot showing the contribution of the bioclimatic variables on the first two PC axes. Abbreviations are explained in Methods. The projection of each arrow on an axis shows its contribution to this axis. Colors show the percentage of contribution (% contrib) of the variables to other axes out of the first principal plane.

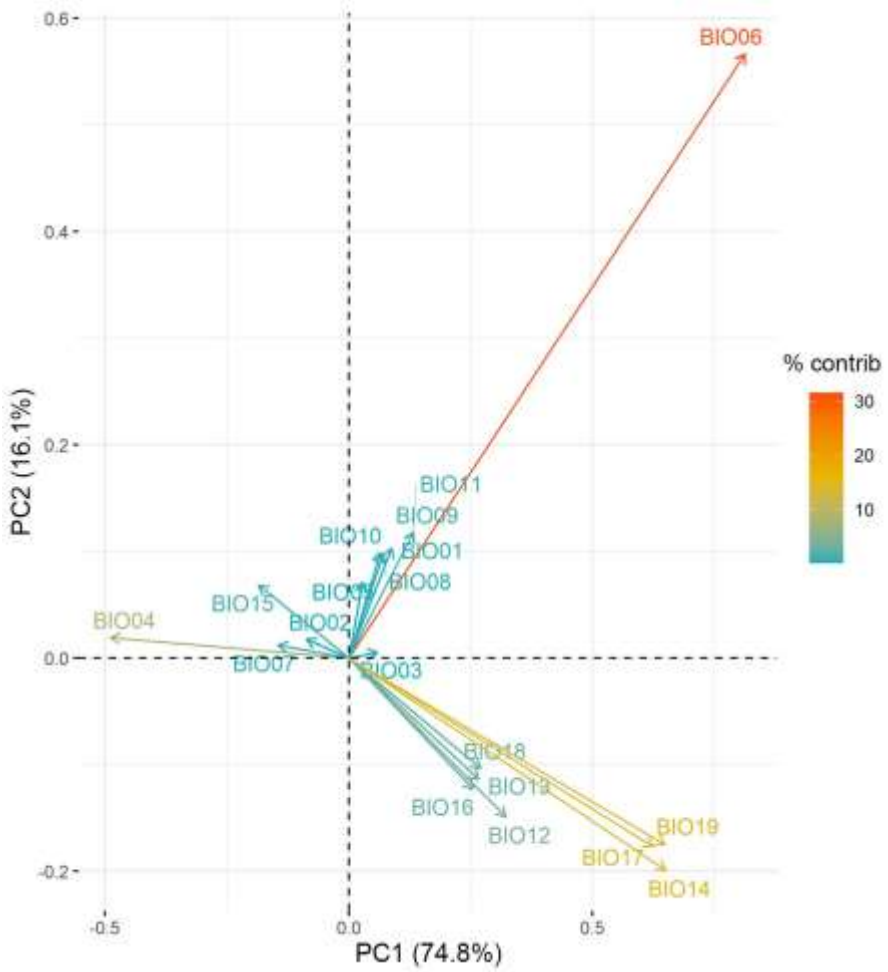

Supplementary Data SD9.— Percentage of variance and eigenvalues for the first two principal components (PC) for each bioclimatic variable. The variables that contributed the most to the PC are shown in bold. Abbreviations are explained in Methods.

Variables	**PC1**	**PC2**
Variance (%)	74.78	16.06
BIO01	0.055	0.139
BIO02	-0.054	0.024
BIO03	0.037	0.007
BIO04	-0.305	0.026
BIO05	0.018	0.095
BIO06	**0.507**	**0.763**
BIO07	-0.091	0.016
BIO08	0.044	0.131
BIO09	0.083	0.159
BIO10	0.040	0.133
BIO11	0.083	0.158
BIO12	0.201	-0.201

BIO13	0.166	-0.153
BIO14	0.406	**-0.268**
BIO15	-0.115	0.092
BIO16	0.159	-0.165
BIO17	0.390	**-0.238**
BIO18	0.169	-0.139
BIO19	0.405	**-0.236**

Supplementary Data SD10.— Log regressions (red line) of relative turbinal surface areas (RTSA, OTSA, and TTSA) sized by skull length versus 19 bioclimatic variables.

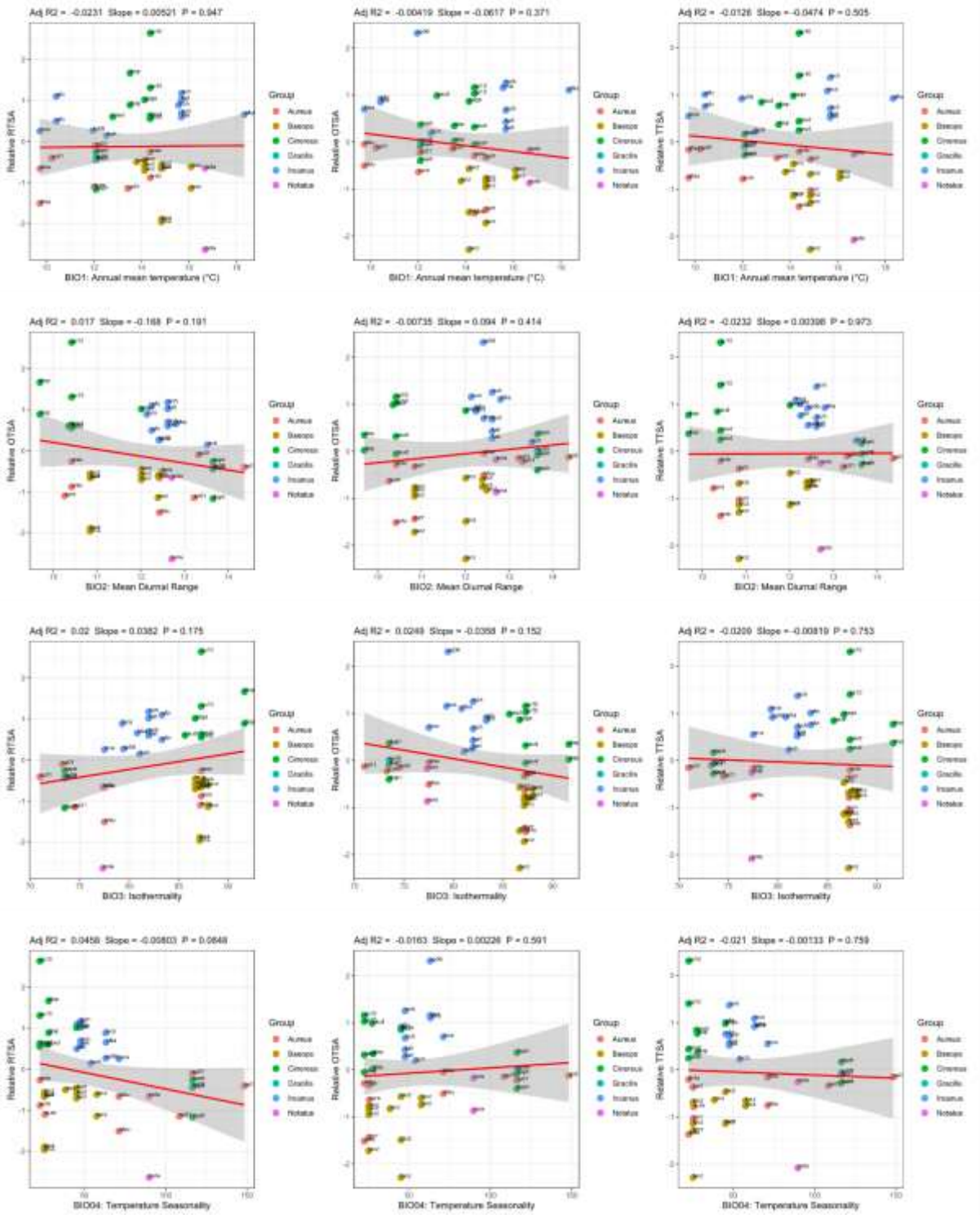

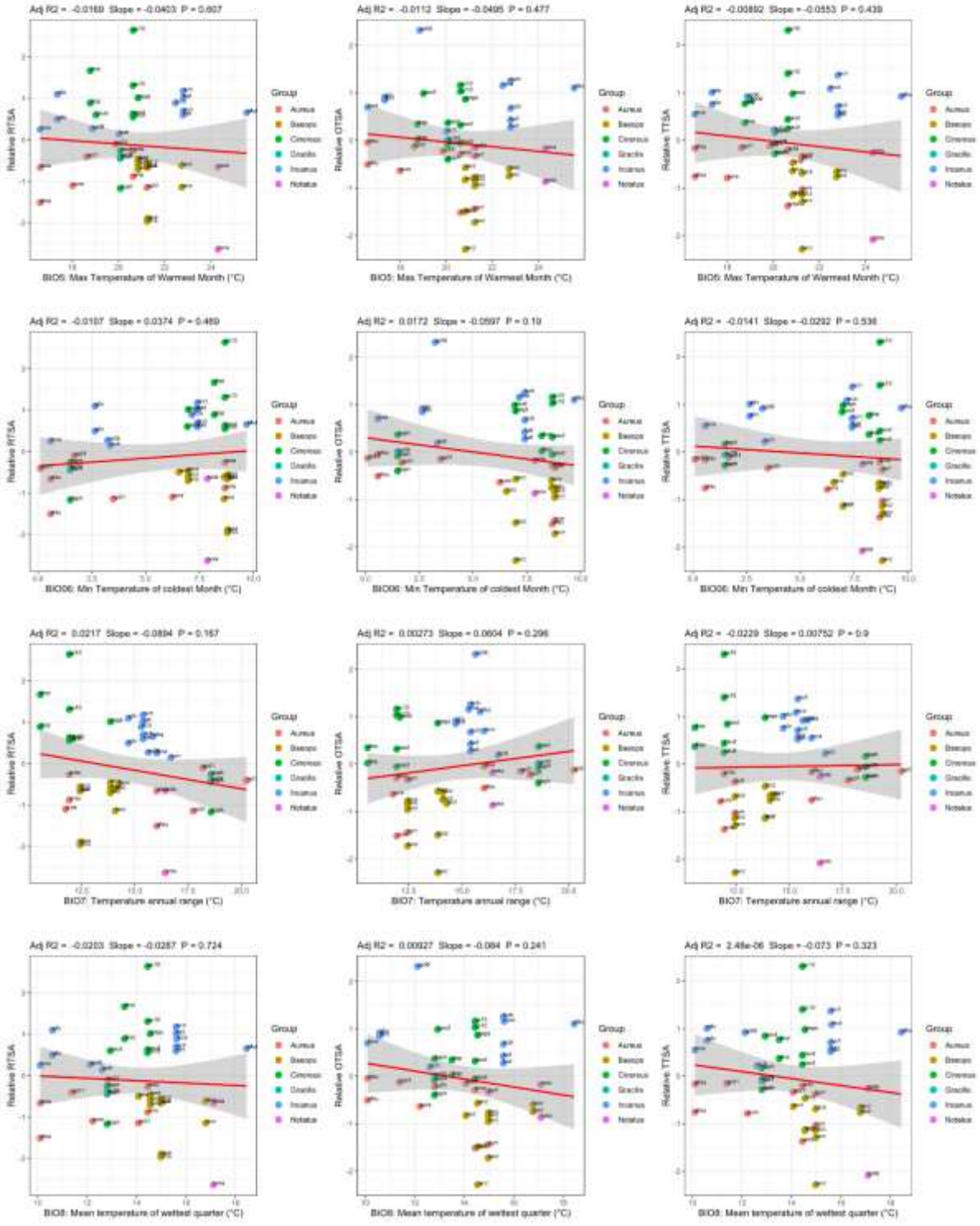
Adj R2 = -0.0169 Slope = -0.0403 P = 0.607
Adj R2 = -0.0112 Slope = -0.0495 P = 0.477
Adj R2 = -0.00892 Slope = -0.0553 P = 0.439
Relative RTSA
Relative CTSA
Relative TTSA
BIO5: Max Temperature of Warmest Month (°C)
Adj R2 = -0.0107 Slope = 0.0374 P = 0.469
Adj R2 = 0.0172 Slope = -0.0597 P = 0.19
Adj R2 = -0.0141 Slope = -0.0292 P = 0.536
BIO06: Min Temperature of coldest Month (°C)
Adj R2 = 0.0217 Slope = -0.0894 P = 0.167
Adj R2 = 0.00273 Slope = 0.0604 P = 0.296
Adj R2 = -0.0229 Slope = 0.00752 P = 0.9
BIO7: Temperature annual range (°C)
Adj R2 = -0.0203 Slope = -0.0287 P = 0.724
Adj R2 = 0.00927 Slope = -0.084 P = 0.241
Adj R2 = 2.48e-06 Slope = -0.073 P = 0.323
BIO8: Mean temperature of wettest quarter (°C)
Group
Aureus
Baeops
Cinereus
Gracilis
Insanus
Notatus

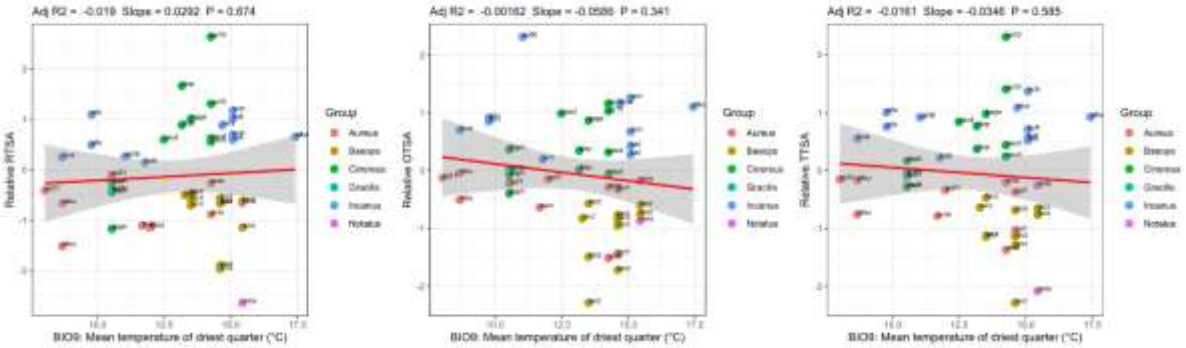
Adj R2 = -0.019 Slope = 0.0292 P = 0.674
Adj R2 = -0.00162 Slope = -0.0586 P = 0.341
Adj R2 = -0.0161 Slope = -0.0346 P = 0.585
Relative RTSA
Relative OTSA
Relative TTSA
BIO9: Mean temperature of driest quarter (°C)
Group
Aureus
Baeops
Cinereus
Gracilis
Insanus
Notatus

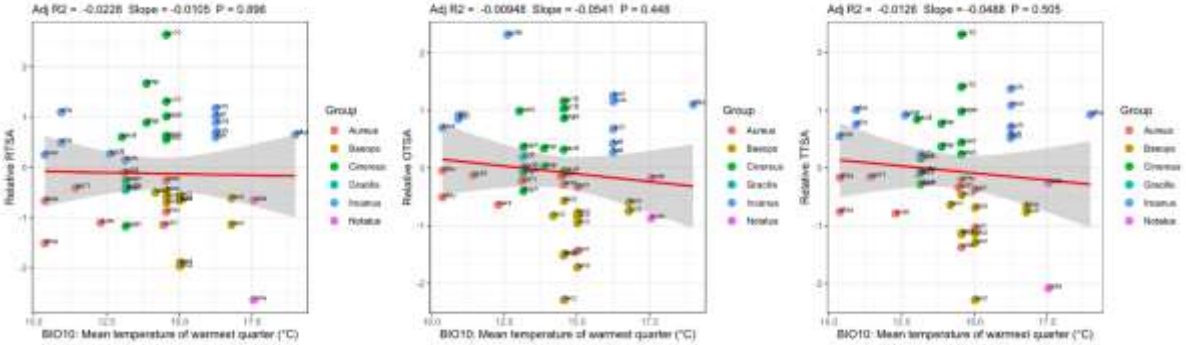
Adj R2 = -0.0228 Slope = -0.0105 P = 0.896
Adj R2 = -0.00948 Slope = -0.0541 P = 0.448
Adj R2 = -0.0126 Slope = -0.0488 P = 0.505
Relative RTSA
Relative OTSA
Relative TTSA
BIO10: Mean temperature of warmest quarter (°C)
Group
Aureus
Baeops
Cinereus
Gracilis
Insanus
Notatus

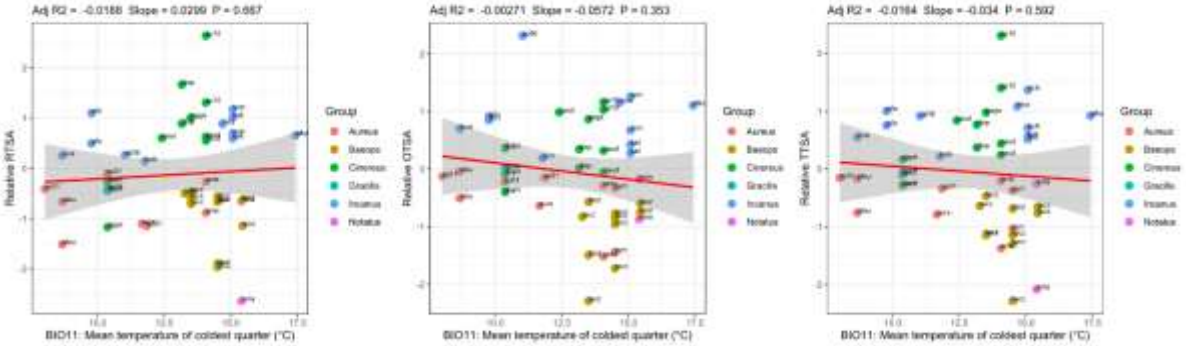
Adj R2 = -0.0188 Slope = 0.0209 P = 0.657
Adj R2 = -0.00271 Slope = -0.0572 P = 0.353
Adj R2 = -0.0184 Slope = -0.034 P = 0.592
Relative RTSA
Relative OTSA
Relative TTSA
BIO11: Mean temperature of coldest quarter (°C)
Group
Aureus
Baeops
Cinereus
Gracilis
Insanus
Notatus

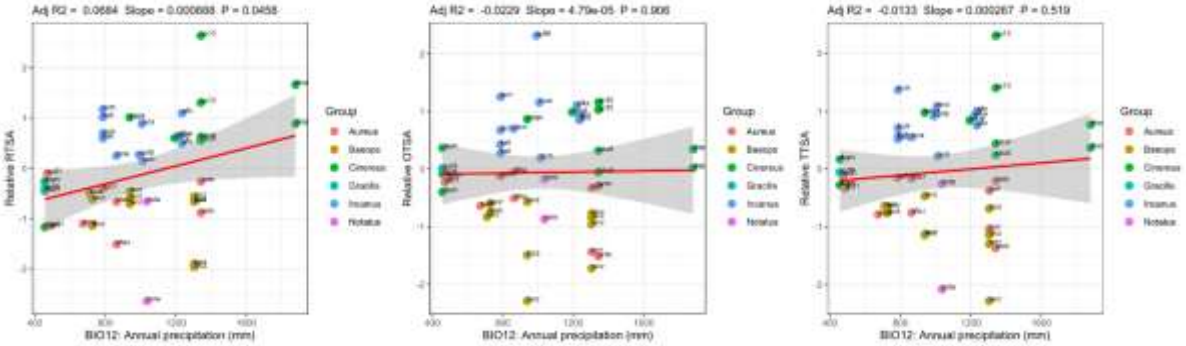
Adj R2 = 0.0684 Slope = 0.000688 P = 0.0458
Adj R2 = -0.0229 Slope = 4.79e-05 P = 0.906
Adj R2 = -0.0133 Slope = 0.000267 P = 0.519
Relative RTSA
Relative OTSA
Relative TTSA
BIO12: Annual precipitation (mm)
Group
Aureus
Baeops
Cinereus
Gracilis
Insanus
Notatus

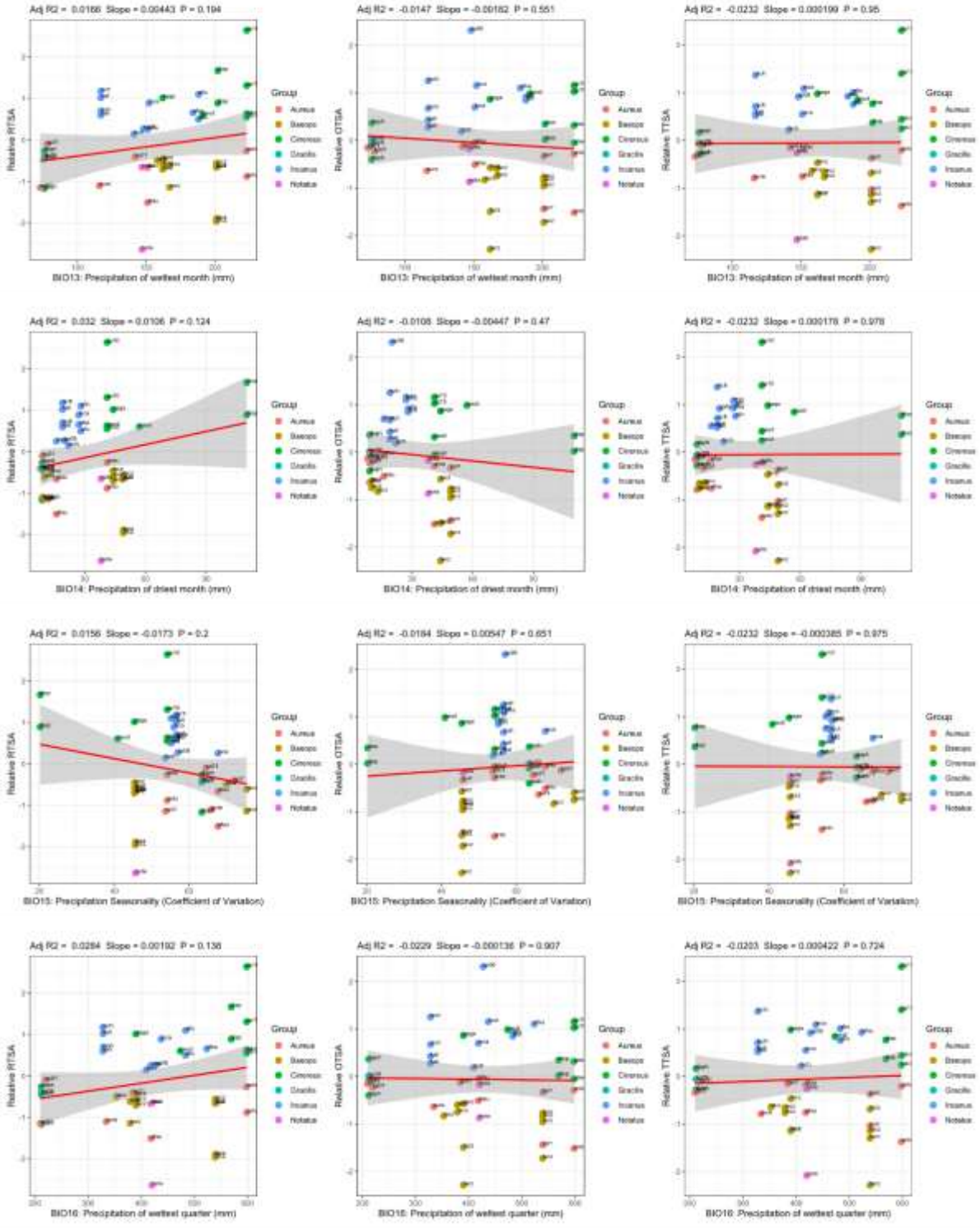
Adj R2 = 0.0166 Slope = 0.00443 P = 0.194
Adj R2 = -0.0147 Slope = -0.00182 P = 0.551
Adj R2 = -0.0232 Slope = 0.000199 P = 0.95
Adj R2 = 0.032 Slope = 0.0106 P = 0.124
Adj R2 = -0.0108 Slope = -0.00447 P = 0.47
Adj R2 = -0.0232 Slope = 0.000178 P = 0.978
Adj R2 = 0.0156 Slope = -0.0173 P = 0.2
Adj R2 = -0.0184 Slope = 0.00547 P = 0.651
Adj R2 = -0.0232 Slope = -0.000385 P = 0.975
Adj R2 = 0.0284 Slope = 0.00192 P = 0.136
Adj R2 = -0.0229 Slope = -0.000136 P = 0.907
Adj R2 = -0.0203 Slope = 0.000422 P = 0.724
Relative RTSA
Relative GTSA
Relative TTSA
BIO13: Precipitation of wettest month (mm)
BIO14: Precipitation of driest month (mm)
BIO15: Precipitation Seasonality (Coefficient of Variation)
BIO16: Precipitation of wettest quarter (mm)
Group
Aureus
Baeops
Cinereus
Gracilis
Insanus
Notatus

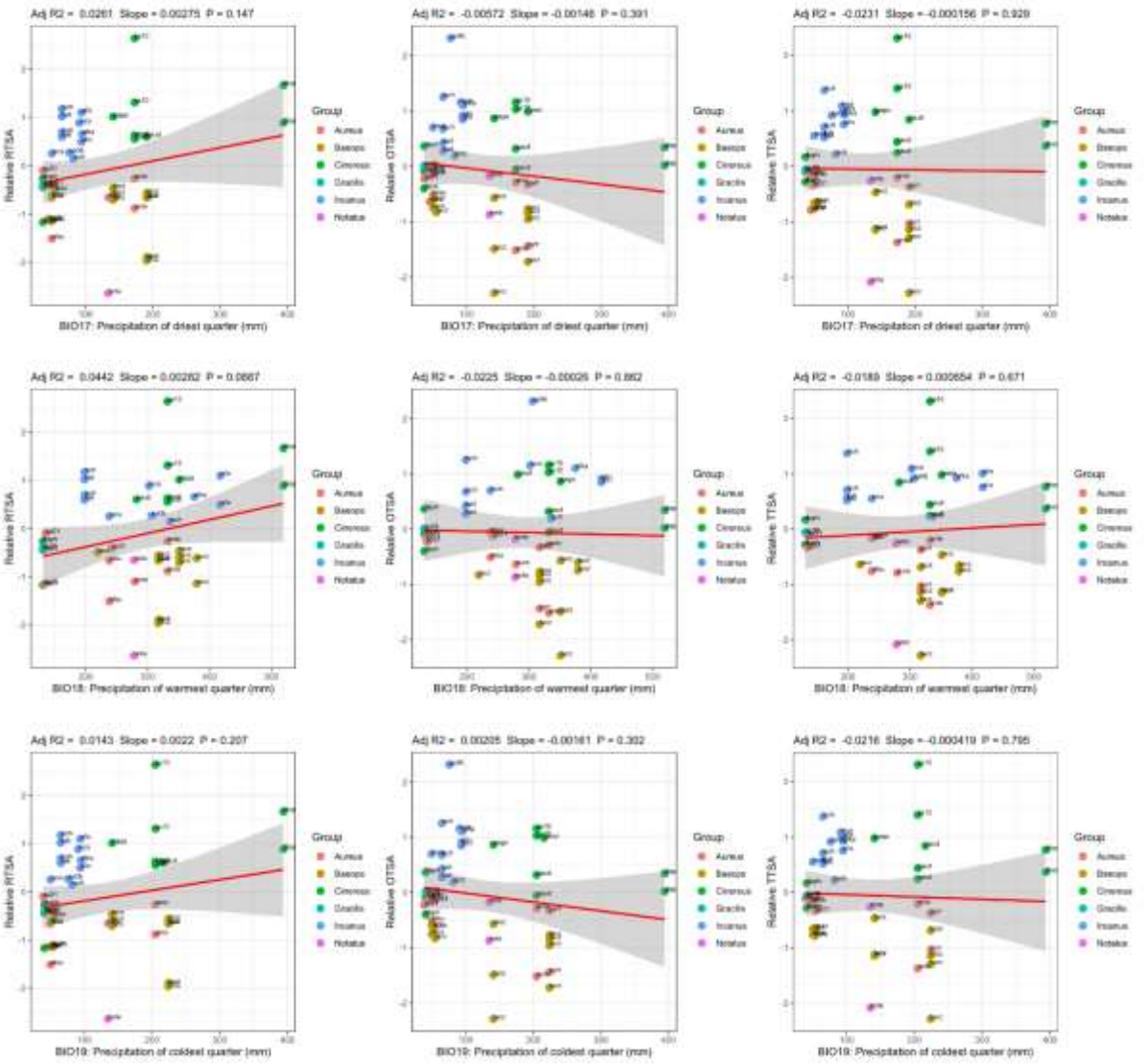
Adj R2 = 0.0261 Slope = 0.00275 P = 0.147
Adj R2 = -0.00572 Slope = -0.00148 P = 0.391
Adj R2 = -0.0231 Slope = -0.000156 P = 0.929
Relative RTSA
Relative GTSA
Relative TTSA
BIO17: Precipitation of driest quarter (mm)
Adj R2 = 0.0442 Slope = 0.00282 P = 0.0887
Adj R2 = -0.0225 Slope = -0.00026 P = 0.882
Adj R2 = -0.0189 Slope = 0.000654 P = 0.671
BIO18: Precipitation of warmest quarter (mm)
Adj R2 = 0.0143 Slope = 0.0022 P = 0.207
Adj R2 = 0.00205 Slope = -0.00161 P = 0.302
Adj R2 = -0.0216 Slope = -0.000419 P = 0.795
BIO19: Precipitation of coldest quarter (mm)
Group
Aureus
Baeops
Cinereus
Gracilis
Insanus
Notatus

Supplementary Data SD11.— Linear regression between elevation (in m) and log-transformed BIO12 variable. Abbreviations for species are shown in Supplementary Data SD3.

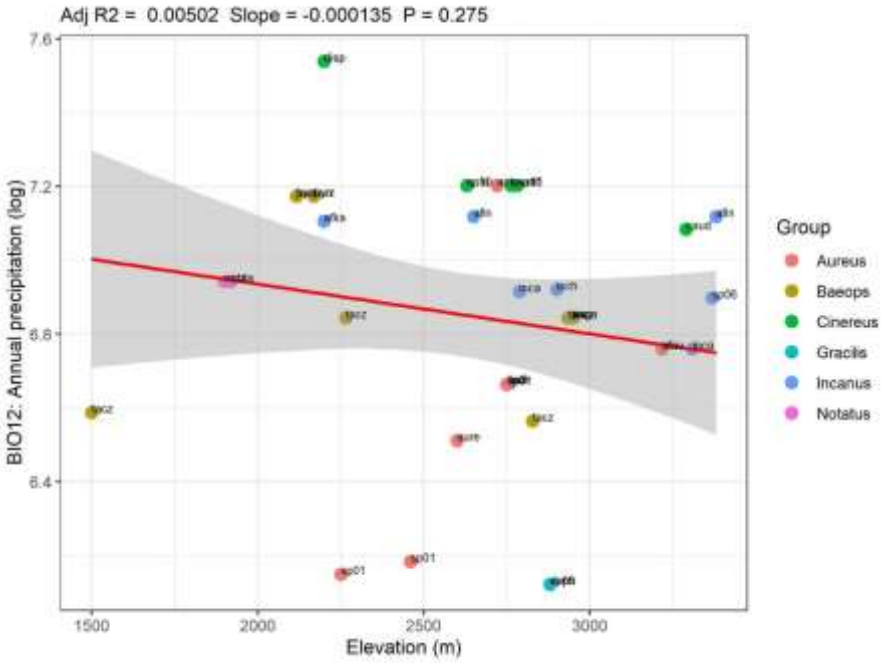

Supplementary Data SD12.— Log regressions (red line) of relative turbinal surface areas (RTSA and OTSA) sized by TTSA versus 19 bioclimatic variables.

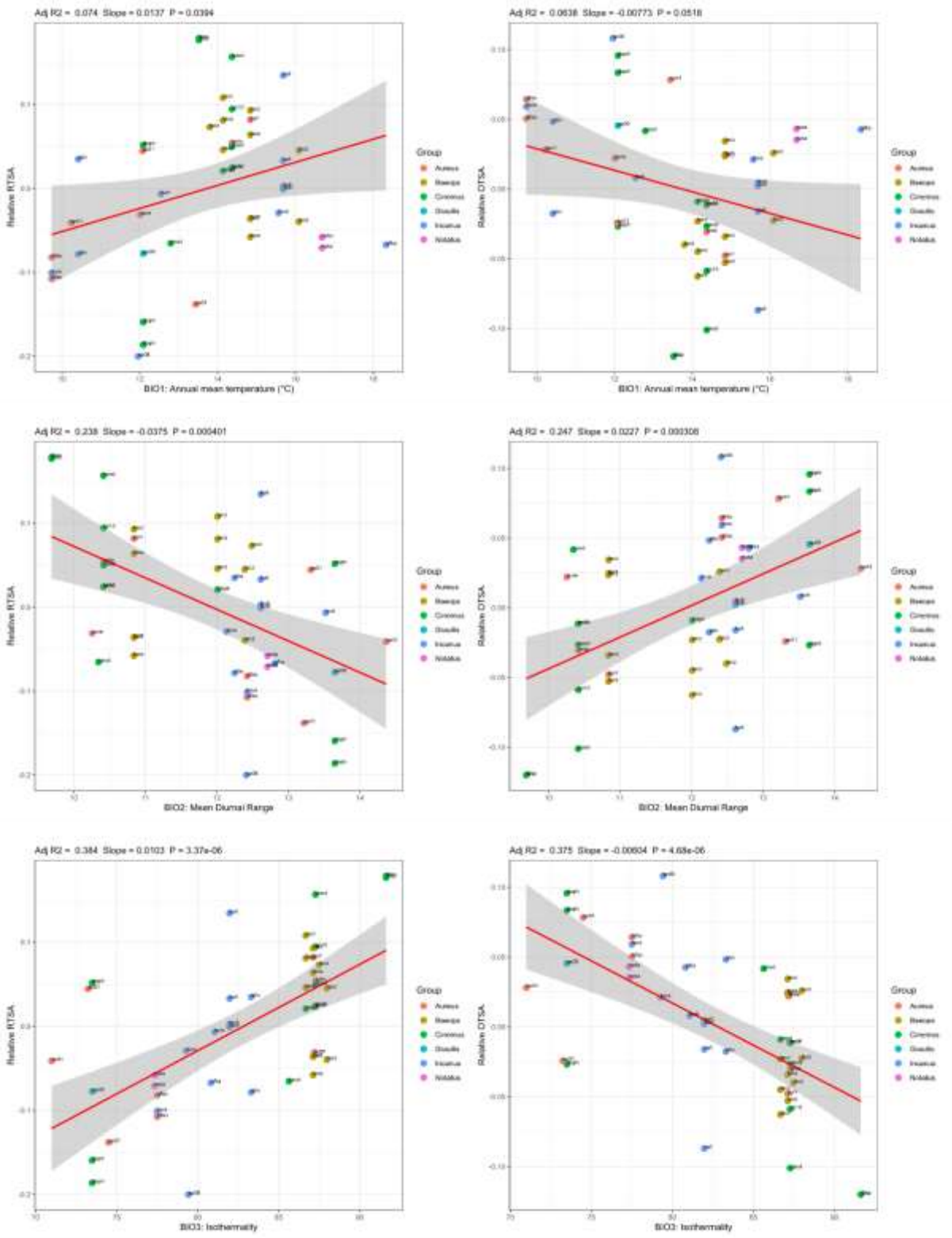

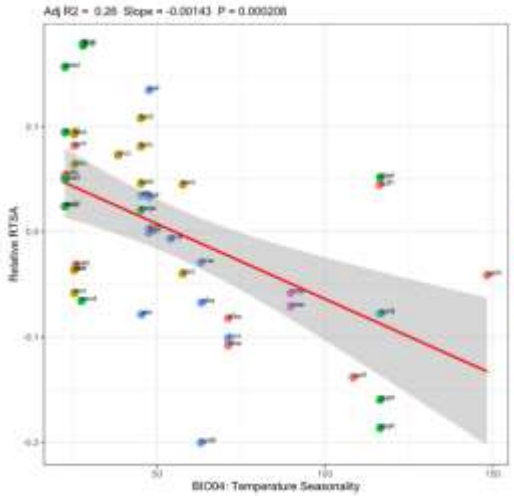
Adj R2 = 0.26 Slope = -0.00143 P = 0.000208
Relative RTSA
BIO04: Temperature Seasonality
Group
Aureus
Baeops
Cinereus
Gouldii
Insulus
NAMiss

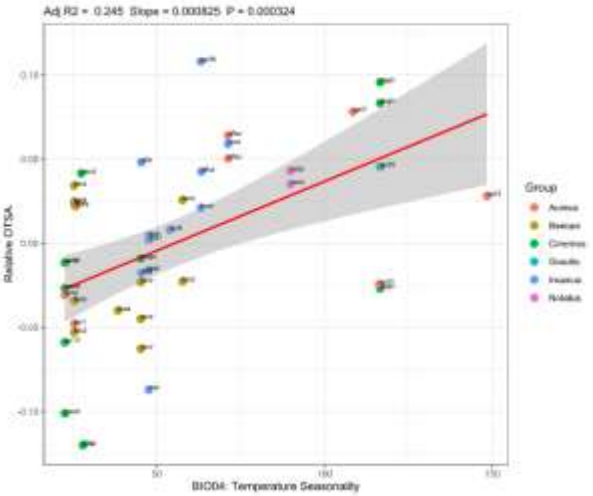
Adj R2 = 0.245 Slope = 0.000825 P = 0.000324
Relative OTSA
BIO04: Temperature Seasonality
Group
Aureus
Baeops
Cinereus
Gouldii
Insulus
NAMiss

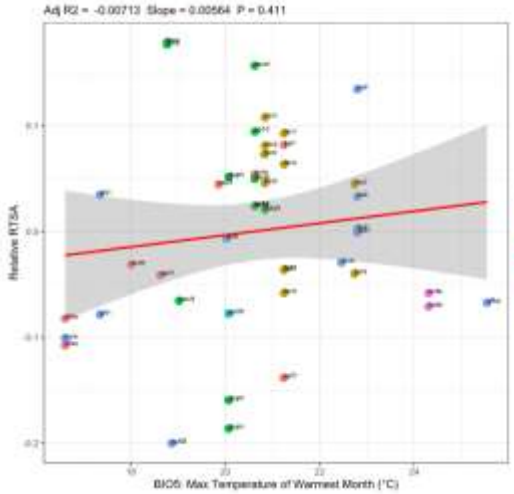
Adj R2 = -0.00713 Slope = 0.00564 P = 0.411
Relative RTSA
BIO5: Max Temperature of Warmest Month (°C)
Group
Aureus
Baeops
Cinereus
Gouldii
Insulus
NAMiss

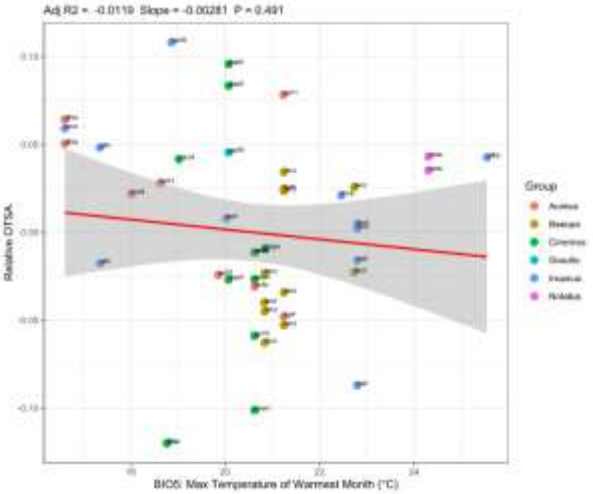
Adj R2 = -0.0119 Slope = -0.00281 P = 0.491
Relative OTSA
BIO5: Max Temperature of Warmest Month (°C)
Group
Aureus
Baeops
Cinereus
Gouldii
Insulus
NAMiss

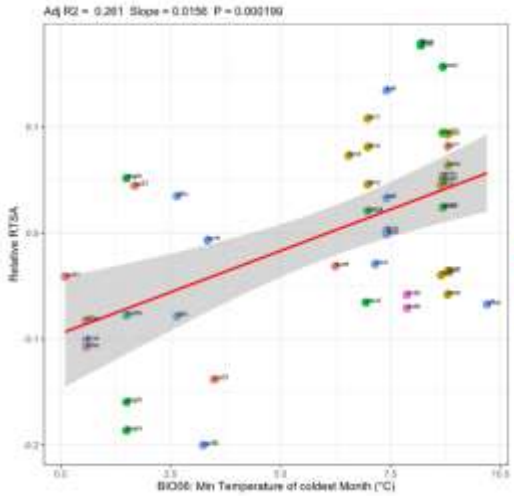
Adj R2 = 0.261 Slope = 0.0158 P = 0.000109
Relative RTSA
BIO06: Min Temperature of coldest Month (°C)
Group
Aureus
Baeops
Cinereus
Gouldii
Insulus
NAMiss

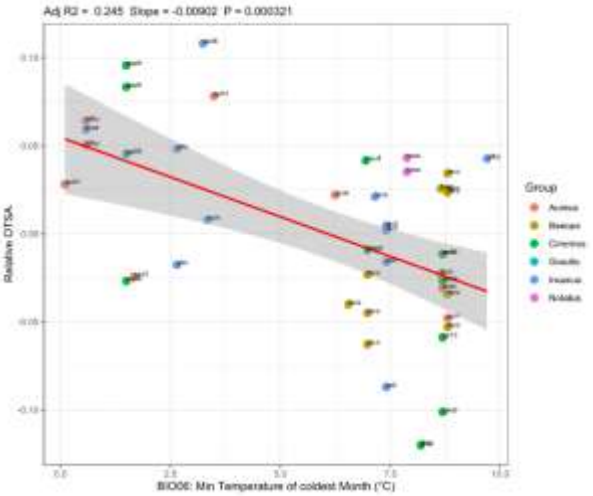
Adj R2 = 0.245 Slope = -0.00902 P = 0.000321
Relative OTSA
BIO06: Min Temperature of coldest Month (°C)
Group
Aureus
Baeops
Cinereus
Gouldii
Insulus
NAMiss

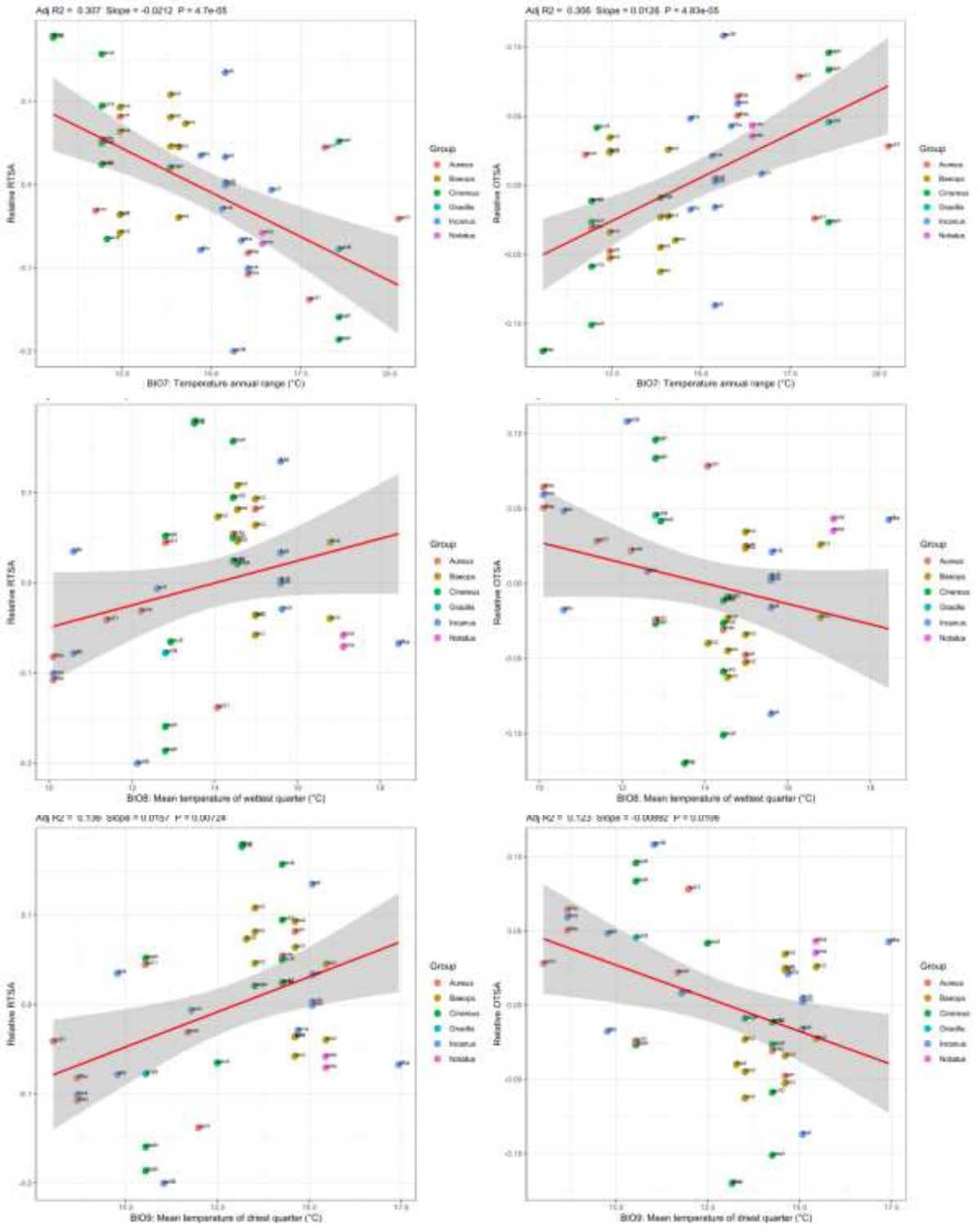
Adj R2 = 0.307 Slope = -0.0212 P = 4.7e-05
Relative RTSA
BIO7: Temperature annual range (°C)
Adj R2 = 0.306 Slope = 0.0126 P = 4.83e-05
Relative OTSA
BIO7: Temperature annual range (°C)
Group
Aureus
Baeops
Cinereus
Ossellis
Incanus
Notatus
Relative RTSA
BIO8: Mean temperature of wettest quarter (°C)
Relative OTSA
BIO8: Mean temperature of wettest quarter (°C)
Relative RTSA
BIO9: Mean temperature of driest quarter (°C)
Relative OTSA
BIO9: Mean temperature of driest quarter (°C)

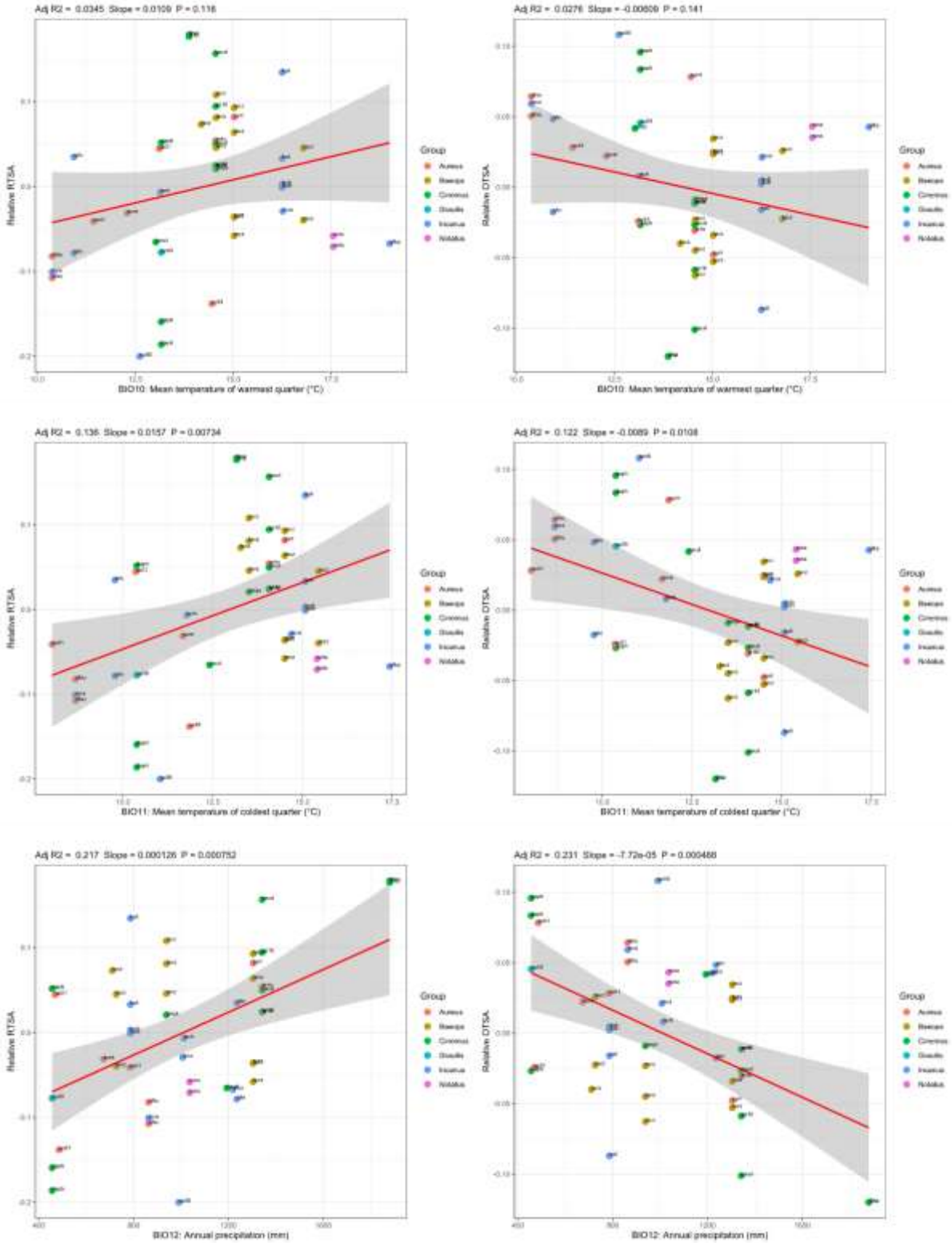
Adj R2 = 0.0345 Slope = 0.0109 P = 0.116
Relative RTSA
BIO10: Mean temperature of warmest quarter (°C)
Adj R2 = 0.0276 Slope = -0.00609 P = 0.141
Relative OTSA
BIO10: Mean temperature of warmest quarter (°C)
Adj R2 = 0.136 Slope = 0.0157 P = 0.00734
Relative RTSA
BIO11: Mean temperature of coldest quarter (°C)
Adj R2 = 0.122 Slope = -0.0089 P = 0.0108
Relative OTSA
BIO11: Mean temperature of coldest quarter (°C)
Adj R2 = 0.217 Slope = 0.000126 P = 0.000752
Relative RTSA
BIO12: Annual precipitation (mm)
Adj R2 = 0.231 Slope = -7.72e-05 P = 0.000488
Relative OTSA
BIO12: Annual precipitation (mm)
Group

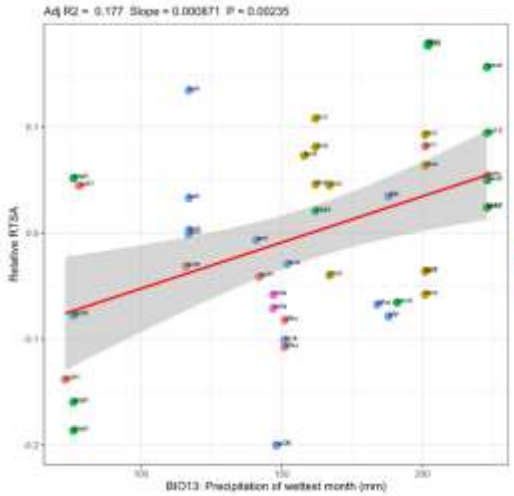
Adj R2 = 0.177 Slope = 0.000871 P = 0.00235
Relative RTSA
BIO13: Precipitation of wettest month (mm)
Group

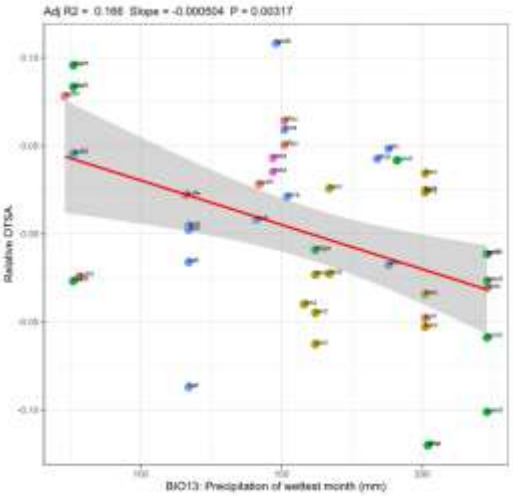
Adj R2 = 0.166 Slope = -0.000504 P = 0.00317
Relative OTSA
BIO13: Precipitation of wettest month (mm)
Group

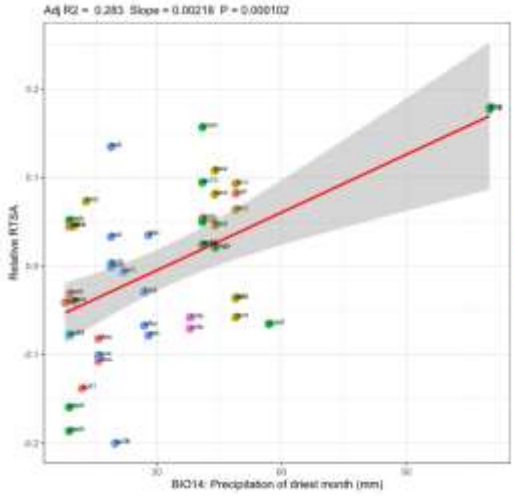
Adj R2 = 0.283 Slope = 0.00218 P = 0.000102
Relative RTSA
BIO14: Precipitation of driest month (mm)
Group

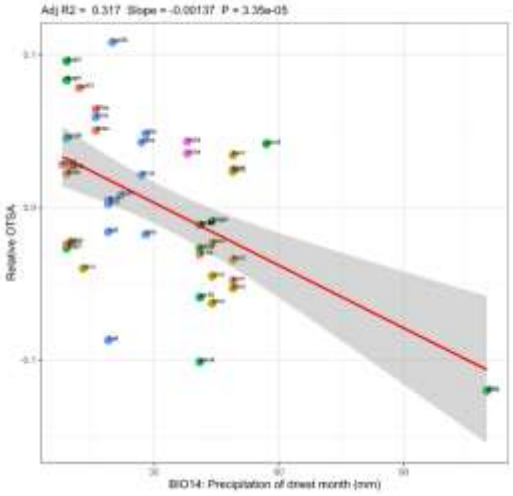
Adj R2 = 0.317 Slope = -0.00137 P = 3.35e-05
Relative OTSA
BIO14: Precipitation of driest month (mm)
Group

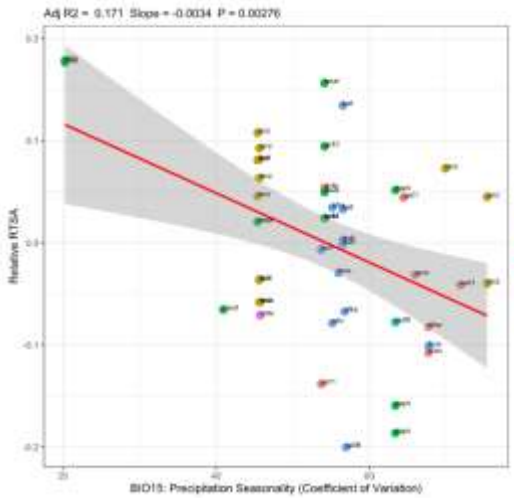
Adj R2 = 0.171 Slope = -0.0034 P = 0.00276
Relative RTSA
BIO15: Precipitation Seasonality (Coefficient of Variation)
Group

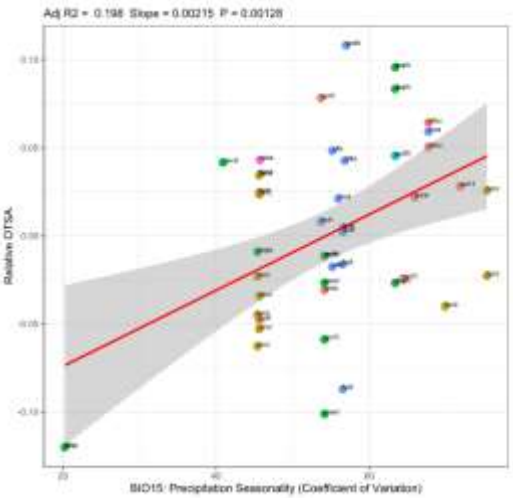
Adj R2 = 0.198 Slope = 0.00215 P = 0.00128
Relative OTSA
BIO15: Precipitation Seasonality (Coefficient of Variation)
Group

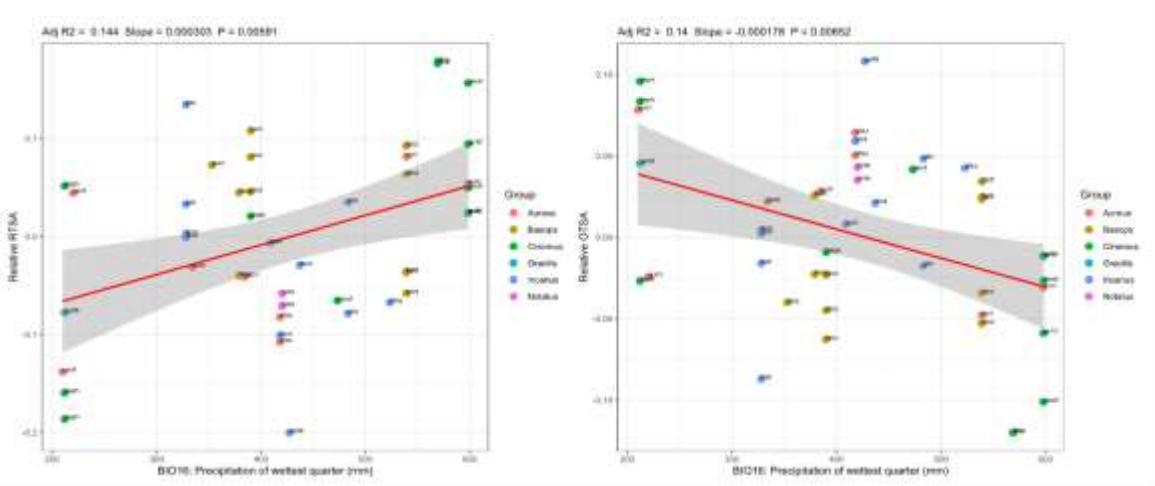
Adj R2 = 0.144 Slope = 0.000303 P = 0.00591
Relative RTSA
BIO16: Precipitation of wettest quarter (mm)
Group
Adj R2 = 0.14 Slope = -0.000178 P = 0.00652
Relative OTSA
BIO16: Precipitation of wettest quarter (mm)
Group

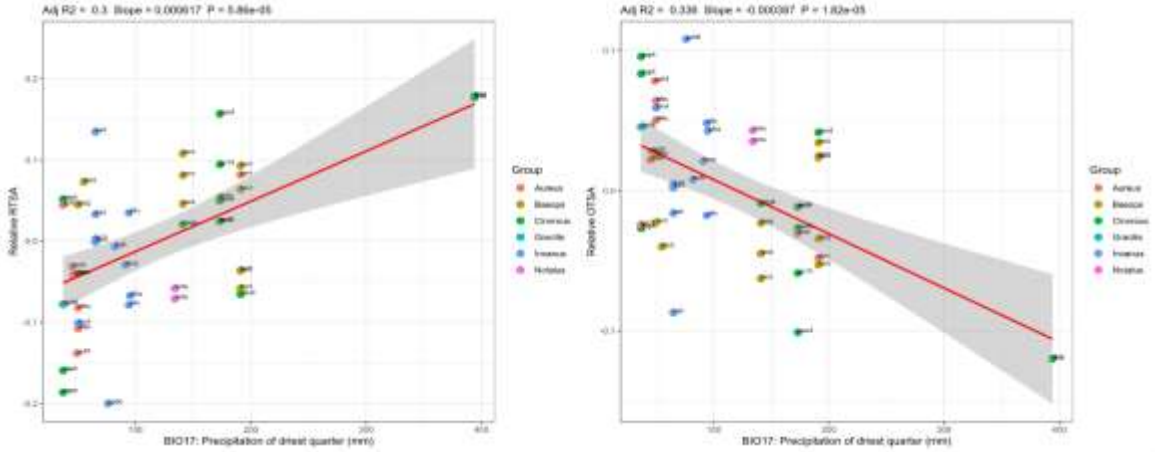
Adj R2 = 0.3 Slope = 0.000617 P = 5.86e-05
Relative RTSA
BIO17: Precipitation of driest quarter (mm)
Group
Adj R2 = 0.338 Slope = -0.000397 P = 1.82e-05
Relative OTSA
BIO17: Precipitation of driest quarter (mm)
Group

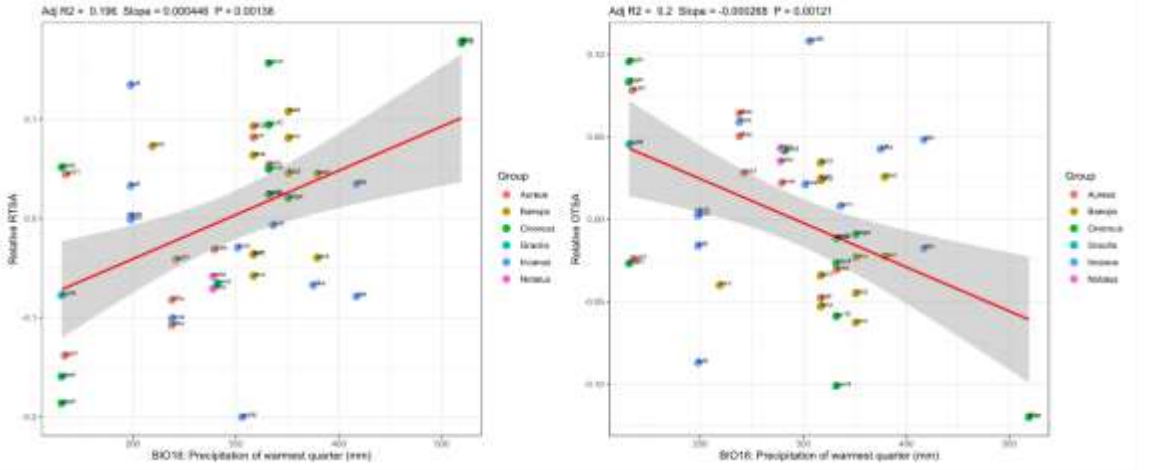
Adj R2 = 0.196 Slope = 0.000446 P = 0.00136
Relative RTSA
BIO16: Precipitation of warmest quarter (mm)
Group
Adj R2 = 0.2 Slope = -0.000268 P = 0.00121
Relative OTSA
BIO16: Precipitation of warmest quarter (mm)
Group

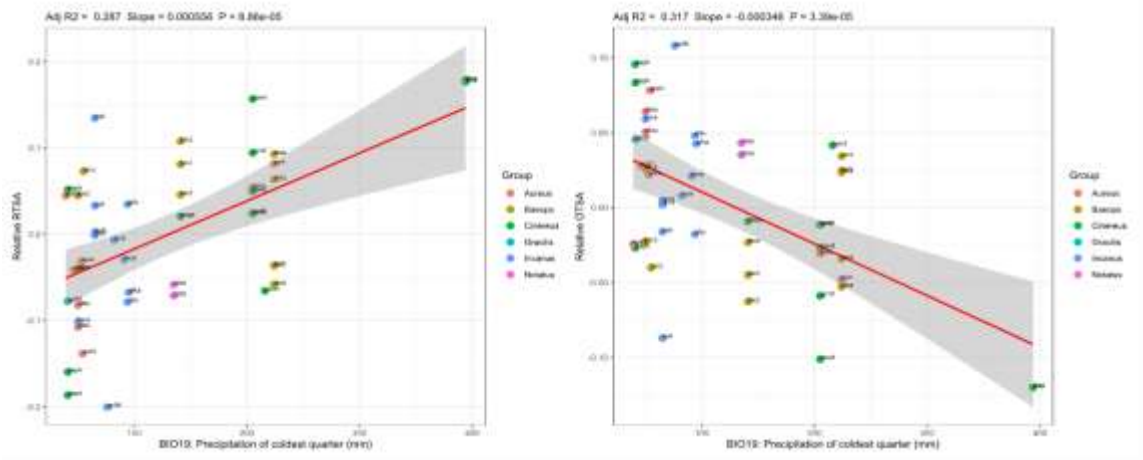
Adj R2 = 0.287 Slope = 0.000556 P = 9.86e-05
Relative RTSA
BIO19: Precipitation of coldest quarter (mm)
Group
Adj R2 = 0.317 Slope = -0.000348 P = 3.39e-05
Relative OTSA
BIO19: Precipitation of coldest quarter (mm)
Group

Extended abstract in French / Résumé étendu en français :

1. Objectifs du travail de thèse

L'objectif général de cette thèse est de proposer un cadre complet sur la monophylie et les limites des espèces du genre *Thomasomys* en utilisant l'analyse phylogénétique, d'analyser les adaptations morphologiques aux environnements de haute altitude et de clarifier le statut taxonomique d'une espèce candidate de *Thomasomys* au sein de la tribu Thomasomyini. Cette thèse est divisée en trois chapitres, chacun avec un objectif spécifique :

1. **Analyses phylogénétiques du genre *Thomasomys* et des limites des espèces :** Utiliser des analyses d'inférence phylogénétique sur des séquences d'ADN pour tester la monophylie du genre *Thomasomys*, évaluer les groupes d'espèces et les espèces candidates proposés par Pacheco (2003, 2015), et examiner la diversité des espèces en utilisant plusieurs méthodes de délimitation d'espèces unilocus.

2. **Étude des adaptations morphologiques chez *Thomasomys* :** Analyser les adaptations morphologiques des os turbinaux des espèces de *Thomasomys*, basées sur l'énoncé de Martinez et al. (2020) pour les espèces de rongeurs de haute altitude, afin de découvrir comment elles correspondent aux défis de l'altitude et de l'environnement, offrant ainsi des perspectives sur les réponses évolutives de *Thomasomys* aux divers habitats de haute altitude.

3. **Évaluation des *Thomasomys* non regroupés et implications taxonomiques pour le genre *Thomasomys* et la tribu Thomasomyini :** Examiner l'espèce candidate *Thomasomys* sp. 4 dans un cadre combiné moléculaire et morphologique, contribuant à la compréhension de *Thomasomys* sensu stricto et, dans l'ensemble, à la composition de la tribu Thomasomyini.

2. Principaux résultats

2.1. Chapitre 1: "Unilocus delimitation methods reveal the underestimated species diversity of *Thomasomys* (Rodentia, Cricetidae)"

- Confirmation de la monophylie et structure phylogénétique de *Thomasomys*: L'étude soutient la monophylie du genre *Thomasomys*, excluant « *Thomasomys* » sp. 4 de cette classification. Le genre forme un clade bien soutenu avec d'autres genres tels que *Chilomys* et *Rhipidomys*, indiquant des relations évolutives étroites. Dix grands clades au sein de *Thomasomys* ont été constamment identifiés à travers les analyses ML et BI, indiquant une structure phylogénétique complexe. Plusieurs espèces au sein de ces clades ont montré des relations paraphylétiques ou polyphylétiques, suggérant des histoires évolutives complexes et des classifications potentielles erronées d'espèces. En outre, l'étude a révélé des distances génétiques notables entre diverses espèces de *Thomasomys*, certaines montrant une variation génétique intraspécifique substantielle. Ces distances fournissent des informations critiques sur la différenciation génétique et le potentiel d'espèces non reconnues au sein du genre.

- Intégration des phylogénies moléculaires et des méthodes de délimitation des espèces : L'étude montre l'efficacité des phylogénies moléculaires et des méthodes exploratoires de délimitation des espèces dans l'évaluation des limites d'espèces. Malgré les débats sur la précision des approches à un seul gène, l'utilisation du gène Cytb s'est avérée efficace pour identifier les espèces potentielles, qui sont souvent validées par des approches multilocus et des méthodes morphologiques traditionnelles. En utilisant des méthodes de délimitation d'espèces unilocus telles que ABGD, ASAP, bPTP et GMYC, l'étude a déduit un nombre plus élevé d'espèces putatives par rapport à celles reconnues par la taxonomie actuelle (81-94 putative espèces contre 40 espèces et 20 espèces candidates initialement délimitées dans cette etude). Cette disparité indique un besoin de révision taxonomique complète du genre. Cette étude préconise l'utilisation de plusieurs loci moléculaires et une approche taxonomique intégrative pour une compréhension complète de la diversité et de l'histoire évolutive du genre.

- Implications biogéographiques : Les principaux clades sont principalement délimités par des caractéristiques géographiques, notamment la zone du Marañón (rivere plus foret sec). Cette découverte souligne le rôle significatif de cette zone en tant que barrière géographique influençant la distribution des espèces et la spéciation de *Thomasomys*. Ainsi que les espèces non résolues de *Thomasomys* présentent des défis pour l'analyse biogéographique, ajoutant de la complexité à notre compréhension des modèles de distribution et de diversification dans la région andine. Les modèles de distribution diversifiés des espèces de *Thomasomys*, incluant à la fois des distributions étendues et un endémisme localisé, soulignent la complexité écologique et l'importance de la conservation du genre.

2.2. Chapitre 2 : "Introduction to the *Thomasomys* (Rodentia: Cricetidae) turbinal bone adaptations: Insights into elevation and environmental challenges"

- Caractérisation des os turbinaux : L'étude montre que les espèces de *Thomasomys*, à travers 45 spécimens analysés par des scans 3D CT, présentent des motifs cohérents dans la complexité et la taille de leurs os turbinaux. Les espèces de *Thomasomys* possèdent deux turbinaux respiratoires (nasoturbinal et maxilloturbinal) dans la partie antérieure du rostre et sept turbinaux olfactifs (lamina semi-circulaire, frontoturbinal 1, frontoturbinal 2, ethmoturbinal I, interturbinal, ethmoturbinal II, et ethmoturbinal III) dans la partie postérieure, chacun avec des variations structurelles. Ces structures sont essentielles pour réchauffer et humidifier l'air inspiré et pour l'olfaction.

- Relations allométriques : Une relation allométrique positive significative a été observée entre les zones de surface turbinaux (respiratoires et olfactives) et la longueur du crâne. Cela suggère que les espèces de *Thomasomys* plus grandes ont proportionnellement des turbinaux plus grands.

- Corrélation des turbinaux : Il existe une corrélation positive entre les surfaces relatives des nasoturbinaux et maxilloturbinaux, et entre les turbinaux respiratoires et olfactifs, suggérant l'absence de trade-off évolutif entre ces structures.

- Impact de l'altitude et des variables bioclimatiques: Les espèces de *Thomasomys* habitant à des altitudes plus basses ont tendance à avoir des turbinaux plus petits par rapport à celles vivant à des altitudes plus élevées. Cela suggère que des turbinaux respiratoires plus grands (dimensionnés par la longueur du crâne) peuvent être une adaptation aux défis des habitats de haute altitude, tels que l'air plus fin et plus froid. Les variables bioclimatiques influencent de manière significative les zones de surface turbinales, en particulier lorsqu'on considère la répartition fonctionnelle des turbinaux (dimensionnée par TTSA).

- Implications méthodologiques dans le dimensionnement des turbinaux : L'étude souligne l'importance de l'ajustement par taille et par surface totale lors de l'évaluation des zones de surface turbinales pour interpréter précisément leur signification morphologique et écologique.

2.3. Chapitre 3: "Three new species of *Thomasomys*-like form from the central Peruvian montane forest and a new perspective of the tribe Thomasomyini"

- Réévaluation de la monophylie de *Thomasomys* et des Thomasomyini : Utilisant à la fois des données morphologiques qualitatives et quantitatives, ainsi que des analyses moléculaires complètes impliquant 13 gènes mitochondriaux et 5 gènes nucléaires, l'étude offre une meilleure compréhension des relations phylogénétiques dans la tribu. Le genre *Thomasomys* a été trouvé monophylétique et étroitement lié à *Rhipidomys*, tandis que les relations entre les autres genres de la tribu restent non résolues complètement. D'autre part, L'étude a également identifié des spécimens ressemblant à *Thomasomys* (« *Thomasomys* » sp. 4) remettant en question les relations évolutives au sein de la tribu des Thomasomyini ou *Rhagomys* a été trouvé comme faisant partie de cette tribu.

- Découverte d'un nouveau genre et de trois nouvelles espèces : L'étude découvre un nouveau genre distinct des genres Thomasomyini typiquement connus (*Aepeomys*, *Chilomys*, *Rhipidomys* et *Thomasomys*), basé sur l'analyse phylogénétique. L'analyse phylogénétique non seulement soutient fortement la monophylie de ce genre, mais révèle également sa divergence moléculaire notable de trois lignées, avec des variances génétiques allant de 5,4% à 6,98%. Ces preuves

établissent fermement qu'elles représentent trois nouvelles espèces endémiques des Yungas centrales du Pérou. L'étude va plus loin en décrivant formellement ces nouvelles espèces (« Oxapampa », « Tarma » et « Satipo »). Ces descriptions sont étayées par une analyse morphologique détaillée, soulignant des caractéristiques qui les distinguent nettement des genres existants dans la tribu Thomasomyini.

- Implications pour la taxonomie : *Thomasomys*, reconnu pour sa grande diversité en morphologie et en taille, aurait pu occulter l'identité distincte de « *Thomasomys* » sp. 4 ainsi que d'autres genres tels que *Aepeomys*, *Chilomys* et *Rhipidomys* dans des approches morphologiques. La découverte et la description de ces espèces ont des implications cruciales pour la taxonomie de la tribu des Thomasomyini et la redéfinition de sa composition. D'autre part, la position basale d'*Aepeomys* au sein de la tribu est essentielle pour définir la composition globale des Thomasomyini, affirmant l'inclusion de *Rhagomys*. Une approche taxonomique conservatrice est préconisée pour éviter l'inflation taxonomique et maintenir la clarté dans la classification des rongeurs sigmodontins.

3. Discussion général

Dans cette étude, Ruelas et al. (2024 : Chapitre 1 ; en prép. : Chapitre 3) ont trouvé que la monophylie de *Thomasomys* est conditionnelle à l'exclusion de « Thomasomys » sp. 4, qui a été trouvé soit apparenté à *Thomasomys*, soit à Rhagomys en utilisant différents ensembles de données moléculaires. De plus, Ruelas et al. (2024 : Chapitre 1) ont corroboré la monophylie des groupes Baeops, Cinereus et Notatus représentés par des clades majeurs dans la phylogénie. En revanche, les groupes Gracilis et Aureus sont paraphylétiques en accord avec des études antérieures (par exemple, Salazar-Bravo & Yates, 2007 ; Lee et al., 2015, 2018 ; Brito et al., 2019 ; Pacheco & Ruelas, 2023). Il est intéressant de noter que l'inclusion de *Thomasomys macrotis* dans le groupe Incanus a conduit à la reconnaissance de ce dernier comme monophylétique, clarifiant ainsi les relations taxonomiques au sein de ces groupes discutés précédemment par Leo et Gardner (1993) et Pacheco (2003, 2015c). De plus, Ruelas et al. (2024 ; Chapitre 1) ont trouvé que les principaux clades des groupes Cinereus et Aureus sont

géographiquement séparés, avec des distributions soit à l'ouest, soit à l'est du fleuve Marañón. Malgré ces avancées, nos connaissances restent incomplètes, en particulier en raison de l'absence de données moléculaires sur plusieurs espèces.

Ruelas et al. (2024 : Chapitre 1) ont également découvert que *T. aureus* s.l. est paraphylétique, comprenant au moins cinq espèces candidates, chacune avec une petite aire de répartition. Cette découverte est cohérente avec le modèle de répartition limitée généralement observé dans ce genre. La délimitation minutieuse de *T. aureus* s.s. fournit des informations cruciales sur la diversité des espèces. Elle suggère que d'autres populations précédemment classées sous l'épithète aureus devraient mériter une distinction d'espèce et être comprises comme faisant probablement partie d'un cas de convergence morphologique. Cela est particulièrement intrigant car les espèces du complexe *T. aureus*, malgré leur similitude externe, sont apparentées à des espèces distinctement différentes, par exemple, *T.* aff. *aureus* « Lambayeque-Cajamarca S » et *T. praetor*. De telles découvertes montrent que les similitudes morphologiques au sein du complexe T. aureus masquent des différences phylogénétiques profondes, prouvant que ces espèces visuellement similaires ont évolué indépendamment. Cette situation dans le complexe *T. aureus* reflète un scénario observé dans le complexe d'espèces Akodon orophilus, initialement vu comme une seule espèce. Des études caryologiques et morphologiques (Jiménez et al., 2013 ; Jiménez & Pacheco, 2016) l'ont révélé comme trois espèces morphologiquement similaires : *A. orophilus*, *A. josemariarguedasi* et *A. kotosh*. Par la suite, une étude moléculaire (Ruelas et al., 2020) les a trouvées non étroitement apparentées, soulignant les limites de l'utilisation de la seule morphologie pour la classification des petits rongeurs.

Malgré les limitations inhérentes, Ruelas et al. (2024 : Chapitre 1) ont fait des progrès significatifs dans l'identification des espèces au sein du genre et ont non seulement identifié plusieurs espèces cryptiques, mais ont également fourni un soutien moléculaire pour certaines espèces candidates précédemment signalées par Pacheco (2003, 2015c) et d'autres auteurs (par exemple, Brito et al., 2019, 2021 ; Lee et al., 2018, 2022 ; Pacheco & Ruelas, 2023). Cette diversité cachée pourrait

doubler le nombre d'espèces connues de *Thomasomys*, améliorant la compréhension de la diversité du genre et aidant à une classification plus précise de ses espèces.

En outre, la découverte d'un nouveau genre au sein des Thomasomyini, « *Thomasomys* » sp. 4, comprenant trois espèces (« Oxapampa », « Tarma », « Satipo »), est un développement important dans le domaine de la taxonomie des sigmodontinés (Ruelas et al. en prép. : Chapitre 3). Ses relations phylogénétiques dans une approche multilocus, cependant, restent ambiguës, car elles varient selon l'ensemble de données et l'analyse utilisés. Selon la méthode, il est soit faiblement supporté comme groupe frère de *Rhagomys* en utilisant des gènes mitochondriaux dans l'analyse de Maximum de Vraisemblance (ML), de *Chilomys* dans l'Inférence Bayésienne (BI), ou de *Thomasomys* avec des gènes nucléaires (Ruelas en prép. : Chapitre 3). Ces découvertes pourraient démontrer que la diversité morphologique extensive trouvée chez *Thomasomys* a éclipsé les caractéristiques morphologiques uniques d'autres genres de Thomasomyini, tels que *Aepeomys*, *Chilomys*, *Rhipidomys*, et « *Thomasomys* » sp. 4. Ruelas et al. (en prép. : Chapitre 3) soulignent les défis significatifs pour définir avec précision les limites des espèces et des genres au sein du clade *Thomasomys* sensu Pacheco (2003). Ils ont observé que « *Thomasomys* » sp. 4 et les espèces du groupe Incanus et *Aepeomys*, qui partagent des turbinaux complexes et enroulés, pourraient présenter une évolution convergente en raison de l'habitation à des altitudes similaires mais à des distributions différentes. En particulier, la variation des traits morphologiques et les contraintes posées par les caractéristiques d'échantillons limités ont conduit à une sous-estimation des identités distinctes des espèces au sein de ce complexe. Cela soulève la possibilité de deux chemins distincts de diversification morphologique au sein du groupe, un pour *Rhagomys* et un autre pour *Aepeomys*, *Chilomys*, *Rhipidomys*, *Thomasomys* et « *Thomasomys* » sp. 4. La disparité morphologique significative entre ces deux groupes a été notée par divers auteurs (par exemple, Luna, 2015 ; Pardiñas et al., 2022) et est attribuée à la spécialisation de *Rhagomys* dans les habitats de sous-bois denses, tels que les roseaux, les bambous et une végétation similaire. Cette divergence morphologique marquée a été un facteur clé dans la décision d'établir Rhagomyini comme une tribu distincte uniquement pour *Rhagomys*.

Cependant, Ruelas et al. (en prép. : Chapitre 3) remettent en question cette décision, grâce à un échantillonnage de gènes plus complet (13 gènes mitochondriaux et 5 gènes nucléaires), plaidant pour la reclassification de Rhagomys au sein de Thomasomyini. Les preuves phylogénétiques suggèrent que Thomasomyini, incluant *Rhagomys* — qu'il soit positionné comme basal, groupe frère d'un autre genre thomasomyine, ou avec des relations non résolues — forme systématiquement une lignée bien soutenue. Cette perspective s'aligne avec la proposition initiale de D'Elía et al. (2006) et Pacheco et al. (2015), et préconise une approche taxonomique conservatrice mettant l'accent sur la stabilité, la clarté et la signification biologique. L'intégration des données écologiques dans les discussions améliore la compréhension de la signification évolutive et adaptative de ces groupements taxonomiques, garantissant que les décisions taxonomiques reflètent à la fois les relations génétiques et les adaptations écologiques. Cette approche holistique fournit un cadre complet pour étudier la tribu diverse et complexe des Thomasomyini. En minimisant les changements taxonomiques brusques, cette approche met en évidence des différences biologiques significatives et des relations évolutives au sein de la tribu, facilitant ainsi une compréhension plus fine des dynamiques évolutives au sein des Thomasomyini et contribuant à une taxonomie raffinée et précise. Cette stratégie conservatrice garantit que les classifications taxonomiques reflètent les histoires évolutives, améliorant ainsi la recherche dans divers domaines scientifiques.

Tous les genres au sein de la tribu Thomasomyini, y compris *Aepeomys*, *Chilomys*, *Thomasomys*, et « *Thomasomys* » sp. 4, sont endémiques des forêts montagnardes et des páramos, certaines espèces de *Rhipidomys* et *Rhagomys* étant également endémiques de ces habitats de haute altitude. Cette distribution a conduit à la désignation informelle de la tribu comme « thomasomines andins » (Pacheco, 2003). Ces espèces, en particulier celles du genre *Thomasomys*, sont hautement spécialisées pour survivre dans des environnements plus frais et de haute altitude, habitant généralement entre 2000 et 3500 mètres (Ruelas et al. 2024 : Chapitre 1).

Thomasomys, reconnu pour sa diversité au sein de la sous-famille des Sigmodontinae, montre une adaptabilité significative dans ces habitats. Ruelas (en rév. : Chapitre 2), se concentrant sur leurs adaptations de haute altitude, examine particulièrement le rôle de la taille des surfaces turbinales et révèle une forte corrélation entre la taille des surfaces turbinales (lorsqu'elles sont ajustées à la longueur du crâne), l'altitude et les précipitations annuelles, suggérant des adaptations pour une fonction respiratoire efficace en haute altitude. Cela s'aligne avec des études sur d'autres petits mammifères dans des environnements de haute altitude, qui se concentrent sur les adaptations du taux métabolique, de la respiration, de la capacité d'oxygène dans le sang et de la rétention d'humidité (par exemple, Arias-Reyes et al., 2021 ; Martinez et al., 2020 ; Schippers et al., 2012 ; Withers et al., 2016a). Les espèces plus grandes de *Thomasomys* présentent une surface respiratoire moins importante par rapport à leur taille (c'est-à-dire les espèces du groupe Aureus), une tendance cohérente avec les espèces caniformes plus grandes (Green et al., 2012). L'étude souligne également les influences potentielles du régime alimentaire, de l'habitat et de l'âge sur la morphologie turbinale, mettant en évidence des domaines pour de futures recherches. Cependant, il existe une corrélation minimale entre les surfaces turbinales et les variables bioclimatiques, soulignant l'influence du régime alimentaire et de l'habitat (par exemple, type de forêt). D'autre part, Ruelas (en rév. : Chapitre 2) a identifié une corrélation entre l'OTSA (ajustée à la TTSA) et les variables bioclimatiques, suggérant une adaptation évolutive de la proportion olfactive aux pressions environnementales, cruciale pour la survie dans divers écosystèmes montagnards. Cela souligne le rôle critique de l'olfaction dans le succès écologique de *Thomasomys*, mettant en lumière ses adaptations évolutives aux habitats de haute altitude. La recherche continue sur leurs traits morphologiques et physiologiques est essentielle pour comprendre les mécanismes derrière leur succès.

La corrélation significative observée entre les turbinaux respiratoires et olfactifs remet en question la vision traditionnelle d'un compromis entre ces structures, suggérant une potentielle co-dépendance (Green et al., 2012 ; Martinez et al., 2018, 2020 ; Van Valkenburgh et al., 2011). En outre, Ruelas et al. (en rév. : Chapitre 2) soulignent l'importance d'ajuster la taille des turbinaux, en particulier

par la longueur du crâne (SL) et la surface totale des turbinaux (TTSA), pour des évaluations précises et des insights sur les modèles évolutifs. Cette approche est fondamentale pour distinguer les espèces et déchiffrer leurs adaptations évolutives et écologiques. Ruelas et al. (en rév. : Chapitre 2) ont montré que l'ajustement par SL met en évidence comment l'altitude influence le développement turbinal, reliant les structures turbinales à la taille corporelle et aux changements allométriques potentiels. En revanche, l'ajustement par TTSA met en évidence les adaptations fonctionnelles aux facteurs environnementaux, soulignant l'impact notable des variables bioclimatiques sur les proportions turbinales (par exemple, Green et al., 2012 ; Martinez et al., 2018, 2020 ; Mitchell et al., 2023 ; Porto et Enfin, Ruelas et al. (en rév. : Chapitre 2) propose que la radiation adaptative et le succès de Thomasomys dans des habitats de haute altitude difficiles pourraient constituer une réponse évolutive significative à de nouveaux environnements. Des études moléculaires complètes et des recherches comparatives avec d'autres mammifères de haute altitude sont nécessaires pour pleinement étayer cette hypothèse.

Les recherches futures sur *Thomasomys* doivent prioriser l'inclusion des holotypes afin d'élucider ou de clarifier le statut des espèces candidates identifiées dans ce travail et par d'autres auteurs (Ruelas et al., en cours). Cette approche est cruciale pour *Thomasomys*, où les espèces sont souvent supposées occuper des aires de distribution très limitées, et les spécimens des localités voisines sont rares. De plus, la grande diversité morphologique au sein du genre complique les efforts taxonomiques, rendant difficile la vérification de l'exactitude de l'identification des espèces dans les collections récentes ou des spécimens utilisés pour des comparaisons provenant de collections scientifiques. Par exemple, la classification des espèces et des espèces candidates au sein du groupe Aureus, précédemment identifiées comme *T. aureus* d'Équateur, nécessite une réévaluation pour déterminer si elles représentent des espèces distinctes valides ou des candidates, ou si elles font partie de *T. aureus* s.s., qui n'est connu que par une peau sans crâne. Bien que d'autres spécimens aient été utilisés pour représenter *T. aureus* s.s. dans les phylogénies moléculaires et morphologiques, avec leur localité posée comme la localité type probable, la véritable localité type reste incertaine. De même, la

validité de T. *nicefori*, débattue par certains comme synonyme de *T. popayanus* (e.g., Voss 2003, Pacheco 2015c), nécessite une clarification.

La découverte de plusieurs clades pour *T. kalinowskii* ou *T. ischyrus* par Ruelas et al. (2024 : Chapitre 1 ; en prép. : Chapitre 3) souligne encore la nécessité d'un examen détaillé. Cependant, obtenir des séquences à partir des holotypes, dont beaucoup ont été collectés et décrits il y a plus d'un siècle (Tableau 1), présente un défi significatif. Les méthodes de préparation et les conditions de stockage de ces spécimens influenceront considérablement la faisabilité de l'extraction d'ADN viable pour les analyses moléculaires. De plus, toutes les espèces candidates nécessitent une révision taxonomique approfondie pour confirmer leur statut d'espèces distinctes valides. Pour les espèces et les candidates précédemment caractérisées par Pacheco (2003, 2015c), ce processus est facilité par les données morphologiques existantes. Cette focalisation stratégique sur l'intégration des holotypes et la révision taxonomique complète est essentielle pour faire progresser notre compréhension de la diversité des *Thomasomys* et garantir une délimitation précise des espèces au sein de ce genre complexe.al., 2013 ; Weaver & Grossnickle, 2020).

4. Conclusions

Cette étude révèle la monophylie de *Thomasomys* dans une approche unilocus et multilocus, sous réserve d'exclure « *Thomasomys* » sp. 4, suggérant un nouveau genre. Les principaux clades au sein de *Thomasomys*, tels que Baeops, Cinereus et Notatus, sont confirmés comme monophylétiques, tandis que les groupes Gracilis et Aureus apparaissent paraphylétiques. L'inclusion de *T. macrotis* dans le groupe Incanus clarifie sa monophylie, abordant les ambiguïtés taxonomiques précédentes. La ségrégation géographique des groupes Cinereus et Aureus par la rivière Marañón souligne la complexité de la spéciation de *Thomasomys*. La paraphylie de *T. aureus* s.l., révélant cinq espèces candidates, souligne la diversité mais aussi les gammes de distribution limitées du genre, suggérant un besoin de délimitation prudente des espèces et de prise en compte de la convergence morphologique.

Cette étude marque également une avancée significative dans notre compréhension du genre *Thomasomys*, révélant une diversité cachée qui pourrait potentiellement doubler le nombre d'espèces reconnues au sein de ce genre. Ces découvertes soulignent l'importance des analyses moléculaires et morphologiques dans la compréhension de la diversité des espèces, particulièrement dans les genres ayant des histoires taxonomiques complexes comme *Thomasomys*.

La découverte du nouveau genre « *Thomasomys* » sp. 4 dans les Yungas péruviens et l'examen détaillé des os turbinaux chez Thomasomys et les genres apparentés suggèrent des adaptations évolutives en réponse aux pressions environnementales andines pour les membres andins des Thomasomyini. Les découvertes de l'étude sur les structures osseuses turbinales de *Thomasomys* suggèrent des adaptations évolutives pour une fonction respiratoire efficace dans des environnements de haute altitude, avec des implications pour comprendre le succès écologique de *Thomasomys* à travers des écosystèmes montagnards variés.

Les recherches futures devraient se concentrer sur l'incorporation d'holotypes pour clarifier le statut des espèces candidates, des analyses biogéographiques complètes pour comprendre la diversification andine, et l'examen des barrières géographiques dans la spéciation. Cette approche intégrative améliorera notre compréhension de la biodiversité andine et du succès évolutif de *Thomasomys* dans des habitats de haute altitude.